Dissertation zur Erlangung des Doktorgrades
der Fakultät für Chemie und Pharmazie
der Ludwig-Maximilians-Universität München

Structure-based design and synthesis of novel CLK1 inhibitors

Angelina Evelyn Dauser (geb. Welsch)
aus
Augsburg

2022

Erklärung

Diese Dissertation wurde im Sinne von § 7 der Promotionsordnung vom 28. November 2011 von Herrn Prof. Dr. Franz Bracher betreut.

Eidesstattliche Versicherung

Diese Dissertation wurde eigenständig und ohne unerlaubte Hilfe erarbeitet.

München, 15.06.2022

.....

Angelina Dauser

Dissertation eingereicht am 15.06.2022

1. Gutachter: Prof. Dr. Franz Bracher

2. Gutachter: Prof. Dr. Franz Paintner

Mündliche Prüfung am 01.08.2022

Danksagung

An erster Stelle möchte ich mich bei meinem Doktorvater Herrn Prof. Dr. Franz Bracher bedanken – dafür, dass er mich in seinen Arbeitskreis aufgenommen und diese Dissertation überhaupt ermöglicht hat, sowie für die stete Unterstützung und Förderung. Zudem gilt mein herzlichster Dank allen Mitgliedern der Promotionskommission, insbesondere Herrn Prof. Dr. Franz Paintner für die Übernahme des Koreferats.

Auch bei meinen Kooperationspartnern möchte ich mich bedanken: für die Anfertigung der Co-Kristallstrukturen bei Prof. Dr. Oded Livnah (Hebrew University Jerusalem) und für die Auswertung dieser bei Dr. Michael Meyer (MBC-Statistik), für die DSF Messungen bei Prof. Dr. Stefan Knapp (Goethe Universität Frankfurt) und für die CLK1 Testung bei Dr. Jens Peter von Kries (FMP Berlin).

Vielen Dank an Dr. Lars Allmendinger und Claudia Glas für die Messung der zahlreichen NMRs sowie an Dr. Werner Spahl für die Messung all der Massen. Des Weiteren möchte ich mich bei Anna Niedrig für die Messung einer jeden HPLC Reinheit bedanken und bei Martina Stadler für die Durchführung der MTT- und Agardiffusionstests. Danke auch allen Studenten, die einen Beitrag zu dieser Arbeit geleistet haben – insbesondere Francesca Donà, Lukas Finger und Moritz Kornmayer.

Nicht nur für das tapfere Korrekturlesen geht ein ganz besonderer Dank an Dr. Desirée Heerdegen und Dr. Susanne Rautenberg – ohne eure Bereitschaft Wissen zu teilen und zu helfen, eure Geduld und euer immer offenes Ohr wäre diese Arbeit niemals entstanden. Auch Dr. Carina Glas und Charlotte Leser danke ich vielmals für ihre Ratschläge und den ein oder anderen (notwendigen) Schubs in die richtige Richtung.

Allen aktuellen und ehemaligen Mitgliedern des AK Bracher möchte ich für die schöne Zeit und die gute Arbeitsatmosphäre danken und Herrn Dr. Jürgen Krauss außerdem für die tolle Zusammenarbeit in der Lehre. Das Doktorandendasein hat mich nicht nur viele Nerven gekostet, sondern mir auch wahnsinnig viele schöne Momente und Freundschaften beschert. Ich bin unendlich froh, dass ich diese Zeit in unserem Relatively Nice Network erleben durfte.

Für ihre ganz besondere Freundschaft möchte ich mich außerdem bei Marion & Michaela bedanken, auf die ich mich seit dem ersten (Schul- bzw. Uni-) Tag immer verlassen kann.

Der größte Dank gebührt jedoch meiner Familie. Meinen großen Brüdern Alexander & Andreas. Meinen Eltern – Manuela & Joachim – für ihre immerwährende Liebe und die bedingungslose Unterstützung in allen Lebenslagen. Und meinem Mann Tobias, der mir an jedem Tag ein Lächeln in Gesicht zaubert und mich daran erinnert, niemals aufzugeben.

Ich danke euch von ganzem Herzen.

FÜR MEINE MAMA

Table of contents

1 Introduction

As a consequence of the FDA approval of Gleevec (imatinib mesylate) in 2001, PHILIP COHEN posed the prophesying question “Protein kinases – the major drug targets of the twenty-first century?”[1] and 20 years later it is apparent, how right he was about that.

Although the true future meaning of this drug was not evaluable at the time of approval, the treatment of chronic myelogenous leukemia (CML) with the protein kinase inhibitor imatinib (**Figure 1**) was surely considered as a milestone from the very beginning. Protein kinases, despite known to be over-activated and over-expressed in several malignant tumors, were formerly said to be “undruggable”, since the very early ATP competitive inhibitors were lacking both, potency and selectivity. However, when the bisindolyl maleimide staurosporine was identified as nanomolar inhibitor of protein kinase C in 1986[2], it became plausible to overcome the first issue. While this natural product isolated from *Streptomyces staurosporeus*[3] is still highly unselective, it could be further developed and the semi-synthetic *N*-benzoyl derivative midostaurin even became FDA approved in 2017[4]. Thus, neither imatinib nor midostaurin inhibit just a single kinase and this “unspecificity” even has synergistic effects in cancer treatment[4-5].

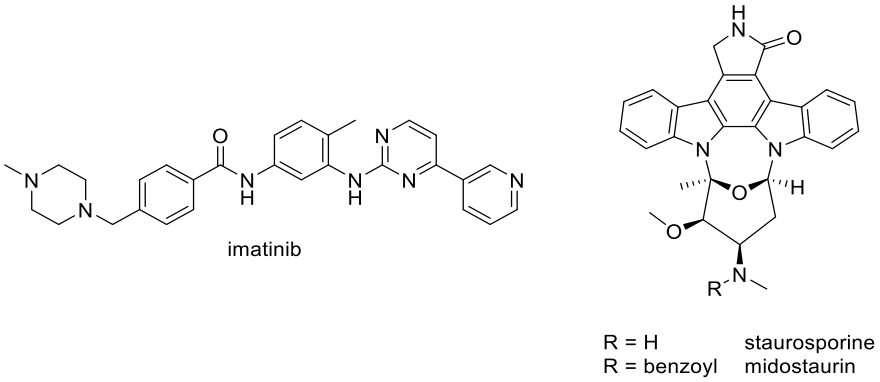

Figure 1. Structure of the kinase inhibitors imatinib, staurosporine and midostaurin.

The very first, in 1999, FDA approved kinase inhibitor was immunosuppressant rapamycin, that was found to target mTOR[6]. However, imatinib was the first drug to be developed for a specific kinase, the BCR-ABL tyrosine kinase, which is constitutively activated in Philadelphia chromosome-positive CML patients resulting in uncontrolled growth of leukemic cells. This breakthrough in therapy was not just an unprecedented proof to emphasize the potential of target-based medicinal chemistry, but even changed the lives of so many patients. A disease,

which had been rare due to very bad prognosis, has just become (not curable but at least) manageable[1, 7].

In the subsequent two decades several FDA approvals of kinase inhibitors followed, resulting in overall 73 drugs until September 2021[8]. The major part of these drugs still covers cancer indications, but also other therapeutic areas are already accessed, such as rheumatoid arthritis, ulcerative colitis, fibrosis or ocular hypertension, and many more are addressed in clinical trials[8]. The major drawback of kinase inhibitors in antitumor therapy is, similar to other approaches, the development of resistance by mutation. This affords constant improvement of inhibitors leading e.g. to dasatinib, nilotinib and ponatinib as therapeutic options for imatinib-resistant CML[7]. Besides optimizing ligands, this problem can also be counteracted from a mechanistic point of view. The mode of action of approved kinase inhibitors relies mainly (for approx. 80%) on orthosteric binding, which implies ATP competitive kinetics at either an active or inactive conformation in the ATP site, but also allosteric and covalent inhibitors now gain more attention[9].

The human kinome comprises 518 protein kinases with manifold relevance for biochemical processes[10]. An essential component in signal transduction is the phosphorylation of effector proteins by protein kinases (and *vice versa* the dephosphorylation by phosphatases). Protein kinases utilize ATP (or rarely GTP) to transfer the *γ*-phosphate group onto the hydroxyl group of serine/threonine or tyrosine residues of their specific substrates and thereby cause a conformational change which corresponds to activation or deactivation. The regulation of the protein kinases themselves can be achieved by the intracellular action of other protein kinases within a transduction cascade, but in the case of membrane-bound receptor tyrosine kinases also upon binding of the respective ligands (such as growth factors like EGF, PDGF or VEGF) at the extracellular binding domain[11].

Taking into consideration, that protein kinases differ under various aspects, the aforementioned challenges that had to be overcome to develop orthosteric inhibitors arise from their most important commonness: ATP as co-substrate. This endogenous ligand is fixed in the binding pocket by several distinct hydrogen bonds of the adenine, the ribose and the phosphate moiety (**Figure 2**)[12-13]. Small molecule inhibitors commonly resemble the adenine unit and therefore hinder ATP at acquiring the needed position by blocking the pocket most deep inside the hinge region. While competing with very high intracellular ATP concentrations (up to 10 mM) is a hurdle regarding the inhibitor's potency, the strong structural and sequence similarity of various kinases due to the highly conserved ATP binding domain makes selectivity even more pivotal[11]. This issue can be addressed with inhibitors that besides the adenine pocket additionally protrude into adjacent alternative regions, which are not occupied by ATP, such as the hydrophobic pockets[11, 14].

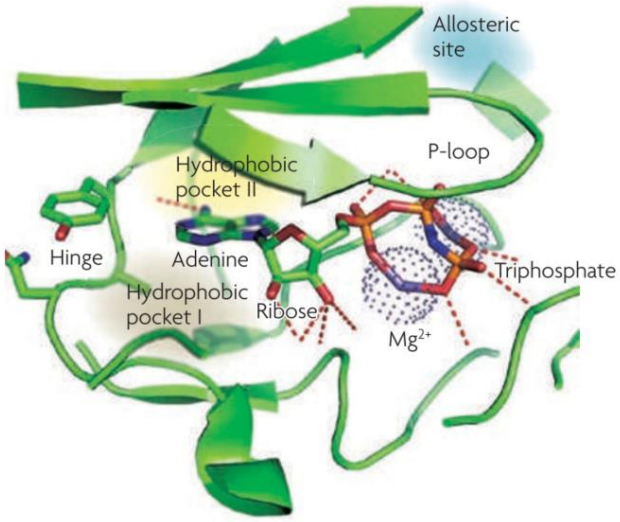

Figure 2. Illustration of ATP in complex with serine/threonine kinases AKT1 (red dotted lines indicate hydrogen bonds). Reproduced with permission from Springer Nature[12].

A sort of selectivity is inevitably required, since the more than 500 protein kinases are ubiquitous and involved in almost all biological functions, ranging from cell cycle regulation, movement and differentiation over metabolism to gene transcription[11]. Highly specific kinase inhibitors could therefore not only have less adverse side effects for patients, but are also needed as chemical tools to elucidate the biological relevance of all of these kinases, from which many are up to now underexplored.

This applies for example to the Cdc2-like kinases (CLKs). CLK1 (initially named STY) was first described in 1991[15-16], but the role of the CLK family is not fully unraveled until today. The four isoforms (CLK1-4) show high homology and are phylogenetically categorized in the CMGC group together with the cyclin-dependent kinases (CDKs), mitogen-activated protein kinases (MAPKs) and glycogen synthase kinases (GSKs)[17-18]. Under structural aspects, the CLKs share a kinase typical *N*-terminal lobe (consisting of five *β*-sheets and one *α*-helix) and *C*-terminal lobe (consisting of six *α*-helices including the LAMMER amino acid motif) linked to each other by the hinge region, which contains the ATP binding site[19]. While CLK1, CLK2 and CLK4 consist of roughly 500 amino acids, CLK3 has some additional elements resulting in a length of 638 amino acids[20]. Like all LAMMER kinases, the CLKs possess dual specificity, which means that they can act as serine/threonine as well as tyrosine kinases[15, 21]. The latter function, however, is limited to autophosphorylation. CLKs are found in nearly all human tissues, although their expression levels differ. For example, levels of CLK3 are very high in

the cytoplasm of spermatozoa[22], whereas CLK1 is ubiquitous and in particular located in nuclei[21].

Less is known about the “direct” participation of CLKs in processes such as cell growth and division, but their capability to regulate splicing is well documented and demonstrates the potential to be involved in nearly all biological processes indirectly[23]. Splicing, which refers to the processing of pre-mRNA to mature mRNA, is the elimination of non-coding areas (introns) and ligation of coding areas (exons) of the primary transcript prior to translation into the protein. This mechanism is important in refutation of the “one gene, one polypeptide chain” hypothesis[24]. Since pre-mRNA processing can not only follow the path of constitutive splicing, but also several modes of alternative splicing (**Figure 3**)[25], one gene can result in several different mRNAs and therefore one gene can code for several proteins depending on the splice variant.

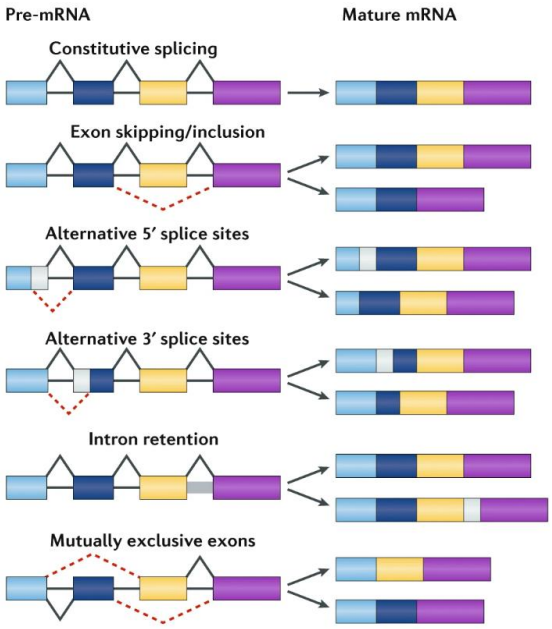

Figure 3. Schematic procedure of constitutive splicing and five common modes of alternative splicing (exon skipping/inclusion, alternative 5’ or 3’ splice sites, intron retention and mutually exclusive exons). Reproduced with permission from Springer Nature[25].

The spliceosome, which is the machinery responsible for the splicing process, consists of proteins and uridine rich small nuclear RNAs, that form a ribonucleoprotein complex. Its assembly is promoted by serine and arginine rich splicing factors, the SR proteins[26], that are in turn regulated by CLKs. For example, the localization and phosphorylation of the SR protein SRSF1 is mainly controlled by CLK1 (**Figure 4**)[19]. Enriching of this splicing factor in the nucleus can be achieved by formation of a complex with the CLK1 in the cytoplasm, which enables nuclear import of both components *via* transportin SR2 (TRN-SR2)[27], or by provoking

release of SRSF1 from nuclear speckles[28]. A ternary complex of SRSF1, CLK1 and another kinase, the serine/arginine-protein kinase (SRPK1), needs to be formed to achieve full phosphorylation of the splicing factor, which is then released and provokes spliceosome assembly[29]. This whole system is highly sensitive and hypo- as well as hyperphosphorylation of the SR proteins strongly impair splicing[28]. Activity of CLK1 is dependent on factors, such as body temperature or stress, and regulated upon a complex network, which involves *inter alia* also alternative splicing of the *clk1* gene itself[30-31]. Taken all of this into consideration, it becomes apparent that dysregulation of splicing can have many reasons and many consequences. Thus, it can in general be associated with a variety of diseases, ranging from cancer[32] to neurological[33], immune-associated[34], cardiovascular[35] and metabolic diseases[36].

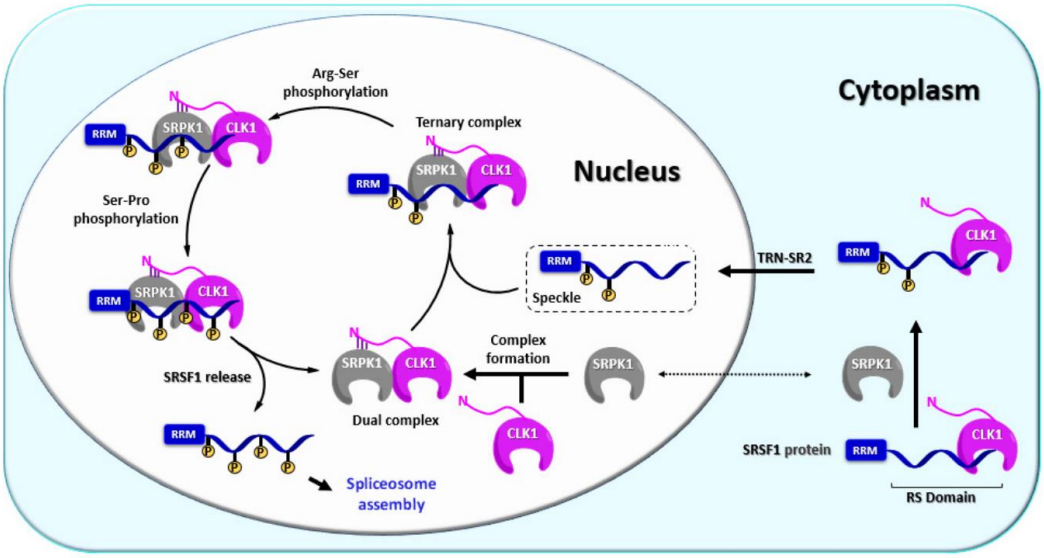

Figure 4. Schematic mechanism of regulation of spliceosome assembly by SRSF1, CLK1 and SRPK1[19].

Relevance of the CLKs and in particular of CLK1, was observed for several of the abovementioned disease areas. Predominantly, it was mentioned in oncological contexts. Only recently, in 2021, it was found, that CLK1 is upregulated in pancreatic cancer and promotes growth and metastasis thereof by affecting splicing[37]. Likewise, it was demonstrated that the CLK1/CLK4 inhibitor TG003[38] (**Figure 5**, left) reduced cell proliferation and induced apoptosis in prostate cancer cells *in vitro*, while it caused widespread changes in splicing of cancer-associated genes[39]. CLK1 knockdown experiments confirmed, that the observed effects were not mainly due to off-targets but CLK1 inhibition, and a xenograft mouse model indicated that TG003 can also prevent *in vivo* tumor growth[39]. Furthermore CLK1 was identified as potential

therapeutic target in gastric cancer[40], whereas CLK2 was found to be especially promising for breast cancer[41] and CLK3 for hepatocellular carcinoma[42]. With SM08502 (**Figure 5**, center) the first CLK inhibitor has even entered phase I clinical trial for advanced solid tumors (castration-resistant prostate cancer, non-small cell lung cancer and colorectal cancer)[43-44]. It was discovered in gastrointestinal cancer models, that the antitumor effect of SM08502 results from a reduction of Wnt signaling, which is aberrantly activated in several tumors, and alteration of splicing of Wnt pathway genes[45]. While this perfectly meets the hypothesis of CLKs being responsible for splicing, SM08502 was found in this study to be a pan CLK/DYRK inhibitor with nanomolar IC_{50} values for all CLK and DYRK isoforms and some further kinases of the CMGC and other subfamilies (in total approx. 20 kinases). Hence, it remained poorly understood, the interplay of which kinases is responsible for the favorable impact, although a particular contribution of CLK2 and CLK3 was assumed[45].

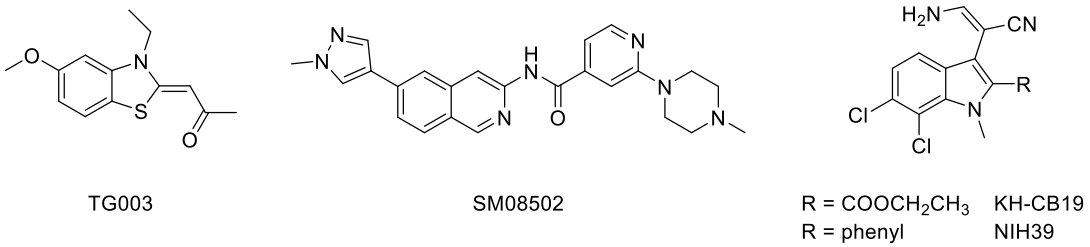

Figure 5. Structure of CLK inhibitors TG003[38], SM08502[45], KH-CB19[46-47] and NIH39[48].

Another potential therapeutic area linked to the CLKs, and again also to the closely related DYRK family, are neurodegenerative diseases. Hyperphosphorylation and aggregation of tau protein is a key factor for e.g. ALZHEIMER's disease or frontotemporal and DOWN syndrome dementia[49]. Thus, dysregulation of splicing of the *tau* gene is one aspect within this pathology[50] and involvement of CLKs was demonstrated[51-53]. Of the DYRKs especially DYRK1A has significant impact on tauopathies by direct phosphorylation of tau proteins or as well by regulation of splicing[54]. The close homology of both families and the fact that most small molecules target several isoforms thereof hamper the understanding of the role of each kinase also in this context, for which only very recently a DYRK1A-selective inhibitor was identified[55].

Lastly, infectious diseases shall be mentioned. The risk of emerging viral diseases was not unknown or unforeseeable when the COVID-19 pandemic hit the world. However, it demonstrated impressively the importance of taking imminent infectious diseases seriously and investigating therapeutic options foresightedly. One particular challenge therefore is the

high mutability and adaptability of viruses, which in many cases cause fast development of resistance. A promising approach to at least decrease this risk is to target not only virus factors, such as structural and nonstructural proteins like viral enzymes involved in replication, but additionally also host factors[56]. Besides reinforcing protective immune response (therapeutically utilized by interferon therapy), host-directed antiviral mechanisms also refer to impacting structures of the host organism, which the virus needs for efficient internalization, replication or persisting. Since different pathogens are dependent on the same host factors, this approach also provides the possibility of broad-spectrum antiviral agents[56].

Within this context the CLK1 was repeatedly identified as host factor, in particular for influenza A virus (IAV)[57-58], West Nile virus[59] and Chikungunya virus (CHIKV)[60]. Regarding the relatively small genome of viruses, it is not surprising that these pathogens also take advantage of alternative splicing. It is known for example for IAV, that the same viral pre-mRNA gives rise to membrane protein M1 ("unspliced") and ion channel M2 ("spliced" variant)[61-62]. Participation of the CLK1 in this process was first described by KARLAS *et al.*[57], when treatment with TG003 resulted not only in decreased IAV replication *in vitro* but also reduced levels of M2 mRNA and protein. This was further confirmed by CLK1 knockdown experiments with siRNA and in CLK1 deficient mice[63]. Inhibition of IAV replication was also achieved with the CLK1 inhibitors KH-CB19[46-47] and NIH39[48] (**Figure 5**, right), which were developed within the BRACHER group. However, their impact on splicing was different. While NIH39 promoted splicing, KH-CB19 caused no change in the M1/M2 ratio, but both lead to decreased expression of M1 and M2, as well as of other proteins[63]. A possible explanation therefore is, that the mentioned inhibitors affect the CLK isoforms differentially[48] and this remarkably emphasizes the susceptibility of IAV to any changes in this sensitive balance.

A genome-wide loss-of-function screening then revealed CLK1 also as host factor for CHIKV[60]. Of in total 156 proviral and 41 antiviral host factors, 6 were identified as highly promising druggable targets, since their inhibition correlated with good antiviral activity but low toxicity. One of these was the CLK1, for which the relevance was again validated with CLK1 deficient mice *in vivo*, that developed in contrast to the control group nearly no paralysis upon CHIKV infection[57]. These experiments further indicated that the CLK1 is at least temporarily dispensable for the host, making it even more appealing as drug target[60, 63].

Chikungunya fever – the mosquito-borne infectious disease caused by CHIKV – is widespread in (sub)tropical regions, but not very familiar in Europe. However, this could change rather quickly. The ECDC reported 516 cases of chikungunya virus disease in the EU/EEA in 2019[64]. None was a result of autochthonous transmissions and approx. 80% were "imported" by travellers infected in Asia (mainly Thailand, Myanmar and India). This tallies entirely with the only 59 cases reported in 2020, when the global mobility was massively impaired due to the COVID-19 pandemic[65]. However, in former years also several hundred autochthonous

transmissions as a result of viraemic travel-related cases were already noticed in Europe, most recently in France and Italy in 2017[66-67]. Since the alpha-virus is transmitted by mosquitoes of the *Aedes* species (*Ae. aegypti* and *Ae. albopictus*), its spreading and persisting is likely to be continued with its vectors adapting to previously unaffected regions. This is facilitated by climate change and applies not only to CHIKV but also to other pathogens potentially establishing in our latitudes (e.g. Dengue virus, Zika virus and yellow fever virus), that may represent a major challenge in the future[68-69].

Systematically, CHIKV belongs to the *Togaviridae* family and is a single-stranded positive-sense RNA enveloped virus[70]. It was first recognized and isolated in the 1950s in Tanzania[71] and subsequently multiple small-scale outbreaks occurred in Africa and Asia in the following 50 years. A large outbreak commenced in 2004 in Kenya and infested several countries bordering the Indian Ocean with more than 2 million cases in total in the following few years[72-73]. Within this time a genetic adaption of the virus enhanced infectivity and transmissibility by *Ae. albopictus*[74], which caused also the first local transmissions in Europe and attracted global attention. In 2013 the first outbreaks were also documented in the Caribbean territories and today CHIKV disease is endemic in large parts of Africa, Southeast Asia, the Indian subcontinent, the Pacific Region and the (sub)tropical regions of the Americas[72, 75].

After transmission by a bite of an infected mosquito, CHIKV is replicated first within the skin, from where it is disseminated through the blood circuit particularly to the liver, lymphatic system, brain, muscles and joints[76]. Clinical manifestation then occurs after an incubation time of 2 – 12 days by a sudden onset of illness including high fever, headache, rash, arthralgia, myalgia and gastrointestinal symptoms[72]. The acute phase is mainly marked by the incapacitating joint pain, giving the disease its name – meaning "that which bends up"[71]. Although it is self-limiting in the majority of cases and the mortality is generally low, severe manifestations such as encephalitis, myocarditis and hepatitis occur occasionally and roughly 30 – 40% of infected persons suffer from a protracted chronic course with recurrent joint pain for several months or even years[76]. This is, first and foremost, a burden for the affected patients but from the economic point of view also for the health care system. CHIKV disease can only be treated symptomatically with analgesic, antipyretic and anti-inflammatory drugs, since no prophylactic or specific therapeutic treatment is available[72]. Although clinical research is advanced regarding the development of vaccines, especially since Valneva's candidate VLA1553 has completed its phase III trial in March 2022[77], there still is an urgent need to develop specific antiviral drugs and the involvement of CLK1 in CHIKV pathology makes it one promising novel target therefore.

To sum it up, the relevance of CLKs and especially of CLK1 for a variety of diseases has to be further investigated to understand the complex biochemical and pharmacological processes, as well as regulation and functions of these kinases in general. Diverse inhibitor chemotypes with nanomolar IC_{50} values were published already. However, as reviewed in literature in 2020 by MOYANO *et al.*[19], many suffer from off-target activities or are missing selectivity profiling data and results from cellular assays. Whereas inhibitors with high subtype selectivity could help to exploit the role and contribution of each CLK isoform, closely related inhibitors which target also other kinases could have synergistic biological effects. For both purposes there is a need to develop novel chemotypes of inhibitors, for which structure-activity relationships are comprehensively investigated regarding their activity and selectively.

2 Objective

Kinase inhibitors derived from natural products and related heterocyclic organic molecules have quite a tradition in the group of PROF. DR. FRANZ BRACHER. A large number of compounds synthesized within the group was already found to be inhibitors of several kinases, e.g. CDK1[78-81], DYRK1[82], PIM kinases[46, 83] and CLK1[46, 48, 82]. A cooperation with the group of PROF. DR. ODED LIVNAH (The Hebrew University of Jerusalem, Israel) allowed to start a more target-based approach to CLK1 inhibitors, as these cooperation partners are not just able to isolate the target protein, but can perform co-crystallization experiments with potential inhibitors[84]. This can reveal the binding mode and interactions of the crystallized ligand with the protein, but also give insight into the electronic and spatial conditions and surrounding residues. Following this approach, DR. CHRISTIAN AIGNER did a systematic variation of indole KH-CB19 (*cf.* **Figure 5**), which is a potent and highly specific inhibitor of CLK1 and CLK4[46-47]. He could replace the labile enaminonitrile moiety by heteroaromatic amines, that are hydrolytically stable and share the same binding mode[85].

In addition to indole KH-CB19, the screening of a substance library of the BRACHER group by DR. JENS PETER VON KRIES at the Leibniz-Forschungsinstitut für Molekulare Pharmakologie (FMP, Berlin, Germany) evinced β-carboline **1** as very promising hit for CLK1 inhibition (**Figure 6**, left). β-Carboline **1** was formerly synthesized by DR. TIM TREMMEL as intermediate, when he was elaborating new synthetic routes to 6-substituted canthin-4-ones[86]. Besides having a submicromolar IC_{50} value (< 0.05 µM) as CLK1 inhibitor in the mobility shift assay, the lead structure **1** and its methyl analogue **2** (IC_{50} = 1.2 µM) were also co-crystallized already in complex with CLK1. Since both ligands show the same binding mode in the ATP-binding pocket and are only marginally shifted (**Figure 6**, right), the ideal basis for a structure-based optimization of the lead structure was given.

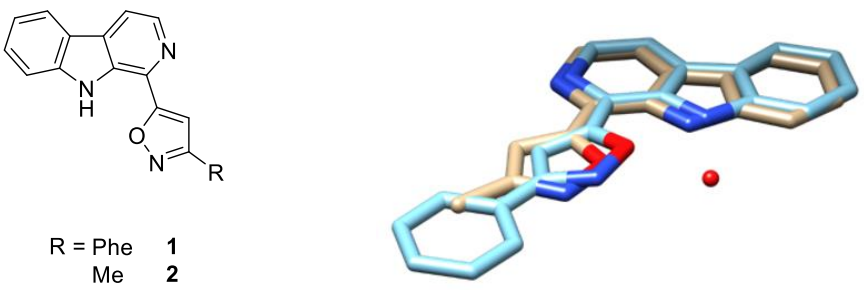

Figure 6. Structure of lead structure **1** and its methyl analogue **2** (left) and superposition of the orientation of both ligands (**1** blue, **2** beige) in the ATP-binding pocket of CLK1 (right) (protein not shown). A water molecule (red sphere) is involved in an intramolecular hydrogen bond.

Basing on the analysis of the aforementioned co-crystal structures by DR. MICHAEL MEYER (MBC-Statistik, Falkensee, Germany), it was aimed at further developing inhibitors of this chemotype. The almost coplanar orientation of the 1-aryl-β-carbolines **1** and **2** is fixed by an intramolecular hydrogen bond between the NH (indole) and the O (isoxazole), whereby also a water molecule is involved. Surprisingly, the crystal structure did not show any direct hydrogen bonds to the protein, but at different positions short distances of roughly 3.0 – 3.6 Å between donor and acceptor atoms of the protein and nonpolar atoms of the lead structure were observed (**Figure 7**). Therefore, the introduction of corresponding acceptor and donor groups into hit **1** was estimated to be capable of establishing further interactions and this could possibly improve affinity, activity and selectivity.

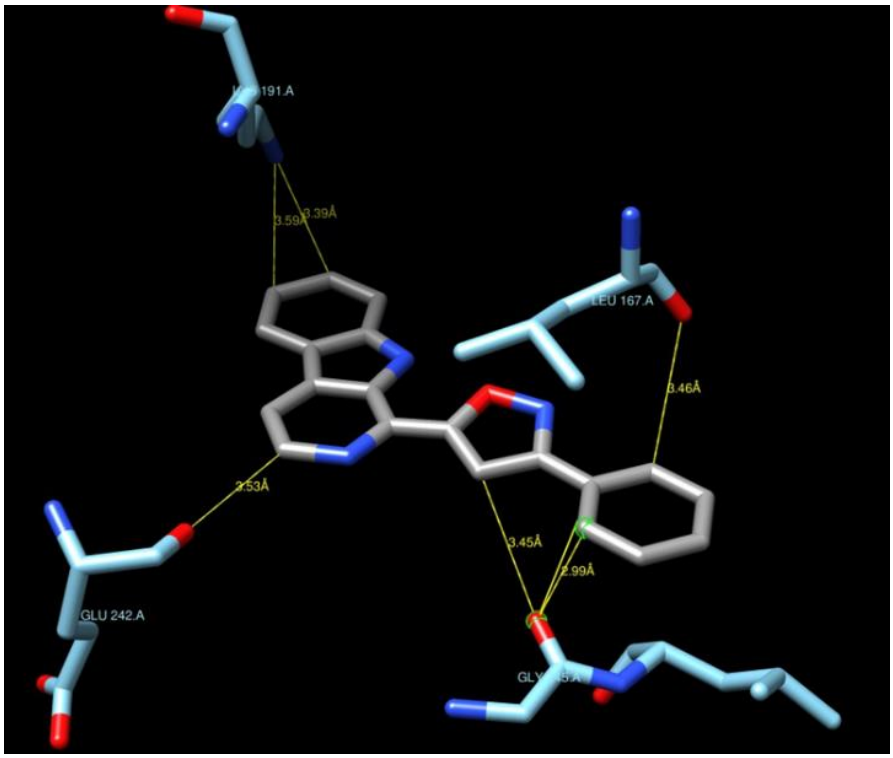

Figure 7. CLK1 (blue) in complex with lead structure **1** (grey). Yellow lines indicate short distances between nonpolar atoms of the ligand and donor or acceptor atoms of the protein.

Additionally, the crystal structures with ligand **1** and **2** revealed areas, which are not yet occupied by the ligand. This suggests, which substructures could be enlarged with additional substituents to even better fill the binding pocket.

With regard to these considerations, the aim of this thesis was to synthesize different sets of structural analogues of lead structure **1**. Besides the introduction of polar groups or additional residues, the relevance of the different structural elements and heteroatoms and the tolerance

regarding the replacement by structurally related motifs were to be examined. With not just more complex but also simplified molecules in hand it should be determined, which substructures are crucial for the affinity and inhibitory activity.

While the concrete intentions and retrosynthetic considerations are described at the beginning of each chapter, **Figure 8** shows a summary of envisaged analogues. Such as the molecule can be divided in three parts, the modifications respectively comprise a variation of the phenyl group, the isoxazole moiety or the β-carboline motif. Therefore, some of the analogues should presumably not only have beneficial properties, but would in their entirety also allow the discussion of structure-activity relationships.

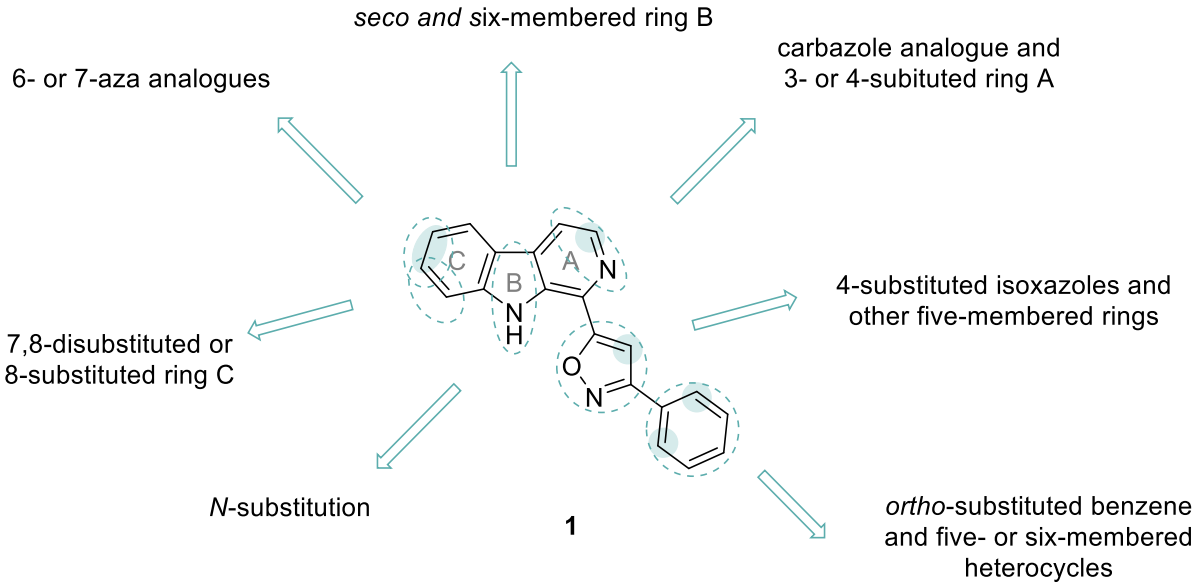

Figure 8. Structure of lead structure **1** and envisaged analogues thereof. Nonpolar atoms of the ligand for which short distances to donor or acceptor atoms of the protein were observed are marked with blue spheres.

3 Results and discussion

In the following chapters, the synthesis of lead structure **1** and analogues which are variations of the phenyl (3.1), the isoxazole (3.2) and the *β*-carboline moiety (3.3) will be discussed in the order stated. Concrete aims from considerations upon the co-crystal structure and retrosynthetic approaches are described respectively at the begin of each (sub)chapter. The results from the biological testing will then be outlined and assessed for all analogues collectively at long last (3.4).

3.1 Lead structure 1 and variations of the phenyl ring

Following the published approach[86], the key step regarding the synthesis of lead structure **1** and also the envisaged variations of the phenyl ring is a HUISGEN cycloaddition (**Scheme 1**). The therefore required dipolarophile, arylacetylene **3**, can be prepared from (pseudo)halide building blocks (**C**). Nitrile oxides (**B**), which act as 1,3-dipoles, allow the introduction of various (hetero)aromatic substituents at C-3' and are accessible by (formal) oxidation of the respective oximes (**A**).

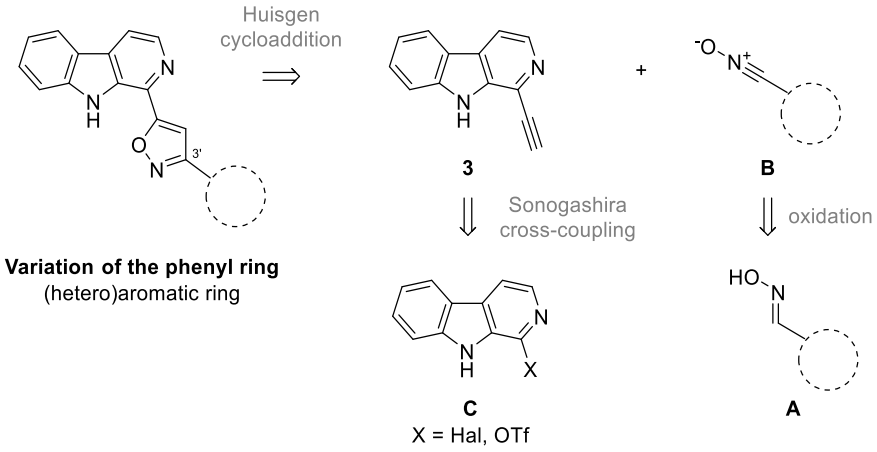

Scheme 1. Retrosynthesis of lead structure **1** (phenyl ring) and variations with modified (hetero)aromatic substituents at C-3'.

3.1.1 Synthesis of lead structure **1**

Synthesis of lead structure **1** was conducted similar or identical to published procedures. However, the conducted syntheses will be outlined in brief as improvements, alterations and additional findings were fundamental for syntheses of miscellaneous variations and expanded the scope of accessible analogues.

To begin with, another approach to the required *β*-carbolinone building block **5** was followed. Formerly this intermediate was synthesized within the BRACHER group following the two-step procedure of HILDEBRAND[86-87]. This approach starts from tryptamine and triphosgene and gives an intermediary isocyanate, which cyclizes upon treatment with hydrobromic acid (**Scheme 2**)[87].

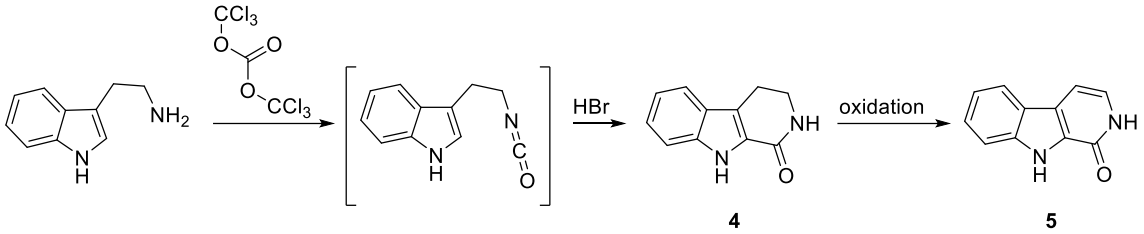

Scheme 2. Synthesis of *β*-carbolinone **5** according to HILDEBRAND[87].

The obtained 1,2,3,4-tetrahydro-1-oxo-*β*-carboline **4** is subsequently dehydrogenated with palladium on carbon[87] or 2,3-dichloro-5,6-dicyano-1,4-benzoquinone (DDQ)[88] to pyridone **5**. However, this approach has some major drawbacks. The first step affords an excess of toxic phosgene. Modifying the equivalents of this reactant to avoid this hazard, drastically reduced the yield (to approx. 35% instead of 74%). Additionally, the subsequent aromatization is poorly reproducible with palladium on carbon and the use of DDQ is inevitably linked to very large amounts of hydroquinone side product, which complicates purification on a large scale[88].

Therefore, a different approach was followed. LA REGINA *et al.*[89] found that the acid catalyzed cyclization of amides, generated from indole-2-carboxylic acid and 2-aminoacetaldehyde dimethyl acetal, can progress from 1- or 3-position of the indole precursor and that the predominant route depends on the employed acid. According to their studies, polyphosphoric acid (PPA) showed the highest selectivity for the cyclization in 3-position and **5** was isolated almost quantitatively (98% yield, 2% yield of side product **7**). As their experiments were conducted on a rather small scale (1.0 mmol), the procedure was to be tested and optimized for the larger scale.

The coupling of indole-2-caboxylic acid and 2-aminoacetaldehyde dimethyl acetal was conducted with DCC as coupling reagent (instead of the more expensive BOP used by LA REGINA *et al*.[89]) (**Scheme 3**). DCC was found to be superior to EDC hydrochloride, when reactions were conducted on a large scale (60 mmol). The major part of the poorly soluble DCC urea could be partitioned off simply by filtration and subsequent flash column chromatography readily gave amide **6** (69% yield). The cyclization with polyphosphoric acid afforded *β*-carbolinone **5** indeed as major product. It was accompanied to very little extent by the expected side product **7**, whereby the cyclization had proceeded in 1-position. The work-up

procedure was somehow more laborious on a larger scale (18.5 mmol) than described in the publication. Hydrolysis of the polyphosphoric acid in the tar-like reaction mixture resulted in formation of vast amounts of precipitate, which was found to contain **5**. As this product is soluble in ethyl acetate only to a minor extent and huge quantities of this solvent would have been needed, the precipitate was collected by filtration and washed with methanol instead. This filtrate was then combined with the organic phases from extracting the aqueous solution, and flash column chromatography allowed purification and simple separation of both pyridones **5** (50% yield) and **7** (approx. 5% yield).

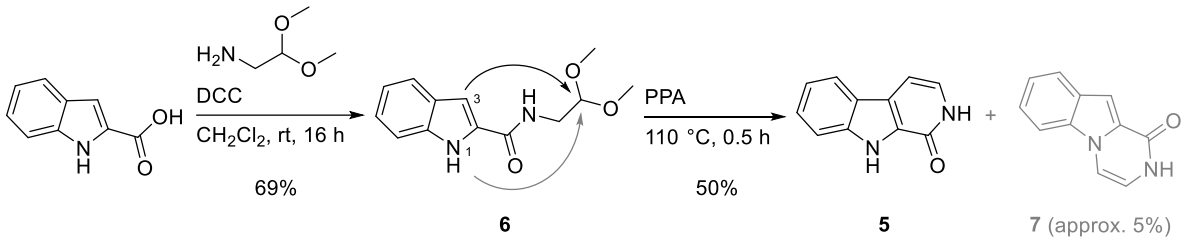

Scheme 3. Synthesis of *β*-carbolinone **5** *via* amide coupling and PPA mediated cyclization.

β-Carbolinone **5** can then be further functionalized to (pseudo)halide building blocks, which are required for SONOGASHIRA cross-couplings. To do so, bromide **8** (88% yield) was accessed following the established procedure of HILDEBRAND using phosphorus oxybromide in anisole[90] (**Scheme 4**). The subsequent cross-coupling with trimethylsilylacetylene was described by TREMMEL[91-92]. Repetition of his procedure, however, revealed that some alterations could improve feasibility. First, the reaction mixture was filtered over celite to remove the catalyst before an aqueous work-up was conducted to simplify the extraction process. Second, since TMS-protected alkyne **9** and bromide **8** show very similar chromatographic behaviour and are barely separable with flash column chromatography, the crude mixture was directly desilylated with potassium carbonate in methanol[93] and purification is achieved on the stage of terminal alkyne **3** (70% yield over two steps). This was especially beneficial, since desilylation of the very labile TMS-protected alkyne **9** already occurred partially during flash column chromatography.

In addition, also the respective triflate **10** was synthesized following the procedure of ROGGERO *et al.*[88] (81% yield) and its utility for the SONOGASHIRA cross-couplings with trimethylsilylacetylene was examined. HILDEBRAND had synthesized the same triflate already earlier, but it was accompanied by the *N*-9 triflated *β*-carbolinone in his experiment[94]. Also the SONOGASHIRA cross-coupling was already attempted by HILDEBRAND, but the reaction failed with copper(I) iodide and $PdCl_2(PPh_3)_2$ in a mixture of triethylamine and dimethylformamide

(at 55 – 100 °C)[95]. SCOTT and STILLE[96] have demonstrated, that lithium chloride can expand the scope of cross-coupling reactions by impacting oxidative addition. Therefore, additive lithium chloride was used under otherwise equal conditions[97] and **10** indeed underwent SONOGASHIRA cross-coupling. Arylacetylene **3** was then obtained after TMS cleavage (40% yield over two steps). Although the yield is relatively poor in comparison to the route starting from bromide **8**, this finding opens up new possibilities, since not all precursors of intended analogues can be brominated.

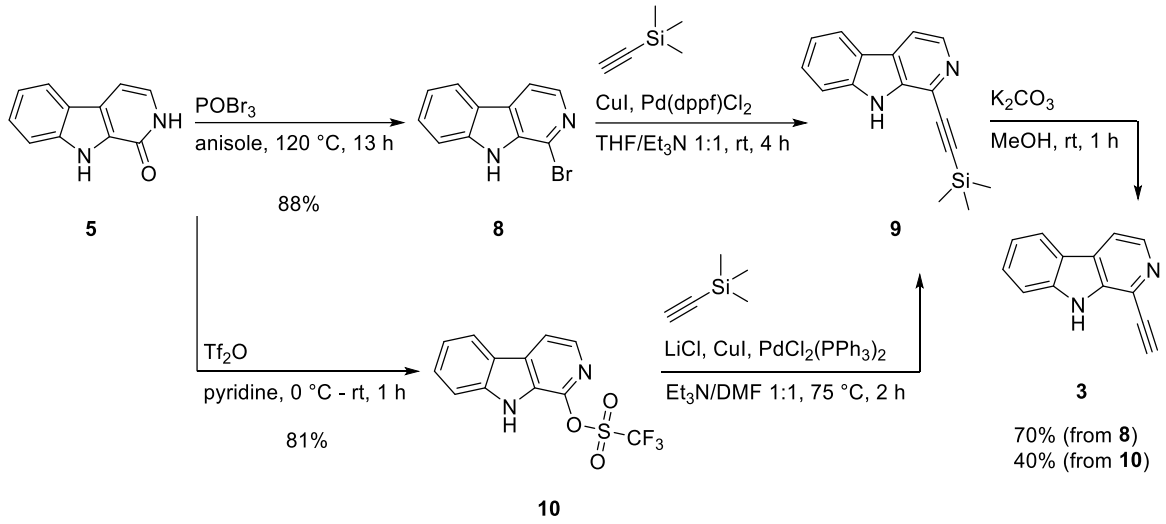

Scheme 4. Synthesis of arylacetylene **3** from bromide **8** and triflate **10**.

ROLF HUISGEN was the first, who recognized the general applicability of the 1,3-dipolar cycloaddition, which is also referred to as (3+2)-cycloaddition, to synthesize five-membered heterocycles. He comprehensively investigated mechanism and kinetics of this reaction between a 1,3-dipole and a dipolarophile[98-99]. The concerted reaction proceeds *via* a cyclic electron shift, whereby two new *σ*-bonds are formed (**Scheme 5**). 1,3-Dipoles possess a zwitterionic structure with an incomplete octet of electrons and a positive charge on the one side (a) and a lone pair of electrons with a negative charge on the other side (c). These structures are stabilized by mesomeric dislocation, as depicted exemplarily for nitrile oxides[98]. The most commonly employed dipolarophiles are alkenes and alkynes.

Scheme 5. Cyclic electron shift between a 1,3-dipole (abc) and a dipolarophile (de) (left) and mesomeric stabilization of nitrile oxides (right)[98].

Depending on the chosen components various five-membered heterocycles are accessible *via* the HUISGEN cycloaddition. For example, nitrile oxides lead to isoxazolines with alkenes and to isoxazoles with alkynes. In general, the reaction of unsymmetrical dipolarophiles can form two regioisomeric products, since the addition can progress from both sides of the multiple bond. However, it was also realized by HUISGEN already in 1963, that in contrast to other 1,3-dipoles the reaction of benzonitrile oxide with terminal alkenes or alkynes gives only 3,5-disubstituted isoxazol(in)es[99]. Since this observation was not dependent on the electronic nature of the dipolarophile's substituent, it was assumed that steric reasons prevail[99].

The final step to obtain lead structure **1** is such a cycloaddition with benzonitrile oxide. TREMMEL used a one-pot protocol, in which (*E*)-benzaldehyde oxime was first reacted with *N*-chlorosuccinimide (NCS), followed by the addition of arylacetylene **3** and triethylamine to generate the nitrile oxide *in situ* and initiate the HUISGEN cycloaddition[91]. With this procedure he received isoxazole **1** in 40% yield.

In order to improve the 1,3-dipolar cycloaddition, it was first attempted to split the protocol into two separate steps (**Scheme 6**). Therefore, hydroxymoyl chloride **11** was isolated (89% yield)[100]. Milder conditions were then chosen for the *in situ* nitrile oxide synthesis and subsequent cycloaddition, since benzonitrile oxide tends to dimerization[99]. Isoxazole **1** was obtained, but the yield (37%) was not improved.

Another, very convenient method to conduct 1,3-dipolar cycloadditions was described by JAWALEKAR *et al*.[101] and applied within the BRACHER group repeatedly by PLESCH[102]. Thereby, the hypervalent iodine reagent [bis(trifluoracetoxy)iodo]benzene (PIFA) is used to generate the nitrile oxide species from the respective oxime *in situ*. JAWALEKAR *et al*.[101] found that this oxidation proceeds very rapidly. The best results regarding the formation of isoxazoles were achieved in a mixture of methanol and water (5:1) and using a small excess of oxime and PIFA (1.5 eq each), whereby the oxidant is added portion wise (3 x 0.5 eq with an interval of 2 h) to diminish dimerization[101].

By applying this procedure to benzaldehyde oxime and arylacetylene **3**, the synthesis of isoxazole **1** was greatly improved (85% yield).

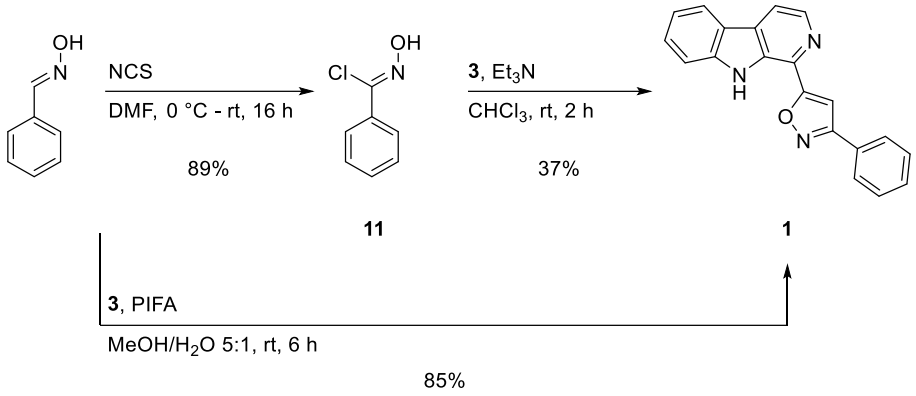

Scheme 6. Synthesis of isoxazole **1** *via* HUISGEN cycloaddition.

3.1.2 Syntheses of variations with substituted phenyl rings and heteroaromatic residues

As first set of analogues, the phenyl ring of lead structure **1** was to be altered. TREMMEL had synthesized also the related 3-methyl and 3-ethyl isoxazole analogues, but both were rather inferior regarding the CLK1 inhibitory activity (IC_{50} = 1.2 µM for both in the mobility shift assay) compared to 3-phenyl isoxazole **1** (IC_{50} < 0.05 µM). Therefore, only residues with a similar size than phenyl were envisaged. On the one side, marginally smaller bioisosters, such as furan and thiophene, were to be introduced. On the other side, also replacement by a pyridyl residue and substituted phenyl rings were to be investigated. The crystal structure revealed, that for the introduction of substituents especially the *ortho*-position is of interest (*cf.* **Figure 7**). Donor groups like -OH and -NH_2 could establish a hydrogen bond with the acceptor carbonyl oxygen of LEU 167 or GLY 245. Same could presumably be achieved with the NH of a 2-substituted pyrrole.

In addition, it was striven for a “clickable” analogue to be tested in a yeast three-hybrid (Y3H) system in the group of Dr. SIMONE MOSER to identify potential further (off-)targets[103]. Therefore, it was necessary to implement an acetylene group, which can be linked to the trimethoprim based probe for the assay, without affecting the affinity towards the CLK1. According to the crystal structure, several areas are unoccupied within the binding pocket, but the phenyl ring is particularly relevant, as it is directed outward of the binding pocket (**Figure 9**). Thus, introduction of the acetylene group in *para*-position of the phenyl residue was assumed to be most expedient as it could protrude into the solvent.

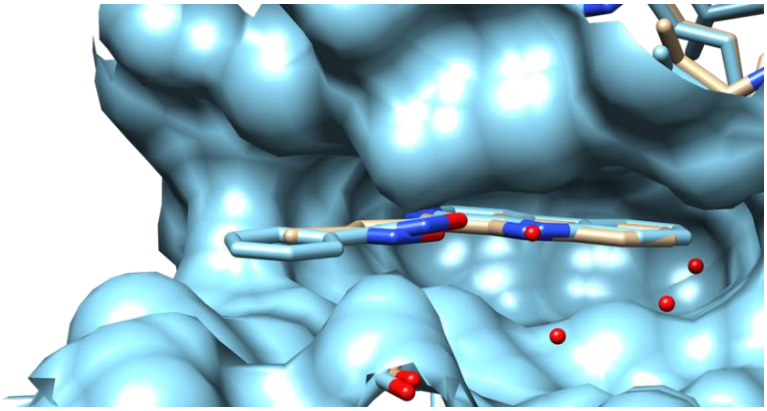

Figure 9. Surface of the CLK1 (blue) in complex with lead structure **1** (blue) and methyl analogue **2** (grey) showing the orientation of the phenyl residue out of the binding pocket. Water molecules (red spheres) indicate further unoccupied areas within the binding pocket.

To synthesize variations with substituted phenyl and heteroaromatic residues in analogy to lead structure **1**, various arylaldehydes were converted into the corresponding oximes in very good yields (75 – 99%) by condensation with hydroxylamine (**Scheme 7**). For this purpose a general procedure of LOHRER was followed employing hydroxylamine hydrochloride and sodium acetate[104]. Interestingly, while all six-membered rings gave selectively (*E*)-configured oximes (**12-15**), thiophene **16** and pyrrole **18** were obtained as (*Z*)-configured oximes only, and furan **17** as a mixture of both (*E*/*Z* ratio 1.0:1.8 determined *via* ^{1}H NMR spectrum).

Next, the HUISGEN cycloaddition of the oximes, or rather the corresponding nitrile oxides, with arylacetylene **3** was investigated and all results are summarized below (**Scheme 7**).

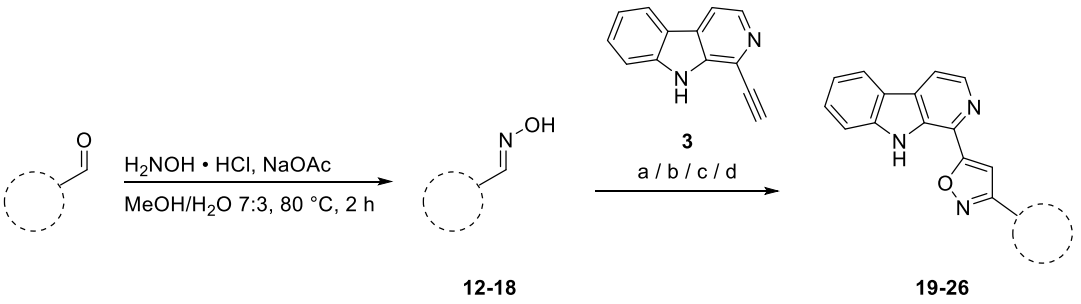

method a: 1. NCS 1.1 eq, oxime 1.1 eq, pyridine 0.05 eq, $CHCl_3$/TCE, 50 °C, 1 h; 2. **3**, Et_3N 1.2 eq, rt - 50 °C, 3 h
method b: **3**, PIFA 1.5 eq, oxime 1.5 eq, MeOH/H_2O 5:1, rt, 16 h
method c: **3**, PIFA 10 eq, oxime 10 eq, MeOH/H_2O 5:1, rt, 1 - 7 d
method d: 1. NCS 1.1 eq, oxime 1.1 eq, pyridine 0.2 eq, DMF, 0 °C - rt, 20 h; 2. **3**, Et_3N 1.1 eq, 0 °C - rt, 18 h

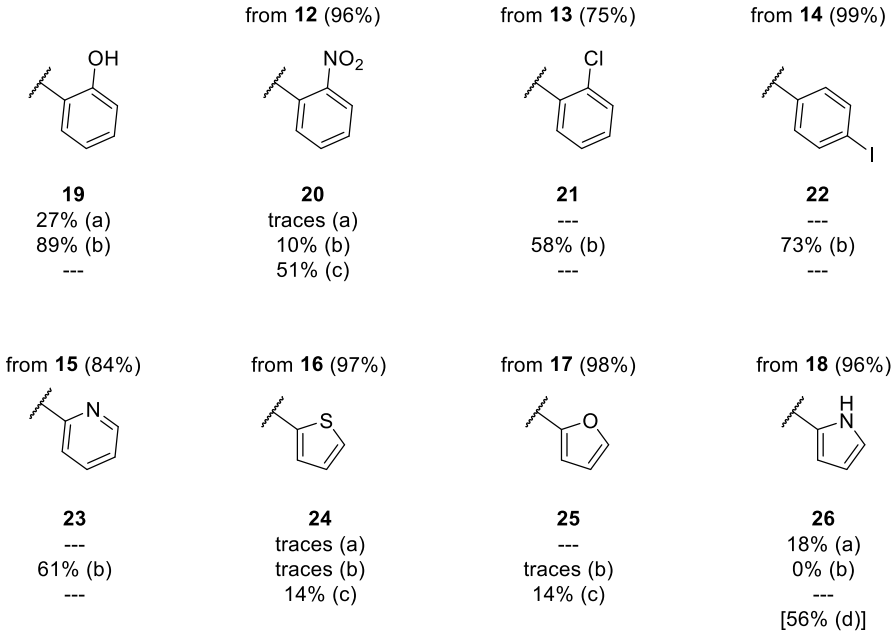

Scheme 7. Syntheses of variations with substituted phenyl and heteroaromatic residues *via* HUISGEN cycloaddition. Yields of oxime syntheses are given above the illustrated residues, whereas yields of subsequent cycloadditions are given below for each of the applied methods.

Initial experiments were conducted with salicylaldehyde oxime and nitro compound **12** similar to the procedure of TREMMEL[86] by generating the hydroxymoyl chlorides *in situ* in chloroform or trichloroethane (method a). However, the outcome of this initial reaction already remained unclear. TLC and MS analysis had little informative value as it could not be distinguished, if the chlorination had proceeded only barely or if the hydroxymoyl chlorides decompose rapidly. Therefore, the reaction sequence was continued and alkyne **3** and triethylamine were added after 1 h. 2-Nitrophenyl analogue **20** was only observed in traces among starting material and various unidentified side products. In contrast, the cycloaddition was successful for the 2-hydroxyphenyl analogue and isoxazole **19** could be isolated (27% yield). However, also this compound was accompanied by various poorly separable side products, from which one is an

additionally chlorinated product according to HRMS analysis. This could result from ring chlorination through NCS due to the activating hydroxyl group. A similar observation was made by PLESCH with a furan substituent, which is likewise electron rich[102].

To circumvent this and broaden the substrate scope, the use of PIFA was investigated (method b). JAWALEKER *et al.*[101] have used none of the intended oximes, but by applying their procedure the synthesis of various phenyl variations was achieved. The yield of 2-hydroxyphenyl analogue **19** was improved (89%) and 2-nitrophenyl analogue **20** (10% yield) was isolable. Additionally, 2-chlorophenyl analogue **21** (58%), 4-iodophenyl analogue **22** (73%) and 2-pyridyl analogue **23** (61%) were all prepared in good yields.

However, the envisaged isoxazoles bearing five-membered heteroaromatic rings could not be synthesized. Traces of thiophene **24** and furan **25** were observed, whereas the pyrrole residue obviously withstands the oxidative conditions not at all[105]. JAWALEKER *et al.*[101] could improve the conversion in one example by increasing the amount of oxime and PIFA. By doing so (method c), also the yield of 2-nitrophenyl analogue **20** was improved (51%) and thiophene **24** (14% yield) as well as furan **25** (14% yield) could be isolated, although purification was really hampered by the excess of reagents.

Synthesis of pyrrole **26** was still pending and therefore it was returned to the initially used procedure. With this (method a), the isoxazole synthesis was achieved (18% yield), but the received quantity was too small. A literature search revealed only very few examples of HUISGEN cycloadditions with oxime **18**. However, it was noticed, that BHOSALE *et al*.[106] applied milder conditions in another solvent (without pyridine in DMF, 0° C – rt). Several test reactions were run and the best result was obtained, when a combination of both procedures was used with prolonged reaction times (method d). With this method, synthesis of isoxazole **26** (56% yield) was achieved. (Similar optimization studies are likely to also improve the yield of thiophene **24** and furan **25**. However, as the obtained quantities were sufficient, no further reactions were conducted.)

Two of the analogues synthesized *via* HUISGEN cycloaddition were further modified. To synthesize a “clickable” ligand for the Y3H screening[103], iodide **22** was subjected to SONOGASHIRA cross-coupling with trimethylsilylacetylene. Subsequent desilylation then gave arylacetylene **27** (88% yield over two steps) (**Scheme 8**).

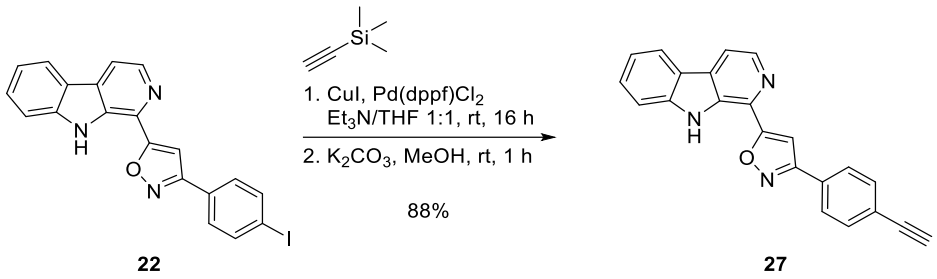

Scheme 8. Synthesis of arylacetylene **27** from iodide **22** *via* SONOGASHIRA cross-coupling.

Furthermore, it was envisaged to reduce the nitro group of **20** to the corresponding amino function. While this is generally achievable with a variety of reducing agents, also the isoxazole ring is susceptible to reductive cleavage[107]. By choosing very mild conditions[108] and using zinc granules instead of zinc dust, it was ensured that the isoxazole ring remained intact, while the reduction to aniline **28** (39% yield) proceeded (**Scheme 9**).

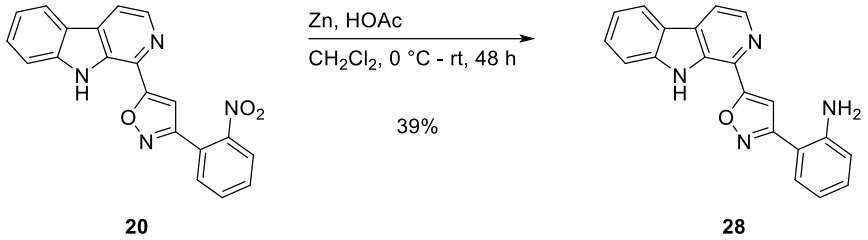

Scheme 9. Synthesis of aniline **28** from nitroarene **20** *via* reduction.

3.2 Variations of the isoxazole

The second intention was to vary the isoxazole moiety, which links the *β*-carboline with the phenyl residue in the lead structure **1**. As mentioned in the beginning an entire substance library from previous work of the BRACHER group was tested at the FMP (Berlin) in the group of DR. JENS PETER VON KRIES, and these screening results have demonstrated, that six-membered heteroaromatic rings possess only very limited activity compared to the isoxazole. This could presumably be due to the very distinct, almost planar orientation of the ligand, which is a consequence of the intramolecular hydrogen bond between the NH (indole) and the O (isoxazole) (*cf.* **Figure 6**).

However, the potential of other five-membered heterocycles was to be investigated, which could adopt the same geometry (**Figure 10**). The relevance of the isoxazole nitrogen was low according to the crystal structure, therefore the respective 2,4-disubstituted furan was envisaged. Substitution of the oxygen by less polar sulfur atoms, such as in isothiazole or thiophene, or by nitrogen might affect or not affect the planarity and orientation of the ligand by rotation of the single bond. Nitrogen containing five-membered rings are multifarious and comprise for example a 1,2,3-triazole, a 3,5-disubstituted pyrazole and an isomeric isoxazole, where the positions of the substituents are interchanged. Furthermore, also the opposite side, which corresponds to C-4' of the isoxazole and is oriented towards the protein in the crystal structure, was to be modified. On the one side further acceptor groups as being present in oxa(dia)zoles should be implemented to examine the tolerance regarding size and electron density. On the other side donor groups such as the NH of an imidazole or a 4-aminoisoxazole possess a clear rationale, since they could establish a hydrogen bond to the acceptor carbonyl oxygen of GLY 245. By synthesizing the latter, further 4-substituted isoxazoles should be accessed and investigated.

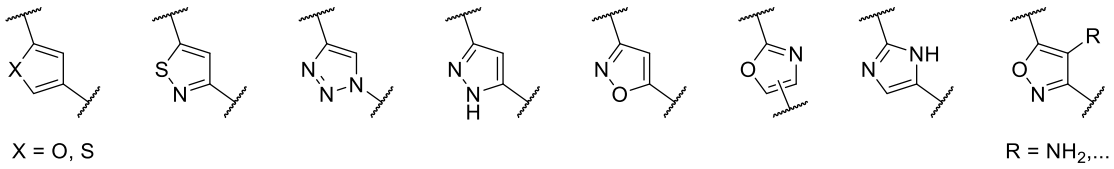

Figure 10. Overview of envisaged five-membered heterocycles.

3.2.1 Replacement of the isoxazole by other five-membered heterocycles

At first, a variety of other five-membered heterocycles should be synthesized, which affords several different synthetic approaches.

3.2.1.1 Syntheses of other five-membered heterocycles *via* HUISGEN cycloaddition

As already described, the 1,3-dipolar cycloaddition of alkynes and nitrile oxides leads to the formation of isoxazoles. Besides this, other 1,3-dipols than nitrile oxides can be used to generate other five-membered heterocycles: triazoles are accessible from azides, pyrazoles from diazo intermediates and isoxazolines from nitrones. Therefore, the use of different phenyl substituted 1,3-dipoles (**A**) in cycloaddition reactions with arylacetylene **3** gives analogues with the corresponding heterocycles instead of isoxazole (**Scheme 10**).

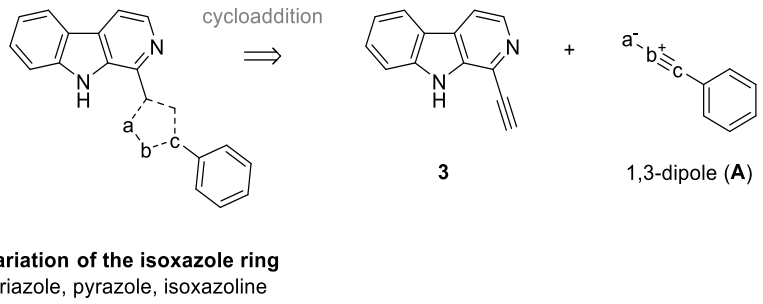

Scheme 10. Retrosynthesis of variations of the isoxazole group with other 5-membered heterocycles accessible *via* HUISGEN cycloaddition.

The first analogue synthesized of this set is triazole **29** (**Scheme 11**). The therefore needed phenyl azide can be prepared with different methods, e.g. the diazotation of aniline and subsequent treatment with sodium azide[109] or the "diazotization" of phenylhydrazine[110]. However, as phenyl azide is highly instable and reactive, a more recent protocol was chosen, whereby the 1,3-dipole is generated *in situ* from phenyl boronic acid and sodium azide with copper(II) sulfate. While the general procedure of TAO *et al.*[111] described the azide formation under mild conditions at room temperature in methanol, TLC indicated no considerable conversion after 16 h. At elevated temperature (55 °C) the azide synthesis was in contrast completed after 3 h. For the following cycloaddition reaction, alkyne **3** was then added besides Na-L-ascorbate to generate the copper(I) catalyst. Although generally known as perfect example for click chemistry, even with a phenyl azide excess (2.0 eq) the formation of triazole **29** worked rather mediocre (39% yield).

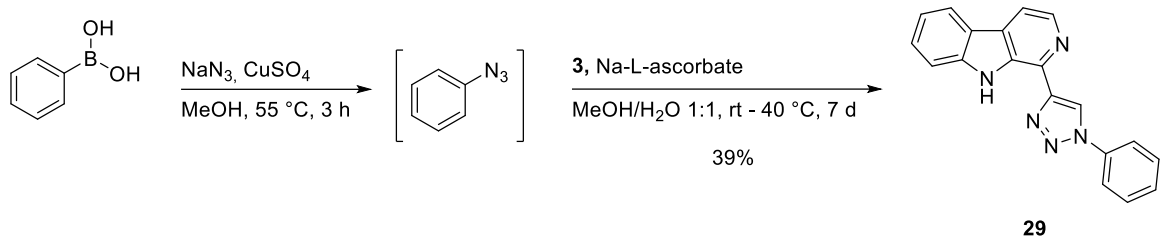

Scheme 11. Synthesis of triazole **29** from phenylboronic acid.

Next, pyrazole **31** was prepared (**Scheme 12**). According to AGGARWAL *et al.*[112], it would have been possible to apply a one-pot synthesis from benzaldehyde, but they mentioned even better yields when the appropriate tosylhydrazone was preformed. Therefore, tosylhydrazone **30** was synthesized from benzaldehyde and *p*-toluenesulfonyl hydrazide and isolated[113] and then used to generate the labile phenyldiazomethane *in situ*. After deprotonation, the tosylhydrazone anion decomposed at elevated temperatures resulting in the 1,3-dipole[114], which reacted with alkyne **3** to pyrazole **31** (49% yield).

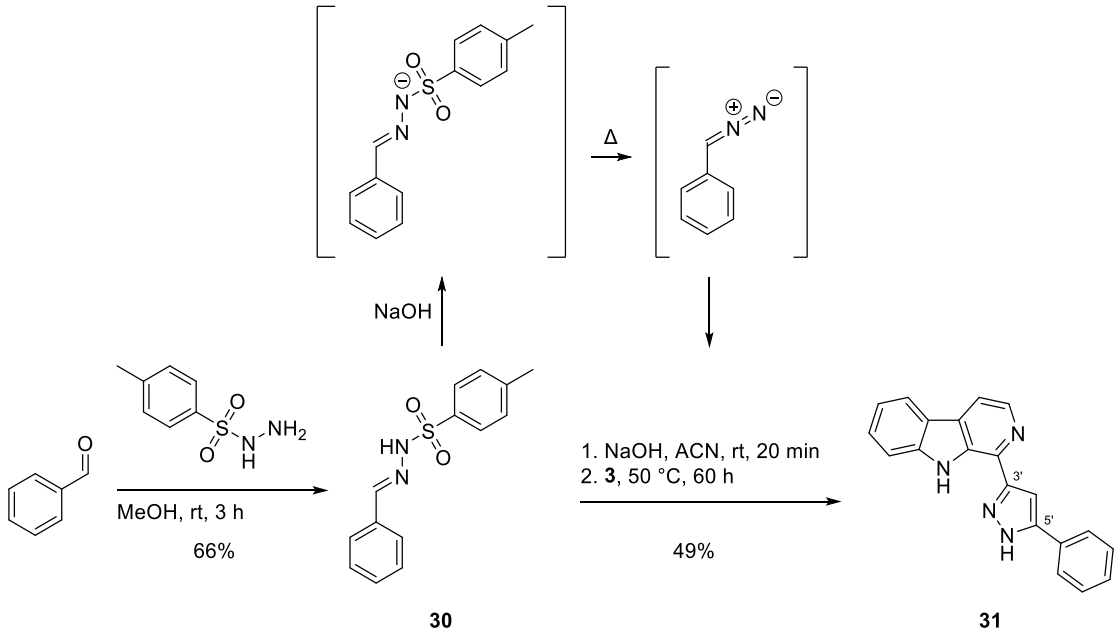

Scheme 12. Synthesis of pyrazole **31** from benzaldehyde.

Due to prototropic exchange, the formation of two tautomeric forms of pyrazoles is possible depending on the NH position. However, ^{1}H NMR analysis of pyrazole **31** in DMSO-d_6 showed only a single set of signals. This could be either due to the presence of only one tautomer or a mixture of both with a high interconversion rate. The relatively broad signals in the ^{13}C NMR

spectrum for C-3' and C-5' support the latter hypothesis[115]. A NOESY experiment indicated the illustrated tautomer, as a weak signal between the pyrazole-NH and 2''-H/6''-H was observed, but this does not exclude also the presence of the other tautomer.

Another envisaged analogue was isoxazoline **33** (**Scheme 13**). In contrast to the aforementioned ones, this 2,3-dihydroisoxazole is not aromatic and therefore has a differing molecular geometry as well as an asymmetric carbon atom. The required nitrone **32** was prepared from benzaldehyde and *N*-methylhydroxylamine hydrochloride[116], but the following cycloaddition with arylacetylene **3** in toluene (**Table 1**, entry 1) did not lead to the formation of isoxazoline **33**. This was not absolutely unexpected as the used alkyne is neither highly strained, such as cyclooctyne derivatives[117], or highly reactive, such as methyl propiolate[118]. A Chinese patent describes the facile synthesis of 3,5-diaryl substituted 2,3-dihydroisoxazoles in various solvents with the help of different bases[119], but none of the conditions tested, even at elevated temperatures and with prolonged reaction times (**Table 1**, entry 2 – 4), gave traces of the desired product.

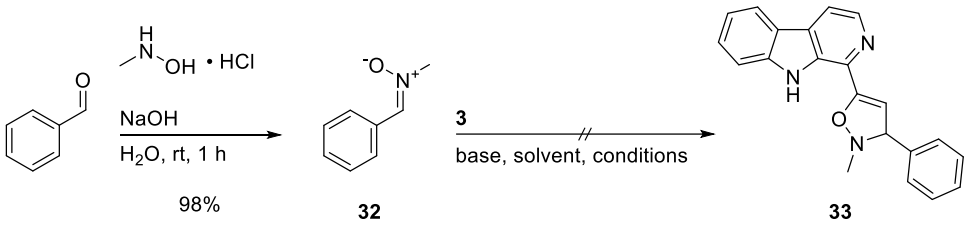

Scheme 13. Attempted synthesis of isoxazoline **33** from benzaldehyde.

Table 1. Reaction conditions tested for the HUISGEN cycloaddition of nitrone **32** and alkyne **3**.

entry	base	solvent	conditions
1	-	toluene	125 °C, 4 d
2	K_2CO_3	acetonitrile	rt – 50 °C, 5 d
3	K_2CO_3	acetonitrile	100 °C, 3 d (pressure tube)
4	KOH	methylene chloride	rt, 5 d

In contrast to other 1,3-dipoles, nitrones are less reactive and within this subgroup, *N*-methyl-*C*-phenyl-nitrone (**32**) was shown to be a nitrone with only weak "willingness" to add to dipolarophiles[99]. This can be explained by the *trans*-configuration of the organic residues to each other regarding the CN double bond. In comparison, 3,4-dihydroisoquinoline *N*-oxide, adds 200 times faster to ethyl crotonate in toluene due to its cyclic structure, which stabilizes the *cis*-configuration of the organic residues[99].

Although this would have been a promising alternative nitrone, no further attempts were made to synthesize any isoxazolines, as the size of the phenyl residue should not be changed too much and the flexibility to rotate around the single bond should be maintained.

Another interesting variation of the isoxazole group, which is accessible *via* HUISGEN cycloaddition, is inverse isoxazole **34**, whereby the substituents at C-3' and C-5' are interchanged. Compared to the synthesis of isoxazole **1**, building blocks with the converse residues are needed. Therefore, phenylacetylene is the alkyne component, whereas a nitrile oxide derived from *β*-carboline-1-carbaldehyde oxime (**35**) is used as 1,3-dipole (**Scheme 14**). This oxime can be synthesized from the corresponding aldehyde **36**, which in turn can be prepared from styrene **37** *via* ozonolysis.

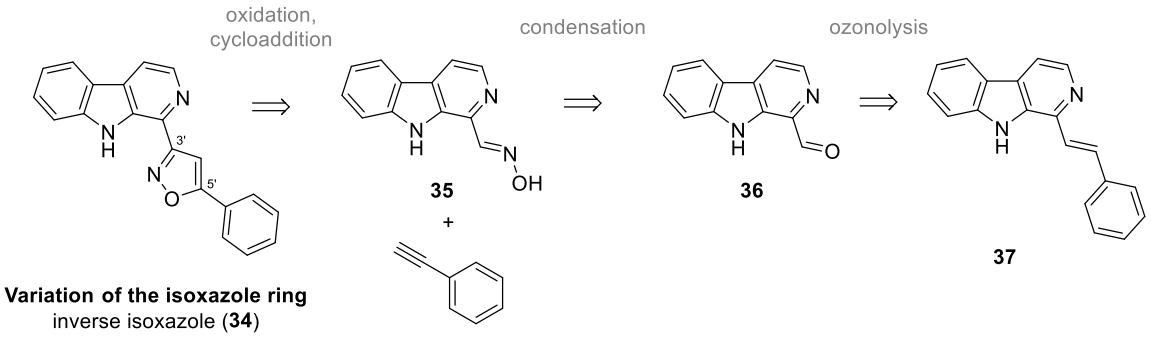

Scheme 14. Retrosynthesis of inverse isoxazole **34** *via* HUISGEN cycloaddition.

1-Formyl *β*-carboline (**36**), also known as kumujian C, is a natural alkaloid isolated from the wood of *Picrasma quassioides*[120]. Several strategies for synthesizing it were published, e.g. *via* PICTET-SPENGLER reaction of tryptamine with dimethoxyglyoxal and subsequent dehydrogenation and acetal cleavage[121] or oxidation of harmane with SeO_2[122]. Additionally ozonolysis of *N*-PMB protected benzalharman to the corresponding aldehyde was described[123]. The protective group was needed for the subsequent reaction with an aryl lithium compound, but assumed to be irrelevant for the ozonolysis.

Hence, the same protocol, which implied the use of Sudan III as an ozonizable dye to indicate the selective cleavage of the olefinic linkage[124], was used to generate 1-formyl *β*-carboline (**36**) from benzalharman (**37**), which was available in sufficient quantities from a former project[125]. The ozonolysis was found to be completed within 5 min and reductive work-up with dimethyl sulfide gave aldehyde **36** (55% yield) (**Table 2**, entry 1). The importance of the indicator, monitoring the completion of the reaction by colour change, was demonstrated, when the reaction was accidently run for too long (15 min) and the yield substantially decreased to

21%. Besides dimethyl sulfide other reducing agents can be used to generate aldehydes from the intermediate ozonides, but neither zinc in acetic acid (**Table 2**, entry 2) nor triphenylphosphine (**Table 2**, entry 3) were as efficient.

Table 2. Synthesis of aldehyde **36** *via* ozonolysis of benzalharman (**37**) with different reductive work-up procedures.

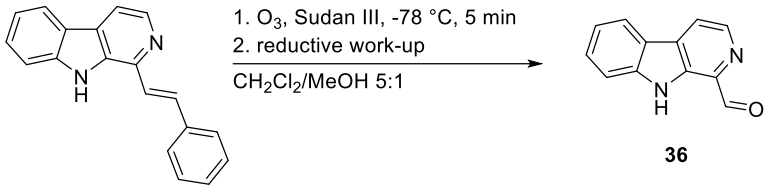

37 **36**

entry	reductive work-up	yield
1	Me_2S, -78 °C – rt, 16 h	55%
2	Zn, HOAc, rt, 2 h	15%
3	PPh_3, -78 °C – rt, 48 h	40%

Next the oxime synthesis and cycloaddition was to be examined. SINGH *et al.*[126] prepared one example of a related "inverse" isoxazole from a *β*-carboline-1-carbaldehyde that was additionally *N*-methyl and ethyl 3-carboxylate substituted. While the condensation with hydroxylamine could be applied to aldehyde **36** to give (*E*)-oxime **35** quantitatively, several attempts for the subsequent preparation of the hydroxymoyl chloride **38** and isoxazole **34** failed (**Scheme 15**). First, it was tried to prepare the hydroxymoyl chloride **38** with NCS in DMF at room temperature, but no conversion was indicated by TLC analysis. Rising the temperature to 40 °C and adding pyridine did also not lead to full consumption of the starting material, but several new spots were observed. Therefore, it was tried to proceed with the reaction cascade and phenylacetylene and triethylamine were added. The formation of isoxazole **34** could be detected with MS, but no sufficient quantities could be isolated. Presumably already the chlorination was inefficient. This could be due to side reactions, such as ring chlorination of the *β*-carboline[127], or an interference of the NH group. The reaction was repeated in chloroform, but this did also not lead to an improvement. Again another method to generate the nitrile oxide *in situ* was needed and the protocol of JAWALEKAR *et al.*[101] using PIFA as oxidant was applied once more successfully and gave isoxazole **34** (43% yield).

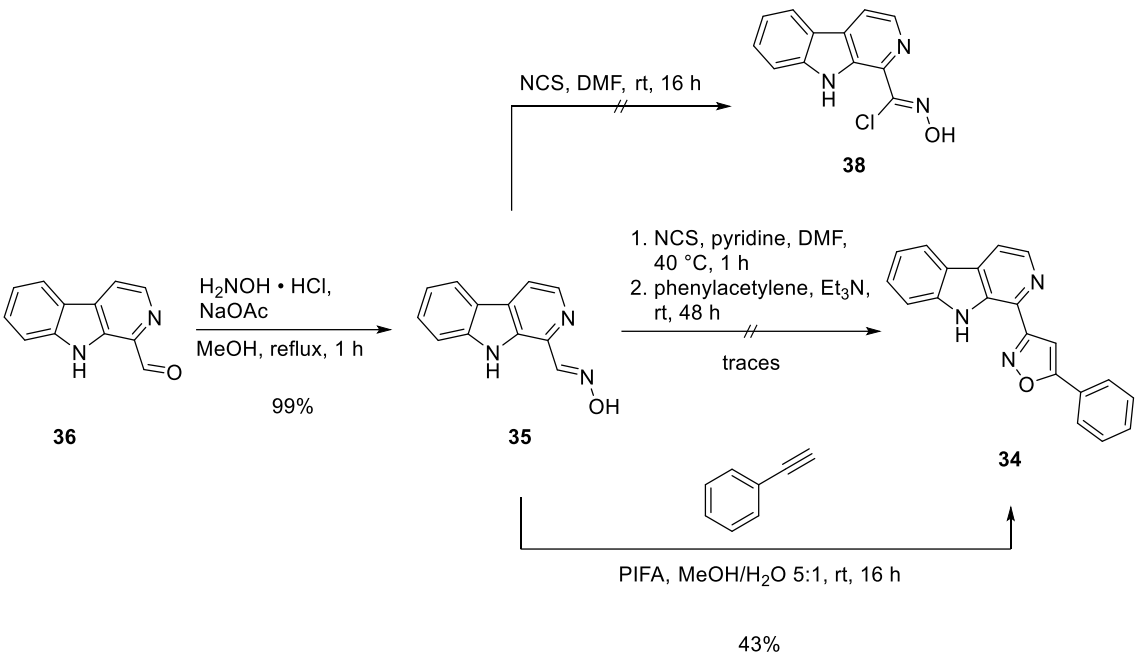

Scheme 15. Synthesis of inverse isoxazole **34** from aldehyde **36**.

3.2.1.2 Syntheses of five-membered heterocycles from open-chained intermediates

In addition to the intermolecular HUISGEN cycloaddition, several other five-membered heterocycles are accessible *via* intramolecular cyclization reactions starting from bifunctional open-chained intermediates.

The first envisaged analogue of this subset was isothiazole **39**, in which sulfur replaces the oxygen atom of the isoxazole lead structure (**Scheme 16**). In general, isothiazoles are accessible from the respective open-chained enamino ketones. After generating the thioketone by displacing O by S, oxidative ring closure leads to formation of the isothiazole ring. The therefore required enamino ketone **40** can be generated from the corresponding isoxazole **1** *via* reductive cleavage of the N-O bond.

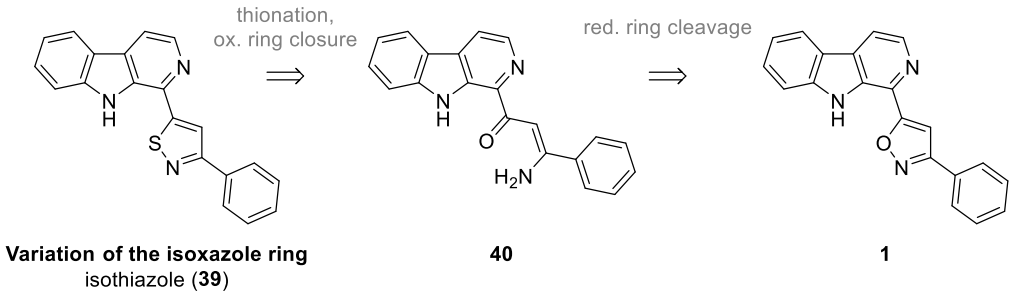

Scheme 16. Retrosynthesis of isothiazole **39** from isoxazole **1**.

The preparation of enamino ketone **40** from lead structure **1** was already described by TREMMEL as intermediate for the synthesis of canthin-4-ones. However, when the hydrogenation was run under the published conditions with palladium on carbon (**Table 3**, entry 1[86]), reductive isoxazole cleavage was only achieved in traces according to TLC and ASAP analysis. When the reaction conditions were more forcing, the conversion was improved, but even after 4 d the starting material/product ratio was only 1:1 according to ^{1}H NMR analysis (**Table 3**, entry 2). The presence of a base is often required, but KAMLAH[128] made other observations recently, when she could only cleave a 3,4,5-trisubstituted isoxazole without the addition of a base. For isoxazole **1** this was not expedient (**Table 3**, entry 3), but full conversion was achieved, when KOH was replaced by Cs_2CO_3[128] and a mixture of methanol and ethyl acetate was used as solvent mixture, in which **1** showed greatly enhanced solubility. Enamino ketone **40** was then isolated in a yield of 67% (**Table 3**, entry 4).

Table 3. Reaction conditions for the synthesis of enamino ketone **40** from isoxazole **1**.

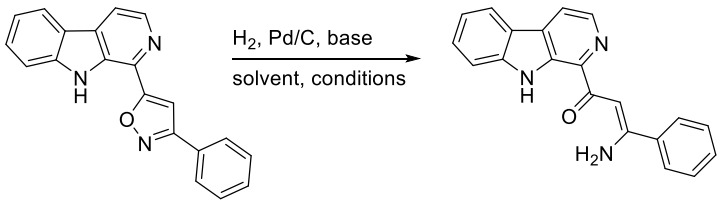

1 **40**

entry	base	solvent	conditions	yield
1	KOH	EtOH	1 bar (H_2), rt, 16 h	traces
2	KOH	EtOH	20 bar (H_2), 30 °C, 4 d	n.d.*
3	-	EtOH	1 bar (H_2), rt, 18 h	-
4	Cs_2CO_3	MeOH/EtOAc 1:1	30 bar (H_2), rt, 16 h	67%

(*Yield was not determined due to bad separability of starting material and product, but 1:1 ratio was observed in ^{1}H NMR analysis.)

Next, the isothiazole synthesis was approached. Thionation reagents such as LAWESSON'S reagent or P_4S_{10} can be used for the transformation of ketones into thioketones. The latter one was shown to be more efficient in the presence of a base and in solvents more polar than toluene[129]. The ring closure can then be accomplished by oxidants such as sulfur or *p*-chloranil[130].

Following a procedure of PLESCH[102], the synthesis of isothiazole **39** was accomplished (**Scheme 17**). Enamino ketone **40** was treated with P_4S_{10} in the presence of $NaHCO_3$. After 16 h TLC analysis showed no remaining starting material, but multiple other spots indicating degradation in a non-specific manner[130]. Nevertheless, the addition of *p*-chloranil resulted in

the formation of the envisaged isothiazole **39** (17% yield). In order to increase the yield, repetition of the thionation with LAWESSON'S reagent was attempted, but this did not show any improvement regarding the degradation. Thus, the reaction sequence was not continued.

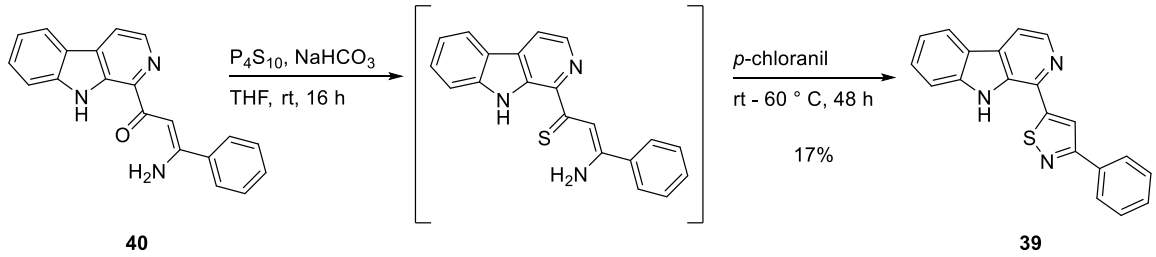

Scheme 17. Synthesis of isothiazole **39** from enamino ketone **40**.

The next intention was the synthesis of analogues, for which C-4' is replaced by heteroatoms, such as in oxazoles or oxadiazoles. In general, those rings can be generated from different open-chained intermediates (**A**) by intramolecular cyclocondensation or oxidative ring closure (**Scheme 18**). These intermediates are in turn accessible from carboxylic acid **41** or aldehyde **36**, which can both be prepared from benzalharman (**37**) by oxidative cleavage (*cf.* 3.2.1.1). In total, four analogues were envisaged: the 2,4- and 2,5-disbstituted 1,3-oxazoles **46** and **43**, which differ in the position of the phenyl ring, and the 1,2,4- oxadiazole **48** and 1,3,4-oxadiazole **50** with their altering order of heteroatoms.

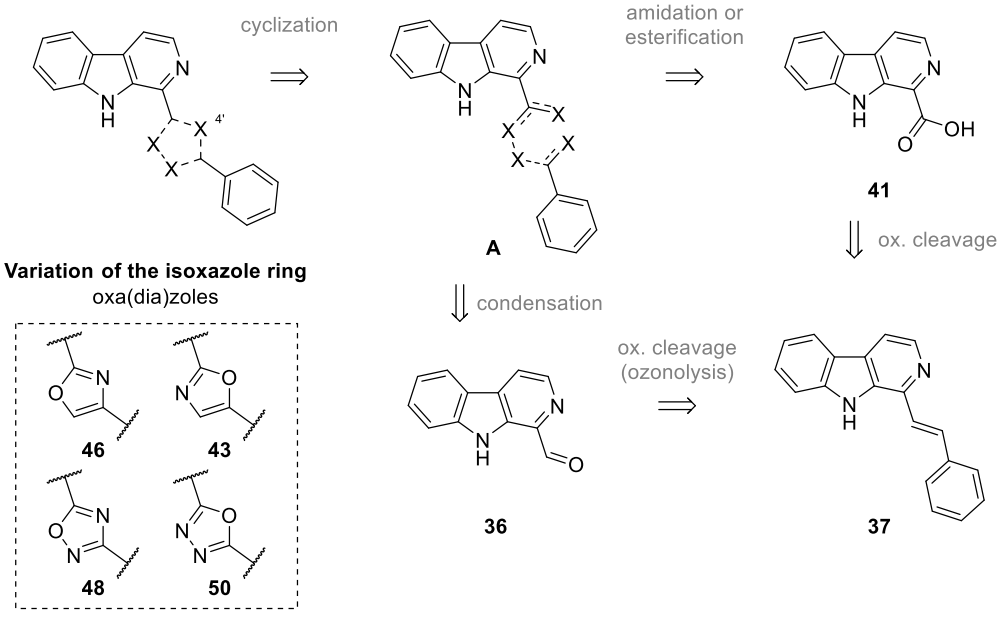

Scheme 18. Retrosynthesis of oxa(dia)zoles from benzalharman (**37**).

The conducted oxidative cleavage of benzalharman (**37**) using $KMnO_4$ in acetone was described by MCEVOY *et al.*[131] and gave carboxylic acid **41** in good yield (78%) (**Scheme 19**). Subsequent activation with 1,1'-carbonyldiimidazole (CDI) and coupling with phenylethylamine resulted in amide **42** (62% yield), which was the precursor for an oxidative cyclisation. However, this iodine catalysed oxazole synthesis, which uses TBHP as oxidant and most likely follows a radical pathway[132], failed to give oxazole **43**. Probably the close proximity to the free indole NH impeded the reaction, since this method was only applied to *N*-phenylethylamide derived from pyridine-2-carboxylic acid according to the literature[132].

The ROBINSON-GABRIEL synthesis is a more common approach to substituted oxazoles, which covers the cyclodehydration of *α*-acylamino ketones[133-134]. Based on this, a Russian patent describes a one-pot protocol for the multigram-scale preparation of 2-pyridyl-5-phenyloxazoles from respective pyridinecarboxylic acids and 2-aminoacetophenone hydrochloride making the isolation of the intermediate redundant[135]. For the synthesis of oxazole **43** some adjustments had to be made. The reaction could not be conducted in pure phosphorus(V) oxychloride due to the extremely limited solubility of carboxylic acid **41**. Toluene was added to obtain at least an inviscid suspension. Additionally, a pressure tube was used to not distil off any phosphorus(V) oxychloride prior to completeness of the reaction sequence, since it possesses dual functions as activation and dehydration reagent. After stirring for 16 h at 105 °C, residual intermediate *α*-acylamino ketone **44** was still present, but the conversion to 2,5-disubstituted oxazole **43** was completed after 40 h (39% yield).

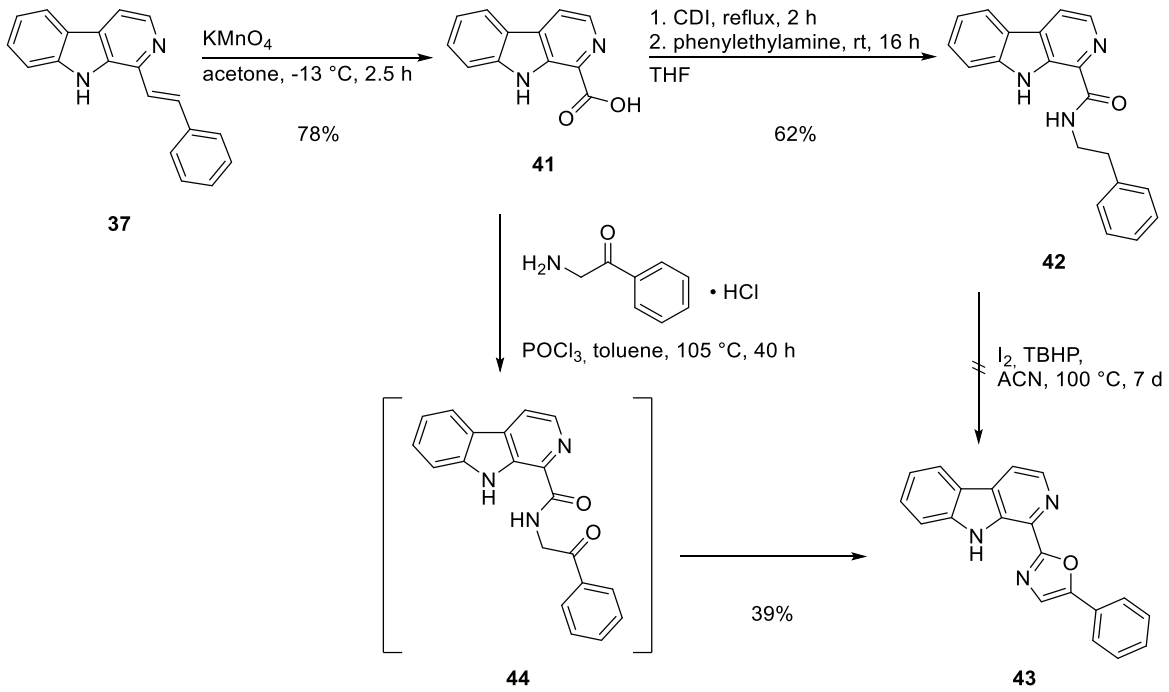

Scheme 19. Synthesis of 2,5-disubstituted oxazole **43** from styrene **37**.

The corresponding 2,4-disubstituted oxazole **46** was accessible from the same precursor **41** (**Scheme 20**). Following a protocol of REDDY *et al.*[136], nucleophilic substitution of phenacyl bromide was attempted, but due to the extremely poor solubility of carboxylic acid **41**, formation of ester **45** was only achieved at elevated temperature. No side products, e.g. caused by *N*-alkylation, were detected by TLC analysis and the crude product showed only negligible impurities in ^{1}H NMR analysis after extraction. However, the yield dropped dramatically after flash column chromatography (32%). As phenacyl esters are used as photocleavable protective groups[137] and linkers[138-139], (photo)lability of ester **45** is also a plausible explanation for degradation.

Condensation of such phenacyl esters with ammonium acetate results in oxazoles in only relatively low yields, because the respective imidazoles can form as well. To prevent this side reaction, HUANG *et al.*[140] described an improved approach by using acetamide and boron trifluoride etherate. With this procedure, oxazole **46** was synthesized (31% yield) among several unidentified side products.

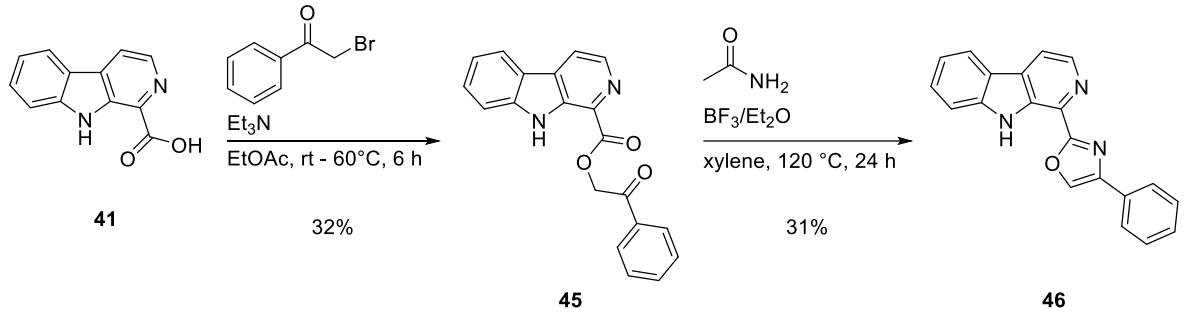

Scheme 20. Synthesis of 2,4-disubstituted oxazole **46** from carboxylic acid **41**.

The 1,2,4-oxadiazole **48** was prepared following a one-pot procedure of SHARONOVA *et al.*[141], which consists of three steps: activation of the carboxylic acid with CDI, coupling with an amidoxime to the respective *O*-acylamidoxime, and base-catalysed cyclodehydration. According to the published method, the entire reaction cascade can be conducted in DMSO at room temperature. However, in the case of carboxylic acid **41**, activation could only be achieved at elevated temperature, due to the aforementioned, very limited solubility (**Scheme 21**). As cooling to room temperature resulted in the formation of a large amount of precipitate again, the coupling with amidoxime **47**, which was synthesized from benzonitrile and hydroxylamine hydrochloride[142], was also run at elevated temperature. This led to the intermediary *O*-acylamidoxime, even though a small amount of oxadiazole **48** was detected at this stage already. Treatment with KOH then resulted in the complete conversion to 1,2,4-oxadiazole **48** (46% yield).

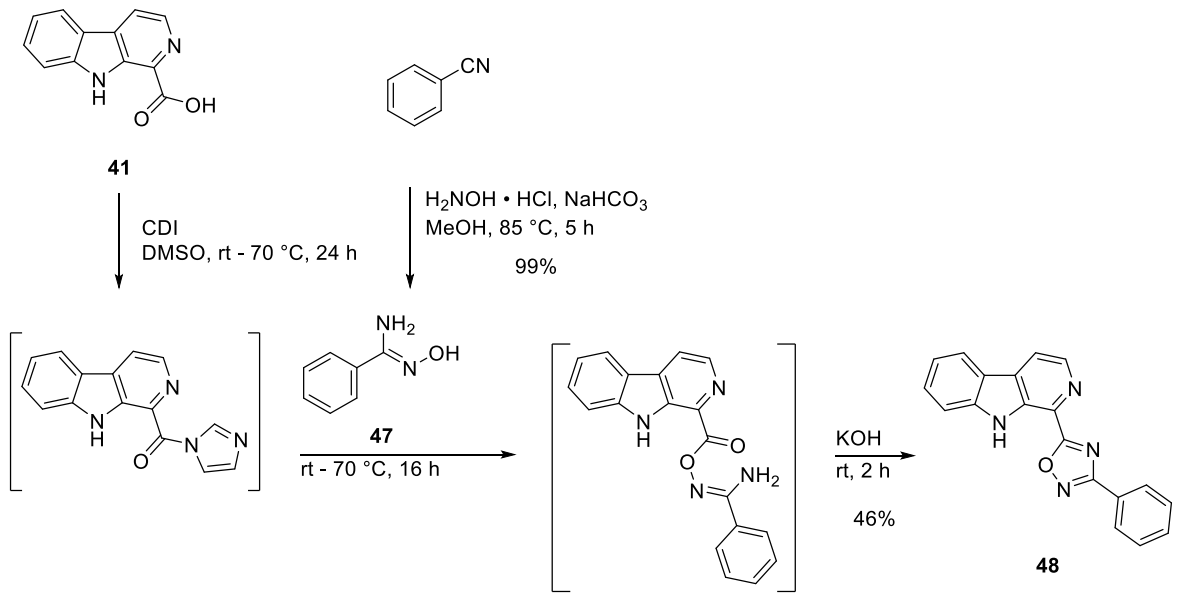

Scheme 21. Synthesis of 1,2,4-oxadiazole **48** from carboxylic acid **41**.

The synthesis of envisaged 1,3,4-oxadiazole **50** was performed as described in literature (**Scheme 22**)[143]. After condensation of aldehyde **36** and benzoylhydrazine, the intermediary benzoylhydrazone **49** was subjected to oxidative cyclisation using iodine and Cs_2CO_3. In contrast to the literature, oxadiazole **50** (63% yield) was however not obtained pure after filtration, requiring subsequent purification by flash column chromatography.

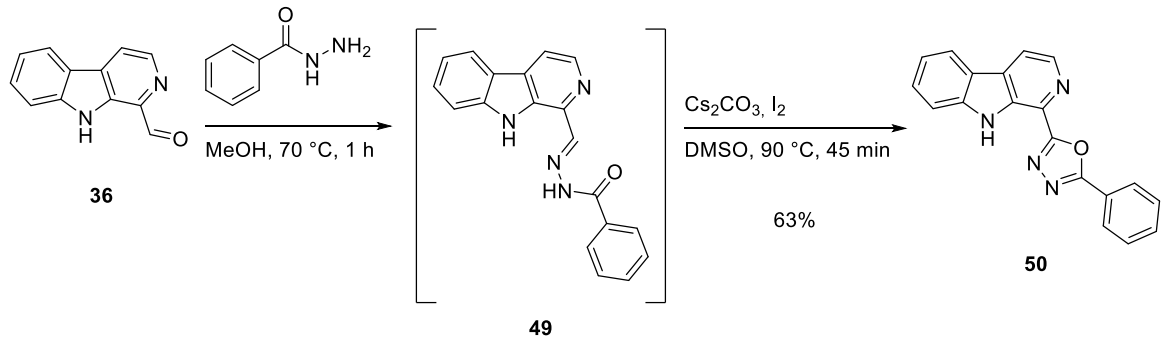

Scheme 22. Synthesis of 1,3,4-oxadiazole **50** from aldehyde **36**.

Besides the variety of analogues described to this point containing other five membered heterocycles as variations of the isoxazole ring, also an acetylene analogue was synthesized. SONOGASHIRA cross-coupling of bromide **8** with phenylacetylene was conducted to obtain alkyne **51** (69% yield) (**Scheme 23**). This very simple variation can be seen as an

open-chained analogue (isoster), which has an acetylene linker instead of a five-membered heterocycle between the phenyl residue and the *β*-carboline motif.

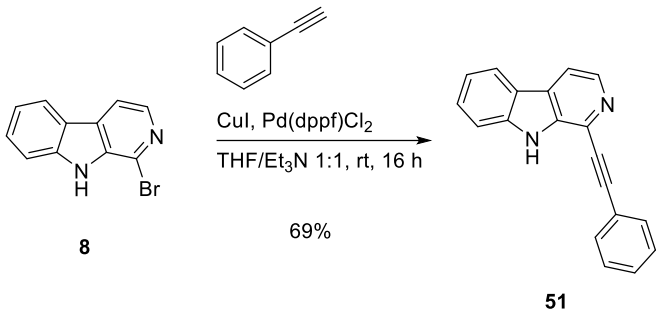

Scheme 23. Synthesis of phenylacetylene **51** from bromide **8**.

3.2.1.3 Syntheses of variations with other five-membered heterocycles than isoxazole *via* PICTET-SPENGLER reaction

Another intensively investigated method to synthesize 1-substituted *β*-carbolines in general is the dehydrogenation of respective 1,2,3,4-tetrahydro-*β*-carbolines. These intermediates (**B**) can be obtained *via* PICTET-SPENGLER reaction of tryptamine and (hetero)aromatic aldehydes (**A**), whereby with the latter the desired variation of the isoxazole moiety (five-membered heterocycle with a phenyl substituent) is introduced (**Scheme 24**). In contrast to the previous analogues, this approach is particularly advantageous for heterocycles, which cannot straightforwardly be synthesized from the aforementioned precursors.

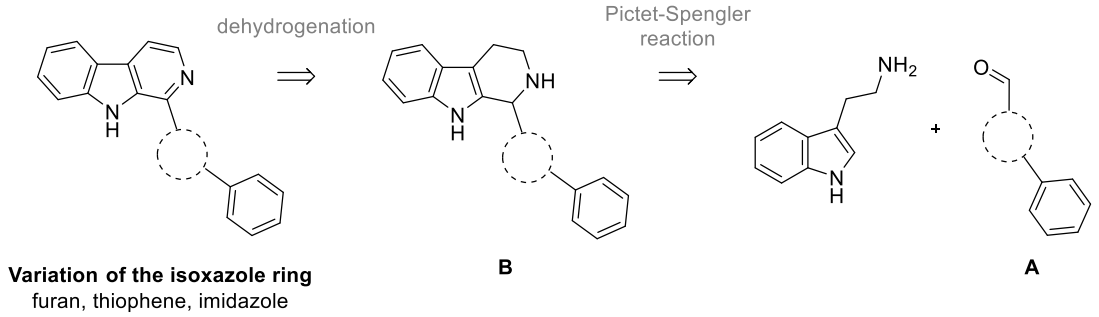

Scheme 24. Retrosynthesis of variations of the isoxazole group with other 5-membered heterocycles accessible *via* PICTET-SPENGLER reaction and dehydrogenation.

To confirm the feasibility of this strategy, it was at first utilized for the synthesis of lead structure **1**. The required arylaldehyde **53** was prepared similar to literature (**Scheme 25**): HUISGEN cycloaddition of propargyl alcohol and benzonitrile oxide (derived from hydroxymoyl chloride

11 with triethylamine) gave alcohol **52**[144] (79% yield), which was further oxidized following a SWERN protocol to aldehyde **53**[145] (84% yield).

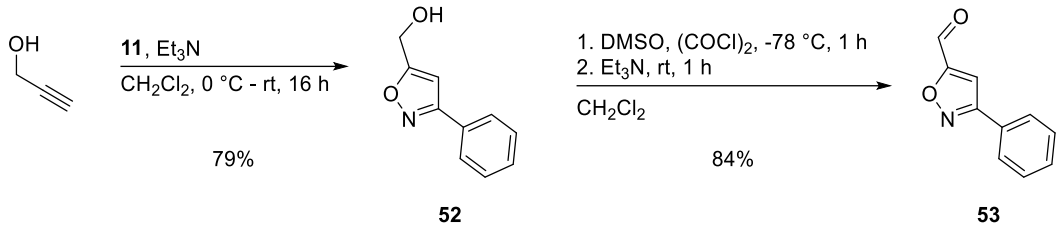

Scheme 25. Synthesis of aldehyde **53** *via* HUISGEN cycloaddition and SWERN oxidation.

Next, the PICTET-SPENGLER reaction was elaborated. This reaction comprises two steps in general (**Scheme 26**), whereby the first step is the condensation of an amine, such as tryptamine, with an aldehyde group. The formed imine can then undergo an intramolecular cyclization to the respective 1-substituted 1,2,3,4-tetrahydro-*β*-carboline. This step is facilitated by BRØNSTED or LEWIS acids, as the iminum ion is more electrophilic than the corresponding imine[146].

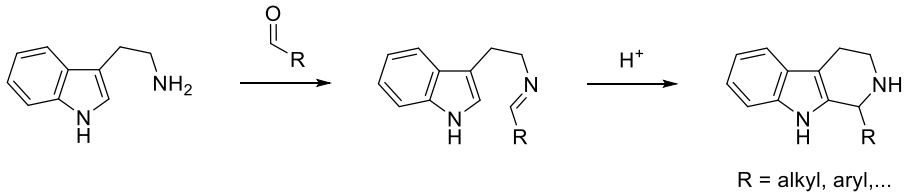

Scheme 26. PICTET-SPENGLER reaction of tryptamine.

Initially, an acid-promoted protocol[147] was tried to synthesize tetrahydro-*β*-carboline **54**. This was promising also with regard to the isoxazole analogues, as the conditions were used in literature for the synthesis of various 1-substituted 1,2,3,4-tetrahydro-*β* carbolines derived from benzaldehydes, but also from thiophene- and furancarbaldehydes[148-149]. However, the treatment of tryptamine and aldehyde **53** in methylene chloride with trifluoroacetic acid at 0 °C and the subsequent warming to room temperature, resulted only in traces of tetrahydro-*β*-carboline **54**, even after stirring for 48 h (according to TLC and HRMS analysis) (**Scheme 27**).

Instead of screening various solvents, acids and reaction conditions to optimize the conversion, another type of PICTET-SPENGLER reaction was utilized. Although it is not the most common approach, PICTET-SPENGLER reactions can also be conducted without acid in high-

boiling solvents, e.g. xylene or toluene[146], as high temperature can obviously overcome the energy barrier even in the case of imines derived from electron-rich (hetero)arylaldehydes[150]. However, the formation of traces of acid *in situ* by air oxidation of the aldehyde is possibly a facilitating contribution[151]. In general, this approach was particularly beneficial for the intended variations, as it would also enable the subsequent dehydrogenation of tetrahydro-*β*-carbolines to the fully aromatic derivatives to be carried out one-pot by the addition of sulfur or palladium on carbon[152-153].

RAJKUMAR *et al.*[153] synthesized, for example, 1-(thiophen-2-yl)-9*H*-pyrido[3,4-*b*]indole with such a one-pot reaction to elaborate *β*-carbolines as directing group in ruthenium(II)-catalyzed C-H arylation. When the first step of their general procedure, stirring tryptamine and (hetero)arylaldehyde in anisole at 120 °C for 2 h, was applied to aldehyde **53**, TLC indicated the full conversion of the aldehyde to a quite polar substance, which was after flash column chromatography identified indeed as tetrahydro-*β*-carboline **54** (63% yield). When the reaction was repeated and after 2 h palladium on carbon was added and the mixture was heated to 140 °C for 24 h, the tetrahydro-*β*-carboline **54** was fully dehydrogenated to give *β*-carboline **1** in equal and satisfying yield (63%).

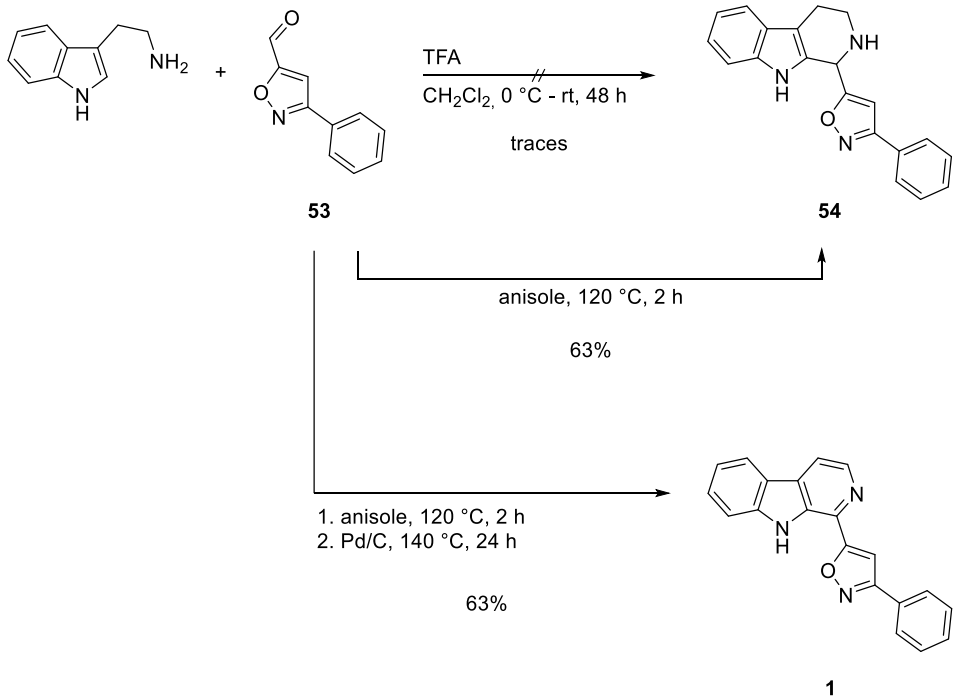

Scheme 27. Synthesis of 1,2,3,4-tetrahydro analogue **54** *via* PICTET-SPENGLER reaction and lead structure **1** by subsequent dehydrogenation.

The developed method should also be applied to the synthesis of analogues, which contain a furan, thiophene and imidazole ring instead of the isoxazole.

The required furan aldehyde **55** and thiophene aldehyde **56** could easily be prepared according to literature in good yields *via* SUZUKI cross-coupling of bromoarylaldehydes and phenyl boronic acid[154] (**Scheme 28**). With aldehyde **55** once again an acid-promoted protocol was tried[148], but treatment with trifluoroacetic acid did not lead to the formation of tetrahydro-*β*-carboline **57** (according to HRMS). The fast transition of the brownish solution to a black slurry and the plethora of spots on the TLC plate indicated the decomposition of furan **55**, probably due to acid-lability. When the abovementioned acid-free one-pot reaction was applied to aldehydes **55** and **56** respectively, both envisaged *β*-carbolines were obtained: furan **58** (18% yield) and thiophene **59** (23% yield). Although the yields fell short of expectations compared to **1** (63% yield), they were somehow acceptable for a one-pot three step procedure (condensation, cyclization and dehydrogenation).

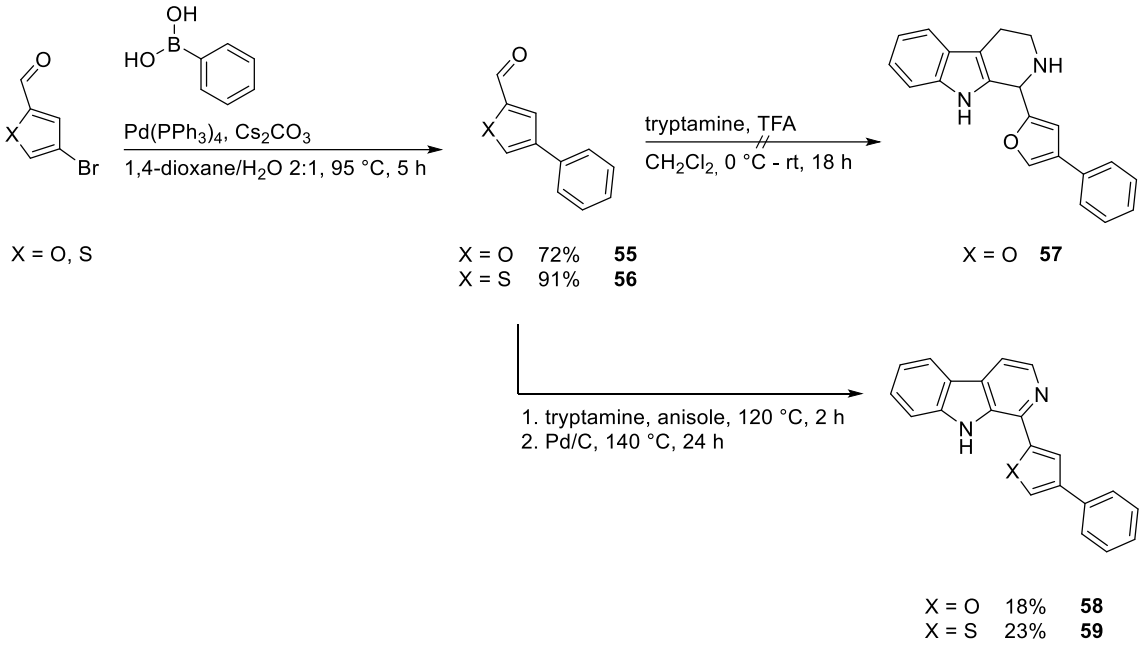

Scheme 28. Synthesis of furan **58** and thiophene **59** *via* SUZUKI cross-coupling, PICTET-SPENGLER reaction and subsequent dehydrogenation.

The DEBUS-RADZISZEWSKI imidazole synthesis is a well-known strategy for the synthesis of substituted imidazoles. Over 100 years ago, it was observed, that the condensation of glyoxal and formaldehyde with two equivalents of ammonia results in imidazole[155]. When substituted 1,2-dicarbonyl components, aldehydes and amines are used, differently substituted imidazoles are accessible. For disubstituted imidazoles such as **60**, phenylglyoxal (commercially available as monohydrate) is the required 1,2-dicarbonyl component.

Initially, a direct synthesis of **60** from aldehyde **36** was attempted[156-157]. Therefore, phenylglyoxal monohydrate was reacted with ammonium acetate and aldehyde **36**, but no

formation of imidazole **60** was observed (**Scheme 29**). As phenylglyoxal can react as both, dicarbonyl and aldehyde component, obviously the condensation with itself to **61** takes place, as described by KHALILI *et al.*[158] and confirmed by HRMS.

In contrast, the DEBUS-RADZISZEWSKI imidazole synthesis could be applied to the synthesis of aldehyde **62**, following a patent starting from phenylglyoxal monohydrate and 2,2-dimethoxyacetaldehyde[159]. After condensation, the intermediary dimethyl acetal was cleaved with aqueous hydrochloric acid to give the free aldehyde (62% yield). This aldehyde was then subjected to the acid-free PICTET-SPENGLER reaction and one-pot dehydrogenation, which was run at further elevated temperature[160]. Purification of imidazole **60** (19% yield) was difficult due to its limited solubility in various organic solvents. TLC demonstrated a broadened, not clearly defined spot and dragging of the compound was also a challenge for flash column chromatography.

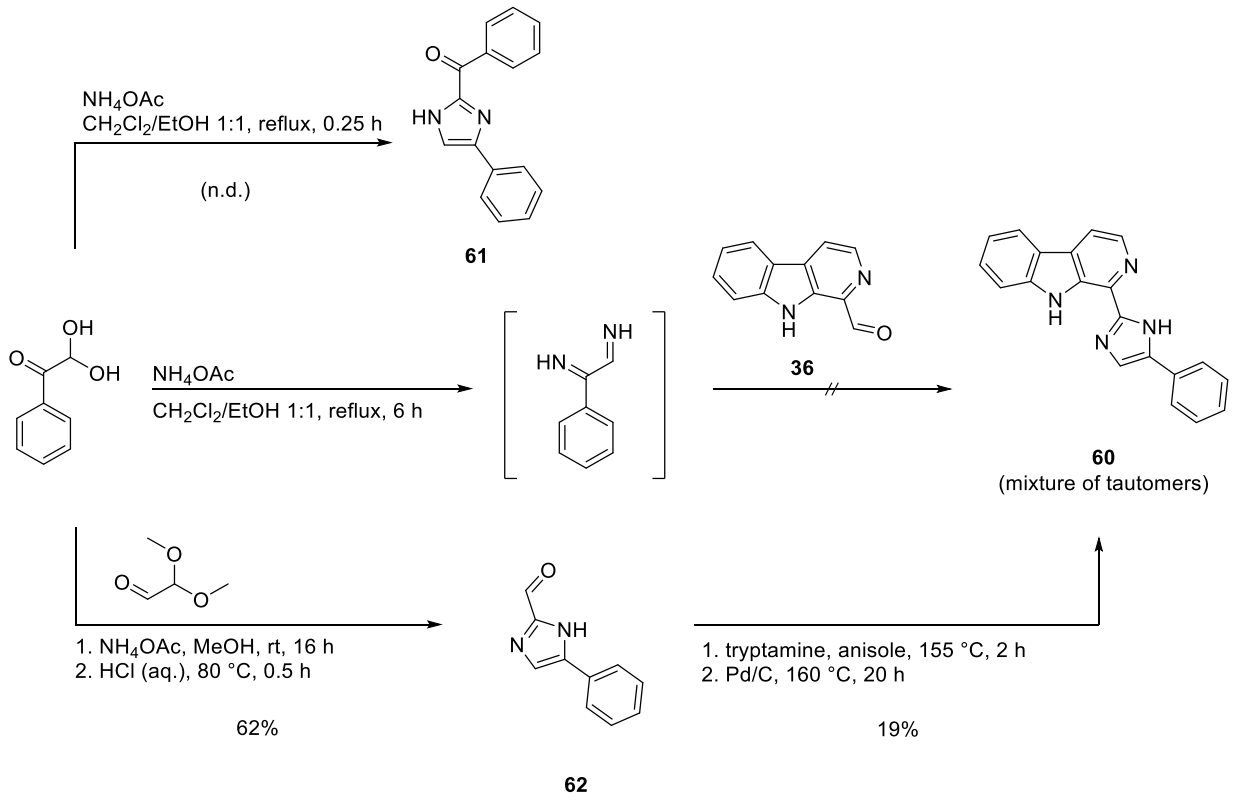

Scheme 29. Synthesis of imidazole **60** *via* DEBUS-RADZISZEWSKI imidazole synthesis, PICTET-SPENGLER reaction and subsequent dehydrogenation.

^{1}H NMR analysis showed, that all signals (besides one very broad singlet >12 ppm) were doubled, but this was difficult to assess as some signals were overlapping. Also imidazoles can occur in two tautomeric forms due to protopic exchange of the NH and – in contrast to pyrazole **31** – this time the interconversion rate is obviously slow enough to observe both in a

ratio of 1:5 in ^{1}H NMR analysis in DMSO-d_6 under standard conditions (25 °C, 400 MHz). It could not be assigned, which tautomeric form is predominant and similar to KHALILI *et al.*[158] both can be stabilized by intramolecular hydrogen bonds (**Figure 11**, top). As the exchange rate is related to temperature, the ^{1}H NMR spectra were also recorded at elevated temperatures (**Figure 11**, bottom). At 50 °C and 80 °C a difference is already observed and the doubled signals start merging. At 100 °C some signals are still not fully overlapping, resulting in a slightly bulbous shape, while full coalescence is achieved at 120 °C, when only a single set of signals is remaining.

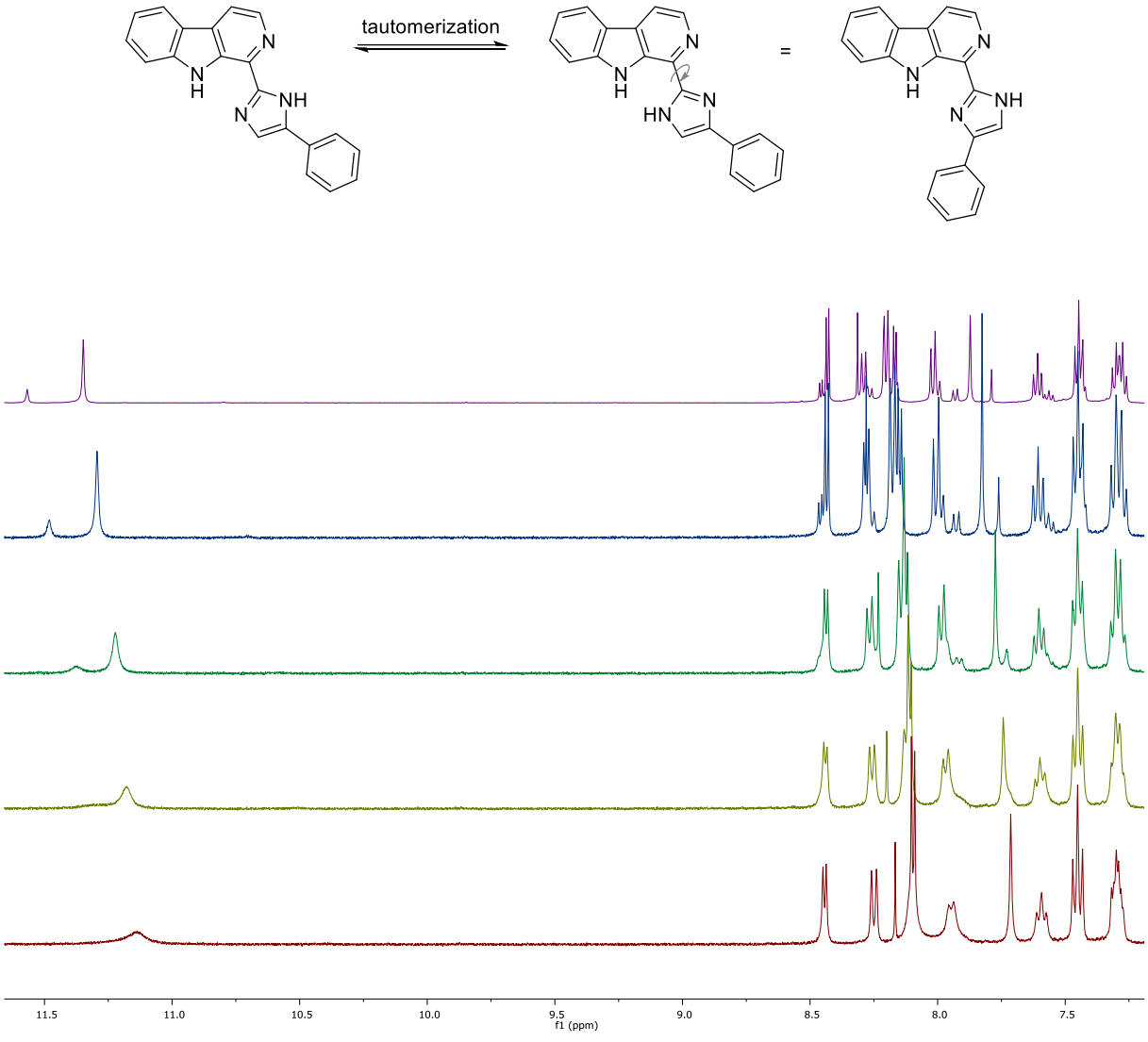

Figure 11. Tautomeric forms of imidazole **60** (top) and ^{1}H NMR spectra recorded at 25 °C (purple), 50 °C (blue), 80 °C (green), 100 °C (yellow) and 120 °C (red) (bottom).

3.2.2 Studies towards isoxazoles with additional substituents at C-4'

After synthesizing diverse five-membered heterocycles, the 4-substitued isoxazoles should next be investigated. Gaining access to 4-aminoisoxazole **63** was a key objective in terms of the introduction of donor groups onto lead structure **1** (*cf.* **Figure 7**). It seemed highly promising according to docking experiments performed by DR. MICHAEL MEYER (MBC-Statistik, Falkensee, Germany), that the 4'-amino group could be capable of establishing a hydrogen bond with the backbone carbonyl oxygen of GLY 245 (**Figure 12**).

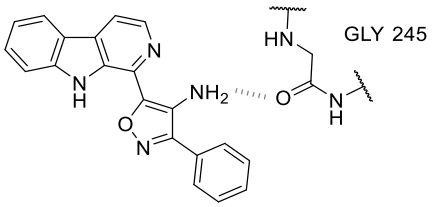

63

Figure 12. Illustration of the potential hydrogen bond (dotted line), which could hypothetically be formed between the 4-aminoisoxazole **63** and GLY 245.

3.2.2.1 Attempted synthesis of 4-aminoisoxazole **63** *via* reduction of the corresponding nitro compound

The presumably most widely used method to generate primary aromatic amines is the reduction of the corresponding nitroarenes. In the case of 4-aminoisoxazole **63**, the suitable precursor is 4-nitro isoxazole **64** (**Scheme 30**). Since selective nitration at C-4' of lead structure **1** is not feasible, this precursor should be synthesized *via* (3+2)-cycloaddition of benzonitrile oxide and (the enol form of) *α*-nitro ketone **65**.

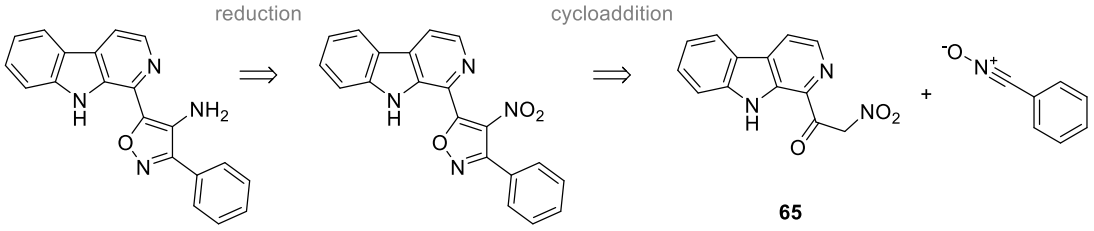

Variation of the isoxazole ring
4-amino isoxazole (**63**)

64

65

Scheme 30. Retrosynthesis of 4-aminoisoxazole **63** *via* reduction of 4-nitro isoxazole **64**.

α-Nitro ketones can generally be accessed from nitromethane and activated carboxylic acids. BAKER *et al.*[161] showed that the reaction of the nitromethane anion and *N*-acylimidazoles,

which are generated from carboxylic acids upon reaction with CDI, results in *C*-acylation (rather than *O*-acylation). Thus, for the preparation of *α*-nitro ketone **65**, carboxylic acid **41** was activated to receive the intermediary *N*-acylimidazole, which was then reacted with preformed sodium methanenitronate (prepared by the reaction of sodium hydride with dry nitromethane) (**Scheme 31**). As the activated intermediate of **41** is not sufficiently soluble, the suspension was transferred, while it was still hot and inviscid enough to be drawn up and injected by syringe. The resulting *α*-nitro ketone **65** (61% yield) could then be purified solely by extraction at different pH values due to the rather acidic methylene group. In basic aqueous solution, the anion was predominant and remained in the aqueous phase, while organic substances, such as imidazole, were partitioned off with methylene chloride. When pH 1 was subsequently adjusted, the then uncharged form could be moved to the organic layer. Although *α*-nitro ketones can possibly undergo keto-enol and nitro-*aci*-nitro tautomerism, ^{1}H NMR analysis clearly showed a single set of signals and the singlet of the methylene group with the integral of 2 H was a further confirmation of the depicted structure of **65**.

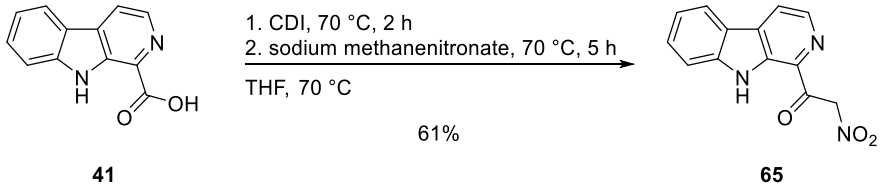

Scheme 31. Synthesis of *α*-nitro ketone **65**.

Next, the isoxazole synthesis was attempted. DAL PIAZ *et al.*[162] found, that *α*-nitro ketones can react as dipolarophiles in cycloaddition reactions with nitrile oxides. In contrast to the cycloadditions mentioned so far, the corresponding enolates of the ketones lead to the formation of hydroxyisoxazolines, which are then dehydrated to isoxazoles. When *α*-nitro ketone **65** and hydroxymoyl chloride **11** were used as described in the procedure of DAL PIAZ *et al*.[162] (**Table 4**, entry 1), no cycloaddition to isoxazole **64** occurred. Neither varying the temperature (**Table 4**, entry 2), nor the solvent and base system (**Table 4**, entry 3 – 6) lead to any conversion of the dipolarophile. Obviously, the generated nitrile oxide is more prone to undergo competing side reactions, such as dimerization[99].

Table 4. Attempted synthesis of 4-nitro isoxazole **64** from *α*-nitro ketone **65**.

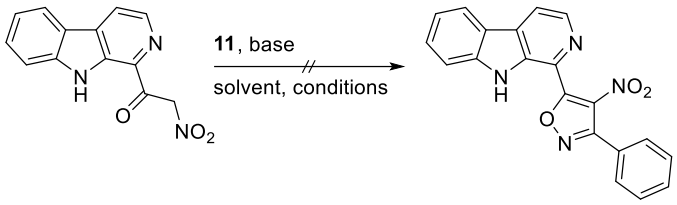

65 **64**

entry	base	solvent	conditions	yield
1	Et_3N	EtOH	-10 °C – rt, 18 h	-
2	Et_3N	EtOH	80 °C, 8 h	-
3	Et_3N	MeOH	0 °C, 16 h	-
4	Et_3N	$CHCl_3$	rt, 24 h	-
5	Cs_2CO_3	EtOH	-10 °C – rt, 18 h	-
6	NaH	THF	-10 °C – rt, 18 h	-

As there are only very few examples[162-164] of 4-nitro isoxazoles synthesized following this approach and none of them contained pyridine or indole substructures, no further attempts were made. Additionally, it was assumed, that an alternative synthesis route *via* CURTIUS rearrangement would give access to further interesting analogues, such as an ester and a carboxylic acid.

3.2.2.2 Synthesis of 4-aminoisoxazole **63** *via* CURTIUS rearrangement

Besides nitroarenes, other suitable precursors for the synthesis of primary aromatic amines are carboxylic acids. These can be converted into intermediary acyl azides and then subjected to degradation reactions such as the CURTIUS rearrangement. For 4-aminoisoxazole **63** the required carboxylic acid **66** is, again, approachable *via* HUISGEN cycloaddition (**Scheme 32**). To obtain this 3,4,5-trisubtituted isoxazole no terminal alkyne, but ethyl propiolate **67** is required. This dipolarophile should be accessible *via* SONOGASHIRA cross-coupling of bromide **8**.

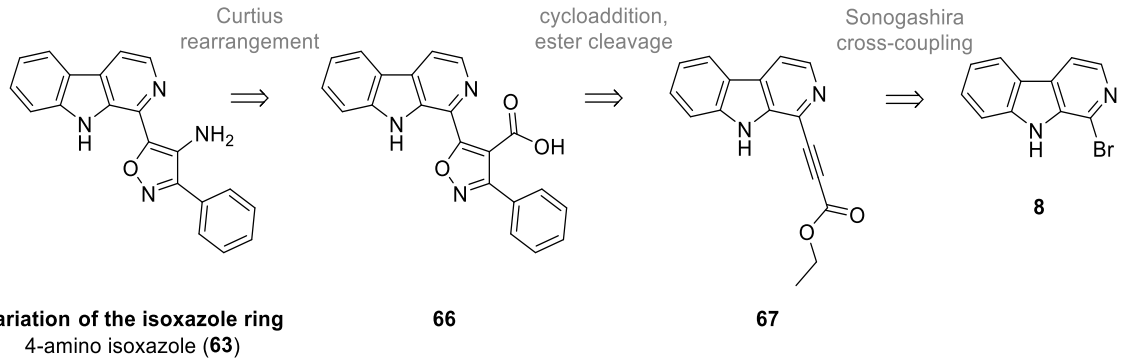

Scheme 32. Retrosynthesis of 4-aminoisoxazole **63** *via* CURTIUS rearrangement of carboxylic acid **66**.

Initially, SONOGASHIRA cross-coupling of bromide **8** with ethyl propiolate was attempted under the same conditions as described for the previous couplings with TMS-acetylene and phenylacetylene (**Scheme 33**). Full conversion of bromide **8** to a more polar substance occurred according to TLC analysis. However, ASAP analysis showed a characteristic isotope pattern (*m/z* = 345 and 347 $[M+H]^+$, ratio approx. 1:1), which indicates that the bromine remained unaffected and no alkyne **67** has formed. NMR and HRMS confirmed that instead an *aza*-MICHAEL addition of ethyl propiolate to the indole NH occurred and the resulting alkene **68** was obtained as *E*/*Z* mixture (in a ratio of 1.0:0.27 determined *via* ^{1}H NMR spectrum). HILDEBRAND[165] made similar observations for the corresponding 1-chloro-*β*-carboline and ethyl propiolate, but received only *E*-configured alkene. Although aryl bromides are generally more reactive towards SONOGASHIRA cross-couplings than the respective chlorides, bromide **8** obviously also undergoes the *aza*-MICHAEL addition selectively.

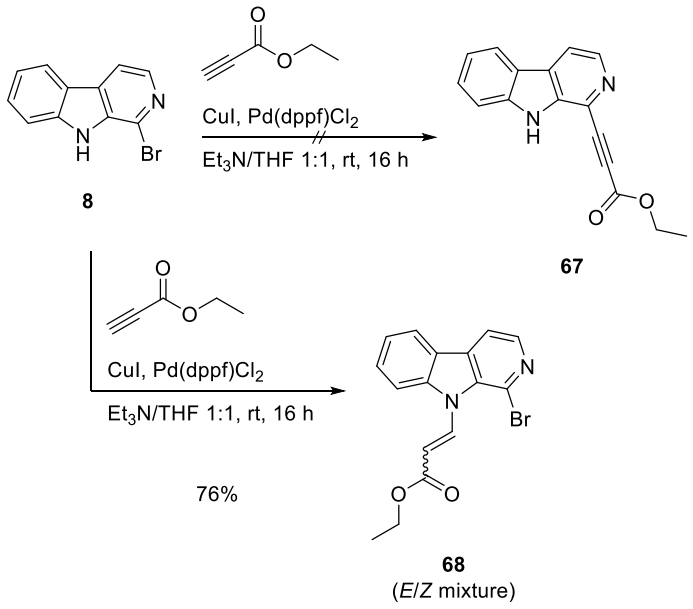

Scheme 33. Attempted synthesis of ethyl propiolate **67** *via* SONOGASHIRA cross-coupling.

To circumvent this, a protective group for *N*-9 of the *β*-carboline should be introduced. The 4-aminoisoxazole **63** is accessible from the *N*-protected ethyl propiolate (**B**) with the same reaction cascade described for the unprotected intermediate plus an additional deprotection step, which could be performed at any stage (**Scheme 34**). It was assumed that the SONOGASHIRA cross-coupling with ethyl propiolate can be achieved with the *N*-9 protected bromide (**A**), which can in turn be synthesized from bromide **8**.

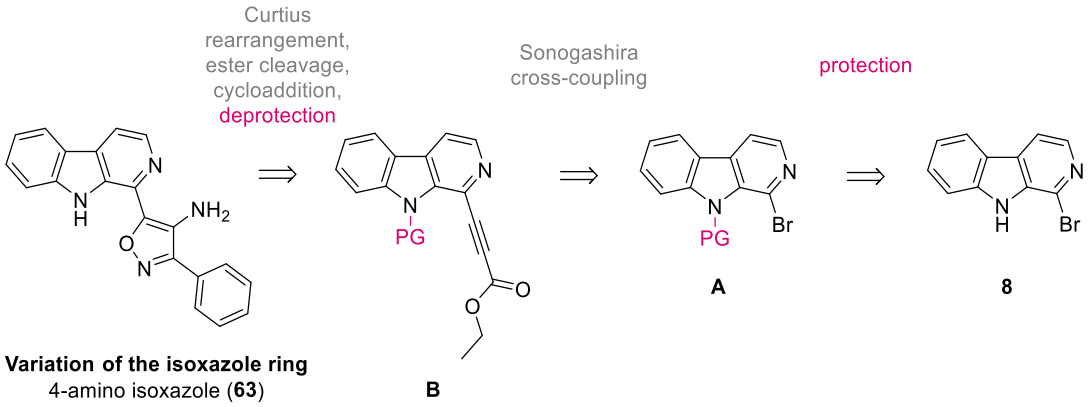

Scheme 34. Retrosynthesis of 4-aminoisoxazole **63** *via* CURTIUS rearrangement with using a *N*-9 protective group (PG).

The protective group of first choice for the indole NH was the “SEM” group, which corresponds to the 2-(trimethylsilyl)ethoxymethyl group. It can be introduced easily by deprotonation of the NH and subsequent nucleophilic substitution of SEM-chloride[137]. The resulting amino acetal derivative is relatively stable and can later on be cleaved by treatment with acids or fluoride ions, whereby the latter is very selective and more common[137]. Additionally, SEM as *N*-protective group was used within the BRACHER group successfully in a variety of related issues[79-80, 83, 91, 128].

Protection of *β*-carboline **8** was achieved in almost quantitative yield under standard conditions (**Scheme 35**). When the protected bromide **69** was then subjected to SONOGASHIRA cross-coupling with ethyl propiolate, there was no conversion to internal alkyne **70** and the starting material was entirely recovered by flash column chromatography. However, also another substance was isolated, which was identified as ether **71**. This finding is consistent with the reports of WINTERFELDT[166] and MCCULLOCH *et al.*[167], who describe that amines, such as triethylamine, mediate the transformation of acetylenic esters to symmetrical ethers like **71**, if only traces of water are present. The SONOGASHIRA cross-coupling is generally performed under inert gas atmosphere and with anhydrous solvents to exclude oxygen and water. Despite this, traces of water were obviously still present as the reagents were not further dried.

Subsequently, an amine-free protocol using cesium carbonate instead was attempted with ethyl propiolate[168]. However, conversion of **69** still remained marginal and internal alkyne **70** was isolated in a yield of less than 5%. Obviously the electron withdrawing ester group directly attached to the alkyne impedes efficient SONOGASHIRA cross-coupling substantially and the aforementioned side-reactions were only of secondary relevance for the failure.

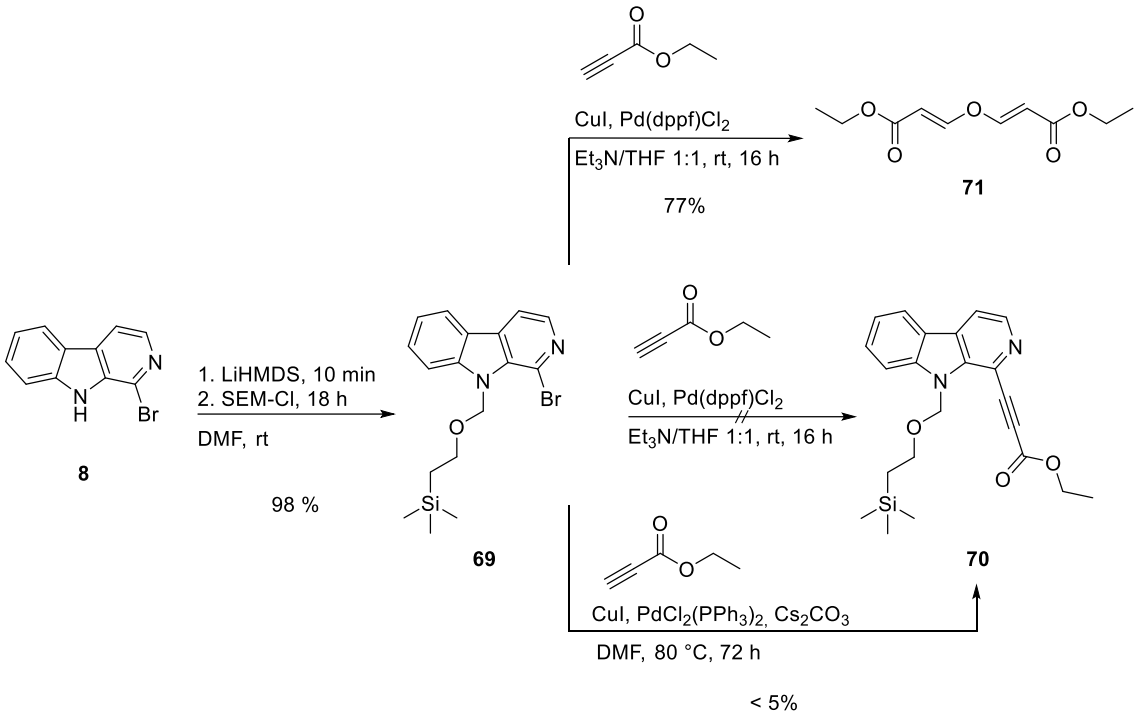

Scheme 35. Synthesis of alkyne **70** *via* SONOGASHIRA cross-coupling of bromide **69** and ethyl propiolate.

Therefore, internal alkyne **70** was pursued by a two-step procedure. SONOGASHIRA cross-coupling of protected bromide **69** and TMS-acetylene followed by desilylation gave terminal alkyne **72** (88% yield over two steps) (**Scheme 36**). The completion of the ethyl propiolate motif was then achieved by deprotonation of the terminal alkyne and subsequent ethoxycarbonylation with ethyl chloroformate[169], and finally propiolate **70** was obtained in satisfying yield (57%).

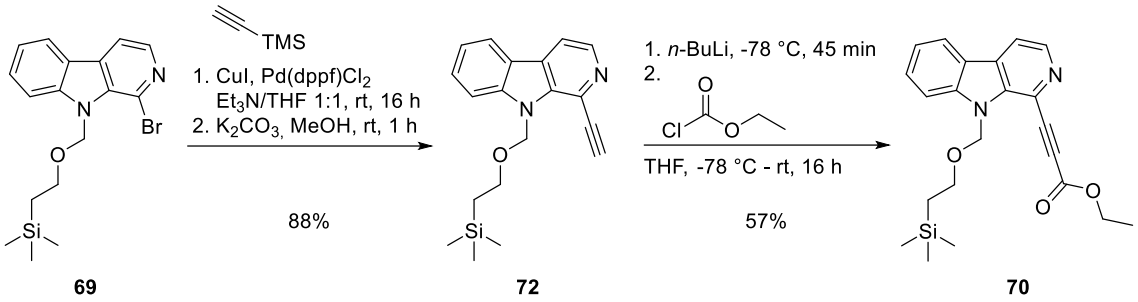

Scheme 36. Synthesis of alkyne **70** *via* SONOGASHIRA cross-coupling of bromide **69** and TMS-acetylene, followed by TMS-cleavage and ethoxycarbonylation.

Next, the 1,3-dipolar cycloaddition was performed to generate isoxazole **73** (**Scheme 37**). The use of benzaldehyde oxime and PIFA was again superior (69% yield) to the procedure with hydroxymoyl chloride **11** and triethylamine (45% yield).

The possibility of forming isoxazole-4- and isoxazole-5-carboxylates was already investigated by HUISGEN *et al*.[170], who described that the methyl ester of propiolic acid gives preferentially isoxazole-5-carboxylate. However, they found that substitution at the terminal alkyne results in a reversed orientation and esters of phenylpropiolic acid give almost selectively isoxazole-4-carboxylates. In accordance with this, only one isomer was isolable here, and its structure was determined as 3,4,5-substituted isoxazole **73** with NMR analysis. The routine experiments had no sufficient informative value to distinguish between the two possible isomers, since no ^{3}J-coupling to the isoxazole C-4' and C-5' are existent. However, a NOESY experiment demonstrated the proximity of the ethyl ester to the 2''-H/6''-H of the phenyl ring. That is only compliant with the illustrated isoxazole-4-carboxylate, as the two residues would not be adjacent in case of the isoxazole-5-carboxylate, for which the substituents at C-4' and C-5' are interchanged. Additionally, this substitution pattern was confirmed retrospectively at several of the following stages when ^{3}J-coupling to the isoxazole C-4' or C-5' was observed, e.g. for aminal **80** or amines **79** and **63**.

Initially, simultaneous ester cleavage and SEM-deprotection was attempted with hydrochloric acid to receive carboxylic acid **66** in the next step. However, the ester remained entirely unaffected and SEM was only removed in traces.

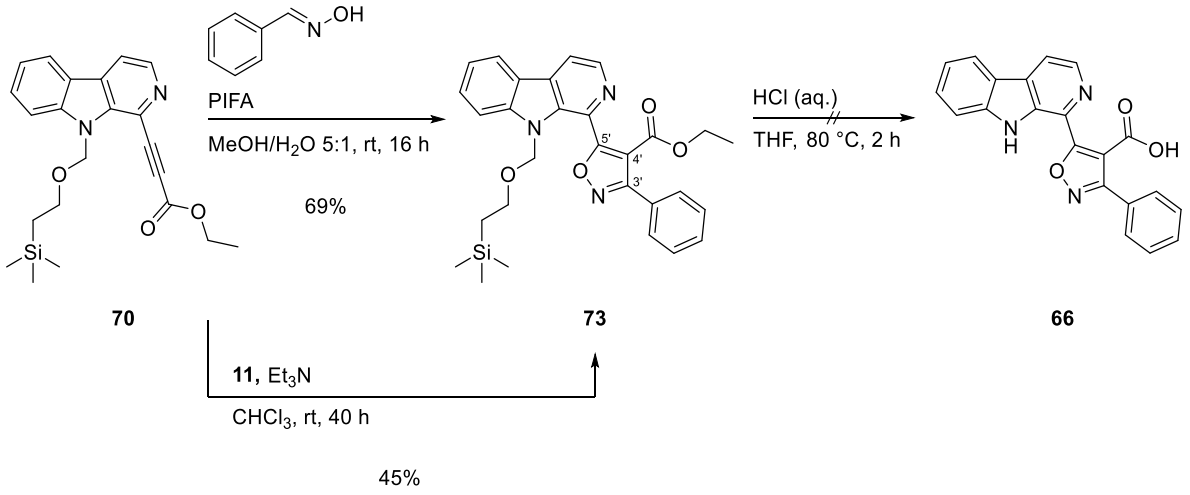

Scheme 37. Synthesis of 4-substituted isoxazole **73** *via* HUISGEN cycloaddition and attempted simultaneous ester cleavage and SEM-deprotection.

Therefore, it was planned to cleave the protective group first and then subsequently hydrolyze the ester under alkaline conditions (**Scheme 38**). SEM-cleavage was much more tedious than expected and not achieved with fluoride ions. Tetra-*n*-butylammonium fluoride (TBAF) was tried solely[91] (**Table 5**, entry 1) and in combination with ethylenediamine as formaldehyde scavenger[137, 171] (**Table 5**, entry 2), but both attempts were effectless. Also hydrogen fluoride, as aqueous HF in THF[79] (**Table 5**, entry 3) and HF in pyridine[172] (**Table 5**, entry 4), did not lead to any conversion. Since the SEM group in **73** is obviously resistant towards fluoride ions, its cleavage was attempted with acids. As the aforementioned treatment with hydrochloric acid achieved deprotection at least in traces, more forcing conditions were chosen (**Table 5**, entry 5). TLC analysis indicated formation of deprotected ester **74**, but also several side products. In contrast to this, the use of trifluoroacetic acid and ammonia[173] was expedient (**Table 5**, entry 6). Although residual starting material was still present, ester **74** was finally found to be the main component. With regards to a deprotection, the yield (69%) surely is mendable. However, the recovered starting material (approx. 20%) could be subjected to the SEM-cleavage again. Next, the ester group was hydrolyzed, but treatment with KOH resulted in the formation of two products. The envisaged carboxylic acid **66** was accompanied by a side product (ratio 1.0:0.15 according to ^{1}H NMR spectrum), which could not be identified at this stage. Due to the very poor solubility of both substances, the crude product was directly subjected to a modified CURTIUS rearrangement.

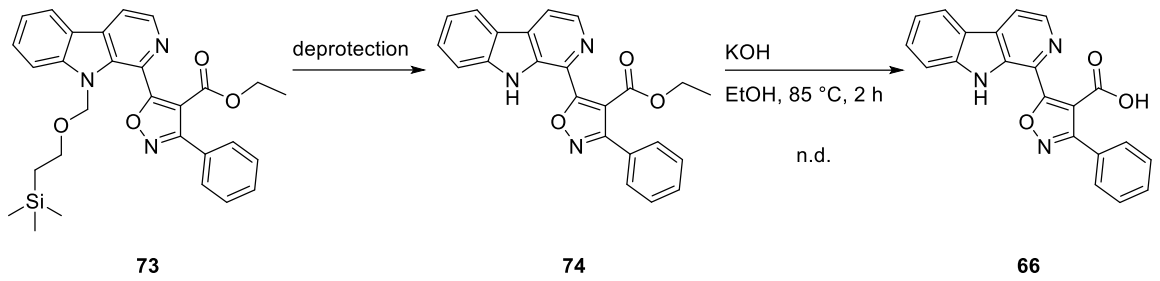

Scheme 38. Synthesis of carboxylic acid **66** from ester **73**.

Table 5. Reaction conditions for the SEM cleavage of **73**.

entry	deprotection	yield
1	TBAF, THF, reflux, 40 h	-
2	TBAF, ethylenediamine, THF, reflux, 16 h	-
3	HF (aq. 40%), THF, rt, 40 h	-
4	HF (70% in pyridine), EtOAc, rt, 40 h	-
5	HCl (aq.), THF/EtOH 1:1, 110 °C, 24 h	n.d.
6	1. TFA, CH_2Cl_2, rt, 16 h; 2. NH_3, rt, 0.5 h	69%

First discovered by CURTIUS[174], the rearrangement of acyl azides to isocyanates and their further transformation was extensively investigated in the past century (**Scheme 39**). The required acyl azides are accessible from carboxylic acids and derivatives, e.g. by treatment of acid chlorides with sodium azide or acyl hydrazides with nitrous acid[175]. Heating then leads to rearrangement with loss of nitrogen and the resulting isocyanates can undergo consecutive reactions with nucleophiles. For example, water gives intermediary carbamic acids, which upon release of carbon dioxide result in primary amines, while alcohols give carbamates[174]. Especially *tert*-butanol can be useful in this context to generate *N*-Boc protected amines, that can then be cleaved at a later stage.

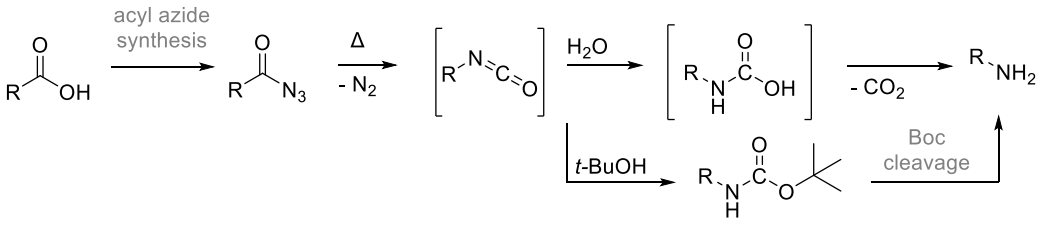

Scheme 39. Overview of the sequence of the CURTIUS rearrangement.

One particularly important simplification of the original approach has been published by SHIOIRI *et al*.[176], who found diphenylphosphoryl azide (DPPA) as azidation reagent (**Figure**

13). With their modified CURTIUS rearrangement, carboxylic acids are directly transformed to the *N*-Boc protected amines. Hence, isolation of the rather unstable acyl azides becomes redundant with this one-pot reaction. From a mechanistic point of view, DPPA generates the acyl azide in the presence of triethylamine *in situ* and *tert*-butanol functions as both, solvent and nucleophile to attack the isocyanate.

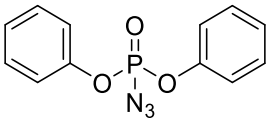

Figure 13. Structure of diphenylphosphoryl azide (DPPA), which can be used for the modified CURTIUS rearrangement[176].

Following the procedure of REITER[177], the modified CURTIUS rearrangement of carboxylic acid **66** however, did not lead to the formation of envisaged *N*-Boc protected amino isoxazole **75** (**Scheme 40**). TLC analysis indicated complete conversion to the former side product of **66**. HRMS suggested formal dehydration of **66** and ^{1}H NMR showed signals for eleven aromatic protons, but no NH signal. Presumably, the intermediary acyl azide reacts not as CURTIUS precursor, but as activated carboxylic acid. Promoted by the close proximity, the indole NH then undergoes intramolecular amide coupling to lactam **76**. This fits with the observation as side product in the alkaline ester cleavage of **74** at elevated temperatures. Obviously, also the ethyl ester is activated to some extent towards the amidation. Due to the extremely poor solubility of the obtained substance, it was not possible to run ^{13}C and 2D NMR experiments to verify the postulated structure. However, treatment of carboxylic acid **66** with the coupling reagent HBTU resulted in formation of the same substance according to TLC and MS analysis and confirmed the hypothesis.

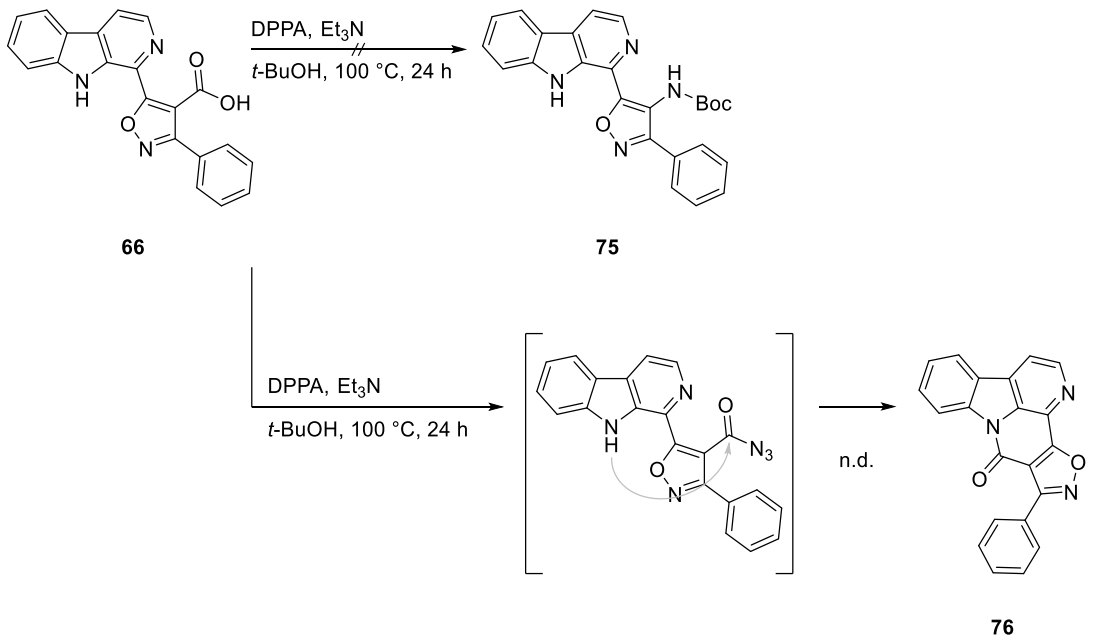

Scheme 40. Attempted synthesis of *N*-Boc amine **75** *via* modified CURTIUS rearrangement. (**76** was not characterized due to extremely poor solubility.)

This intramolecular cyclization is obviously preventable, if the *N*-9 protective group is cleaved from amines (**B**) – successively or simultaneously with Boc – only after the CURTIUS rearrangement (**Scheme 41**). Therefore, *N*-9 protected carboxylic acids (**A**) are used, whereby SEM is again the first choice.

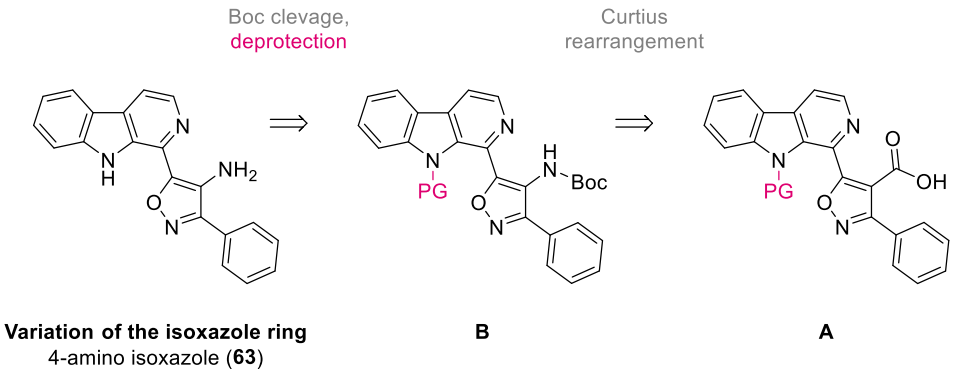

Scheme 41. Retrosynthesis of 4-aminoisoxazole **63** *via* CURTIUS rearrangement of *N*-9 protected carboxylic acids.

Alkaline hydrolysis of *N*-SEM protected ester **73** gave carboxylic acid **77** (96% yield), which was also subjected to the modified CURTIUS rearrangement[177] (**Scheme 42**). TLC analysis showed again complete conversion and the product was this time identified as *N*-Boc aminoisoxazole **78** with ASAP analysis. The crude product, obtained from aqueous acidic and basic workup, was directly used for the next step.

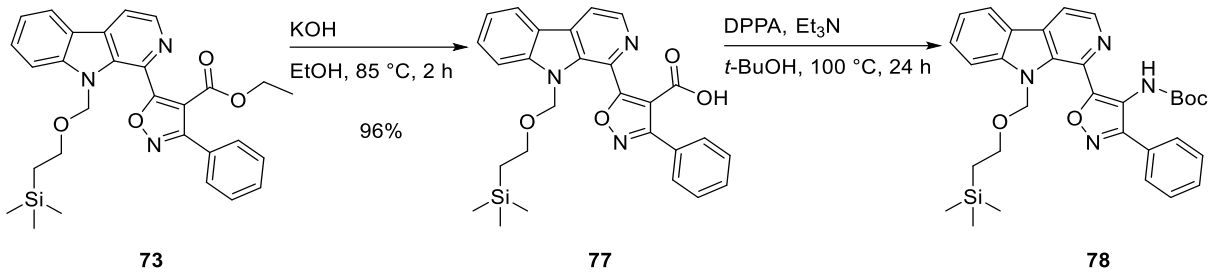

Scheme 42. Synthesis of *N*-Boc amine **78** from ester **73** *via* ester hydrolysis and CURTIUS rearrangement.

Boc cleavage was attempted with HCl in 1,4-dioxane (**Scheme 43**). However, the solubility of *N*-Boc amine **78** was limited and after 16 h, ASAP analysis indicated only marginal conversion resulting in traces of amine **79** and another hitherto unknown side product. To improve the solubility and accelerate the reaction, the mixture was diluted with ethanol and stirred at elevated temperature for 3 h. By doing so, complete consumption of the starting material was achieved and the former side product obtained as a sole product. However, MS as well as NMR analysis revealed that it was not amine **63**, but cyclic aminal **80**.

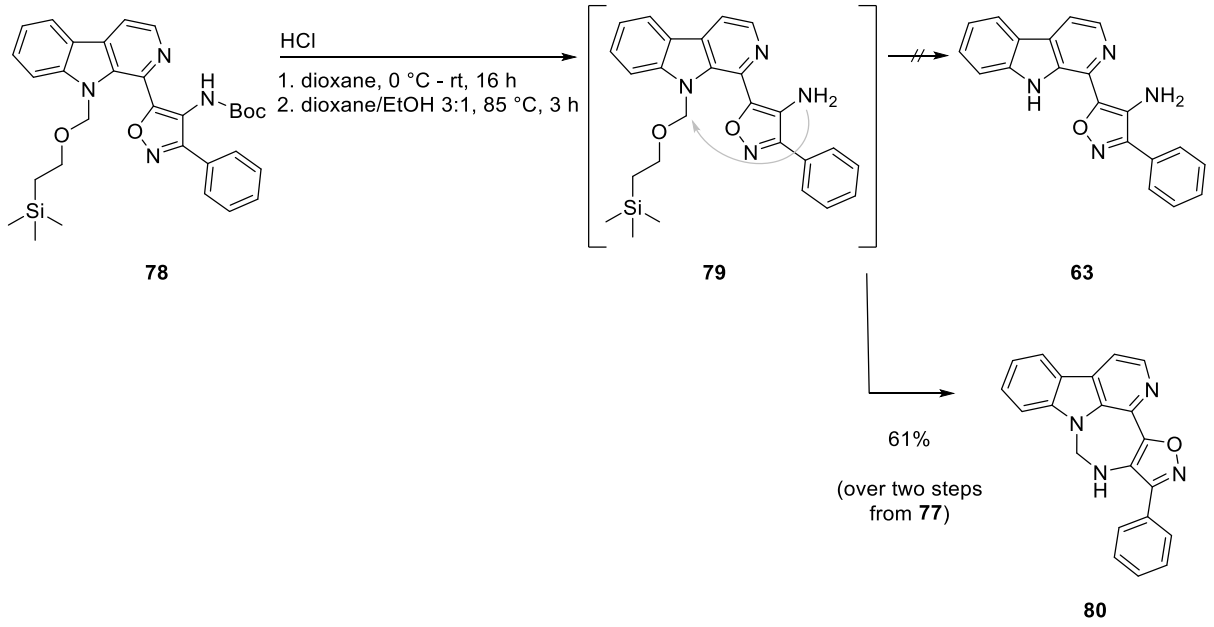

Scheme 43. Synthesis of cyclic aminal **80** from *N*-Boc amine **78**.

While almost all signals of the SEM group were missing in the ^{1}H NMR spectrum, the *N*-9 was obviously still substituted, as no downfield singlet for the indole NH was present. Besides signals for eleven aromatic protons, a doublet at 5.36 ppm (2H, J = 6.2 Hz) and a triplet at

4.39 ppm (1H, *J* = 6.2 Hz) were observed. The latter of these neighbouring protons was shown to be bound to a heteroatom in the HSQC spectrum and HMQC spectrum demonstrated ^3J-coupling to the isoxazole C-3' and C-5'. In contrast, the CH_2 group was shown to couple over three bonds with C-4' of the isoxazole and C-8a and C-9a of the *β*-carboline. With all these observations taken into consideration, the only plausible explanation is the formation of an aminal between *N*-9 and the 4'-amino group with the "formaldehyde unit" of SEM.

Although unexpected at first, several notices support this hypothesis. Obviously, Boc cleavage occurs initially. This was confirmed with closer reaction monitoring by MS analysis, which demonstrated that over time only starting material **78**, amine **79** and aminal **80**, but no fully SEM deprotected intermediate, were present. However, SEM deprotection with acids generally follows the mechanism of acetal cleavage. The ether is protonated and elimination of an alcohol then causes the formation of an iminium ion. Instead of water, which results in the formation of a hemiaminal and subsequent hydrolysis to formaldehyde, also other nucleophiles can attack this intermediate. In the case of **79**, this is obviously the 4'-amino group, which causes the formation of aminal **80**. This intramolecular cyclisation seems to be highly favoured due to the spatial proximity of the 4'-amino group and the generally limited basicity of the 4-aminoisoxazole moiety, for which a pK_a value of approx. 1.5 (calculated with ACD/Labs)[178-179] explains the presence of sufficient amounts of unprotonated species.
In accordance with this, BUSACCA *et al*.[180] made a similar observation, when they investigated the cleavage of *N*-SEM *β*-carbolines (**Scheme 44**). They found that deprotection with hydrochloric acid in (deuterated) ethanol, was accompanied by the formation of a (deuterated) hydroxyethyl ether, which can be explained by the reaction of (deuterated) ethanol with the intermediary iminium species.

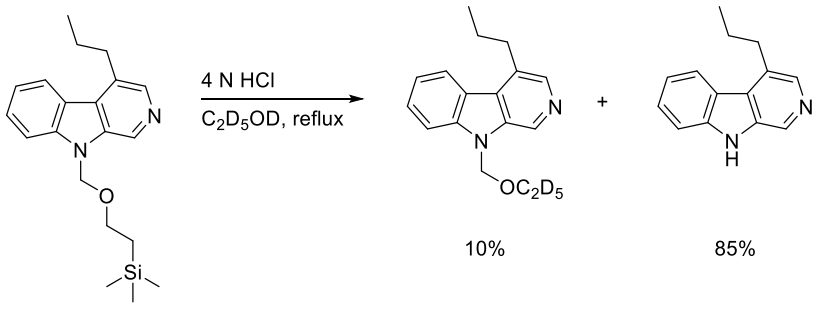

Scheme 44. According to BUSACCA *et al.*[180], SEM cleavage with hydrochloric acid in deuterated ethanol gives deuterated hydroxyethyl ether besides the unprotected species.

Further attempts were carried out. However, repetition of the cleavage of *N*-Boc amine **78** with aqueous hydrochloric acid in ethanol resulted again solely in the formation of intermediary

amine **79** and aminal **80** according to MS. Traces of both were even found, when *N*-Boc amine **78** was treated with TBAF and ethylenediamine in THF at 60 °C, although mainly starting material was observed after 48 h. Obviously, the 4-amino group is really prone to undergo this intramolecular cyclization.

As cyclic aminals could also be hydrolysed in acidic aqueous solution in some cases[181-182], the cleavage was also attempted for **80**. However, no conversion was achieved with hydrochloric acid in a mixture of ethanol and water (**Table 6**, entry 1) and formic acid (**Table 6**, entry 2). Sulfuric acid[183], in contrast, led to decomposition of the starting material (**Table 6**, entry 3). Additionally, the SEM deprotection protocol with trifluoroacetic acid and ammonia was tried, but again aminal **80** remained completely unaffected (**Table 6**, entry 4).

Table 6. Attempted aminal hydrolysis of **80**.

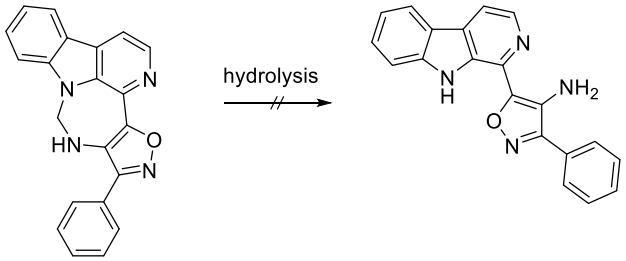

80 **63**

entry	hydrolysis	yield
1	HCl, EtOH/H_2O 1:1, 100 °C, 16 h	-
2	HCOOC, rt, 4 d, then 105 °C, 8 h	-
3	H_2SO_4, H_2O, rt – 100 °C, 24 h	decomposition
4	1. TFA, CH_2Cl_2, rt, 16 h; 2. NH_3, rt, 0.5 h	-

Since SEM turned out not to be ideal due to its ability to form a cyclic aminal and its resistivity regarding the cleavage, other protective groups were investigated. They should be attachable to ester **74** and withstand the subsequent ester hydrolysis.

N-Boc is known as a rather labile protective group, which is usually deprotected with acids[137]. Within the synthesis of amine **63**, it was particularly interesting as a double *N*-Boc protected intermediate amine was very likely to be easily cleavable. Its lability towards alkaline conditions is described, but less extensively investigated[137].

As a patent[184] mentioned the selective methyl ester cleavage besides a *N*-9 Boc protected *β*-carboline, this approach was attempted. Boc protection[185] of *β*-carboline **74** with Boc anhydride gave ester **81** (79% yield) (**Scheme 45**). Initially, the subsequent ester cleavage was attempted with 1.0 eq of an aqueous potassium hydroxide solution in ethanol at room

temperature. However, after 1 h no conversion at all has been achieved. When the temperature was raised to 60 °C and the reaction mixture stirred for further 1 h, TLC and MS analysis revealed the formation of two products, besides large amounts of residual starting material: envisaged carboxylic acid **82**, but also additionally Boc cleaved product **66**. Although this identified Boc as an unsuitable protective group regarding the synthesis of amino isoxazole **63**, the use of excess potassium hydroxide allowed the preparation of analytically pure carboxylic acid **66** (95% yield), which was not achieved from ester **74** directly but also intended to be tested as CLK1 inhibitor.

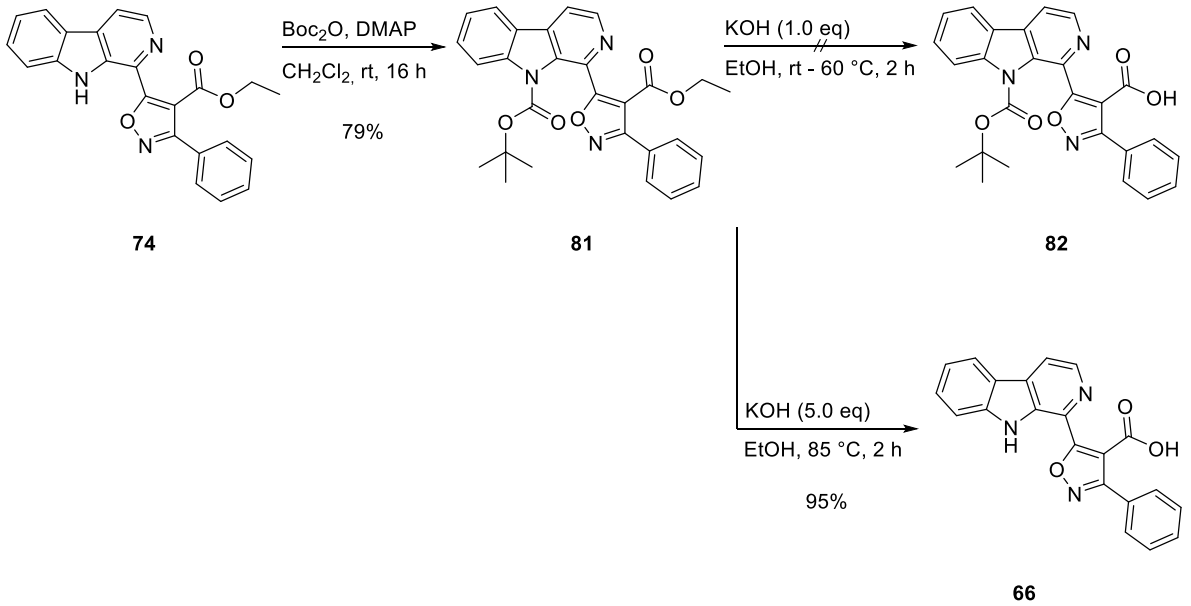

Scheme 45. Synthesis of carboxylic acid **66** from *N*-Boc substituted ester **81**.

Another class of protective groups, which would definitely withstand the ester cleavage, contains *N*-benzyl derivatives, such as benzyl itself or *p*-methyoxybenzyl. As it was assumed that their great stability could again cause problems, when it comes to deprotection, preliminary tests were conducted and are briefly outlined.

1-Bromo-*β*-carboline (**8**) was used as test molecule, since it is substituted at C-1 and was available in large quantities. NH-Substitution[186] was achieved with sodium hydride and the respective benzyl halides (**Scheme 46**). The reaction with benzyl bromide gave *N*-benzyl *β*-carboline **83** (60% yield) and the reaction with 4-methoxybenzyl chloride gave *N*-PMB *β*-carboline **84** (85% yield).

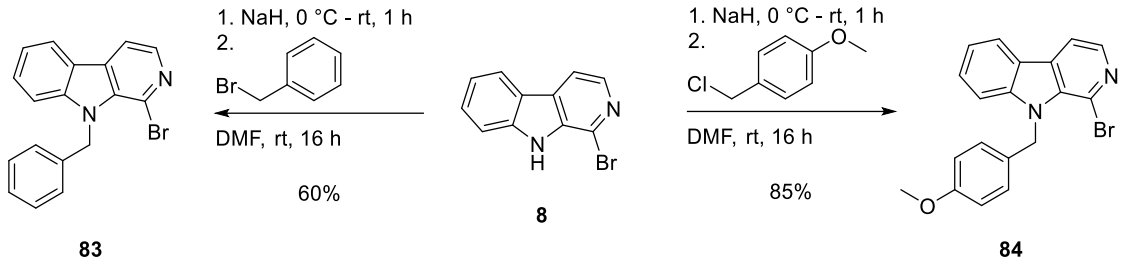

Scheme 46. Synthesis of *N*-benzyl *β*-carboline **83** and *N*-PMB *β*-carboline **84**.

Next, suitable conditions for the cleavage were examined. The conducted reactions were monitored by TLC and MS analysis, respectively. Debenzylation was attempted first, but as hydrogenolysis was not an option for the envisaged intermediate isoxazole, only other, less widely used methods were tried. However, aluminum chloride in anisole[187] (**Table 7**, entry 1) as well as potassium *tert*-butoxide and oxygen in DMSO[188] (**Table 7**, entry 2) did not lead to conversion of *N*-benzyl derivative **83**, even after much prolonged reaction times. PMB cleavage of **84** was attempted with DDQ in toluene[189], but also not achieved with this procedure (**Table 7**, entry 3). Conversely, the use of trifluoroacetic acid in anisole was expedient[190]. When the reaction was run at elevated temperature, encouragingly, the formation of deprotected *β*-carboline **8** was observed after 4 h. However, after further 8 h the reaction was still not complete and the starting material/product ratio was only approx. 1:1 (**Table 7**, entry 4). When, in contrast, the reaction was run at room temperature with supplementary sulfuric acid[191], already after 2 h full conversion had taken place (**Table 7**, entry 5).

Table 7. Attempted deprotection of *N*-benzyl *β*-carbolines **83** and **84**.

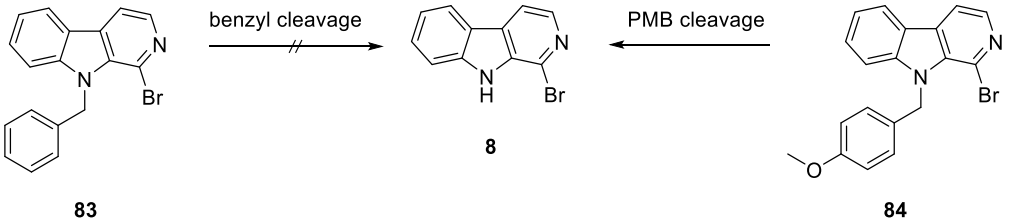

entry	starting material	cleavage conditions	observation
1	**83**	$AlCl_3$, anisole, rt, 7 d	only **83**
2	**83**	*t*BuOK, O_2, DMSO, rt, 4 d	only **83**
3	**84**	DDQ, toluene, 115 °C, 16 h	only **84**
4	**84**	TFA, anisole, 135 °C, 12 h	**84**/**8** (ratio 1:1)
5	**84**	TFA, H_2SO_4, anisole, rt, 2 h	only **8**

Since the PMB group seemed to be a promising protective group, it should next be applied to the synthesis of amine **63**. PMB was introduced onto **74** *via* NH-substitution with sodium hydride and 4-methoxybenzyl chloride (**Scheme 47**). While the reaction seemed to had proceeded smoothly at first sight, two substances with very similar chromatographic behavior were found to be present. ^{1}H NMR and MS analysis were used to identify these as ethyl ester **85** and PMB ester **86**. As the 4-methoxybenzyl chloride used for this reaction had been stored in the fridge for several years already, it was presumably partially hydrolyzed and the resulting alcohol then participated in transesterification. As both esters lead to the same envisaged carboxylic acid, the obtained mixture was subjected to alkaline ester cleavage and gave **87** (69% yield over two steps).

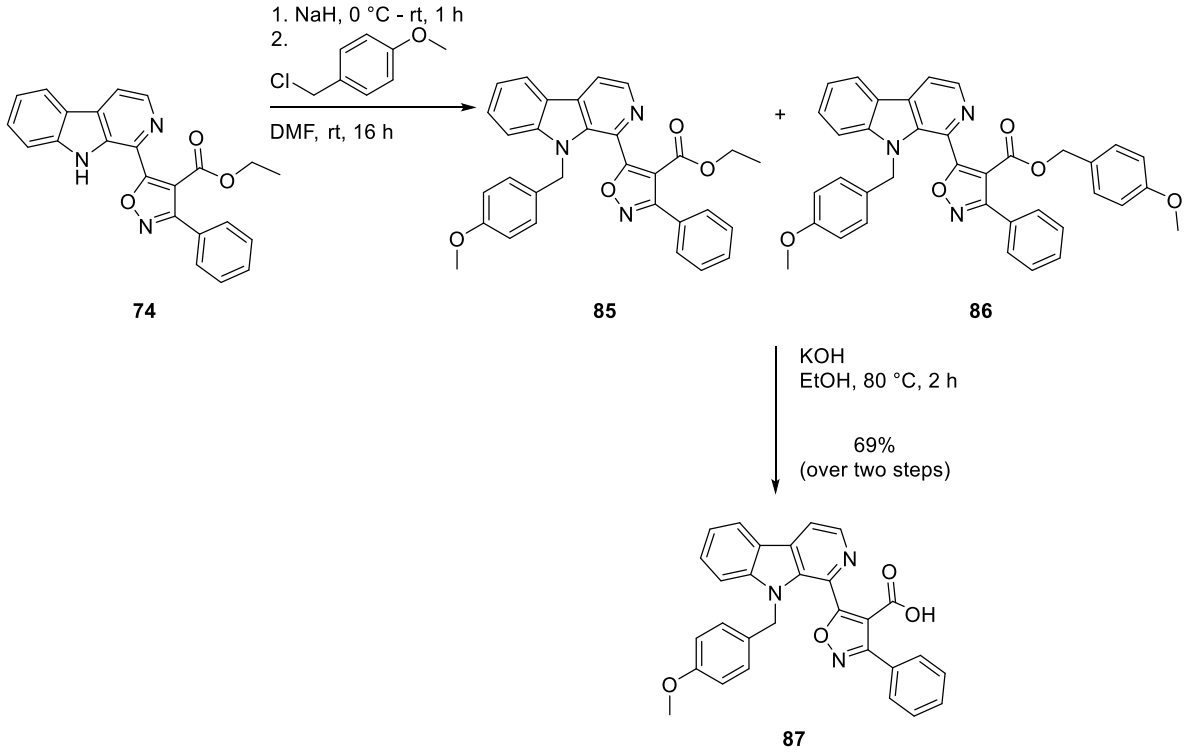

Scheme 47. Synthesis of carboxylic acid **87** *via* *N*-substitution and alkaline ester hydrolysis.

The modified CURTIUS rearrangement of carboxylic acid **87** in *tert*-butanol gave *N*-Boc protected amine **88** (86% yield), which should then be deprotected (**Scheme 48**). However, the treatment with trifluoroacetic acid and sulfuric acid in anisole did not result in the formation of amino isoxazole **63**. TLC analysis indicated immediate decomposition, as already after 5 min no defined substance was observable anymore. When in contrast only trifluoroacetic acid was used, the reaction progress could be monitored with MS and TLC analysis. After 15 min at room temperature, the major proportion of starting material **88** was solely *N*-Boc

cleaved to amine **89**. When the temperature was raised, complete conversion to another substance was achieved after 1 h, but it turned out to be again not the desired amino isoxazole **63**. PMB deprotection has not proceeded, but amidation of the amino group with trifluoroacetic acid resulted in amide **90** according to MS analysis. The reaction mixture was stirred for further 17 h under reflux, but the PMB group remained rather unchanged and only traces of deprotected trifluoroacetamide **91** were found.

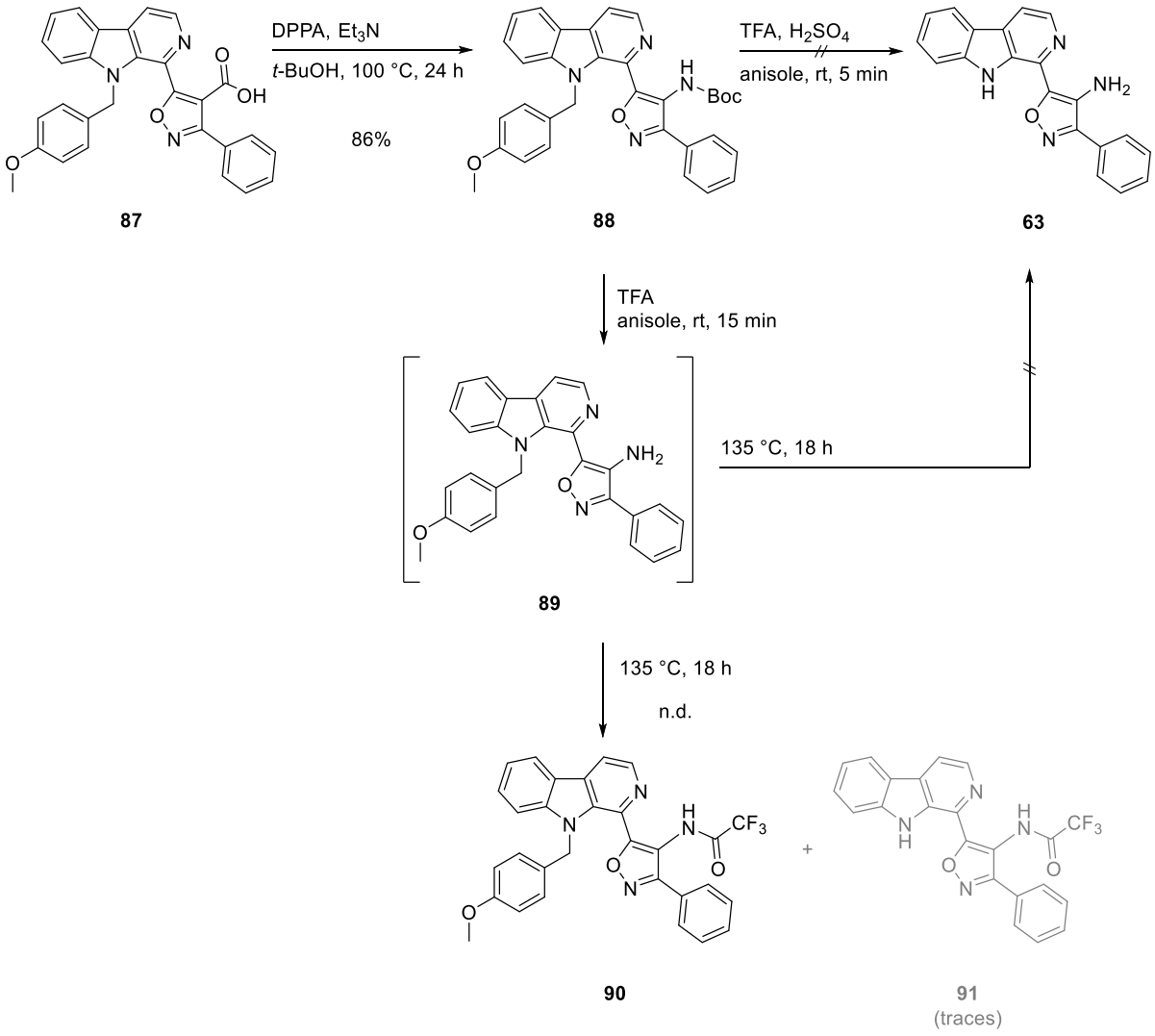

Scheme 48. Attempted synthesis of amino isoxazole **63** from *N*-9 PMB protected carboxylic acid **87**.

Although the failure of this approach was another setback, it opened a new perspective. The use of a protective group for the 4-aminoisoxazole (**B**), which is cleaved after the *N*-9 protective group (**A**), can also circumvent the described undesired reactions, such as aminal or lactam formation (**Scheme 49**). The findings from the aforementioned attempts to synthesize amino

isoxazole **63** already suggest the most expedient strategy: to use SEM as *N*-9 protective group and mask the 4-aminoisoxazole as trifluoroacetamide.

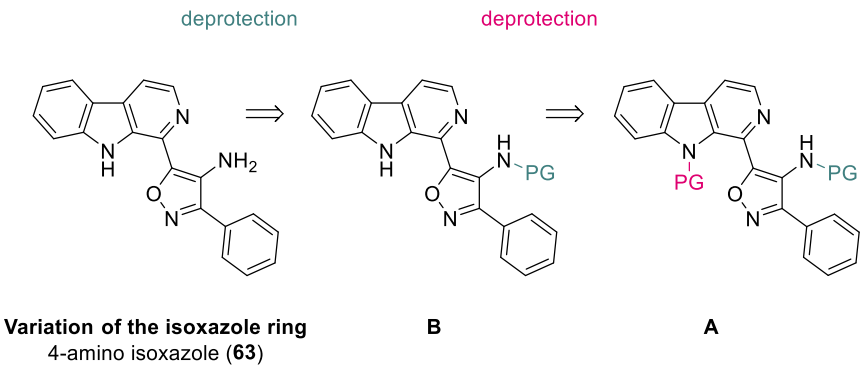

Scheme 49. Retrosynthesis of 4-aminoisoxazole **63** *via* CURTIUS rearrangement using *N*-9 and 4-NH_2 protective groups.

To synthesize the intended intermediate, a slightly modified procedure[192] was used this time for the modified CURTIUS rearrangement of carboxylic acid **77** (**Scheme 50**). Instead of *tert*-butanol, which directly attacks the intermediary isocyanate **92** to form a carbamate, THF was used as inert solvent. Subsequent treatment with water then gave primary amine **79** (68% yield).

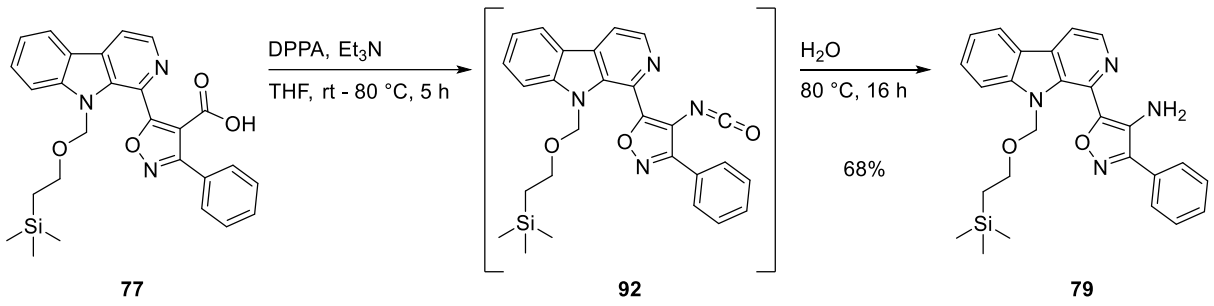

Scheme 50. Synthesis of 4-aminoisoxazole **79** from carboxylic acid **77**.

Although the masking of amines as trifluoroacetamides is a rather unusual strategy, this protective group perfectly meets the requirements. It decreases the nucleophilicity of the amino group, which will prevent formation of a cyclic aminal in the course of the SEM deprotection. Additionally, it withstands the treatment with trifluoroacetic acid, but can in the following be removed easily with other acids or under basic conditions[137].

Introduction with trifluoroacetic anhydride and 4-(dimethylamino)pyridine (DMAP)[193] gave amide **93** (84% yield) (**Scheme 51**). Subsequent *N*-9 SEM cleavage with the established method using TFA and ammonia then resulted in β-carboline **91** (66% yield).

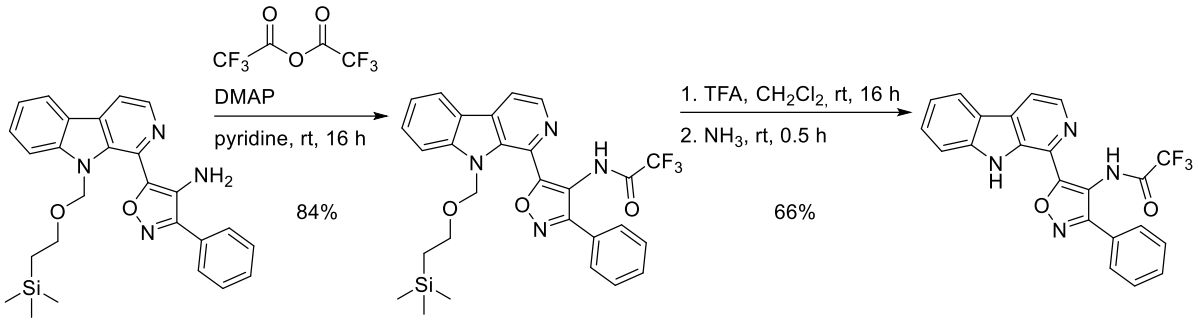

Scheme 51. Synthesis of trifluoroacetamide **91**.

The last step pending was the trifluoroacetamide cleavage. As trifluoroacetamides are known to be susceptible to basic conditions, K_2CO_3 in methanol/water under reflux[194] was tried first, but gave only traces of the envisaged deprotected amine **63** (**Table 8**, entry 1). Also ammonia in refluxing methanol[194] was not expedient. After 3 h, the conversion was insufficient, but the product was clearly observable with TLC analysis (**Table 8**, entry 2). However, when the reaction time was prolonged to 24 h, no defined substance was present anymore, indicating again decomposition (**Table 8**, entry 3). Also procedures for acid mediated cleavage of trifluoroacetamides are found in literature. For example, KING *et al.*[195] used hydrochloric acid in methanol at 65 °C, after basic conditions had failed. As other attempts to generate amine **63** also led to degradation (aminal cleavage and PMB cleavage with sulfuric acid), it is conceivable that the envisaged product maybe has actually formed, but is rather unstable. Therefore, the acidic cleavage was conducted, but milder conditions were chosen. When amide **91** was treated with anhydrous hydrochloric acid in methanol at room temperature, the formation of amine **63** was again observed with TLC analysis after 2 h. This time, prolonging the reaction time to 16 h did not lead to decomposition, but complete conversion. Finally, with this procedure synthesis of amine **63** was achieved (69% yield) (**Table 8**, entry 4).

Table 8. Synthesis of amine **63** from trifluoroacetamide **91**.

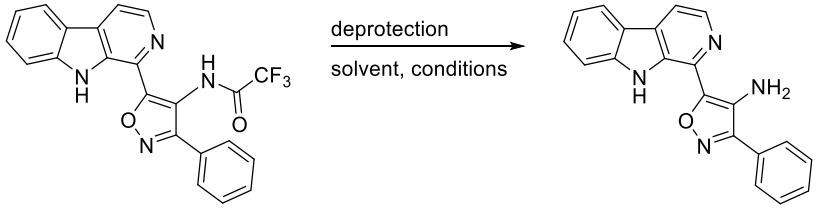

WEA-148 **WEA-151**

entry	deprotection	solvent	conditions	yield
1	K_2CO_3	MeOH/H_2O 15:1	70 °C, 16 h	traces
2	NH_3 (aq.)	MeOH	70 °C, 3 h	traces
3	NH_3 (aq.)	MeOH	70 °C, 24 h	decomposition
4	HCl	MeOH	rt, 16 h	69%

3.3 Variations of the *β*-carboline nucleus

3.3.1 *N*-9 substituted *β*-carbolines

As already mentioned (in chapter 3.2), the NH group of the *β*-carboline is involved in stabilizing the almost planar orientation of the ligand by an intramolecular hydrogen bond (*cf.* **Figure 6**). In contrast to the isoxazole variations, for which it was taken into account that the formation of this hydrogen bond is somehow allowed, the NH was now to be substituted to intentionally impede this, in order to gain deeper insight into the SAR. Thus, in a first step simply a methyl group should be introduced, which could promote rotation of the single bond and result in another orientation and therefore could or could not lead to a change of affinity and activity. Additionally, WURZLBAUER has shown, that propargyl and cyanomethyl residues at *N*-9 of *β*-carbolines can be beneficial regarding the kinase-inhibitory activity towards CLK1 and the related DYRKs, when she investigated harmine analogues[82]. Although no crystal structure data was available for these at the active site of the CLK1, it should be examined, if these modifications eventually improve the activity of lead structure **1**.

The envisaged *N*-9 alkylated analogues of lead structure **1** can be generated thereof *via* nucleophilic substitution (**Scheme 52**). Hence, the *β*-carboline is deprotonated first and subsequently treated with the respective alkyl halide.

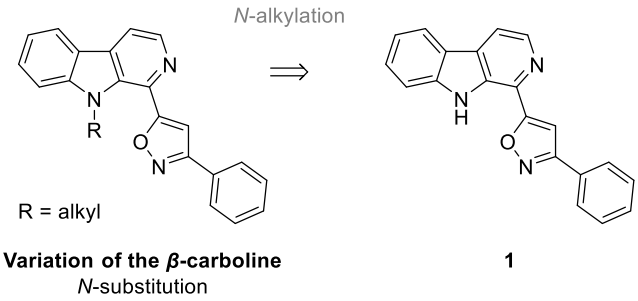

Scheme 52. Retrosynthesis of *N*-9 alkylated analogues.

As described for the *N*-9 benzyl and PMB protection[186], the *N*-9 substitution of lead structure **1** was achieved with sodium hydride and selected alkyl halides (**Scheme 53**). While the reactions with iodomethane and propargyl bromide proceeded smoothly to *N*-methyl derivative **94** (59% yield) and *N*-propargyl derivative **95** (75% yield), only limited conversion was observed with bromoacetonitrile at room temperature after 16 h. Also further addition of the alkyl halide and elevated temperature[82] did not lead to full consumption of the starting material. This indicated insufficient deprotonation with sodium hydride in the first step, which could be due to degradation of the reagent by residual water in this particular reaction mixture.

Nevertheless, the reaction was not repeated, since *N*-cyanomethyl derivative **96** was obtained in a sufficient yield (32%) after separation from starting material **1** (approx. 40%).

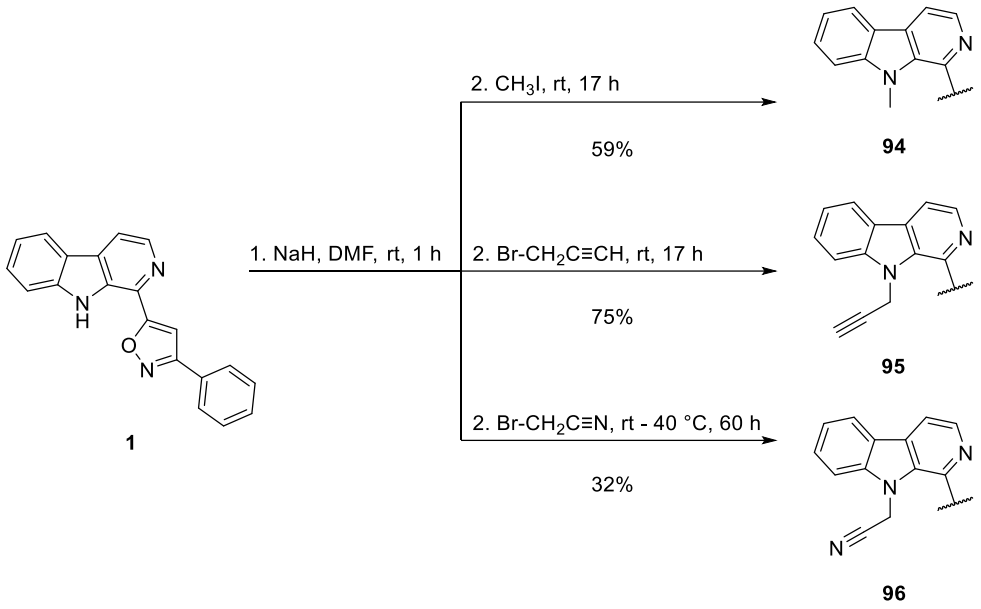

Scheme 53. Synthesis of *N*-alkyl derivatives **94**, **95** and **96** from lead structure **1**.

3.3.2 Ring A substituted *β*-carbolines

Next, substitution at ring A of the *β*-carboline moiety was to be investigated. Although the binding pocket is relatively restricted “upwards” (*cf.* **Figure 9**), this also exhibits short distances between the ligand and protein (**Figure 14**). Substitution in 3-position seemed especially promising, since the carbonyl oxygen of GLU 242 can act as hydrogen bond acceptor. Therefore, donor groups such as OH and NH_2 should be introduced onto the *β*-carboline directly or with a C-1 spacer.

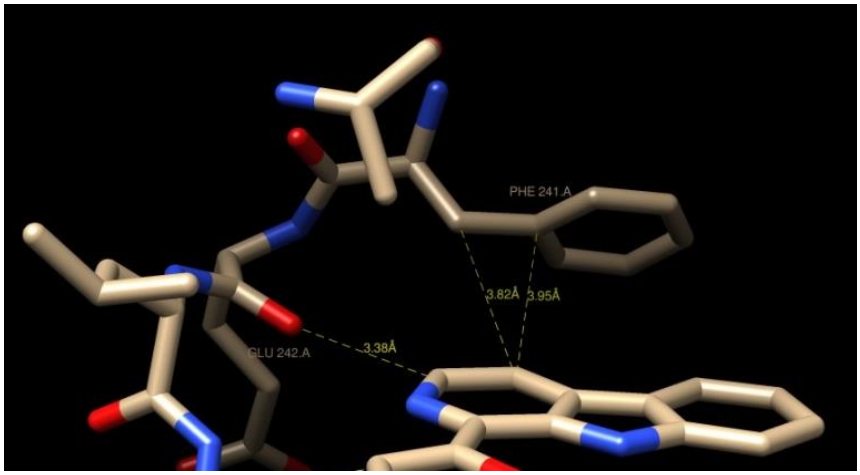

Figure 14. Detailed short distances (indicated by yellow lines) between ring A of the *β*-carboline moiety of lead structure **1** and CLK1.

Since only very recently new chemistry was developed within the BRACHER group to introduce residues on the 3- and 4-positions of *β*-carbolines[128, 196-197], a 4-dimethylaminocarbonyl derivative was additionally envisaged. Although there are no donor groups present in the protein to form a hydrogen bond with the carbonyl oxygen, the methyl groups could participate in hydrophobic interactions.

3.3.2.1 Synthesis of 3-substituted analogues

The central building block to introduce donor groups onto C-3 of the *β*-carboline moiety is the corresponding 3-methoxycarbonyl-*β*-carboline **97** (**Scheme 54**). Hydrolysis of the ester function gives carboxylic acid **98** and subsequent CURTIUS rearrangement aminopyridine **99**. Further envisaged analogues with a slightly greater distance between the pyridine ring and the donor group are carboxamide **100** and hydroxymethyl compound **101**, which are accessible respectively *via* amidation or reduction of ester **97**. A very established approach towards the synthesis of 3-alkoxycarbonyl substituted *β*-carbolines is the PICTET-SPENGLER reaction. Likewise to tryptamine, also tryptophan esters can participate in this condensation and ring closure with aldehydes, such as **53**, and give the 3-substituted *β*-carbolines after dehydrogenation.

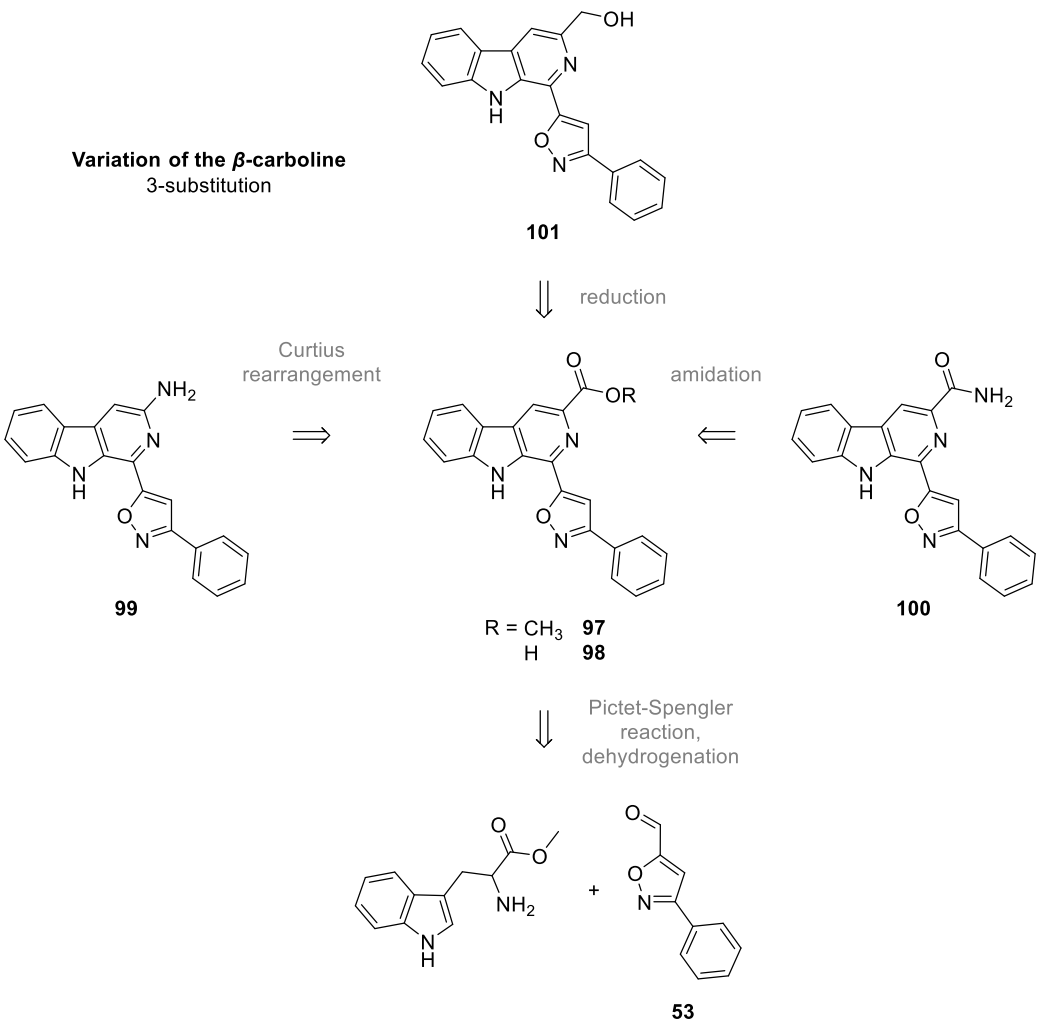

Scheme 54. Retrosynthesis of 3-substituted analogues from tryptophan esters.

In contrast to tryptamine, the PICTET-SPENGLER reaction of tryptophan derivatives gives rise to diastereomeric mixtures of 1,2,3,4-tetrahydro-*β*-carbolines. While the configuration of the later C-3 is preserved from the amino acid, the planar iminium intermediate allows the formation of both, *cis* and *trans* configured products[198]. This is, however, irrelevant for syntheses like the following, when actually the fully aromatic *β*-carboline is pursued.

Following the method of a patent[199], which described the synthesis of an isomer of the probably most prominent tetrahydro-*β*-carboline, tadalafil, L-tryptophan methyl ester hydrochloride was reacted with aldehyde **53** (**Scheme 55**). Reaction monitoring with TLC-MS analysis revealed the complete conversion of both starting materials to three new components. One was fluorescing (at 365 nm excitation), but only present in traces. According to MS analysis, this referred to *β*-carboline **97**. The two others showed very similar chromatographic behaviour and the same *m/z*, which matched the two diastereomeric tetrahydro-*β*-carbolines **102**. These components were not separated or even isolated, but directly oxidized with potassium permanganate[200]. With this, 3-methoxycarbonyl-*β*-carboline **97** could be received

in good yield (59%) with a one-pot reaction. Purification was accomplished with two simple filtration steps, exploiting the variable solubility in organic solvents, which was also fundamental for the following reactions. While its good solubility in methylene chloride allowed the separation of manganese dioxide, the removal of other impurities was achieved by resuspension in methanol, in which **97** was only very poorly soluble and obtained as precipitate.

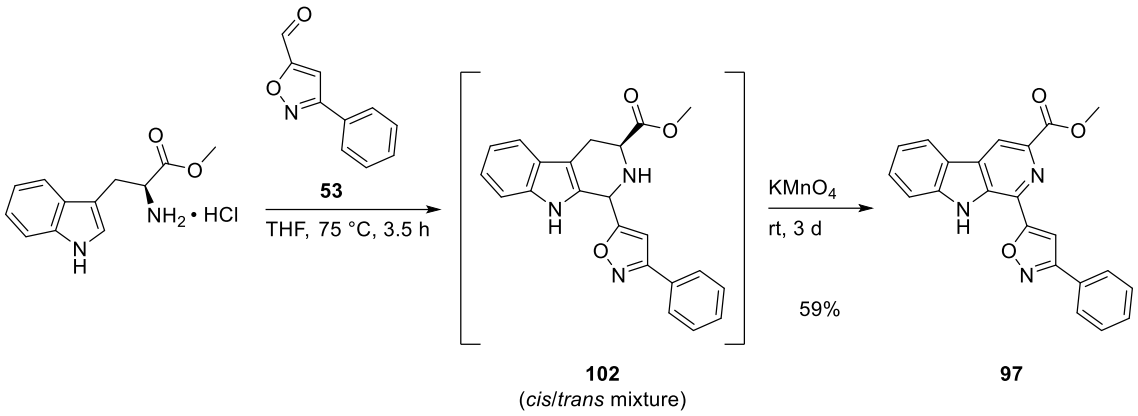

Scheme 55. Synthesis of *β*-carboline **97** *via* PICTET-SPENGLER reaction and dehydrogenation.

Hydrolysis of ester **97** was achieved from a suspension in THF with aqueous potassium hydroxide solution and gave carboxylic acid **98** in nearly quantitative yield (**Scheme 56**). Subsequent modified CURTIUS rearrangement using DPPA and generation of the respective amine by the addition of water[192], was a straight forward approach to 3-amino-*β*-carboline **99** (46% yield).

In contrast, amide coupling[201] of carboxylic acid **98** with ammonium carbonate failed and only the starting material was recovered. However, aminolysis of ester **97** was successful, resulting in the desired amide **100** in 80% yield. Initially, aqueous ammonia solution was used, but gave only traces of amide **100** and mainly carboxylic acid **98** (after 8 h at 100 °C). When ammonia in methanol was used instead, the desired conversion proceeded very well. Due to limited solubility of both, starting material and product in methanol, the reaction mixture permanently remained a suspension. Hence, traces of the residual ester **97** could be removed by washing the precipitate with methylene chloride, giving pure amide **100**.

Reduction of ester functions to the corresponding hydroxymethyl analogues are most commonly performed with lithium aluminum hydride in ethereal solvents. However, the very limited solubility of ester **97** in THF prompted the use of sodium borohydride. “Activated” with calcium chloride, its scope is significantly widened[202] and it can be used in a mixture of ethanol and methylene chloride[203] and thus gave alcohol **101** (87% yield).

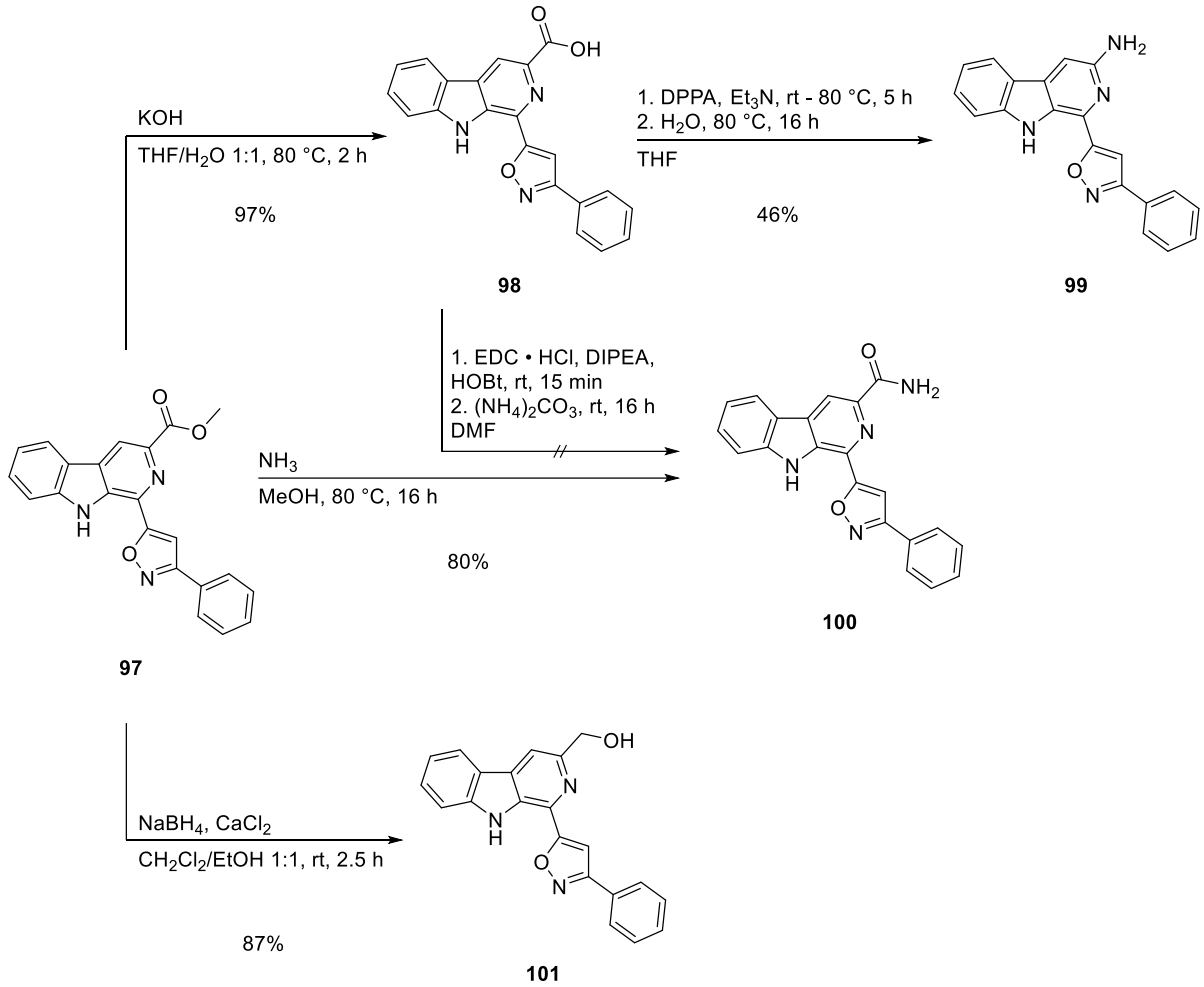

Scheme 56. Synthesis of 3-substituted analogues from ester **97**.

3.3.2.2 Attempted synthesis of 4-substituted analogue **103**

The 4-dimethylaminocarbonyl derivative **103** should be accessible *via* a protocol developed very recently in the BRACHER group (**Scheme 57**). Thereby, ring A of the *β*-carboline is built up by the condensation of ammonia with a keto and an enamino group. The introduction of the latter onto ketone **104** should be achievable with BREDERECK'S reagent, which later on corresponds to C-3 of the *β*-carboline. The indole structure is envisaged *via* an *aza*-alkylation/MICHAEL addition cascade reaction of sulfonamide **105** and *α*-bromoketone **106**. UNTERGEHRER[196] and THEES[197] developed this method for the synthesis of some 1,4-disubstituted *β*-carbolines. However, this approach was not fully exploited until finalization of this project and the general applicability remained vague. The sole employed aromatic residue at C-1 of the *β*-carboline was a phenyl ring, which possesses very different size and electronic properties compared to the phenylisoxazole moiety.

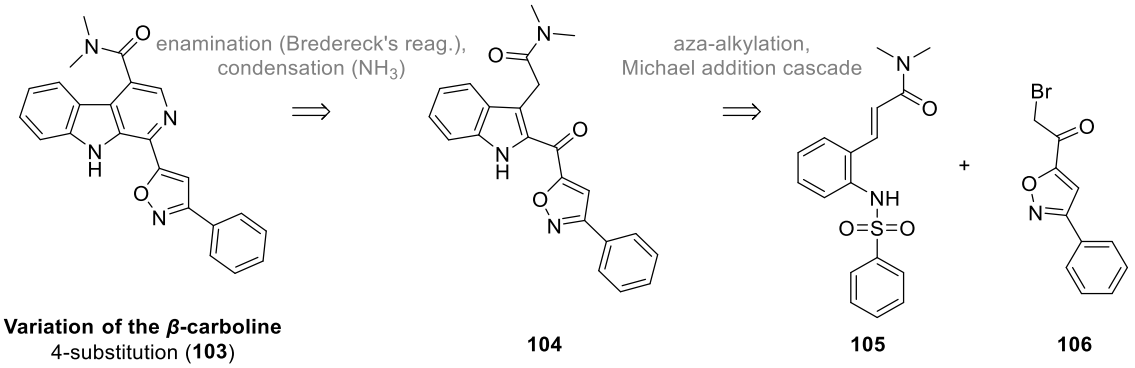

Scheme 57. Retrosynthesis of 4-subtituted analogue **103**.

The sulfonamide intermediate **105**, which was generously provided by KATHARINA THEES[197] and synthesized *via* HECK reaction and *N*-sulfonylation from 2-iodoaniline, was subjected to the *aza*-alkylation/MICHAEL addition cascade reaction (**Scheme 58**). This sequence is based on the diketoindole synthesis of KIM *et al.*[204], who proposed from a mechanistic point of view, that triethylamine leads to *N*-alkylation and MICHAEL addition to an intermediary indoline and treatment with DBU then initiates the desulfonation to the respective indole.

THEES and UNTERGEHRER aimed at expanding the substrate scope to MICHAEL systems with other electron withdrawing groups than ketones such as the envisaged amide. In a first attempt, the reaction was performed following the general procedure of UNTERGEHRER precisely[196] using 1.5 eq each of triethylamine and *α*-bromoketone **106**. This gave, after DBU treatment, indole **104** in 19% yield. However, while sulfonamide **105** was not fully consumed, no residual *α*-bromoketone was present. This indicates degradation and at the same time greatly decreased reactivity towards the *N*-alkylation compared to phenacyl bromide. When the reaction was modified, so that triethylamine and a greater excess of *α*-bromoketone **106** were added repetitively (3 x 1.0 eq, stirring for 0.5 h each time at 60 °C; then DBU treatment), the yield could be significantly improved (54%).

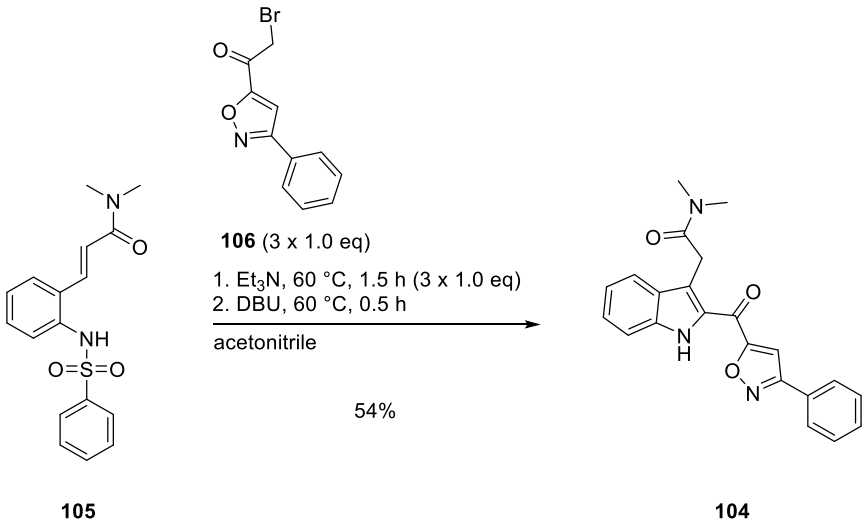

Scheme 58. Synthesis of indole **104** *via aza*-alkylation/MICHAEL addition cascade reaction.

BREDERECK'S reagent (*tert*-butoxybis(dimethylamino)methane) has been widely used for the enamination of active methylene groups. This reagent is advantageous over other approaches, as thermal decomposition results in the generation of both required components *in situ*: *tert*-butoxide and the iminium species (**Scheme 59**). The strongly basic alkoxide can deprotonate the active methylene group, which then subsequently attacks the iminium ion. This corresponds to the introduction of one carbon atom and gives the envisaged enamine after *β*-elimination of dimethylamine. The utility of this reagent was demonstrated in several natural product total syntheses[205].

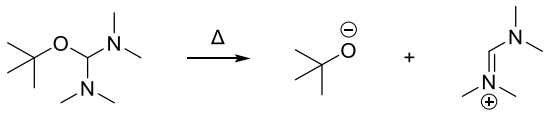

Scheme 59. Thermal decomposition of BREDERECK'S reagent.

In the case of indole **104** the active methylene group is a vinylogous 1,3-dicarbonyl substructure, which was assumed to be sufficiently CH-acidic. Treatment with BREDERECK'S reagent, however, did not lead to any conversion to enamine **107**. Although different temperatures and increasing amounts of the reagent were tried, only starting material was recovered (**Scheme 60**). As this reaction worked well, when conducted by THEES with the corresponding phenyl residue (70% yield)[197], the reason for this failure is likely to be the phenylisoxazole moiety. Possibly, the electron rich substituent decreases the CH-acidity.

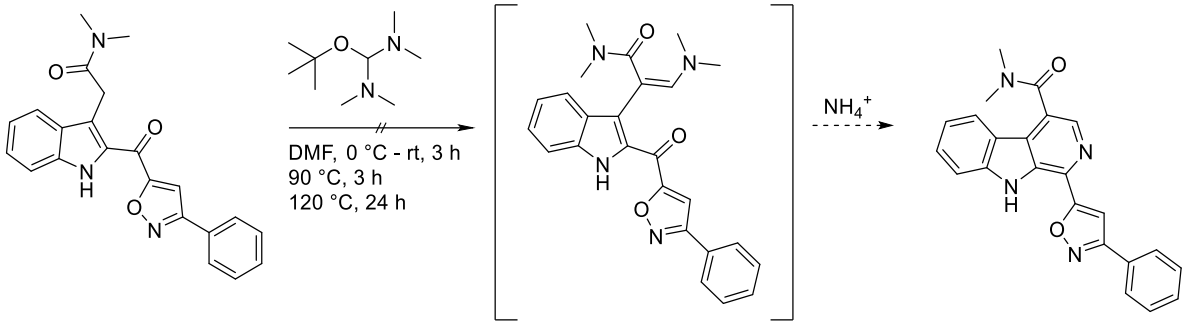

104 107 103

Scheme 60. Attempted synthesis of 4-substituted analogue **103** with BREDERECK'S reagent.

As a positive effect of the 4-substitution in terms of target affinity is highly questionable, no further attempts were made to synthesize amide **103** or related analogues with formylation reagents, such as ethyl formate. However, also with indole **104** an interesting compound was accessed. It can be seen as a more flexible, truncated analogue of the lead structure **1**, whereby the keto function replaces C-1 and the pyridine nitrogen.

3.3.3 Other tricyclic heteroarenes and ring C substituted *β*-carbolines

Other tricyclic heteroarenes and ring C substituted *β*-carbolines were investigated for several reasons. For one thing the relevance of the pyridine nitrogen in lead structure **1** was to be examined. A very weak hydrogen bond was observed between the pyridine nitrogen of methyl analogue **2** and LEU 244 in the co-crystal structure, but the significance for lead structure **1** remained unclear. To examine this, a carbazole as well as a phenothiazine analogue were pursued, from which the latter has also modified geometry.

Furthermore, the presence of substituents was not just promising at ring A but also at ring C. The 7,8-dichloro motif is familiar from bauerine alkaloids and indole KH-CB19 (**Figure 15**, left), where it is even involved in the formation of a dual halogen bond with the hinge region of protein kinases (**Figure 15**, right)[47]. Although the orientation of KH-CB19 is twisted, it was envisaged to introduce this motif in lead structure **1**, as reorientation was observed in many other ligands.

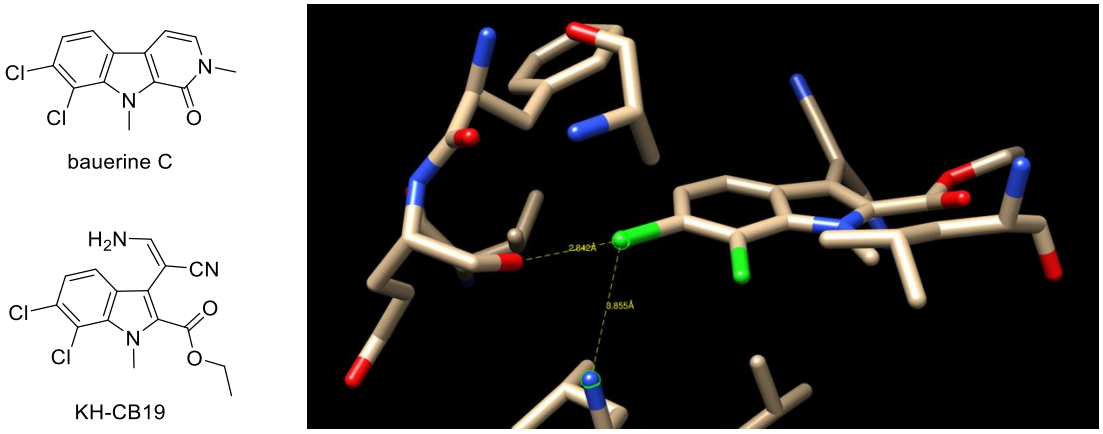

Figure 15. Structures of bauerine C and KH-CB19 (left) and illustration of the halogen bonds (yellow lines) formed between KH-CB19 and the hinge region of CLK1 (right).

The crystal structure with ligand **2** revealed that especially the 8-position provides plenty of space, which is filled by other inhibitors, such as KH-CB19 (*cf.* **Figure 17** in chapter 3.3.4). Additionally, two water molecules are present in 4 – 5 Å distance in this region of the protein, which could be displaced by donor groups to interact with the backbone oxygen of GLU 292 or ASN 293 (**Figure 16**). Molecular modelling (performed by DR. MICHAEL MEYER, MBC-Statistik, Falkensee, Germany) suggested that either a five-membered heteroarene with a NH function, such as pyrazole, or a propargylamine or alcohol could fit well.

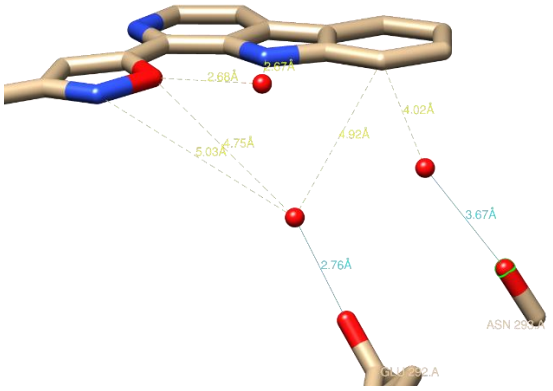

Figure 16. Detailed short distances (indicated by yellow lines) between C-8 of ring C of the *β*-carboline moiety of ligand **2** and the CLK1. Water molecules (red spheres) are nearby.

The other tricyclic heteroarenes and ring C substituted *β*-carbolines can be approached with the same reaction sequence as described for lead structure **1** (**Scheme 61**). The isoxazole is thereby built up *via* HUISGEN cycloaddition of arylacetylenes (**B**), which are in turn synthesized from the corresponding (pseudo)halides (**A**). However, these (pseudo)halides (**A**) can also

serve as key intermediates, when the phenylisoxazole moiety is introduced as a whole *via* SUZUKI cross-coupling. The required boronic acid pinacol ester **108** can therefore be prepared again *via* HUISGEN cycloaddition from alkynylboronates and benzonitrile oxide.

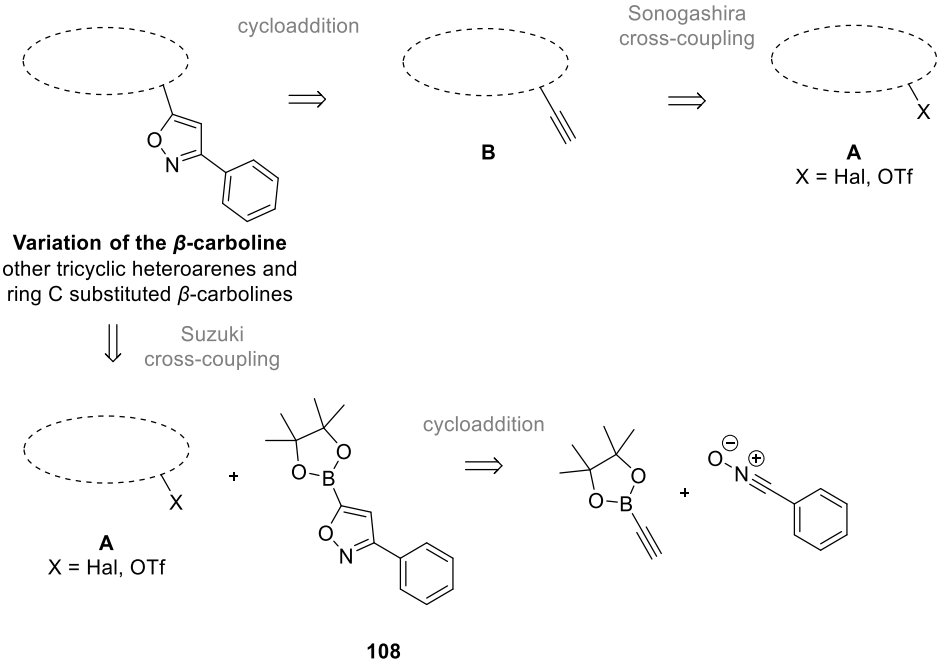

Scheme 61. Retrosynthesis of analogues with modified heteroaromatic tricycles.

3.3.3.1 Studies towards the use of boronic acid pinacol ester **108**

The use of a boronic acid derivatives, such as **108**, can be advantageous, as it paves the way to introduce the phenylisoxazole moiety directly onto aromatic (pseudo)halides. This approach could spare several steps compared to the previously used procedure. However, the building block has to meet the requirement of being stable enough in general, but readily reactive in SUZUKI cross-couplings. While the corresponding free boronic acid of **108** was reported to be very easily deboronated already in 1966[206], the properties of its related boronates remained ambiguous. DAVIES *et al.*[207] and MOORE *et al.*[208] intensively investigated the synthesis of isoxazoleboronic acid pinacol esters *via* cycloaddition of alkynylboronates with nitrile oxides. While internal alkynes gave the 3,4,5-trisubstituted isoxazoles with the boronic acid derivative in 4-position, the terminal alkyne led to 3,5-disubstituted analogues with the boronic acid derivative in 5-position. Unfortunately, to demonstrate the utility of these building blocks in SUZUKI cross-couplings the authors chose only isoxazole-4-boronic acid derivatives. Two patents however use isoxazole-5-boronic acid derivative **108**[209-210], which prompted to do the same.

Synthesis was accomplished from hydroxymoyl chloride **11** and 2-ethynyl-4,4,5,5-tetramethyl-1,3,2-dioxaborolane similar to the procedure of DAVIES *et al.*[207] and ^{1}H NMR analysis of the crude product confirmed formation of the envisaged boronic acid pinacol ester **108** with slight impurities (**Scheme 62**). The attempt to purify it by flash column chromatography (as stated in the publication), resulted in protodeboronation and only 3-phenylisoxazole (**109**) was isolated (approx. 55% yield). This was somehow surprising, as MOORE *et al.*[208] mention this sensitivity only for 3-halo analogues, but specifically not for the phenyl substituent. In another attempt, crude **108** was directly subjected to SUZUKI cross-coupling with 1-bromo-*β*-carboline (**8**) under standard conditions[211]. ^{1}H NMR analysis of the crude mixture showed only traces of lead structure **1**, whereas 3-phenylisoxazole (**109**) and bromide **8** were the main components.

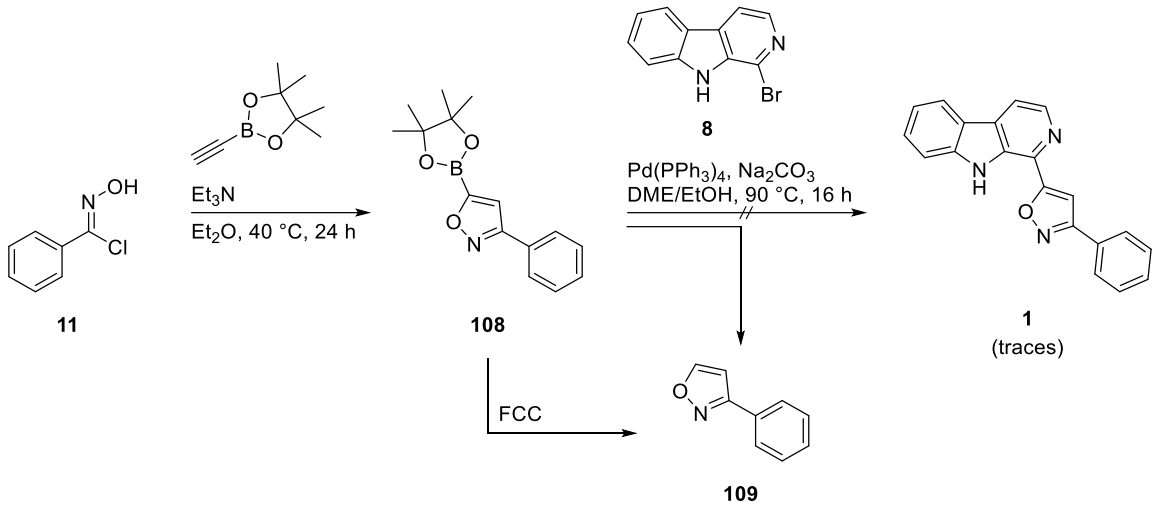

Scheme 62. Attempted synthesis of lead structure **1** *via* SUZUKI cross-coupling with boronic acid pinacol ester **108**.

A publication of GROB *et al*.[212] indicates that other groups were facing similar problems. They report the synthesis of the respective *N*-methyliminodiacetic acid (MIDA) masked boronic acids and highlight their superiority compared to pinacol esters in terms of stability. However, they had to perform tedious optimization of reaction conditions for the SUZUKI cross-coupling to circumvent competing protodeboronation even of those MIDA esters. Therefore, this approach was not followed further, as the general applicability to more complex substrates remained uncertain and the required catalysts as well as the MIDA alkynylboronate are rather expensive.

3.3.3.2 Syntheses *via* SONOGASHIRA cross-coupling and cycloaddition from tricyclic heteroaromatic precursors

The other tricyclic heteroarenes and ring C substituted *β*-carbolines were then approached *via* SONOGASHIRA cross-coupling and HUISGEN cycloaddition from the respective (pseudo)halides. The synthesis of these key intermediates and their further transformation will consecutively be described in the following.

The first envisaged tricyclic heteroarene was the phenothiazine moiety. While bromination of phenothiazine proceeds in the first place *para* to the nitrogen in 3-position[213], HALLBERG *et al.*[214] described the synthesis of 1-chloro- and 1-bromo-phenothiazine *via* lithiation and subsequent halogenation. Following their procedure, treatment of phenothiazine with *n*-butyllithium generated the dilithio species **110**[215], which was then reacted with 1,2-dibromoethane[216] to bromide **111**[214] (50% yield) (**Scheme 63**). Replacement of the electrophile by 1,2-diiodoethane gave also the corresponding 1-iodinated analogue **112** (43% yield), of which the constitution was confirmed by ^{1}H NMR and NOE analysis.

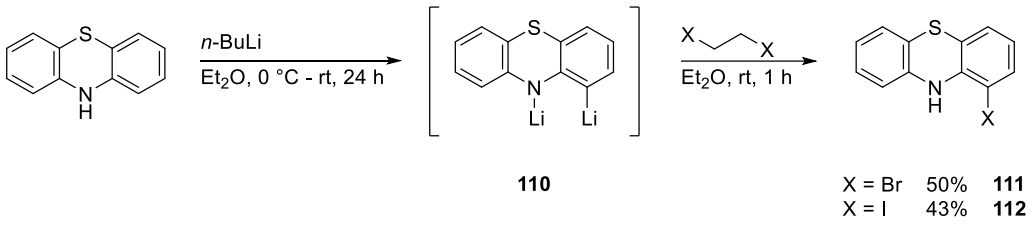

Scheme 63. Synthesis of 1-halogenated phenothiazines **111** and **112** *via* lithiation and halogenation.

Next, the SONOGASHIRA cross-coupling of both aryl halides was investigated, but a literature search revealed no examples for SONOGASHIRA cross-couplings of phenothiazines in 1-position. KRÄMER *et al.*[217] performed a few with *N*-alkylated 3-bromo phenothiazines and trimethylsilylacetylene in piperidine. However, these conditions failed for bromide **111** (**Scheme 64**). In contrast to this, the procedure of a Chinese patent[218] led to at least partial conversion to alkyne **113**, when it was applied to iodide **112** and trimethylsilyl acetylene. As even after 40 h not all iodide was consumed, the reaction was stopped. After TMS cleavage with potassium carbonate, arylacetylene **114** was obtained (45% yield over two steps). The last step was the cycloaddition. Since the PIFA method was superior in nearly all compared reactions hitherto, it was initially also applied to **114**. However, this resulted only in traces of isoxazole **115** according to TLC-MS analysis among residual starting material and several other components. Most likely, the hypervalent iodine reagent does not only lead to oxidation of benzaldehyde oxime, but also of the phenothiazine. This consideration is supported by the

use of related reagents for the transformation of phenothiazine to phenothiazin-3-one[219]. When in contrast hydroxymoyl chloride **11** and triethylamine were used for the cycloaddition, isoxazole **115** could be obtained (31% yield).

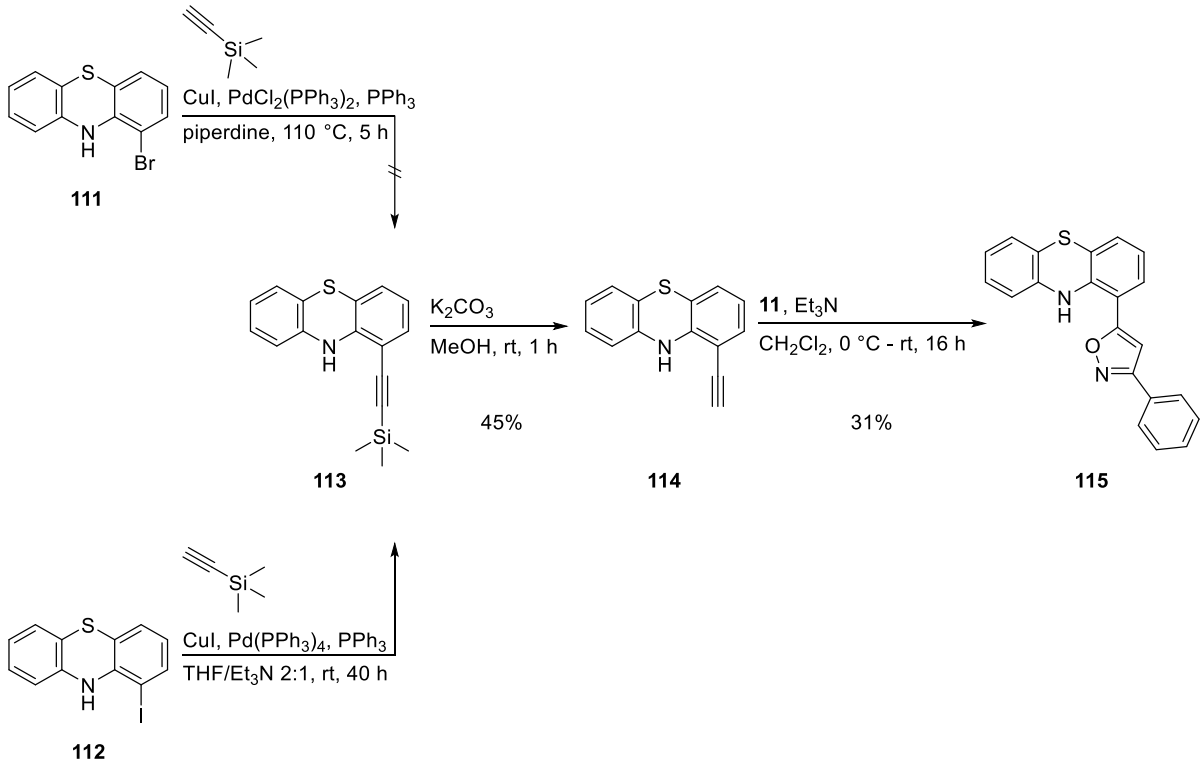

Scheme 64. Synthesis of 1-substiued phenothiazine **115** *via* SONOGASHIRA cross-coupling and HUISGEN cycloaddition.

The next envisaged tricyclic heteroarene was the carbazole, which corresponds to the 2-desaza analogue of lead structure **1**. Since bromide **117** has already successfully been employed in various SUZUKI and STILLE cross-coupling reactions within the BRACHER group[79, 83, 211], it was also chosen as building block for the SONOGASHIRA cross-coupling.

The preparation of bromide **117** was accomplished by repeating the established BORSCHE-DRECHSEL carbazole synthesis[79, 83, 211] (**Scheme 65**). At first, FISCHER indole synthesis[220-221] of 2-bromophenylhydrazine hydrochloride and cyclohexanone gave tetrahydrocarbazole **116** (89% yield), which was then dehydrogenated with *p*-chloranil and resulted in carbazole **117** (72% yield)[222].

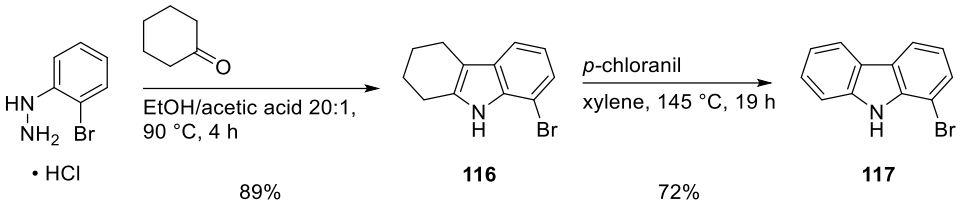

Scheme 65. Synthesis of bromide **117** *via* BORSCHE-DRECHSEL carbazole synthesis.

Then, the SONOGASHIRA cross-coupling of bromide **117** and trimethylsilylacetylene was studied. Application of the conditions, which have proven successful for the respective 1-bromo-*β*-carboline **8**, gave only traces of arylacetylene **118** (**Table 9**, entry 1). Considering the enhanced electrophilic properties of pyridine in *ortho*-position in contrast to phenyl, it deemed necessary to use more forcing conditions. When palladium(II) acetate and triphenylphosphine were used in a mixture of THF and isopropylamine at 60 °C[223], only little improvement was achieved (**Table 9**, entry 2). However, the use of $PdCl_2(PPh_3)_2$ in pure triethylamine at 80 °C[224] lead to complete conversion (**Table 9**, entry 3).

Table 9. SONOGASHIRA cross-coupling of bromide **117**.

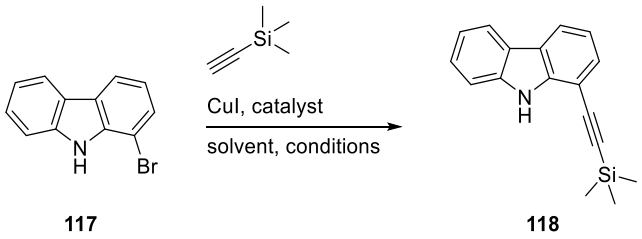

entry	catalyst	solvent	conditions	observation
1	$Pd(dppf)Cl_2$	THF/Et_3N 1:1	rt, 16 h	traces (TLC-MS)
2	$Pd(OAc)_2$, PPh_3	THF/iPr_2NH 1:4	60 °C, 16 h	< 10% (^1H NMR)
3	$PdCl_2(PPh_3)_2$	Et_3N	80 °C, 24 h	full conversion (TLC)

With these conditions and subsequent desilylation, arylacetylene **119** was then synthesized (55% yield over two steps) (**Scheme 66**). The HUISGEN cycloaddition was conducted once more with the PIFA method. However, to achieve full consumption of the starting material, the addition of PIFA and benzaldehyde oxime (1.5 eq each) was repeated. The stated relatively low yield of isoxazole **120** (21%) did not arise from insufficient conversion, but difficulties during purification. In contrast to *β*-carboline **1**, carbazole **120** is much less polar. Therefore, the isolation by flash column chromatography and recrystallization was hampered by the presence of large quantities of organic compounds derived from PIFA and benzaldehyde oxime. Since

a sufficient amount of isoxazole **120** was obtained analytically pure, no more efforts were made to separate the mixed fractions.

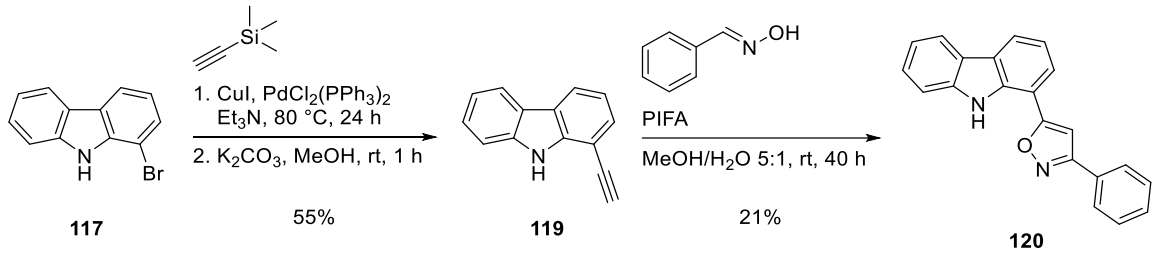

Scheme 66. Synthesis of 1-substiued carbazole **120** *via* SONOGASHIRA cross-coupling and HUISGEN cycloaddition.

Next, synthesis of the 7,8-dichloro-*β*-carboline was approached. Preparation of the required bromide building block **124** was already described by WURZLBAUER[82] based on previous studies[46, 78].

Tetrahydro-1-oxo-*β*-carboline **122** was synthesized following the two-step procedure of POHL[78]. At first, 3-ethoxycarbonyl-2-piperidone was hydrolysed and subjected to a JAPP-KLINGEMAN reaction[225-226] with diazotised 2,3-dichloroaniline (**Scheme 67**). The resulting hydrazone **121** (60% yield) was then treated with formic acid to undergo FISCHER cyclisation[220]. As stated by HUBER[46], tetrahydro-*β*-carboline **122** was accompanied by its *N*-formyl analogue, which could by cleaved with sodium hydroxide to give solely *N*-unsubstituted tetrahydro-*β*-carboline **122** (43% yield).

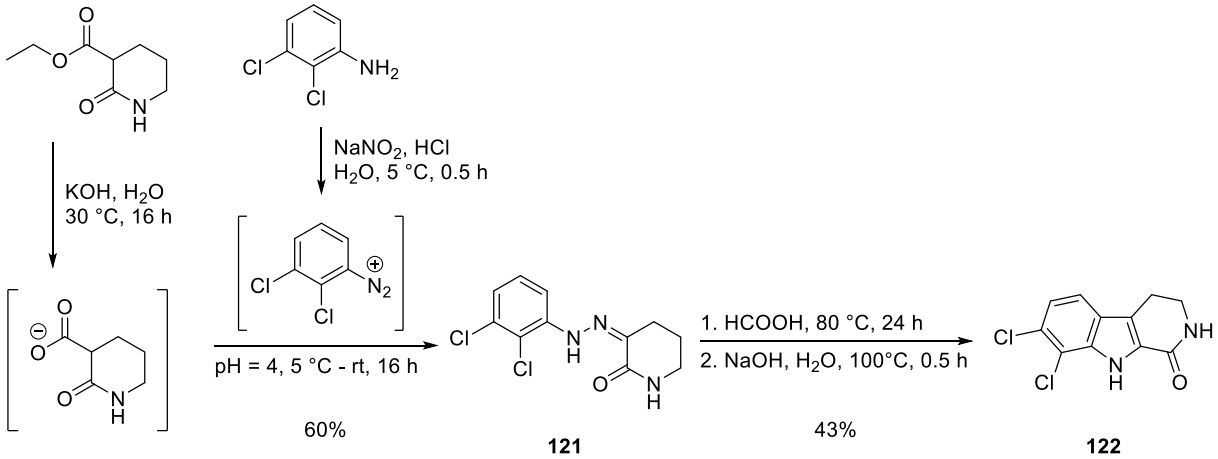

Scheme 67. Synthesis of 1,2,3,4-tetrahydro 1-oxo-*β*-carboline **122** *via* JAPP-KLINGEMANN reaction and FISCHER cyclisation.

The dehydrogenation was performed following the procedure of WURZLBAUER[82] with small alterations (**Scheme 68**). Decreasing the amount of DDQ (from 2.0 to 1.2 eq) still led to complete conversion and simplified the purification of *β*-carbolinone **123** (63% yield). Then, bromination was achieved with phosphorus oxybromide in anisole giving bromide **124**[82] (75% yield).

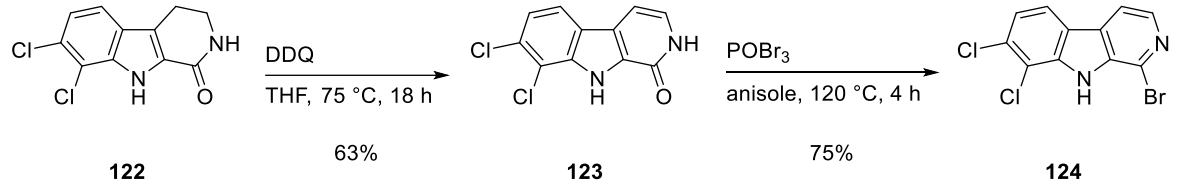

Scheme 68. Synthesis of bromide **124** *via* dehydrogenation and bromination.

WURZLBAUER[82] has used bromide **124** within the synthesis of 7,8-dichloro annomontine to introduce a methyl ketone *via* STILLE cross-coupling with tributyl(1-ethoxyvinyl)tin. This time it should be subjected to SONOGASHIRA cross-coupling with trimethylsilyl acetylene. Initially, triethylamine and THF were used as solvent mixture as usual. However, bromide **124** showed only poor solubility and arylacetylene **125** was obtained in only 6% yield after TMS deprotection. The conversion was improved when THF was replaced by DMF in the first step (52% yield), which obviously also enhanced solubility (**Scheme 69**). HUISGEN cycloaddition with the PIFA method then gave 7,8-dichloro analogue **126** (88% yield).

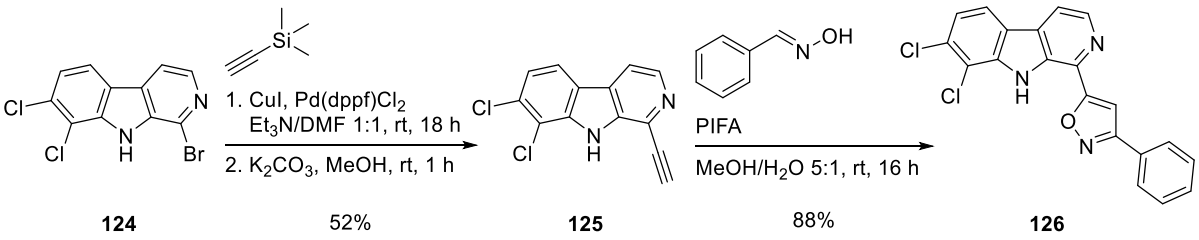

Scheme 69. Synthesis of isoxazole **126** *via* SONOGASHIRA cross-coupling and HUISGEN cycloaddition.

With the procedure described for 7,8-dichloro analogue **126**, also other substitution patterns of ring C could be synthesized. Instead of utilizing the various 1,2,3,4-tetrahydro-1-oxo-*β*-carbolines with chloro-, bromo-, methyl-, methoxy- and alkoxycarbonyl-substituents described by POHL[78], more specific analogues were envisaged. These larger and more complex residues in 8-position, such as propargyl alcohol or amine and pyrazole, do not

tolerate all reactions included in the sequence. To circumvent their incompatibility and establish an access to versatile substituents, it was striven for a pseudo(halide) intermediate, which can be modified *via* cross-coupling reactions. However, this functional group has to be introduced only after implying the 1-substituent. To do so, the respective triflate **127** can easily be accessed from the corresponding phenol and this, in turn, can be generated from 8-methoxy analogue **128** *via* ether cleavage (**Scheme 70**). To sum it up, the methyl ether substituent is not just an interesting analogue, but in addition perfectly meets the requirement of a phenol protecting group. It is supposed to be resistant towards all required reagents and conditions, but later on selectively cleavable.

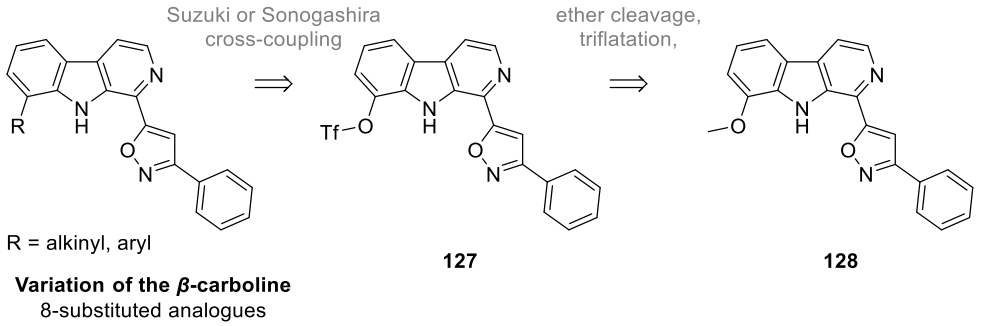

Scheme 70. Retrosynthesis of 8-substituted analogues from methyl ether **128**.

Preparation of the 1,2,3,4-tetrahydro-1-oxo-*β*-carboline **130** was already described by SÓTI *et al.*[227] within the synthesis of 7-methoxytryptamine. While the JAPP-KLINGEMANN reaction generated hydrazone **129** (68% yield) as described, the procedure for the FISCHER cyclisation had to be adjusted (**Scheme 71**). Following their experimental part, the reaction was initially conducted in refluxing formic acid over a course of 4 h. This, however, caused not only ring formation, but mostly also *N*-2 formylation. The subsequent hydrolysis, as described for the 7,8-dichloro analogue, using sodium hydroxide was not feasible. Even after just 30 min, also extensive lactam cleavage[227] had proceeded. WURZLBAUER faced the same problem, when she synthesized the respective 7-methoxy analogue, which she tried to solve by stirring the crude product in an ethanolic potassium hydroxide solution at room temperature[82]. However, no conclusions were drawn regarding an improvement of the yield, that remained poor in her case (14%). In contrast to this, closer reaction monitoring revealed, that the cyclisation is completed already after 1 h, while *N*-formylation is nearly negligible at that time. The excess of formic acid was simply evaporated and 1,2,3,4-tetrahydro-1-oxo-*β*-carboline **130** was obtained in acceptable yield (53%) after flash column chromatography.

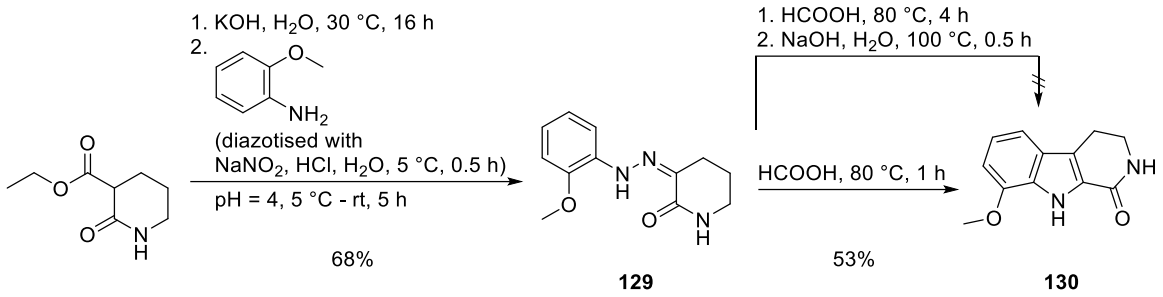

Scheme 71. Synthesis of 1,2,3,4-tetrahydro 1-oxo-*β*-carboline **130** *via* JAPP-KLINGEMANN reaction and FISCHER cyclisation.

Next, dehydrogenation was achieved with *p*-chloranil giving *β*-carbolinone **131** (56% yield), which then again needed to be functionalized at C-1 (**Scheme 72**). In this case, bromination is not an option. The method of HILDEBRAND[90], which has proven successful for bromides **8** and **124**, implies the use of anisole as solvent. This is necessary to prevent additional ring bromination at ring A and ring C of the *β*-carboline, because thermal decomposition of phosphorus oxybromide results in the formation of bromine. Therefore, anisole functions not only as solvent, but also as bromine scavenger. As the methoxy substituent of **131** likewise increases the electron density of the *β*-carboline, ring bromination is probably no longer sufficiently suppressed by anisole. WURZLBAUER experienced this for the 8-methoxy substituent and therefore switched to the corresponding chloride[82]. However, **131** was to be converted into triflate **132**, as the prospects for the subsequent SONOGASHIRA cross-coupling reaction seemed more promising. Treatment with trifluoromethanesulfonic anhydride in pyridine[88] yielded triflate **132** (93%) without any indices of a related *N*-2 or *N*-9 triflated regioisomeric byproduct.

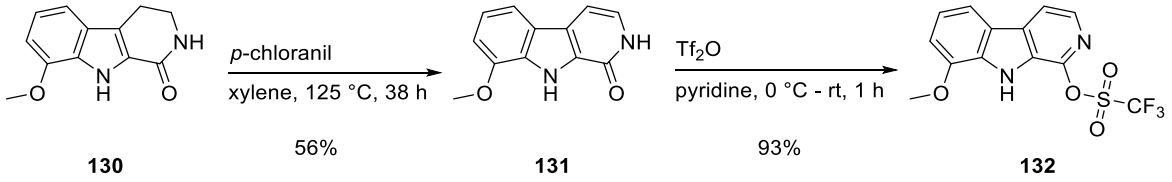

Scheme 72. Synthesis of triflate **132** *via* dehydrogenation and triflation.

Applying again the conditions of ZHENG *et al.*[97], which included lithium chloride, SONOGASHIRA cross-coupling of triflate **132** proceeded smoothly and subsequent TMS deprotection gave arylacetylene **133** (68% yield over two steps) (**Scheme 73**). HUISGEN cycloaddition with the PIFA method was also high yielding in the case of **128** (86%).

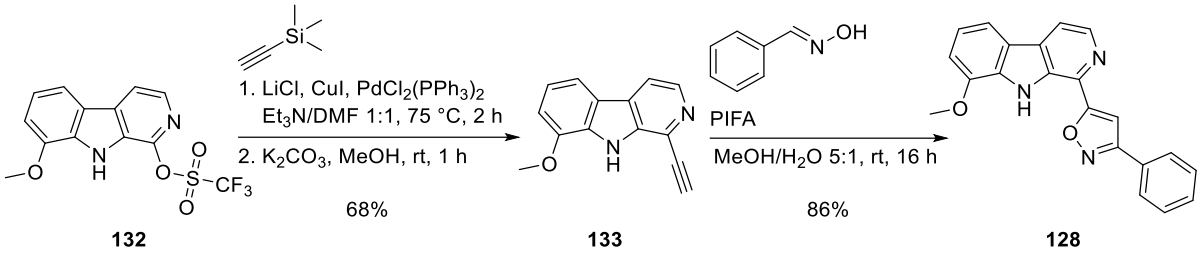

Scheme 73. Synthesis of isoxazole **128** *via* SONOGASHIRA cross-coupling and HUISGEN cycloaddition.

After introducing the phenylisoxazole moiety in 1-position, the transformation of the 8-methoxy substituent had to be realized. Several approaches of aryl methyl ether cleavage are known[137], however the initial attempts were not expedient. Boron tribromide[228], which is probably the most commonly used reagent for this purpose, gave traces of phenol **134** according to TLC-MS analysis, when the reaction was performed with 10 eq at room temperature for several days (**Table 10**, entry 1). Surprisingly, harsher reaction conditions (20 eq, 40 °C) did not lead to a significant improvement (**Table 10**, entry 2). Pyridine hydrochloride[229] has been successfully employed for demethylation of a 6-methoxy-*β*-carboline, after boron tribromide and other reagents have failed according to recent literature[152]. However, in the case of **128** no conversion at all was observed, neither neat (**Table 10**, entry 3) nor with additional pyridine as co-solvent (**Table 10**, entry 4). Hydrobromic acid was at first tried solely[230-231] without success (**Table 10**, entry 5). However, when acetic acid was added[232], the reaction mixture became a clear solution temporarily and conversion was achieved. With this, phenol **134** could finally be accessed (**Table 10**, entry 6). After full conversion and cooling to room temperature, the precipitate, which is likely the hydrobromide salt, was filtered off. Resuspension in dilute aqueous sodium hydroxide solution and extraction with ethyl acetate then gave sufficiently pure **134** (63% yield).

Table 10. Demethylation of ether **128**.

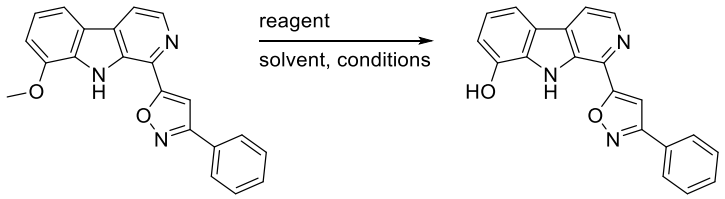

128 **134**

entry	reagent	solvent	conditions	yield
1	BBr_3 (10 eq)	CH_2Cl_2	-78 °C – rt, 7 d	traces
2	BBr_3 (20 eq)	CH_2Cl_2	-78 °C – 40 °C, 3 d	traces
3	pyridine-HCl	-	150 °C, 24 h	-
4	pyridine-HCl	pyridine	130 °C, 16 h	-
5	HBr (aq., 48%)	H_2O	rt – 130 °C, 4 h	-
6	HBr (aq., 48%)	acetic acid	135 °C, 6 h	63%

The subsequent triflation was conducted with trifluoromethanesulfonic anhydride again[233]. When the reaction was run for the first time, triflate **127** was the sole product (approx. 90% yield). However, repetition with a new batch of phenol **134** resulted in a decreased yield of the envisaged product **127** (67%) and the formation of a side product (**Scheme 74**). This could be separated by flash column chromatography and identified by HRMS and NMR analysis as acetate **135** (23% yield). Obviously, residual acetic acid was still present from the previous step. Reaction with trifluoromethanesulfonic anhydride could give a mixed anhydride and related substances, such as trifluoroacetyl triflate[234], were shown to be efficient acylating reagents under similar conditions.

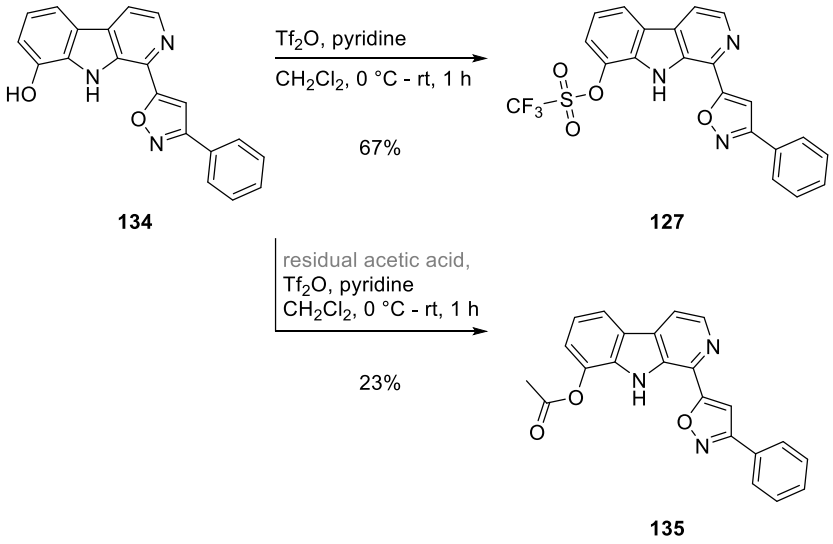

134 **127** **135**

Scheme 74. Synthesis of triflate **127** and acetate **135**.

With triflate **127** in hand, substitution at C-8 *via* cross-coupling reactions could be addressed next. However, since the available amount was limited at this stage after numerous synthesis steps, preliminary test reactions to find suitable conditions were run, which are outlined in brief. Phenyl triflate was therefore used as starting material and several conditions were tested for the SUZUKI cross-coupling with 1*H*-pyrazol-3-ylboronic acid. The reaction failed, when palladium(II) acetate and SPhos were used with potassium phosphate in DMF (**Table 11**, entry 1) or dioxane (**Table 11**, entry 2)[235]. While again no notable conversion was achieved, when tetrakis(triphenylphosphine)palladium(0) was used in a combination with potassium carbonate in a mixture of DMF and ethanol[236] (**Table 11**, entry 3), the use of the same catalyst with sodium carbonate in a mixture of dioxane and water[237] lead to the formation of biaryl **136** (**Table 11**, entry 4, 70% yield).

Table 11. Synthesis of biaryl **136** via SUZUKI cross-coupling.

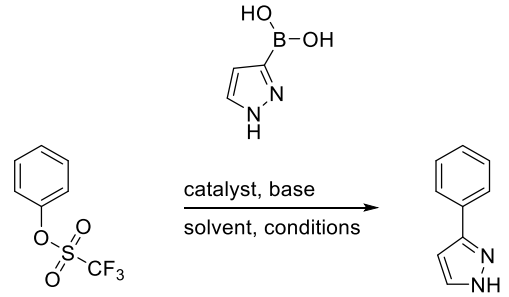

136

entry	catalyst	base	solvent	conditions	yield
1	$Pd(OAc)_2$, SPhos	K_3PO_4	DMF	100 °C, 16 h	-
2	$Pd(OAc)_2$, SPhos	K_3PO_4	dioxane	100 °C, 16 h	traces
3	$Pd(PPh_3)_4$	K_2CO_3	DMF/EtOH 2:1	80 °C, 16 h	-
4	$Pd(PPh_3)_4$	Na_2CO_3	dioxane/H_2O 4:1	85 °C, 20 h	70%

Initially, test reactions for the SONOGASHIRA cross-coupling were also run with phenyl triflate. The outcome was however barely assessable with TLC and MS analysis due to high volatility, limited UV activity and extensive fragmentation. Therefore, triflate **137** was synthesized[238] (96% yield) and used as starting material in a test reaction with trimethylsilyl acetylene (**Scheme 75**). The use of a copper-free procedure (**Table 12**, entry 1) as well as standard conditions (**Table 12**, entry 2)[239] resulted in only limited consumption of the starting material to the envisaged product **139**. The acceleration and improvement of SONOGASHIRA cross-coupling reactions of aromatic triflates by the addition of tetra-*n*-butylammonium iodide was described by POWELL and RYCHNOVSKY already in 1993[240]. This protocol also lead to full

conversion of triflate **137** in only 3 h and arylacetylene **138** was isolated in nearly quantitative yield (**Table 12**, entry 3, 99%).

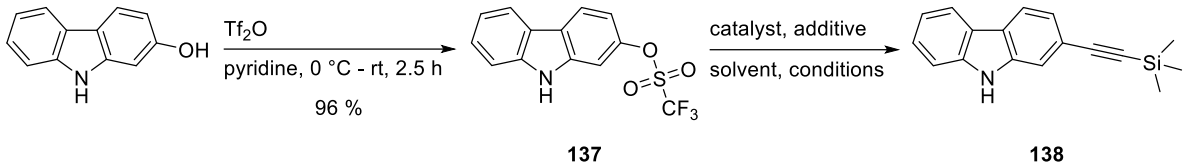

137 **138**

Scheme 75. Synthesis of arylacetylene **138** *via* SONOGASHIRA cross-coupling.

Table 12. Reaction conditions for the SONOGASHIRA cross-coupling between triflate **137** and trimethylsilylacetylene.

entry	catalyst	additive	solvent	conditions	observation
1	$PdCl_2(PPh_3)_2$	-	DMF/Et_3N 14:1	50 °C, 24 h	incomplete conversion
2	$PdCl_2(PPh_3)_2$, CuI	-	DMF/Et_3N 8:1	100 °C, 16 h	incomplete conversion
3	$PdCl_2(PPh_3)_2$, CuI	*n*-Bu_4NI	DMF/Et_3N 5:1	70 °C, 3 h	full conversion (99%)

These optimized conditions were then applied to the synthesis of 2-substitued carbazoles with the intended propargyl residues (**Scheme 76**). While the reaction with propargylamine showed no residual triflate **137** after 3 h, also no arylacetylene **139** was present. The only substance which could be isolated in a noteworthy amount was tetra-*n*-butylammonium iodide. In contrast to this, the *N*-Boc protected analogue **140** (70%) and propargyl alcohol **141** (84%) were isolated in high yields. Subsequent acidic Boc cleavage of **140** under different conditions (trifluoroacetic acid in methylene chloride, aq. HCl in ethyl acetate, HCl in dioxane) did surprisingly again not result in the formation of propargylamine **139**, but in a mixture of several unidentified substances (according to TLC-MS analysis).

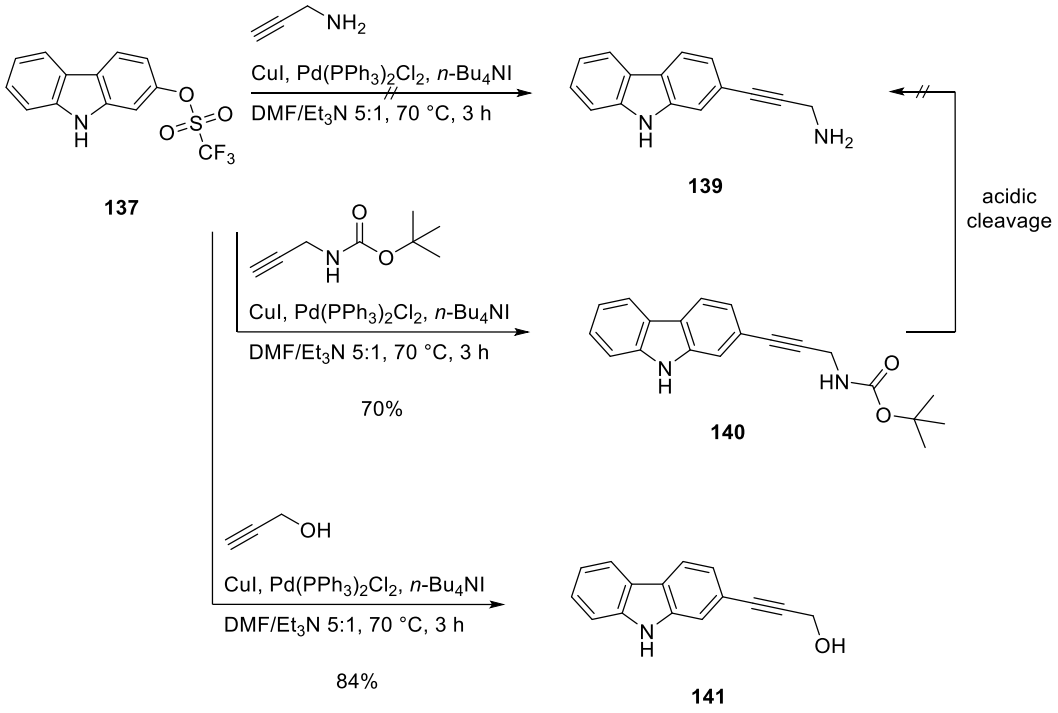

Scheme 76. Model reactions: Attempted synthesis of propargylamine **139** and synthesis of *N*-Boc protected propargylamine **140** and propagyl alcohol **141** *via* SONOGASHIRA cross-coupling.

Consequently, besides 1*H*-pyrazol-3-ylboronic acid, propargyl alcohol was chosen as building block to be introduced onto triflate **127**. The SONOGASHIRA cross-coupling proceeded just as good as the test reaction and gave 8-alkynyl substituted analogue **142** (86% yield) (**Scheme 77**). Conversely, SUZUKI cross-coupling was less effective. While complete conversion was achieved, TLC and MS analysis indicated the formation of two substances with very similar chromatographic behavior, which were presumed to be pyrazole **143** and phenol **134**. Obviously, triflate hydrolysis is a competing side reaction under the applied conditions. ^{1}H NMR analysis of the crude product confirmed this hypothesis. The expected very distinct signals of the pyrazole moiety were observed and could be used to differentiate between the two substances, that were present in a 1.0:0.8 ratio (according to ^{1}H NMR spectrum). However, with laborious flash column chromatograph, which had to be conducted repeatedly, separation of phenol **134** (26% yield) and pyrazole **143** (41% yield) was achieved.

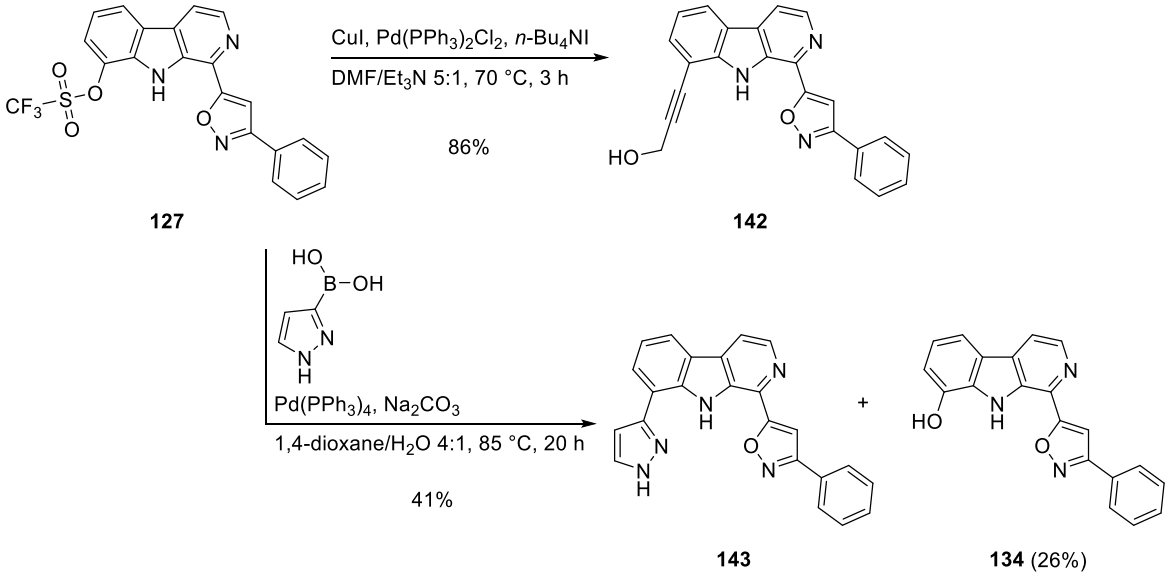

Scheme 77. Synthesis of propargyl alcohol **142** and pyrazole **143** *via* SONOGASHIRA and SUZUKI cross-coupling reactions.

3.3.4 Ring C *aza* and ring B *seco* analogues

The interest in *aza* analogues arose from the comparison of the crystal structures of lead structure **1** and indole KH-CB19. The nitrile group of the latter functions as acceptor for a strong hydrogen bond with LYS 191 (**Figure 17**, left). Superposition of both ligands in their respective orientation within the active centre of the protein demonstrates that the position of the nitrile group roughly corresponds to C-6 or C-7 of the *β*-carboline (**Figure 17**, right).

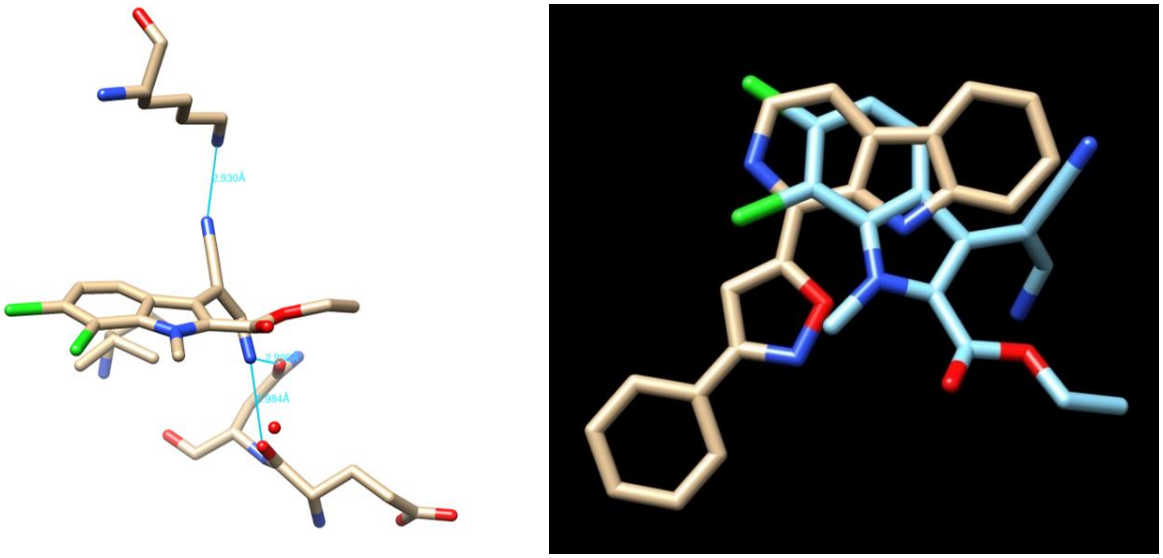

Figure 17. Hydrogen bonds (blue lines) between KH-CB19 and CLK1 (left) and superposition of lead structure **1** (beige) and indole KH-CB19 (blue) in the active centre of the CLK1 (right).

In order to enable a correspondent interaction with CLK1, the introduction of an acceptor group onto lead structure **1** was pursued by replacing the phenyl ring C with a pyridine, which gives 6- and 7-aza analogues **145** and **144**, respectively (**Figure 18**). Since a hydrogen bond with LYS 191 was found to be established also by several other CLK1 inhibitors, this modification was highly promising.

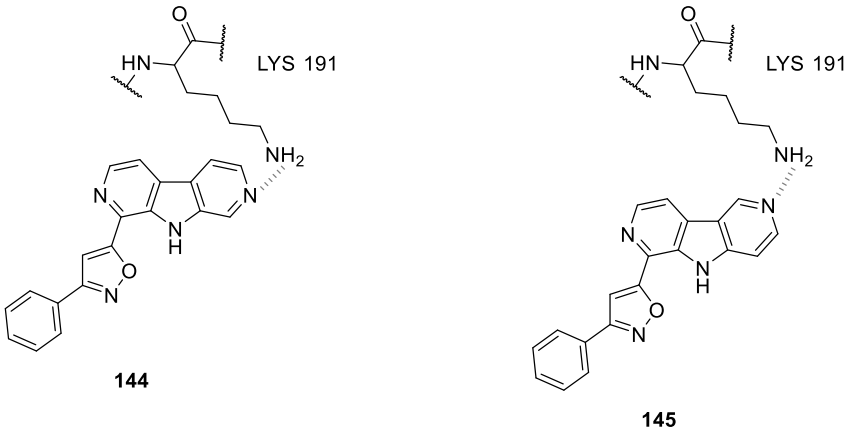

Figure 18. Illustration of the potential hydrogen bond (dotted line), which could hypothetically be formed between 7-aza analogue **144** or 6-aza analogue **145** and LYS 191.

Furthermore, s*eco* analogues, which are in this context diarylamines that lack the direct connection between ring A and ring C, were envisaged. Since these are much more flexible than the rigid *β*-carboline, it was assumed, that they could adopt the same orientation or an even more favored position than lead structure **1**.

3.3.4.1 Attempted synthesis of 7-aza analogue **144** from pyridone precursor **151**[a]

As described in the previous chapter, also the envisaged 6- and 7-aza analogues should be accessible from the respective pyridones (**D**) (**Scheme 78**). However, a new efficient approach to these building blocks had to be developed. This was carried out by FRANCESCA DONÀ in the course of her master thesis under my supervision[201]. Similar to KAMLAH[241], the *β*-carboline motif, or to be more precise ring A, should be built up by intramolecular cyclization of an ethoxyvinyl side chain with a carbonyl group under incorporation of ammonia. While KAMLAH used ketoindoles and ended up with 1-alkyl and aryl substituted *β*-carbolines, aza-*β*-carboline-1-ones should be synthesizable from azaindoles bearing an ester or a carboxamide function at C-2 (**C**). The introduction of the ethoxyvinyl residue can be performed *via* SUZUKI or STILLE cross-coupling of 3-brominated azaindoles (**B**), which can in turn be synthesized from azaindole esters (**A**) by ring halogenation.

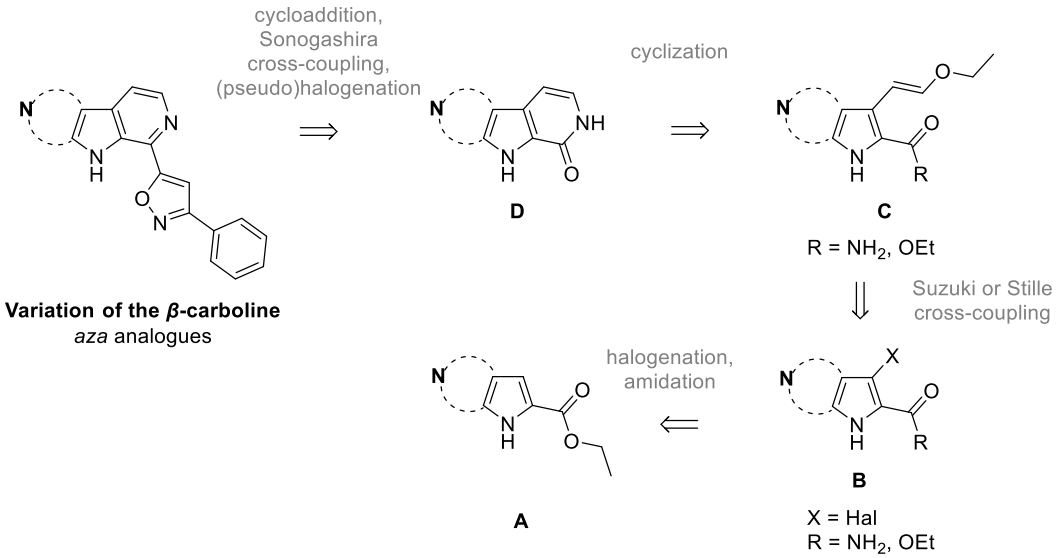

Scheme 78. Retrosynthesis of aza analogues from azaindoles.

FRANCESCA DONÀ focused on the synthesis of 7-aza-*β*-carboline-1-one (**151ª**) and comprehensively described different approaches thereto within her thesis. Hence, only the essential findings and optimized reaction conditions will be briefly presented in the following.

The 6-azaindole building block **147ª** was synthesized following literature procedures *via* REISSERT indole synthesis[242] with small alterations (**Scheme 79**). Pyruvate **146ª** (70% yield) was generated from 4-methyl-3-nitropyridine with sodium ethoxide and diethyl oxalate[243] and reductive cyclization was found to be most efficiently achieved with iron in acetic acid[244] (74% yield).

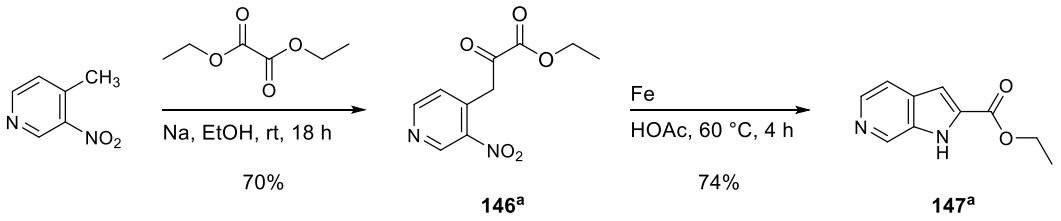

Scheme 79. Synthesis of 6-azaindole **147ª** *via* REISSERT indole synthesis.

Bromination at C-3 of 6-azaindole **147ª** could be carried out with pyridinium tribromide in pyridine as described in a patent[245] (82% yield[201]), but *N*-bromosuccinimide in DMF was found to be even more convenient to generate bromide **148ª** (93% yield) (**Scheme 80**). The transformation of the ester to the amide function was conducted by alkaline hydrolysis (98%

yield) and subsequent amide coupling with ammonium carbonate[246] to carboxamide **149ᵃ** (61% yield).

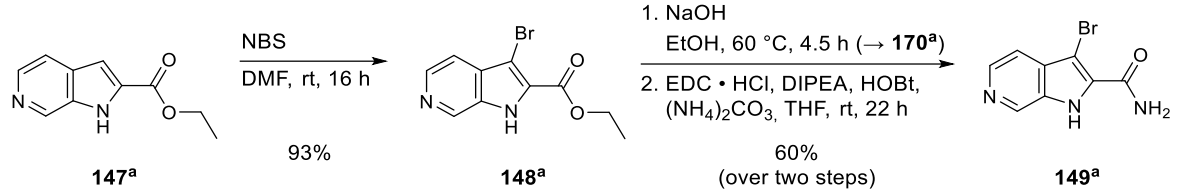

Scheme 80. Synthesis of carboxamide **149ᵃ** from 6-azaindole **147ᵃ**.

Initially, the intended intermediate should carry the caboxamide function, as cyclization to the pyridone with the ethoxyvinyl side chain then is easily enabled by treatment with acid. A similar approach was applied successfully within the synthesis of isoquinoline alkaloids in the BRACHER group recently[247].

However, several attempted SUZUKI and STILLE cross-couplings of bromide **149ᵃ** with (*E*)-2-ethoxyvinylboronic acid pinacol ester and (*Z*)-tributyl[2-ethoxyethenyl]stannane[128] have failed to yield enol ether **150ᵃ** or, after treatment of the crude product with trifluoroacetic acid[247], pyridone **151ᵃ** (**Scheme 81**).

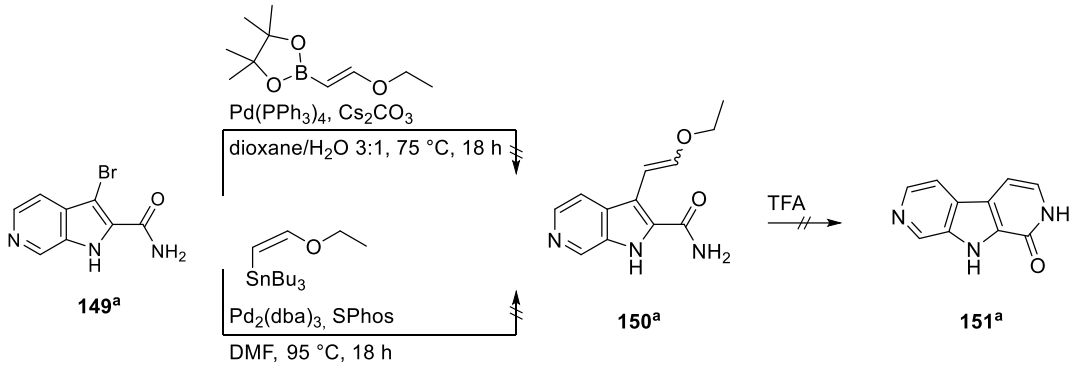

Scheme 81. Attempted synthesis of pyridone **151ᵃ** from carboxamide **149ᵃ**.

Since the cross-coupling reactions seemed to be completely ineffective for bromide **149ᵃ**, conceivably due to complexation of the catalyst, the approach was modified in several ways. For one thing, synthesis of a *N*-1 SEM protected analogue of **149ᵃ** was performed, which could indeed be transformed to the respective enol ether and pyridone **151ᵃ**. However, the reaction showed poor reproducibility regarding the yields, and the use of a protecting group should generally be avoided.

Therefore, the cross-coupling reaction was implemented already on the stage of ester **148ª**. STILLE as well as SUZUKI cross-couplings were initially hampered by extensive debromination. However, this could be prevented in the latter reaction, when the temperature was raised from 75 °C to 95 °C and only enol ether **152ª** was obtained (57% yield) (**Scheme 82**). To construct the pyridone ring A from the enol ether and ester group, in contrast to the carboxamide, condensation with ammonia has to proceed before the cyclization. Several attempts therefore failed using ammonia and various acids, before it was finally achieved with an ammonium acetate melt[248]. Although the very poor solubility greatly impeded work up and purification, pyridone **151ª** was finally obtained in good yield (69%) with an efficient synthesis.

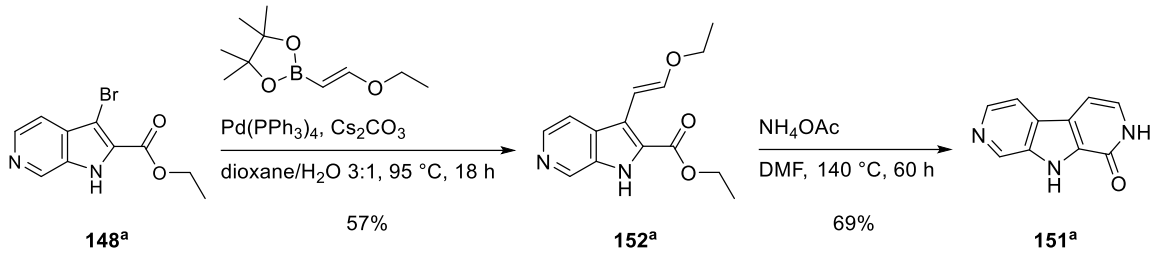

Scheme 82. Synthesis of pyridone **151ª** from ester **148ª**.

Individual functionalization of the pyridine (ring C) and pyridone (ring A) due to their differing reactivity could allow a general access to various substituted 7-aza-*β*-carbolines, which are generally poorly explored. However, substitution at C-1 was most relevant since the synthesis of 7-aza analogue **144** was pursued. Initially, bromination of pyridone **151ª** was attempted with phosphorus oxybromide in anisole[90] (**Scheme 83**). No homogenous reaction mixture was obtained and no conversion at all was achieved under the common (120 °C, 4 h) or more forcing conditions (160 °C, 14 h), and when dioxane was utilized as cosolvent (120 °C, 4 h). Next, phosphorus oxychloride was tried to synthesize chloride **154**, but again no reaction took place (with and without catalytic *N*,*N*-dimethylaniline[87]).

Pyridone **151ª** turned out not to be a convenient building block due to very poor solubility and reactivity. Though, it was found to be at least slightly soluble in pyridine and therefore treated with trifluoromethanesulfonic anhydride[88] to generate pseudohalide **155**. The reaction was closely monitored by TLC and MS analysis. With 1.0 eq of trifluoromethanesulfonic anhydride the conversion was marginal, but as soon as further 0.5 eq were added, two products with very similar chromatographic behavior were generated, which were according to MS analysis a mono-triflate and a twofold triflated side product. Pyridone **151ª** was only fully consumed with addition of another 0.5 eq of trifluoromethanesulfonic anhydride. Both products were not separable by flash column chromatography, but NMR analysis of fractions, which contained

mainly the mono-triflated species, clearly confirmed the formation of **155** (approx. 35% yield, calculated from ^{1}H NMR). The structure of the side product could not be analyzed in detail, but additional formation of an *N*-9 triflamide **156** is plausible (approx. 15% yield, calculated from ^{1}H NMR). Noteworthy, none of the *β*-carboline triflates (**10** and **132**), which were prepared likewise with 2.0 eq of trifluoromethanesulfonic anhydride were accompanied by a twofold triflated side product.

The mixture of triflates was next subjected to SONOGASHIRA cross-coupling with trimethylsilylacetylene, and subsequent desilylation resulted in arylacetylene **157** as sole product in 20% yield over three steps (from pyridone **151[a]**). The following cycloaddition with (*E*)-benzaldehyde oxime using PIFA lead to formation of isoxazole **144** to some extent (approx. 30% yield). However, the quantity was too small and the product could not be sufficiently purified.

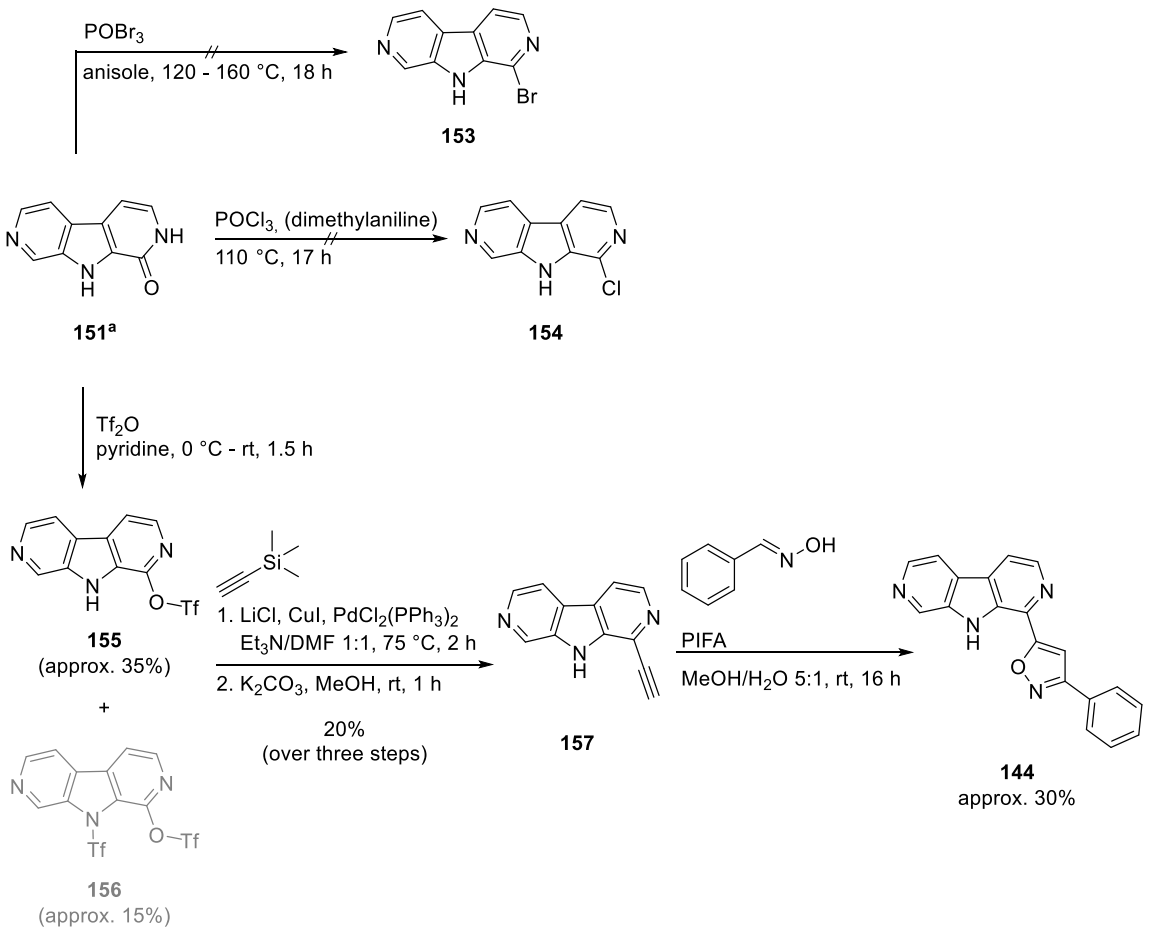

Scheme 83. Synthesis of 7-aza-*β*-carboline analogue **144** from pyridone **151[a]**.

One further attempt was made to improve this approach by introducing again a SEM protecting group onto the indole NH. This could not only avoid the formation of an *N*-9 triflamide, but also enhance solubility.

Therefore, 6-azaindole **148[a]** was protected using SEM chloride (73% yield) and subsequent SUZUKI cross-coupling with (*E*)-2-ethoxyvinylboronic acid pinacol ester was even superior (76% yield) in comparison to the unprotected indole (**Scheme 84**). However, the cyclization with the ammonium acetate melt failed. Consumption of enol ether **158** was very slow and only resulted in degradation, probably due to instability of SEM. According to HRMS analysis neither pyridone **159** nor the deprotected pyridone **151[a]** were found to be present.

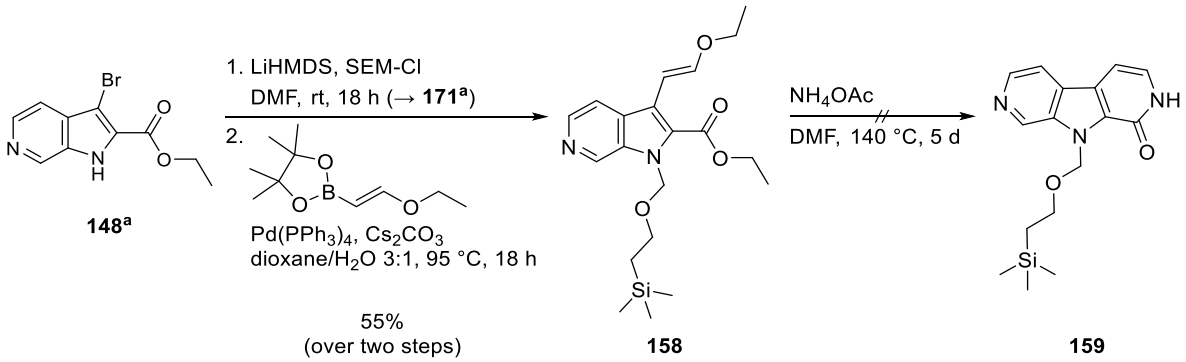

Scheme 84. Attempted synthesis of *N*-9 SEM protected pyridone **159**.

In summary, an efficient route towards 7-aza-*β*-carboline-1-one (**151[a]**) was developed, but the further functionalization of this building block turned out to be inconvenient. Therefore, it was not expanded to other azaindole carboxylates, which carry the nitrogen in another position. Instead of repeating the laborious and low yielding sequence to synthesize 7-aza analogue **144**, another more general approach towards *aza* analogues was developed.

3.3.4.2 Synthesis of *seco* analogues *via* BUCHWALD-HARTWIG *N*-arylation and 6- and 7-aza analogues from *seco* precursors

In context with another approach to the *aza* analogues, also the envisaged diarylamines, that can be seen as *seco* analogues with a cleaved ring B, were addressed. These are accessible from aminopyridine **160[b]** *via* *N*-arylation (**Scheme 85**). In contrast to the rather complex variations of ring C of the *β*-carbolines, this allows the straightforward introduction of various residues mimicking ring C from the same building block. Once again, the phenylisoxazole substituent can be introduced onto the respective bromide (**A**) *via* SONOGASHIRA cross-coupling and HUISGEN cycloaddition. As interference of the amino group was possible, also

the utilization of a nitro group as precursor of the primary amine was to be elaborated. This was carried out by LUKAS FINGER in the course of his bachelor thesis under my supervision[249].

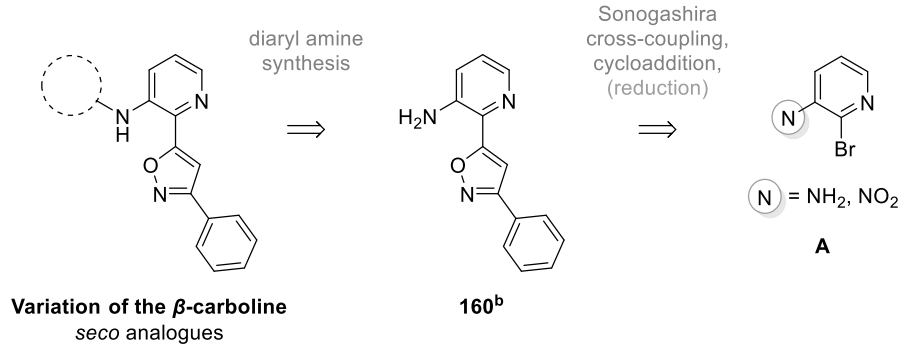

Scheme 85. Retrosynthesis of *seco* analogues from bromopyridines.

In addition, this route can also provide direct access to the envisaged 6- and 7-aza analogues (**Scheme 86**). Intramolecular HECK-like cyclization can achieve ring closure to connect ring A and ring C, if the used diarylamines are halogenated in *ortho*-position (**A**). This consequently results in construction of ring B and formation of the aza-*β*-carboline motif.

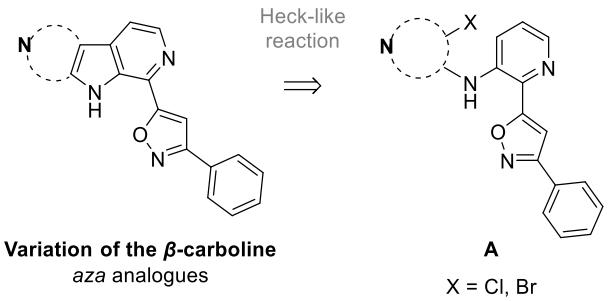

Scheme 86. Retrosynthesis of aza analogues from diarylamine intermediates.

LUKAS FINGER comprehensively investigated the synthesis of *seco* analogue **162b** and variations thereof. He described in detail the individual approaches and compared different methods. Hence, in the following his findings will be presented briefly and only the optimized reaction conditions will be depicted.

Synthesis of isoxazole **160b** was initially approached from 3-amino-2-bromopyridine and 2-bromo-3-nitropyridine, respectively. While starting from the nitropyridine requires an

additional step, because it has to be reduced to the amine at a later stage, it was assumed, that the electron withdrawing effect could be beneficial regarding the SONOGASHIRA cross-coupling. Nevertheless, it was found, that also the aminopyridine undergoes coupling with trimethylsilylacetylene efficiently as described in a patent[250] (74% yield) (**Scheme 87**). TMS-cleavage to receive arylacetylene **161^{b}** was found to work even better with potassium carbonate (99% yield) than with tetra-*n*-butylammonium fluoride[250] (70% yield).

Next, the isoxazole synthesis was investigated. Only very few examples of HUISGEN cycloaddition reactions of arylacetylenes with amino groups in *ortho*-position were found in literature, from which all use hydroxymoyl chlorides as intermediates[251-252]. However, applying the NCS/triethylamine procedure[104], gave isoxazole **160^{b}** only in low yield (28%), whereas the PIFA method[101] was again superior (66% yield). This demonstrates once more the reagent's broad applicability and compatibility with various functional groups.

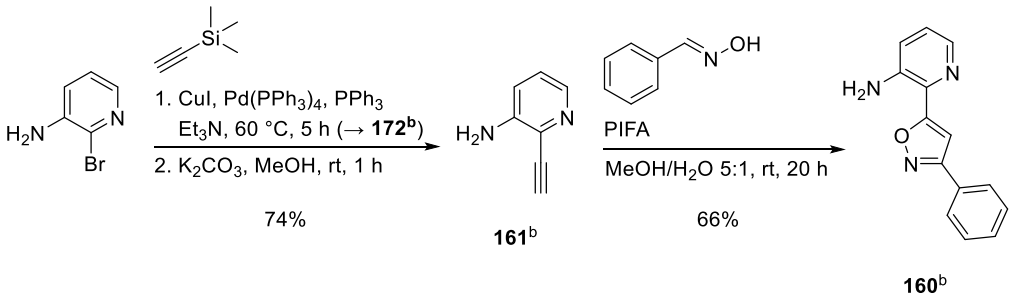

Scheme 87. Synthesis of isoxazole **160^{b}** from 3-amino-2-bromopyridine *via* SONOGASHIRA cross-coupling and HUISGEN cycloaddition.

To build up the envisaged diarylamine motif several reactions can be utilized, from which the CHAN-LAM cross-coupling and BUCHWALD-HARTWIG amination were conducted for the synthesis of *seco* analogue **162^{b}** comparatively. The copper(II)-mediated cross-coupling with phenylboronic acid, following the procedure of MAZU *et al.*[253], resulted in only slow and incomplete conversion to diarylamine **162^{b}** (28% yield). In contrast, the cross-coupling with iodobenzene under Pd(dba)$_2$/Xantphos catalysis[254] was highly efficient and gave diarylamine **162^{b}** in 86% yield (**Scheme 88**). Hence, the BUCHWALD-HARTWIG *N*-arylation was the method of choice for further *seco* compounds: pyridines **163^{b}** (57% yield) and **164^{b}** (71% yield) as well as 3-methoxy-phenyl analogue **165^{b}** (29% yield) were synthesized from respective halides.

Additionally, *ortho*-halogenated diarylamines **166^{b}** (99% yield) and **167** (90% yield) were prepared as precursors for the 7-aza-*β*-carboline **144**. In both cases, coupling took place in very good yield selectively at the iodide in 3-position, although the bromide/chloride is situated at the activated 4-position.

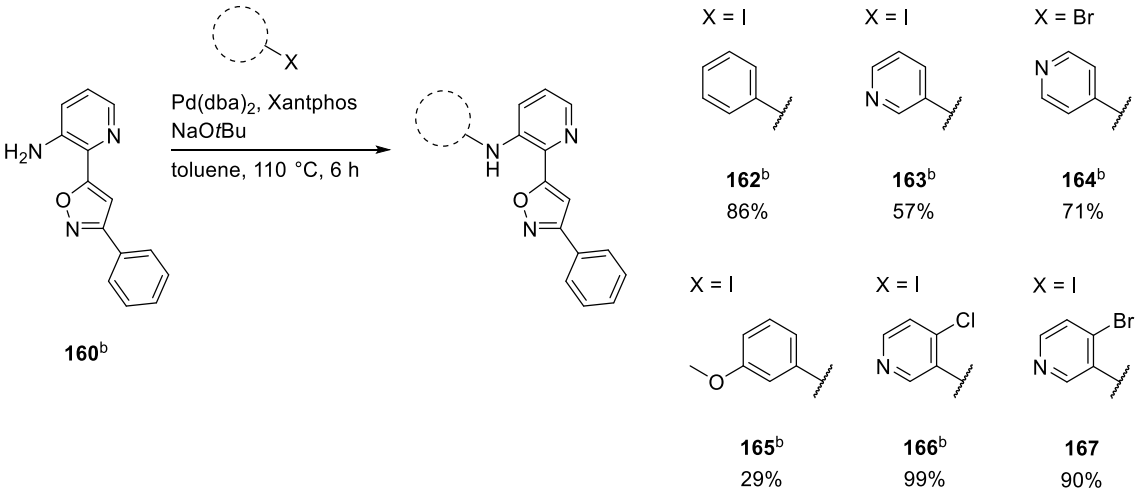

Scheme 88. Synthesis of *seco* analogues **162[b]**, **163[b]**, **164[b]**, **165[b]**, **166[b]** and **167** from aminopyridine **160[b]** *via* BUCHWALD-HARTWIG *N*-arylation.

NAMJOSHI *et al.*[255] investigated the synthesis of 3-substituted *β*-carbolines from related *seco* precursors. Initially, they attempted direct CH activation/oxidative coupling cyclization of non-halogenated diarylamines, which was without avail. However, they accomplished the synthesis *via* an intramolecular HECK-like cyclization of the respective chloride. Since the cyclization can proceed in both *ortho*-positions of their building blocks, they obtained a mixture of *β*- and *δ*-carbolines.

This approach is particularly interesting for the synthesis of 1-substituted related aza-*β*-carbolines, such as **144**, that can result in only one product. NAMJOSHI *et al.*[255] screened a few conditions, from which some resulted in no reaction, dechlorination or decomposition, and found that a combination of tri-*tert*-butylphosphonium tetrafluoroborate as ligand and potassium carbonate as base in dimethylacetamide at 120 °C gave the best results. The same conditions at slightly elevated temperature (130 °C) were actually used in a patent[256] for the synthesis of a 7-aza-*β*-carboline from a chloro precursor and seemed therefore very promising. Hence, chloride **166[b]** was subjected to the intramolecular HECK-like cyclization, but the conversion was low (**Table 13**, entry 1[b]). Starting material was still present after 24 h and besides the envisaged 7-aza-*β*-carboline **144** also extensive dechlorination occurred. The patent indicated also incomplete conversion, as it mentioned the need to recharge with an additional portion of catalyst and ligand. However, in the case of chloride **166[b]** the conversion still remained poor and the reaction was stopped after 48 h. Both products were roughly generated in a 1:1 ratio in approximately 10% yield each, but purification was impeded due to their similar chromatographic behavior. Next, more forcing conditions were applied and the reaction was run at 140 °C (**Table 13**, entry 2). Full consumption of the starting material was observed and cyclization seemed to prevail over dechlorination, but obviously also decomposition occurred and the yield was still insufficient (approx. 20%). Hence, other

conditions were tried. While sodium *tert*-butoxide in dioxane did not lead to any conversion (**Table 13**, entry 3), the exchange of the ligand by CyJohnPhos and base by DBU[257] gave comparable results (**Table 13**, entry 4, approx. 20% yield). In general, bromides are more reactive towards cross-coupling reactions than chlorides and the same was described for an intramolecular HECK-like cyclization to carbazoles, when both halides could compete[258]. Therefore, bromide **167** was subjected to the aforementioned conditions and the conversion was much improved (**Table 13**, entry 5). Only traces of debrominated side product **163[b]** were found to be present and 7-aza-*β*-carboline **144** was finally obtained in 45% yield.

Table 13. Synthesis of 7-aza analogue **144** from *ortho*-halogenated precursors **166[b]** and **167** *via* intramolecular HECK-like cyclization.

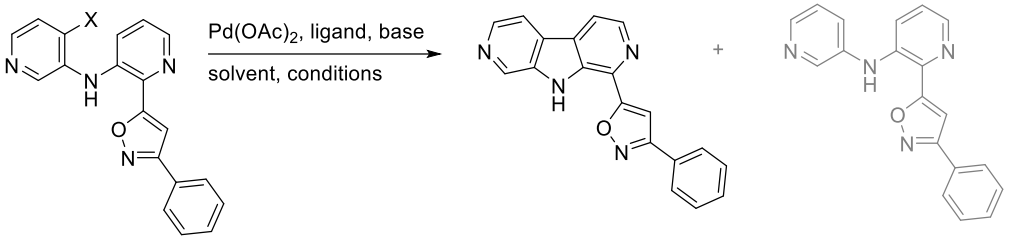

X = Cl **166[b]**
X = Br **167**

144

163[b]

entry	halide	ligand	base	solvent	conditions	observation	yield (144)
1[b]	Cl	[(*t*-Bu)$_3$PH]BF$_4$	K_2CO_3	DMA	120 °C, 48 h	low conversion	approx. 10%
2	Cl	[(*t*-Bu)$_3$PH]BF$_4$	K_2CO_3	DMA	140 °C, 40 h	full conversion	approx. 20%
3	Cl	[(*t*-Bu)$_3$PH]BF$_4$	NaO*t*Bu	dioxane	115 °C, 24 h	no conversion	-
4	Cl	CyJohnPhos	DBU	DMA	130°C, 40 h	full conversion	approx. 20%
5	Br	CyJohnPhos	DBU	DMA	130°C, 40 h	full conversion	45% isolated

([b] Reaction setup and work-up was performed by LUKAS FINGER within his bachelor thesis[249].)

With optimized conditions in hand, this straightforward approach was then also applied to the synthesis of the respective 6-aza analogue **145**. 3-Bromo-4-iodopyridine (**168**) was synthesized similar to literature[259] from 3-bromopyridine by regioselective direct ring lithiation and subsequent iodination (18% yield) (**Scheme 89**). The BUCHWALD-HARTWIG *N*-arylation with aminopyridine **160[b]** then gave *ortho*-halogenated diarylamine **169** (78% yield).

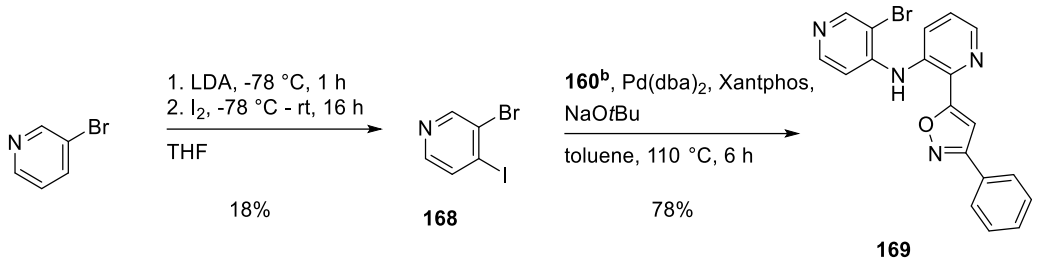

Scheme 89. Synthesis of *seco* analogue **169** from 3-bromopyridine *via* lithiation/iodination and BUCHWALD-HARTWIG *N*-arylation.

Finally, the intramolecular HECK-like cyclization was performed under the optimized reaction conditions. To a very small extent also debromination to side product **164[b]** was observed, but predominantly cyclization proceeded and 6-aza-*β*-carboline **145** was isolated in good yield (51%) (**Scheme 90**).

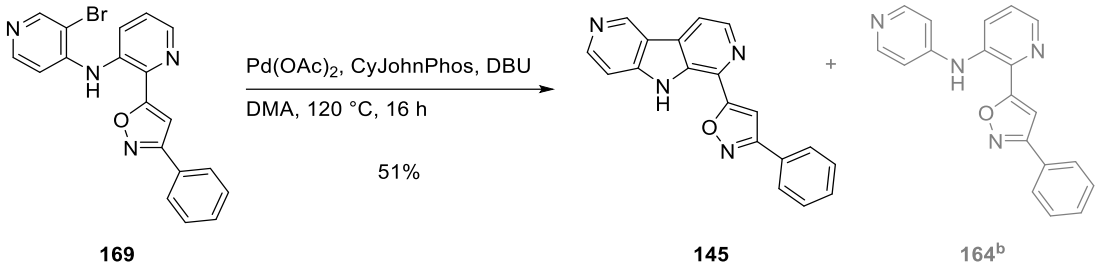

Scheme 90. Synthesis of 6-aza analogue **145** from *ortho*-halogenated precursor **169** *via* intramolecular HECK-like cyclization.

3.4 Results from biological testing

3.4.1 Reevaluation of lead structure **1** as inhibitor of CLK1 and CHIKV replication

The interest in lead structure **1** originally arose from a cooperation with the group of PROF. DR. THOMAS MEYER at the Max Planck Institute for Infection Biology (MPI, Berlin, Germany) and the group of DR. JENS PETER VON KRIES at the Leibniz-Forschungsinstitut für Molekulare Pharmakologie (FMP, Berlin, Germany), who investigated host factors as antiviral targets against IAV and CHIKV[57, 60, 63]. Prior to the beginning of this project, lead structure **1** was in that context identified as promising inhibitor of both, CHIKV replication and CLK1.

The inhibition of CHIKV replication was initially assessed at the MPI and an IC_{50} value below 30 nM was reported for lead structure **1** with an infection model using HEK-293 cells. This cell line was also used for the genome-wide loss-of-function screening that identified CLK1 as host factor[60]. Due to structural and personnel changes it was not possible to further investigate this subject at the MPI at all and it was therefore attempted to verify the anti-CHIKV activity of lead structure **1** in the group of PROF. DR. LEEN DELANG (University of Leuven, Belgium) with a different assay in Vero cells. However, this verification was not accomplished.

Therefore, the focus of this project was placed solely on kinase inhibition. However, also with respect to that, the initially available data from the enzymatic assay had to be revaluated. As already mentioned, the mobility shift assay performed at the FMP suggested a highly potent inhibitor with an IC_{50} value below 50 nM. In brief, this enzymatic assay is based on the change of the net charge of a fluorescence labelled substrate upon phosphorylation by the kinase[260]. The substrate and product have different net charges and are consequently separable by electrophoresis. By measuring the fluorescence signals respectively, the ratio of the readout of both signals, substrate and product, then draws conclusions on the enzyme activity. Generally, this method is reliable and also suitable for autofluorescent compounds, such as most of the synthesized analogues[260-262].

However, the given IC_{50} value, which corresponds to “lower than the lowest measured concentration”, has to be interpreted with caution. First, the reported data suggests only relatively low efficacy of lead structure **1**: at a concentration of 1 µM the residual activity was approx. 45%, which corresponds to only 55% inhibition and is therefore a significant but merely moderate effect. Second, to confirm the potency of lead structure **1** regardless of the low efficacy, the measurement would have to be repeated at lower concentrations. Unfortunately, this was not carried out until finalization of this thesis and therefore neither a defined numerical value could be determined nor the curve progression could be assessed. Since the mobility shift assay was furthermore no longer run regularly at the FMP, it was not a convenient test system to obtain a comparable and comprehensive set of data for the synthesized analogues in a timely manner.

Therefore, other assays were needed to closer examine the true inhibitory potential of lead structure **1** and afterwards also the synthesized analogues. In contrast to enzymatic assays, which quantify the conversion of a substrate to the corresponding product, differential scanning fluorimetry (DSF) – also known as thermal shift assay – is a binding assay, that relies on thermodynamic principles[263]. The melting temperature (T_m) which corresponds to the thermal unfolding of a protein is a characteristic property of each kinase. It is determined with the help of fluorescent dyes such as SYPRO Orange, that binds to hydrophobic regions exposed only by the unfolded protein. Since the interaction with ligands can result in stabilization of the protein and thus in higher melting temperatures, these T_m shifts are a measure for the affinity and indicate inhibitory activity, although there is no direct quantitative correlation[263-265].

The DSF experiments were run in the group of PROF. DR. STEFAN KNAPP at Goethe University (Frankfurt, Germany). CLK1 is a kinase for which also very potent inhibitors have relatively low temperature shifts – for example, the included positive control staurosporine shifts only approx. 11 °C for CLK1, but more than 23 °C for other kinases. However, the measured temperature shift of CLK1 was only 2.9 °C for lead structure **1** and is therefore only marginally significant. As already mentioned, the temperature shifts differ very much among kinases and the comparability with other assays tremendously depends on various assay parameters[266]. In spite of this, a very rough approximation indicates that T_m shifts of greater than 4 °C measured at an inhibitor concentration of 10 µM usually correspond to more than 50% inhibition of kinase activity at an inhibitor concentration of 0.5 µM[265-266]. Although this categorization includes a notable number of false-positives and false-negatives[265], which seem to be particularly relevant for those “low shifting kinases”, this matches the relatively low efficacy of lead structure **1** observed in the mobility shift assay.

Additionally, a radiometric assay was performed at Reaction Biology Europe GmbH (Freiburg, Germany), since radiometric assays are generally seen as gold standard of enzymatic assays. The basis of the ^{33}PanQinase assay is the transfer of ^{33}P-phosphate from radioisotope-labelled ATP to the kinase substrate. The incorporation of ^{33}P is then quantified with a microplate scintillation counter and provides insight into the extent, to which kinase activity is reduced in the presence of an inhibitor[267-268].

Lead structure **1** was tested at a concentration of 1 µM and the residual activity of CLK1 was determined as 42%, which corresponds to 58% inhibition. In general, compounds which cause inhibition greater or equal to 40% are – like lead structure **1** – categorized as moderate inhibitors and compounds which cause inhibition greater or equal to 80% are categorized as highly potent.

Taken together all of these results it becomes apparent, that lead structure **1** has not the outstanding inhibitory properties as assumed at the beginning of this project, but is a moderate inhibitor of CLK1. However, this did not diminish the potential to develop highly potent CLK1

inhibitors and investigate the structure-activity relationships of this chemotype based on the co-crystal of lead structure **1** with CLK1.

3.4.2 Evaluation of the synthesized analogues as CLK1 inhibitors

Although the aforementioned results revealed that the kinase-inhibitory and the antiviral properties of lead structure **1** were initially overestimated, the co-crystal structure with CLK1 (*cf.* **Figure 7**) still provided a rational basis to investigate this inhibitor chemotype towards CLK1. As explained in detail at the beginning of each chapter, the co-crystal structure suggested various approaches to develop advanced inhibitors with beneficial properties.

All synthesized analogues were therefore tested like lead structure **1** in the thermal shift assay (in the group of PROF. DR. STEFAN KNAPP, Goethe University Frankfurt, Germany) and in the radiometric ^{33}PanQinase (Reaction Biology Europe GmbH, Freiburg, Germany) for their CLK1-inhibitory properties. While there is no direct quantitative correlation, it was found in this study, that for the investigated inhibitor chemotype the results of both assays are generally in good agreement with each other: a temperature shift of more than 3 °C at 10 µM inhibitor concentration in the DSF roughly corresponds to equal or greater than 40% CLK1 inhibition at 1 µM inhibitor concentration. Therefore, these values were chosen as threshold to assess the inhibitory potential of all synthesized analogues as significant. Highly potent inhibitors, such as the positive control staurosporine, were expected to display more than 80% CLK1 inhibition and temperature shifts of above 6 – 7 °C.

In total, 10 analogues of lead structure **1** with a modified or replaced phenyl residue were synthesized and tested (**Figure 19**) and all results for these phenyl variations are depicted in **Figure 20**.

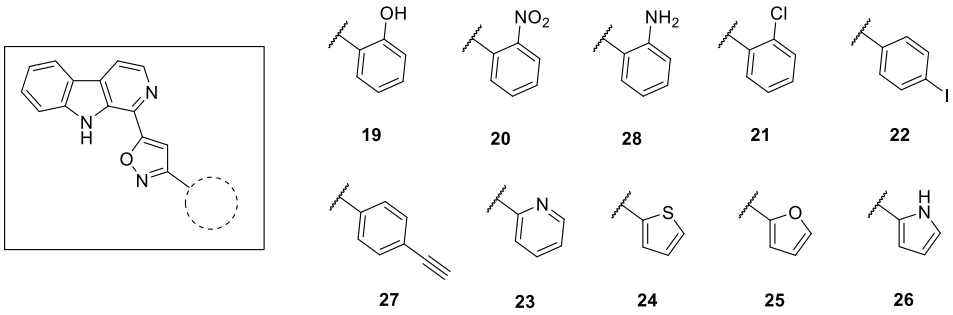

Figure 19. Synthesized analogues with a modified or replaced phenyl residue.

The four *ortho*-substituted analogues can be categorized in two groups. 2-Hydroxyphenyl analogue **19** and 2-chlorophenyl analogue **21** had no significant activity (≤ 10% CLK1 inhibition, 1.4 °C T_m shift), whereas nitro compound **20** (40% inhibition, 2.7 °C T_m shift) and

aniline **28** (41% inhibition, 2.9 °C T_m shift) were close to the limit values in both assays. In contrast to the considerations resulting from the co-crystal structure of lead structure **1** and CLK1, the electronic nature of the substituent and its ability to function as hydrogen bond donor are obviously not pivotal.

The *para*-substituted analogues, 4-iodophenyl analogue **22** and phenylacetylene **27**, showed no remarkable activity in both assays. This was particularly unfavorable, since the intention behind phenylacetylene **27** was the target identification with the Y3H system. Although the confirmation of CLK1 as target of this inhibitor chemotype was now likely to be impossible, it could still point out potential off-targets.

All of the variations for which the phenyl is replaced by heteroaromatic rings were found to be notably active in both assays. The most remarkable variation was furan **25**, which displayed the highest level of inhibition (64%) and the greatest temperature shift (5.0 °C). Whereas the other five-membered heteroarenes, thiophene **24** and pyrrole **26** (3.9 °C and 3.8 °C T_m shift), were superior to pyridine **23** (3.4 °C T_m shift) regarding the temperature shift assay, the latter demonstrated higher inhibition in the enzymatic assay (54% vs. 40 and 46%). In summary, the replacement of the phenyl residue by bioisosteric five- as well as six-membered heteroaromatic rings was shown to be tolerated or have even beneficial properties.

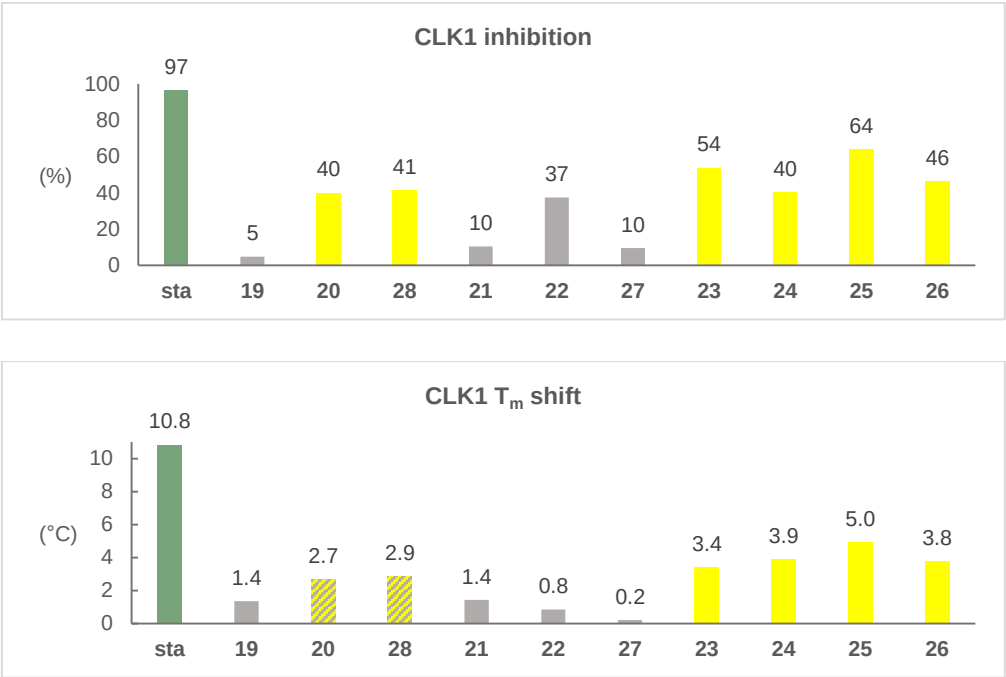

Figure 20. Results of the ^{33}PanQinase assay (top) and the thermal shift assay (bottom) for analogues with a modified or replaced phenyl residue (sta = staurosporine). Yellow bars indicate moderate inhibitors, whereas green bars indicate potent inhibitors. Shaded bars point out discrepancies between the two different assay systems.

Regarding the isoxazole unit, overall 15 analogues of lead structure **1** were investigated: 11 other disubstituted five-membered rings with additional or altered heteroatoms, the phenylacetylene analogue **51** and 3 isoxazoles, which carry a substituent in 4'-position (**Figure 21**). All results for these isoxazole variations are depicted in **Figure 22**.

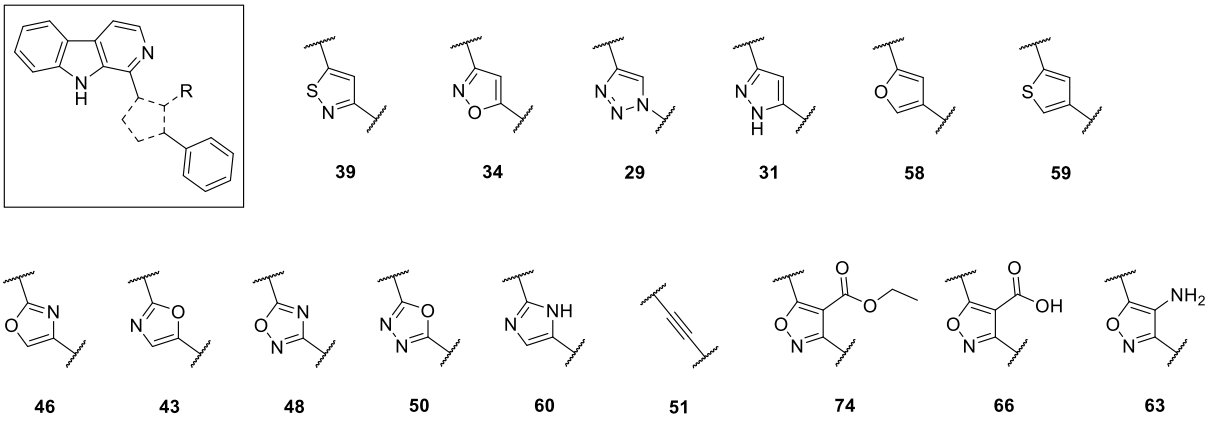

Figure 21. Synthesized analogues with a modified or replaced isoxazole unit.

First, the closely related analogues were analysed. Isothiazole **39** and isomeric isoxazole **34** showed no activity, whereas triazole **29** and pyrazole **31** displayed 57% and 47% inhibition and temperature shifts of 3.7 °C and 3.1 °C. Obviously the oxygen atom can be replaced by nitrogen to maintain kinase-inhibitory activity. This is in accordance with the observed intramolecular hydrogen bond between the NH (indole) and the oxygen (isoxazole) in the co-crystal structure of lead structure **1** and CLK1, which seems to be formable also with the nitrogen atom in this position. Although sulphur is generally also capable of acting as hydrogen bond acceptor, its divergent size and electronic properties are likely to require a different geometry.

In contrast, the isoxazole nitrogen was presumed to be dispensable. However, isomeric isoxazole **34** suggested that no exchange by oxygen was tolerated. Also omission of this heteroatom – by replacement with CH as found in furan **58**, thiophene **59**, imidazole **60** and oxazoles **46** and **43** – lead to no notable activity in the ^{33}PanQinase or in the temperature shift assay. The two oxazoles and imidazole **60** not only support the importance of *N*-2', but also point out that C-4' cannot readily be replaced by heteroatoms. This was not expectable but confirmed by the lacking activity of oxadiazoles **48** and **50**. Although the geometry of these five-membered rings is very similar, it is obviously no longer possible to acquire the needed position in the active center of the enzyme with an additional heteroatom. As last replacement of the isoxazole, phenylacetylene **51** was tested. It showed a temperature shift of 3.3 °C, but no significant CLK1 inhibition (25%).

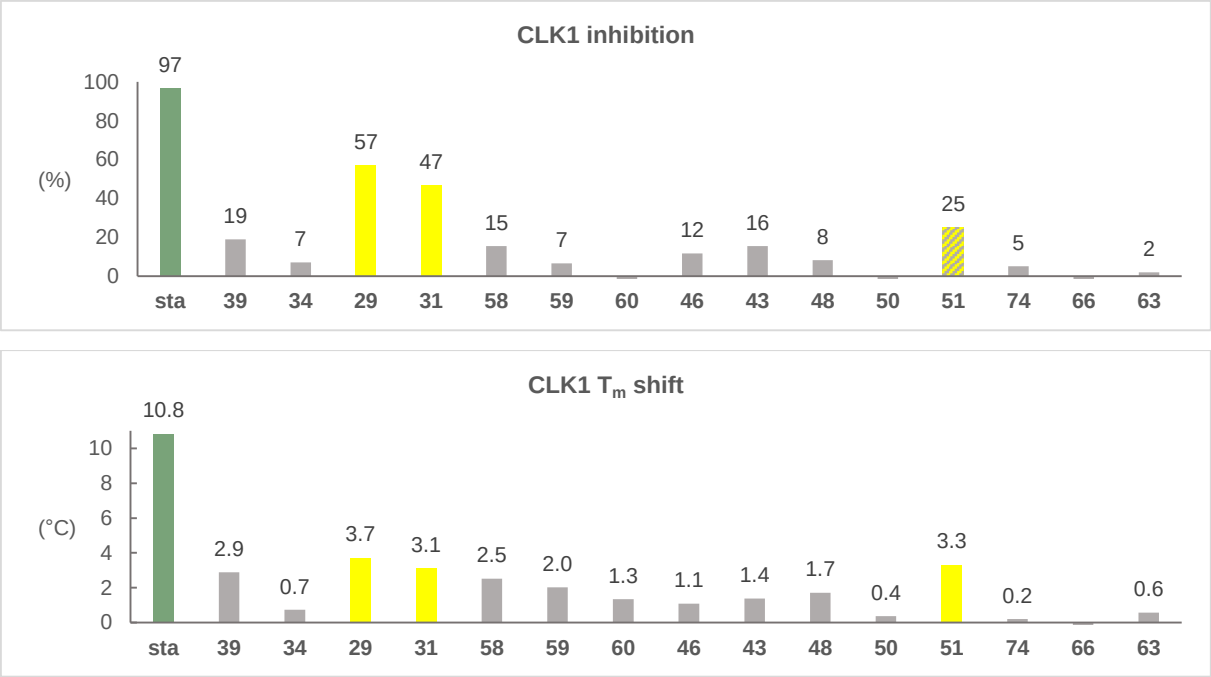

Figure 22. Results of the ^{33}PanQinase assay (top) and the thermal shift assay (bottom) for analogues with a modified or replaced isoxazole unit (sta = staurosporine). Yellow bars indicate moderate inhibitors, whereas green bars indicate potent inhibitors. Shaded bars point out discrepancies between the two different assay systems.

A very promising approach to improve lead structure **1** was according to the co-crystal structure the introduction of donor groups at C-4'. This has turned out to be of no avail for imidazole **60**, but since imidazoles can occur in two tautomeric forms and it was not assignable which form is predominant, a meaningful evaluation of this strategy could only be achieved with 4-substitued isoxazole analogues. However, the two precursors, ester **74** and carboxylic acid **66**, and likewise the envisaged very auspicious 4-aminoisoxazole **63**, displayed no activity at all in both assays. Obviously not only replacement of C-4' by heteroatoms but also substituents at C-4' are absolutely not tolerated regardless of their capability to establish hydrogen bonds.

The first class of variations of the *β*-carboline were the 8 modifications of ring A and the second class were the 6 modifications of ring B (**Figure 23**). All results for these *β*-carboline variations are depicted in **Figure 24**.

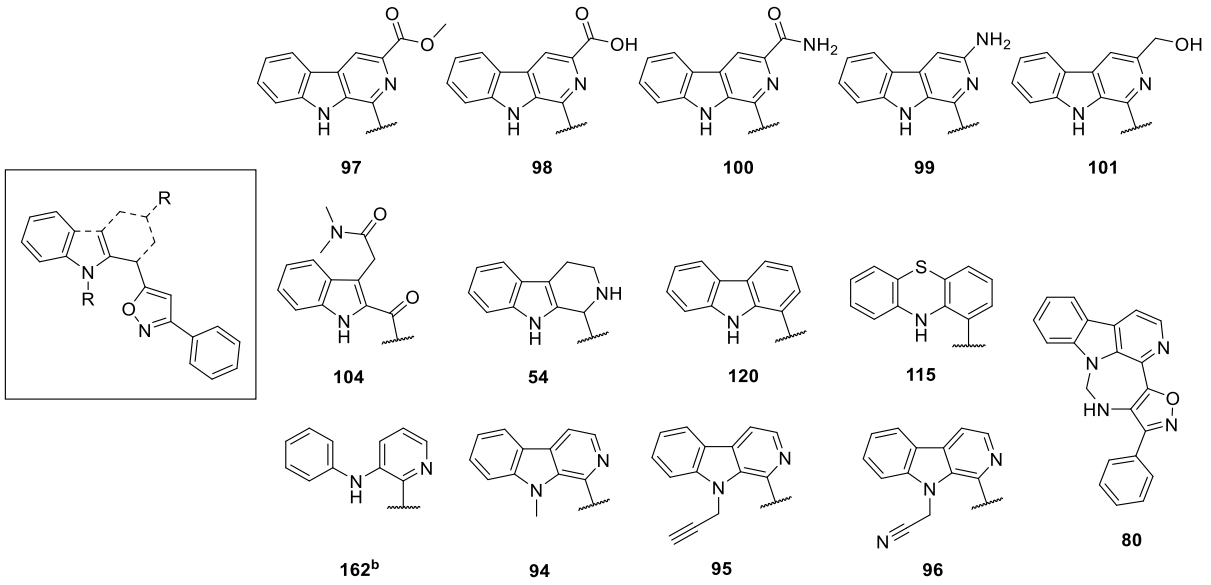

Figure 23. Synthesized analogues with a modified or substituted ring A or ring B.

None of the 3-substituted analogues, which comprise ester **97**, carboxylic acid **98**, carboxamide **100**, amine **99** and hydroxymethyl compound **101**, showed significant activity towards CLK1. Especially the last two variations mentioned seemed highly promising according to the co-crystal structure of **1** with CLK1, but fell short of expectations. Also indole **104** and tetrahydro-*β*-carboline **54** were found to be inactive. In contrast, the 2-desaza analogue, carbazole **120** showed a temperature shift below the limit value (2.5 °C), but 68% CLK1 inhibition. The relevance of *N*-2 of the lead structure therefore seems low.

Phenothiazine **115** and *seco* analogue **162[b]** indicate that no alteration of the size of ring B is allowed and the angle between ring A and ring C is not to be changed. Obviously the enhanced flexibility of the diarylamine impedes the correct orientation.

Regarding the substitution at *N*-9, in contrast to *N*-methyl derivative **94** and *N*-propargyl derivative **95**, only *N*-cyanomethyl derivative **96** turned out to be significantly active with 43% inhibition and a temperature shift of 3.7 °C. Also cyclic aminal **80**, which is “rigidized” but in an orientation at odds to lead structure **1**, displayed no activity. While this generally supports the hypothesis, that the orientation caused by the intramolecular hydrogen bond is crucial, this does not explain the exception regarding *N*-cyanomethyl derivative **96**. Most likely, a completely different orientation in the active center is adapted. This could potentially be driven by the capability of the nitrile group to function as hydrogen bond acceptor.

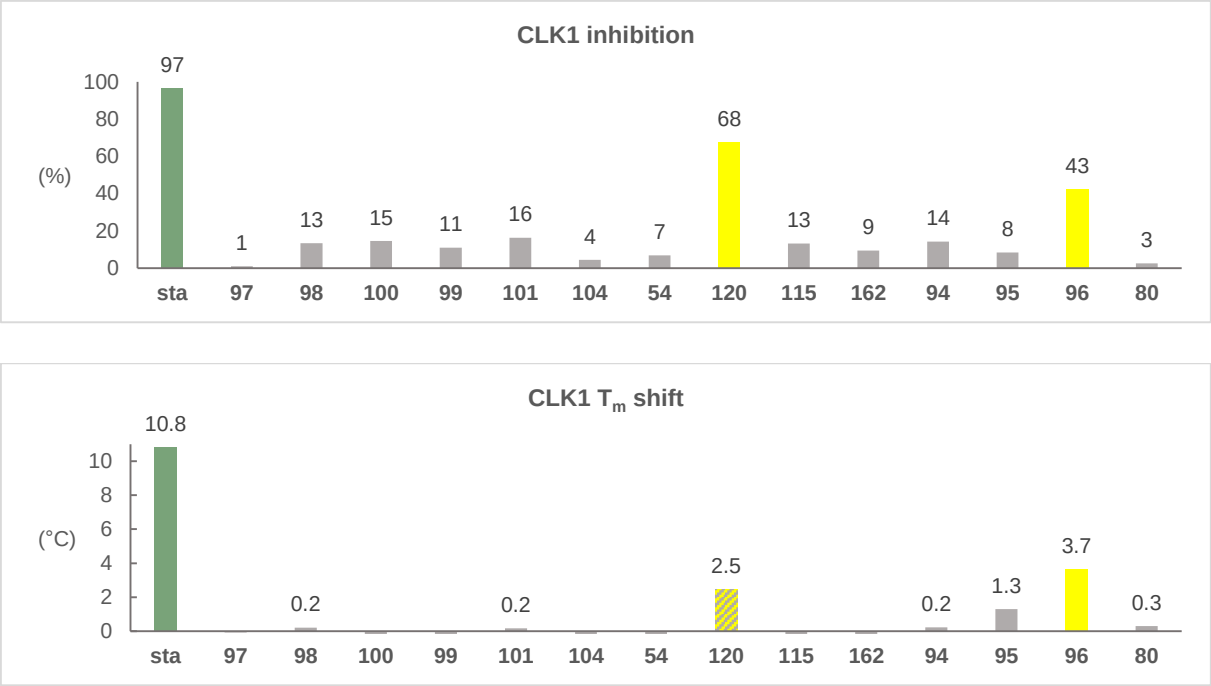

Figure 24. Results of the ^{33}PanQinase assay (top) and the thermal shift assay (bottom) for analogues with a modified or substituted ring A or ring B (sta = staurosporine). Yellow bars indicate moderate inhibitors, whereas green bars indicate potent inhibitors. Shaded bars point out discrepancies between the two different assay systems.

The final set of compounds are 15 variations of the *β*-carboline with a modified or substituted ring C, for which some are additionally ring B *seco* derivatives (**Figure 25**). All results for these variations are depicted in **Figure 26**.

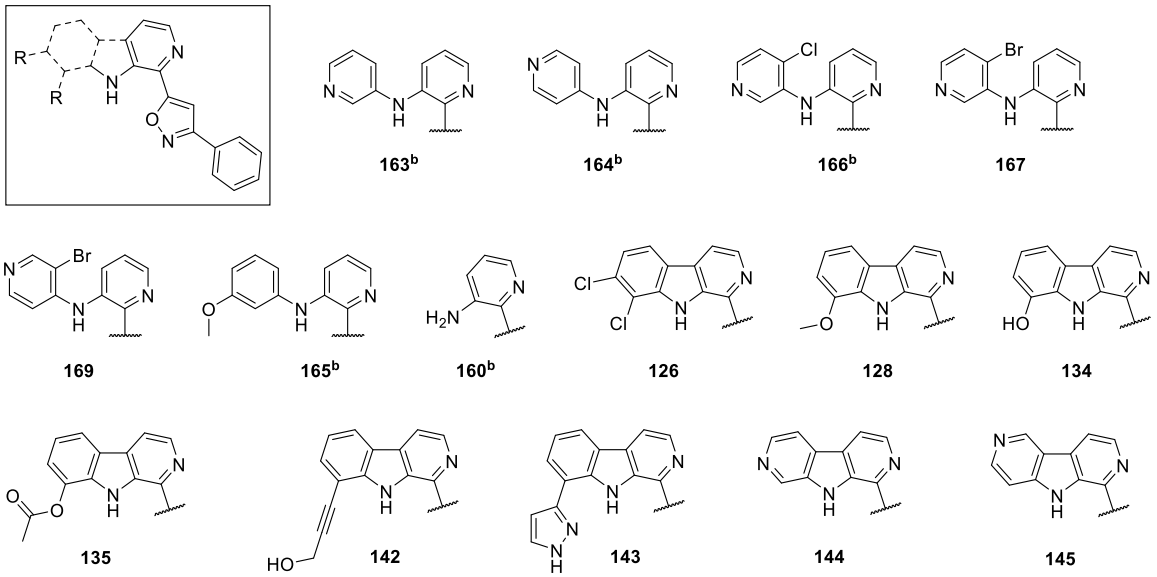

Figure 25. Synthesized analogues with a modified or substituted ring C (and in some cases additionally with a *seco* ring B).

The 6 further *seco* derivatives **163**[b], **164**[b], **165**[b], **166**[b], **167**, and **169** and their mutual precursor **160**[b] were not significantly active. Obviously the introduction of heteroatoms or substituents on the "ring C surrogate" does not facilitate to acquire the needed orientation.

Also substitution at ring C had only very limited positive impact. In contrast to 7,8-dichloro analogue **126**, 8-methoxy analogue **128**, phenol **134**, pyrazole **143** and propargyl alcohol **142**, only acetate **135** showed significant inhibition (67%) and temperature shift (3.1 °C). This was somehow surprising, since the co-crystal data suggests the introduction of hydrogen bond donor groups in a defined distance at C-8. While these analogues, namely propargyl alcohol **142** and pyrazole **143** were now found to be inactive, the acetate residue obviously enhances inhibition, although it can only act as acceptor group.

As final strategy the introduction of acceptor groups into ring C of the *β*-carboline was realized with the last subset, the two *aza* analogues. While 7-aza analogue **144** is close to but below the limit values in both assays (35% inhibition, 2.8 °C T_m shift), with 6-aza analogue **145** finally a highly potent inhibitor was created: with a temperatures shift of 6.4 °C it is the highest shifting of all synthesized compounds and with 95% inhibition it has even comparable activity to staurosporine in the radiometric assay.

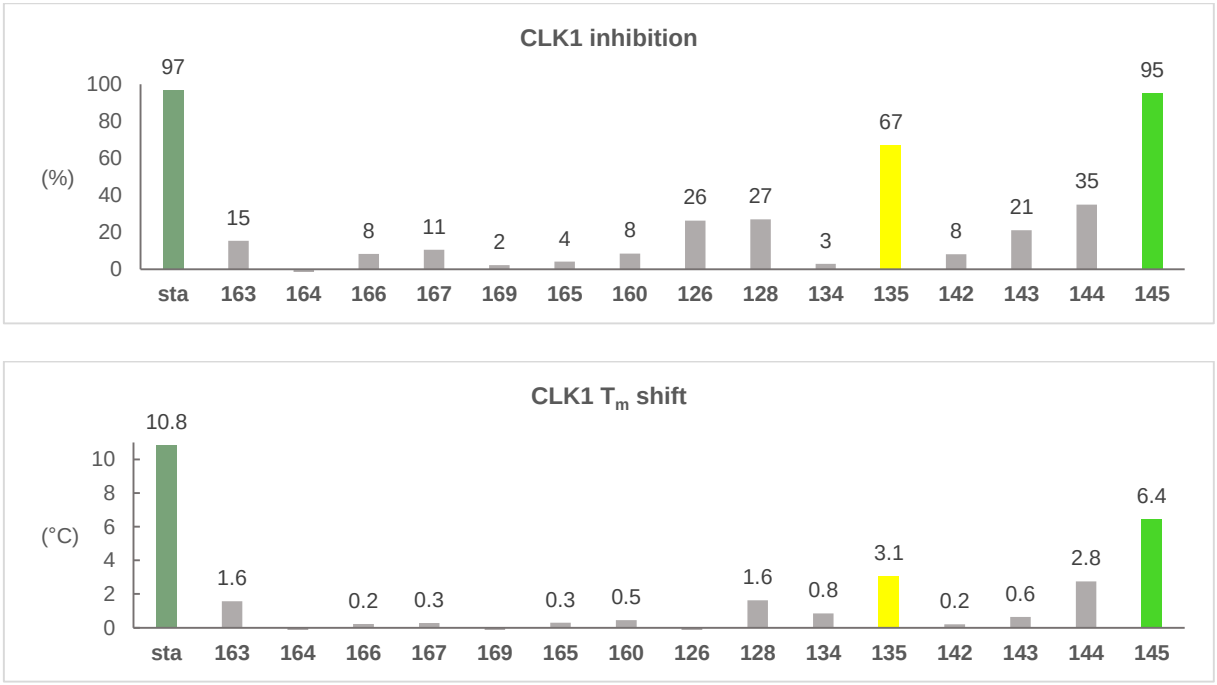

Figure 26. Results of the [33]PanQinase assay (top) and the thermal shift assay (bottom) for analogues with a modified or substituted ring C and in some cases additionally with *seco* ring B (sta = staurosporine). Yellow bars indicate moderate inhibitors, whereas green bars indicate potent inhibitors.

According to this initial testing, replacing C-6 by a nitrogen is a huge advancement of lead structure **1**. To further confirm that with 6-aza-*β*-carboline **145** indeed a really potent CLK1 inhibitor was found, the ^{33}PanQinase assay was also used to determine the IC_{50} value. Starting at a concentration of 100 µM a 10 times serial dilution was performed (up to a concentration of 3 nM) and the residual activity was then measured at each concentration, respectively. Likewise to the positive control staurosporine, which has in this assay an IC_{50} value of 52 nM, for 6-aza analogue **145** indeed an IC_{50} value of 56 nM was determined. This highlights the great potential of 6-aza analogue **145**, which should in the next step also be investigated in cellular assays such as NanoBRET.

In summary, the testing of this comprehensive set of synthesized analogues of lead structure **1** demonstrated, that only small changes are tolerated. Only very few variations have conserved or improved CLK1-inhibitory activtiy and several of the very promising variations suggested by docking experiments based on the co-crystal structure of CLK1 and **1** turned out to be entirely inactive. However, with 6-aza analogue **145** indeed a highly auspicious nanomolar inhibitor of this chemotype was developed from lead structure **1** (**Figure 27**) based on a rational drug design approach, that exhibits great potency and at the same time great efficacy.

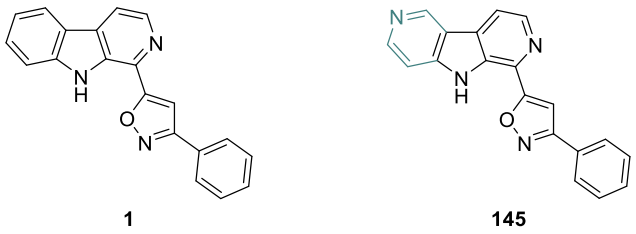

Figure 27. Structure of lead structure **1** in comparison to 6-aza analogue **145**.

3.4.3 Co-crystal structures of CLK1 with selected synthesized analogues

To evaluate whether the synthesized analogues bind in the same manner as lead structure **1**, it was attempted to obtain co-crystal structures of all final compounds with the CLK1 in the group of PROF. DR. ODED LIVNAH (The Hebrew University of Jerusalem, Israel). Previous projects have shown that already small structural alterations of ligands can cause drastic changes regarding the binding mode or a complete loss of affinity. Thus, prediction of the interactions of the synthesized analogues with the protein are difficult and experimental results are of pivotal importance.

However, co-crystallization is a highly complex and time-consuming process. No success is guaranteed even in the case of compounds, for which binding is likely according to the results from the radiometric and temperature shift assay. In total only very few co-crystal structures of synthesized ligands in complex with CLK1 were available already until finalization of this thesis. Although this generally supports the conclusion that the majority of compounds has decreased or lost inhibitory activity because the affinity to the target structure is no longer given, in several cases the co-crystallization was successful according to preliminary analysis, but the final coordinates and data were not yet provided. Encouragingly, this applies to the very promising 6-aza analogue **145**.

GIRAUD *et al.*[269] have investigated the ATP binding mode within the active centre of the CLK1 by docking experiments. They described that binding of the adenine moiety is mainly driven by two hydrogen bonds with GLU 242 and LEU 244 in the hinge region (**Figure 28**)[269]. Inhibitors acquiring similar positions can therefore be seen as ATP-competitive.

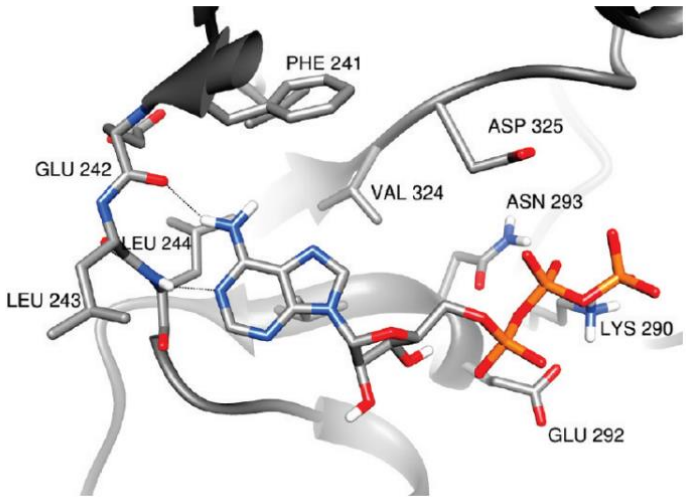

Figure 28. Docking of ATP in the ATP binding pocket of CLK1[269]. Reprinted with permission from Giraud *et al*., *J. Med. Chem*. **2011**, 54, 4474-4489. Copyright 2011 American Chemical Society.

Until finalization of this thesis a comprehensive dataset of co-crystals was only obtained for the variations of the phenyl residue and evaluated in collaboration with DR. MICHAEL MEYER (MBC-Statistik, Falkensee, Germany). Hydroxyphenyl derivative **19**, aniline **28**, pyridine **23**, furan **25** and pyrrole **26** share a binding mode that corresponds closely to the one of lead structure **1**. Superposition of the crystal data, revealed that all of these compounds are only marginally shifted within the active site of the protein (**Figure 29**).

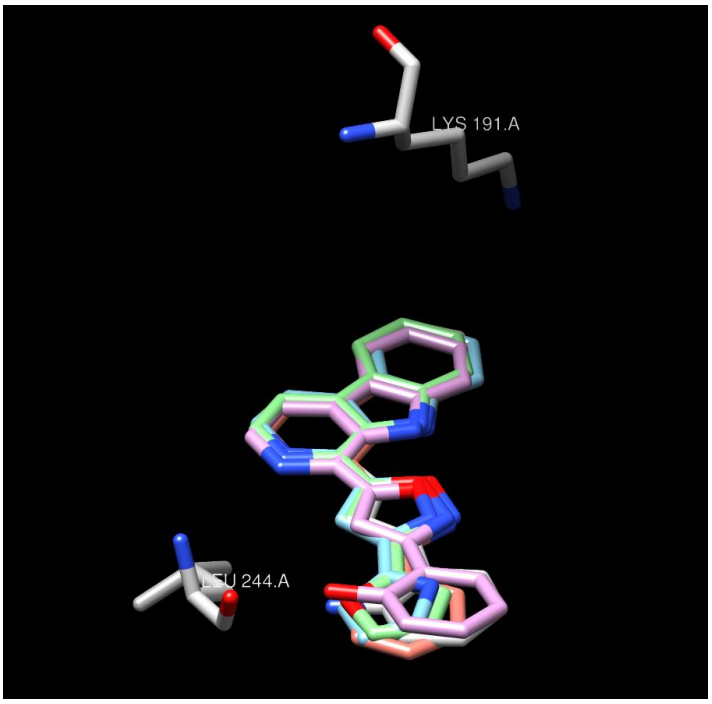

Figure 29. Superposition of hydroxyphenyl derivative **19** (rose), aniline **28** (white), pyridine **23** (orange), furan **25** (green) and pyrrole **26** (blue).

All of these analogues show the expected almost planar orientation (water molecules not shown) and establish a mutual hydrogen bond between the nitrogen of ring A and the backbone NH of LEU 244. The distance is roughly 3.2 – 3.3 Å, as exemplarily depicted for furan **25** (**Figure 30**). This ATP-mimetic hydrogen bond was not observed for lead structure **1**, for which the distance between the protein and *N*-2 is marginally greater. In addition, it should be noticed, that no interaction with LYS 191 is relevant for binding of these compounds.

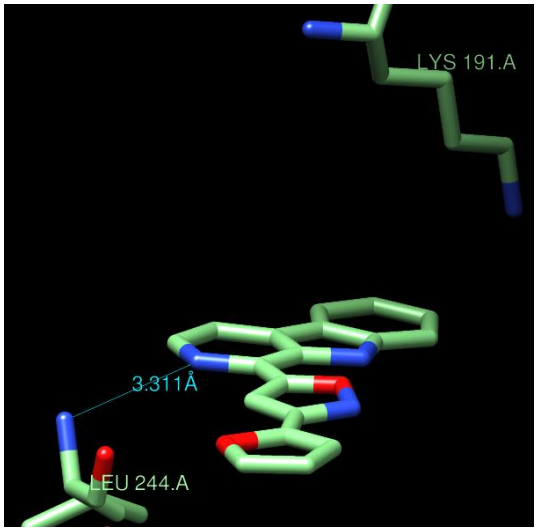

Figure 30. Furan **25** at the active site of the CLK1.

The analogues which carry donor groups in *ortho*-position, namely **19** and **28**, are capable of building an additional hydrogen bond to the same amino acid (LEU 244). Although these substituents were originally intended to form a hydrogen bond with LEU 167 or GLY 245, the co-crystal structure revealed the interaction with the backbone O of LEU 244 (**Figure 31**).

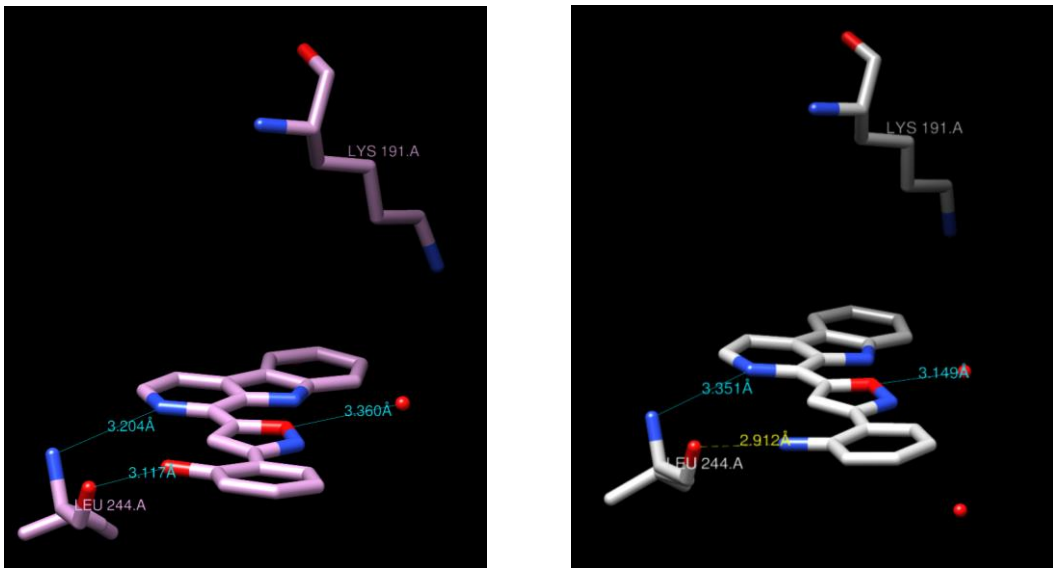

Figure 31. Hydroxyphenyl derivative **19** (left) and aniline **28** (right) at the CLK1.

Taking into account the data from the CLK1 assays, interpretation of the co-crystal structures is difficult. On the one side, several inhibitors with significant enzyme inhibition (≥ 40% in the radiometric assay) were shown to be oriented similar to lead structure **1** and establish a ATP-mimetic hydrogen bond to the hinge region. This is a rational explanation for the activity of the

variations with five-membered heterocycles: furan **25** (64% CLK1 inhibition), pyridine **23** (54% CLK1 inhibition) and pyrrole **26** (46% CLK1 inhibition).
In contrast, the introduction of donor groups in *ortho*-position allowed the formation even of an additional hydrogen bond, but this enhanced affinity is not reflected in enhanced activity. Hydroxyphenyl analogue **19** was found to be inactive (5% CLK1 inhibition), whereas aniline **28** displayed 41% CLK1 inhibition. Obviously this interaction is not detrimental for enzyme inhibition under assay conditions.

Additionally, the binding mode of pyrrole **26** was questioned, since two different co-crystal structures were reported. While both have very similar resolution (1.9 Å and 1.8 Å), one measurement revealed the “standard binding mode” as mentioned earlier (*cf.* **Figure 29**), which closely corresponds to lead structure **1** (**Figure 32**, left). In contrast, a second measurement proposed a completely different orientation, whereby the ligand is flipped (**Figure 32**, right).

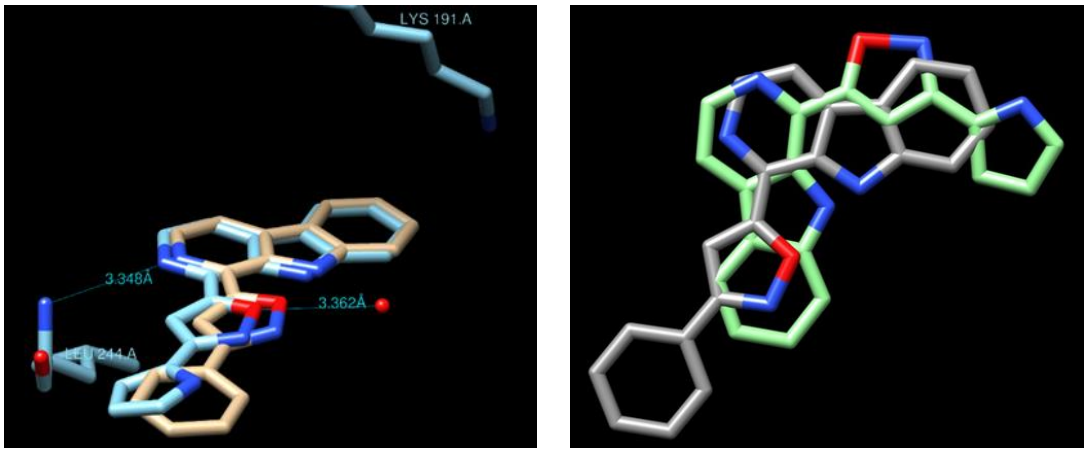

Figure 32. Superposition of lead structure **1** (beige/grey) and pyrrole **26** (blue/green) according to the standard (left) and an alternative binding mode.

The “alternative binding mode” results in the loss of the ATP-mimetic hydrogen bond of the pyridine nitrogen to LEU 244. Only nonpolar atoms are directed thereto, whereas the ligand is fixed by a single hydrogen bond from the pyrrole NH to the side chain of LYS 191 (**Figure 33**).

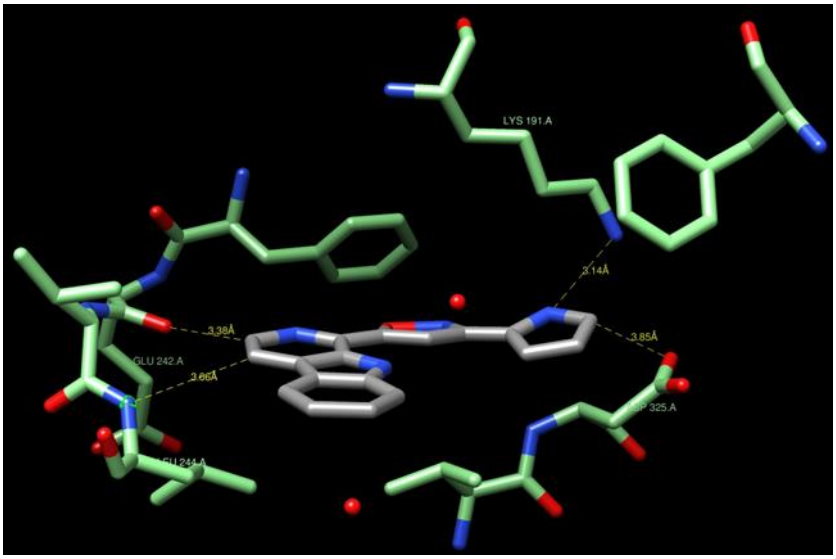

Figure 33. CLK1 (green) in complex with pyrrole **26** (grey) according to the alternative binding mode.

It remained unclear, which is the “more true” orientation, although the “standard binding mode” seems more likely, because it was observed also for the other heteroaromatic rings. However, this discrepancy highlights the importance of experimental results, as prediction of ligand properties is impossible, if already small modifications can unexpectedly cause an altered binding mode or complete loss of affinity.

Unfortunately for the variations of the isoxazole moiety and the *β*-carboline nucleus no final co-crystal data was available until finalization of this thesis. Preliminary analysis of the data however indicated, that up to now five further compounds were found to bind to CLK1: phenylacetylene **51**, diarylamines **164** and **165**, as well as *aza* analogues **144** and **145**.

It seems that phenylacetylene **51** is flipped in comparison to lead structure **1** and *N*-2 can therefore establish a single hydrogen bond with LYS 191 (**Figure 34**).

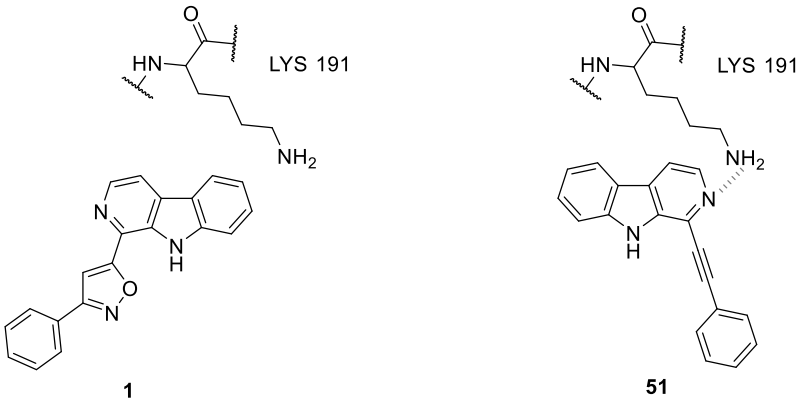

Figure 34. Illustration of the flipped orientation of phenylacetylene **51** in the active center of CLK1 in comparison to lead structure **1**. This enables the formation of a hydrogen bond (dotted line) between *N*-2 and LYS 191 (according to preliminary results).

For 7-aza analogue **144** and 6-aza analogue **145** it was reported that binding occurs in a similar but not identical mode as furan **25**. While this suggests the formation of a hydrogen bond between *N*-2 and LEU 244, it is purely speculative that the strategy to establish an additional hydrogen bond with LYS 191 was possibly fulfilled (**Figure 35**). However, this would be in agreement with the observations for phenylacetylene **51**.

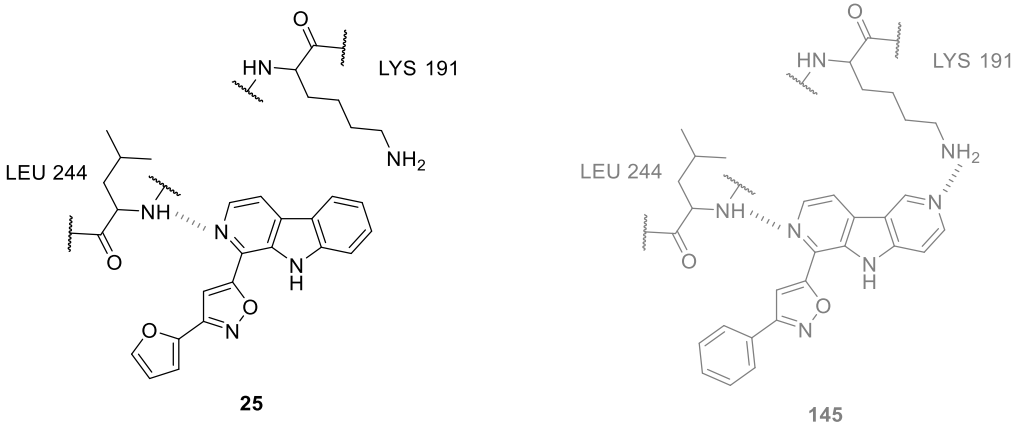

Figure 35. Illustration of the orientation of furan **25** in the active center of CLK establishing a ATP-mimetic hydrogen bond (dotted line) to LEU 244. A similar binding mode of 6-aza analogue **145** (according to preliminary result) could potentially be capable of forming an additional hydrogen bond between *N*-6 and LYS 191.

In summary, final interpretation is yet impossible and it is especially of interest, if the greatly enhanced inhibitory activity of 6-aza analogue **145**, but not 7-aza analogue **144**, will be explainable on the basis of the co-crystal structures. Moreover, further co-crystal structure data will hopefully be obtainable for several more of the synthesized analogues.

3.4.4 Kinase selectivity profiling of the synthesized analogues

Since the structure of the ATP-binding pocket is highly conserved among different families of kinases, selectivity of kinase inhibitors is a main issue. Although in some cases inhibition of several kinases has an additive effect, kinase inhibitors with a certain level of selectivity are pursued. Not only more specific drugs with less adverse effects are striven for, but also chemical tools which help to unravel signal transduction pathways and general relevance in biological contexts.

To investigate the spectrum of targeted kinases of the herein described inhibitor chemotype, DSF experiments were conducted in the group of PROF. DR. STEFAN KNAPP at the Goethe University Frankfurt for all final compounds towards a panel of more than 100 kinases of different subfamilies. In total 23 kinases shifted significantly (≥ 3.0 °C) due to one or more compounds at a concentration of 10 µM (**Table 14**). Although all synthesized analogues are closely related, the targeted kinases and the selectivity observed was very distinct. As expected, the highest number of compounds (10 in total) caused a shift in the melting temperature of CLK1, but also other kinases were influenced repeatedly, such as AAK1, BMP2K, CAMKK2, DYRK and PIM kinases.

The selectivity of 6-aza analogue **145** was clearly of highest interest. **145** was found to have a moderate impact on the melting temperature of some kinases (BMP2K, CSNK1D, CLK3, PIM3, STK17A, ULK3), but exhibited a temperature shift of more than 5 °C besides CLK1 for only further 3 kinases: CAMKK2 (7.8 °C T_m shift), DYRK1A (5.4 °C T_m shift) and DYRK2 (5.5 °C T_m shift). Three further compounds were found to have also high shifts for CAMKK2: pyrazole **31** (7.5 °C T_m shift), acetylene **51** (6.7 °C T_m shift) and furan **58** (7.0 °C T_m shift), of which the latter was even entirely selective among all kinases tested. Several other compounds additionally had moderate effects on the melting temperature of CAMKK2. However, as highlighted by the positive control staurosporine (23.6 °C T_m shift), this kinase generally displays much greater shifts than e.g. CLK1 and the threshold values are therefore presumably not suitable. This was further investigated and confirmed with the ^{33}PanQinase assay (Reaction Biology Europe GmbH, Freiburg, Germany). A small selection of 8 compounds, which are according to the temperature shift assay potential inhibitors of CAMKK2 (**1**, **25**, **26**, **29**, **31**, **51**, **58**, **145**), was tested for their inhibition with this assay. However, only 6-aza analogue **145** was found to show significant activity at a concentration of 1 µM (76% inhibition), whereas all others were below the limit value of 40% inhibition. In addition, also the inhibitory properties of **145** towards DYRK1A and DYRK2 were assessed with the ^{33}PanQinase assay (Reaction Biology Europe GmbH, Freiburg, Germany). Contrary to the DSF results, it was found, that DYRK1A (93% inhibition) is much more impacted than DYRK2 (51% inhibition).

Table 14. Results of the DSF selectivity profiling (sta = staurosporine). In total all final compounds were tested against a panel of 104 kinases at a concentration of 10 µM. (Values between 3.0 °C and 3.9 °C are marked in yellow, values between 4.0 °C and 5.9 °C in orange and values ≥ 6.0 °C in red.)

	sta	1	20	23	24	25	26	29	31	39	51	58	59	96	98	101	115	120	128	135	145	160	163	164
AAK1	12.9	2.8	1.1	2.7	4.4	4.3	7.9	3.0	4.7	1.5	3.3	2.8	1.0	1.1	0.0	0.3	-0.3	0.8	3.3	2.5	2.9	0.8	0.4	0.2
BMP2K	18.2	1.4	0.9	2.3	3.3	5.0	3.8	1.1	3.8	1.9	3.8	2.2	1.2	0.6	-0.1	0.5	1.6	0.7	2.2	1.1	3.9	1.4	0.4	0.6
CAMKK2	23.6	3.7	0.7	2.4	5.6	5.5	5.7	3.2	7.5	2.3	6.7	7.0	2.2	1.0	0.2	0.3	0.5	1.3	2.7	2.5	7.8	1.3	1.7	0.5
CAMK1D	10.5	-1.6	-0.9	-1.7	-1.7	-1.2	-1.5	-1.7	-1.8	-0.7	-1.1	-1.8	0.2	-4.2	-0.7	0.8	1.7	0.8	1.3	1.0	1.6	3.1	-0.9	1.2
CSNK1D	1.7	1.0	0.1	1.6	0.9	1.3	2.6	0.3	0.6	0.1	0.2	0.2	-0.1	-0.7	0.7	3.8	0.3	1.0	0.5	1.8	4.1	0.1	3.1	3.5
CSNK1E	1.6	n.d.	n.d.	n.d.	n.d.	n.d.	n.d.	n.d.	n.d.	n.d.	n.d.	n.d.	n.d.	n.d.	-0.1	2.7	0.9	n.d.	-0.2	0.6	2.8	0.1	3.3	3.2
CSNK2A1	3.7	0.1	0.6	0.4	0.5	1.3	0.8	0.3	1.9	1.6	2.4	0.9	1.2	-0.1	5.3	0.2	-0.4	1.2	0.3	0.2	1.4	0.6	0.3	0.6
CSNK2A2	4.2	0.4	1.0	0.8	1.1	1.9	1.3	0.4	2.2	1.8	2.4	1.0	1.4	-0.1	4.2	0.8	0.0	1.4	0.4	0.3	2.1	0.9	-0.2	0.7
CHEK2	16.6	0.1	0.3	0.1	0.3	0.6	1.1	0.3	1.5	2.0	0.6	1.1	1.5	0.4	-0.4	-0.1	3.0	1.7	0.6	-0.6	0.8	0.8	0.5	0.0
CLK1	10.8	2.9	2.7	3.4	3.9	5.0	3.8	3.7	3.1	2.9	3.3	2.5	2.0	3.7	0.2	0.2	-0.4	2.5	1.6	3.1	6.4	0.5	1.6	0.3
CLK3	4.7	1.0	0.6	0.9	1.1	1.7	1.7	1.4	1.7	0.8	0.9	0.9	0.7	1.1	0.7	0.1	0.0	0.6	0.6	1.1	4.0	0.1	0.7	0.2
DCAMKL1	11.4	1.0	1.4	1.2	1.6	1.5	1.7	0.8	3.1	1.9	2.2	0.7	1.9	0.5	-1.3	1.3	-0.6	1.5	-0.1	-0.4	1.2	-0.9	-0.3	-0.4
DYRK1A	10.7	0.2	0.9	0.8	1.8	2.1	2.1	1.8	3.8	3.4	2.9	1.7	2.8	-1.4	2.7	-0.7	-1.5	2.6	1.9	2.3	5.4	-0.2	1.1	1.1
DYRK2	6.9	1.2	3.5	2.2	2.2	2.4	3.4	1.7	2.1	1.0	3.6	1.8	0.5	1.1	0.4	0.9	0.1	0.2	1.6	1.6	5.5	0.2	0.4	0.4
MAPK10	7.4	-0.9	0.4	-0.8	-0.6	-0.9	-0.2	-0.9	0.6	1.4	0.3	-0.8	0.4	n.d.	1.6	-0.1	0.5	0.1	1.8	1.2	2.1	2.1	3.1	1.3
MST3	9.2	1.4	0.6	0.8	1.4	1.1	1.9	1.1	3.6	2.5	2.0	2.1	3.2	0.4	0.5	1.5	1.1	3.3	0.5	0.9	0.1	0.5	-0.3	0.6
PIM1	12.0	1.1	2.6	0.9	1.5	2.8	2.6	0.2	2.5	3.7	2.4	0.7	3.6	-0.6	2.3	-0.1	-0.6	1.9	0.7	0.4	-0.4	0.9	0.5	-0.1
PIM3	17.9	0.8	3.4	1.8	1.9	2.7	3.4	0.5	3.4	6.0	3.5	1.6	2.7	0.4	1.1	0.4	0.5	4.8	0.6	1.2	3.1	0.8	0.7	0.4
STK17A	11.7	-0.1	3.5	0.5	0.5	1.3	1.3	0.3	2.4	2.1	3.0	0.6	1.2	-0.7	0.9	-0.6	0.3	2.5	-0.1	-0.4	4.4	0.5	0.5	-0.9
TOPK	5.8	0.0	0.1	0.1	0.2	1.7	2.4	-0.5	1.2	1.7	3.3	0.9	1.2	-1.7	n.d.	n.d.	n.d.	0.8	n.d.	n.d.	n.d.	n.d.	n.d.	n.d.
TTK	9.1	1.2	0.4	0.4	0.6	0.7	1.1	0.6	2.3	2.4	1.5	0.8	2.2	-2.6	0.5	0.5	0.2	3.0	0.4	1.8	1.6	0.8	1.3	0.8
ULK1	11.3	0.1	0.8	0.1	0.5	1.1	0.7	0.0	1.3	1.6	1.0	0.0	1.0	-0.1	0.4	-0.1	-1.5	1.4	-0.1	-0.4	1.6	0.6	0.1	-0.6
ULK3	17.7	1.9	1.0	2.2	3.9	3.7	4.5	1.4	2.8	0.8	3.3	1.5	0.4	0.9	0.4	-0.2	0.4	-0.2	1.7	1.7	4.3	0.5	0.3	0.0

To sum it up, this first selectivity profiling showed that 6-aza analogue **145** is no broad spectrum protein kinase inhibitor like staurosporine, but targets only few kinase families. As next step to deeply study the potential of 6-aza analogue **145** also further selectivity profiling should be performed. Especially the subtype selectivity towards all CLK and DYRK isoforms has to be comprehensively assessed.

Additionally, the temperature shift assay indicated two other potent and relatively selective inhibitors: isothiazole **39** for PIM3 (6.0 °C T_m shift) and pyrrole **26** for AAK1 (7.9 °C T_m shift). Further investigations should be carried out in the future to confirm these results with enzymatic assays. Besides that, for all other kinases only moderate inhibitory activity could be assumed according to the temperature shift assay. For example, BMP2K was targeted by furan **25** (5.0 °C T_m shift) and PIM3 by carbazole **120** (4.8 °C T_m shift). Remarkably, carboxylic acid **98** was found to be entirely selective towards CSNK2A1 (5.3 °C T_m shift) and CSNK2A2 (4.2 °C T_m shift), for which none of the other synthesized analogues displayed any temperature shift at all.

In summary, the selectivity profiling helped not only to characterize the newly synthesized CLK1 inhibitors, but unraveled also other (potentially even more) affectable targets. Several of the mentioned kinases are considered as important for various biochemical processes and linked to several diseases, especially tumors (**Table 15**).

Table 15. Relevance of the kinases for which notable temperature shifts were observed with DSF.

Kinase	Relevance
AAK1 (Adaptor-associated kinase 1)	Involved in clathrin mediated endocytosis. Inhibitors could be relevant for treatment of neuropathic pain, schizophrenia and Parkinson's disease[270].
BMP2K (BMP-2-inducible protein kinase)	Involved in osteoblast differentiation and clathrin mediated endocytosis; relevant as host factor for HIV[271].
CAMKK2 (Ca^{2+}/calmodulin-dependent protein kinase kinase 2)	Involved in regulation of CAMKs and other kinases and therefore in inflammation, cell proliferation, cell survival etc.; overexpressed in several tumors, e.g. gastric and prostate cancer[272-273].
CAMK1D (Ca^{2+}/calmodulin-dependent protein kinase 1D)	Associated with diabetes; overexpression relevant for e.g. breast cancer[274-275].
CSNK1D and CSNK1E (Casein kinase I isoform δ and Ɛ)	Involved in cell cycle and neuronal processes, e.g. neurotransmitter signaling, and relevant for Alzheimer disease and several tumors, e.g. blood cancer[276-277].
CSNK2A1 and CSNK2A2 (Casein kinase II subunit α and α')	Involved in cell cycle, division, apoptosis, tumorigenesis; overexpressed in several tumors[278].
DYRK (Dual specificity tyrosine-phosphorylation-regulated kinase)	**1A**: Involved in neuronal development and cell cycle control; inhibition e.g. relevant for tumors, Down syndrome, Alzheimer disease[54, 279]. **2**: Involved in cell survival, cancer stem cell formation and metastasis[279-280].
PIM1 and PIM 3 (Serine/threonine-protein kinase Pim-1 and Pim-3)	Involved in cytokine signaling, promote cell growth, proliferation, survival and migration; relevant for P-glycoprotein mediated drug resistance and overexpressed in several tumors[281].

3.4.5 MTT assay

Subsequent characterisation of the synthesized compounds with cellular assays is only feasible, if the relevance of unspecific cytotoxicity is known. Therefore, all final compounds were tested routinely in a MTT assay by MARTINA STADLER in our group for their cytotoxic effects towards HL-60 cells.

Basis of this assay developed by MOSMANN[282] is the metabolic activity of living cells, which is necessarily required to reduce 3-(4,5-dimethylthiazol-2-yl)-2,5-diphenyltetrazoliumbromide (MTT) to the respective formazan (**Scheme 91**).

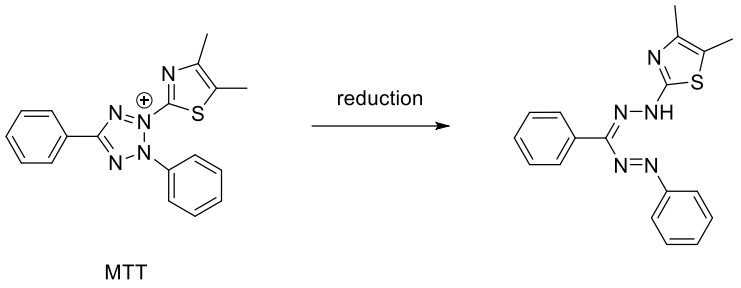

Scheme 91. Reduction of MTT to a blue formazan derivative by metabolically active cells.

Early considerations directly linked this reaction to the presence of active mitochondria, but it was described later, that also extramitochondrial reduction occurs[283]. However, NADH and NADPH were found to be crucial[283]. The reductive cleavage of MTT's tetrazolium ring generates a formazan derivative with an intense blue color, of which the absorbance can be measured photometrically at 570 nm[282]. Since the amount of generated formazan is directly proportional to the number of metabolically active cells, the MTT assay allows to draw conclusions on cell viability. Thus, if cytotoxicity is determined, no information about the responsible mode of action is gained.

All final compounds were tested initially at a single concentration (100 µM) and, if cytotoxicity was observed, IC_{50} values were determined. As positive control the detergent Triton X-100 was used, which causes total cell lysis.

Substances, which exhibit IC_{50} value of ≤ 5.0 µM are classified as highly cytotoxic, comparable with the chemotherapeutic agent cisplatin. Although CLK inhibition is also linked to strong antitumor activity against several cancer cell lines, this was generally not relevant in HL-60 cells, which made it a suitable cell line for cytotoxicity testing. The very potent CLK1/4 inhibitor indole KH-CB19 for example had an IC_{50} value of approx. only 30 µM in this MTT assay[46], which corresponds to weak activity.

Table 16. Results of the MTT assay. (Compounds which displayed moderate/strong cytotoxic effects are marked in light orange/orange.)

Compound	IC_{50} (µM)
1	> 100
19	15
20	> 100
21	> 100
22	10
23	> 100
24	> 100
25	> 100
26	> 100
27	> 100
28	> 100
29	> 100
31	46
34	> 100
39	> 100
43	> 100
46	> 100
48	> 100
50	> 100

Compound	IC_{50} (µM)
51	12
54	> 100
58	44
59	> 100
60	> 100
63	> 100
66	> 100
74	> 100
80	> 100
94	> 100
95	> 100
96	> 100
97	3.5
98	16
99	> 100
100	> 100
101	> 100
104	> 100
120	> 100

Compound	IC_{50} (µM)
115	> 100
126	> 100
128	> 100
134	> 100
135	> 100
142	> 100
143	> 100
144	> 100
145	> 100
160[b]	> 100
162[b]	> 100
163[b]	> 100
164[b]	> 100
165[b]	> 100
166[b]	> 100
167	> 100
169	> 100

Of all final compounds only five exhibited noteworthy cytotoxicity. For phenol **19**, iodide **22**, acetylene **51** and carboxylic acid **98**, IC_{50} values indicated moderate effects. The corresponding methyl ester **97**, in contrast, was found to have comparable cytotoxicity to cisplatin. As already mentioned, no conclusions regarding the mechanism can be drawn. However, antitumoral activity towards several cancer cell lines of β-carbolines in general and especially related 3-alkoxycarbonyl-β-carbolines were reported in literature[284-286].

Regarding the future investigation of the synthesized compounds as kinase inhibitors in cellular assays, the cytotoxicity was considered as unproblematic. Whereas cytotoxic ester **97** was found to have no affinity to any of the investigated kinases by DSF, all potential inhibitors were evaluated as only moderate or nontoxic.

3.4.6 Agar diffusion assay

Additionally, all final compounds were tested routinely by MARTINA STADLER in our group for their antimicrobial effect towards several model germs in the agar diffusion assay.

This qualitative assay is based on the formation of zones of growth inhibition. Therefore, test platelets are impregnated with a solution of the compound and placed on agar plates, which contain appropriate growth medium and are incubated with a selected germ. The applied

compound can then diffuse into the medium and inhibit growth of the germ. If zones of inhibition are then present after incubation, antimicrobial effects are determinant.

None of the tested compounds showed any noteworthy antimicrobial effect towards the investigated bacteria (*Escherichia coli*, *Pseudomonas marginalis*, *Straphylococcus equorum*, *Streptococcus entericus*) and fungi (*Yarrowia lipolytica*, *Saccharomyces cerevisiae*). As positive control, tetracycline as broad-spectrum antibiotic and clotrimazole as broad-spectrum antifungal agent were included in all experiments.

3.4.7 Yeast three-hybrid screening with arylacetylene **27**

The Y3H system is a method to identify targets of small molecules, that is intensively investigated in the group of DR. SIMONE MOSER (Pharmaceutical Biology) at our department[103, 287]. In brief, small molecules of interest (such as **27**) are coupled through a linker to trimethoprim based probes (*via* click chemistry or amide coupling), and these combined probes are then responsible for binding to two proteins that are needed to cause transcription of a reporter gene[103]. First, the trimethoprim subunit binds to the anchor protein, the enzyme dihydrofolate reductase, that is fused to the DNA binding domain of a split transcription factor. Second, a variety of potential targets each coupled to the activation domain of the same transcription factor is available for the small molecule subunit to interact with and only if the small molecule binds to one of these potential targets, activation of the reporter gene transcription takes place and the yeast survives. Subsequently, the respective target is then identifiable by DNA sequencing[103].

Although arylacetylene **27** was shown to have no significant CLK1-inhibitory activity, the Y3H screening could still be useful to identify potential off-targets of the herein investigated inhibitor chemotype. Unfortunately, no final results were available until finalization of this thesis, since the experiments could only be started with a delay of several months. Nevertheless, preliminary results indicated quinone reductase 2 (NQO2) as interesting target, which is however not yet validated.

NQO2 is a flavoenzyme highly expressed in liver and kidney cells, that utilizes not NAD(P)H but less common reducing equivalents, such as *N*-ribosylnicotinamide. Its involvement in reducing catechol quinones links it to neurotransmitter homeostasis and therefore neurodegenerative diseases[288]. Furthermore NQO2 could be implicated in drug metabolism (as a toxifying as well as a detoxifying enzyme[289]) and is considered as potential (off-)target of melatonin, resveratrol and some licensed drugs like chloroquine and imatinib, which suggests also a role in malaria and cancer[289-291].

4 Summary

The screening of a substance library, containing various compounds from the BRACHER group which are derived from natural products, identified *β*-carboline **1** as inhibitor of the protein kinase CLK1 and as promising candidate for further development. By co-crystallization with the target enzyme, the orientation of the ligand within the ATP-binding pocket was revealed and it was found that no direct hydrogen bonds to the protein, but several short distances between donor or acceptor groups of the protein and nonpolar atoms of the ligand are existent (**Figure 36**).

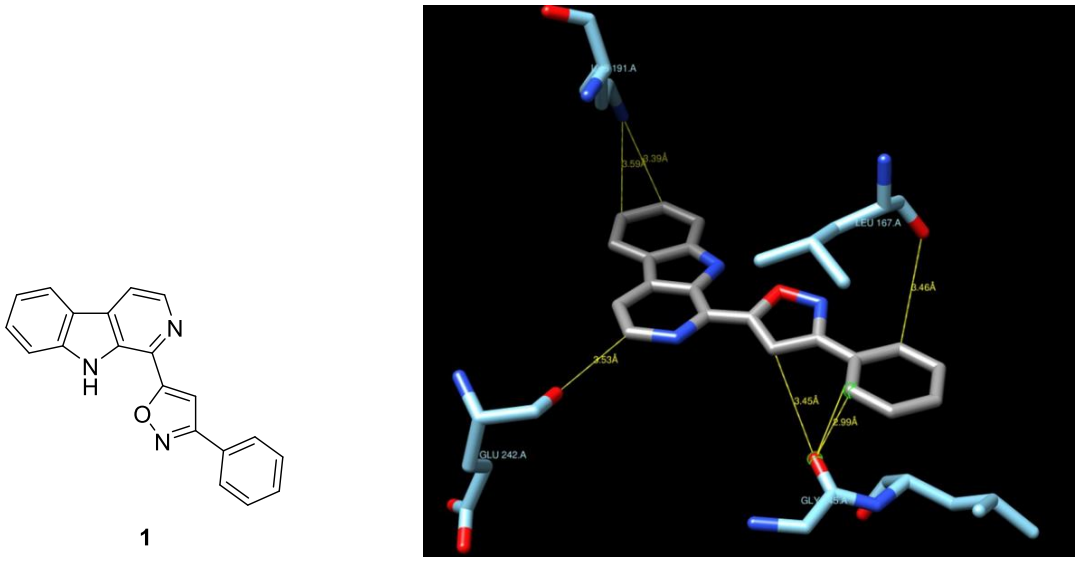

Figure 36. Structure of lead structure **1** (left) and CLK1 (blue) in complex with **1** (grey) (right). Short distances are indicated by yellow lines.

Basing on this, the aim of this thesis was to investigate the structure-activity relationship of this inhibitor chemotype. With a structure-based design and synthesis of several sets of analogues thereof, it was striven for inhibitors with considerably improved activity. Therefore, variation of each part of the molecule – namely the phenyl, the isoxazole and the *β*-carboline moiety – were to be successively pursued. Besides examining the necessity of the present substructures and the tolerance regarding the replacement by structurally related motifs, the introduction of donor or acceptor groups at particular positions was intended purposefully. Since **1** unusually displays no notable interactions with the active centre of the protein according to the obtained co-crystal structure, it was assumed that the analogues which are capable of forming hydrogen bonds will have significantly enhanced affinity to the target and as a result also enhanced CLK1-inhibitory activity.

Synthesis of lead structure **1** was possible according to literature[86]. However, several adaptions were examined to improve feasibility and broaden the substrate scope regarding the intended analogues (**Scheme 92**). *β*-Carbolinone **5** was accessed from indole-2-carboxylic acid by amide coupling with 2-aminoacetaldehyde dimethyl acetal and subsequent acid-mediated cyclization[89], then transformed into the respective bromide **8** (with $POBr_3$ in anisole)[90] and triflate **10** (with Tf_2O)[88]. Both were demonstrated to undergo smooth SONOGASHIRA cross-coupling with trimethylsilylacetylene and terminal alkyne **3** was obtained after desilylation with potassium carbonate[86]. The final HUISGEN cycloaddition to isoxazole **1** with benzonitrile oxide derived from benzaldehyde oxime was achieved by chlorination with NCS and subsequent dehydrohalogenation with triethylamine, but could even be more improved by using PIFA as direct oxidant.

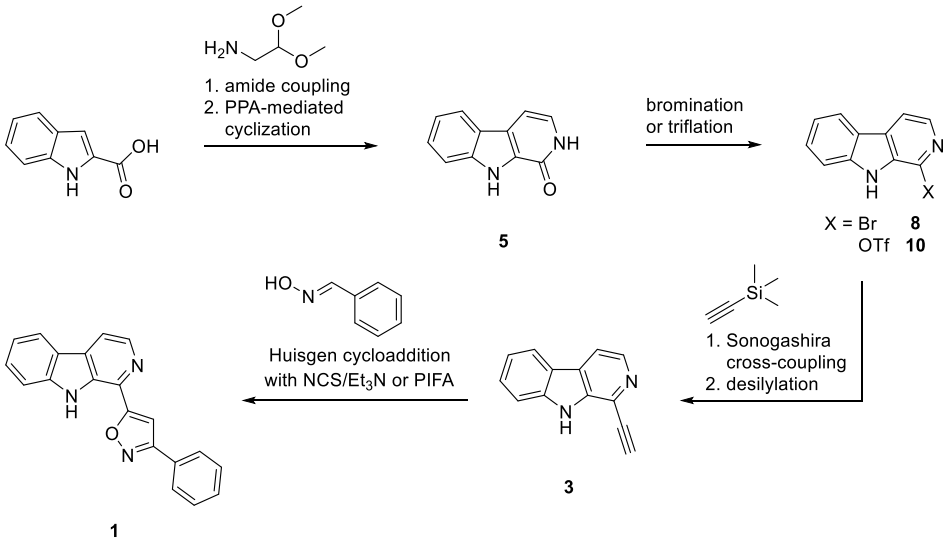

Scheme 92. Overview of the synthesis of building block **3** and lead structure **1**.

The first intended variations of lead structure **1** focussed on the phenyl ring, which was either substituted in *ortho*- or *para*-position or replaced by bioisosteric five- and six-membered heteroaromatic rings. According to the co-crystal structure of **1** in complex with CLK1, donor groups in *ortho*-position could be particularly beneficial, since the formation of a hydrogen bond with LEU 167 or GLY 245 is conceivable.

In close analogy to the synthesis of lead structure **1**, various analogues with a substituted or replaced phenyl ring were accessed (**Scheme 93**). Therefore, several arylaldehydes were transformed into the respective oximes **12** – **18** by condensation with hydroxylamine. Subsequently, the nitrile oxides were generated, again either by a NCS/triethylamine mediated procedure or by using PIFA, and subjected to HUISGEN cycloaddition with arylacetylene **3**.

Although this afforded some tedious optimization, a representative set of analogues was obtained (**19**, **20**, **21**, **22**, **23**, **24**, **25**, **26**). Additionally, the *ortho*-aniline residue **28** was accessed by selective reduction of the nitro group from **20** and the corresponding *para*-acetylene analogue **27** by SONOGASHIRA cross-coupling from iodide **22**. The terminal alkyne was intended to be used as clickable ligand in the Y3H system established in the group of DR. SIMONE MOSER[103] to identify further (off-)targets of this substance class.

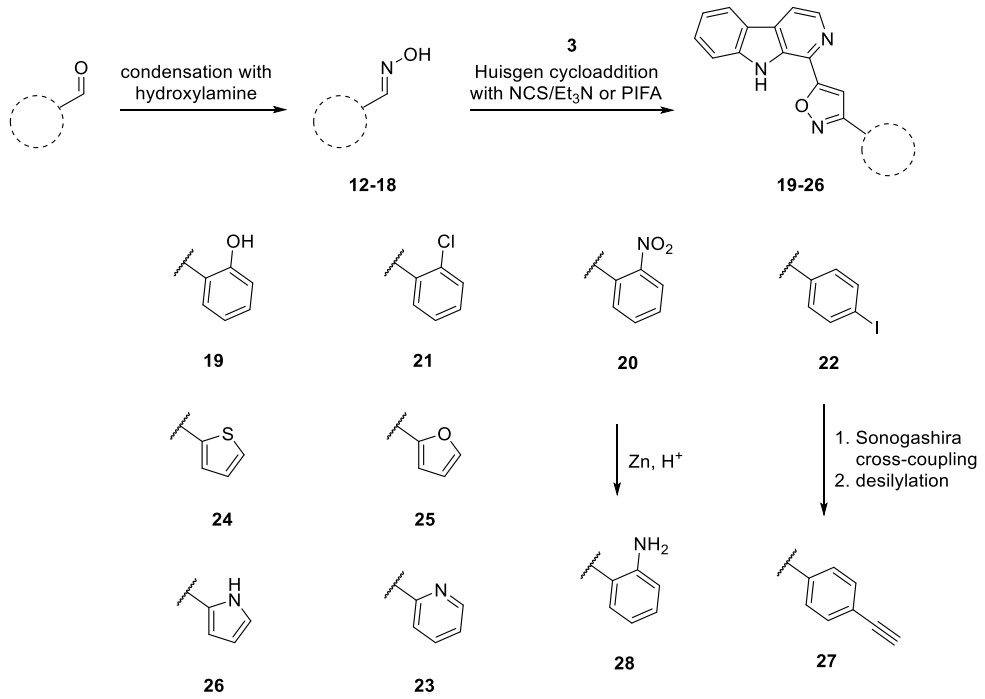

Scheme 93. Overview of the syntheses of variations of the phenyl ring.

The second set of analogues comprises variations of the isoxazole ring, which is (based on co-crystal structure data; *cf.* **Figure 6**) important for the almost co-planar orientation of the ligand due to the formation of an intramolecular hydrogen bond between the isoxazole oxygen and the indole NH. Besides investigating the replacement by many other five-membered heterocycles (containing other as well as less and more heteroatoms) to fully investigate the tolerance and potential of this substructure, especially the C-4' position was of interest. According to the co-crystal structure of CLK1 in complex with isoxazole **1**, a donor group in this position is likely capable of building a hydrogen bond with GLY 245.

For this purpose, alkyne **3** was also used as dipolarophile in HUISGEN reactions with other 1,3-dipoles than nitrile oxides (**Scheme 94**). With phenyl azide the Cu(I)-catalyzed synthesis of triazole **29** was achieved and with phenyldiazomethane pyrazole **31** was accessible. Only preparation of isoxazoline **33** from *N*-methyl-*C*-phenyl-nitrone was not feasible.

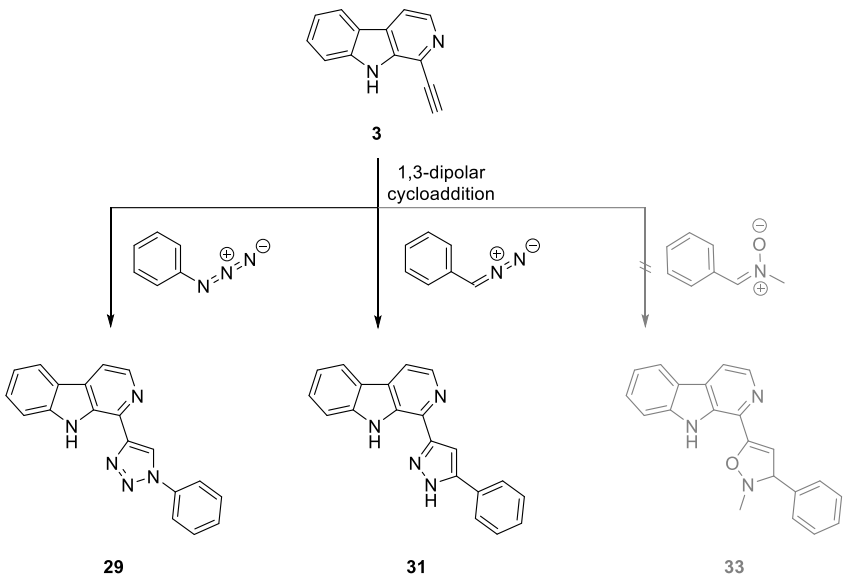

Scheme 94. Overview of the syntheses of variations of the isoxazole *via* HUISGEN cycloaddition from alkyne **3**.

To access further isoxazole analogues, literature-known aldehyde **36** and carboxylic acid **41** were utilized[131] (**Scheme 95**). Both were synthesized from benzalharman (**37**) by oxidative cleavage and employed as precursors in several heterocycle syntheses. To begin with aldehyde **36**, condensation with hydroxylamine gave oxime **35**, which could be converted into the corresponding nitrile oxide and reacted with phenylacetylene to the isomeric isoxazole **34** only by using PIFA but not with NCS/triethylamine. Furthermore, condensation with benzoylhydrazine and iodine-mediated oxidative cyclization afforded literature-known oxadiazole **50**[143].

Carboxylic acid **41** was activated with CDI and after coupling with amidoxime **47** subjected to KOH catalyzed cyclodehydration to give oxadiazole **48**. When the intermediate acylimidazole was reacted with phenylethylamine instead, amide **42** was accessed. However, the subsequent oxidative cyclisation to oxazole **43** was not achieved using iodine and TBHP[132]. In contrast, the one-pot ROBINSON-GABRIEL synthesis starting from carboxylic acid **41** and 2-aminoacetophenone, which uses $POCl_3$ as activating and cyclodehydrating reagent, was expedient. The related oxazole **46** was accessible from carboxylic acid **41** and phenacyl bromide, which gave phenacyl ester **45**, that was reacted with acetamide/boron trifluoride etherate.

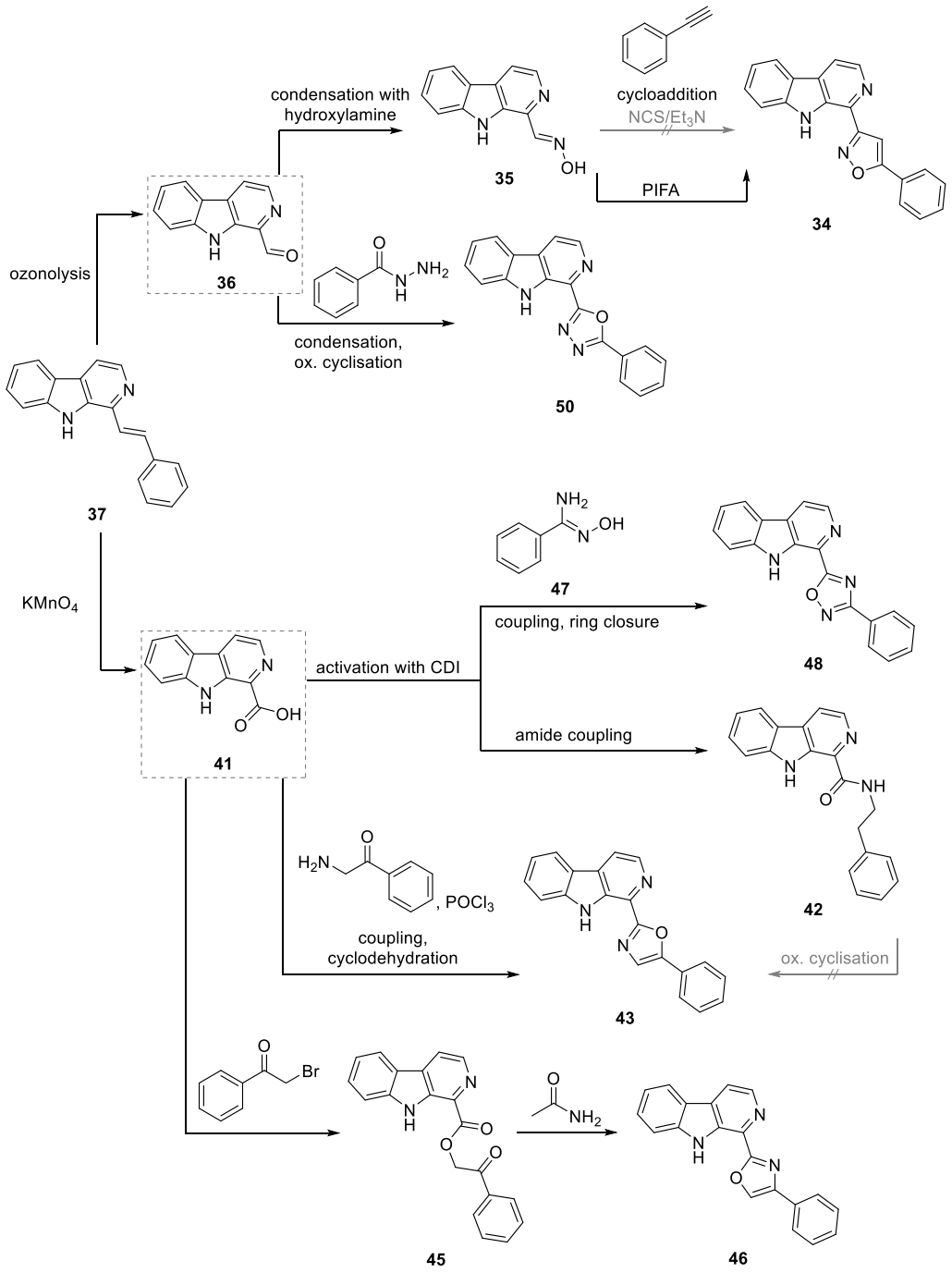

Scheme 95. Overview of the syntheses of variations of the isoxazole from central precursors aldehyde **36** and carboxylic acid **41**.

PICTET-SPENGLER reaction was used to establish an alternative synthesis for lead structure **1** and gain access to furan **58**, thiophene **59** and imidazole **60** (**Scheme 96**). The required aldehydes (**53**, **55**, **56** and **62**) were synthesized according to literature[145, 154, 159] and reacted with tryptamine at elevated temperature. Solely the respective 1,2,3,4-tetrahydro-*β*-carboline analogue **54** was also isolated, all other cyclization products were directly subjected to

Pd-catalyzed dehydrogenation to obtain the fully aromatic derivatives with a one-pot procedure.

Additionally, isoxazole **1** was converted into the corresponding enamino ketone **40** *via* reductive cleavage, and subsequent isothiazole synthesis *via* thionation with P_4S_{10} and *p*-chloranil mediated ring closure gave sulfur analogue **39**. Last but not least, phenylacetylene analogue **51** was synthesized from bromide **8** *via* SONOGASHIRA cross-coupling with phenylacetylene.

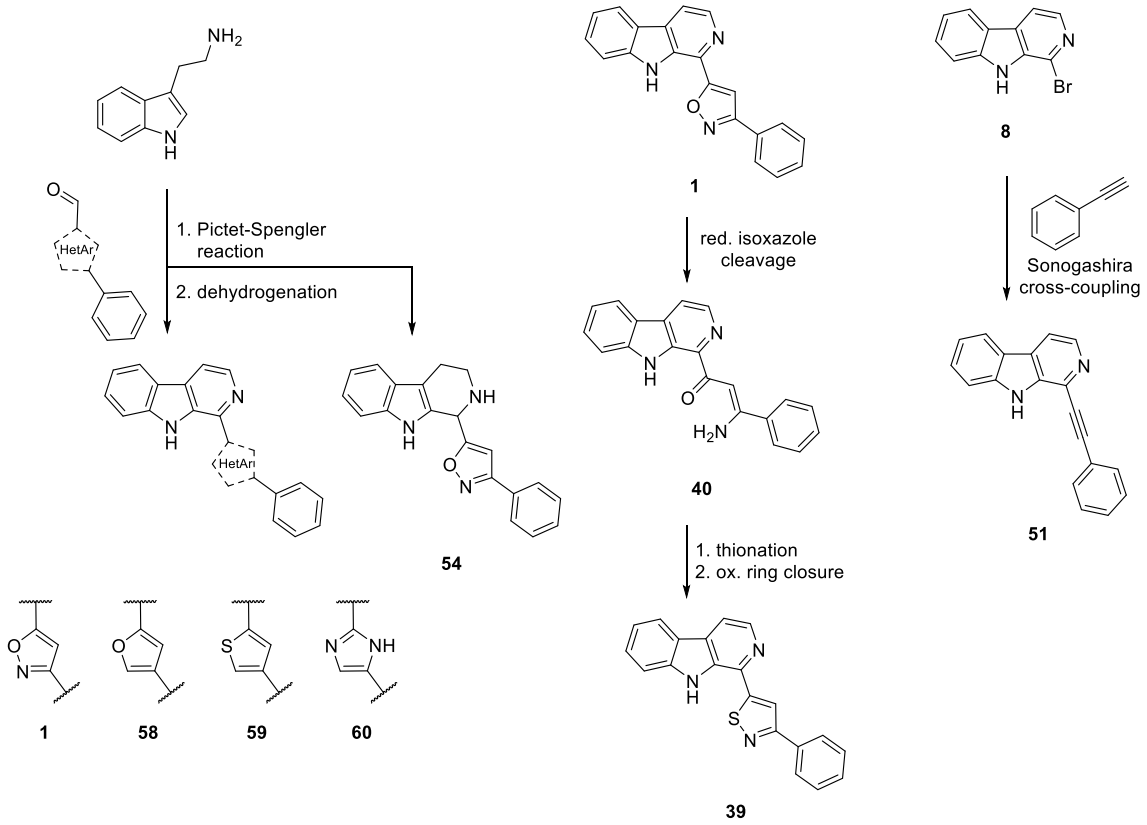

Scheme 96. Overview of the syntheses of further variations of the isoxazole from tryptamine, lead structure **1** and precursor **8**.

In order to synthesize 4-aminoisoxazole analogue **63**, for which dockings based on the co-crystal structure data predicted attractive additional interactions with the CLK1, the initially intended key step was the reduction of the corresponding nitro analogue **64** (**Scheme 97**). For this purpose, *α*-nitro ketone **65** was synthesized, but the 1,3-dipolar cycloaddition with benzonitrile oxide could not be realized. Therefore, an alternative approach was followed, in which the amino group should be generated from the respective carboxylic acid *via* CURTIUS rearrangement using DPPA. Direct synthesis of the needed ethyl propiolates (**67** and **70**) *via* SONOGASHIRA cross-coupling with ethyl propiolate was not feasible, presumably due to the

electron withdrawing ester group directly attached to the alkyne. However, **70** was accessed from SEM-protected 1-bromo-*β*-carboline **69** with trimethylsilylacetylene, desilylation and subsequent ethoxycarbonylation with ethyl chloroformate. Cycloaddition with benzonitrile oxide readily gave 3,4,5-trisubstituted isoxazole **73**, for which SEM cleavage to **74** was only achieved with trifluoroacetic acid, but surprisingly not with fluoride ions. After alkaline ester hydrolysis, CURTIUS rearrangement of carboxylic acid **66** was attempted, but instead of degradation to amine **63**, intramolecular amide formation to **76** proceeded. When in contrast the reactions were run in reverse order, CURTIUS rearrangement of *N*-SEM protected carboxylic acid **77** in *tert*-butanol gave Boc amine **78**. Treatment with hydrochloric acid then resulted in Boc cleavage, but subsequently in the formation of intramolecular aminal **80** with the “formaldehyde unit” of SEM. To circumvent this, several other *N*-9 protective groups (Boc, benzyl, PMB) were investigated, but found to be not suitable. Therefore, it was striven for a 4’-amino protecting group, which withstands the conditions of SEM cleavage and is eliminable in the last step. This was realized by masking amine **79** as trifluoroacetamide **93**. After SEM cleavage with trifluoroacetic acid, trifluoroacetamide cleavage of **91** was achieved with hydrochloric acid in methanol and finally led to 4’-amino analogue **63**.

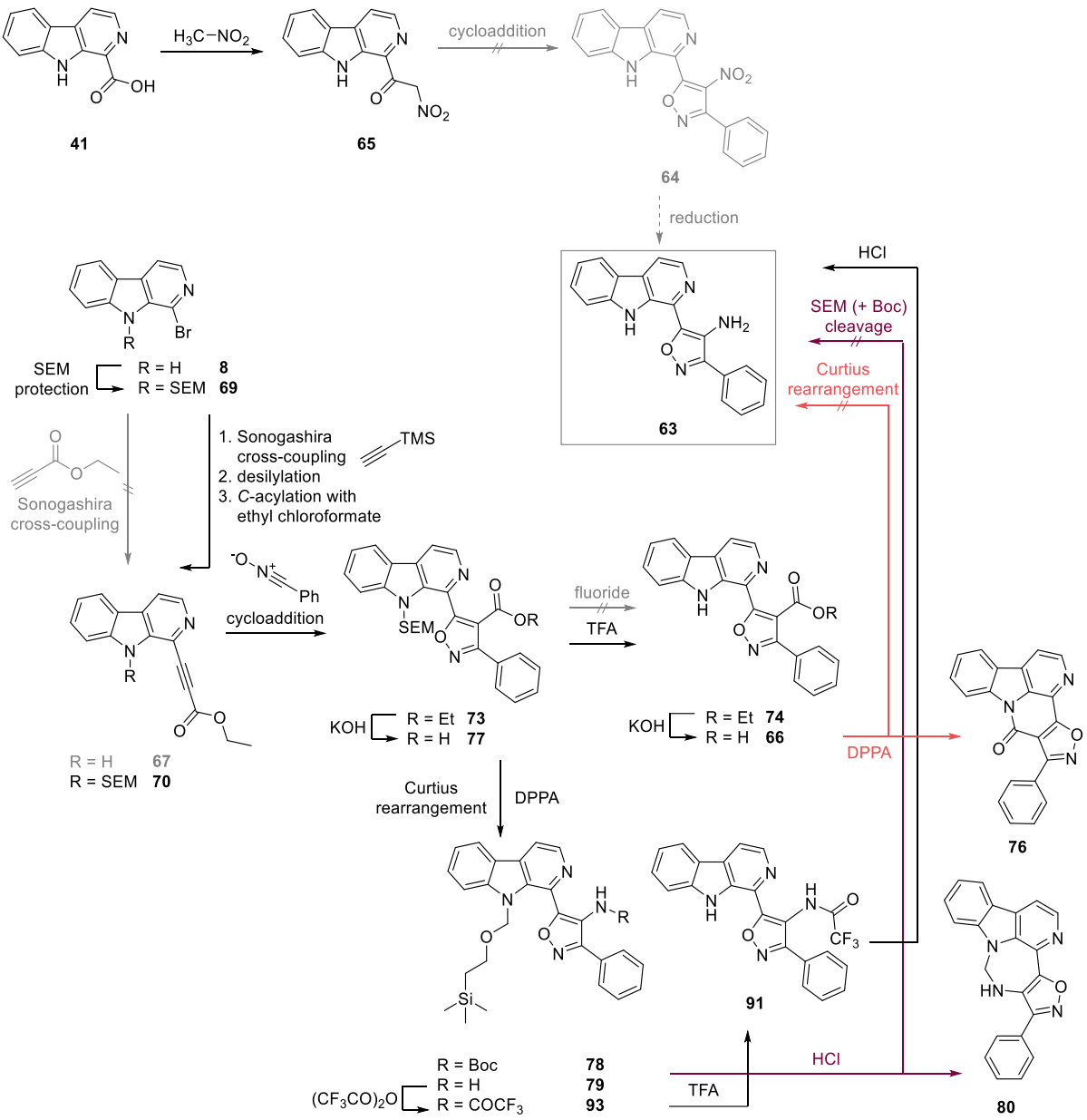

Scheme 97. Overview of the synthesis of 4-aminoisoxazole **63**.

The third and final set of analogues affects the tricyclic *β*-carboline skeleton. Besides investigating the necessity of the present nitrogen atoms, the co-crystal structure indicated several positions, for which the introduction of substituents was highly promising.

Firstly, to further investigate the co-planar orientation of lead structure **1** based on an intramolecular hydrogen bond, the crucial indole NH moiety was eliminated. So, the indole NH was methylated *via* nucleophilic substitution (**94**) (**Scheme 98**). Additionally, *N*-propargyl derivative **95** and *N*-cyanomethyl derivative **96** were synthesized, since both residues showed beneficial properties at *N*-9 of *β*-carbolines investigated as kinase inhibitors in previous studies[82].

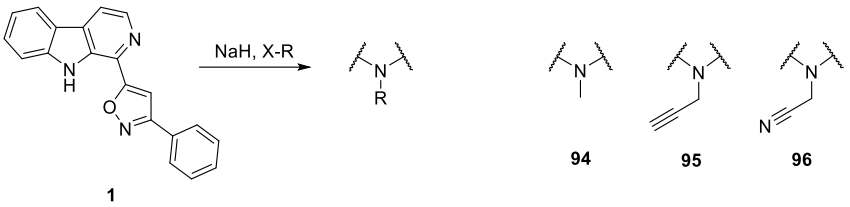

Scheme 98. Overview of the synthesis of *N*-9 substituted analogues.

Regarding ring A, the introduction of substituents was especially auspicious at C-3. Donor groups were assumed to be capable of forming an ATP-mimetic hydrogen bond with the carbonyl oxygen of GLU 242. The access to such analogues was established *via* PICTET-SPENGLER reaction between L-tryptophan methyl ester hydrochloride and aldehyde **53**, which was in turn synthesized in close analogy to literature from propargyl alcohol *via* 1,3-dipolar cycloaddition with benzonitrile oxide[144] and subsequent SWERN oxidation[145] (**Scheme 99**). The following dehydrogenation with potassium permanganate gave 3-methoxycarbonyl analogue **97** directly, which was then further transformed into envisaged donor groups: hydrolysis to carboxylic acid **98** and subsequent CURTIUS rearrangement with DPPA gave aminopyridine **99**, aminolysis with ammonia in methanol resulted in amide **100** and reduction with $NaBH_4/CaCl_2$ lead to hydroxymethyl compound **101**.

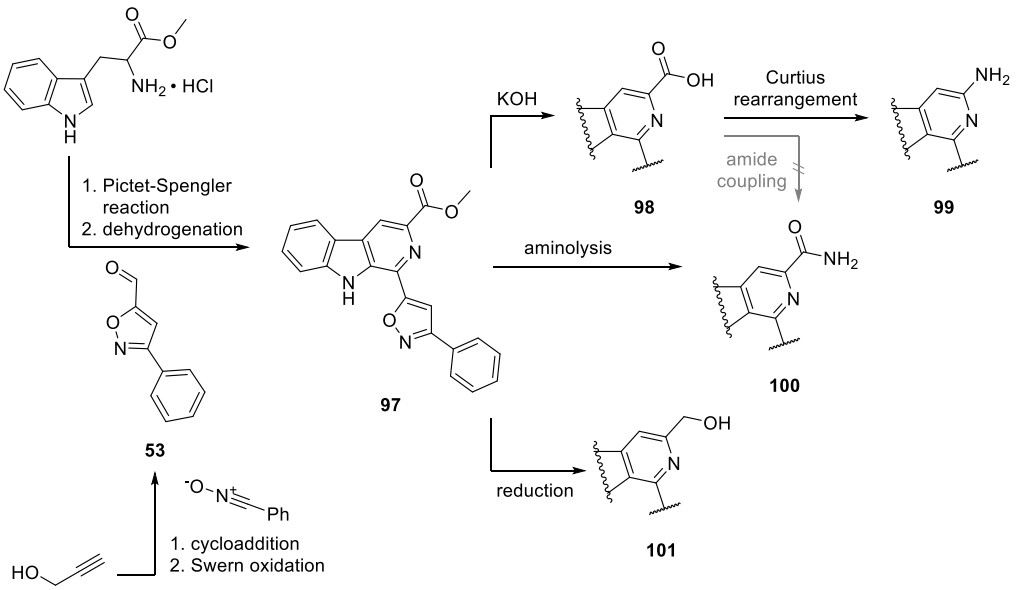

Scheme 99. Overview of the (attempted) synthesis of ring A substituted analogues.

With regard to further variations of the *β*-carboline moiety also several other tricyclic heteroarenes and ring C substituted *β*-carbolines were envisaged for different reasons. First

of all, a carbazole moiety was pursued, since this 2-desaza analogue would allow to evaluate the relevance of the nitrogen atom in ring A. Furthermore, the replacement of the *β*-carboline by phenothiazine was intended. This widely spread tricyclic core structure additionally has different geometry due to the central thiazine ring.
Also variations of ring C were investigated, for which substituents seemed especially interesting at C-7 and C-8. The 7,8-dichloro pattern is familiar from bauerine alkaloids and KH-CB19[46-47]. Donor groups with a short spacer at C-8 could interact with the backbone oxygen of GLU 292 or ASN 293. Also the introduction of acceptor atoms into ring C was very promising according to the co-crystal data. An additional nitrogen replacing C-6 or C-7, could enable a hydrogen bond with the side chain of LYS 191.

To access these multifarious analogues the corresponding (pseudo)halide building blocks were generated (**Scheme 100**). While several of these precursors could be synthesized following literature or related procedures *via* lithiation and halogenation (**111**, **112**), BORSCHE-DRECHSEL carbazole synthesis (**117**) or JAPP-KLINGEMANN reaction (**124**, **132**), a new approach was to be developed for the 7-aza analogue **155**. Starting from 4-methyl-3-nitropyridine and ethyl pyruvate, literature-known ester **148**[a] was accessed *via* REISSERT indole synthesis and bromination with NBS, and subsequently transformed to amide **149[a]**. The key step was the construction of ring A by introduction of an ethoxyvinyl side-chain and subsequent ring closure. Since neither the STILLE nor the SUZUKI cross-coupling was achieved at the stage of amide **149[a]**, the side chain was then already introduced at the stage of ester **148**[a]. However, cyclization of **152[a]** then affords condensation with ammonia, which was only achieved with an ammonium acetate melt. Subsequent bromination and chlorination of the pyridone moiety failed and triflation was only very low yielding, making the extremely poorly soluble 7-aza-*β*-carboline-1-one (**151[a]**) not a convenient building block to further investigate the underexplored class of 7-aza-*β*-carbolines.
Introduction of the phenylisoxazole residue on these (pseudo)halides was initially intended *via* SUZUKI cross-coupling with boronic acid pinacol ester **108**. As this was, however, not feasible due to extensive protodeboronation, the well-established combination of SONOGASHIRA cross-coupling with trimethylsilylacetylene, desilylation and HUISGEN cycloaddition with benzonitrile oxide was applied. With this sequence, phenothiazine **115**, carbazole **120**, 7,8-dichloro-*β*-carboline **126** and 8-methoxy-*β*-carboline **128** were accessed. The latter was subsequently converted to the corresponding phenol **134** *via* ether cleavage with HBr in acetic acid. Triflation and cross-coupling with suitable building blocks then allowed the introduction of the envisaged donor groups: propargyl alcohol **142** *via* SONOGASHIRA and pyrazole **143** *via* SUZUKI cross-coupling.

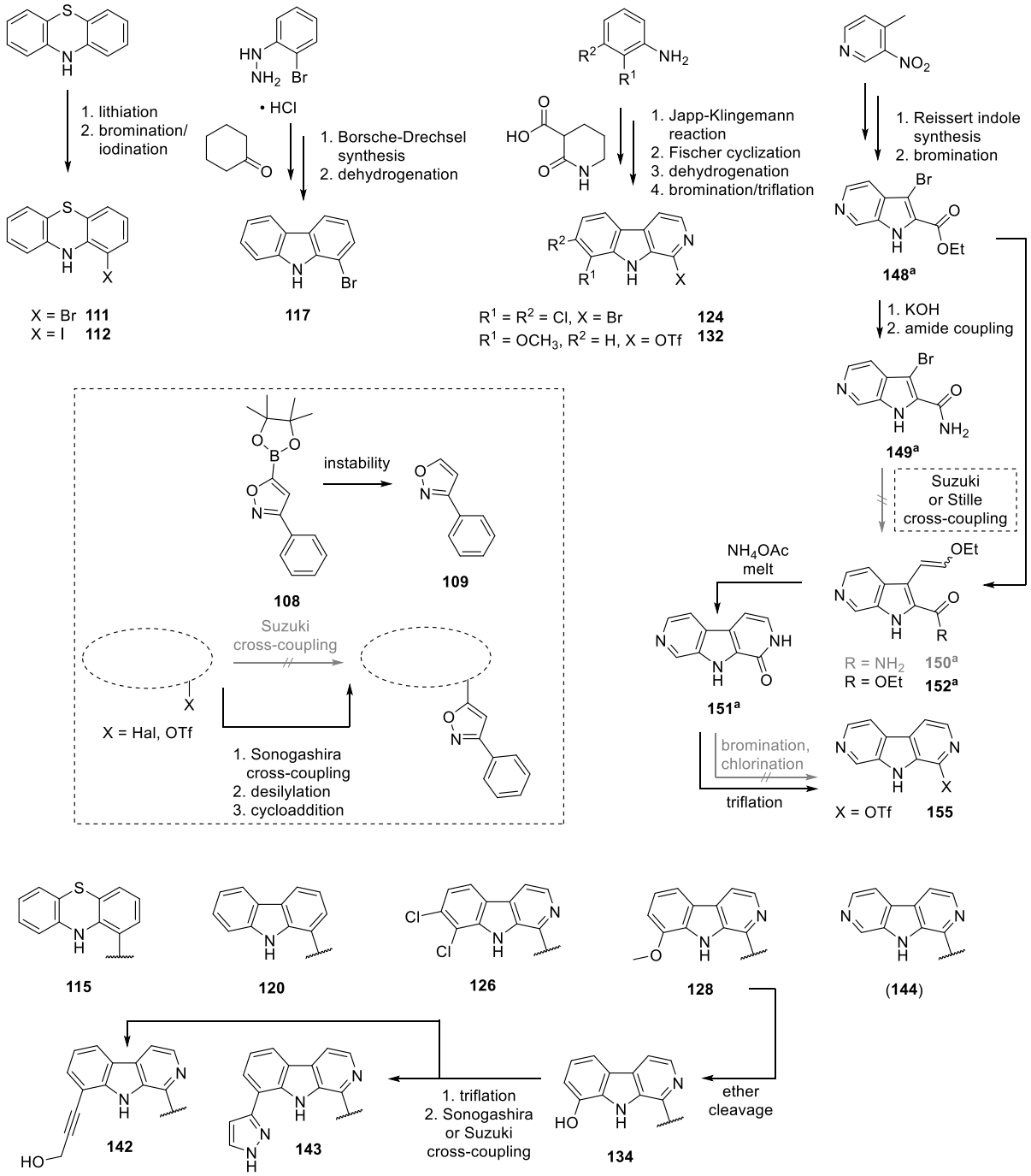

Scheme 100. Overview of the synthesis of other tricyclic heteroarenes and ring C substituted analogues from (pseudo)halide precursors.

Also synthesis of 7-aza analogue **144** was achieved with the aforementioned procedure, but suffered from low yields and substantial loss of substance, which hampered the isolation of analytical pure final compound. Therefore, another approach was followed, that additionally gave access to the more flexible ring B *seco* derivatives (**Scheme 101**). The phenyl isoxazole residue was introduced at first onto 3-amino-2-bromopyridine, which corresponds to ring A of the *β*-carboline. BUCHWALD-HARTWIG *N*-arylation of amine **160[b]** with aryl halides was then utilized to generate *seco* analogue **162[b]** and several related diarylamines (**163[b]**, **164[b]**, **165[b]**,

166[b], **167**, **169**). Key step for construction of the aza-*β*-carboline motif was an intramolecular HECK-like cyclization of the *ortho*-halogenated precursors to connect ring A and ring C. Initially, synthesis of 7-aza analogue **144** was attempted with chloride **166[b]**, but impeded by competing dechlorination. The procedure was significantly improved and readily gave 7-aza-*β*-carboline **144** by employing bromide **167**. Likewise, this method could be applied to prepare 6-aza-*β*-carboline **145** from bromide **169**.

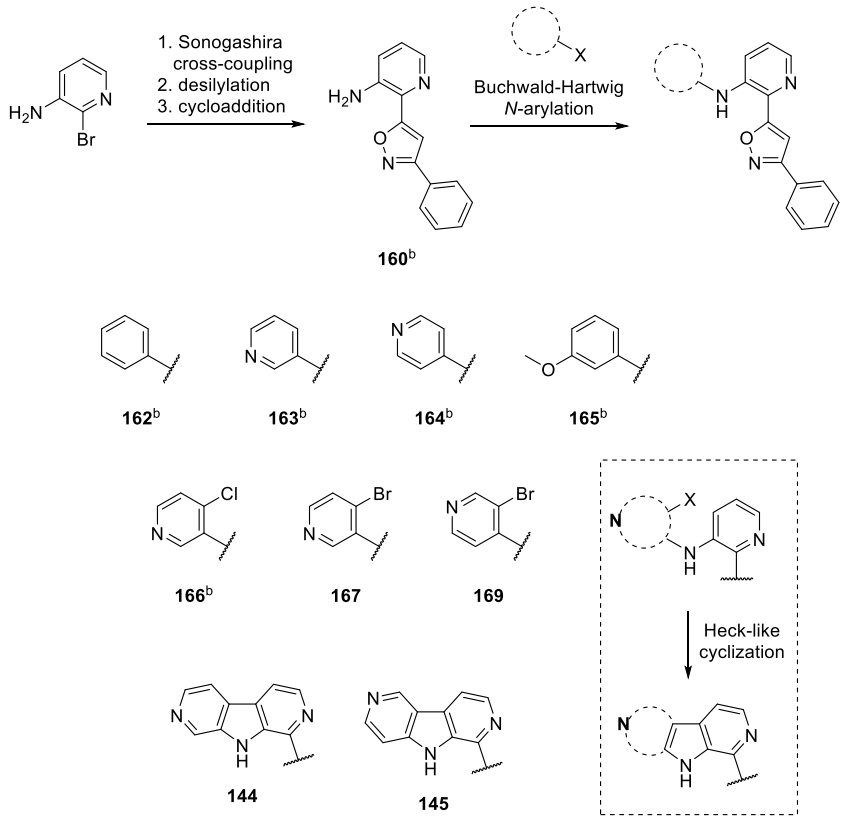

Scheme 101. Overview of the synthesis of *seco* and *aza* analogues *via* BUCHWALD-HARTWIG *N*-arylation.

In total, 10 variations of the phenyl ring, 15 variations of the isoxazole moiety and 29 variations of the *β*-carboline nucleus were synthesized and their CLK1 inhibitory activity was determined in the ^{33}PanQinase assay (Reaction Biology Europe GmbH, Freiburg, Germany). Additionally, their affinity towards CLK1 and more than 100 further kinases was assessed with DSF experiments (in the group of PROF. DR. STEFAN KNAPP, Goethe University Frankfurt, Germany) and co-crystallization with the target enzyme was achieved with some of these ligands (in the group of PROF. DR. ODED LIVNAH, The Hebrew University of Jerusalem, Israel).

In summary, the biological testing of these analogues revealed that only few structural changes of lead structure **1** are tolerated to maintain or improve CLK1 inhibitory activity. According to

the radiometric assay, which measured the enzyme inhibition at a concentration of 1 µM, besides lead structure **1**, further 11 synthesized analogues were found to be moderate inhibitors (40 – 80% inhibition), whereas only 6-aza analogue **145** was classified as very potent inhibitor (> 80% inhibition) (**Figure 37**). These results were all in all reflected well in the temperature shift assay with CLK1, for which nearly all moderate inhibitors caused a temperature shift of 3 – 5 °C and only 6-aza analogue **145** of more than 6 °C.

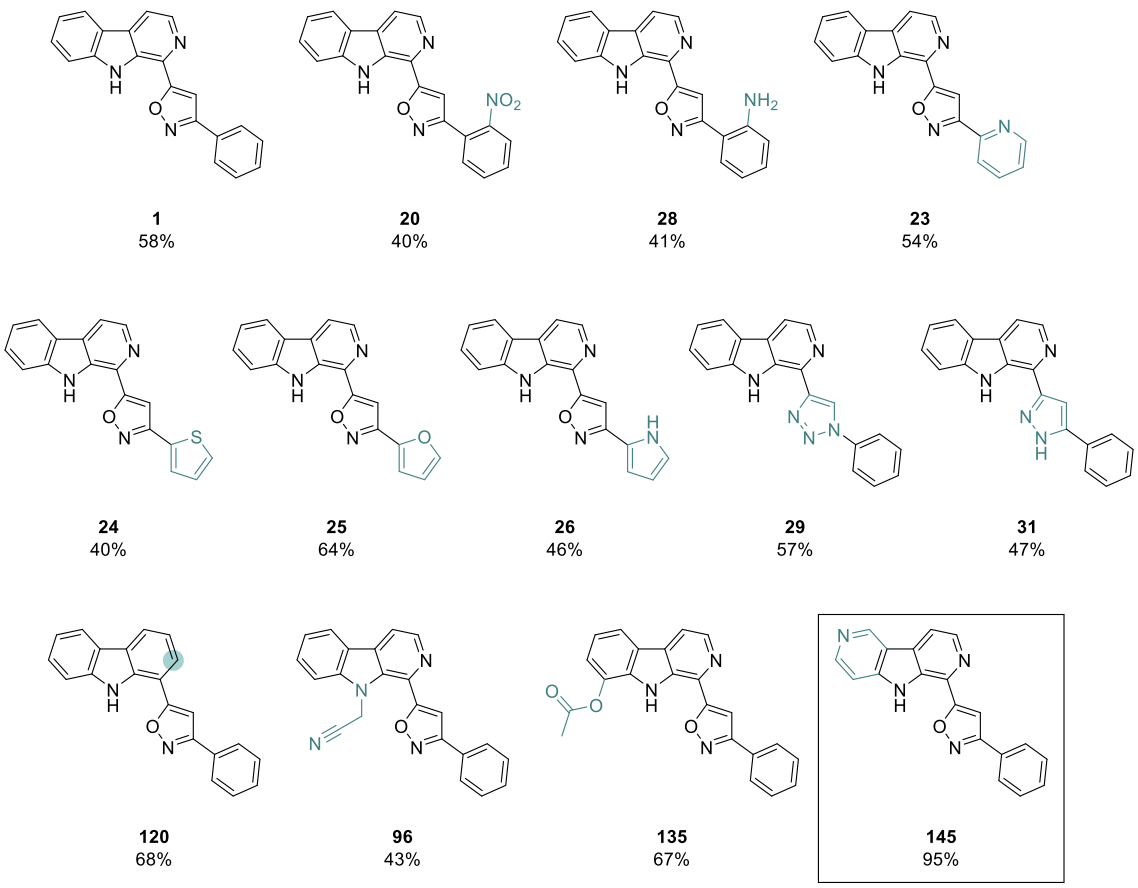

Figure 37. Overview of lead structure **1** and synthesized analogues, which were identified as moderate or potent CLK1 inhibitors with the ^{33}PanQinase assay. The respectively measured CLK1 inhibition in % is given below each structure.

Taken this into consideration, it becomes apparent, that the rational synthesis of inhibitors based on considerations of the co-crystal structure of ligand **1** at the active site of the CLK1 is challenging. Several expectedly highly promising modifications, which were assumed to enable further interactions with the protein, fell short of expectations and several minor changes unexpectedly resulted in a complete loss of activity and affinity as summarized in **Figure 38**.

The highest variability and tolerance towards modifications was observed for the phenyl ring. Replacement by five- and six-membered heteroaromatic rings was tolerated well regarding the CLK1 inhibitory activity and co-crystal structures of several of these ligand (pyridine **23**, furan **25**, pyrrole **26**) with the protein revealed a mutual orientation similar to lead structure **1**, but the establishment of a ATP-mimetic hydrogen bond between *N*-2 and LEU 244. In contrast, substitution in *para*-position resulted in a loss of activity and affinity, whereas substitution in *ortho*-position has to be considered differentially. The introduction of donor groups in this position was assumed to be particularly beneficial due to potential further interactions. While this seems to be accomplished according to the co-crystal structures of hydroxyphenyl analogue **19** and aniline **28**, that demonstrate an additional hydrogen bond to LEU 244, this advancement was not reflected in enhanced activity. While aniline **28** has decreased activity, like its nitro precursor **20**, hydroxyphenyl analogue **19** is entirely inactive.

Regarding the isoxazole moiety, it was figured out that this substructure is a lot more susceptible to structural changes. Only triazole **29** and pyrazole **31** still displayed inhibitory activity. While this suggests the replaceability of *O*-1' and C-3' by nitrogen, all other alterations were not tolerated. This comprises the replacement of *O*-1' by sulphur, *N*-2' by oxygen or methine and C-4' by oxygen or nitrogen, although the relevance of the latter two positions was considered as low from the co-crystal structure of isoxazole **1**. Also the introduction of a donor group at C-4', such as realized with imidazole **60** and 4'-aminoisoxazole **63**, did not fulfil the intended task to interact with GLY 245, but resulted in entirely inactive analogues. Unfortunately, until finalization of this thesis no co-crystal structures for any of these variations could be obtained. Only phenylacetylene **51** was found in complex with CLK1, which occurs according to preliminary analysis not in a binding mode similar to lead structure **1**, but in a flipped orientation that enables the formation of a hydrogen bond between *N*-2 and LYS 191.

Also the *β*-carboline nucleus was found to not readily tolerate broad alterations. Although this is in contradiction to the results from co-crystal structures of the phenyl variations, the relevance of *N*-2 was assumed to be low for *β*-carboline **1**, which could explain the conserved activity of carbazole **120**. Substitution was not conducive as planned at various positions: the highly promising introduction of donor groups at C-3, such as present in aminopyridine **99**, which could theoretically establish even two ATP-mimetic hydrogen bonds with the protein, was not beneficial. Same was observed for the donor groups at C-8, that were realized with propargyl alcohol **142** and pyrazole **143** and intended to interact with GLU 292 or ASN 293. Also several other substituents at C-3, C-7 and C-8 were not tolerated, but surprisingly acetate **135** was found to still have inhibitory activity. Ring B (the pyrrole substructure of the *β*-carboline) should also not be changed – as demonstrated with phenothiazine **115** and the many *seco* derivatives – and further, substitution at *N*-9 obviously hinders the co-planar

orientation of the ligand. However, *N*-cyanomethyl derivative **96** was found to be a moderate inhibitor.

In contrast to the aforementioned unsuccessful strategies to promote interaction with the protein by additional donor groups and therefore enhance inhibitory activity, this objective was finally achieved by the introduction of an acceptor group at ring C of the *β*-carboline. While the replacement of C-7 by nitrogen is not beneficial, such replacement of C-6 creates a highly potent CLK1 inhibitor: 6-aza analogue **145** was found to have comparable efficacy (95% inhibition) and potency (IC_{50} = 56 nM) to staurosporine (97% inhibition, IC_{50} = 52 nM) in the enzymatic assay. The final results from the co-crystallization of both *aza* analogues (**144** and **145**) are not yet available, but a binding mode similar to furan **25** was already reported. This indicates the ATP-mimetic hydrogen bond between *N*-2 and LEU 244, but does not yet allow to draw conclusions, if the improved kinase-inhibitory activity of **145** can be explained by formation of the intended interaction with LYS 191.

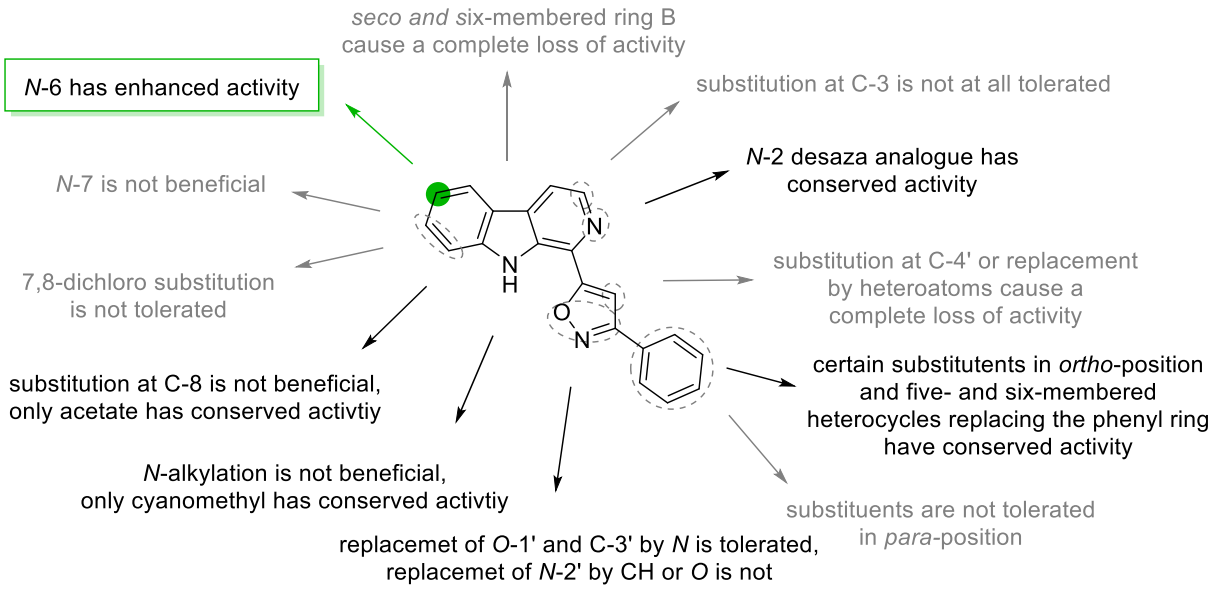

Figure 38. Summary of the outcome from the biological testing of all synthesized analogues of lead structure **1**.

At long last, a rational approach led to the advancement of the moderate CLK1 inhibitor **1** to the highly promising inhibitor **145**. Initial selectivity profiling with DSF against a panel of 104 kinases from different families further revealed that in total only 9 other kinases are potential targets of **145**. However, apart from DYRK1A, DYRK2 and CAMKK, all measured temperature shifts were below 5 °C and therefore only moderate effects are presumable. Besides further investigating the selectivity, especially towards all CLK and DYRK isoforms, the next essential step is to study the inhibitory potential of 6-aza-*β*-carboline **145** also in cellular assays.

5 Experimental Part

5.1 Materials and methods

5.1.1 General reaction conditions and reagents

Oxygen- and moisture-sensitive reactions were run in oven-dried glassware under N_2 atmosphere using SCHLENK line technique. All chemicals and reagents were purchased from commercial sources (abcr, Fischer Scientific, Merck, Sigma-Aldrich, TCI, Th. Geyer) and used without further purification. Solvents were also purchased from commercial sources, used without further purification or purified and dried by distillation and stored over molecular sieves, if needed. Phase separation filters (MN 617 WA) were purchased from Macherey-Nagel.

5.1.2 Reaction monitoring and purification

Monitoring of all reactions and fraction control was performed by thin layer chromatography (TLC) on POLYGRAM SIL G/UV254 silica gel polyester sheets (0.2 mm silica gel, 40 x 80 mm, Macherey-Nagel). Visualization was achieved with UV light irradiation (254 nm or 365 nm) or one of the following TLC staining reagents: CAM (ceric ammonium molybdate), DNPH (2,4-dinitrophenylhydrazine) or EHRLICH's reagent (4-(dimethylamino)-benzaldehyde). If needed, direct mass analysis from TLC plates using Plate Express and direct mass analysis from solid and liquid samples using atmospheric solids analysis probe (ASAP) on an expression Compact Mass Spectrometer (Advion) with atmospheric pressure chemical ionization (APCI) was performed for further reaction monitoring or compound identification.
Flash column chromatography was run on silica gel (pore size 60 Å, particle size 0.040 – 0.063 mm) purchased from Merck or Macherey-Nagel. Isolated yields were determined after work-up and purification by flash column chromatography or recrystallization, if needed.

5.1.3 Compound characterisation

Retardation factors (R_f) were determined by TLC analysis using the eluents as described for the single products.
Melting points were measured with a Büchi B-540 Melting Point Apparatus in capillary tubes. Values are reported in °C and are uncorrected.
Nuclear magnetic resonance (NMR) spectroscopy was performed by the NMR Analytics Group of the Department of Pharmacy (Dr. LARS ALLMENDINGER and co-workers). All NMR spectra (^{1}H, ^{13}C, DEPT, H-H-COSY, HSQC/HMQC, HMBC) were recorded on an Avance III 400 MHz Bruker BioSpin or Avance III 500 MHz Bruker BioSpin device at room temperature, unless otherwise stated. Chemical shifts δ are reported in parts per million (ppm) and refer to the residual solvent peak of chloroform-*d*, DMSO-d_6, methanol-d_4 or methylene chloride-d_2. The signals in the ^{1}H and ^{13}C NMR spectra were assigned using COSY, DEPT, HSQC/HMQC,

HMBC and, if needed, NOE spectra. Multiplicities are abbreviated as s = singlet, d = doublet, t = triplet, q = quartet, m = multiplet (and derivatives thereof) and coupling constants *J* are reported in Hz. The software MestReNova (Mestrelab Research S.L.) was used to analyze all spectra.

Infrared spectra were recorded on a Perkin Elmer FT-IR BXII/1000 spectrometer with Smiths ATR sensor. Wavenumbers of absorption bands were assigned with the software Spectrum (PerkinElmer) and are reported in cm^{-1}.

High resolution mass spectrometry was performed by the LMU Mass Spectrometry Service (Dr. WERNER SPAHL and co-workers). Spectra were recorded on a Jeol JMS-700 MStation or JMS GC Mate II device at 250 °C and electron energy of 70 eV for electron impact ionization (EI) and on a Thermo Finnigan LTQ device at 250 °C for electron spray ionization (ESI). Observed molecular ions are reported in *m/z* units.

Analytical HPLC measurements were performed on a HP Agilent 1100 HPLC system with a diode array detector. Purity was determined at 210 nm and 254 nm by applying the following methods and is reported in %.

Method 1:

Agilent Poroshell 120 EC-C18 (2.7 µm, 3.0 x 100 mm), temp. 50 °C, flow 0.5 – 1.0 mL/min

a) 80% acetonitrile, 20% water; injection vol. 10 µL
b) 70% acetonitrile, 29.9% water, 0.1% formic acid; injection vol. 10 µL
c) 50% acetonitrile, 49.9% water, 0.1% THF; injection vol. 2 – 5 µL
d) 50% acetonitrile, 49.9% water, 0.1% formic acid; injection vol. 10 µL

Method 2:

Agilent Zorbax Eclipse Plus C18 (5.0 µm, 4.6 x 150 mm), temp. 50 °C, injection vol. 10 µL

a) 80% methanol, 20% water, pH 9; flow 1.2 mL/min
b) 80% methanol, 20% water; flow 1.0 mL/min
c) 70% acetonitrile, 30% water; flow 1.5 mL/min
d) 70% acetonitrile, 29.9% water, 0.1% formic acid; flow 1.0 mL/min
e) 50% acetonitrile, 50% water; flow 1.0 mL/min
f) 30% acetonitrile, 69.9% water, 0.1% formic acid; flow 1.0 mL/min
g) 20% → 80% acetonitrile in water; flow 1.0 mL/min
h) 20% → 90% acetonitrile + 0.1% formic acid in water; temp. 25 °C, flow 1.0 mL/min
i) 5% → 95% acetonitrile in phosphate buffer (0.03 M, pH 3.5) with octane-1-sulfonic acid sodium salt (1 mg/L); flow 1.5 mL/min

Method 3:

Raptor Biphenyl (5.0 µm, 4.6 x 150 mm) temp. 50 °C, injection vol. 10 µL,

20% → 95% methanol in water; flow 1.0 mL/min

5.1.4 Nomenclature and numbering

All compounds are titled with the systematic name following IUPAC recommendations. Compounds, which were (first) synthesized by undergraduate students under my supervision and are described also within their theses, are marked with letters in superscript as follows.

a: Master thesis of FRANCESCA DONÀ[201]

b: Bachelor thesis of LUKAS FINGER[249]

Numbering is based on IUPAC rules, though the apostrophes are not in accordance with the priority of the root systems, but constantly remain as in the depicted order for all analogues.

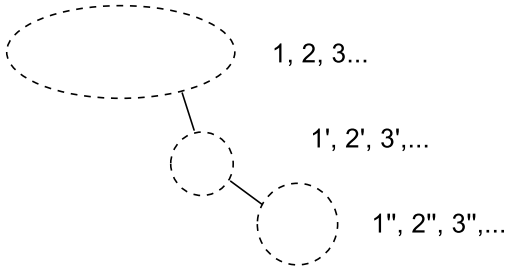

5.2 General synthetic procedures

I: SONOGASHIRA cross-coupling reactions

a: SONOGASHIRA cross-coupling of bromopyridines and aryl iodide 22 with alkynes

The respective aryl halide (1.0 eq) was dissolved or suspended under N_2 atmosphere in anhydrous triethylamine (3 – 9 mL/mmol halide) and anhydrous THF (3 – 10 mL/mmol halide) and the reaction mixture was stirred at room temperature. CuI (0.2 eq) was added and the mixture was purged with N_2 for 5 – 10 min. Then, $Pd(dppf)Cl_2$ (0.05 eq) was added and again the mixture was purged with N_2 for 5 – 10 min. A degassed solution of the respective alkyne (1.2 – 2.0 eq) in anhydrous THF was added dropwise and the reaction mixture stirred at room temperature for 3.5 – 20 h. After diluting with ethyl acetate, the mixture was filtered through a pad of celite and the pad was washed with ethyl acetate. Sat. aq. NaCl solution was added to the filtrate and the phases were separated. The aq. phase was further extracted with ethyl acetate, the combined organic layers were dried over Na_2SO_4, filtered and the solvent was removed *in vacuo*. The crude TMS-protected alkynes were used without further purification, while the other crude products were purified by flash column chromatography.

b: SONOGASHIRA cross-coupling of pyridyl triflates with trimethylsilylacetylene

The respective triflate (1.0 eq), LiCl (3.0 eq), CuI (0.1 eq) and $Pd(PPh_3)_2Cl_2$ (0.08 eq) were dissolved in anhydrous DMF/triethylamine (1.1:1, 20 mL/mmol triflate) under N_2 atmosphere in a pressure tube. The solution was stirred for 10 min at room temperature, before trimethylsilylacetylene (7.0 eq) was added. The reaction mixture was purged with N_2 for 10 min and, after sealing the tube, stirred at 75 °C for 2 h and at room temperature for further 16 h. After diluting with ethyl acetate (10 mL), the mixture was filtered through a pad of silica and the pad was washed with ethyl acetate (100 mL). Sat. aq. NaCl solution (50 mL) was added to the filtrate and the phases were separated. The aq. phase was further extracted with ethyl acetate (2 x 50 mL) and the combined organic layers were dried using a phase separation filter. The solvent was removed *in vacuo* and the TMS-protected alkynes were used without further purification.

c: SONOGASHIRA cross-coupling of aryl triflates with alkynes

The respective triflate (1.0 eq), tetra-*n*-butylammonium iodide (3.0 eq) and $Pd(PPh_3)_2Cl_2$ (0.1 eq) were dissolved in anhydrous DMF/triethylamine (5:1, 5 – 10 mL/mmol triflate) under N_2 atmosphere in a pressure tube. The solution was stirred for 10 min at room temperature, before CuI (0.3 eq) was added. Then, the reaction mixture was purged with N_2 for 10 min and the respective alkyne (2.0 eq) was added. The tube was sealed and the mixture stirred at 70 °C for 3 h and at room temperature for further 16 h. After diluting with water (20 mL), the mixture was extracted with methylene chloride (3 x 20 mL) and the combined organic layers were dried

using a phase separation filter. The solvent was removed *in vacuo* and the residue purified by flash column chromatography.

II: TMS deprotection

The appropriate TMS-protected alkyne (1.0 eq) was dissolved in methanol (5 – 20 mL/mmol alkyne) and K_2CO_3 (3.3 eq) was added. After stirring for 1 h at room temperature, sat. aq. NaCl solution (40 mL/mmol alkyne) was added and the mixture was extracted with ethyl acetate (3 x 10 mL/mmol alkyne). The combined organic layers were dried using a phase separation filter or dried over Na_2SO_4 and filtered. The solvent was removed *in vacuo* and the residue purified by flash column chromatography.

III: HUISGEN cycloaddition of alkynes and nitrile oxides

a: Using [bis(trifluoracetoxy)iodo]benzene and oximes (1.5 eq)

The respective alkyne (1.0 eq) and oxime (1.5 eq) were dissolved or suspended in methanol/water (5:1, 10 mL/mmol alkyne). [Bis(trifluoroacetoxy)iodo]benzene (0.5 eq) was added initially and further 0.5 eq every 2 h (until in total 1.5 eq were added), while stirring the reaction mixture at room temperature. After stirring for additional 2 – 20 h, the reaction mixture was diluted with ethyl acetate (40 mL/mmol alkyne) and filtered through a pad of silica. The pad was washed with ethyl acetate (50 – 150 mL), the filtrate concentrated *in vacuo* and the residue purified by flash column chromatography.

b: Using [bis(trifluoracetoxy)iodo]benzene and oximes (10 eq)

The respective alkyne (1.0 eq) and oxime (10 eq) were dissolved or suspended in methanol/water (5:1, 10 mL/mmol alkyne). [Bis(trifluoroacetoxy)iodo]benzene (0.5 eq) was added initially and further 0.5 eq every 30 min (until in total 10 eq were added), while stirring the reaction mixture at room temperature. After stirring for additional 1 – 7 d, the mixture was diluted with ethyl acetate (40 mL/mmol alkyne) and filtered through a pad of silica. The pad was washed with ethyl acetate (50 – 150 mL), the filtrate concentrated *in vacuo* and the residue purified by flash column chromatography.

IV: PICTET-SPENGLER reaction of arylaldehydes and tryptamine

The respective aldehyde (1.0 eq) and tryptamine (1.0 eq) were dissolved in anisole (10 mL/mmol aldehyde) and the solution was stirred at 120 °C for 2 h. Then, palladium on carbon (10 wt.%, 0.5 eq) was added, the reaction mixture was stirred at 140 °C for 24 h and, after cooling to room temperature, filtered through a pad of celite. The pad was washed with methanol or ethyl acetate, the filtrate concentrated *in vacuo* and the residue purified by flash column chromatography.

V: Oxime synthesis

The respective aldehyde (1.0 eq), hydroxylamine hydrochloride (1.6 eq) and sodium acetate (2.0 eq) were dissolved in methanol/water (7:3, 2 mL/mmol) and the solution was stirred at 90 °C for 2 h. After cooling to room temperature, the reaction mixture was diluted with water (50 mL) and extracted with ethyl acetate (3 x 20 mL). The combined organic layers were dried over Na_2SO_4 and filtered. The solvent was removed *in vacuo* and the oximes were used without further purification or purified by flash column chromatography, as described below for the single products.

VI: SUZUKI-MIYAURA cross-couplings

a: SUZUKI-MIYAURA cross-coupling of bromoarylaldehydes with phenyl boronic acid

The respective bromoarylaldehyde (1.0 eq), phenylboronic acid (1.2 eq) and Cs_2CO_3 (2.5 eq) were dissolved or suspended in degassed 1,4-dioxane/water (2:1, 15 mL/mmol aldehyde) under N_2 atmosphere. The reaction mixture was stirred for 5 min at room temperature, before $Pd(PPh_3)_4$ (0.05 eq) was added, then purged with N_2 for 5 min and stirred at 100 °C for 5 h. After cooling to room temperature, the mixture was partitioned between methylene chloride (20 mL) and sat. aq. NaCl solution (40 mL). The aq. phase was further extracted with methylene chloride (3 x 20 mL) and the combined organic layers were dried over Na_2SO_4 and filtered. The solvent was removed *in vacuo* and the residue purified by flash column chromatography.

b: SUZUKI-MIYAURA cross-coupling of aryl triflates with 1*H*-pyrazol-3-ylboronic acid

The respective aryl triflate (1.0 eq), 1*H*-pyrazol-3-ylboronic acid hydrate (1.2 – 2.0 eq), Na_2CO_3 (3.0 eq) and $Pd(PPh_3)_4$ (0.04 – 0.05 eq) were dissolved or suspended in degassed 1,4-dioxane/water (4:1, 12.5 – 15 mL/mmol triflate) under N_2 atmosphere in a pressure tube. The suspension was purged with N_2 for 5 min at room temperature, before the tube was sealed and the reaction mixture stirred at 85 °C for 16 – 20 h. After cooling to room temperature, the mixture was partitioned between ethyl acetate and sat. aq. NaCl solution. The aq. phase was further extracted with ethyl acetate and the combined organic layers were dried using a phase separation filter. The solvent was removed *in vacuo* and the crude product purified by flash column chromatography.

c: SUZUKI-MIYAURA cross-coupling of 3-bromo-6-azaindoles with (*E*)-2-ethoxyvinylboronic acid pinacol ester

The respective 3-bromo-6-azaindole (1.0 eq), $Pd(PPh_3)_4$ (0.1 eq) and (*E*)-2-ethoxyvinylboronic acid pinacol ester (2.0 eq) were dissolved or suspended in degassed 1,4-dioxane (6 mL/mmol aryl bromide) under N_2 atmosphere and the mixture stirred at room temperature for 10 min. A solution of Cs_2CO_3 (5.0 eq) in degassed water (2 mL/mmol aryl bromide) was added and the

reaction mixture was stirred at 95 °C for 18 h. After cooling to room temperature, the mixture was filtered through a pad of celite. The pad was washed with ethyl acetate and sat. aq. NH_4Cl solution was added to the filtrate. The phases were separated and the aq. phase further extracted with ethyl acetate. The combined organic layers were dried over Na_2SO_4, filtered and concentrated *in vacuo* and the crude product was purified by flash column chromatography.

VII: NH-Substitution of *β*-carbolines and 6-azaindoles

a: SEM protection

The respective *β*-carboline or 6-azaindole (1.0 eq) was dissolved in anhydrous DMF (1.2 – 2.5 mL/mmol *β*-carboline or 6-azaindole) under N_2 atmosphere. Lithium bis(trimethylsilyl)amide (1 M in THF, 1.1 eq) was slowly added and the reaction mixture stirred at room temperature for 10 min, before 2-(chloromethoxy)ethyltrimethylsilane (SEM chloride) (1.1 eq) was added. The mixture was stirred for further 18 h, then diluted with sat. aq. NaCl solution and extracted with ethyl acetate. The combined organic layers were dried over Na_2SO_4, filtered and concentrated *in vacuo* and the crude product was purified by flash column chromatography.

b: Benzyl and PMB protection

The respective *β*-carboline (1.0 eq) was dissolved in anhydrous DMF (16 – 20 mL/mmol *β*-carboline) under N_2 atmosphere and the solution was cooled to 0 °C. Sodium hydride (60% dispersion in mineral oil, 2.0 eq) was added and the reaction mixture was warmed to room temperature and stirred for 1 h. Then, a solution of the respective benzyl halide (1.1 – 1.9 eq) in anhydrous DMF (0.5 mL) under N_2 atmosphere was added dropwise. After stirring for 16 h, the mixture was diluted with water and extracted with methylene chloride. The combined organic layers were dried over Na_2SO_4, filtered and concentrated *in vacuo* and the crude product was purified by flash column chromatography.

c: Further NH-substitutions

The respective *β*-carboline (1.0 eq) was dissolved in anhydrous DMF (20 mL/mmol *β*-carboline) under N_2 atmosphere, then sodium hydride (60% dispersion in mineral oil, 1.1 – 2.0 eq) was added and the reaction mixture was stirred for 1 h at room temperature. Then, a solution of the respective alkyl halide (1.2 – 1.4 eq) in anhydrous DMF (0.5 mL) under N_2 atmosphere was added dropwise. After stirring for 16 h, the mixture was diluted with water (30 mL) and extracted with methylene chloride (3 x 30 mL). The combined organic layers were washed with sat. aq. NaCl solution (30 mL) and aq. LiCl solution (5%, 60 mL). The aq. LiCl phase was reextracted with methylene chloride (2 x 30 mL) and the combined organic layers were dried over Na_2SO_4, filtered and concentrated *in vacuo*. The crude product was purified by flash column chromatography.

VIII: Alkaline hydrolysis of 4-isoxazolecarboxylic acid esters

The respective carboxylic acid ester (1.0 eq) was dissolved or suspended in ethanol (25 mL/mmol ester). KOH (5.0 eq) was added and the reaction mixture stirred for 2 h at 85 °C. After cooling to room temperature, the solvent was removed *in vacuo*. The residue was resuspended in water (50 mL/mmol ester) and the pH was adjusted to 1 with aq. HCl (2 M). As described for the single products in detail, the aq. phase was then either extracted with methylene chloride or the precipitate was collected by filtration.

IX: SEM deprotection

The respective *N*-SEM protected *β*-carboline (1.0 eq) was dissolved in methylene chloride (40 mL/mmol *β*-carboline) and cooled to 0 °C. Trifluoroacetic acid (4 mL/mmol *β*-carboline) was added dropwise, the reaction mixture was slowly warmed to room temperature and stirred for 16 h. The solvent was removed *in vacuo* and the residue was redissolved at 0 °C in aq. ammonia (25%, 40 mL/mmol *β*-carboline) and methylene chloride (40 mL/mmol *β*-carboline). After stirring for 30 min at room temperature, the mixture was diluted with water (30 mL/mmol *β*-carboline) and extracted with methylene chloride (30 mL/mmol *β*-carboline). The combined organic layers were dried using a phase separation filter and concentrated *in vacuo* and the crude product was purified by flash column chromatography.

X: CURTIUS rearrangements

a: Formation of *N*-Boc amines

The respective carboxylic acid (1.0 eq) was dissolved in *tert*-butanol (10 mL/mmol, dried over 3 Å molecular sieves) under N_2 atmosphere in a pressure tube. Diphenyl phosphoryl azide (1.0 eq) and triethylamine (1.0 eq) were added and the tube was sealed. The solution was stirred at 100 °C for 24 h and, after cooling to room temperature, partitioned between aq. HCl (1 M, 50 mL/mol) and ethyl acetate (50 mL/mol). The aq. phase was further extracted with ethyl acetate (2 x 50 mL/mol), the combined organic layers were washed with sat. aq. $NaHCO_3$ solution (50 mL/mol) and dried using a phase separation filter. The solvent was removed *in vacuo* and the crude product was used without further purification or purified as described for the single products.

b: Formation of primary amines

The respective carboxylic acid (1.0 eq) was dissolved or suspended in anhydrous THF (6 mL/mmol carboxylic acid) under N_2 atmosphere in a pressure tube. Triethylamine (2.3 eq) and diphenyl phosphoryl azide (1.15 eq) were added and the tube was sealed. The mixture was stirred at room temperature for 3 h and subsequently at 80 °C for 2 h. After cooling to

room temperature, water (1.0 mL) was added and the reaction mixture stirred at 80 °C for 15 h. The work-up procedure was performed as described for the single products.

XI: C-1 Halogenation of 10*H*-phenothiazine

Phenothiazine (1.0 eq) was dissolved in anhydrous diethyl ether (10 mL/mmol phenothiazine) under N_2 atmosphere and cooled to 0 °C, then *n*-butyllithium (2.5 M in hexanes, 2.25 eq) was added dropwise and the reaction mixture was slowly warmed to room temperature. After stirring for 24 h, a solution of the respective ethylene 1,2-dihalide (1.1 eq) in anhydrous diethyl ether (0.5 mL/mmol dihalide) under N_2 atmosphere was added. The mixture was stirred for further 24 h at room temperature and, after the addition of ice water (40 mL/mmol phenothiazine), extracted with ethyl acetate (3 x 40 mL/mmol phenothiazine). The combined organic layers were dried using a phase separation filter, the solvent was removed *in vacuo* and the residue purified by flash column chromatography.

XII: BUCHWALD-HARTWIG *N*-arylation of aminopyridine 160[b]

Aminopyridine **160[b]** (1.0 eq), $Pd(dba)_2$ (0.04 – 0.05 eq), Xantphos (0.08 – 0.09 eq), NaO*t*Bu (2.0 eq) and the respective aryl halide (1.0 – 3.0 eq) were suspended in anhydrous toluene (5 mL/mmol aminopyridine) under N_2 atmosphere. The reaction mixture was stirred at 110 °C for 6 h and, after cooling to room temperature, filtered through a pad of celite. The pad was washed with ethyl acetate (50 – 100 mL), the filtrate concentrated *in vacuo* and the residue purified by flash column chromatography.

XIII: HECK-like cyclization of brominated diarylamines

The respective bromide (1.0 eq), $Pd(OAc)_2$ (0.2 eq) and CyJohnPhos (0.2 eq) were suspended in anhydrous DMA (2 mL/mmol bromide) under N_2 atmosphere in a pressure tube. The suspension was purged with N_2 for 10 min at room temperature, before DBU (2.0 eq) was added. The tube was sealed and the reaction mixture stirred at 130 °C for 20 h. After cooling to room temperature, the mixture was diluted with methylene chloride (50 mL). Water (50 mL) and sat. aq. NaCl solution (50 mL) were added, and the pH was adjusted to 12 with aq. NaOH solution (2 M). The phases were separated and the aq. phase was further extracted with methylene chloride (2 x 50 mL). The combined organic layers were dried using a phase separation filter, the solvent was removed *in vacuo* and the residue purified by flash column chromatography.

5.3 Synthetic procedures and analytical data

5.3.1 Lead structure **1** and variations of the phenyl ring

_N_-(2,2-Dimethoxyethyl)-1_H_-indole-2-carboxamide (6)[89]

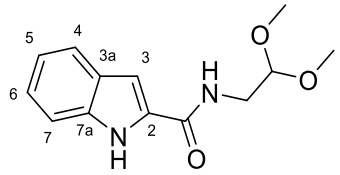

$C_{13}H_{16}N_2O_3$

M_r = 248.28 g/mol

Indole-2-carboxylic acid (9.67 g, 60.0 mmol, 1.0 eq) and aminoacetaldehyde dimethyl acetal (7.20 mL, 66.0 mmol, 1.1 eq) were dissolved in methylene chloride (60 mL) and cooled to 0 °C. *N*,*N*‘-Dicyclohexylcarbodiimide (12.4 g, 60.0 mmol, 1.0 eq) was added in portions, then the reaction mixture was warmed to room temperature and stirred for 20 h. The precipitate was filtered and washed with methylene chloride (150 mL). The solvent of the filtrate was removed *in vacuo* and the residue purified by flash column chromatography (25% → 40% ethyl acetate in hexanes) to give amide **6** as white solid (10.3 g, 41.5 mmol, 69%).

R_f = 0.13 (25% ethyl acetate and 1% acetic acid in hexanes).

Melting point = 130 °C (lit.[292] 130 – 131 °C).

^{1}H NMR (500 MHz, chloroform-*d*) δ (ppm) = 9.60 (s, 1H, NH), 7.66 (dq, *J* = 8.0, 0.9 Hz, 1H, 4-H), 7.45 (dq, *J* = 8.2, 0.9 Hz, 1H, 7-H), 7.29 (ddd, *J* = 8.2, 7.0, 1.1 Hz, 1H, 6-H), 7.14 (ddd, *J* = 8.0, 7.0, 1.0 Hz, 1H, 5-H), 6.90 (dd, *J* = 2.2, 1.0 Hz, 1H, 3-H), 6.48 (t, *J* = 6.1 Hz, 1H, CONH), 4.53 (t, *J* = 5.3 Hz, 1H, CH), 3.67 (dd, *J* = 5.9, 5.3 Hz, 2H, CH_2), 3.46 (s, 6H, OCH_3).

^{13}C NMR (126 MHz, chloroform-*d*) δ (ppm) = 161.9 (CO), 136.5 (C-7a), 130.6 (C-2), 127.8 (C-3a), 124.7 (C-6), 122.1 (C-4), 120.8 (C-5), 112.1 (C-7), 102.9 (CH), 102.5 (C-3), 54.9 (OCH_3), 41.4 (CH_2).

IR (ATR) $\tilde{\nu}$ (cm^{-1}) = 3306, 3238, 1633, 1555, 1419, 1312, 1302, 1266, 1189, 1101, 1060, 1042, 818, 745.

HRMS (EI) (*m/z*) = calculated for $C_{13}H_{16}N_2O_3^{\cdot+}$ $[M]^{\cdot+}$ 248.1156, found 248.1156.

Purity (HPLC, method 2e) > 95% (λ = 210 nm), > 95% (λ = 254 nm).

2,9-Dihydro-1*H*-pyrido[3,4-*b*]indol-1-one (5)[89]

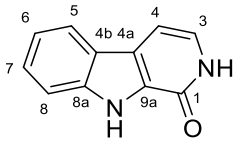

$C_{11}H_8N_2O$

M_r = 184.20 g/mol

Similar to literature[89], amide **6** (4.59 g, 18.5 mmol, 1.0 eq) was suspended in polyphosphoric acid (38.0 g, 158 mmol, 8.6 eq) and stirred at 110 °C for 30 min. After cooling to room temperature, the resinous mass was neutralized with sat. aq. Na_2CO_3 solution. The precipitate was filtered and the filtrate was extracted with ethyl acetate (3 x 300 mL). The combined organic layers were dried over Na_2SO_4, filtered and concentrated *in vacuo*. Additionally, the precipitate from the initial filtration was washed with methanol (400 mL) and the solvent of this filtrate was removed *in vacuo*. Both residues were united and purified by flash column chromatography (50% ethyl acetate in hexanes → 100% ethyl acetate → 3% methanol in ethyl acetate) to give *β*-carbolinone **5** as ochre solid (1.69 g, 9.19 mmol, 50%).

R_f = 0.40 (7% ethanol in methylene chloride).

Melting point = 265 °C (lit.[89] 251 – 252 °C).

^{1}H NMR (400 MHz, DMSO-d_6) δ (ppm) = 11.92 (s, 1H, 9-NH), 11.38 (s, 1H, 2-NH), 8.02 (dq, *J* = 8.0, 1.0 Hz, 1H, 5-H), 7.51 (dt, *J* = 8.3, 1.0 Hz, 1H, 8-H), 7.40 (ddd, *J* = 8.3, 7.0, 1.2 Hz, 1H, 7-H), 7.17 (ddd, *J* = 8.0, 7.0, 1.0 Hz, 1H, 6-H), 7.10 – 7.04 (m, 1H, 3-H), 6.98 (d, *J* = 6.8 Hz, 1H, 4-H).

^{13}C NMR (101 MHz, DMSO-d_6) δ (ppm) = 155.7 (CO), 139.0 (C-8a), 128.0 (C-9a), 126.2 (C-7), 124.5 (C-3), 124.2 (C-4a), 122.0 (C-4b), 121.3 (C-5), 119.5 (C-6), 112.4 (C-8), 99.7 (C-4).

IR (ATR) $\tilde{\nu}$ (cm^{-1}) = 3109, 3962, 2843, 1640, 1444, 1326, 1232, 952, 831, 738.

HRMS (EI) (*m/z*) = calculated for $C_{11}H_8N_2O^{\cdot+}$ $[M]^{\cdot+}$ 184.0632, found 184.0630.

Purity (HPLC, method 2e) > 95% (λ = 210 nm), > 95% (λ = 254 nm).

1-Bromo-9*H*-pyrido[3,4-*b*]indole (8)[90]

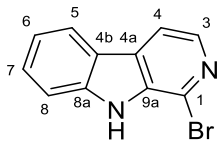

$C_{11}H_7BrN_2$

M_r = 247.10 g/mol

Similar to literature[90], phosphorus(V) oxybromide (9.0 g, 32 mmol, 7.0 eq) was dissolved in anisole (9.0 mL) and this solution added to *β*-carbolinone **5** (829 mg, 4.50 mmol, 1.0 eq). The reaction mixture was stirred at 120 °C for 13 h, slowly cooled to room temperature and stirred for further 16 h. The mixture was cautiously neutralized with sat. aq. Na_2CO_3 solution and extracted with ethyl acetate (3 x 200 mL). The combined organic layers were dried over Na_2SO_4, filtered and concentrated *in vacuo*. The crude product was purified by flash column chromatography (10% → 20% ethyl acetate in hexanes) to give bromide **8** as pale yellow solid (981 mg, 3.97 mmol, 88%).

R_f = 0.35 (20% ethyl acetate in hexanes).

Melting point = 155 °C (lit.[90] 152 °C).

^{1}H NMR (400 MHz, chloroform-*d*) δ (ppm) = 8.50 (s, 1H, NH), 8.23 (d, *J* = 5.2 Hz, 1H, 3-H), 8.10 (dq, *J* = 7.9, 0.9 Hz, 1H, 5-H), 7.91 (dd, *J* = 5.2, 0.7 Hz, 1H, 4-H), 7.62 – 7.55 (m, 2H, 7-H, 8-H), 7.33 (ddd, *J* = 8.0, 6.4, 1.7 Hz, 1H, 6-H).

^{13}C NMR (101 MHz, chloroform-*d*) δ (ppm) = 139.9 (C-8a), 139.3 (C-3), 135.0 (C-9a), 130.1 (C-4a), 129.2 (C-7), 124.7 (C-1), 122.3 (C-5), 122.2 (C-4b), 121.0 (C-6), 114.7 (C-4), 112.1 (C-8).

IR (ATR) $\tilde{\nu}$ (cm^{-1}) = 3157, 1626, 1545, 1500, 1452, 1321, 1236, 1182, 1149, 1039, 824, 730.

HRMS (ESI) (*m/z*) = calculated for $C_{11}H_8{}^{79}BrN_2^+$ $[M+H]^+$ 246.9866, found 246.9865.

Purity (HPLC, method 2e) > 95% (λ = 210 nm), > 95% (λ = 254 nm).

1-Ethynyl-9*H*-pyrido[3,4-*b*]indole (3)[86]

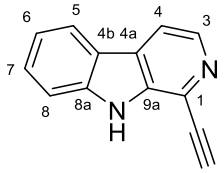

$C_{13}H_8N_2$

M_r = 192.22 g/mol

Method A: Following **General Procedure Ia**, bromide **8** (1.20 g, 4.85 mmol, 1.0 eq), CuI (193 mg, 1.01 mmol, 0.2 eq), Pd(dppf)Cl_2 (181 mg, 0.247 mmol, 0.05 eq) and trimethylsilylacetylene (0.816 mL, 5.77 mmol, 1.2 eq, dissolved in 4.0 mL anhydrous THF) were used in anhydrous triethylamine (15 mL) and anhydrous THF (11 mL). After stirring for 3.5 h, the reaction was completed. The celite pad was washed with ethyl acetate (200 mL) and the extraction was performed with water (150 mL) and ethyl acetate (3 x 50 mL).
The crude TMS-protected intermediate **9** (R_f = 0.39, 20% ethyl acetate in hexanes) was desilylated, following **General Procedure II**, with K_2CO_3 (2.21 g, 16.0 mmol, 3.3 eq) in methanol (40 mL). The crude product was purified by flash column chromatography (20% → 40% ethyl acetate in hexanes) to give terminal alkyne **3** as light brown solid (652 mg, 3.39 mmol, 70% over two steps).

Method B: Following **General Procedure Ib**, triflate **10** (0.380 g, 1.20 mmol, 1.0 eq), LiCl (0.15 g, 3.6 mmol, 3.0 eq), Pd(PPh_3)$_2Cl_2$ (67 mg, 0.096 mmol, 0.08 eq), CuI (23 mg, 0.12 mmol, 0.1 eq) and trimethylsilylacetylene (1.19 mL, 8.40 mmol, 7.0 eq) were used in anhydrous DMF/triethylamine (25 mL).
The crude TMS-protected intermediate **9** was desilylated, following **General Procedure II**, with K_2CO_3 (0.654 g, 3.96 mmol, 3.3 eq) in methanol (10 mL). The crude product was purified by flash column chromatography (40% ethyl acetate in hexanes) to give terminal alkyne **3** as light brown solid (95.0 mg, 0.494 mmol, 41% over two steps).

R_f = 0.24 (40% ethyl acetate in hexanes).

Melting point = 163 °C (lit.[86] 174 °C).

^{1}H NMR (400 MHz, methylene chloride-d_2) δ (ppm) = 8.65 (s, 1H, NH), 8.43 (d, J = 5.2 Hz, 1H, 3-H), 8.16 (dq, J = 7.9, 0.9 Hz, 1H, 5-H), 7.98 (dd, J = 5.2, 0.7 Hz, 1H, 4-H), 7.62 – 7.56 (m, 2H, 7-H, 8-H), 7.33 (ddd, J = 8.0, 4.9, 3.2 Hz, 1H, 6-H), 3.63 (s, 1H, CCH).

^{13}C NMR (126 MHz, methylene chloride-d_2) δ (ppm) = 140.6 (C-8a), 140.2 (C-3), 138.4 (C-9a), 129.4 (C-7), 129.2 (C-4a), 125.9 (C-1), 122.4 (C-5), 122.1 (C-4b), 121.0 (C-6), 115.6 (C-4), 112.1 (C-8), 82.2 (C<u>C</u>H), 80.0 (<u>C</u>CH).

IR (ATR) $\tilde{\nu}$ (cm^{-1}) = 3289, 3054, 2007, 1625, 1561, 1498, 1452, 1424, 1321, 1227, 1065, 826, 738, 667.

HRMS (EI) (*m/z*) = calculated for $C_{13}H_8N_2^{\cdot+}$ $[M]^{\cdot+}$ 192.0682, found 192.0684.

Purity (HPLC, method 2e) > 95% (λ = 210 nm), > 95% (λ = 254 nm).

3-Phenyl-5-(9*H*-pyrido[3,4-*b*]indol-1-yl)isoxazole (1)[86]

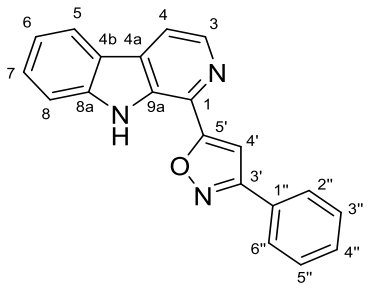

$C_{20}H_{13}N_3O$

M_r = 311.34 g/mol

Method A: Following **General Procedure IIIa**, alkyne **3** (100 mg, 0.520 mmol, 1.0 eq), (*E*)-benzaldehyde oxime (94.5 mg, 0.780 mmol, 1.5 eq) and [bis(trifluoroacetoxy)iodo]benzene (335 mg, 0.780 mmol, 1.5 eq) were used in methanol/water (5.2 mL). After stirring for additional 2 h, the reaction was completed. The crude product was purified by flash column chromatography (15% → 20% ethyl acetate in hexanes) to give isoxazole **1** as yellow solid (138 mg, 0.443 mmol, 85%).

Method B: Alkyne **3** (192 mg, 1.00 mmol, 1.0 eq) and *N*-hydroxybenzimidoyl chloride (233 mg, 1.50 mmol, 1.5 eq) were dissolved in anhydrous chloroform (2.0 mL) under N_2 atmosphere. The solution was stirred at room temperature, while triethylamine (0.209 mL, 1.50 mmol, 1.5 eq) was added dropwise over 15 min. After stirring the reaction mixture at room temperature for 2 h, it was partitioned between water (60 mL) and methylene chloride (30 mL) and the aq. phase was further extracted with methylene chloride (2 x 30 mL). The combined organic layers were dried over Na_2SO_4, filtered and concentrated *in vacuo*. The crude product was purified by flash column chromatography (15% → 25% ethyl acetate in hexanes) to give isoxazole **1** as pale yellow solid (115 mg, 0.370 mmol, 37%).

Method C: Following **General Procedure IV**, aldehyde **53** (86.6 mg, 0.500 mmol, 1.0 eq), tryptamine (80.1 mg, 0.500 mmol, 1.0 eq) and palladium on carbon (10 wt. %, 266 mg, 0.250 mmol, 0.5 eq) were used in anisole (5.0 mL). The celite pad was washed with ethyl acetate (50 mL). The crude product was purified by flash column chromatography (20% ethyl acetate in hexanes) to give *β*-carboline **1** as yellow solid (97.4 mg, 0.313 mmol, 63%).

R_f = 0.26 (20% ethyl acetate in hexanes).

Melting point = 172 °C (lit.[86] 166 °C).

^{1}H NMR (400 MHz, methylene chloride-d_2) δ (ppm) = 9.62 (s, 1H, NH), 8.54 (d, *J* = 5.1 Hz, 1H, 3-H), 8.18 (dq, *J* = 7.9, 0.9 Hz, 1H, 5-H), 8.05 (dd, *J* = 5.0, 0.8 Hz, 1H, 4-H), 7.97 – 7.93 (m, 2H, 2''-H, 6''-H), 7.66 – 7.60 (m, 2H, 7-H, 8-H), 7.56 – 7.50 (m, 3H, 3''-H, 4''-H, 5''-H), 7.43 (s, 1H, 4'-H), 7.34 (ddd, J = 8.0, 5.8, 2.3 Hz, 1H, 6-H).

^{13}C NMR (101 MHz, methylene chloride-d_2) δ (ppm) = 171.3 (C-5‘), 163.4 (C-3‘), 141.2 (C-8a), 139.7 (C-3), 133.2 (C-9a), 131.3 (C-4a), 130.7 (C-4‘‘), 130.3 (C-1), 129.6 (C-7), 129.4 (C-3‘‘, C-5‘‘), 129.2 (C-1‘‘), 127.3 (C-2‘‘, C-6‘‘), 122.1 (C-5), 121.3 (C-4b), 121.0 (C-6), 116.4 (C-4), 112.3 (C-8), 100.3 (C-4‘).

IR (ATR) $\tilde{\nu}$ (cm^{-1}) = 3229, 2927, 1609, 1556, 1440, 1428, 1399, 1286, 1238, 1223, 811, 755.

HRMS (EI) (*m/z*) = calculated for $C_{20}H_{13}N_3O^{\cdot+}$ $[M]^{\cdot+}$ 311.1054, found 311.1053.

Purity (HPLC, method 2a) > 95% (λ = 210 nm), > 95% (λ = 254 nm).

(*E*)-2-Nitrobenzaldehyde oxime (12)[293]

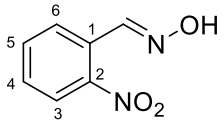

$C_7H_6N_2O_3$

M_r = 166.14 g/mol

Following **General Procedure V**, 2-nitrobenzaldehyde (1.51 g, 10.0 mmol, 1.0 eq), hydroxylamine hydrochloride (1.11 g, 16.0 mmol, 1.6 eq) and sodium acetate (1.64 g, 20.0 mmol, 2.0 eq) were used in methanol/water (20 mL). The crude product was purified by flash column chromatography (20% → 25% ethyl acetate in hexanes) to give oxime **12** as white solid (1.59 g, 9.56 mmol, 96%).

R_f = 0.22 (100% methylene chloride).

Melting point = 101 °C (lit.[293] 100 – 101 °C).

^{1}H NMR (400 MHz, DMSO-d_6) δ (ppm) = 11.77 (s, 1H, OH), 8.41 (s, 1H, CHN), 8.04 (dd, *J* = 8.2, 1.3 Hz, 1H, 3-H), 7.88 (dd, *J* = 7.8, 1.5 Hz, 1H, 6-H), 7.76 (td, *J* = 7.6, 1.3 Hz, 1H, 5-H), 7.64 (td, *J* = 7.8, 1.5 Hz, 1H, 4-H).

^{13}C NMR (101 MHz, DMSO-d_6) δ (ppm) = 147.6 (C-2), 144.8 (CHN), 133.6 (C-5), 130.2 (C-4), 128.4 (C-6), 127.2 (C-1), 124.6 (C-3).

IR (ATR) $\tilde{\nu}$ (cm^{-1}) = 3255, 1518, 1487, 1344, 1318, 1210, 1145, 977, 960, 851, 740, 693.

HRMS (ESI) (*m/z*) = calculated for $C_7H_5N_2O_3^-$ $[M-H]^-$ 165.0306, found 165.0306.

Purity (HPLC, method 2h) > 93% (λ = 210 nm), > 95% (λ = 254 nm).

(*E*)-2-Chlorobenzaldehyde oxime (13)[294]

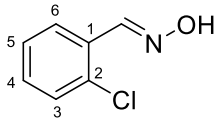

C_7H_6ClNO

M_r = 155.58 g/mol

Following **General Procedure V**, 2-chlorobenzaldehyde (703 mg, 5.00 mmol, 1.0 eq), hydroxylamine hydrochloride (556 mg, 8.00 mmol, 1.6 eq) and sodium acetate (820 mg, 10.0 mmol, 2.0 eq) were used in methanol/water (10 mL). The crude product was purified by flash column chromatography (10% ethyl acetate in hexanes) to give oxime **13** as white solid (584 ng, 3.75 mmol, 75%).

R_f = 0.45 (100% methylene chloride).

Melting point = 73 °C (lit.[294] 72 – 74 °C).

^{1}H NMR (400 MHz, DMSO-d_6) δ (ppm) = 11.68 (s, 1H, OH), 8.36 (s, 1H, CHN), 7.82 (dd, *J* = 7.6, 1.9 Hz, 1H, 6-H), 7.50 (dd, *J* = 7.9, 1.4 Hz, 1H, 3-H), 7.41 (td, *J* = 7.7, 2.0 Hz, 1H, 4-H), 7.39 – 7.35 (m, 1H, 5-H).

^{13}C NMR (101 MHz, DMSO-d_6) δ (ppm) = 144.5 (CHN), 132.2 (C-2), 130.9 (C-4), 130.3 (C-1), 129.8 (C-3), 127.5 (C-5), 126.8 (C-6).

IR (ATR) $\tilde{\nu}$ (cm^{-1}) = 3273, 1480, 1441, 1311, 1284, 1211, 1050, 1035, 971, 949, 872, 745, 708.

HRMS (EI) (*m/z*) = calculated for $C_7H_6ClNO^{\cdot+}$ $[M]^{\cdot+}$ 155.0133, found 155.0131.

Purity (HPLC, method 2e) > 95% (λ = 210 nm), > 95% (λ = 254 nm).

(*E*)-4-Iodobenzaldehyde oxime (14)[295]

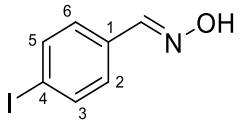

C_7H_6INO

M_r = 247.04 g/mol

Following **General Procedure V**, 4-iodobenzaldehyde (232 mg, 1.00 mmol, 1.0 eq), hydroxylamine hydrochloride (111 mg, 1.60 mmol, 1.6 eq) and sodium acetate (164 mg, 2.00 mmol, 2.0 eq) were used in methanol/water (2.0 mL). Without further purification, pure oxime **14** was obtained as pale yellow solid (248 mg, 1.00 mmol, quantitative).

R_f = 0.36 (100% methylene chloride).

Melting point = 116 °C (lit.[295] 111 – 112 °C).

^{1}H NMR (400 MHz, DMSO-d_6) δ (ppm) = 11.35 (s, 1H, OH), 8.10 (s, 1H, CHN), 7.80 – 7.72 (m, 2H, 3-H, 5-H), 7.42 – 7.34 (m, 2H, 2-H, 6-H).

^{13}C NMR (101 MHz, DMSO-d_6) δ (ppm) = 147.4 (CHN), 137.5 (C-3, C-5), 132.6 (C-1), 128.3 (C-2, C-6), 95.7 (C-4).

IR (ATR) $\tilde{\nu}$ (cm^{-1}) = 3246, 1584, 1480, 1392, 1310, 1003, 965, 949, 926, 865, 810.

HRMS (EI) (*m/z*) = calculated for $C_7H_6INO^{\cdot+}$ $[M]^{\cdot+}$ 246.9489, found 246.9489.

Purity (HPLC, method 2e) > 95% (λ = 210 nm), > 94% (λ = 254 nm).

(*E*)-Picolinaldehyde oxime (15)[296]

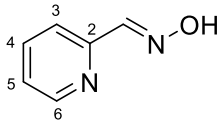

$C_6H_6N_2O$

M_r = 122.13 g/mol

Following **General Procedure V**, 2-pyridinecarboxaldehyde (536 mg, 5.00 mmol, 1.0 eq), hydroxylamine hydrochloride (556 mg, 8.00 mmol, 1.6 eq) and sodium acetate (820 mg, 10.0 mmol, 2.0 eq) were used in methanol/water (10 mL). The crude product was purified by flash column chromatography (20% → 25% ethyl acetate in hexanes) to give oxime **15** as white solid (512 ng, 4.19 mmol, 84%).

R_f = 0.10 (20% ethyl acetate in hexanes).

Melting point = 114 °C (lit.[296] 114 °C).

^{1}H NMR (400 MHz, DMSO-d_6) δ (ppm) = 11.66 (s, 1H, OH), 8.61 – 8.53 (m, 1H, 6-H), 8.07 (s, 1H, CHN), 7.84 – 7.80 (m, 1H, 4-H), 7.78 (dt, *J* = 6.8, 0.7 Hz, 1H, 3-H), 7.37 (ddd, *J* = 6.8, 4.9, 1.8 Hz, 1H, 5-H).

^{13}C NMR (101 MHz, DMSO-d_6) δ (ppm) = 152.1 (C-2), 149.4 (C-6), 148.9 (CHN), 136.8 (C-4), 123.9 (C-5), 119.8 (C-3).

IR (ATR) $\tilde{\nu}$ (cm^{-1}) = 2804, 1592, 1564, 1514, 1434, 1320, 1154, 976, 960, 943, 768, 735.

HRMS (EI) (*m/z*) = calculated for $C_6H_6N_2O^{\cdot+}$ $[M]^{\cdot+}$ 122.0475, found 122.0475.

Purity (HPLC, method 2i) > 95% (λ = 210 nm), > 94% (λ = 254 nm).

(*Z*)-Thiophene-2-carbaldehyde oxime (16)[297]

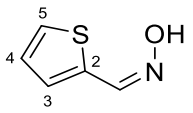

C_5H_5NOS

M_r = 127.16 g/mol

Following **General Procedure V**, 2-thiophenecarboxaldehyde (0.467 mL, 5.00 mmol, 1.0 eq), hydroxylamine hydrochloride (556 mg, 8.00 mmol, 1.6 eq) and sodium acetate (820 mg, 10.0 mmol, 2.0 eq) were used in methanol/water (10 mL). The crude product was purified by flash column chromatography (20% ethyl acetate in hexanes) to give oxime **16** as white solid (617 mg, 4.85 mmol, 97%).

R_f = 0.24 (100% methylene chloride).

Melting point = 137 °C (lit.[297] 136 – 138 °C).

^{1}H NMR (400 MHz, DMSO-d_6) δ (ppm) = 11.85 (s, 1H, OH), 7.84 (d, *J* = 1.0 Hz, 1H, CHN), 7.73 (dt, *J* = 5.1, 1.2 Hz, 1H, 5-H), 7.47 (dd, *J* = 3.7, 1.3 Hz, 1H, 3-H), 7.13 (dd, *J* = 5.1, 3.7 Hz, 1H, 4-H).

^{13}C NMR (101 MHz, DMSO-d_6) δ (ppm) = 139.8 (CHN), 131.1 (C-2), 131.1 (C-3), 131.0 (C-5), 126.2 (C-4).

IR (ATR) $\tilde{\nu}$ (cm^{-1}) = 2750, 1631, 1433, 1416, 1347, 1306, 1232, 1213, 1051, 941, 799, 712.

HRMS (EI) (*m/z*) = calculated for $C_5H_5NOS^{\cdot+}$ $[M]^{\cdot+}$ 127.0087, found 127.0087.

Purity (HPLC, method 2h) > 95% (λ = 210 nm), > 95% (λ = 254 nm).

Furan-2-carbaldehyde oxime (17)[298]

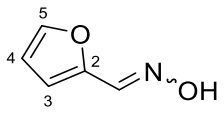

$C_5H_5NO_2$

M_r = 111.10 g/mol

Following **General Procedure V**, furan-2-carboxaldehyde (0.414 mL, 5.00 mmol, 1.0 eq), hydroxylamine hydrochloride (556 mg, 8.00 mmol, 1.6 eq) and sodium acetate (820 mg, 10.0 mmol, 2.0 eq) were used in methanol/water (10 mL). The crude product was purified by flash column chromatography (25% ethyl acetate in hexanes) to give oxime **17** as an *E*/*Z* mixture (*E*/*Z* ratio 1:1.8 determined *via* ^{1}H NMR spectrum) as white solid (542 mg, 4.88 mmol, 98%).

R_f = 0.32 (100% methylene chloride).

Melting point = 89 °C (lit.[298] 89 – 91 °C).

^{1}H NMR (400 MHz, DMSO-d_6) δ (ppm) = 11.79 (s, 1H, OH (*Z*)), 11.23 (s, 1H, OH (*E*)), 8.01 (s, 1H, CHO (*E*)), 7.75 (dd, *J* = 1.7, 0.8 Hz, 1H, 5-H (*Z*)), 7.74 (dd, *J* = 1.8, 0.8 Hz, 1H, 5-H (*E*)), 7.52 (s, 1H, CHO (*Z*)), 7.21 – 7.17 (m, 1H, 3-H (*Z*)), 6.71 – 6.68 (m, 1H, 3-H (*E*)), 6.63 (ddd, *J* = 3.5, 1.8, 0.8 Hz, 1H, 4-H (*Z*)), 6.56 (dd, *J* = 3.4, 1.8 Hz, 1H, 4-H (*E*)).

^{13}C NMR (101 MHz, DMSO-d_6) δ (ppm) = 147.9 (C-2 (*E*)), 145.4 (C-2 (*Z*)), 144.2 (C-5 (*E*)), 143.4 (C-5 (*Z*)), 138.9 (CHO (*E*)), 135.5 (CHO (*Z*)), 116.4 (C-3 (*Z*)), 112.2 (C-4 (*Z*)), 111.7 (C-4 (*E*)), 111.6 (C-3 (*E*)).

IR (ATR) $\tilde{\nu}$ (cm^{-1}) = 2852, 1645, 1477, 1443, 1376, 1144, 1016, 967, 820, 808, 746.

HRMS (EI) (*m*/*z*) = calculated for $C_5H_5NO_2^{\cdot+}$ $[M]^{\cdot+}$ 111.0315, found 111.0316.

Purity (HPLC) n.d.

(*Z*)-1*H*-Pyrrole-2-carbaldehyde oxime (18)[299]

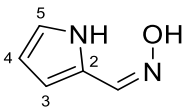

$C_5H_6N_2O$

M_r = 110.12 g/mol

Following **General Procedure V**, pyrrole-2-carboxaldehyde (476 mg, 5.00 mmol, 1.0 eq), hydroxylamine hydrochloride (556 mg, 8.00 mmol, 1.6 eq) and sodium acetate (820 mg, 10.0 mmol, 2.0 eq) were used in methanol/water (10 mL). Without further purification, pure oxime **18** was obtained as pale yellow solid (526 mg, 4.78 mmol, 96%).

R_f = 0.07 (100% methylene chloride).

Melting point = 166 °C (lit.[299] 165 – 166 °C).

^{1}H NMR (400 MHz, DMSO-d_6) δ (ppm) = 11.16 (s, 1H, NH), 11.12 (s, 1H, OH), 7.26 (s, 1H, CHO), 6.88 (td, *J* = 2.7, 1.5 Hz, 1H, 5-H), 6.55 (ddd, *J* = 3.8, 2.3, 1.5 Hz, 1H, 3-H), 6.11 (dt, *J* = 3.6, 2.4 Hz, 1H, 4-H).

^{13}C NMR (101 MHz, DMSO-d_6) δ (ppm) = 137.2 (CHO), 124.0 (C-2), 121.0 (C-5), 114.0 (C-3), 108.5 (C-4).

IR (ATR) $\tilde{\nu}$ (cm^{-1}) = 3426, 3410, 2763, 1644, 1461, 1429, 1412, 1303, 1276, 1083, 916, 832, 741.

HRMS (EI) (*m/z*) = calculated for $C_5H_6N_2O^{\cdot+}$ $[M]^{\cdot+}$ 110.0475, found 110.0470.

Purity (HPLC, method 2h) > 95% (λ = 210 nm), > 95% (λ = 254 nm).

2-(5-(9*H*-Pyrido[3,4-*b*]indol-1-yl)isoxazol-3-yl)phenol (19)

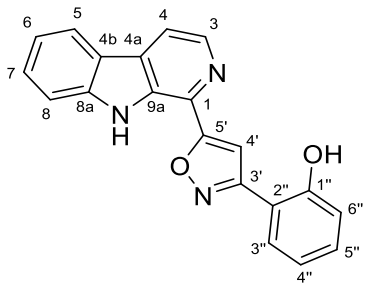

$C_{20}H_{13}N_3O_2$

M_r = 327.34 g/mol

Method A: Following **General Procedure IIIa**, alkyne **3** (48.1 mg, 0.250 mmol, 1.0 eq), 2-hydroxybenzaldoxime (51 mg, 0.38 mmol, 1.5 eq) and [bis(trifluoroacetoxy)iodo]benzene (161 mg, 0.375 mmol, 1.5 eq) were used in methanol/water (2.5 mL). After stirring for additional 16 h, the reaction was completed. The crude product was purified two times by flash column chromatography (15% ethyl acetate in hexanes, 100% methylene chloride) to give isoxazole **19** as white solid (73.1 mg, 0.223 mmol, 89%).

Method B: *N*-Chlorosuccinimide (59 mg, 0.44 mmol, 1.1 eq) was suspended in anhydrous chloroform (1.0 mL) under N_2 atmosphere, then anhydrous pyridine (0.002 mL, 0.020 mmol, 0.05 eq, dissolved in 0.02 mL anhydrous chloroform) and 2-hydroxybenzaldoxime (60 mg, 0.44 mmol, 1.1 eq) were added. The solution was stirred for 30 min at room temperature and for 1 h at 50 °C. Alkyne **3** (76.9 mg, 0.400 mmol, 1.0 eq) was added in one portion and anhydrous triethylamine (0.067 mL, 0.480 mmol, 1.2 eq, dissolved in 0.25 mL anhydrous chloroform) dropwise over 15 min. The reaction mixture was stirred at 50 °C for 3 h and, after cooling to room temperature, partitioned between water (15 mL) and methylene chloride (10 mL). The aq. phase was further extracted with methylene chloride (2 x 10 mL) and the combined organic layers were dried over Na_2SO_4 and filtered. The solvent was removed *in vacuo* and the crude product purified by flash column chromatography (20% ethyl acetate in hexanes) to give isoxazole **19** as white solid (35.8 mg, 0.109 mmol, 27%).

R_f = 0.28 (20% ethyl acetate in hexanes).

Melting point = 222 °C.

^{1}H NMR (400 MHz, DMSO-d_6) δ (ppm) = 11.87 (s, 1H, NH), 10.27 (s, 1H, OH), 8.53 (d, *J* = 5.0 Hz, 1H, 3-H), 8.34 – 8.30 (m, 2H, 4-H, 5-H), 7.90 (dd, *J* = 7.8, 1.8 Hz, 1H, 3‘‘-H), 7.85 – 7.80 (m, 1H, 8-H), 7.68 (s, 1H, 4‘-H), 7.62 (ddd, *J* = 8.3, 7.1, 1.2 Hz, 1H, 7-H), 7.38 (ddd, *J* = 8.7, 7.3, 1.8 Hz, 1H, 5‘‘-H), 7.32 (ddd, *J* = 8.1, 7.1, 1.0 Hz, 1H, 6-H), 7.09 (dd, *J* = 8.2, 1.1 Hz, 1H, 6‘‘-H), 6.99 (td, *J* = 7.5, 1.1 Hz, 1H, 4‘‘-H).

^{13}C NMR (101 MHz, DMSO-d_6) δ (ppm) = 168.7 (C-5‘), 160.5 (C-3‘), 155.8 (C-1‘‘), 141.6 (C-8a), 138.5 (C-3), 132.1 (C-9a), 131.6 (C-5‘‘), 130.4 (C-1 or C-4a), 129.6 (C-1 or C-4a), 128.9 (C-7), 128.7 (C-3‘‘), 121.8 (C-5), 120.3 (C-4b), 120.1 (C-6), 119.5 (C-4‘‘), 116.8 (C-6‘‘), 116.3 (C-4), 114.9 (C-2‘‘), 113.0 (C-8), 103.1 (C-4‘).

IR (ATR) $\tilde{\nu}$ (cm^{-1}) = 3390, 3234, 1618, 1557, 1406, 1382, 1368, 1324, 1299, 1231, 936, 828, 800, 740.

HRMS (ESI) (*m/z*) = calculated for $C_{20}H_{14}N_3O_2^+$ $[M+H]^+$ 328.1081, found 328.1080.

Purity (HPLC, method 1a) > 95% (λ = 210 nm), > 95% (λ = 254 nm).

3-(2-Nitrophenyl)-5-(9*H*-pyrido[3,4-*b*]indol-1-yl)isoxazole (20)

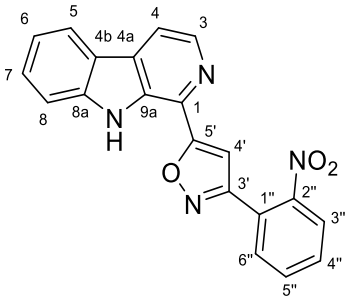

$C_{20}H_{12}N_4O_3$

M_r = 356.34 g/mol

Following **General Procedure IIIb**, alkyne **3** (48.1 mg, 0.250 mmol, 1.0 eq), oxime **12** (415 mg, 2.50 mmol, 10 eq) and [bis(trifluoroacetoxy)iodo]benzene (1.08 g, 2.50 mmol, 10 eq) were used in methanol/water (2.5 mL). After stirring for additional 16 h, the reaction was completed. The crude product was purified two times by flash column chromatography (20% → 25% ethyl acetate in hexanes, 100% methylene chloride) to give isoxazole **20** as yellow solid (45.2 mg, 0.127 mmol, 51%).

R_f = 0.36 (40% ethyl acetate in hexanes).

Melting point = 209 °C.

^{1}H NMR (400 MHz, methylene chloride-d_2) δ (ppm) = 9.59 (s, 1H, NH), 8.55 (d, *J* = 5.1 Hz, 1H, 3-H), 8.21 (dq, *J* = 7.9, 0.9 Hz, 1H, 5-H), 8.09 (dd, *J* = 5.1, 0.7 Hz, 1H, 4-H), 8.03 (ddd, *J* = 8.1, 1.2, 0.6 Hz, 1H, 3‘‘-H), 7.84 – 7.76 (m, 2H, 5‘‘-H, 6‘‘-H), 7.71 (ddd, *J* = 8.0, 6.7, 2.3 Hz, 1H, 4‘‘-H), 7.68 – 7.62 (m, 2H, 7-H, 8-H), 7.37 (ddd, *J* = 8.0, 6.1, 2.0 Hz, 1H, 6-H), 7.24 (s, 1H, 4‘-H).

^{13}C NMR (101 MHz, methylene chloride-d_2) δ (ppm) = 171.4 (C-5‘), 161.0 (C-3‘), 149.3 (C-2‘‘), 141.2 (C-8a), 139.4 (C-3), 133.4 (C-5‘‘), 133.3 (C-9a), 132.0 (C-6‘‘), 131.4 (C-1), 131.4 (C-4‘‘), 129.9 (C-4a), 129.7 (C-7), 124.9 (C-3‘‘), 124.1 (C-1‘‘), 122.2 (C-5), 121.4 (C-4b), 121.1 (C-6), 116.6 (C-4), 112.3 (C-8), 102.3 (C-4‘).

IR (ATR) $\tilde{\nu}$ (cm^{-1}) = 3457, 1611, 1523, 1430, 1347, 1295, 1227, 1139, 1117, 1063, 951, 923, 786, 750.

HRMS (ESI) (*m/z*) = calculated for $C_{20}H_{13}N_4O_3^+$ $[M+H]^+$ 357.0983, found 357.0981.

Purity (HPLC, method 1c) > 95% (λ = 210 nm), > 95% (λ = 254 nm).

3-(2-Chlorophenyl)-5-(9*H*-pyrido[3,4-*b*]indol-1-yl)isoxazole (21)

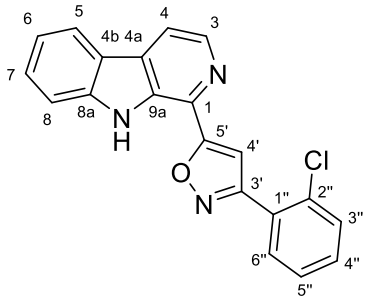

$C_{20}H_{12}ClN_3O$

M_r = 345.79 g/mol

Following **General Procedure IIIa**, alkyne **3** (48.1 mg, 0.250 mmol, 1.0 eq), oxime **13** (58 mg, 0.38 mmol, 1.5 eq) and [bis(trifluoroacetoxy)iodo]benzene (161 mg, 0.375 mmol, 1.5 eq) were used in methanol/water (2.5 mL). After stirring for additional 16 h, the reaction was completed. The crude product was purified by flash column chromatography (10% → 20% ethyl acetate in hexanes) to give isoxazole **21** as pale yellow solid (49.9 mg, 0.144 mmol, 58%).

R_f = 0.61 (40% ethyl acetate in hexanes).

Melting point = 186 °C.

^{1}H NMR (400 MHz, methylene chloride-d_2) δ (ppm) = 9.63 (s, 1H, NH), 8.56 (d, J = 5.1 Hz, 1H, 3-H), 8.21 (dq, J = 7.9, 0.9 Hz, 1H, 5-H), 8.08 (dd, J = 5.1, 0.8 Hz, 1H, 4-H), 7.88 – 7.79 (m, 1H, 6‘‘-H), 7.70 – 7.56 (m, 3H, 7-H, 8-H, 3‘‘-H), 7.52 (s, 1H, 4‘-H), 7.46 (pd, J = 7.4, 1.8 Hz, 2H, 4‘‘-H, 5‘‘-H), 7.36 (ddd, J = 8.0, 6.5, 1.6 Hz, 1H, 6-H).

^{13}C NMR (101 MHz, methylene chloride-d_2) δ (ppm) = 170.7 (C-5‘), 162.2 (C-3‘), 141.2 (C-8a), 139.8 (C-3), 133.5 (C-9a or C-2‘‘), 133.3 (C-9a or C-2‘‘), 131.6 (C-4‘‘), 131.4 (C-6‘‘), 131.3 (C-4a), 130.9 (C-3‘‘), 130.3 (C-1), 129.6 (C-7), 128.5 (C-1‘‘), 127.6 (C-5‘‘), 122.2 (C-5), 121.4 (C-4b), 121.0 (C-6), 116.5 (C-4), 112.3 (C-8), 103.5 (C-4‘).

IR (ATR) $\tilde{\nu}$ (cm^{-1}) = 3228, 2923, 1609, 1555, 1497, 1444, 1426, 1396, 1285, 1237, 1114, 1051, 950, 812.

HRMS (ESI) (*m/z*) = calculated for $C_{20}H_{13}{}^{35}ClN_3O^+$ $[M+H]^+$ 346.0742, found 346.0742.

Purity (HPLC, method 1b) > 95% (λ = 210 nm), > 95% (λ = 254 nm).

3-(4-Iodophenyl)-5-(9*H*-pyrido[3,4-*b*]indol-1-yl)isoxazole (22)

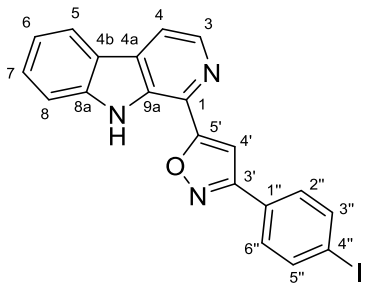

$C_{20}H_{12}IN_3O$

M_r = 437.24 g/mol

Following **General Procedure IIIa**, alkyne **3** (96.1 mg, 0.500 mmol, 1.0 eq), oxime **14** (185 mg, 0.750 mmol, 1.5 eq) and [bis(trifluoroacetoxy)iodo]benzene (323 mg, 0.750 mmol, 1.5 eq) were used in methanol/water (5.0 mL). After stirring for additional 20 h, the reaction was completed. The crude product was purified by flash column chromatography (15% → 20% ethyl acetate in hexanes) to give isoxazole **22** as yellow solid (159 mg, 0.365 mmol, 73%).

R_f = 0.29 (20% ethyl acetate in hexanes).

Melting point = 203 °C.

^{1}H NMR (500 MHz, methylene chloride-d_2) δ (ppm) = 9.59 (s, 1H, NH), 8.55 (d, *J* = 5.1 Hz, 1H, 3-H), 8.20 (dq, *J* = 7.9, 1.0 Hz, 1H, 5-H), 8.07 (dd, *J* = 5.0, 0.8 Hz, 1H, 4-H), 7.90 – 7.87 (m, 2H, 3‘‘-H, 5‘‘-H), 7.72 – 7.69 (m, 2H, 2‘‘-H, 6‘‘-H), 7.67 – 7.65 (m, 1H, 8-H), 7.65 – 7.62 (m, 1H, 7-H), 7.42 (s, 1H, 4‘-H), 7.36 (ddd, *J* = 8.0, 6.5, 1.6 Hz, 1H, 6-H).

^{13}C NMR (126 MHz, methylene chloride-d_2) δ (ppm) = 171.7 (C-5’), 162.7 (C-3’), 141.2 (C-8a), 139.8 (C-3), 138.7 (C-3’’, C-5’’), 133.2 (C-9a), 131.4 (C-1), 130.1 (C-4a), 129.7 (C-7), 128.9 (C-2’’, C-6’’), 128.8 (C-1’’), 122.2 (C-5), 121.4 (C-4b), 121.1 (C-6), 116.5 (C-4), 112.3 (C-8), 100.1 (C-4’), 96.8 (C-4’’).

IR (ATR) $\tilde{\nu}$ (cm^{-1}) = 3124, 1608, 1554, 1492, 1431, 1418, 1321, 1286, 1234, 1005, 948, 809, 747.

HRMS (EI) (*m/z*) = calculated for $C_{20}H_{12}IN_3O^{\cdot+}$ $[M]^{\cdot+}$ 437.0020, found 437.0018.

Purity (HPLC, method 2a) > 95% (λ = 210 nm), > 95% (λ = 254 nm).

3-(Pyridin-2-yl)-5-(9*H*-pyrido[3,4-*b*]indol-1-yl)isoxazole (23)

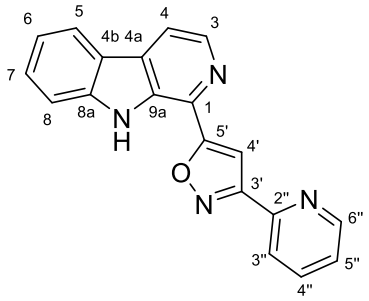

$C_{19}H_{12}N_4O$

M_r = 312.33 g/mol

Following **General Procedure IIIa**, alkyne **3** (48.1 mg, 0.250 mmol, 1.0 eq), oxime **15** (46 mg, 0.38 mmol, 1.5 eq) and [bis(trifluoroacetoxy)iodo]benzene (161 mg, 0.375 mmol, 1.5 eq) were used in methanol/water (2.5 mL). After stirring for additional 16 h, the reaction was completed. The crude product was purified by flash column chromatography (40% ethyl acetate and 0.5% triethylamine in hexanes) and subsequent recrystallization (from ethyl acetate/hexanes) to give isoxazole **23** as ochre solid (47.9 mg, 0.153 mmol, 61%).

R_f = 0.18 (40% ethyl acetate in hexanes).

Melting point = 226 °C.

^{1}H NMR (400 MHz, methylene chloride-d_2) δ (ppm) = 9.61 (s, 1H, NH), 8.76 (ddd, *J* = 4.8, 1.9, 1.0 Hz, 1H, 6‘‘-H), 8.57 (d, *J* = 5.1 Hz, 1H, 3-H), 8.21 (dq, *J* = 7.9, 0.9 Hz, 1H, 5-H), 8.14 (dt, *J* = 7.9, 1.1 Hz, 1H, 3‘‘-H), 8.08 (dd, *J* = 5.0, 0.7 Hz, 1H, 4-H), 7.87 (td, *J* = 7.7, 1.8 Hz, 1H, 4‘‘-H), 7.67 (s, 1H, 4‘-H), 7.67 – 7.60 (m, 2H, 7-H, 8-H), 7.42 (ddd, *J* = 7.6, 4.9, 1.2 Hz, 1H, 5‘‘-H), 7.36 (ddd, *J* = 8.0, 6.6, 1.5 Hz, 1H, 6-H).

^{13}C NMR (101 MHz, methylene chloride-d_2) δ (ppm) = 171.4 (C-5‘), 163.4 (C-3‘), 150.4 (C-6‘‘), 148.7 (C-2‘‘), 141.2 (C-8a), 139.8 (C-3), 137.3 (C-4‘‘), 133.2 (C-9a), 131.3 (C-1), 130.4 (C-4a), 129.6 (C-7), 125.1 (C-5‘‘), 122.2 (C-3‘‘), 122.0 (C-5), 121.4 (C-4b), 121.0 (C-6), 116.4 (C-4), 112.3 (C-8), 101.2 (C-4‘).

IR (ATR) $\tilde{\nu}$ (cm^{-1}) = 3319, 1607, 1555, 1490, 1451, 1401, 1364, 1289, 1216, 1067, 996, 839, 750.

HRMS (ESI) (*m/z*) = calculated for $C_{19}H_{13}N_4O^+$ $[M+H]^+$ 313.1084, found 313.1083.

Purity (HPLC, method 1c) > 95% (λ = 210 nm), > 95% (λ = 254 nm).

5-(9*H*-Pyrido[3,4-*b*]indol-1-yl)-3-(thiophen-2-yl)isoxazole (24)

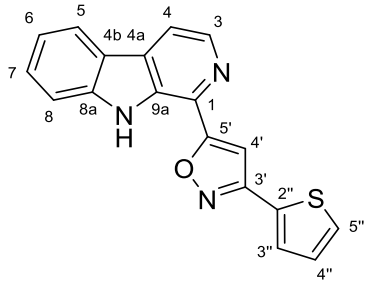

$C_{18}H_{11}N_3OS$

M_r = 317.37 g/mol

Following **General Procedure IIIb**, alkyne **3** (48.1 mg, 0.250 mmol, 1.0 eq), oxime **16** (318 mg, 2.50 mmol, 10 eq) and [bis(trifluoroacetoxy)iodo]benzene (1.08 g, 2.50 mmol, 10 eq) were used in methanol/water (2.5 mL). After stirring for additional 6 d, the reaction was completed. The crude product was purified by flash column chromatography (15% ethyl acetate in hexanes) and subsequent recrystallization (from chloroform/hexanes) to give isoxazole **24** as pale yellow solid (10.8 mg, 0.0340 mmol, 14%).

R_f = 0.22 (20% ethyl acetate in hexanes).

Melting point = 183 °C.

^{1}H NMR (500 MHz, methylene chloride-d_2) δ (ppm) = 9.58 (s, 1H, NH), 8.55 (d, *J* = 5.1 Hz, 1H, 3-H), 8.21 (dq, *J* = 8.0, 1.0 Hz, 1H, 5-H), 8.08 (dd, *J* = 5.1, 0.8 Hz, 1H, 4-H), 7.69 – 7.61 (m, 3H, 7-H, 8-H, 3‘‘-H), 7.52 (dd, *J* = 5.0, 1.1 Hz, 1H, 5‘‘-H), 7.38 (s, 1H, 4‘-H), 7.36 (ddd, *J* = 7.9, 6.6, 1.4 Hz, 1H, 6-H), 7.21 (dd, *J* = 5.1, 3.6 Hz, 1H, 4‘‘-H).

^{13}C NMR (126 MHz, methylene chloride-d_2) δ (ppm) = 171.3 (C-5‘), 158.7 (C-3‘), 141.2 (C-8a), 139.8 (C-3), 133.3 (C-9a), 131.4 (C-1 or C-2‘‘), 130.8 (C-1 or C-2‘‘), 130.1 (C-4a), 129.7 (C-3‘‘), 128.6 (C-7), 128.4 (C-5‘‘), 128.3 (C-4‘‘), 122.2 (C-5), 121.4 (C-4b), 121.1 (C-6), 116.6 (C-4), 112.3 (C-8), 100.3 (C-4‘).

IR (ATR) $\tilde{\nu}$ (cm^{-1}) = 3450, 3056, 1608, 1564, 1462, 1422, 1391, 1321, 1296, 1227, 1132, 1054, 906, 849, 798, 740.

HRMS (ESI) (*m/z*) = calculated for $C_{18}H_{12}N_3OS^+$ $[M+H]^+$ 318.0696, found 318.0695.

Purity (HPLC, method 1c) > 95% (λ = 210 nm), > 95% (λ = 254 nm).

3-(Furan-2-yl)-5-(9*H*-pyrido[3,4-*b*]indol-1-yl)isoxazole (25)

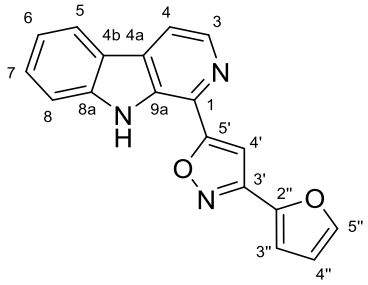

$C_{18}H_{11}N_3O_2$

M_r = 301.31 g/mol

Following **General Procedure IIIb**, alkyne **3** (48.1 mg, 0.250 mmol, 1.0 eq), oxime **17** (287 mg, 2.50 mmol, 10 eq) and [bis(trifluoroacetoxy)iodo]benzene (1.08 g, 2.50 mmol, 10 eq) were used in methanol/water (2.5 mL). After stirring for additional 7 d, the reaction was completed. The crude product was purified by flash column chromatography (10% → 20% ethyl acetate in hexanes) and subsequent recrystallization (from chloroform/hexanes) to give isoxazole **25** as pale yellow solid (10.8 mg, 0.0358 mmol, 14%).

R_f = 0.31 (25% ethyl acetate in hexanes).

Melting point = 177 °C.

^{1}H NMR (400 MHz, methylene chloride-d_2) δ (ppm) = 9.58 (s, 1H, NH), 8.55 (d, *J* = 5.1 Hz, 1H, 3-H), 8.20 (dq, *J* = 7.9, 0.9 Hz, 1H, 5-H), 8.08 (dd, *J* = 5.1, 0.7 Hz, 1H, 4-H), 7.70 – 7.59 (m, 3H, 7-H, 8-H, 5‘‘-H), 7.39 – 7.35 (m, 1H, 6-H), 7.35 (s, 1H, 4‘-H), 7.04 (dd, *J* = 3.4, 0.8 Hz, 1H, 3‘‘-H), 6.62 (dd, *J* = 3.4, 1.8 Hz, 1H, 4‘‘-H).

^{13}C NMR (101 MHz, methylene chloride-d_2) δ (ppm) = 171.1 (C-5‘), 155.7 (C-3‘), 144.8 (C-5‘‘), 144.5 (C-2‘‘), 141.2 (C-8a), 139.8 (C-3), 133.3 (C-9a), 131.4 (C-1), 130.1 (C-4a), 129.7 (C-7), 122.2 (C-5), 121.4 (C-4b), 121.1 (C-6), 116.6 (C-4), 112.3 (C-8), 112.2 (C-4‘‘), 111.5 (C-3‘‘), 99.8 (C-4‘).

IR (ATR) $\tilde{\nu}$ (cm^{-1}) = 3462, 3093, 1609, 1557, 1493, 1425, 1380, 1286, 1231, 1137, 1064, 1012, 887, 726.

HRMS (ESI) (*m/z*) = calculated for $C_{18}H_{12}N_3O_2^+$ $[M+H]^+$ 302.0925, found 302.0923.

Purity (HPLC, method 1c) > 95% (λ = 210 nm), > 95% (λ = 254 nm).

5-(9*H*-Pyrido[3,4-*b*]indol-1-yl)-3-(1*H*-pyrrol-2-yl)isoxazole (26)

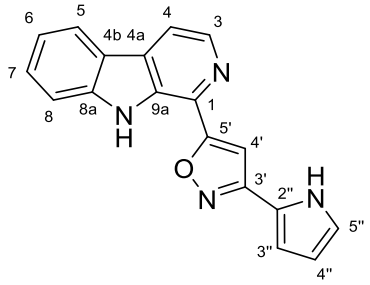

$C_{18}H_{12}N_4O$

M_r = 300.32 g/mol

N-Chlorosuccinimide (37 mg, 0.28 mmol, 1.1 eq) and oxime **18** (30 mg, 0.28 mmol, 1.1 eq) were dissolved anhydrous DMF (0.5 mL) under N_2 atmosphere and stirred at 0 °C. Then anhydrous pyridine (0.004 mL, 0.05 mmol, 0.2 eq) was added and the reaction mixture was stirred at 0 °C for 0.5 h and at room temperature for further 20 h. Alkyne **3** (48.1 mg, 0.250 mmol, 1.0 eq) was added in one portion and, after stirring for 5 min, anhydrous triethylamine (0.038 mL, 0.28 mmol, 1.1 eq) dropwise over 10 min. The suspension was stirred for 16 h at room temperature and then partitioned between water (20 mL) and methylene chloride (20 mL). The aq. phase was further extracted with methylene chloride (2 x 20 mL) and the combined organic layers were dried using a phase separation filter. The solvent was removed *in vacuo* and the crude product purified two times by flash column chromatography (20% → 25% ethyl acetate in hexanes, 100% methylene chloride → 0.1% methanol in methylene chloride) to give isoxazole **26** as white solid (33.8 mg, 0.113 mmol, 56%).

R_f = 0.44 (40% ethyl acetate in hexanes).

Melting point = 180 °C (decomposition).

^{1}H NMR (400 MHz, DMSO-d_6) δ (ppm) = 11.80 (s, 1H, 9-NH), 11.73 (s, 1H, 1''-NH), 8.52 (d, *J* = 5.0 Hz, 1H, 3-H), 8.34 – 8.29 (m, 2H, 4-H, 5-H), 7.82 (d, *J* = 8.2 Hz, 1H, 8-H), 7.62 (ddd, *J* = 8.3, 7.1, 1.2 Hz, 1H, 7-H), 7.56 (s, 1H, 4'-H), 7.32 (td, *J* = 7.5, 7.1, 1.0 Hz, 1H, 6-H), 7.03 (td, *J* = 2.7, 1.5 Hz, 1H, 5''-H), 6.83 (ddd, *J* = 3.9, 2.5, 1.5 Hz, 1H, 3''-H), 6.25 (dt, *J* = 3.6, 2.5 Hz, 1H, 4''-H).

^{13}C NMR (101 MHz, DMSO-d_6) δ (ppm) = 168.6 (C-5'), 156.3 (C-3'), 141.5 (C-8a), 138.5 (C-3), 132.1 (C-9a), 130.4 (C-1 or C-4a), 129.5 (C-1 or C-4a), 128.9 (C-7), 121.8 (C-5), 121.5 (C-5''), 120.3 (C-4b), 120.1 (C-6), 120.0 (C-2''), 116.3 (C-4), 112.9 (C-8), 110.3 (C-3''), 109.3 (C-4''), 100.1 (C-4').

IR (ATR) $\tilde{\nu}$ (cm^{-1}) = 3606, 3256, 2922, 1613, 1453, 1428, 1385, 1324, 1291, 1230, 1135, 1122, 1031 884, 745, 722.

HRMS (ESI) (*m/z*) = calculated for $C_{18}H_{13}N_4O^+$ $[M+H]^+$ 301.1084, found 301.1085.

Purity (HPLC, method 1a) > 95% (λ = 210 nm), > 95% (λ = 254 nm).

3-(4-Ethynylphenyl)-5-(9*H*-pyrido[3,4-*b*]indol-1-yl)isoxazole (27)

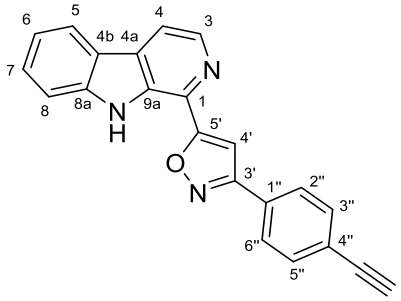

$C_{22}H_{13}N_3O$

M_r = 335.37 g/mol

Following **General Procedure Ia**, iodide **22** (144 mg, 0.330 mmol, 1.0 eq), CuI (13 mg, 0.069 mmol, 0.2 eq), Pd(dppf)Cl_2 (12 mg, 0.017 mmol, 0.05 eq) and trimethylsilylacetylene (0.093 mL, 0.66 mmol, 2.0 eq, dissolved in 0.25 mL anhydrous THF) were used in anhydrous triethylamine (3.0 mL) and anhydrous THF (3.0 mL). After stirring for 20 h, the reaction was completed. The celite pad was washed with ethyl acetate (100 mL) and the extraction was performed with sat. aq. NaCl solution (50 mL) and ethyl acetate (2 x 50 mL).
The crude TMS-protected intermediate (R_f = 0.50, 20% ethyl acetate in hexanes; HRMS (EI) (m/z) = calculated for $C_{25}H_{21}N_3OSi^{\cdot+}$ $[M]^{\cdot+}$ 407.1449, found 407.1442) was desilylated, following **General Procedure II**, with K_2CO_3 (180 mg, 1.09 mmol, 3.3 eq) in methanol (7.0 mL). The crude product was purified by flash column chromatography (100% methylene chloride) to give terminal alkyne **27** as off-white solid (96.8 mg, 0.289 mmol, 88% over two steps).

R_f = 0.35 (20% ethyl acetate in hexanes).

Melting point = 241 °C.

^{1}H NMR (400 MHz, DMSO-d_6) δ (ppm) = 11.86 (s, 1H, NH), 8.54 (d, *J* = 5.0 Hz, 1H, 3-H), 8.35 – 8.30 (m, 2H, 4-H, 5-H), 8.11 – 8.06 (m, 2H, 2‘‘-H, 6‘‘-H), 7.86 (s, 1H, 4‘-H), 7.82 (dt, *J* = 8.3, 0.9 Hz, 1H, 8-H), 7.72 – 7.66 (m, 2H, 3‘‘-H, 5‘‘-H), 7.63 (ddd, *J* = 8.3, 7.1, 1.2 Hz, 1H, 7-H), 7.32 (ddd, *J* = 8.0, 7.1, 1.0 Hz, 1H, 6-H), 4.40 (s, 1H, CCH).

^{13}C NMR (101 MHz, DMSO-d_6) δ (ppm) = 169.9 (C-5’), 161.8 (C-3’), 141.5 (C-8a), 138.5 (C-3), 132.5 (C-3’’, C-5’’), 132.2 (C-9a), 130.5 (C-1 or C-4a), 129.3 (C-1 or C-4a), 129.0 (C-7), 128.7 (C-1’’), 127.0 (C-2’’, C-6’’), 123.7 (C-4’’), 121.8 (C-5), 120.3 (C-4b), 120.1 (C-6), 116.6 (C-4), 112.9 (C-8), 100.7 (C-4’), 83.0 (CCH), 82.7 (CCH).

IR (ATR) $\tilde{\nu}$ (cm^{-1}) = 3463, 3166, 2097, 1613, 1553, 1494, 1433, 1421, 1288, 1229, 949, 917, 839, 806, 740.

HRMS (EI) (*m/z*) = calculated for $C_{22}H_{13}N_3O^{\cdot+}$ $[M]^{\cdot+}$ 335.1054, found 335.1054.

Purity (HPLC, method 2a) > 95% (λ = 210 nm), > 95% (λ = 254 nm).

2-(5-(9*H*-Pyrido[3,4-*b*]indol-1-yl)isoxazol-3-yl)aniline (28)

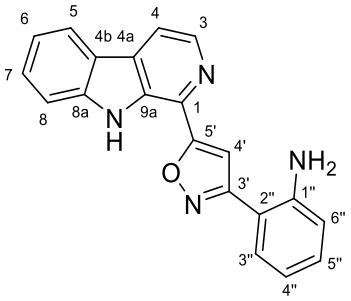

$C_{20}H_{14}N_4O$

M_r = 326.36 g/mol

Nitro compound **20** (44.5 mg, 0.125 mmol, 1.0 eq) was dissolved in methylene chloride (1.0 mL) and the solution was cooled to 0 °C. Then zinc granules (490 mg, 7.50 mmol, 60 eq) and acetic acid (0.11 ml, 2.0 mmol, 16 eq) were added. The reaction mixture was slowly warmed to room temperature, stirred for 48 h, then diluted with methylene chloride (20 mL) and filtered. The filtrate was washed with sat. aq. $NaHCO_3$ solution (50 mL) and the aq. phase further extracted with methylene chloride (2 x 30 mL). The combined organic layers were dried over Na_2SO_4, filtered and concentrated *in vacuo*. The crude product was purified by flash column chromatography (40% ethyl acetate in hexanes) to give aniline **28** as pale orange solid (15.9 mg, 0.049 mmol, 39%).

R_f = 0.60 (40% ethyl acetate in hexanes).

Melting point = 244 °C (decomposition).

^{1}H NMR (500 MHz, DMSO-d_6) δ (ppm) = 11.81 (s, 1H, NH), 8.55 (d, *J* = 5.1 Hz, 1H, 3-H), 8.35 – 8.30 (m, 2H, 4-H, 5-H), 7.85 – 7.79 (m, 3H, 8-H, 4‘-H, 3‘‘-H), 7.63 (ddd, *J* = 8.3, 7.1, 1.2 Hz, 1H, 7-H), 7.36 – 7.30 (m, 1H, 6-H), 7.23 (ddd, *J* = 8.3, 7.0, 1.6 Hz, 1H, 5‘‘-H), 6.90 (dd, *J* = 8.2, 1.2 Hz, 1H, 6‘‘-H), 6.74 – 6.69 (m, 1H, 4‘‘-H), 6.42 – 6.36 (m, 2H, NH_2).

^{13}C NMR (126 MHz, DMSO-d_6) δ (ppm) = 167.5 (C-5‘), 163.4 (C-3‘), 147.0 (C-1‘‘), 141.5 (C-8a), 138.5 (C-3), 132.2 (C-9a), 130.8 (C-5‘‘), 130.4 (C-1 or C-4a), 129.8 (C-3‘‘), 129.4 (C-1 or C-4a), 129.0 (C-7), 121.8 (C-5), 120.3 (C-4b), 120.1 (C-6), 116.5 (C-4), 116.0 (C-6‘‘), 115.8 (C-4‘‘), 112.9 (C-8), 109.9 (C-2‘‘), 101.1 (C-4‘).

IR (ATR) $\tilde{\nu}$ (cm^{-1}) = 3421, 3318, 2920, 1611, 1554, 1433, 1424, 1391, 1282, 1231, 929, 802, 762, 743.

HRMS (ESI) (*m/z*) = calculated for $C_{20}H_{15}N_4O^+$ $[M+H]^+$ 327.1241, found 327.1240.

Purity (HPLC, method 2a) > 95% (λ = 210 nm), > 95% (λ = 254 nm).

5.3.2 Variations of the isoxazole

1-(1-Phenyl-1*H*-1,2,3-triazol-4-yl)-9*H*-pyrido[3,4-*b*]indole (29)

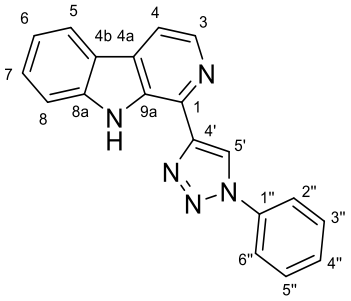

$C_{19}H_{13}N_5$

M_r = 311.35 g/mol

Phenylboronic acid (31 mg, 0.25 mmol, 1.0 eq), sodium azide (18 mg, 0.28 mmol, 1.1 eq) and $CuSO_4$ (4.0 mg, 0.025 mmol, 0.1 eq) were dissolved in methanol (1.0 mL) and stirred at 55 °C for 3 h (= phenyl azide solution). Water (1.0 mL), alkyne **3** (48.1 mg, 0.250 mmol, 1.0 eq) and sodium L-ascorbate (25 mg, 0.13 mmol, 0.5 eq) were added and the mixture stirred for 72 h at room temperature. Then, the abovementioned phenyl azide solution (1.0 eq) was prepared again and added to the reaction mixture besides water (1.0 mL) and sodium L-ascorbate (25 mg, 0.13 mmol, 0.5 eq). The mixture was stirred for further 72 h, then diluted with aq. NH_3 solution (1 M, 100 mL) and extracted with ethyl acetate (3 x 70 mL). The combined organic layers were dried over Na_2SO_4, filtered and concentrated *in vacuo*. The crude product was purified two times by flash column chromatography (1% methanol in methylene chloride, 100% chloroform) to give triazole **29** as pale yellow solid (30.6 mg, 0.0983 mmol, 39%).

R_f = 0.23 (1% methanol in methylene chloride).

Melting point = 166 °C.

^{1}H NMR (500 MHz, methylene chloride-d_2) δ (ppm) = 10.57 (s, 1H, NH), 8.86 (s, 1H, 5‘-H), 8.46 (d, *J* = 5.2 Hz, 1H, 3-H), 8.20 (dq, *J* = 7.8, 0.9 Hz, 1H, 5-H), 7.99 (dd, *J* = 5.2, 0.7 Hz, 1H, 4-H), 7.94 – 7.89 (m, 2H, 2‘‘-H, 6‘‘-H), 7.69 (dt, *J* = 8.2, 0.9 Hz, 1H, 8-H), 7.65 – 7.60 (m, 3H, 7-H, 3‘‘-H, 5‘‘-H), 7.56 – 7.51 (m, 1H, 4‘‘-H), 7.33 (ddd, *J* = 8.0, 7.0, 1.0 Hz, 1H, 6-H).

^{13}C NMR (126 MHz, methylene chloride-d_2) δ (ppm) = 150.0 (C-4‘), 141.1 (C-8a), 139.0 (C-3), 137.4 (C-1‘‘), 133.6 (C-1 or C-9a), 133.5 (C-1 or C-9a), 130.3 (C-3‘‘, C-5‘‘), 130.1 (C-4a), 129.5 (C-4‘‘), 129.0 (C-7), 122.1 (C-5), 121.6 (C-4b), 121.0 (C-2‘‘, C-6‘‘), 120.4 (C-6), 120.4 (C-5‘), 114.7 (C-4), 112.4 (C-8).

IR (ATR) $\tilde{\nu}$ (cm^{-1}) = 3612, 3427, 3403, 2918, 2206, 1627, 1574, 1505, 1490, 1420, 1366, 1352, 1285, 1267, 1029, 746.

HRMS (ESI) (*m/z*) = calculated for $C_{19}H_{14}N_5^+$ $[M+H]^+$ 312.1244, found 312.1247.

Purity (HPLC, method 2a) > 95% (λ = 210 nm), > 95% (λ = 254 nm).

1-(5-Phenyl-1*H*-pyrazol-3-yl)-9*H*-pyrido[3,4-*b*]indole (31)

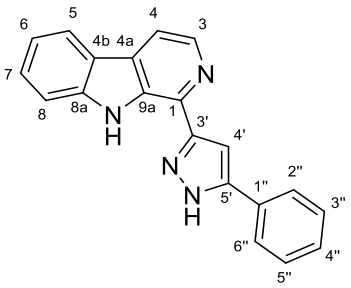

$C_{20}H_{14}N_4$

M_r = 310.36 g/mol

Benzaldehyde *p*-toluenesulfonylhydrazone (**30**) (68 mg, 0.25 mmol, 1.0 eq) was dissolved in acetonitrile (1.0 mL). Aq. NaOH solution (5 M, 0.050 mL, 0.25 mmol, 1.0 eq) was added and the reaction mixture stirred for 20 min at room temperature (= tosylhydrazone anion solution). Then, a solution of alkyne **3** (48.1 mg, 0.250 mmol, 1.0 eq) in acetonitrile (1.0 mL) was added and the mixture was stirred at 50 °C. An additional portion of the abovementioned tosylhydrazone anion solution (1.0 eq) was prepared and added to the reaction mixture after 24 h (1.0 eq) and 40 h (0.5 eq). After stirring for additional 6 h, the mixture was diluted with water (15 mL) and extracted with ethyl acetate (3 x 15 mL). The combined organic layers were dried over Na_2SO_4, filtered and concentrated *in vacuo*. The crude product was purified two times by flash column chromatography (40% ethyl acetate and 1% triethylamine in hexanes, 100% chloroform → 2.5% methanol in chloroform) to give pyrazole **31** as pale yellow solid (38.2 mg, 0.123 mmol, 49%).

R_f = 0.18 (40% ethyl acetate in hexanes).

Melting point = 224 °C.

^{1}H NMR (500 MHz, methylene chloride-d_2) δ (ppm) = 10.79 (s, 1H, 1‘-NH), 10.37 (s, 1H, 9-NH), 8.49 (d, *J* = 5.2 Hz, 1H, 3-H), 8.19 (dd, *J* = 7.9, 1.0 Hz, 1H, 5-H), 7.97 (d, *J* = 5.2 Hz, 1H, 4-H), 7.76 – 7.70 (m, 2H, 2‘‘-H, 6‘‘-H), 7.64 (dt, *J* = 8.2, 1.0 Hz, 1H, 8-H), 7.58 (ddd, *J* = 8.2, 7.0, 1.2 Hz, 1H, 7-H), 7.52 – 7.45 (m, 3H, 4‘-H, 3‘‘-H, 5‘‘-H), 7.44 – 7.40 (m, 1H, 4‘‘-H), 7.31 (ddd, *J* = 7.9, 7.0, 1.1 Hz, 1H, 6-H).

^{13}C NMR (126 MHz, methylene chloride-d_2) δ (ppm) = 154.4 (C-3‘), 144.9 (C-5‘), 141.2 (C-8a), 139.0 (C-3), 135.9 (C-1), 133.6 (C-9a), 129.9 (C-1‘‘), 129.8 (C-3’’, C-5’’), 129.7 (C-4a), 129.4 (C-4‘‘), 128.9 (C-7), 126.1 (C-2‘‘, C-6‘‘), 122.2 (C-5), 122.0 (C-4b), 120.5 (C-6), 114.6 (C-4), 112.4 (C-8), 101.9 (C-4‘).

IR (ATR) $\tilde{\nu}$ (cm^{-1}) = 3433, 3223, 2918, 1623, 1574, 1563, 1452, 1431, 1416, 1359, 1315, 1253, 1228, 981, 813, 732.

HRMS (ESI) (*m/z*) = calculated for $C_{20}H_{15}N_4^+$ $[M+H]^+$ 311.1292, found 311.1290.

Purity (HPLC, method 2a) > 95% (λ = 210 nm), > 95% (λ = 254 nm).

9*H*-Pyrido[3,4-*b*]indole-1-carbaldehyde (36)[90]

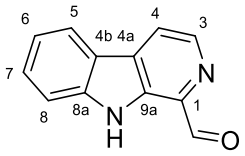

$C_{12}H_8N_2O$

M_r = 196.20 g/mol

Benzalharman (**37**) (2.50 g, 9.25 mmol, 1.0 eq) and Sudan III (0.005 mg, 0.01 mmol, 0.001 eq) were dissolved in methylene chloride/methanol (5:1, 240 mL). The reaction mixture was cooled to -78 °C and purged with N_2 for 15 min. Then, ozone was passed through (flow rate 60 L/h, 50 W), until the colour changed to yellow (5 min). The solution was again purged with N_2 for 30 min and dimethyl sulfide (7.50 mL, 101 mmol, 11 eq) was slowly added. The mixture was stirred at -78 °C for 1 h, at 0 °C for 2 h and at room temperature further 16 h. The solvent was removed *in vacuo* and the crude product was purified by flash column chromatography (20% ethyl acetate in hexanes) to give aldehyde **36** as yellow solid (994 mg, 5.07 mmol, 55%).

R_f = 0.27 (20% ethyl acetate in hexanes).

Melting point = 202 °C (lit.[90] 202 °C).

^{1}H NMR (500 MHz, chloroform-*d*) δ (ppm) = 10.35 (s, 1H, CHO), 10.08 (s, 1H, NH), 8.64 (d, *J* = 5.0 Hz, 1H, 3-H), 8.19 – 8.12 (m, 2H, 4-H, 5-H), 7.65 – 7.56 (m, 2H, 7-H, 8-H), 7.36 (ddd, *J* = 8.0, 6.8, 1.2 Hz, 1H, 6-H).

^{13}C NMR (126 MHz, chloroform-*d*) δ (ppm) = 195.9 (CHO), 141.4 (C-8a), 139.8 (C-3), 136.1 (C-1), 135.4 (C-9a), 131.8 (C-4a), 129.7 (C-7), 122.1 (C-5), 121.3 (C-6), 120.6 (C-4b), 119.5 (C-4), 112.2 (C-8).

IR (ATR) $\tilde{\nu}$ (cm^{-1}) = 3378, 2915, 2827, 1681, 1449, 1433, 1274, 1199, 1121, 1057, 739.

HRMS (EI) (*m/z*) = calculated for $C_{12}H_8N_2O^{\cdot+}$ $[M]^{\cdot+}$ 196.0632, found 196.0631.

Purity (HPLC, method 1c) > 95% (λ = 210 nm), > 95% (λ = 254 nm).

(*E*)-9*H*-Pyrido[3,4-*b*]indole-1-carbaldehyde oxime (35)

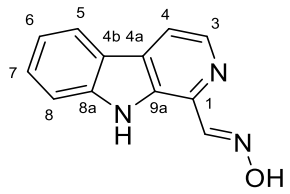

$C_{12}H_9N_3O$

M_r = 211.22 g/mol

Hydroxylamine hydrochloride (130 mg, 1.88 mmol, 1.25 eq) and sodium acetate (154 mg, 1.88 mmol, 1.25 eq) were dissolved in methanol (15 mL). Then, aldehyde **36** (294 mg, 1.50 mmol, 1.0 eq) was added and the suspension stirred at 75 °C for 1 h. After cooling to room temperature, the solvent was removed *in vacuo* and the residue resuspended in water (50 mL). The precipitate was filtered and washed with diethyl ether (25 mL) to give oxime **35** as ochre solid (313 mg, 1.48 mmol, 99%).

R_f = 0.33 (40% ethyl acetate in hexanes).

Melting point = 230 °C.

^{1}H NMR (400 MHz, DMSO-d_6) δ (ppm) = 11.65 (s, 1H, OH), 10.98 (s, 1H, NH), 8.45 (s, 1H, CHN), 8.40 (d, *J* = 5.1 Hz, 1H, 3-H), 8.26 (dd, *J* = 7.8, 1.1 Hz, 1H, 5-H), 8.15 (d, *J* = 5.1 Hz, 1H, 4-H), 7.81 (dd, *J* = 8.2, 0.9 Hz, 1H, 8-H), 7.56 (ddd, *J* = 8.3, 7.1, 1.2 Hz, 1H, 7-H), 7.28 (ddd, *J* = 8.0, 7.1, 1.0 Hz, 1H, 6-H).

^{13}C NMR (101 MHz, DMSO-d_6) δ (ppm) = 150.8 (CHN), 140.9 (C-8a), 138.1 (C-3), 135.6 (C-1), 132.4 (C-9a), 128.7 (C-4a), 128.3 (C-7), 121.6 (C-5), 120.5 (C-4b), 119.9 (C-6), 115.1 (C-4), 113.0 (C-8).

IR (ATR) $\tilde{\nu}$ (cm^{-1}) = 3430, 2851, 1628, 1571, 1494, 1428, 1376, 1322, 1233, 1131, 1069, 989, 819, 735.

HRMS (EI) (*m/z*) = calculated for $C_{12}H_9N_3O^{\cdot+}$ $[M]^{\cdot+}$ 211.0741, found 211.0737.

Purity (HPLC, method 2e) > 95% (λ = 210 nm), > 95% (λ = 254 nm).

5-Phenyl-3-(9*H*-pyrido[3,4-*b*]indol-1-yl)isoxazole (34)

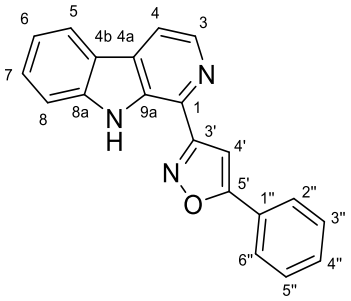

$C_{20}H_{13}N_3O$

M_r = 311.34 g/mol

Similar to **General Procedure IIIa**, phenylacetylene (0.10 mL, 0.94 mmol, 1.25 eq), oxime **35** (158 mg, 0.750 mmol, 1.0 eq) and [bis(trifluoroacetoxy)iodo]benzene (484 mg, 1.13 mmol, 1.5 eq) were used in methanol/water (5.0 mL). After stirring for additional 16 h, the reaction was completed. The crude product was purified two times by flash column chromatography (25% ethyl acetate in hexanes, 100% methylene chloride) to give isoxazole **34** as pale yellow solid (99.4 mg, 0.319 mmol, 43%).

R_f = 0.79 (40% ethyl acetate in hexanes).

Melting point = 166 °C.

^{1}H NMR (400 MHz, methylene chloride-d_2) δ (ppm) = 9.99 (s, 1H, NH), 8.56 (d, *J* = 5.1 Hz, 1H, 3-H), 8.20 (dq, *J* = 7.9, 0.9 Hz, 1H, 5-H), 8.07 (dd, *J* = 5.1, 0.7 Hz, 1H, 4-H), 7.97 – 7.90 (m, 2H, 2‘‘-H, 6‘‘-H), 7.67 – 7.58 (m, 2H, 7-H, 8-H), 7.57 – 7.50 (m, 3H, 3‘‘-H, 4‘‘-H, 5‘‘-H), 7.47 (s, 1H, 4‘-H), 7.34 (ddd, *J* = 8.0, 6.9, 1.3 Hz, 1H, 6-H).

^{13}C NMR (101 MHz, methylene chloride-d_2) δ (ppm) = 170.3 (C-5‘), 165.1 (C-3‘), 141.1 (C-8a), 139.3 (C-3), 134.2 (C-9a), 131.6 (C-1), 130.9 (C-4‘‘), 130.4 (C-4a), 129.5 (C-3‘‘, C-5‘‘), 129.3 (C-7), 127.7 (C-1‘‘), 126.3 (C-2‘‘, C-6‘‘), 122.1 (C-5), 121.6 (C-4b), 120.8 (C-6), 116.3 (C-4), 112.4 (C-8), 98.7 (C-4‘).

IR (ATR) $\tilde{\nu}$ (cm^{-1}) = 3425, 3051, 1628, 1568, 1490, 1453, 1361, 1262, 1143, 943, 828, 732.

HRMS (EI) (*m/z*) = calculated for $C_{20}H_{13}N_3O^{\cdot+}$ $[M]^{\cdot+}$ 311.1054, found 311.1054.

Purity (HPLC, method 1b) > 95% (λ = 210 nm), > 95% (λ = 254 nm).

(*Z*)-3-Amino-3-phenyl-1-(9*H*-pyrido[3,4-*b*]indol-1-yl)prop-2-en-1-one (40)[86]

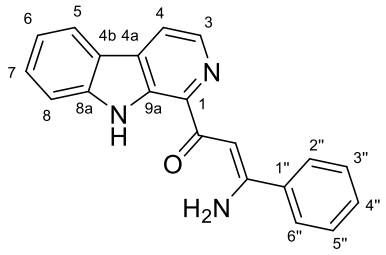

$C_{20}H_{15}N_3O$

M_r = 313.36 g/mol

Isoxazole **1** (62.3 mg, 0.200 mmol, 1.0 eq) was dissolved in ethyl acetate/methanol (1:1, 2.0 mL), before Cs_2CO_3 (65 mg, 0.20 mmol, 1.0 eq) and palladium on carbon (10 wt.%, 21 mg, 0.020 mmol, 0.1 eq) were added. Hydrogenation was performed under 35 bar H_2 pressure at 30 °C for 16 h. The reaction mixture was filtered through a pad of celite and the pad was washed with ethyl acetate/methanol (1:1, 25 mL). The filtrate was concentrated *in vacuo* and the residue purified by flash column chromatography (20% ethyl acetate in hexanes) to give enamino ketone **40** as yellow solid (41.8 mg, 0.133 mmol, 67%).

R_f = 0.45 (40% ethyl acetate in hexanes).

Melting point = 221 °C (lit.[86] 221 °C).

^{1}H NMR (500 MHz, chloroform-*d*) δ (ppm) = 10.74 (s, 1H, NH), 10.48 (s, 1H, NH_2), 8.52 (d, *J* = 4.9 Hz, 1H, 3-H), 8.16 (d, *J* = 7.8 Hz, 1H, 5-H), 8.08 (d, *J* = 5.0 Hz, 1H, 4-H), 7.80 – 7.74 (m, 2H, 2‘‘-H, 6‘‘-H), 7.62 – 7.56 (m, 2H, 7-H, 8-H), 7.54 – 7.46 (m, 3H, 3‘‘-H, 4‘‘-H, 5‘‘-H), 7.31 (dq, *J* = 8.0, 4.4 Hz, 1H, 6-H), 7.20 (s, 1H, CH), 5.58 (s, 1H, NH_2).

^{13}C NMR (126 MHz, chloroform-*d*) δ (ppm) = 191.2 (CO), 163.4 (CNH_2), 141.1 (C-8a), 138.5 (C-1), 138.0 (C-3), 137.5 (C-1‘‘), 136.0 (C-9a), 131.2 (C-4a), 131.0 (C-4‘‘), 129.1 (C-3‘‘, C-5‘‘), 128.9 (C-7), 126.7 (C-2‘‘, C-6‘‘), 121.9 (C-5), 121.0 (C-4b), 120.2 (C-6), 117.5 (C-4), 112.0 (C-8), 91.7 (CH).

IR (ATR) $\tilde{\nu}$ (cm^{-1}) = 3405, 2919, 2850, 1985, 1600, 1588, 1559, 1524, 1484, 1380, 1281, 1213, 1132, 1073, 1061, 810, 734.

HRMS (EI) (*m/z*) = calculated for $C_{20}H_{15}N_3O^{\cdot+}$ $[M]^{\cdot+}$ 313.1210, found 313.1211.

Purity (HPLC, method 2a) > 95% (λ = 210 nm), > 95% (λ = 254 nm).

3-Phenyl-5-(9*H*-pyrido[3,4-*b*]indol-1-yl)isothiazole (39)

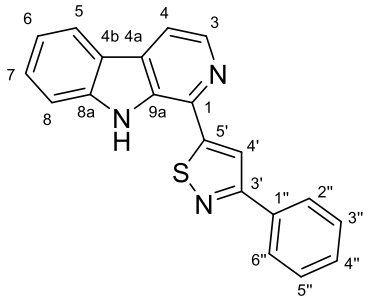

$C_{20}H_{13}N_3S$

M_r = 327.41 g/mol

Enamino ketone **40** (78.3 mg, 0.250 mmol, 1.0 eq) and $NaHCO_3$ (21 mg, 0.25 mmol, 1.0 eq) were suspended in anhydrous THF (2.5 mL) under N_2 atmosphere. Phosphorus pentasulfide (83 mg, 0.38 mmol, 1.5 eq) was added and the reaction mixture was stirred at room temperature for 16 h. Anhydrous THF (2.0 mL) and *p*-chloranil (92 mg, 0.38 mmol, 1.5 eq) were added and the mixture was stirred at room temperature for 40 h and at 65 °C for 6 h. After cooling to room temperature, it was diluted with water (50 mL) and extracted with ethyl acetate (3 x 20 mL). The combined organic layers were dried over $MgSO_4$, filtered and concentrated *in vacuo*. The crude product was purified three times by flash column chromatography (20% acetone in hexanes, 100% methylene chloride, 50% methylene chloride in chloroform) to give isothiazole **39** as white solid (14.1 mg, 0.0431 mmol, 17%).

R_f = 0.41 (20% ethyl acetate in hexanes).

Melting point = 197 °C.

^{1}H NMR (500 MHz, methylene chloride-d_2) δ (ppm) = 8.69 (s, 1H, NH), 8.53 (d, *J* = 5.2 Hz, 1H, 3-H), 8.21 (dq, *J* = 7.9, 0.9 Hz, 1H, 5-H), 8.18 (s, 1H, 4‘-H), 8.13 – 8.08 (m, 2H, 2‘‘-H, 6‘‘ H), 8.06 (dd, *J* = 5.2, 0.7 Hz, 1H, 4-H), 7.68 (dt, *J* = 8.2, 1.0 Hz, 1H, 8-H), 7.64 (ddd, *J* = 8.2, 6.9, 1.2 Hz, 1H, 7-H), 7.56 – 7.51 (m, 2H, 3‘‘-H, 5‘‘-H), 7.50 – 7.45 (m, 1H, 4‘‘-H), 7.38 (ddd, *J* = 7.9, 6.9, 1.2 Hz, 1H, 6-H).

^{13}C NMR (101 MHz, methylene chloride-d_2) δ (ppm) = 168.8 (C-3‘), 167.3 (C-5‘), 141.2 (C-8a), 140.0 (C-3), 135.3 (C-1‘‘), 134.3 (C-1), 132.5 (C-9a), 131.7 (C-4a), 129.8 (C-7 or C-4‘‘), 129.6 (C-7 or C-4‘‘), 129.3 (C-3‘‘, C-5‘‘), 127.3 (C-2‘‘, C-6‘‘), 122.2 (C-5), 122.1 (C-4b), 121.4 (C-6), 118.0 (C-4‘), 116.0 (C-4), 112.4 (C-8).

IR (ATR) $\tilde{\nu}$ (cm^{-1}) = 3228, 2919, 2850, 1497, 1455, 1424, 1403, 1321, 1227, 1205, 1012, 847, 832, 748.

HRMS (EI) (*m/z*) = calculated for $C_{20}H_{13}N_3S^{\cdot+}$ $[M]^{\cdot+}$ 327.0825, found 327.0827.

Purity (HPLC, method 2a) > 95% (λ = 210 nm), > 95% (λ = 254 nm).

_N_-Phenethyl-9_H_-pyrido[3,4-_b_]indole-1-carboxamide (42)[300]

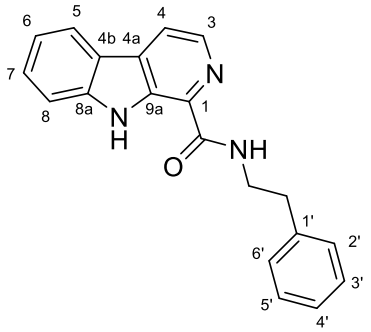

$C_{20}H_{17}N_3O$

M_r = 315.38 g/mol

Carboxylic acid **41** (53.1 mg, 0.250 mmol, 1.0 eq) and 1,1'-carbonyldiimidazole (49 mg, 0.30 mmol, 1.2 eq) were suspended in anhydrous THF (3.0 mL) under N_2 atmosphere and the reaction mixture was stirred at 70 °C for 2 h. After cooling to room temperature, a solution of 2-phenylethylamine (0.038 mL, 0.30 mmol, 1.2 eq) in anhydrous THF (0.5 mL) was added to the activated carboxylic acid (R_f = 0.16, 40% ethyl acetate in hexanes). The mixture was stirred for 18 h at room temperature, then diluted with sat. aq. NaCl solution (20 mL) and extracted with ethyl acetate (3 x 20 mL). The combined organic layers were dried over Na_2SO_4, filtered and concentrated *in vacuo*. The crude product was purified by flash column chromatography (15% → 20% ethyl acetate in hexanes) to give amide **42** as pale yellow oil (49.0 mg, 0.155 mmol, 62%), which solidified in the cold (2 – 8°C).

R_f = 0.68 (40% ethyl acetate in hexanes).

Melting point = 94 °C.

^{1}H NMR (500 MHz, chloroform-*d*) δ (ppm) = 10.32 (s, 1H, 9-NH), 8.35 (d, *J* = 5.1 Hz, 1H, 3-H), 8.27 (s, 1H, CONH), 8.14 (dq, *J* = 7.9, 0.9 Hz, 1H, 5-H), 8.08 (dd, *J* = 5.1, 0.7 Hz, 1H, 4-H), 7.59 (ddd, *J* = 8.1, 6.9, 1.1 Hz, 1H, 7-H), 7.55 (dt, *J* = 8.2, 1.1 Hz, 1H, 8-H), 7.36 – 7.29 (m, 5H, 6-H, 2'-H, 3'-H, 5'-H, 6'-H), 7.26 – 7.23 (m, 1H, 4'-H, collapses with chloroform peak), 3.84 – 3.77 (m, 2H, $NHCH_2$), 3.02 (t, *J* = 7.3 Hz, 2H, $NHCH_2\underline{CH_2}$).

^{13}C NMR (126 MHz, chloroform-*d*) δ (ppm) = 166.7 (CONH), 141.2 (C-8a), 139.1 (C-1'), 137.4 (C-3), 135.7 (C-9a), 132.2 (C-1 or C-4a), 131.5 (C-1 or C-4a), 129.3 (C-7), 129.0 (C-2', C-6'), 128.8 (C-3', C-5'), 126.7 (C-4'), 122.0 (C-5), 120.8 (C-4b), 120.4 (C-6), 117.9 (C-4), 112.0 (C-8), 40.7 ($NHCH_2$), 36.3 ($NHCH_2\underline{CH_2}$).

IR (ATR) $\tilde{\nu}$ (cm^{-1}) = 3343, 2923, 1648, 1624, 1522, 1491, 1449, 1370, 1318, 1243, 1218, 1205, 728, 697.

HRMS (ESI) (*m/z*) = calculated for $C_{20}H_{17}N_3O^+$ $[M+H]^+$ 316.1445, found 316.1445.

Purity (HPLC, method 2c) > 95% (λ = 210 nm), > 95% (λ = 254 nm).

5-Phenyl-2-(9*H*-pyrido[3,4-*b*]indol-1-yl)oxazole (43)

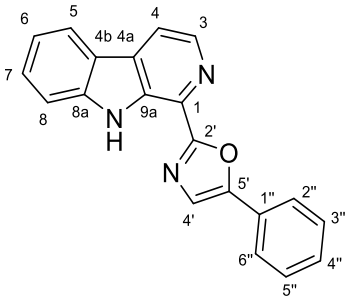

$C_{20}H_{13}N_3O$

M_r = 311.34 g/mol

Carboxylic acid **41** (106 mg, 0.500 mmol, 1.0 eq) and 2-aminoacetophenone hydrochloride (85.6 mg, 0.500 mmol 1.0 eq) were suspended in toluene (2.5 mL) in a pressure tube. Phosphorus(V) oxychloride (0.375 mL, 4.00 mmol, 8.0 eq) was added and the reaction mixture stirred at 105 °C for 16 h. Then, another portion of phosphorus(V) oxychloride (0.375 mL, 4.00 mmol, 8.0 eq) was added and the mixture stirred for further 24 h at 105 °C. After cooling to room temperature, it was added dropwise to aq. NaOH solution (1 M, 50 mL) and vigorously stirred for 15 min. The mixture was extracted with ethyl acetate (3 x 30 mL) and the combined organic layers were dried over Na_2SO_4, filtered and concentrated *in vacuo*. The crude product was purified two times by flash column chromatography (50% → 65% methylene chloride in hexanes, methylene chloride) to give oxazole **43** as yellow solid (61.0 mg, 0.196 mmol, 39%).

R_f = 0.55 (40% ethyl acetate in hexanes).

Melting point = 179 °C.

^{1}H NMR (400 MHz, methylene chloride-d_2) δ (ppm) = 10.44 (s, 1H, NH), 8.58 (d, *J* = 5.1 Hz, 1H, 3-H), 8.21 (dq, *J* = 7.9, 0.9 Hz, 1H, 5-H), 8.09 (dd, *J* = 5.1, 0.7 Hz, 1H, 4-H), 7.89 – 7.84 (m, 2H, 2‘‘-H, 6‘‘-H), 7.70 – 7.66 (m, 2H, 8-H, 4‘-H), 7.62 (ddd, *J* = 8.2, 7.0, 1.2 Hz, 1H, 7-H), 7.54 – 7.48 (m, 2H, 3‘‘-H, 5‘‘-H), 7.44 – 7.39 (m, 1H, 4‘‘-H), 7.35 (ddd, *J* = 8.0, 6.9, 1.2 Hz, 1H, 6-H).

^{13}C NMR (101 MHz, methylene chloride-d_2) δ (ppm) = 160.5 (C-2‘), 152.2 (C-5‘), 141.1 (C-8a), 139.3 (C-3), 134.6 (C-9a), 130.4 (C-1), 129.4 (C-3‘‘, C-5‘‘), 129.3 (C-4a), 129.3 (C-7), 129.3 (C-4‘‘), 128.1 (C-1‘‘), 125.0 (C-2‘‘, C-6‘‘), 123.7 (C-4‘), 122.2 (C-5), 121.7 (C-4b), 120.8 (C-6), 116.4 (C-4), 112.4 (C-8).

IR (ATR) $\tilde{\nu}$ (cm^{-1}) = 3403, 1627, 1491, 1448, 1318, 1253, 1224, 1172, 1070, 943, 817, 757.

HRMS (EI) (*m/z*) = calculated for $C_{20}H_{13}N_3O^{\cdot+}$ $[M]^{\cdot+}$ 311.1054, found 311.1055.

Purity (HPLC, method 2a) > 95% (λ = 210 nm), > 95% (λ = 254 nm).

2-Oxo-2-phenylethyl 9*H*-pyrido[3,4-*b*]indole-1-carboxylate (45)

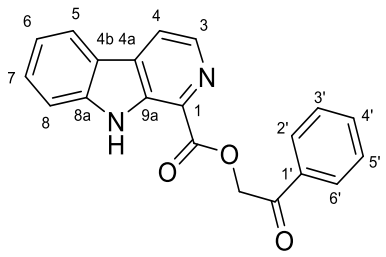

$C_{20}H_{14}N_2O_3$

M_r = 330.34 g/mol

Carboxylic acid **41** (106 mg, 0.500 mmol, 1.0 eq) was suspended in ethyl acetate (3.0 mL), then 2-bromoacetophenone (99.5 mg, 0.500 mmol, 1.0 eq) and triethylamine (0.091 ml, 0.65 mmol, 1.3 eq) were added and the mixture stirred at 60 °C for 5 h. After cooling to room temperature, the mixture was partitioned between water (15 mL) and ethyl acetate (10 mL). The aq. phase was further extracted with ethyl acetate (2 x 10 mL) and the combined organic layers were dried over Na_2SO_4, filtered and concentrated *in vacuo*. The crude product was purified by flash column chromatography (40% → 60% ethyl acetate in hexanes) to give ester **45** as white solid (50.8 mg, 0.154 mmol, 32%).

R_f = 0.11 (40% ethyl acetate in hexanes).

Melting point = 219 °C.

^{1}H NMR (500 MHz, methylene chloride-d_2) δ (ppm) = 10.45 (s, 1H, NH), 8.60 (d, J = 4.9 Hz, 1H, 3-H), 8.23 – 8.17 (m, 2H, 4-H, 5-H), 8.09 – 8.02 (m, 2H, 2‘-H, 6‘-H), 7.73 – 7.66 (m, 2H, 8-H, 4‘-H), 7.64 (ddd, J = 8.2, 6.9, 1.2 Hz, 1H, 7-H), 7.61 – 7.55 (m, 2H, 3‘-H, 5‘-H), 7.35 (ddd, J = 8.0, 6.9, 1.2 Hz, 1H, 6-H), 5.81 (s, 2H, CH_2).

^{13}C NMR (126 MHz, methylene chloride-d_2) δ (ppm) = 192.9 (CO), 165.5 (COO), 141.3 (C-8a), 139.4 (C-3), 137.8 (C-9a), 134.7 (C-4‘), 134.4 (C-1‘), 132.0 (C-4a), 129.8 (C-7), 129.5 (C-3‘, C-5‘), 128.3 (C-2‘, C-6‘), 122.2 (C-5), 121.3 (C-4b), 121.0 (C-6), 119.2 (C-4), 112.4 (C-8), 67.6 (CH_2). Signal for C-1 not observed.

IR (ATR) $\tilde{\nu}$ (cm^{-1}) = 3292, 2925, 1748, 1681, 1625, 1596, 1425, 1369, 1309, 1284, 1236, 1171, 1151, 969, 934, 765.

HRMS (EI) (*m/z*) = calculated for $C_{20}H_{14}N_2O_3^{\cdot+}$ $[M]^{\cdot+}$ 330.0999, found 330.1000.

Purity (HPLC) n.d.

4-Phenyl-2-(9*H*-pyrido[3,4-*b*]indol-1-yl)oxazole (46)

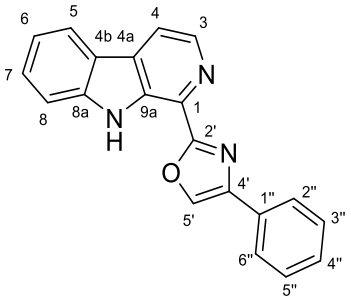

$C_{20}H_{13}N_3O$

M_r = 311.34 g/mol

Ester **45** (66.1 mg, 0.200 mmol, 1.0 eq) and acetamide (59 mg, 1.0 mmol, 5.0 eq) were suspended in xylene (2.0 mL) in a pressure tube. Boron trifluoride diethyl etherate (0.020 mL, 0.16 mmol, 0.8 eq) was added and the reaction mixture stirred at 120 °C for 24 h. After cooling to room temperature, cold water (20 mL) was added and extracted with ethyl acetate (3 x 20 mL). The combined organic layers were washed with sat. aq. NaCl solution (20 mL), dried over Na_2SO_4, filtered and concentrated *in vacuo*. The crude product was purified two times by flash column chromatography (100% methylene chloride, 100% chloroform → 10% methylene chloride in chloroform) to give oxazole **46** as white solid (19.5 mg, 0.0626 mmol, 31%).

R_f = 0.38 (20% ethyl acetate in hexanes).

Melting point = 199 °C.

^{1}H NMR (500 MHz, methylene chloride-d_2) δ (ppm) = 10.42 (s, 1H, NH), 8.57 (d, *J* = 5.1 Hz, 1H, 3-H), 8.22 (dd, *J* = 7.9, 1.0 Hz, 1H, 5-H), 8.21 (s, 1H, 5‘-H), 8.11 (d, *J* = 5.1 Hz, 1H, 4-H), 8.00 – 7.95 (m, 2H, 2‘‘-H, 6‘‘-H), 7.74 (dd, *J* = 8.2, 0.9 Hz, 1H, 8-H), 7.65 (ddd, *J* = 8.2, 7.0, 1.2 Hz, 1H, 7-H), 7.56 – 7.51 (m, 2H, 3‘‘-H, 5‘‘-H), 7.45 – 7.41 (m, 1H, 4‘‘-H), 7.36 (ddd, *J* = 8.0, 7.1, 1.0 Hz, 1H, 6-H).

^{13}C NMR (101 MHz, methylene chloride-d_2) δ (ppm) = 161.1 (C-2‘), 142.3 (C-4‘), 141.1 (C-8a), 139.4 (C-3), 134.6 (C-5‘), 134.5 (C-9a), 131.1 (C-1), 130.6 (C-1‘‘), 129.4 (C-7), 129.3 (C-3‘‘, C-5‘‘), 129.1 (C-4a), 128.9 (C-4‘‘), 126.1 (C-2‘‘, C-6‘‘), 122.3 (C-5), 121.8 (C-4b), 120.9 (C-6), 116.6 (C-4), 112.5 (C-8).

IR (ATR) $\tilde{\nu}$ (cm^{-1}) = 3405, 3095, 1624, 1490, 1430, 1390, 1315, 1242, 1217, 1165, 1123, 1065, 942, 837, 748.

HRMS (EI) (*m/z*) = calculated for $C_{20}H_{13}N_3O^{\cdot+}$ $[M]^{\cdot+}$ 311.1054, found 311.1057.

Purity (HPLC, method 2a) > 95% (λ = 210 nm), > 95% (λ = 254 nm).

3-Phenyl-5-(9*H*-pyrido[3,4-*b*]indol-1-yl)-1,2,4-oxadiazole (48)

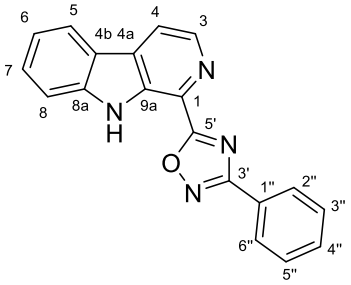

$C_{19}H_{12}N_4O$

M_r = 312.33 g/mol

Carboxylic acid **41** (91.2 mg, 0.430 mmol, 1.0 eq) and 1,1'-carbonyldiimidazole (84 mg, 0.52 mmol, 1.2 eq) were suspended in anhydrous DMSO (1.0 mL) under N_2 atmosphere. The reaction mixture was stirred at 70 °C for 2 h and at room temperature for 16 h. Then a solution of benzamidoxime (**47**) (64 mg, 0.47 mmol, 1.1 eq) in anhydrous DMSO (0.2 mL) was added dropwise to the activated carboxylic acid (R_f = 0.16, 40% ethyl acetate in hexanes). The mixture was stirred for further 6 h at 70 °C and for 16 h at room temperature, before NaOH (21 mg, 0.52 mmol, 1.2 eq) was added. After stirring for 2 h, the reaction mixture was diluted with cold water (20 mL) and sat. aq. NaCl solution (30 mL) and extracted with ethyl acetate (3 x 50 mL). The combined organic layers were dried over Na_2SO_4, filtered and concentrated *in vacuo*. The crude product was purified by flash column chromatography (15% → 20% ethyl acetate in hexanes) to give oxadiazole **48** as white solid (62.1 mg, 0.199 mmol, 46%).

R_f = 0.65 (40% ethyl acetate in hexanes).

Melting point = 218 °C.

^{1}H NMR (500 MHz, chloroform-*d*) δ (ppm) = 10.00 (s, 1H, NH), 8.68 (d, *J* = 5.0 Hz, 1H, 3-H), 8.29 – 8.25 (m, 2H, 2‘‘-H, 6‘‘-H), 8.17 (dd, *J* = 8.0, 1.0 Hz, 1H, 5-H), 8.15 (d, *J* = 5.0 Hz, 1H, 4-H), 7.68 (dt, *J* = 8.2, 1.2 Hz, 1H, 8-H), 7.65 (ddd, *J* = 8.2, 6.7, 1.2 Hz, 1H, 7-H), 7.60 – 7.56 (m, 3H, 3‘‘-H, 4‘‘-H, 5‘‘-H), 7.36 (ddd, *J* = 8.0, 6.7, 1.3 Hz, 1H, 6-H).

^{13}C NMR (126 MHz, chloroform-*d*) δ (ppm) = 173.8 (C-5‘), 168.8 (C-3‘), 140.8 (C-8a), 140.0 (C-3), 135.3 (C-9a), 131.7 (C-4‘‘), 131.4 (C-4a), 129.8 (C-7), 129.1 (C-3‘‘, C-5‘‘), 127.8 (C-2‘‘, C-6‘‘), 126.7 (C-1‘‘), 125.8 (C-1), 122.2 (C-5), 121.3 (C-4b), 121.2 (C-6), 118.4 (C-4), 112.2 (C-8).

IR (ATR) $\tilde{\nu}$ (cm^{-1}) = 3410, 3241, 1628, 1556, 1446, 1358, 1246, 1220, 1185, 1072, 847, 736, 696, 686.

HRMS (EI) (*m/z*) = calculated for $C_{19}H_{12}N_4O^{\cdot+}$ $[M]^{\cdot+}$ 312.1006, found 312.1007.

Purity (HPLC, method 2a) > 95% (λ = 210 nm), > 95% (λ = 254 nm).

2-Phenyl-5-(9*H*-pyrido[3,4-*b*]indol-1-yl)-1,3,4-oxadiazole (50)[143]

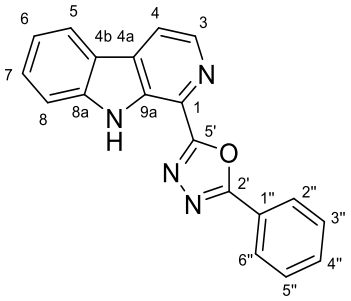

$C_{19}H_{12}N_4O$

M_r = 312.33 g/mol

Similar to literature[143], aldehyde **36** (98.1 mg, 0.500 mmol, 1.0 eq) and benzoic acid hydrazide (72.9 mg, 0.525 mmol, 1.05 eq) were dissolved in methanol (6.0 mL) and the reaction mixture was stirred at 75 °C for 1 h. The solvent was removed *in vacuo* and the crude hydrazone **49** (R_f = 0.04**,** 40% ethyl acetate in hexanes) was redissolved in DMSO (3.0 mL). Then Cs_2CO_3 (489 mg, 1.50 mmol, 3.0 eq) and iodine (190 mg, 0.750 mmol, 1.5 eq) were added, the mixture was stirred at 90 °C for 1 h and, after cooling to room temperature, diluted with cold water (10 mL) and sat. aq. $Na_2S_2O_3$ solution (10 mL). It was extracted with ethyl acetate (3 x 30 mL) and the combined organic layers were dried over Na_2SO_4, filtered and concentrated *in vacuo*. The crude product was purified by flash column chromatography (20% → 25% ethyl acetate in hexanes) to give oxadiazole **50** as white solid (98.2 mg, 0.314 mmol, 63%).

R_f = 0.20 (20% ethyl acetate in hexanes).

Melting point = 237 °C (lit.[143] 209 – 211 °C).

^{1}H NMR (500 MHz, chloroform-*d*) δ (ppm) = 10.22 (s, 1H, NH), 8.66 (d, *J* = 5.1 Hz, 1H, 3-H), 8.32 – 8.29 (m, 2H, 2‘-H, 6‘-H), 8.18 (dq, *J* = 7.9, 0.9 Hz, 1H, 5-H), 8.12 (dd, *J* = 5.0, 0.8 Hz, 1H, 4-H), 7.65 – 7.62 (m, 2H, 7-H, 8-H), 7.60 – 7.54 (m, 3H, 3‘-H, 4‘-H, 5‘-H), 7.35 (ddd, *J* = 8.0, 5.0, 3.1 Hz, 1H, 6-H).

^{13}C NMR (126 MHz, chloroform-*d*) δ (ppm) = 165.0 (C-2‘), 164.0 (C-5‘), 140.9 (C-8a), 139.5 (C-3), 134.9 (C-9a), 132.3 (C-4‘), 130.8 (C-4a), 129.6 (C-7), 129.2 (C-3‘, C-5‘), 127.6 (C-2‘, C-6‘), 125.9 (C-1), 123.6 (C-1‘‘), 122.1 (C-5), 121.3 (C-4b), 121.0 (C-6), 117.4 (C-4), 112.3 (C-8).

IR (ATR) $\tilde{\nu}$ (cm^{-1}) = 3411, 3062, 1629, 1538, 1492, 1449, 1431, 1397, 1318, 1283, 1250, 1224, 744, 722, 687.

HRMS (EI) (*m/z*) = calculated for $C_{19}H_{12}N_4O^{\cdot+}$ $[M]^{\cdot+}$ 312.1006, found 312.1003.

Purity (HPLC, method 2a) > 95% (λ = 210 nm), > 95% (λ = 254 nm).

1-(Phenylethynyl)-9*H*-pyrido[3,4-*b*]indole (51)

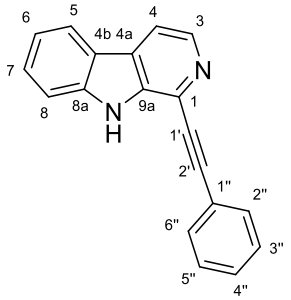

$C_{19}H_{12}N_2$

M_r = 268.32 g/mol

Following **General Procedure Ia**, bromide **8** (98.8 mg, 0.400 mmol, 1.0 eq), CuI (16 mg, 0.084 mmol, 0.2 eq), Pd(dppf)Cl_2 (15 mg, 0.020 mmol, 0.05 eq) and phenylacetylene (0.060 mL, 0.55 mmol, 1.4 eq, dissolved in 0.6 mL anhydrous THF) were used in anhydrous triethylamine (2.4 mL) and anhydrous THF (2.0 mL). After stirring for 18 h, the reaction was completed. The celite pad was washed with ethyl acetate (50 mL) and the extraction was performed with sat. aq. NaCl solution (50 mL) and ethyl acetate (3 x 25 mL). The crude product was purified two times by flash column chromatography (15% → 20% ethyl acetate in hexanes, methylene chloride) to give alkyne **51** as pale yellow solid (74.1 mg, 0.276 mmol, 69%).

R_f = 0.16 (20% ethyl acetate in hexanes).

Melting point = 229 °C.

^{1}H NMR (500 MHz, methylene chloride-d_2) δ (ppm) = 8.99 (s, 1H, NH), 8.49 (s, 1H, 3-H), 8.17 (dt, *J* = 8.0, 0.9 Hz, 1H, 5-H), 7.97 (d, *J* = 5.0 Hz, 1H, 4-H), 7.65 – 7.61 (m, 3H, 8-H, 2‘‘-H, 6‘‘-H), 7.60 (ddd, *J* = 8.2, 6.7, 1.2 Hz, 1H, 7-H), 7.42 – 7.37 (m, 3H, 3‘‘-H, 4‘‘-H, 5‘‘-H), 7.33 (ddd, *J* = 8.0, 6.6, 1.4 Hz, 1H, 6-H).

^{13}C NMR (126 MHz, methylene chloride-d_2) δ (ppm) = 140.8 (C-8a), 140.4 (C-3), 138.1 (C 9a), 132.5 (C-2’’, C-6’’), 129.7 (C-4’’), 129.4 (C-7), 129.3 (C-4a), 129.1 (C-3’’, C-5’’), 127.3 (C-1), 122.7 (C-1’’), 122.5 (C-5), 122.3 (C-4b), 121.0 (C-6), 115.3 (C-4), 112.3 (C-8), 94.4 (C 2’), 85.8 (C-1’).

IR (ATR) $\tilde{\nu}$ (cm^{-1}) = 3054, 2208, 1625, 1560, 1499, 1492, 1453, 1427, 1276, 1239, 826, 742, 687.

HRMS (EI) (*m/z*) = calculated for $C_{19}H_{12}N_2^{\cdot+}$ $[M]^{\cdot+}$ 268.0995, found 268.0995.

Purity (HPLC, method 2b) > 95% (λ = 210 nm), > 95% (λ = 254 nm).

(3-Phenylisoxazol-5-yl)methanol (52)[144]

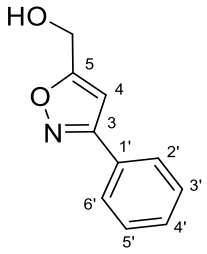

$C_{10}H_9NO_2$

M_r = 175.19 g/mol

Propargyl alcohol (0.76 mL, 13 mmol, 1.3 eq) and *N*-hydroxybenzimidoyl chloride (1.56 g, 10.0 mmol, 1.0 eq) were dissolved in methylene chloride (20 mL). The solution was stirred at 0 °C, while triethylamine (1.53 mL, 11.0 mmol, 1.1 eq) was added dropwise over 30 min. After stirring the reaction mixture at room temperature for 16 h, water (20 mL) was added and the phases were separated. The aq. phase was further extracted with methylene chloride (2 x 20 mL) and the combined organic layers were dried using a phase separation filter. The solvent was removed *in vacuo* and the crude product purified two times by flash column chromatography (20% ethyl acetate in hexanes, 1% methanol in methylene chloride) to give isoxazole **52** as white solid (1.38 g, 7.88 mmol, 79%).

R_f = 0.18 (20% ethyl acetate in hexanes).

Melting point = 54 °C (lit.[144] 52 – 54 °C).

^{1}H NMR (400 MHz, chloroform-*d*) δ (ppm) = 7.81 – 7.76 (m, 2H, 2‘-H, 6‘-H), 7.48 – 7.42 (m, 3H, 3‘-H, 4’-H, 5’-H), 6.56 (d, J = 0.9 Hz, 1H, 4-H), 4.81 (dd, J = 6.4, 0.8 Hz, 2H, CH_2), 2.56 (t, J = 6.4 Hz, 1H, OH).

^{13}C NMR (101 MHz, chloroform-*d*) δ (ppm) = 172.0 (C-5), 162.6 (C-3), 130.3 (C-4’), 129.1 (C-3’, C-5’), 129.0 (C-1’), 127.0 (C-2‘, C-6‘), 100.2 (C-4), 56.7 (CH_2).

IR (ATR) $\tilde{\nu}$ (cm^{-1}) = 3244, 3104, 1608, 1405, 1183, 1041, 988, 950, 899, 837, 766, 691.

HRMS (EI) (*m/z*) = calculated for $C_{10}H_9NO_2^{\cdot+}$ $[M]^{\cdot+}$ 175.0628, found 175.0626.

Purity (HPLC, method 2e) > 95% (λ = 210 nm), > 95% (λ = 254 nm).

3-Phenylisoxazole-5-carbaldehyde (53)[145]

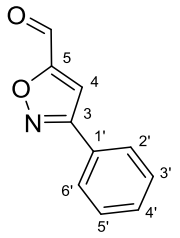

$C_{10}H_7NO_2$

M_r = 173.17 g/mol

Similar to literature[145], anhydrous DMSO (1.94 mL, 27.3 mmol, 2.6 eq) was dissolved in anhydrous methylene chloride (40 mL) under N_2 atmosphere and stirred at -78 °C for 15 min. Then a solution of oxalyl chloride (1.16 mL, 13.7 mmol, 1.3 eq) in anhydrous methylene chloride (7.0 mL) was added slowly and the reaction mixture was stirred at -78 °C for 15 min, before a solution of alcohol **52** (1.84 g, 10.5 mmol, 1.0 eq) in anhydrous methylene chloride (14 mL) was added dropwise. After stirring the mixture at -78°C for 1 h, anhydrous triethylamine (6.22 mL, 44.6 mmol, 4.25 eq) was added. The reaction mixture was warmed to room temperature and stirred for 1 h. After addition of sat. aq. $NaHCO_3$ solution (80 mL), it was extracted with methylene chloride (3 x 60 mL) and the combined organic layers were dried using a phase separation filter. The solvent was removed *in vacuo* and the crude product purified by flash column chromatography (10% ethyl acetate in hexanes) to give aldehyde **53** as white solid (1.52 g, 8.77 mmol, 84%).

R_f = 0.59 (20% ethyl acetate in hexanes).

Melting point = 70 °C (lit.[145] 73 – 74 °C).

^{1}H NMR (400 MHz, chloroform-*d*) δ (ppm) = 10.04 (s, 1H, CHO), 7.87 – 7.83 (m, 2H, 2'-H, 6'-H), 7.52 – 7.49 (m, 3H, 3'-H, 4'-H, 5'-H), 7.29 (s, 1H, 4-H).

^{13}C NMR (101 MHz, chloroform-*d*) δ (ppm) = 178.5 (CHO), 166.3 (C-5), 163.2 (C-3), 130.8 (C-4'), 129.2 (C-3', C-5'), 127.7 (C-1'), 126.9 (C-2', C-6'), 106.5 (C-4).

IR (ATR) $\tilde{\nu}$ (cm^{-1}) = 2963, 1702, 1574, 1439, 1368, 1278, 1175, 1082, 927, 828, 165, 690.

HRMS (EI) (*m/z*) = calculated for $C_{10}H_7NO_2^{\cdot+}$ $[M]^{\cdot+}$ 173.0472, found 173.0472.

Purity (HPLC, method 3) > 95% (λ = 210 nm), > 95% (λ = 254 nm).

3-Phenyl-5-(2,3,4,9-tetrahydro-1*H*-pyrido[3,4-*b*]indol-1-yl)isoxazole (54)

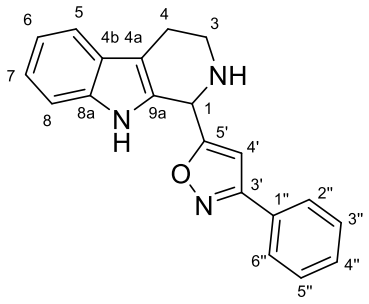

$C_{20}H_{17}N_3O$

M_r = 315.37 g/mol

3-Phenylisoxazole-5-carbaldehyde (**53**) (86.6 mg, 0.500 mmol, 1.0 eq) and tryptamine (80.1 mg, 0.500 mmol, 1.0 eq) were dissolved in anisole (5.0 mL). The solution was stirred at 120 °C for 2 h and, after cooling to room temperature, the solvent was removed *in vacuo*. The crude product was purified by flash column chromatography (50% ethyl acetate in hexanes) and subsequent recrystallization (from ethyl acetate) to give tetrahydro-*β*-carboline **54** as pale rose crystals (98.8 mg, 0.313 mmol, 63%).

R_f = 0.16 (50% ethyl acetate in hexanes).

Melting point = 192 °C.

^{1}H NMR (400 MHz, DMSO-d_6) δ (ppm) = 10.84 (s, 1H, 9-NH), 7.89 – 7.84 (m, 2H, 2''-H, 6''-H), 7.52 – 7.46 (m, 3H, 3''-H, 4''-H, 5''-H), 7.44 (dd, *J* = 7.8, 1.1 Hz, 1H, 5-H), 7.31 (dt, *J* = 8.0, 1.0 Hz, 1H, 8-H), 7.06 (ddd, *J* = 8.1, 7.0, 1.3 Hz, 1H, 7-H), 6.98 (ddd, *J* = 8.0, 7.0, 1.1 Hz, 1H, 6-H), 6.80 (s, 1H, 4'-H), 5.39 (s, 1H, 1-H), 3.16 (s, 1H, 2-NH), 3.12 – 3.00 (m, 2H, 3-H), 2.69 (t, *J* = 5.6 Hz, 2H, 4-H).

^{13}C NMR (101 MHz, DMSO-d_6) δ (ppm) = 174.2 (C-5'), 161.6 (C-3'), 135.9 (C-8a), 131.3 (C-9a), 130.1 (C-4''), 129.1 (C-3'', C-5''), 128.7 (C-1''), 126.6 (C-4b), 126.6 (C-2'', C-6''), 121.1 (C-7), 118.4 (C-6), 117.8 (C-5), 111.3 (C-8), 108.8 (C-4a), 100.4 (C-4'), 48.6 (C-1), 40.2 (C-3, collapses with DMSO peak), 21.9 (C-4).

IR (ATR) $\tilde{\nu}$ (cm^{-1}) = 3328, 1598, 1578, 1454, 1403, 1306, 1265, 1114, 924, 856, 829, 772, 746, 692.

HRMS (EI) (*m/z*) = calculated for $C_{20}H_{18}N_3O^+$ $[M+H]^+$ 316.1445, found 316.1448.

Purity (HPLC, method 2a) > 95% (λ = 210 nm), > 95% (λ = 254 nm).

4-Phenylfuran-2-carbaldehyde (55)[154]

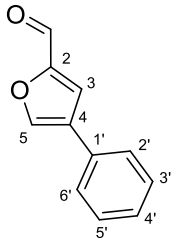

$C_{11}H_8O_2$

M_r = 172.18 g/mol

Following **General Procedure VIa**, 4-bromofuran-2-carboxaldehyde (350 mg, 2.00 mmol, 1.0 eq), phenylboronic acid (293 mg, 2.40 mmol, 1.2 eq), Cs_2CO_3 (1.63 g, 5.00 mmol, 2.5 eq) and $Pd(PPh_3)_4$ (119 mg, 0.100 mmol, 0.05 eq) were used in degassed 1,4-dioxane/water (30 mL). The crude product was purified by flash column chromatography (4% ethyl acetate in hexanes) to give biaryl **55** as yellow oil (249 mg, 1.45 mmol, 72%).

R_f = 0.24 (5% ethyl acetate in hexanes).

^{1}H NMR (500 MHz, chloroform-*d*) δ (ppm) = 9.71 (d, J = 0.7 Hz, 1H, CHO), 7.95 (t, J = 0.8 Hz, 1H, 5-H), 7.53 – 7.50 (m, 3H, 3-H, 2‘-H, 6‘-H), 7.45 – 7.41 (m, 2H, 3‘-H, 5‘-H), 7.37 – 7.33 (m, 1H, 4‘-H).

^{13}C NMR (126 MHz, chloroform-*d*) δ (ppm) = 178.3 (CHO), 153.7 (C-2), 143.8 (C-5), 130.6 (C-1’), 129.5 (C-4), 129.3 (C-3’, C-5’), 128.3 (C-4’), 126.1 (C-2’, C-6’), 119.0 (C-3).

IR (ATR) $\tilde{\nu}$ (cm^{-1}) = 3129, 1763, 1674, 1522, 1477, 1334, 1147, 1049, 942, 926, 755, 691.

HRMS (EI) (*m/z*) = calculated for $C_{11}H_8O_2^{\cdot+}$ $[M]^{\cdot+}$ 172.0519, found 172.0517.

Purity (HPLC, method 2e) > 81% (λ = 210 nm), > 92% (λ = 254 nm).

4-Phenylthiophene-2-carbaldehyde (56)[301]

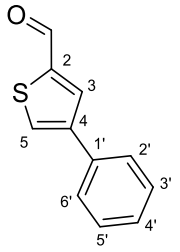

$C_{11}H_8OS$

M_r = 188.24 g/mol

Following **General Procedure VIa**, 4-bromothiophene-2-carboxaldehyde (382 mg, 2.00 mmol, 1.0 eq), phenylboronic acid (293 mg, 2.40 mmol, 1.2 eq), Cs_2CO_3 (1.63 g, 5.00 mmol, 2.5 eq) and $Pd(PPh_3)_4$ (119 mg, 0.100 mmol, 0.05 eq) were used in degassed 1,4-dioxane/water (30 mL). The crude product was purified by flash column chromatography (5% ethyl acetate in hexanes) to give biaryl **56** as pale yellow solid (343 mg, 1.82 mmol, 91%).

R_f = 0.18 (5% ethyl acetate in hexanes).

Melting point = 69 °C (lit.[301] 68 – 69 °C).

^{1}H NMR (400 MHz, chloroform-*d*) δ (ppm) = 9.98 (d, J = 1.3 Hz, 1H, CHO), 8.04 (d, J = 1.5 Hz, 1H, 3-H), 7.86 (t, J = 1.4 Hz, 1H, 5-H), 7.61 – 7.57 (m, 2H, 2‘-H, 6‘-H), 7.47 – 7.42 (m, 2H, 3‘-H, 5‘-H), 7.39 – 7.34 (m, 1H, 4‘-H).

^{13}C NMR (101 MHz, chloroform-*d*) δ (ppm) = 183.1 (CHO), 144.6 (C-2), 143.8 (C-4), 134.9 (C-3), 134.5 (C-1’), 129.8 (C-5), 129.2 (C-3’, C-5’), 128.2 (C-4’), 126.5 (C-2’, C-6’).

IR (ATR) $\tilde{\nu}$ (cm^{-1}) = 2836, 1669, 1536, 1430, 1368, 1244, 1190, 1175, 1156, 859, 757, 696.

HRMS (EI) (*m/z*) = calculated for $C_{11}H_8OS^{\cdot+}$ $[M]^{\cdot+}$ 188.0291, found 188.0290.

Purity (HPLC, method 2e) > 95% (λ = 210 nm), > 95% (λ = 254 nm).

1-(4-Phenylfuran-2-yl)-9*H*-pyrido[3,4-*b*]indole (58)

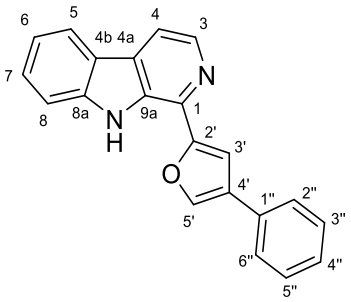

$C_{21}H_{14}N_2O$

M_r = 310.36 g/mol

Following **General Procedure IV**, 4-phenylfuran-2-carbaldehyde (**55**) (86.1 mg, 0.500 mmol, 1.0 eq), tryptamine (80.1 mg, 0.500 mmol, 1.0 eq) and palladium on carbon (10 wt.%, 266 mg, 0.250 mmol, 0.5 eq) were used in anisole (5.0 mL). The celite pad was washed with methanol (50 mL). The crude product was purified two times by flash column chromatography (10% → 15% ethyl acetate in hexanes, 100% methylene chloride) to give *β*-carboline **58** as yellow solid (28.0 mg, 0.0902 mmol, 18%).

R_f = 0.27 (20% ethyl acetate in hexanes).

Melting point = 170 °C.

^{1}H NMR (500 MHz, methylene chloride-d_2) δ (ppm) = 9.49 (s, 1H, NH), 8.45 (d, *J* = 5.1 Hz, 1H, 3-H), 8.17 (dd, *J* = 7.8, 1.1 Hz, 1H, 5-H), 8.04 (d, *J* = 0.9 Hz, 1H, 5‘-H), 7.92 (d, *J* = 5.2 Hz, 1H, 4-H), 7.66 – 7.63 (m, 3H, 8-H, 2‘‘-H, 6‘‘-H), 7.62 – 7.58 (m, 2H, 7-H, 3‘-H), 7.46 – 7.42 (m, 2H, 3‘‘-H, 5‘‘-H), 7.35 – 7.31 (m, 2H, 6-H, 4‘‘-H).

^{13}C NMR (126 MHz, methylene chloride-d_2) δ (ppm) = 156.2 (C-2‘), 141.1 (C-8a), 139.6 (C-3), 139.2 (C-5‘), 133.7 (C-1), 132.3 (C-1‘‘), 132.0 (C-9a), 130.7 (C-4a), 129.5 (C-3‘‘, C-5‘‘), 129.3 (C-4‘), 129.2 (C-7), 128.1 (C-4‘‘), 126.5 (C-2‘‘, C-6‘‘), 122.2 (C-5), 121.8 (C-4b), 120.7 (C-6), 114.4 (C-4), 112.2 (C-8), 107.8 (C-3‘).

IR (ATR) $\tilde{\nu}$ (cm^{-1}) = 3055, 1627, 1564, 1450, 1420, 1316, 1232, 929, 822, 742.

HRMS (EI) (*m/z*) = calculated for $C_{21}H_{14}N_2O^{\cdot+}$ $[M]^{\cdot+}$ 310.1101, found 310.1101.

Purity (HPLC, method 2b) > 95% (λ = 210 nm), > 95% (λ = 254 nm).

1-(4-Phenylthiophen-2-yl)-9*H*-pyrido[3,4-*b*]indole (59)

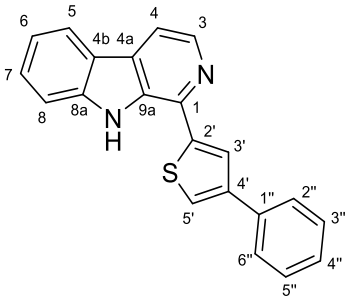

$C_{21}H_{14}N_2S$

M_r = 326.42 g/mol

Following **General Procedure IV**, 4-phenylthiophene-2-carbaldehyde (**56**) (94.1 mg, 0.500 mmol, 1.0 eq), tryptamine (80.1 mg, 0.500 mmol, 1.0 eq) and palladium on carbon (10 wt.%, 266 mg, 0.250 mmol, 0.5 eq) were used in anisole (5.0 mL). The celite pad was washed with methanol (50 mL). The crude product was purified by flash column chromatography (5% → 10% ethyl acetate in hexanes) and subsequent recrystallization (from methylene chloride/hexanes) to give *β*-carboline **59** as pale yellow solid (38.1 mg, 0.117 mmol, 23%).

R_f = 0.44 (20% ethyl acetate in hexanes).

Melting point = 174 °C.

^{1}H NMR (400 MHz, chloroform-*d*) *δ* (ppm) = 8.86 (s, 1H, NH), 8.52 (d, *J* = 5.2 Hz, 1H, 3-H), 8.15 (dq, *J* = 7.9, 0.9 Hz, 1H, 5-H), 7.98 (d, *J* = 1.4 Hz, 1H, 3'-H), 7.91 (dd, *J* = 5.2, 0.7 Hz, 1H, 4-H), 7.65 – 7.61 (m, 2H, 2''-H, 6''-H), 7.58 (dd, *J* = 4.6, 1.1 Hz, 3H, 7-H, 8-H, 5'-H), 7.43 – 7.38 (m, 2H, 3''-H, 5''-H), 7.36 – 7.29 (m, 2H, 6-H, 4''-H).

^{13}C NMR (101 MHz, chloroform-*d*) *δ* (ppm) = 143.6 (C-2' or C-4'), 143.4 (C-2' or C-4'), 140.7 (C-8a), 139.5 (C-3), 137.1 (C-1), 135.8 (C-1''), 132.5 (C-9a), 130.7 (C-4a), 129.0 (C-3'', C-5''), 128.9 (C-7), 127.6 (C-4''), 126.6 (C-2'', C-6''), 124.4 (C-3'), 122.2 (C-5), 122.1 (C-4b), 121.9 (C-5'), 120.8 (C-6), 114.1 (C-4), 112.0 (C-8).

IR (ATR) $\tilde{\nu}$ (cm^{-1}) = 3058, 1625, 1562, 1471, 1454, 1322, 1255, 1233, 883, 826, 744, 728.

HRMS (EI) (*m/z*) = calculated for $C_{21}H_{14}N_2S^{\cdot+}$ $[M]^{\cdot+}$ 326.0873, found 326.0855.

Purity (HPLC, method 2b) > 95% (λ = 210 nm), > 95% (λ = 254 nm).

4-Phenyl-1*H*-imidazole-2-carbaldehyde (62)[159]

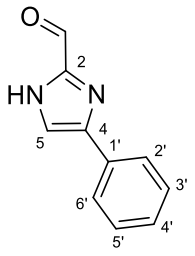

$C_{10}H_8N_2O$

M_r = 172.19 g/mol

Similar to literature[159], phenylglyoxal monohydrate (152 mg, 1.00 mmol, 1.0 eq) was dissolved in methanol (1.7 mL). Then 2,2-dimethoxyacetaldehyde solution (60% in water, 0.347 mL, 2.30 mmol, 2.3 eq) and a solution of ammonium acetate (301 mg, 3.90 mmol, 3.9 eq) in methanol (1.7 mL) were added and the reaction mixture was stirred at room temperature for 16 h, before the solvent was removed *in vacuo*.

The residue, containing the crude dimethyl acetal (R_f = 0.66, 40% ethyl acetate in hexanes; HRMS (EI) (*m/z*) = calculated for $C_{12}H_{14}N_2O_2^{\cdot+}$ $[M]^{\cdot+}$ 218.1050, found 218.1060), was resuspended in aq. HCl (2 M, 2.5 mL) and stirred at 80 °C for 30 min. After cooling to room temperature, the mixture was diluted with water (3.0 mL) and extracted with ethyl acetate (5.0 mL). The organic phase was discarded, the aq. phase basified with aq. NaOH solution (9 M, 1.0 mL) and extracted with ethyl acetate (3 x 20 mL). The combined organic layers dried using a phase separation filter and the solvent was removed *in vacuo* to give sufficiently pure imidazole **62** as light brown solid (107 mg, 0.624 mmol, 62%).

R_f = 0.26 (20% ethyl acetate in toluene).

Melting point = 174 °C.

^{1}H NMR (400 MHz, DMSO-d_6) δ (ppm) = 13.71 (s, 1H, NH), 9.69 (s, 1H, CHO), 8.03 (s, 1H, 5-H), 7.96 – 7.84 (m, 2H, 2‘‘-H, 6‘‘-H), 7.42 (dd, *J* = 8.3, 7.0 Hz, 2H, 3‘‘-H, 5‘‘-H), 7.30 (t, *J* = 7.4 Hz, 1H, 4‘‘-H).

^{13}C NMR (101 MHz, DMSO-d_6) δ (ppm) = 181.2 (CHO), 146.2 (C-2), 142.2 (C-4), 132.5 (C-1‘), 128.7 (C-3‘, C-5‘), 127.5 (C-4‘), 125.0 (C-2‘, C-6‘), 122.1 (C-5).

IR (ATR) $\tilde{\nu}$ (cm^{-1}) = 2830, 2679, 1511, 1467, 1371, 1307, 1283, 1171, 1085, 962, 901, 846, 748, 694.

HRMS (EI) (*m/z*) = calculated for $C_{10}H_8N_2O^{\cdot+}$ $[M]^{\cdot+}$ 172.0632, found 172.0631.

Purity (HPLC, method 3) > 95% (λ = 210 nm), > 95% (λ = 254 nm).

1-(5-Phenyl-1*H*-imidazol-2-yl)-9*H*-pyrido[3,4-*b*]indole (60)

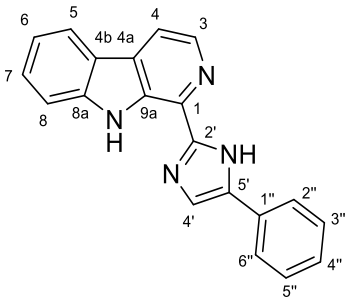

$C_{20}H_{14}N_4$

M_r = 310.36 g/mol

Similar to **General procedure IV**, 4-phenyl-1*H*-imidazole-2-carbaldehyde (**62**) (172 mg, 1.00 mmol, 1.0 eq) and tryptamine (160 mg, 1.00 mmol, 1.0 eq) were suspended in anisole (45 mL) and the solution was stirred at 155 °C for 2 h. After cooling to room temperature, palladium on carbon (10 wt.%, 266 mg, 0.250 mmol, 0.25 eq) was added. The reaction mixture was stirred at 160 °C for 40 h and, after cooling to room temperature, filtered through a pad of celite. The pad was washed with methanol (100 mL) and the filtrate concentrated *in vacuo*. The crude product was purified two times by flash column chromatography (15% → 20% ethyl acetate in hexanes, 50% methylene chloride in chloroform) to give *β*-carboline **60** as yellow solid (59.4 mg, 0.191 mmol, 19%).

R_f = 0.37 (20% ethyl acetate in toluene).

Melting point = 213 °C.

^{1}H NMR (400 MHz, DMSO-d_6, 373 K) δ (ppm) = 12.84 (s, 1H, 1‘-NH), 11.18 (s, 1H, 9-NH), 8.44 (d, *J* = 5.2 Hz, 1H, 3-H), 8.26 (d, *J* = 7.9 Hz, 1H, 5-H), 8.21 – 8.05 (m, 3H, 4-H, 2‘‘-H, 6‘‘-H), 7.97 (d, *J* = 8.3 Hz, 1H, 8-H), 7.74 (s, 1H, 4‘-H), 7.60 (t, *J* = 7.8 Hz, 1H, 7-H), 7.49 – 7.42 (m, 2H, 3‘‘-H, 5‘‘-H), 7.34 – 7.26 (m, 2H, 6-H, 4‘‘-H). (Tautomeric ratio 1:5 according to ^{1}H NMR in DMSO-d_6 at 293 K.)

^{13}C NMR (101 MHz, DMSO-d_6, 373 K) δ (ppm) = 145.6 (C-2‘), 141.6 (C-5‘), 140.5 (C-8a), 137.2 (C-3), 134.0 (C-1‘‘), 132.0 (C-1 or C-9a), 131.8 (C-1 or C-9a), 128.7 (C-4a), 127.8 (C-3‘‘, C-5‘‘), 127.7 (C-7), 125.9 (C-4‘‘), 124.6 (C-2‘‘, C-6‘‘), 121.0 (C-5), 120.4 (C-4b), 119.2 (C-6), 114.0 (C-4‘), 113.7 (C-4), 112.5 (C-8).

IR (ATR) $\tilde{\nu}$ (cm^{-1}) = 3349, 3195, 1574, 1552, 1494, 1453, 1443, 1398, 1319, 1249, 1123, 746, 718, 689.

HRMS (ESI) (*m/z*) = calculated for $C_{20}H_{15}N_4^+$ $[M+H]^+$ 311.1292, found 311.1292.

Purity (HPLC, method 2c) > 95% (λ = 210 nm), > 95% (λ = 254 nm).

2-Nitro-1-(9*H*-pyrido[3,4-*b*]indol-1-yl)ethan-1-one (65)

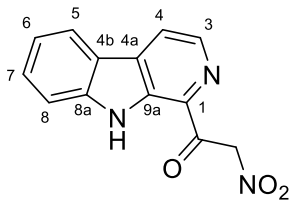

$C_{13}H_9N_3O_3$

M_r = 255.23 g/mol

Carboxylic acid **41** (424 mg, 2.00 mmol, 1.0 eq) and 1,1'-carbonyldiimidazole (389 mg, 2.40 mmol, 1.2 eq) were suspended in anhydrous THF (15 mL) under N_2 atmosphere and the reaction mixture was stirred at 70 °C for 2 h (= activated carboxylic acid; R_f = 0.16, 40% ethyl acetate in hexanes). In another flask, sodium hydride (60% dispersion in mineral oil, 96 mg, 2.4 mmol, 1.2 eq) was suspended in anhydrous THF (4.0 mL), cooled to 0 °C and nitromethane (dried over 4 Å molecular sieves, 0.13 mL, 2.4 mmol, 1.2 eq) was slowly added. The mixture was stirred for 1 h at room temperature, then the activated carboxylic acid was, still slightly warm, added dropwise to the nitromethane anion and the mixture was stirred at 70 °C for 5 h and at room temperature for further 16 h. It was diluted with water (100 mL), extracted with methylene chloride (3 x 50 mL) and these organic phases were discarded. The pH of the aq. phase was adjusted to 1 with aq. HCl (1 M) and it was extracted with methylene chloride (3 x 50 mL). These combined organic layers were dried over Na_2SO_4, filtered and concentrated *in vacuo* to give pure *α*-nitro ketone **65** as yellow solid (313 mg, 1.23 mmol, 61%).

R_f = 0.64 (40% ethyl acetate in hexanes).

Melting point = 170 °C.

^{1}H NMR (400 MHz, DMSO-d_6) δ (ppm) = 12.13 (s, 1H, NH), 8.55 (d, *J* = 4.9 Hz, 1H, 4-H), 8.53 (d, *J* = 4.9 Hz, 1H, 3-H), 8.34 (d, *J* = 7.9 Hz, 1H, 5-H), 7.80 (d, *J* = 8.2 Hz, 1H, 8-H), 7.63 (t, *J* = 7.7 Hz, 1H, 7-H), 7.34 (t, *J* = 7.5 Hz, 1H, 6-H), 6.56 (s, 2H, CH_2).

^{13}C NMR (101 MHz, DMSO-d_6) δ (ppm) = 189.6 (CO), 142.1 (C-8a), 137.8 (C-3), 134.4 (C-9a), 133.1 (C-1), 131.6 (C-4a), 129.4 (C-7), 122.1 (C-5), 120.8 (C-4), 120.7 (C-6), 119.8 (C-4b), 113.1 (C-8), 82.1 (CH_2).

IR (ATR) $\tilde{\nu}$ (cm^{-1}) = 3418, 3014, 1690, 1546, 1493, 1434, 1321, 1290, 1206, 1131, 1109, 1014, 999, 742.

HRMS (ESI) (*m/z*) = calculated for $C_{13}H_8N_3O_3^-$ $[M-H]^-$ 254.0571, found 254.0573.

Purity (HPLC, method 1d) > 95% (λ = 210 nm), > 95% (λ = 254 nm).

Ethyl 3-(1-bromo-9*H*-pyrido[3,4-*b*]indol-9-yl)acrylate (68)

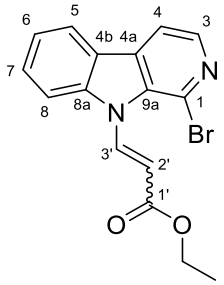

$C_{16}H_{13}BrN_2O_2$

M_r = 345.20 g/mol

Following **General Procedure Ia**, bromide **8** (98.8 mg, 0.400 mmol, 1.0 eq), CuI (16 mg, 0.084 mmol, 0.2 eq), Pd(dppf)Cl_2 (15 mg, 0.020 mmol, 0.05 eq) and ethyl propiolate (0.093 mL, 0.66 mmol, 2.0 eq, dissolved in 0.3 mL anhydrous THF) were used in anhydrous triethylamine (1.5 mL) and anhydrous THF (1.2 mL). After stirring for 16 h, the reaction was completed. The celite pad was washed with ethyl acetate (20 mL) and the extraction was performed with water (15 mL) and ethyl acetate (3 x 15 mL). The crude product was purified by flash column chromatography (10% → 15% ethyl acetate in hexanes) to give alkene **68** as an *E*/*Z* mixture (*E*/*Z* ratio 1.0:0.27 determined *via* ^{1}H NMR spectrum) as yellow solid (105 mg, 0.304 mmol, 76%).

R_f = 0.44 (20% ethyl acetate in hexanes).

Melting point = 70 °C.

^{1}H NMR (400 MHz, chloroform-*d*) δ (ppm) = 9.39 (d, *J* = 14.1 Hz, 1H, 3‘-H (*E*)), 8.30 (d, *J* = 5.0 Hz, 1H, 3-H (*E*)), 8.25 (d, *J* = 5.1 Hz, 1H, 3-H (*Z*)), 8.11 – 8.05 (m, 2H, 5-H (*E*), 5-H (*Z*)), 7.93 – 7.87 (m, 3H, 4-H (*Z*), 4-H (*E*), 8-H (*E*)), 7.79 (d, *J* = 8.7 Hz, 1H, 3‘-H (*Z*)), 7.66 (ddd, *J* = 8.5, 7.2, 1.3 Hz, 1H, 7-H (*E*)), 7.57 (ddd, *J* = 8.4, 7.2, 1.2 Hz, 1H, 7-H (*Z*)), 7.43 (ddd, *J* = 8.0, 7.2, 0.8 Hz, 1H, 6-H (*E*)), 7.32 (dt, *J* = 8.3, 0.9 Hz, 1H, 8-H (*Z*)), 7.34 (ddd, *J* = 8.0, 7.2, 0.9 Hz, 1H, 6-H (*Z*)), 6.32 (d, *J* = 14.1 Hz, 1H, 2‘-H (*E*)), 6.26 (d, *J* = 8.7 Hz, 1H, 2‘-H (*Z*)), 4.34 (q, *J* = 7.2 Hz, 2H, CH_2 (*E*)), 3.93 (q, *J* = 7.1 Hz, 2H, CH_2 (*Z*)), 1.39 (t, *J* = 7.1 Hz, 3H, CH_3 (*E*)), 0.86 (t, *J* = 7.1 Hz, 3H, CH_3 (*Z*)).

^{13}C NMR (101 MHz, chloroform-*d*) δ (ppm) = 166.9 (C-1‘ (*E*)), 164.1 (C-1‘ (*Z*)), 141.7 (C-3 (*E*)), 140.9 (C-8a (*Z*)), 140.5 (C-3 (*Z*)), 140.0 (C-8a (*E*)), 138.8 (C-3‘ (*E*)), 134.9 (C-3‘ (*Z*)), 134.5 (C-9a (*Z*)), 133.9 (C-9a (*E*)), 133.7 (C-4a (*E*)), 132.6 (C-4a (*Z*)), 130.2 (C-7 (*E*)), 129.3 (C-7 (*Z*)), 124.3 (C-1 (*E*)), 124.2 (C-1 (*Z*)), 123.3 (C-6 (*E*)), 123.1 (C-4b (*E*)), 122.0 (C-5 or C-6 (*Z*)), 121.9 (C-5 (*E*)), 121.7 (C-4b (*Z*)), 121.7 (C-5 or C-6 (*Z*)), 118.1 (C-2‘ (*Z*)), 114.4 (C-4 (*Z*)), 114.3 (C-4 (*E*)), 113.6 (C-8 (*E*)), 112.0 (C-8 (*Z*)), 108.7 (C-2‘ (*E*)), 60.9 (CH_2 (*E*)), 60.8 (CH_2 (*Z*)), 14.5 (CH_3 (*E*)), 13.8 (CH_3 (*Z*)).

IR (ATR) $\tilde{\nu}$ (cm^{-1}) = 2925, 1712, 1638, 1536, 1415, 1217, 1172, 1148, 1130, 1025, 969, 956, 771, 746.

HRMS (ESI) (*m/z*) = calculated for $C_{16}H_{14}{}^{79}BrN_2O_2^+$ $[M+H]^+$ 345.0234, found 345.0234.

Purity (HPLC) n.d.

1-Bromo-9-((2-(trimethylsilyl)ethoxy)methyl)-9*H*-pyrido[3,4-*b*]indole (69)

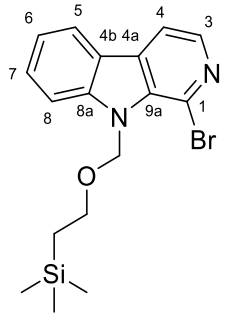

$C_{17}H_{21}BrN_2OSi$

M_r = 377.36 g/mol

Following **General Procedure VIIa**, *β*-carboline **8** (1.98 g, 8.00 mmol, 1.0 eq), lithium bis(trimethylsilyl)amide (1 M in THF, 8.80 mL, 8.80 mmol, 1.1 eq) and SEM chloride (1.56 mL, 8.80 mmol, 1.1 eq) were used in anhydrous DMF (10 mL). The extraction was performed with sat. aq. NaCl solution (100 mL) and ethyl acetate (3 x 100 mL) and the crude product was purified by flash column chromatography (5% → 10% ethyl acetate in hexanes) to give *N*-SEM derivative **69** as pale yellow oil (2.97 g, 7.87 mmol, 98%), which solidified in the cold (2 – 8°C).

R_f = 0.59 (20% ethyl acetate in hexanes).

Melting point = 70 °C.

^{1}H NMR (400 MHz, chloroform-*d*) δ (ppm) = 8.25 (d, *J* = 5.1 Hz, 1H, 3-H), 8.11 (dt, *J* = 8.0, 1.0 Hz, 1H, 5-H), 7.94 (d, *J* = 5.1 Hz, 1H, 4-H), 7.67 (dt, *J* = 8.2, 1.1 Hz, 1H, 8-H), 7.64 (ddd, *J* = 8.4, 6.8, 1.2 Hz, 1H, 7-H), 7.36 (ddd, *J* = 7.9, 6.7, 1.2 Hz, 1H, 6-H), 6.20 (s, 2H, NCH_2), 3.69 – 3.56 (m, 2H, OCH_2), 0.93 – 0.86 (m, 2H, $SiCH_2$), -0.09 (s, 9H, $Si(CH_3)_3$).

^{13}C NMR (101 MHz, chloroform-*d*) δ (ppm) = 142.5 (C-8a), 139.6 (C-3), 134.3 (C-9a), 132.7 (C-4a), 129.4 (C-7), 123.3 (C-1), 121.6 (C-5), 121.5 (C-6), 121.2 (C-4b), 114.5 (C-4), 111.3 (C-8), 72.2 (NCH_2), 65.9 (OCH_2), 18.2 ($SiCH_2$), -1.3 ($Si(CH_3)_3$).

IR (ATR) $\tilde{\nu}$ (cm^{-1}) = 2949, 2923, 2882, 1619, 1534, 1487, 1477, 1433, 1424, 1298, 1218, 1073, 1053, 960, 857, 830.

HRMS (ESI) (*m/z*) = calculated for $C_{17}H_{22}{}^{79}BrN_2OSi^+$ $[M+H]^+$ 377.0680, found 377.0683.

Purity (HPLC, method 2a) > 92% (λ = 210 nm), > 92% (λ = 254 nm).

1-Ethynyl-9-((2-(trimethylsilyl)ethoxy)methyl)-9*H*-pyrido[3,4-*b*]indol (72)

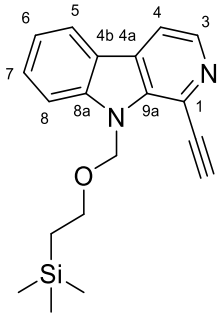

$C_{19}H_{22}N_2OSi$

M_r = 322.48 g/mol

Following **General Procedure Ia**, bromide **69** (2.26 g, 5.98 mmol, 1.0 eq), CuI (239 mg, 1.26 mmol, 0.2 eq), Pd(dppf)Cl_2 (223 mg, 0.305 mmol, 0.05 eq) and trimethylsilylacetylene (1.27 mL, 8.97 mmol, 1.5 eq, dissolved in 6.0 mL anhydrous THF) were used in anhydrous triethylamine (18 mL) and anhydrous THF (14 mL). After stirring for 16 h, the reaction was completed. The celite pad was washed with ethyl acetate (150 mL) and the extraction was performed with sat. aq. NaCl solution (100 mL) and ethyl acetate (3 x 100 mL).
The crude TMS-protected intermediate (R_f = 0.57, 20% ethyl acetate in hexanes; HRMS (EI) (m/z) = calculated for $C_{22}H_{30}N_2OSi_2^{\cdot+}$ $[M]^{\cdot+}$ 394.1892, found 394.1898) was desilylated, following **General Procedure II**, with K_2CO_3 (3.26 g, 20.0 mmol, 3.3 eq) in methanol (50 mL). The crude product was purified by flash column chromatography (15% ethyl acetate in hexanes) to give terminal alkyne **72** as amber oil (1.69 g, 5.25 mmol, 88% over two steps).

R_f = 0.27 (20% ethyl acetate in hexanes).

^{1}H NMR (400 MHz, chloroform-*d*) δ (ppm) = 8.49 (d, *J* = 5.1 Hz, 1H, 3-H), 8.12 (dt, *J* = 7.8, 1.0 Hz, 1H, 5-H), 7.98 (d, *J* = 5.1 Hz, 1H, 4-H), 7.67 (dt, *J* = 8.4, 1.1 Hz, 1H, 8-H), 7.63 (ddd, *J* = 8.3, 6.8, 1.2 Hz, 1H, 7-H), 7.35 (ddd, *J* = 8.0, 6.8, 1.3 Hz, 1H, 6-H), 6.27 (s, 2H, NCH_2), 3.66 – 3.60 (m, 3H, O$\underline{CH_2}CH_2$, CCH), 0.91 – 0.85 (m, 2H, $SiCH_2$), -0.11 (s, 9H, $Si(CH_3)_3$).

^{13}C NMR (101 MHz, chloroform-*d*) δ (ppm) = 142.1 (C-8a), 140.3 (C-3), 137.0 (C-9a), 130.9 (C-4a), 129.3 (C-7), 124.7 (C-1), 121.7 (C-5), 121.3 (C-4b), 121.3 (C-6), 115.3 (C-4), 111.2 (C-8), 82.6 (C$\underline{CH}$), 82.0 ($\underline{C}$CH), 72.5 (NCH_2), 65.9 (O$\underline{CH_2}CH_2$), 18.2 ($SiCH_2$), -1.3 ($Si(CH_3)_3$).

IR (ATR) $\tilde{\nu}$ (cm^{-1}) = 3295, 2951, 2896, 2096, 1621, 1556, 1441, 1420, 1327, 1298, 1282, 1247, 1210, 1066, 1035, 856, 833, 738.

HRMS (EI) (*m/z*) = calculated for $C_{19}H_{22}N_2OSi^{\cdot+}$ $[M]^{\cdot+}$ 322.1496, found 322.1494.

Purity (HPLC, method 2a) > 95% (λ = 210 nm), > 95% (λ = 254 nm).

Ethyl 3-(9-((2-(trimethylsilyl)ethoxy)methyl)-9*H*-pyrido[3,4-*b*]indol-1-yl)propiolate (70)

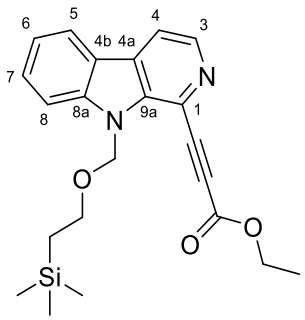

$C_{22}H_{26}N_2O_3Si$

M_r = 394.55 g/mol

Terminal alkyne **72** (1.71 g, 5.30 mmol, 1.0 eq) was dissolved in anhydrous THF (10 mL) under N_2 atmosphere and cooled to -78 °C. Then *n*-butyllithium (2.5 M in hexanes, 2.12 mL, 5.30 mmol, 1.0 eq) was slowly added and the solution was stirred for 45 min. After ethyl chloroformate (0.507 mL, 5.30 mmol, 1.0 eq) was added dropwise, the reaction mixture was stirred at -78 °C for 5 h, slowly warmed to room temperature and stirred for further 16 h. Then the mixture was diluted with water (50 mL) and extracted with ethyl acetate (3 x 50 mL). The combined organic layers were dried using a phase separation filter, the solvent was removed *in vacuo* and the residue purified by flash column chromatography (10% ethyl acetate in hexanes) to give propiolate **70** as amber oil (1.19 g, 3.02 mmol, 57%).

R_f = 0.28 (20% ethyl acetate in hexanes).

^{1}H NMR (400 MHz, chloroform-*d*) δ (ppm) = 8.55 (d, *J* = 5.0 Hz, 1H, 3-H), 8.13 (dt, *J* = 7.9, 1.0 Hz, 1H, 5-H), 8.04 (d, *J* = 5.0 Hz, 1H, 4-H), 7.70 – 7.63 (m, 2H, 7-H, 8-H), 7.37 (ddd, *J* = 8.0, 6.4, 1.7 Hz, 1H, 6-H), 6.20 (s, 2H, NCH_2), 4.35 (q, *J* = 7.2 Hz, 2H, $O\underline{CH_2}CH_3$), 3.74 – 3.66 (m, 2H, $O\underline{CH_2}CH_2$), 1.38 (t, *J* = 7.1 Hz, 3H, $OCH_2\underline{CH_3}$), 0.95 – 0.88 (m, 2H, $SiCH_2$), -0.09 (s, 9H, $Si(CH_3)_3$).

^{13}C NMR (101 MHz, chloroform-*d*) δ (ppm) = 153.7 (CO), 142.2 (C-8a), 140.7 (C-3), 138.3 (C-9a), 131.3 (C-4a), 129.7 (C-7), 122.4 (C-1), 121.8 (C-5), 121.6 (C-6), 121.2 (C-4b), 116.6 (C-4), 111.3 (C-8), 84.6 (CC), 83.1 (CC), 72.9 (NCH_2), 66.1 ($O\underline{CH_2}CH_2$), 62.4 ($O\underline{CH_2}CH_3$), 18.1 ($SiCH_2$), 14.2 ($OCH_2\underline{CH_3}$), -1.4 ($Si(CH_3)_3$).

IR (ATR) $\tilde{\nu}$ (cm^{-1}) = 2952, 2898, 2214, 1705, 1621, 1555, 1441, 1421, 1367, 1311, 1275, 1248, 1200, 1067, 1035, 856, 832, 739.

HRMS (EI) (*m/z*) = calculated for $C_{22}H_{26}N_2O_3Si^{\cdot+}$ $[M]^{\cdot+}$ 394.1708, found 394.1711.

Purity (HPLC, method 2a) > 95% (λ = 210 nm), > 95% (λ = 254 nm).

Ethyl 3-phenyl-5-(9-((2-(trimethylsilyl)ethoxy)methyl)-9*H*-pyrido[3,4-*b*]indol-1-yl)isoxazole-4-carboxylate (73)

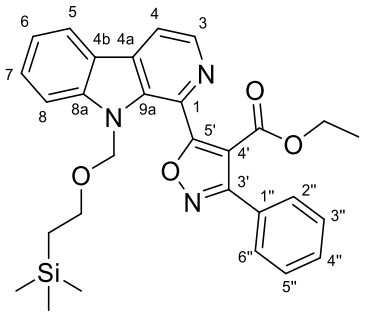

$C_{29}H_{31}N_3O_4Si$

M_r = 513.67 g/mol

Method A: Following **General Procedure IIIa**, alkyne **70** (138 mg, 0.350 mmol, 1.0 eq), (*E*)-benzaldehyde oxime (63.6 mg, 0.525 mmol, 1.5 eq) and [bis(trifluoroacetoxy)iodo]benzene (226 mg, 0.525 mmol, 1.5 eq) were used in methanol/water (3.5 mL). After stirring for additional 16 h, the reaction was completed. The crude product was purified by flash column chromatography (15% → 20% ethyl acetate in hexanes) to give isoxazole **73** as pale yellow oil (124 mg, 0.242 mmol, 69%).

Method B: Alkyne **70** (63.1 mg, 0.160 mmol, 1.0 eq) and *N*-hydroxybenzimidoyl chloride (50 mg, 0.32 mmol, 2.0 eq) were dissolved in chloroform (2.5 mL). The solution was stirred at room temperature and triethylamine (0.045 mL, 0.32 mmol, 2.0 eq, dissolved in 0.5 mL chloroform) was added dropwise over 15 min. After stirring the reaction mixture for 16 h, *N*-hydroxybenzimidoyl chloride (25 mg, 0.16 mmol, 1.0 eq) and triethylamine (0.022 mL, 0.16 mmol, 1.0 eq, dissolved in 0.25 mL chloroform) were added again. The reaction mixture was stirred for further 24 h and then partitioned between water (10 mL) and methylene chloride (10 mL). The aq. phase was further extracted with methylene chloride (2 x 10 mL) and the combined organic layers were dried over Na_2SO_4, filtered and concentrated *in vacuo*. The crude product was purified two times by flash column chromatography (20% ethyl acetate in hexanes, 65% methylene chloride in hexanes) to give isoxazole **73** as pale yellow oil (37.0 mg, 0.0720 mmol, 45%).

$\mathbf{R_f}$ = 0.23 (20% ethyl acetate in hexanes).

^{1}H NMR (400 MHz, chloroform-*d*) δ (ppm) = 8.65 (d, J = 5.1 Hz, 1H, 3-H), 8.20 (dt, J = 7.9, 1.1 Hz, 1H, 5-H), 8.15 (d, J = 5.1 Hz, 1H, 4-H), 7.85 – 7.81 (m, 2H, 2‘‘-H, 6‘‘-H), 7.66 (ddd, J = 8.3, 6.9, 1.2 Hz, 1H, 7-H), 7.60 (dt, J = 8.3, 0.9 Hz, 1H, 8-H), 7.53 – 7.48 (m, 3H, 3‘‘-H, 4‘‘-H, 5‘‘-H), 7.39 (ddd, J = 8.0, 6.9, 1.1 Hz, 1H, 6-H), 5.43 (s, 2H, NCH_2), 3.94 (q, J = 7.1 Hz, 2H, $O\underline{CH_2}CH_3$), 3.30 – 3.20 (m, 2H, $O\underline{CH_2}CH_2$), 0.79 – 0.72 (m, 2H, $SiCH_2$), 0.68 (t, J = 7.1 Hz, 3H, $OCH_2\underline{CH_3}$), -0.15 (s, 9H, $Si(CH_3)_3$).

^{13}C NMR (101 MHz, chloroform-*d*) δ (ppm) = 172.2 (C-5‘), 162.8 (C-3‘), 161.1 (CO), 142.3 (C-8a), 139.6 (C-3), 135.5 (C-9a), 131.6 (C-1), 130.5 (C-4a), 130.3 (C-4‘‘), 129.7 (C-2‘‘, C-6‘‘), 129.6 (C-7), 128.4 (C-3‘‘, C-5‘‘), 128.0 (C-1‘‘), 121.9 (C-5), 121.4 (C-6), 121.4 (C-4b), 116.4 (C-4), 112.0 (C-4‘), 110.6 (C-8), 73.4 (NCH_2), 66.0 ($O\underline{CH_2}CH_2$), 60.8 ($O\underline{CH_2}CH_3$), 17.7 ($SiCH_2$), 13.4 ($OCH_2\underline{CH_3}$), -1.4 ($Si(CH_3)_3$).

IR (ATR) $\tilde{\nu}$ (cm^{-1}) = 2952, 2896, 1726, 1622, 1554, 1444, 1418, 1248, 1213, 1138, 1100, 1071, 1024, 857, 834, 741.

HRMS (EI) (*m/z*) = calculated for $C_{29}H_{31}N_3O_4Si^{\cdot+}$ $[M]^{\cdot+}$ 513.2079, found 513.2058.

Purity (HPLC, method 2a) > 95% (λ = 210 nm), > 95% (λ = 254 nm).

Ethyl 3-phenyl-5-(9*H*-pyrido[3,4-*b*]indol-1-yl)isoxazole-4-carboxylate (74)

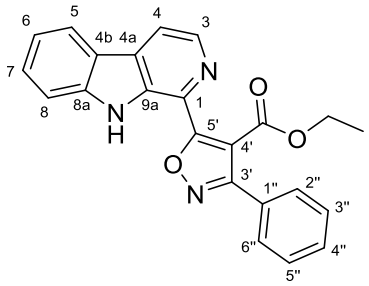

$C_{23}H_{17}N_3O_3$

M_r = 383.41 g/mol

Following **General Procedure IX**, *N*-SEM derivative **73** (121 mg, 0.235 mmol) and trifluoroacetic acid (0.9 mL) were used in methylene chloride (9.0 mL). The crude product was purified by flash column chromatography (15% ethyl acetate in hexanes) to give unprotected *β*-carboline **74** as pale yellow solid (62.0 mg, 0.162 mmol, 69%).

R_f = 0.40 (20% ethyl acetate and 1% acetic acid in hexanes).

Melting point = 194 °C.

^{1}H NMR (500 MHz, chloroform-*d*) δ (ppm) = 9.40 (s, 1H, NH), 8.53 (d, *J* = 5.0 Hz, 1H, 3-H), 8.16 (dd, *J* = 7.8, 1.0 Hz, 1H, 5-H), 8.03 (dd, *J* = 5.0, 0.7 Hz, 1H, 4-H), 7.89 – 7.80 (m, 2H, 2‘‘-H, 6‘‘-H), 7.65 – 7.59 (m, 2H, 7-H, 8-H), 7.54 – 7.48 (m, 3H, 3‘‘-H, 4‘‘-H, 5‘‘-H), 7.35 (ddd, *J* = 8.1, 6.3, 1.8 Hz, 1H, 6-H), 4.47 (q, *J* = 7.1 Hz, 2H, CH_2), 1.34 (t, *J* = 7.1 Hz, 3H, CH_3).

^{13}C NMR (126 MHz, chloroform-*d*) δ (ppm) = 168.4 (C-5‘), 163.7 (CO), 161.3 (C-3‘), 140.8 (C-8a), 139.6 (C-3), 133.5 (C-9a), 131.2 (C-1), 130.6 (C-4‘‘), 129.5 (C-7), 129.1 (C-4a), 129.0 (C-3‘‘, C-5‘‘), 128.3 (C-2‘‘, C-6‘‘), 128.0 (C-1‘‘), 122.0 (C-5), 121.2 (C-4b), 120.9 (C-6), 116.6 (C-4), 112.0 (C-8), 110.9 (C-4‘), 62.3 (CH_2), 14.1 (CH_3).

IR (ATR) $\tilde{\nu}$ (cm^{-1}) = 3355, 1722, 1618, 1430, 1368, 1322, 1286, 1272, 1230, 1186, 1140, 1120, 1061, 840, 748, 728.

HRMS (ESI) (*m/z*) = calculated for $C_{23}H_{18}N_3O_3^+$ $[M+H]^+$ 384.1343, found 384.1343.

Purity (HPLC, method 2b) > 95% (λ = 210 nm), > 95% (λ = 254 nm).

3-Phenyl-5-(9-((2-(trimethylsilyl)ethoxy)methyl)-9*H*-pyrido[3,4-*b*]indol-1-yl)isoxazole-4-carboxylic acid (77)

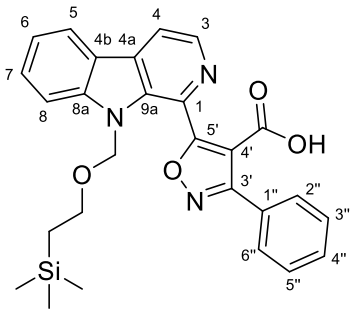

$C_{27}H_{27}N_3O_4Si$

M_r = 485.61 g/mol

Following **General Procedure VIII**, ester **73** (334 mg, 0.650 mmol, 1.0 eq) and KOH (182 mg, 3.25 mmol, 5.0 eq) were used in ethanol (15 mL). The aq. phase was extracted with methylene chloride (3 x 30 mL) and the combined organic layers were dried using a phase separation filter. The solvent was removed *in vacuo* to give pure carboxylic acid **77** as yellow solid (302 mg, 0.622 mmol, 96%).

R_f = 0.00 (20% ethyl acetate in hexanes).

Melting point = 139 °C.

^{1}H NMR (500 MHz, chloroform-*d*) δ (ppm) = 8.59 (d, *J* = 5.2 Hz, 1H, 3-H), 8.28 (d, *J* = 5.2 Hz, 1H, 4-H), 8.24 (dd, *J* = 7.9, 1.0 Hz, 1H, 5-H), 7.84 – 7.78 (m, 2H, 2‘‘-H, 6‘‘-H), 7.76 (ddd, *J* = 8.3, 6.9, 1.2 Hz, 1H, 7-H), 7.71 (dd, *J* = 8.4, 0.9 Hz, 1H, 8-H), 7.54 – 7.48 (m, 3H, 3‘‘-H, 4‘‘-H, 5‘‘-H), 7.47 (ddd, *J* = 7.9, 7.0, 1.0 Hz, 1H, 6-H), 5.95 (s, 2H, NCH_2), 3.20 – 3.11 (m, 2H, $O\underline{CH_2}CH_2$), 0.69 – 0.60 (m, 2H, $SiCH_2$), -0.20 (s, 9H, $Si(CH_3)_3$). Signal for COOH not observed.

^{13}C NMR (126 MHz, chloroform-*d*) δ (ppm) = 166.7 (COOH or C-5‘), 165.2 (C-3‘), 161.3 (COOH or C-5‘), 144.1 (C-8a), 136.8 (C-3), 135.4 (C-1), 134.6 (C-9a), 130.9 (C-7), 130.3 (C-4‘‘), 129.8 (C-2‘‘, C-6‘‘), 129.5 (C-4a), 128.3 (C-3‘‘, C-5‘‘), 127.8 (C-1‘‘), 122.3 (C-6), 122.2 (C-5), 121.0 (C-4b), 117.7 (C-4), 112.0 (C-4‘), 111.7 (C-8), 75.3 (NCH_2), 66.4 ($O\underline{CH_2}CH_2$), 17.6 ($SiCH_2$), -1.5 ($Si(CH_3)_3$).

IR (ATR) $\tilde{\nu}$ (cm^{-1}) = 2921, 1712, 1598, 1547, 1417, 1338, 1302, 1222, 1161, 1108, 1084, 1028, 919, 853, 830, 745.

HRMS (ESI) (*m/z*) = calculated for $C_{27}H_{26}N_3O_4Si^-$ $[M-H]^-$ 484.1698, found 484.1700.

Purity (HPLC, method 2d) > 95% (λ = 210 nm), > 95% (λ = 254 nm).

6-Phenyl-7,8-dihydro-4-oxa-3,5,7,8a-tetraazaazuleno[4,5,6-*jk*]fluorene (80)

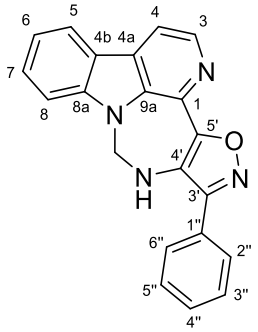

$C_{21}H_{14}N_4O$

M_r = 338.37 g/mol

Following **General Procedure Xa**, carboxylic acid **77** (97.1 mg, 0.200 mmol, 1.0 eq), triethylamine (0.028 mL, 0.20 mmol, 1.0 eq) and diphenyl phosphoryl azide (0.043 mL, 0.20 mmol, 1.0 eq) were used in *tert*-butanol (2.0 mL).

The crude *N*-Boc amine **78** (R_f = 0.64, 40% ethyl acetate and 1% triethylamine in hexanes) was suspended at 0 °C in HCl solution (4 M in 1,4-dioxan, 3.0 mL) and stirred at room temperature for 16 h, before ethanol (1.0 mL) was added and the reaction mixture stirred at 90 °C for 3 h. After cooling to room temperature, water (20 mL) was added and the pH adjusted to 9 with sat. aq. Na_2CO_3 solution. The mixture was extracted with methylene chloride (3 x 15 mL) and the combined organic layers were dried using a phase separation filter. The solvent was removed *in vacuo* and the crude product purified two times by flash column chromatography (40% ethyl acetate in hexanes, 100% methylene chloride → 0.5% methanol in methylene chloride) and subsequent recrystallization (from chloroform) to give aminal **80** as light brown solid (41.2 mg, 0.122 mmol, 61% over two steps).

R_f = 0.28 (40% ethyl acetate and 1% triethylamine in hexanes).

Melting point = 181 °C (decomposition).

^{1}H NMR (400 MHz, chloroform-*d*) δ (ppm) = 8.62 (d, *J* = 5.1 Hz, 1H, 3-H), 8.15 (dt, *J* = 7.9, 1.0 Hz, 1H, 5-H), 7.98 – 7.92 (m, 2H, 2‘‘-H, 6‘‘-H), 7.87 (d, *J* = 5.2 Hz, 1H, 4-H), 7.62 (ddd, *J* = 8.4, 7.1, 1.2 Hz, 1H, 7-H), 7.56 – 7.48 (m, 4H, 8-H, 3‘‘-H, 4‘‘-H, 5‘‘-H), 7.35 (ddd, *J* = 7.9, 7.1, 0.9 Hz, 1H, 6-H), 5.40 (d, *J* = 6.2 Hz, 2H, CH_2), 4.38 (t, *J* = 6.2 Hz, 1H, NH).

^{13}C NMR (101 MHz, chloroform-*d*) δ (ppm) = 157.7 (C-3‘), 156.8 (C-5‘), 140.8 (C-8a), 140.8 (C-3), 135.3 (C-9a), 131.8 (C-1), 130.8 (C-4a), 130.2 (C-4‘‘), 129.1 (C-7), 129.1 (C-3‘‘, C-5‘‘), 128.4 (C-1‘‘), 128.1 (C-2‘‘, C-6‘‘), 126.4 (C-4‘), 122.3 (C-5), 121.7 (C-4b), 121.1 (C-6), 114.3 (C-4), 110.0 (C-8), 58.2 (CH_2).

IR (ATR) $\tilde{\nu}$ (cm^{-1}) = 3288, 3054, 1621, 1488, 1445, 1429, 1325, 1226, 1130, 1013, 885, 776, 742, 689.

HRMS (ESI) (*m/z*) = calculated for $C_{21}H_{15}N_4O^+$ $[M+H]^+$ 339.1241, found 339.1237.

Purity (HPLC, method 2b) > 95% (λ = 210 nm), > 95% (λ = 254 nm).

Ethyl 5-(9-(*tert*-butoxycarbonyl)-9*H*-pyrido[3,4-*b*]indol-1-yl)-3-phenylisoxazole-4-carboxylate (81)

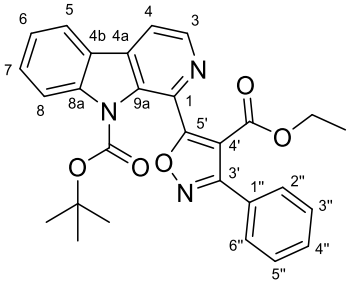

$C_{28}H_{25}N_3O_5$

M_r = 383.41 g/mol

β-Carboline **74** (46.0 mg, 0.120 mmol, 1.0 eq) was dissolved in anhydrous methylene chloride (2.3 mL) under N_2 atmosphere. 4-(Dimethylamino)pyridine (2.9 mg, 0.024 mmol, 0.2 eq) and di-*tert*-butyl dicarbonate (2 M in methylene chloride, 0.090 mL, 0.18 mmol, 1.5 eq) were added and the resulting mixture was stirred at room temperature for 18 h. The solvent was removed *in vacuo* and the crude product purified by flash column chromatography (100% methylene chloride) to give *N*-Boc derivative **81** as pale yellow semi-solid (45.7 mg, 0.0945 mmol, 79%).

R_f = 0.25 (20% ethyl acetate in hexanes).

^{1}H NMR (400 MHz, chloroform-*d*) δ (ppm) = 8.75 (d, *J* = 5.0 Hz, 1H, 3-H), 8.15 (dd, *J* = 8.5, 0.9 Hz, 1H, 8-H), 8.12 (dt, *J* = 7.7, 1.0 Hz, 1H, 5-H), 8.05 (d, *J* = 5.0 Hz, 1H, 4-H), 7.81 – 7.72 (m, 2H, 2‘‘-H, 6‘‘-H), 7.65 (ddd, *J* = 8.5, 7.3, 1.3 Hz, 1H, 7-H), 7.53 – 7.47 (m, 3H, 3‘‘-H, 4‘‘-H, 5‘‘-H), 7.47 – 7.43 (m, 1H, 6-H), 4.02 (q, *J* = 7.1 Hz, 2H, CH_2), 1.59 (s, 9H, $C(CH_3)_3$), 0.80 (t, *J* = 7.1 Hz, 3H, CH_3).

^{13}C NMR (101 MHz, chloroform-*d*) δ (ppm) = 172.5 (C-5‘), 162.3 (C-4‘), 161.7 ($\underline{C}OOCH_2$), 149.8 ($\underline{C}OOC$), 142.7 (C-3), 139.9 (C-8a), 134.6 (C-1 or C-4a), 134.3 (C-1 or C-4a), 134.1 (C-9a), 130.5 (C-7), 130.0 (C-4‘‘), 129.5 (C-2‘‘, C-6‘‘), 128.6 (C-1‘‘), 128.3 (C-3‘‘, C-5‘‘), 123.8 (C-6), 123.3 (C-4b), 121.4 (C-5), 115.8 (C-8), 115.7 (C-4), 110.3 (C-4‘), 85.6 ($\underline{C}(CH_3)_3$), 60.9 (CH_2), 28.1 ($C(\underline{C}H_3)_3$), 13.5 (CH_3).

IR (ATR) $\tilde{\nu}$ (cm^{-1}) = 2980, 1725, 1443, 1405, 1302, 1256, 1147, 1125, 1098, 1040, 1022, 837, 745, 694.

HRMS (EI) (*m/z*) = calculated for $C_{28}H_{25}N_3O_5^{\cdot+}$ $[M]^{\cdot+}$ 483.1789, found 483.1780.

Purity (HPLC, method 2c) > 95% (λ = 210 nm), > 95% (λ = 254 nm).

3-Phenyl-5-(9*H*-pyrido[3,4-*b*]indol-1-yl)isoxazole-4-carboxylic acid (66)

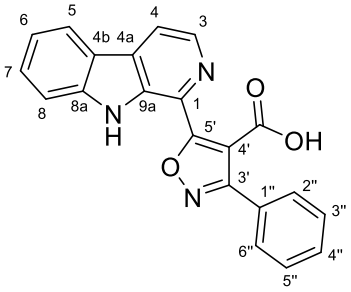

$C_{21}H_{13}N_3O_3$

M_r = 355.35 g/mol

Following **General Procedure VIII**, ester **81** (41.1 mg, 0.085 mmol, 1.0 eq) and KOH (23.8 mg, 0.425 mmol, 5.0 eq) were used in ethanol (2.0 mL). The precipitate was filtered, washed with water (10 mL) and dried to give pure carboxylic acid **66** as yellow solid (28.7 mg, 0.0810 mmol, 95%).

R_f = 0.23 (40% ethyl acetate in hexanes).

Melting point = 254 °C.

^{1}H NMR (500 MHz, DMSO-d_6) δ (ppm) = 12.31 (s, 1H, NH), 8.63 (d, *J* = 5.3 Hz, 1H, 3-H), 8.58 (d, *J* = 5.2 Hz, 1H, 4-H), 8.42 (d, *J* = 7.9 Hz, 1H, 5-H), 7.86 (d, *J* = 8.2 Hz, 1H, 8-H), 7.75 – 7.68 (m, 3H, 7-H, 2‘‘-H, 6‘‘-H), 7.60 – 7.53 (m, 3H, 3‘‘-H, 4‘‘-H, 5‘‘-H), 7.39 (t, *J* = 7.5 Hz, 1H, 6-H). Signal for COOH not observed.

^{13}C NMR (126 MHz, DMSO-d_6) δ (ppm) = 166.9 (COOH or C-5), 164.2 (C-3‘), 161.6 (COOH or C-5), 142.8 (C-8a), 136.2 (C-3), 133.1 (C-9a), 132.8 (C-4a), 130.5 (C-7 or C-4‘‘), 130.4 (C-7 or C-4‘‘), 129.7 (C-2‘‘, C-6‘‘), 128.7 (C-3‘‘, C-5‘‘), 128.6 (C-1‘‘), 127.6 (C-1), 122.8 (C-5), 121.3 (C-6), 120.4 (C-4b), 118.8 (C-4), 113.7 (C-8), 112.0 (C-4‘).

IR (ATR) $\tilde{\nu}$ (cm^{-1}) = 3204, 2920, 1709, 1692, 1553, 1499, 1442, 1326, 1303, 1232, 1083, 969, 744, 695.

HRMS (ESI) (*m/z*) = calculated for $C_{21}H_{12}N_3O_3^-$ $[M-H]^-$ 354.0884, found 354.0887.

Purity (HPLC, method 2b) > 95% (λ = 210 nm), > 95% (λ = 254 nm).

9-Benzyl-1-bromo-9*H*-pyrido[3,4-*b*]indole (83)

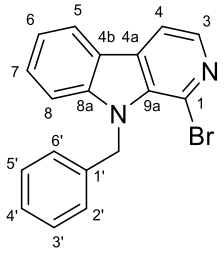

$C_{18}H_{13}BrN_2$

M_r = 337.22 g/mol

Following **General Procedure VIIb**, *β*-carboline **8** (49.4 mg, 0.200 mmol, 1.0 eq), sodium hydride (60% dispersion in mineral oil, 16 mg, 0.40 mmol, 2.0 eq) and benzyl bromide (38 mg, 0.22 mmol, 1.1 eq) were used in anhydrous DMF (4.0 mL). The extraction was performed with water (30 mL) and methylene chloride (3 x 30 mL) and the crude product was purified by flash column chromatography (15% ethyl acetate in hexanes) to give *N*-benzyl derivative **83** as yellow solid (40.1 mg, 0.119 mmol, 60%).

R_f = 0.43 (20% ethyl acetate in hexanes).

Melting point = 139 °C.

^{1}H NMR (400 MHz, chloroform-*d*) δ (ppm) = 8.24 (d, *J* = 5.1 Hz, 1H, 3-H), 8.19 – 8.13 (m, 1H, 5-H), 7.98 (d, *J* = 5.1 Hz, 1H, 4-H), 7.57 (ddd, *J* = 8.4, 7.1, 1.2 Hz, 1H, 7-H), 7.42 (d, *J* = 8.3 Hz, 1H, 8-H), 7.34 (t, *J* = 7.5 Hz, 1H, 6-H), 7.31 – 7.22 (m, 3H, 3‘-H, 4‘-H, 5‘-H), 7.11 – 7.04 (m, 2H, 2‘-H, 6‘-H), 6.08 (s, 2H, CH_2).

^{13}C NMR (101 MHz, chloroform-*d*) δ (ppm) = 142.5 (C-8a), 139.0 (C-3), 137.7 (C-1‘), 134.3 (C-9a), 131.9 (C-4a), 129.4 (C-7), 128.9 (C-3‘, C-5‘), 127.6 (C-4‘), 126.2 (C-2‘, C-6‘), 123.0 (C-1), 121.7 (C-5), 121.0 (C-6), 120.9 (C-4b), 114.6 (C-4), 110.8 (C-8), 47.5 (CH_2).

IR (ATR) $\tilde{\nu}$ (cm^{-1}) = 2923, 2852, 1621, 1532, 1448, 1431, 1351, 1296, 1183, 1054, 845, 727.

HRMS (EI) (*m/z*) = calculated for $C_{18}H_{13}BrN_2^{\cdot+}$ $[M]^{\cdot+}$ 336.0257, found 336.0257.

Purity (HPLC, method 2c) > 95% (λ = 210 nm), > 95% (λ = 254 nm).

1-Bromo-9-(4-methoxybenzyl)-9*H*-pyrido[3,4-*b*]indole (84)

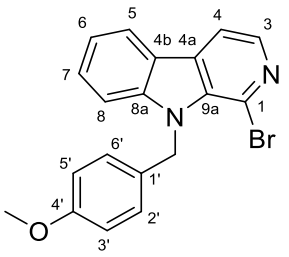

$C_{19}H_{15}BrN_2O$

M_r = 367.25 g/mol

Following **General Procedure VIIb**, *β*-carboline **8** (98.8 mg, 0.400 mmol, 1.0 eq), sodium hydride (60% dispersion in mineral oil, 32 mg, 0.80 mmol, 2.0 eq) and 4-methoxybenzyl chloride (0.060 mL, 0.44 mmol, 1.1 eq) were used in anhydrous DMF (7.5 mL). The extraction was performed with water (30 mL) and methylene chloride (3 x 30 mL) and the crude product was purified by flash column chromatography (15% ethyl acetate in hexanes) to give *N*-PMB derivative **84** as yellow solid (125 mg, 0.341 mmol, 85%).

R_f = 0.33 (20% ethyl acetate in hexanes).

Melting point = 141 °C.

^{1}H NMR (500 MHz, chloroform-*d*) δ (ppm) = 8.23 (d, *J* = 5.0 Hz, 1H, 3-H), 8.14 (dt, *J* = 8.0, 1.0 Hz, 1H, 5-H), 7.97 (d, *J* = 5.0 Hz, 1H, 4-H), 7.57 (ddd, *J* = 8.4, 7.2, 1.2 Hz, 1H, 7-H), 7.43 (dt, *J* = 8.4, 0.9 Hz, 1H, 8-H), 7.33 (ddd, *J* = 7.8, 7.0, 0.9 Hz, 1H, 6-H), 7.06 – 7.01 (m, 2H, 2‘-H, 6‘-H), 6.83 – 6.78 (m, 2H, 3‘-H, 5‘-H), 6.01 (s, 2H, NCH_2), 3.75 (s, 3H, OCH_3).

^{13}C NMR (126 MHz, chloroform-*d*) δ (ppm) = 159.1 (C-4‘), 142.5 (C-8a), 138.9 (C-3), 134.2 (C-9a), 131.9 (C-4a), 129.7 (C-1‘), 129.3 (C-7), 127.5 (C-2‘, C-6‘), 122.9 (C-1), 121.7 (C-5), 120.9 (C-6, C-4b), 114.5 (C-4), 114.3 (C-3‘, C-5‘), 110.9 (C-8), 55.4 (OCH_3), 46.9 (NCH_2).

IR (ATR) $\tilde{\nu}$ (cm^{-1}) = 2925, 2836, 1611, 1532, 1512, 1436, 1293, 1251, 1174, 1158, 1053, 1030, 846, 745, 726.

HRMS (EI) (*m/z*) = calculated for $C_{19}H_{15}{}^{79}BrN_2O^{\cdot+}$ $[M]^{\cdot+}$ 366.0363, found 366.0366.

Purity (HPLC, method 2c) > 95% (λ = 210 nm), > 95% (λ = 254 nm).

5-(9-(4-Methoxybenzyl)-9*H*-pyrido[3,4-b]indol-1-yl)-3-phenylisoxazole-4-carboxylic acid (87)

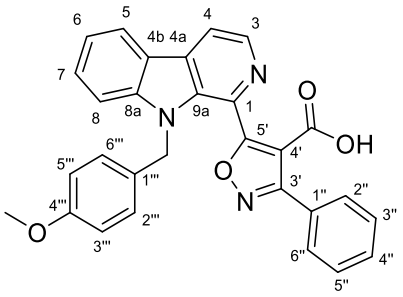

$C_{29}H_{21}N_3O_4$

M_r = 475.50 g/mol

Following **General Procedure VIIb**, *β*-carboline **74** (69.0 mg, 0.180 mmol, 1.0 eq), sodium hydride (60% dispersion in mineral oil, 14 mg, 0.36 mmol, 2.0 eq) and 4-methoxybenzyl chloride (0.046 mL, 0.34 mmol, 1.9 eq) were used in anhydrous DMF (3.0 mL). The extraction was performed with water (15 mL) and methylene chloride (3 x 15 mL). The crude product was purified by flash column chromatography (20% → 35% ethyl acetate in hexanes) to give a mixture of *N*-PMB derivatives **85** (R_f = 0.31, 40% ethyl acetate in hexanes; HRMS (ESI) (*m/z*) = calculated for $C_{31}H_{26}N_3O_4^+$ $[M+H]^+$ 504.1918, found 504.1916) and **86** (R_f = 0.31, 40% ethyl acetate in hexanes; HRMS (ESI) (*m/z*) = calculated for $C_{37}H_{30}N_3O_5^+$ $[M+H]^+$ 596.2180, found 596.2178).

Following **General Procedure VIII**, the mixture of esters **85** and **86** and KOH (51 mg, 0.90 mmol, 5.0 eq) were used in ethanol (5.0 mL). The aq. phase was extracted with methylene chloride (3 x 10 mL) and the combined organic layers were dried using a phase separation filter. The residue was redissolved in aq. NaOH solution (2 M, 10 mL), diluted with water (40 mL) and extracted with diethyl ether (3 x 15 mL). These organic phases were discarded. The pH of the aq. phase was adjusted to 1 with aq. HCl (37%) and it was extracted with methylene chloride (3 x 20 mL) again. The combined organic layers were dried using a phase separation filter and the solvent was removed *in vacuo* to give pure carboxylic acid **87** as yellow semi-solid (59.2 mg, 0.124 mmol, 69% over two steps).

R_f = 0.07 (40% ethyl acetate in hexanes).

^{1}H NMR (400 MHz, chloroform-*d*) δ (ppm) = 8.51 (d, *J* = 5.2 Hz, 1H, 3-H), 8.31 – 8.25 (m, 2H, 4-H, 5-H), 7.81 – 7.71 (m, 3H, 7-H, 2‘‘-H, 6‘‘-H), 7.68 – 7.62 (m, 1H, 8-H), 7.55 – 7.44 (m, 4H, 6-H, 3‘‘-H, 4‘‘-H, 5‘‘-H), 6.62 (s, 4H, 2‘‘‘-H, 3‘‘‘-H, 4‘‘‘-H, 5‘‘‘-H), 5.76 (s, 2H, CH_2), 3.66 (s, 3H, OCH_3). Signal for COOH not observed.

^{13}C NMR (101 MHz, chloroform-*d*) δ (ppm) = 166.3 (COOH or C-5‘), 165.2 (C-3‘), 160.9 (COOH or C-5‘), 159.5 (C-4‘‘‘), 144.6 (C-8a), 136.1 (C-3), 135.1 (C-1 or C-9a), 134.9 (C-1 or

C-9a), 131.0 (C-7), 130.3 (C-4‘‘), 129.8 (C-2‘‘, C-6‘‘), 128.9 (C-4a), 128.3 (C-3‘‘, C-5‘‘), 127.8 (C-1‘‘), 127.2 (C-2‘‘‘, C-6‘‘‘), 127.0 (C-1‘‘‘), 122.2 (C-5), 121.9 (C-6), 120.7 (C-4b), 117.6 (C-4), 114.3 (C-3‘‘‘, C-5‘‘‘), 111.7 (C-4‘), 111.4 (C-8), 55.4 (OCH_3), 49.3 (CH_2).

IR (ATR) $\tilde{\nu}$ (cm^{-1}) = 2929, 1711, 1612, 1512, 1460, 1417, 1296, 1246, 1198, 1175, 1030, 906, 727.

HRMS (ESI) (*m/z*) = calculated for $C_{29}H_{20}N_3O_4^-$ $[M-H]^-$ 474.1459, found 474.1457.

Purity (HPLC, method 2i) > 95% (λ = 210 nm), > 95% (λ = 254 nm).

tert-Butyl (5-(9-(4-methoxybenzyl)-9*H*-pyrido[3,4-*b*]indol-1-yl)-3-phenylisoxazol-4-yl)carbamate (88)

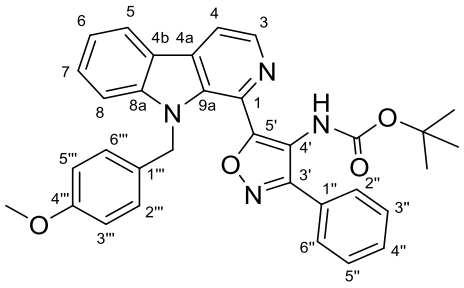

$C_{33}H_{30}N_4O_4$

M_r = 546.63 g/mol

Following **General Procedure Xa**, carboxylic acid **87** (45.2 mg, 0.0950 mmol, 1.0 eq), triethylamine (0.013 mL, 0.095 mmol, 1.0 eq) and diphenyl phosphoryl azide (0.021 mL, 0.095 mmol, 1.0 eq) were used in *tert*-butanol (1.0 mL). The crude product was purified by flash column chromatography (25% ethyl acetate in hexanes) to give *N*-Boc amine **88** as orange oil (44.4 mg, 0.0812 mmol, 86%), which solidified in the cold (2 – 8°C).

R_f = 0.51 (40% ethyl acetate in hexanes).

Melting point = 137 °C.

^{1}H NMR (400 MHz, chloroform-*d*) δ (ppm) = 8.58 (d, J = 5.0 Hz, 1H, 3-H), 8.22 (d, J = 7.8 Hz, 1H, 5-H), 8.11 (d, J = 5.0 Hz, 1H, 4-H), 7.86 – 7.80 (m, 2H, 2''-H, 6''-H), 7.64 – 7.59 (m, 1H, 7-H), 7.53 – 7.45 (m, 4H, 8-H, 3''-H, 4''-H, 5''-H), 7.37 (t, J = 7.5 Hz, 1H, 6-H), 7.09 (s, 1H, NH), 6.88 – 6.76 (m, 2H, 2'''-H, 6'''-H), 6.69 – 6.63 (m, 2H, 3'''-H, 5'''-H), 5.64 (s, 2H, NCH_2), 3.66 (s, 3H, OCH_3), 1.13 (s, 9H, $C(CH_3)_3$).

^{13}C NMR (126 MHz, chloroform-*d*) δ (ppm) = 159.6 (C-3'), 159.0 (C-4'''), 158.9 (C-5' or COO), 153.1 (C-5' or COO), 143.1 (C-8a), 138.8 (C-3), 135.1 (C-9a), 132.2 (C-4a), 130.3 (C-1''), 129.8 (C-4''), 129.5 (C-1, C-7), 128.8 (C-1'''), 128.8 (C-3'', C-5''), 127.6 (C-2'', C-6''), 127.4 (C-2''', C-6'''), 121.7 (C-5), 121.3 (C-4b), 120.8 (C-6), 117.4 (C-4'), 115.8 (C-4), 114.2 (C-3''', C-5'''), 111.0 (C-8), 81.0 ($\underline{C}(CH_3)_3$), 55.2 (OCH_3), 48.0 (NCH_2), 27.9 ($C(\underline{CH_3})_3$).

IR (ATR) $\tilde{\nu}$ (cm^{-1}) = 2932, 1713, 1614, 1513, 1444, 1413, 1366, 1273, 1246, 1198, 1156, 1034, 741, 693.

HRMS (ESI) (m/z) = calculated for $C_{33}H_{31}N_4O_4^+$ $[M+H]^+$ 547.2340, found 547.2339.

Purity (HPLC, method 2c) > 95% (λ = 210 nm), > 95% (λ = 254 nm).

3-Phenyl-5-(9-((2-(trimethylsilyl)ethoxy)methyl)-9*H*-pyrido[3,4-*b*]indol-1-yl)isoxazol-4-amine (79)

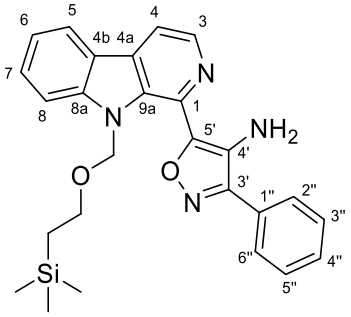

$C_{26}H_{28}N_4O_2Si$

M_r = 456.62 g/mol

Following **General Procedure Xb**, carboxylic acid **77** (257 mg, 0.530 mmol, 1.0 eq), triethylamine (0.17 mL, 1.2 mmol, 2.3 eq) and diphenyl phosphoryl azide (0.13 mL, 0.61 mmol, 1.15 eq) were used in THF (3.0 mL). The reaction mixture was diluted with water (15 mL) and extracted with ethyl acetate (3 x 30 mL). The combined organic layers were washed with sat. aq. $NaHCO_3$ (30 mL) and sat. aq. NaCl solution (30 mL) and dried using a phase separation filter. The solvent was evaporated *in vacuo* and the crude product purified by flash column chromatography (20% ethyl acetate in hexanes) to give amine **79** as yellow oil (164 mg, 0.360 mmol, 68%), which solidified in the cold (2 – 8°C).

R_f = 0.66 (40% ethyl acetate in hexanes).

Melting point = 83 °C.

^{1}H NMR (400 MHz, chloroform-*d*) δ (ppm) = 8.57 (dd, *J* = 5.0, 0.7 Hz, 1H, 3-H), 8.16 (dq, *J* = 7.8, 0.9 Hz, 1H, 5-H), 7.98 (dd, *J* = 5.0, 0.7 Hz, 1H, 4-H), 7.93 – 7.85 (m, 2H, 2‘‘-H, 6‘‘-H), 7.73 – 7.67 (m, 1H, 8-H), 7.64 (ddd, *J* = 8.6, 6.7, 1.2 Hz, 1H, 7-H), 7.59 – 7.49 (m, 3H, 3‘‘-H, 4‘‘-H, 5‘‘-H), 7.40 – 7.33 (m, 1H, 6-H), 6.05 (s, 2H, NCH_2), 4.53 (s, 2H, NH_2), 3.35 – 3.21 (m, 2H, $O\underline{CH_2}CH_2$), 0.72 (m, 2H, $SiCH_2$), -0.20 (d, *J* = 0.7 Hz, 9H, $Si(CH_3)_3$).

^{13}C NMR (101 MHz, chloroform-*d*) δ (ppm) = 156.5 (C-3’), 149.9 (C-5’), 143.1 (C-8a), 139.1 (C-3), 133.9 (C-9a), 133.7 (C-1), 132.7 (C-4a), 129.9 (C-4‘’), 129.3 (C-3‘’, C-5‘’), 129.2 (C-7), 129.0 (C-1‘’), 127.8 (C-2‘’, C-6‘’), 126.5 (C-4’), 122.0 (C-4b), 121.4 (C-5), 121.3 (C-6), 114.3 (C-4), 111.9 (C-8), 74.5 (NCH_2), 65.8 ($O\underline{CH_2}CH_2$), 17.8 ($SiCH_2$), -1.5 ($Si(CH_3)_3$).

IR (ATR) $\tilde{\nu}$ (cm^{-1}) = 3406, 3330, 2952, 1631, 1552, 1444, 1400, 1368, 1248, 1196, 1074, 1055, 855, 829, 748.

HRMS (ESI) (*m/z*) = calculated for $C_{26}H_{29}N_4O_2Si^+$ $[M+H]^+$ 457.2055, found 457.2052.

Purity (HPLC, method 2c) > 95% (λ = 210 nm), > 95% (λ = 254 nm).

2,2,2-Trifluoro-*N*-(3-phenyl-5-(9-((2-(trimethylsilyl)ethoxy)methyl)-9*H*-pyrido[3,4-*b*]indol-1-yl)isoxazol-4-yl)acetamide (93)

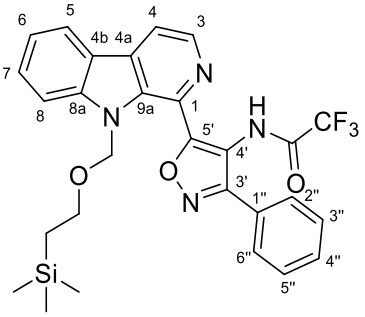

$C_{28}H_{27}F_3N_4O_3Si$

M_r = 552.63 g/mol

Amine **79** (155 mg, 0.340 mmol, 1.0 eq) and 4-(dimethylamino)pyridine (62 mg, 0.51 mmol, 1.5 eq) were dissolved in anhydrous pyridine (1.7 mL) under N_2 atmosphere. Trifluoroacetic Anhydride (0.071 mL, 0.51 mmol, 1.5 eq) was slowly added and the reaction mixture stirred at room temperature for 16 h, diluted with ethyl acetate (50 mL) and washed with sat. aq. $NaHCO_3$ solution (25 mL), water (2 x 25 mL) and sat. aq. NaCl solution (15 mL). The organic layer was dried using a phase separation filter and the solvent removed *in vacuo.* The crude product was purified by flash column chromatography (20% ethyl acetate in hexanes) to give amide **93** as yellow solid (157 mg, 0.285 mmol, 84%).

R_f = 0.21 (20% ethyl acetate in hexanes).

Melting point = 162 °C.

^{1}H NMR (500 MHz, chloroform-*d*) δ (ppm) = 10.45 (s, 1H, CONH), 8.47 (d, *J* = 5.0 Hz, 1H, 3-H), 8.18 (dt, *J* = 7.8, 0.9 Hz, 1H, 5-H), 8.07 (d, *J* = 5.0 Hz, 1H, 4-H), 7.73 – 7.70 (m, 2H, 2‘‘-H, 6‘‘-H), 7.70 – 7.67 (m, 2H, 7-H, 8-H), 7.47 – 7.43 (m, 3H, 3’’-H, 4’’-H, 5’’-H), 7.40 (ddd, *J* = 7.9, 5.0, 3.0 Hz, 1H, 6-H), 5.84 (s, 2H, NCH_2), 3.39 – 3.30 (m, 2H, $O\underline{CH_2}CH_2$), 0.80 – 0.70 (m, 2H, $SiCH_2$), -0.17 (s, 9H $Si(CH_3)_3$).

^{13}C NMR (126 MHz, chloroform-*d*) δ (ppm) = 160.7 (C-3’), 159.2 (C-5’), 155.4 (q, J_{CF} = 38.0 Hz, CONH), 143.1 (C-8a), 138.9 (C-3), 134.5 (C-9a), 133.3 (C-4a), 130.3 (C-7), 130.0 (C-1), 129.9 (C-4’’), 128.9 (C-3’’, C-5’’), 128.2 (C-1’’), 127.5 (C-2’’, C-6’’), 121.7 (C-5), 121.7 (C-6), 121.4 (C-4b), 116.3 (C-4), 115.9 (q, J_{CF} = 288.1 Hz, CF_3), 114.1 (C-4‘), 111.5 (C-8), 74.5 (NCH_2), 66.1 ($O\underline{CH_2}CH_2$), 17.8 ($SiCH_2$), -1.5 ($Si(CH_3)_3$).

IR (ATR) $\tilde{\nu}$ (cm^{-1}) = 2954, 1737, 1622, 1447, 1410, 1212, 1179, 1148, 1074, 833, 740, 693.

HRMS (ESI) (*m/z*) = calculated for $C_{28}H_{27}F_3N_4O_3Si^+$ $[M+H]^+$ 553.1877, found 553.1875.

Purity (HPLC, method 2g) > 95% (λ = 210 nm), > 95% (λ = 254 nm).

2,2,2-Trifluoro-*N*-(3-phenyl-5-(9*H*-pyrido[3,4-*b*]indol-1-yl)isoxazol-4-yl)acetamide (91)

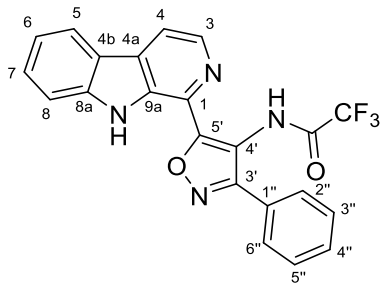

$C_{22}H_{13}F_3N_4O_2$

M_r = 422.37 g/mol

Following **General Procedure IX**, *N*-SEM derivative **93** (138 mg, 0.250 mmol) and trifluoroacetic acid (1.0 mL) were used in methylene chloride (10 mL). The crude product was purified two times by flash column chromatography (35% methylene chloride in hexanes, 100% methylene chloride) to give unprotected *β*-carboline **91** as pale yellow solid (70.0 mg, 0.166 mmol, 66%).

R_f = 0.45 (100% methylene chloride).

Melting point = 179 °C.

^{1}H NMR (500 MHz, chloroform-*d*) δ (ppm) = 10.81 (s, 1H, CONH), 9.44 (s, 1H, 9-NH), 8.54 (d, *J* = 5.1 Hz, 1H, 3-H), 8.18 (d, *J* = 7.9 Hz, 1H, 5-H), 8.05 (d, *J* = 5.1 Hz, 1H, 4-H), 7.71 – 7.66 (m, 2H, 2''-H, 6''-H), 7.65 (dd, *J* = 6.6, 1.2 Hz, 1H, 7-H), 7.62 (dt, *J* = 8.1, 1.3 Hz, 1H, 8-H), 7.53 – 7.45 (m, 3H, 3''-H, 4''-H, 5''-H), 7.38 (ddd, *J* = 8.0, 6.6, 1.5 Hz, 1H, 6-H).

^{13}C NMR (126 MHz, chloroform-*d*) δ (ppm) = 158.8 (C-3‘), 157.9 (C-5‘), 155.3 (q, J_{CF} = 38.3 Hz, CONH), 140.9 (C-8a), 138.8 (C-3), 132.6 (C-9a), 131.4 (C-1 or C-4a), 130.4 (C-1 or C-4a), 130.3 (C-4‘‘), 129.9 (C-7), 128.8 (C-1‘‘), 128.8 (C-3‘‘, C-5‘‘), 127.5 (C-2‘‘, C-6‘‘), 122.1 (C-5), 121.2 (C-6), 121.0 (C-4b), 116.2 (C-4), 115.9 (q, J_{CF} = 288.2 Hz, CF_3), 115.0 (C-4’), 112.2 (C-8).

IR (ATR) $\tilde{\nu}$ (cm^{-1}) = 3386, 3269, 1720, 1453, 1245, 1232, 1187, 1168, 1160, 911, 740, 720, 698.

HRMS (ESI) (*m/z*) = calculated for $C_{22}H_{14}F_3N_4O_2^+$ $[M+H]^+$ 423.1064, found 423.1061.

Purity (HPLC, method 2b) > 93% (λ = 210 nm), > 93% (λ = 254 nm).

3-Phenyl-5-(9*H*-pyrido[3,4-*b*]indol-1-yl)isoxazol-4-amine (63)

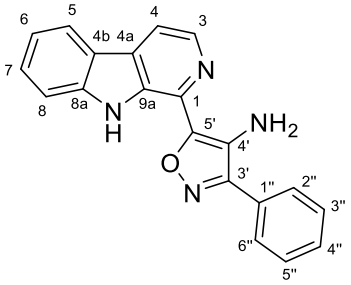

$C_{20}H_{14}N_4O$

M_r = 326.36 g/mol

Trifluoroacetamide **91** (50.7 mg, 0.120 mmol) was dissolved in methanol (7.0 mL) and HCl solution (1.25 M in methanol, 3.0 mL) was slowly added. The reaction mixture was stirred at room temperature for 16 h. The solvent was evaporated *in vacuo* and the residue resuspended in water (15 mL). After adjusting pH 8 with sat. aq. $NaHCO_3$ solution, it was extracted with methylene chloride (3 x 10 mL) and the combined organic layers were dried using a phase separation filter. The solvent was removed *in vacuo* and the crude product purified by flash column chromatography (100% chloroform) to give amine **63** as yellow solid (26.9 mg, 0.0824 mmol, 69%).

R_f = 0.41 (20% ethyl acetate and 1% triethylamine in hexanes).

Melting point = 161 °C.

^{1}H NMR (500 MHz, chloroform-*d*) δ (ppm) = 9.50 (s, 1H, NH), 8.50 (d, *J* = 5.2 Hz, 1H, 3-H), 8.16 (dt, *J* = 7.8, 0.9 Hz, 1H, 5-H), 7.93 – 7.86 (m, 3H, 4-H, 2‘‘-H, 6‘‘-H), 7.62 – 7.59 (m, 2H, 7-H, 8-H), 7.59 – 7.51 (m, 3H, 3‘‘-H, 4‘‘-H, 5‘‘-H), 7.33 (ddd, *J* = 8.0, 5.3, 2.8 Hz, 1H, 6-H), 4.94 (s, 2H, NH_2).

^{13}C NMR (126 MHz, chloroform-*d*) δ (ppm) = 156.1 (C-3‘), 149.7 (C-5‘), 140.6 (C-8a), 138.7 (C-3), 133.8 (C-1), 131.5 (C-9a), 130.1 (C-4‘‘), 129.9 (C-4a), 129.4 (C-3‘‘, C-5‘‘), 128.9 (C-7), 128.7 (C-1‘‘), 127.8 (C-2‘‘, C-6‘‘), 126.6 (C-4‘), 121.8 (C-5), 121.3 (C-4b), 120.5 (C-6), 113.6 (C-4), 112.0 (C-8).

IR (ATR) $\tilde{\nu}$ (cm^{-1}) = 3364, 3285, 1635, 1559, 1492, 1453, 1422, 1378, 1325, 1236, 1198, 1075, 946, 816, 773, 739, 698.

HRMS (EI) (*m/z*) = calculated for $C_{20}H_{15}N_4O^{\cdot+}$ $[M]^{\cdot+}$ 326.1162, found 326.1157.

Purity (HPLC, method 2b) > 95% (λ = 210 nm), > 95% (λ = 254 nm).

5.3.3 Variations of the *β*-carboline

5-(9-Methyl-9*H*-pyrido[3,4-*b*]indol-1-yl)-3-phenylisoxazole (94)

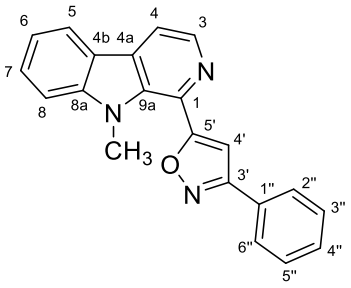

$C_{21}H_{15}N_3O$

M_r = 325.37 g/mol

Following **General Procedure VIIc**, *β*-carboline **1** (74.1 mg, 0.238 mmol, 1.0 eq), sodium hydride (60% dispersion in mineral oil, 19 mg, 0.48 mmol, 2.0 eq) and iodomethane (0.02 mL, 0.3 mmol, 1.2 eq) were used in anhydrous DMF (5.0 mL). The crude product was purified two times by flash column chromatography (20% ethyl acetate in hexanes, 100% methylene chloride) to give *N*-methyl derivative **94** as pale yellow solid (45.3 mg, 0.139 mmol, 59%).

R_f = 0.47 (2% methanol in methylene chloride).

Melting point = 157 °C.

^{1}H NMR (400 MHz, methylene chloride-d_2) δ (ppm) = 8.55 (d, *J* = 5.1 Hz, 1H, 3-H), 8.22 (dt, *J* = 7.8, 1.0 Hz, 1H, 5-H), 8.12 (d, *J* = 5.0 Hz, 1H, 4-H), 8.00 – 7.94 (m, 2H, 2‘‘-H, 6‘‘-H), 7.68 (ddd, *J* = 8.4, 7.1, 1.2 Hz, 1H, 7-H), 7.58 – 7.47 (m, 4H, 8-H, 3‘‘-H, 4‘‘-H, 5‘‘-H), 7.36 (ddd, *J* = 8.0, 7.1, 0.9 Hz, 1H, 6-H), 7.15 (s, 1H, 4‘-H), 3.79 (s, 3H, CH_3).

^{13}C NMR (101 MHz, methylene chloride-d_2) δ (ppm) = 170.3 (C-5‘), 163.3 (C-3‘), 143.4 (C-8a), 138.9 (C-3), 136.1 (C-9a), 131.4 (C-1), 130.6 (C-4a), 130.6 (C-4‘‘), 129.5 (C-7), 129.4 (C-3‘‘, C-5‘‘), 129.4 (C-1‘‘), 127.3 (C-2‘‘, C-6‘‘), 121.9 (C-5), 121.1 (C-4b), 120.7 (C-6), 116.3 (C-4), 110.4 (C-8), 103.4 (C-4‘), 32.6 (CH_3).

IR (ATR) $\tilde{\nu}$ (cm^{-1}) = 3035, 1609, 1547, 1463, 1450, 1440, 1410, 1396, 1293, 1229, 1125, 906, 802, 734.

HRMS (EI) (*m/z*) = calculated for $C_{21}H_{15}N_3O^{\cdot+}$ $[M]^{\cdot+}$ 325.1210, found 325.1210.

Purity (HPLC, method 1b) > 95% (λ = 210 nm), > 95% (λ = 254 nm).

3-Phenyl-5-(9-(prop-2-yn-1-yl)-9*H*-pyrido[3,4-*b*]indol-1-yl)isoxazole (95)

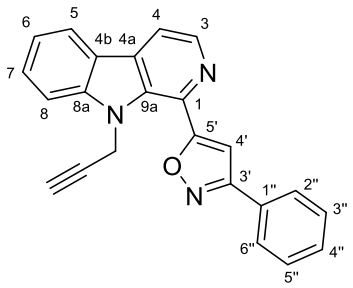

$C_{23}H_{15}N_3O$

M_r = 349.39 g/mol

Following **General Procedure VIIc**, *β*-carboline **1** (77.8 mg, 0.250 mmol, 1.0 eq), sodium hydride (60% dispersion in mineral oil, 11 mg, 0.28 mmol, 1.1 eq) and propargyl bromide (80% in toluene, 0.040 mL, 0.35 mmol, 1.4 eq) were used in anhydrous DMF (5.0 mL). The crude product was purified by flash column chromatography (20% → 25% ethyl acetate in hexanes) to give *N*-propargyl derivative **95** as pale rose solid (65.8 mg, 0.188 mmol, 75%).

R_f = 0.16 (20% ethyl acetate in hexanes).

Melting point = 152 °C.

^{1}H NMR (500 MHz, chloroform-*d*) δ (ppm) = 8.62 (d, *J* = 5.0 Hz, 1H, 3-H), 8.20 (dt, *J* = 7.8, 1.0 Hz, 1H, 5-H), 8.10 (d, *J* = 5.0 Hz, 1H, 4-H), 7.99 – 7.94 (m, 2H, 2‘‘-H, 6‘‘-H), 7.70 (ddd, *J* = 8.2, 7.1, 1.2 Hz, 1H, 7-H), 7.63 (d, *J* = 8.3 Hz, 1H, 8-H), 7.55 – 7.47 (m, 3H, 3‘‘-H, 4‘‘-H, 5‘‘-H), 7.40 (ddd, *J* = 7.9, 7.1, 0.9 Hz, 1H, 6-H), 7.25 (s, 1H, 4’-H), 5.10 (d, *J* = 2.5 Hz, 2H, CH_2), 2.20 (t, *J* = 2.5 Hz, 1H, CCH).

^{13}C NMR (126 MHz, chloroform-*d*) δ (ppm) = 169.5 (C-5‘), 163.1 (C-3‘), 142.2 (C-8a), 139.5 (C-3), 134.6 (C-9a), 132.3 (C-4a), 130.5 (C-1), 130.2 (C-4‘‘), 129.5 (C-7), 129.1 (C-3‘‘, C-5‘‘), 128.9 (C-1‘‘), 127.0 (C-2‘‘, C-6‘‘), 121.7 (C-5), 121.5 (C-4b), 121.2 (C-6), 116.1 (C-4), 110.5 (C-8), 103.1 (C-4‘), 77.7 (C$\underline{C}$CH), 73.0 (C$\underline{C}$H), 35.0 (CH_2).

IR (ATR) $\tilde{\nu}$ (cm^{-1}) = 3252, 2116, 1614, 1554, 1439, 1422, 1397, 1300, 1201, 1051, 819, 772, 735, 694.

HRMS (EI) (*m/z*) = calculated for $C_{23}H_{15}N_3O^{\cdot+}$ $[M]^{\cdot+}$ 349.1210, found 349.1208.

Purity (HPLC, method 2b) > 95% (λ = 210 nm), > 95% (λ = 254 nm).

2-(1-(3-Phenylisoxazol-5-yl)-9*H*-pyrido[3,4-*b*]indol-9-yl)acetonitrile (96)

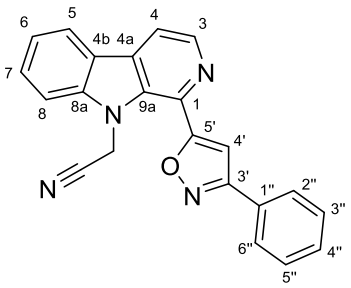

$C_{22}H_{14}N_4O$

M_r = 350.38 g/mol

Similar to **General Procedure VIIc**, *β*-carboline **1** (78.0 mg, 0.250 mmol, 1.0 eq), sodium hydride (60% dispersion in mineral oil, 20 mg, 0.50 mmol, 2.0 eq) and bromoacetonitrile (0.025 mL, 0.36 mmol, 1.4 eq) were used in anhydrous DMF (5.0 mL). In contrast to the general procedure, another amount of bromoacetonitrile (0.025 mL, 0.36 mmol, 1.4 eq) was added after 16 h and the mixture stirred for further 72 h at room temperature and 4 h at 40 °C. Then the work-up was performed and the crude product was purified two times by flash column chromatography (15% → 20% ethyl acetate in hexanes, 100% methylene chloride) to give *N*-cyanomethyl derivative **96** as white solid (28.4 mg, 0.0811 mmol, 32%).

R_f = 0.10 (20% ethyl acetate in hexanes).

Melting point = 198 °C.

^{1}H NMR (400 MHz, methylene chloride-d_2) δ (ppm) = 8.65 (d, *J* = 5.0 Hz, 1H, 3-H), 8.25 (dt, *J* = 7.8, 1.0 Hz, 1H, 5-H), 8.14 (d, *J* = 5.0 Hz, 1H, 4-H), 8.02 – 7.96 (m, 2H, 2‘‘-H, 6‘‘-H), 7.77 (ddd, *J* = 8.4, 7.2, 1.2 Hz, 1H, 7-H), 7.61 (dt, *J* = 8.3, 0.8 Hz, 1H, 8-H), 7.59 – 7.51 (m, 3H, 3‘‘-H, 4‘‘-H, 5‘‘-H), 7.48 (ddd, *J* = 8.0, 7.2, 0.9 Hz, 1H, 6-H), 7.33 (s, 1H, 4‘-H), 5.26 (s, 2H, CH_2).

^{13}C NMR (101 MHz, methylene chloride-d_2) δ (ppm) = 169.5 (C-5‘), 163.8 (C-3‘), 142.2 (C-8a), 141.0 (C-3), 134.7 (C-9a), 133.1 (C-4a), 130.9 (C-1), 130.8 (C-7), 130.4 (C-4‘‘), 129.5 (C-3‘‘, C-5‘‘), 129.0 (C-1‘‘), 127.4 (C-2‘‘, C-6‘‘), 122.5 (C-6), 122.4 (C-5), 122.2 (C-4b), 116.6 (C-4), 115.0 (CN), 110.4 (C-8), 103.9 (C-4‘), 34.4 (CH_2).

IR (ATR) $\tilde{\nu}$ (cm^{-1}) = 3052, 2164, 1977, 1611, 1554, 1442, 1433, 1416, 1202, 1128, 910, 896, 858, 739.

HRMS (EI) (*m/z*) = calculated for $C_{22}H_{14}N_4O^{\cdot+}$ $[M]^{\cdot+}$ 350.1163, found 350.1161.

Purity (HPLC, method 1b) > 95% (λ = 210 nm), > 95% (λ = 254 nm).

Methyl 1-(3-phenylisoxazol-5-yl)-9*H*-pyrido[3,4-*b*]indole-3-carboxylate (97)

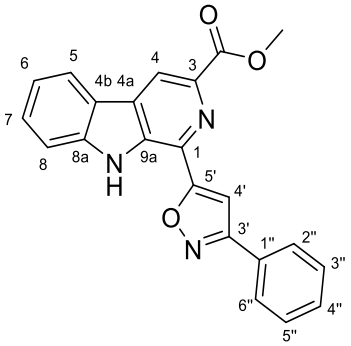

$C_{22}H_{15}N_3O_3$

M_r = 369.38 g/mol

3-Phenylisoxazole-5-carbaldehyde (**53**) (520 mg, 3.00 mmol, 1.0 eq) and L-tryptophan methyl ester hydrochloride (764 mg, 3.00 mmol, 1.0 eq) were suspended in THF (10 mL). The reaction mixture was stirred at 75 °C for 3.5 h and, after cooling to room temperature, $KMnO_4$ (1.19 g, 7.50 mmol, 2.5 eq) was added. The suspension was stirred at room temperature for 3 d and filtered through a pad of celite. The pad was washed with methylene chloride (200 mL) and the filtrate concentrated *in vacuo*. The crude product was resuspended in methanol (50 mL), the precipitate was filtered, washed with methanol (50 mL) and dried to give *β*-carboline **97** as pale yellow solid (650 mg, 1.76 mmol, 59%).

R_f = 0.31 (25% ethyl acetate in hexanes).

Melting point = 246 °C.

^{1}H NMR (400 MHz, chloroform-*d*) δ (ppm) = 9.80 (s, 1H, NH), 8.93 (d, *J* = 0.7 Hz, 1H, 4-H), 8.22 (dd, *J* = 7.9, 1.0 Hz, 1H, 5-H), 7.98 – 7.90 (m, 2H, 2''-H, 6''-H), 7.69 – 7.63 (m, 2H, 7-H, 8-H), 7.58 (s, 1H, 4'-H), 7.55 – 7.48 (m, 3H, 3''-H, 4''-H, 5''-H), 7.41 (ddd, *J* = 8.0, 5.6, 2.5 Hz, 1H, 6-H), 4.10 (s, 3H, OCH_3).

^{13}C NMR (101 MHz, chloroform-*d*) δ (ppm) = 169.9 (C-5'), 166.2 (CO), 163.3 (C-3'), 141.1 (C-8a), 138.1 (C-3), 134.3 (C-9a), 131.5 (C-1 or C-4a), 130.6 (C-4''), 130.0 (C-7), 129.7 (C-4a or C-1''), 129.2 (C-3'', C-5''), 128.6 (C-1 or C-1''), 127.2 (C-2'', C-6''), 122.2 (C-5), 121.7 (C-6), 121.4 (C-4b), 118.8 (C-4), 112.4 (C-8), 101.4 (C-4'), 53.0 (OCH_3).

IR (ATR) $\tilde{\nu}$ (cm^{-1}) = 3463, 3166, 1613, 1553, 1433, 1421, 1288, 1260, 1229, 949, 840, 806, 740.

HRMS (ESI) (*m/z*) = calculated for $C_{22}H_{16}N_3O_3^+$ $[M+H]^+$ 370.1187, found 370.1188.

Purity (HPLC, method 2a) > 95% (λ = 210 nm), > 95% (λ = 254 nm).

1-(3-Phenylisoxazol-5-yl)-9*H*-pyrido[3,4-*b*]indole-3-carboxylic acid (98)

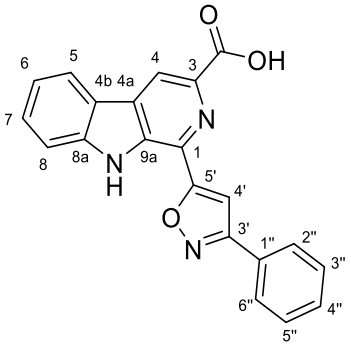

$C_{21}H_{13}N_3O_3$

M_r = 355.35 g/mol

Ester **97** (443 mg, 1.20 mmol, 1.0 eq) was suspended in THF (7.0 mL) and a solution of KOH (337 mg, 6.00 mmol, 5.0 eq) in water (7.0 mL) was added. The reaction mixture was stirred at 80 °C for 2 h. After cooling to room temperature, the solvent was evaporated *in vacuo*. The residue was resuspended in water (10 mL) and acidified with aq. HCl (2 M, 3.0 mL). The precipitate was filtered, washed with water (50 mL) and dried to give carboxylic acid **98** as pale yellow solid (411 mg, 1.16 mmol, 97%).

R_f = 0.08 (40% ethyl acetate in hexanes).

Melting point = 285 °C.

^{1}H NMR (400 MHz, DMSO-d_6) δ (ppm) = 12.92 (s, 1H, COOH), 12.26 (s, 1H, NH), 9.07 (s, 1H, 4-H), 8.49 (d, *J* = 7.9 Hz, 1H, 5-H), 8.12 – 8.04 (m, 2H, 2''-H, 6''-H), 7.97 (s, 1H, 4'-H), 7.87 (d, *J* = 8.2 Hz, 1H, 8-H), 7.68 (ddd, *J* = 8.3, 7.1, 1.2 Hz, 1H, 7-H), 7.64 – 7.56 (m, 3H, 3''-H, 4''-H, 5''-H), 7.43 – 7.35 (m, 1H, 6-H).

^{13}C NMR (101 MHz, DMSO-d_6) δ (ppm) = 168.9 (C-5'), 166.2 (COOH), 162.5 (C-3'), 142.0 (C-8a), 137.3 (C-3), 133.4 (C-9a), 131.0 (C-4a), 130.6 (C-4''), 129.5 (C-7), 129.3 (C-3'', C-5''), 128.7 (C-1 or C-1''), 128.3 (C-1 or C-1''), 126.8 (C-2'', C-6''), 122.3 (C-5), 120.9 (C-6), 120.7 (C-4b), 118.3 (C-4), 113.3 (C-8), 101.6 (C-4').

IR (ATR) $\tilde{\nu}$ (cm^{-1}) = 3215, 2924, 1759, 1614, 1555, 1381, 1351, 1325, 901, 766, 743, 690.

HRMS (ESI) (*m/z*) = calculated for $C_{21}H_{12}N_3O_3^-$ $[M-H]^-$ 354.0884, found 354.0887.

Purity (HPLC, method 2f) > 95% (λ = 210 nm), > 95% (λ = 254 nm).

1-(3-Phenylisoxazol-5-yl)-9*H*-pyrido[3,4-*b*]indol-3-amine (99)

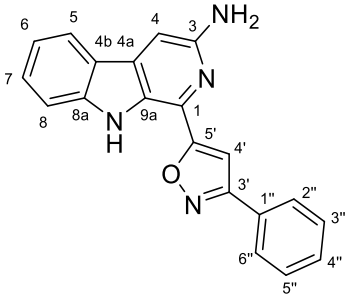

$C_{20}H_{14}N_4O$

M_r = 326.36 g/mol

Following **General Procedure Xb**, carboxylic acid **98** (107 mg, 0.300 mmol, 1.0 eq), triethylamine (0.096 mL, 0.69 mmol, 2.3 eq) and diphenyl phosphoryl azide (0.074 mL, 0.35 mmol, 1.15 eq) were used in THF (2.0 mL). The reaction mixture was partitioned between ethyl acetate (50 mL) and aq. HCl (1 M, 50 mL). Aq. NaOH solution (2 M, 60 mL) was added and the phases were separated. The aq. phase was further extracted with ethyl acetate (3 x 50 mL), the combined organic layers were dried using a phase separation filter and the solvent was evaporated *in vacuo*. The crude product was purified by flash column chromatography (40% ethyl acetate in hexanes) to give amine **99** as yellow solid (45.0 mg, 0.138 mmol, 46%).

R_f = 0.32 (40% ethyl acetate in hexanes).

Melting point = 179 °C.

^{1}H NMR (400 MHz, DMSO-d_6) δ (ppm) = 11.10 (s, 1H, NH), 8.09 (d, *J* = 7.8 Hz, 1H, 5-H), 8.06 – 7.98 (m, 2H, 2''-H, 6''-H), 7.63 (d, *J* = 8.2 Hz, 1H, 8-H), 7.62 – 7.55 (m, 3H, 3''-H, 4''-H, 5''-H), 7.55 – 7.47 (m, 2H, 7-H, 4'-H), 7.32 (s, 1H, 4-H), 7.16 (t, *J* = 7.5 Hz, 1H, 6-H), 5.68 (s, 2H, NH_2).

^{13}C NMR (101 MHz, DMSO-d_6) δ (ppm) = 169.8 (C-5'), 162.2 (C-3'), 152.6 (C-3), 142.9 (C-8a), 134.2 (C-4a), 130.4 (C-4''), 129.2 (C-3'', C-5''), 128.8 (C-7), 128.6 (C-1''), 127.3 (C-9a), 126.8 (C-2'', C-6''), 125.4 (C-1), 121.7 (C-5), 120.1 (C-4b), 119.0 (C-6), 112.3 (C-8), 100.2 (C-4), 99.7 (C-4').

IR (ATR) $\tilde{\nu}$ (cm^{-1}) = 3397, 3327, 1615, 1561, 1466, 1444, 1397, 1323, 1233, 801, 765, 737.

HRMS (ESI) (*m/z*) = calculated for $C_{20}H_{15}N_4O^+$ $[M+H]^+$ 327.1241, found 327.1241.

Purity (HPLC, method 2a) > 95% (λ = 210 nm), > 95% (λ = 254 nm).

1-(3-Phenylisoxazol-5-yl)-9*H*-pyrido[3,4-*b*]indole-3-carboxamide (100)

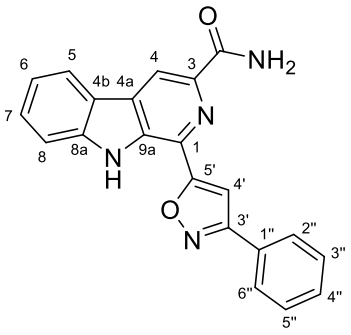

$C_{21}H_{14}N_4O_2$

M_r = 354.37 g/mol

Ester **97** (49.9 mg, 0.135 mmol) was suspended in ammonia solution (7 M in methanol, 2.0 mL) in a pressure tube and the suspension was stirred at 80 °C for 16 h. After cooling to room temperature, the precipitate was filtered, washed with methanol (5.0 mL) and methylene chloride (5.0 mL) and dried to give amide **100** as off-white solid (38.1 mg, 0.108 mmol, 80%).

R_f = 0.20 (40% ethyl acetate in hexanes).

Melting point = 346 °C (decomposition).

^{1}H NMR (400 MHz, DMSO-d_6) δ (ppm) = 12.20 (s, 1H, NH), 8.99 (s, 1H, 4-H), 8.47 (dt, *J* = 7.9, 1.0 Hz, 1H, 5-H), 8.44 (d, *J* = 3.0 Hz, 1H, $CONH_2$), 8.30 (s, 1H, 4'-H), 8.08 – 8.01 (m, 2H, 2''-H, 6''-H), 7.91 – 7.85 (m, 1H, 8-H), 7.74 (d, *J* = 3.0 Hz, 1H, $CONH_2$), 7.70 – 7.59 (m, 4H, 7-H, 3''-H, 4''-H, 5''-H), 7.37 (ddd, *J* = 8.0, 7.1, 1.0 Hz, 1H, 6-H).

^{13}C NMR (101 MHz, DMSO-d_6) δ (ppm) = 170.0 (C-5'), 166.8 (CO), 162.9 (C-3'), 142.6 (C-8a), 140.4 (C-3), 133.3 (C-9a), 131.9 (C-4a), 131.1 (C-4''), 129.8 (C-7, C-3'', C-5''), 128.9 (C-1 or C-1''), 128.90 (C-1 or C-1''), 127.2 (C-2'', C-6''), 122.7 (C-5), 121.2 (C-4b), 121.2 (C-6), 115.6 (C-4), 113.7 (C-8), 102.3 (C-4').

IR (ATR) $\tilde{\nu}$ (cm^{-1}) = 3476, 3361, 3231, 1684, 1569, 1551, 1442, 1382, 1318, 1238, 897, 760, 740, 684.

HRMS (ESI) (*m/z*) = calculated for $C_{21}H_{15}N_4O_2^+$ $[M+H]^+$ 355.1190, found 355.1191.

Purity (HPLC, method 2a) > 95% (λ = 210 nm), > 95% (λ = 254 nm).

(1-(3-Phenylisoxazol-5-yl)-9*H*-pyrido[3,4-b]indol-3-yl)methanol (101)

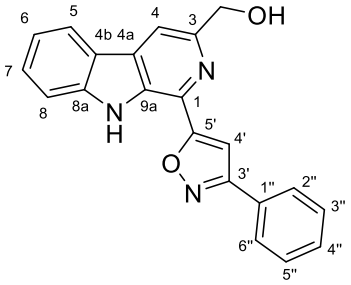

$C_{21}H_{15}N_3O_2$

M_r = 341.37 g/mol

Ester **97** (49.9 mg, 0.135 mmol, 1.0 eq) and pulverized calcium chloride (30 mg, 0.27 mmol, 2.0 eq) were dissolved in methylene chloride/ethanol (1:1, 3.0 mL) under N_2 atmosphere. Sodium borohydride (25.5 mg, 0.675 mmol, 5 eq) was added and the reaction mixture stirred at room temperature for 2.5 h. Water (2.0 mL) was added and the solvent removed *in vacuo*. The residue was cautiously treated with aq. HCl (1 M, 20 mL), then ethyl acetate (60 mL) and aq. NaOH solution (2 M, 10 mL) were added. The phases were separated and the organic layer dried using a phase separation filter. The solvent was removed *in vacuo* and the crude product purified by recrystallization (from methanol/methylene chloride) to give alcohol **101** as yellow crystals (40.1 mg, 0.117 mmol, 87%).

R_f = 0.39 (40% ethyl acetate in hexanes).

Melting point = 234 °C.

^{1}H NMR (400 MHz, DMSO-d_6) δ (ppm) = 11.76 (s, 1H, NH), 8.37 (s, 1H, 4-H), 8.34 (d, *J* = 7.9 Hz, 1H, 5-H), 8.13 – 8.05 (m, 2H, 2''-H, 6''-H), 7.80 (dt, *J* = 8.2, 0.9 Hz, 1H, 8-H), 7.77 (s, 1H, 4'-H), 7.66 – 7.56 (m, 4H, 7-H, 3''-H, 4''-H, 5''-H), 7.31 (ddd, *J* = 8.0, 7.1, 1.0 Hz, 1H, 6-H), 5.54 (t, *J* = 5.8 Hz, 1H, OH), 4.84 (d, *J* = 5.8 Hz, 2H, CH_2).

^{13}C NMR (101 MHz, DMSO-d_6) δ (ppm) = 169.6 (C-5'), 162.4 (C-3'), 151.1 (C-3), 141.9 (C-8a), 131.4 (C-1 or C-9a), 131.3 (C-1 or C-9a), 130.5 (C-4''), 129.2 (C-3'', C-5''), 128.9 (C-7), 128.5 (C-4a or C-1''), 127.9 (C-4a or C-1''), 126.8 (C-2'', C-6''), 121.8 (C-5), 120.4 (C-4b), 120.0 (C-6), 113.1 (C-4), 112.8 (C-8), 100.5 (C-4'), 64.4 (CH_2).

IR (ATR) $\tilde{\nu}$ (cm^{-1}) = 3261, 1610, 1552, 1500, 1464, 1437, 1394, 1316, 1278, 1240, 1004, 764, 741, 682.

HRMS (ESI) (*m/z*) = calculated for $C_{21}H_{16}N_3O_2^-$ $[M+H]^-$ 342.1238, found 342.1241.

Purity (HPLC, method 2a) > 95% (λ = 210 nm), > 95% (λ = 254 nm).

_N_,_N_-Dimethyl-2-(2-(3-phenylisoxazole-5-carbonyl)-1_H_-indol-3-yl)acetamide (104)

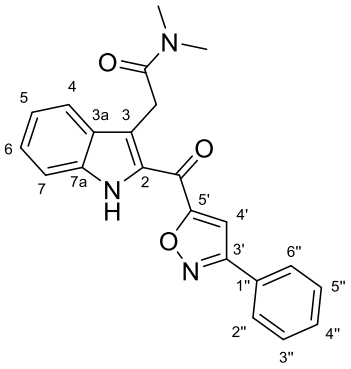

$C_{22}H_{19}N_3O_3$

M_r = 373.41 g/mol

To a solution of sulfonamide **105**[1] (165 mg, 0.500 mmol, 1.0 eq) in acetonitrile (2.5 mL) was added 2-bromo-1-(3-phenylisoxazol-5-yl)ethan-1-one (**106**) (133 mg, 0.500 mmol, 1.0 eq) and triethylamine (0.070 mL, 0.50 mmol, 1.0 eq) and the reaction mixture was stirred at 60 °C. Further amounts of 2-bromo-1-(3-phenylisoxazol-5-yl)ethan-1-one (**106**) (133 mg, 0.500 mmol, 1.0 eq) and triethylamine (0.070 mL, 0.50 mmol, 1.0 eq) were added after 30 min and 1 h (resulting in 3.0 eq of both in total). Then DBU (0.262 mL, 1.75 mmol, 3.5 eq) was added and the reaction mixture stirred at 60 °C for further 30 min. After cooling to room temperature, the mixture was diluted with sat. aq. $NaHCO_3$ solution (30 mL) and extracted with ethyl acetate (3 x 30 mL). The combined organic layers were dried over Na_2SO_4, filtered and concentrated *in vacuo*. The crude product was purified by flash column chromatography (40% → 50% ethyl acetate in hexanes) to give indole **104** as yellow solid (101 mg, 0.270 mmol, 54%).

R_f = 0.35 (40% ethyl acetate in hexanes).

Melting point = 222 °C.

^{1}H NMR (400 MHz, chloroform-*d*) δ (ppm) = 9.99 (s, 1H, NH), 7.91 – 7.83 (m, 2H, 2''-H, 6''-H), 7.72 (d, J = 8.3 Hz, 1H, 4-H), 7.55 – 7.48 (m, 3H, 3''-H, 4''-H, 5''-H), 7.42 (dt, J = 8.3, 1.1 Hz, 1H, 7-H), 7.39 – 7.34 (m, 2H, 6-H, 4'-H), 7.11 (ddd, J = 8.1, 6.7, 1.2 Hz, 1H, 5-H), 4.33 (s, 2H, CH_2), 3.20 (s, 3H, NCH_3), 3.03 (s, 3H, NCH_3).

^{13}C NMR (101 MHz, chloroform-*d*) δ (ppm) = 171.3 (CO), 170.5 (CON), 168.2 (C-5'), 163.0 (C-3'), 137.7 (C-7a), 130.9 (C-4''), 129.6 (C-1''), 129.3 (C-3'', C-5''), 128.2 (C-2 or C-3a), 128.0 (C-2 or C-3a), 127.9 (C-6), 127.1 (C-2'', C-6''), 123.4 (C-3), 121.6 (C-4), 121.4 (C-5), 113.0 (C-7), 107.6 (C-4'), 37.7 (CH_2), 36.0 (NCH_3), 31.1 (NCH_3).

IR (ATR) $\tilde{\nu}$ (cm^{-1}) = 3259, 1621, 1528, 1440, 1403, 1321, 1223, 1155, 1027, 948, 881, 732.

[1] Sulfonamide **105** was generously provided from KATHARINA THEES.

HRMS (EI) (*m/z*) = calculated for $C_{22}H_{19}N_3O_3^{\cdot+}$ $[M]^{\cdot+}$ 373.1421, found 373.1420.

Purity (HPLC, method 2a) > 95% (λ = 210 nm), > 95% (λ = 254 nm).

1-Bromo-10*H*-phenothiazine (111)[214]

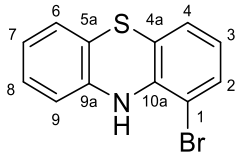

$C_{12}H_8BrNS$

M_r = 278.17 g/mol

Following **General Procedure XI**, phenothiazine (199 mg, 1.00 mmol, 1.0 eq), *n*-butyllithium (2.5 M in hexanes, 0.900 mL, 2.25 mmol, 2.25 eq) and 1,2-dibromoethane (0.095 mL, 1.1 mmol, 1.1 eq) were used. The crude product was purified by flash column chromatography (100% hexanes) to give bromide **111** as white solid (140 mg, 0.501 mmol, 50%).

R_f = 0.58 (5% ethyl acetate in hexanes).

Melting point = 108 °C (lit.[214] 108 – 110 °C).

^{1}H NMR (400 MHz, chloroform-*d*) δ (ppm) = 7.22 (dd, *J* = 8.0, 1.3 Hz, 1H, 2-H), 7.03 (td, *J* = 7.6, 1.5 Hz, 1H, 6-H), 6.99 (dd, *J* = 8.0, 1.6 Hz, 1H, 8-H), 6.92 (dd, *J* = 7.7, 1.3 Hz, 1H, 4-H), 6.87 (td, *J* = 7.6, 1.3 Hz, 1H, 7-H), 6.67 (t, *J* = 7.8 Hz, 1H, 3-H), 6.64 (d, *J* = 1.2 Hz, 1H, 9-H), 6.49 (s, 1H, NH).

^{13}C NMR (101 MHz, chloroform-*d*) δ (ppm) = 141.0 (C-9a), 139.2 (C-10a), 130.7 (C-2), 127.7 (C-6), 126.8 (C-8), 126.1 (C-4), 123.5 (C-7), 123.1 (C-3), 120.1 (C-4a), 118.4 (C-5a), 115.4 (C-9), 109.6 (C-1).

IR (ATR) $\tilde{\nu}$ (cm^{-1}) = 3420, 3334, 1571, 1476, 1439, 1408, 1291, 1126, 1089, 764, 747, 710.

HRMS (EI) (*m/z*) = calculated for $C_{12}H_8{}^{79}BrNS^{\cdot+}$ $[M]^{\cdot+}$ 276.9556, found 276.9554.

Purity (HPLC, method 2c) > 95% (λ = 210 nm), > 95% (λ = 254 nm).

1-Iodo-10*H*-phenothiazine (112)

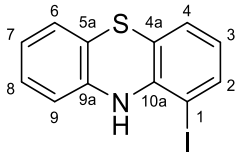

$C_{12}H_8INS$

M_r = 325.17 g/mol

Following **General Procedure XI**, phenothiazine (199 mg, 1.00 mmol, 1.0 eq), *n*-butyllithium (2.5 M in hexanes, 0.900 mL, 2.25 mmol, 2.25 eq) and 1,2-diiodoethane (310 mg, 1.10 mmol, 1.1 eq) were used. The crude product was purified by flash column chromatography (100% hexanes → 3% ethyl acetate in hexanes) to give iodide **112** as pale yellow solid (140 mg, 0.429 mmol, 43%).

R_f = 0.60 (5% ethyl acetate in hexanes).

Melting point = 103 °C.

^{1}H NMR (400 MHz, chloroform-*d*) δ (ppm) = 7.45 (dd, *J* = 8.0, 1.3 Hz, 1H, 2-H), 7.06 – 6.99 (m, 2H, 6-H, 8-H), 6.95 (ddd, *J* = 7.6, 1.3, 0.6 Hz, 1H, 4-H), 6.87 (td, *J* = 7.5, 1.3 Hz, 1H, 7-H), 6.67 (dd, *J* = 7.9, 1.2 Hz, 1H, 9-H), 6.54 (t, *J* = 7.8 Hz, 1H, 3-H), 6.42 (s, 1H, NH).

^{13}C NMR (101 MHz, chloroform-*d*) δ (ppm) = 141.6 (C-9a or C-10a), 141.5 (C-9a or C-10a), 137.1 (C-2), 127.7 (C-6 or C-8), 127.2 (C-4), 126.6 (C-6 or C-8), 123.9 (C-3), 123.5 (C-7), 119.3 (C-4a), 119.0 (C-5a), 115.5 (C-9), 85.1 (C-1).

IR (ATR) $\tilde{\nu}$ (cm^{-1}) = 3326, 1566, 1494, 1475, 1433, 1286, 1125, 1066, 881, 747, 709.

HRMS (EI) (*m/z*) = calculated for $C_{12}H_8INS^{\cdot+}$ $[M]^{\cdot+}$ 324.9417, found 324.9417.

Purity (HPLC, method 2c) > 95% (λ = 210 nm), > 95% (λ = 254 nm).

1-Ethynyl-10*H*-phenothiazine (114)

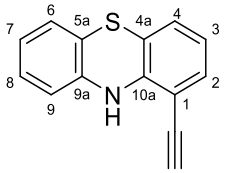

$C_{14}H_9NS$

M_r = 223.29 g/mol

1-Iodo-10*H*-phenothiazine (**112**) (97.6 mg, 0.300 mmol, 1.0 eq) and PPh_3 (8.0 mg, 0.030 mmol, 0.1 eq) were dissolved in anhydrous THF/triethylamine (2:1, 9.0 mL) under N_2 atmosphere and the reaction mixture was stirred at room temperature. CuI (5.7 mg, 0.03 mmol, 0.1 eq) was added and the mixture was purged with N_2 for 5 min. Then, $Pd(PPh_3)_4$ (7 mg, 0.006 mmol, 0.02 eq) was added and the mixture was purged again with N_2 for 5 min. Trimethylsilylacetylene (0.085 mL, 0.60 mmol, 2.0 eq) was added dropwise and the reaction mixture stirred at room temperature for 40 h. Then, it was filtered through a pad of celite and the pad was washed with ethyl acetate (70 mL). The filtrate was washed with sat. aq. NaCl solution (50 mL) and the aq. phase was further extracted with ethyl acetate (2 x 80 mL). The combined organic layers were dried over Na_2SO_4, filtered and concentrated *in vacuo*.
The crude TMS-protected intermediate **113** (R_f = 0.74, 5% ethyl acetate in hexanes) was desilylated, following **General Procedure II**, with K_2CO_3 (164 mg, 0.990 mmol, 3.3 eq) in methanol (5.0 mL). The crude product was purified by flash column chromatography (2% → 5% ethyl acetate in hexanes) to give terminal alkyne **114** as brown semi solid (30.1 mg, 0.135 mmol, 45% over two steps).

R_f = 0.51 (5% ethyl acetate in hexanes).

^{1}H NMR (400 MHz, chloroform-*d*) δ (ppm) = 7.13 (dd, *J* = 7.7, 1.4 Hz, 1H, 2-H), 7.01 (td, *J* = 7.6, 1.5 Hz, 1H, 8-H), 6.95 (m, 2H, 4-H, 6-H), 6.84 (td, *J* = 7.5, 1.3 Hz, 1H, 7-H), 6.74 (t, *J* = 7.7 Hz, 1H, 3-H), 6.65 (s, 1H, NH), 6.60 (dd, *J* = 7.9, 1.2 Hz, 1H, 9-H), 3.49 (s, 1H, CCH).

^{13}C NMR (101 MHz, chloroform-*d*) δ (ppm) = 143.3 (C-10a), 140.7 (C-9a), 130.6 (C-2), 127.6 (C-8), 127.5 (C-6), 126.8 (C-4), 123.2 (C-7), 121.8 (C-3), 118.4 (C-4a), 118.0 (C-5a), 115.2 (C-9), 107.0 (C-1), 84.2 (C<u>C</u>H), 79.2 (<u>C</u>CH).

IR (ATR) $\tilde{\nu}$ (cm^{-1}) = 3260, 2095, 1598, 1562, 1476, 1450, 1435, 1289, 1263, 1127, 893, 774, 743.

HRMS (EI) (*m/z*) = calculated for $C_{14}H_9NS^{\cdot+}$ $[M]^{\cdot+}$ 223.0451, found 223.0451.

Purity (HPLC, method 2i) > 95% (λ = 210 nm), > 95% (λ = 254 nm).

5-(10*H*-Phenothiazin-1-yl)-3-phenylisoxazole (115)

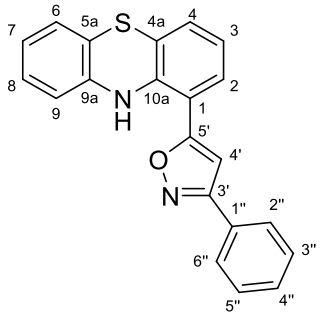

$C_{21}H_{14}N_2OS$

M_r = 342.42 g/mol

Alkyne **114** (40.2 mg, 0.180 mmol, 1.0 eq) and *N*-hydroxybenzimidoyl chloride (42 mg, 0.27 mmol, 1.5 eq) were dissolved in methylene chloride (1.0 mL) and the solution was stirred at 0 °C. Triethylamine (0.038 mL, 0.27 mmol, 1.5 eq, dissolved in 0.3 mL methylene chloride) was added dropwise over 30 min. After stirring the reaction mixture at room temperature for 16 h, it was partitioned between water (10 mL) and methylene chloride (10 mL) and the aq. phase was further extracted with methylene chloride (2 x 10 mL). The combined organic layers were dried using a phase separation filter and the solvent was removed *in vacuo*. The crude product was purified by flash column chromatography (2% ethyl acetate in hexanes) and subsequent recrystallization (from methylene chloride/hexanes) to give isoxazole **115** as yellow crystals (19.3 mg, 0.0564 mmol, 31%).

R_f = 0.32 (5% ethyl acetate in hexanes).

Melting point = 151 °C.

^{1}H NMR (400 MHz, chloroform-*d*) δ (ppm) = 7.90 – 7.85 (m, 2H, 2‘‘-H, 6‘‘-H), 7.82 (s, 1H, NH), 7.55 – 7.48 (m, 3H, 3‘‘-H, 4‘‘-H, 5‘‘-H), 7.33 (dd, *J* = 7.9, 1.5 Hz, 1H, 2-H), 7.09 (dd, *J* = 7.6, 1.4 Hz, 1H, 4-H), 7.04 (td, *J* = 7.7, 1.5 Hz, 1H, 8-H), 7.02 – 6.98 (m, 1H, 6-H), 6.92 – 6.85 (m, 2H, 3-H, 7-H), 6.80 (s, 1H, 4‘-H), 6.71 (dd, *J* = 7.8, 1.2 Hz, 1H, 9-H).

^{13}C NMR (101 MHz, chloroform-*d*) δ (ppm) = 170.4 (C-5’), 162.9, (C-3’), 140.9 (C-9a or C-10a), 140.4 (C-9a or C-10a), 130.5 (C-4’’), 129.2 (C-3’’, C-5’’), 129.1 (C-4), 128.7 (C-1’’), 127.8 (C-8), 127.4 (C-2), 127.1, (C-2’’, C-6’’) 126.8 (C-6), 123.5 (C-7), 122.3 (C-3), 121.0 (C-4a), 118.4 (C-5a), 115.8 (C-9), 112.6 (C-1), 99.9 (C-4’).

IR (ATR) $\tilde{\nu}$ (cm^{-1}) = 3388, 1601, 1571, 1479, 1447, 1425, 1399, 1292, 911, 759, 681.

HRMS (EI) (*m/z*) = calculated for $C_{21}H_{14}N_2OS^{\cdot+}$ $[M]^{\cdot+}$ 342.0822, found 342.0824.

Purity (HPLC, method 2a) > 95% (λ = 210 nm), > 95% (λ = 254 nm).

1-Ethynyl-9*H*-carbazole (119)

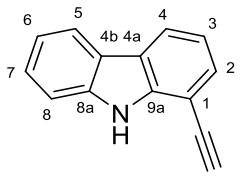

$C_{14}H_9N$

M_r = 191.23 g/mol

1-Bromo-9*H*-carbazole **117** (295 mg, 1.20 mmol, 1.0 eq) was dissolved in anhydrous triethylamine (6.0 mL) under N_2 atmosphere in a pressure tube and the reaction mixture was stirred at room temperature. CuI (23 mg, 0.12 mmol, 0.1 eq) was added and the mixture was purged with N_2 for 5 min. Then, $Pd(PPh_3)_2Cl_2$ (51 mg, 0.072 mmol, 0.06 eq) and trimethylsilylacetylene (0.204 mL, 1.44 mmol, 1.2 eq) were added and the mixture was purged again with N_2 for 5 min. The tube was sealed and the reaction mixture stirred at 80 °C for 24 h. After cooling to room temperature, the mixture was filtered through a pad of celite and the pad was washed with ethyl acetate (50 mL). The filtrate was washed with sat. aq. NaCl solution (50 mL) and the aq. phase was further extracted with ethyl acetate (3 x 50 mL). The combined organic layers were dried using a phase separation filter and concentrated *in vacuo*.
The crude TMS-protected intermediate **118** (R_f = 0.63, 10% ethyl acetate in hexanes) was desilylated, following **General Procedure II**, with K_2CO_3 (654 mg, 3.96 mmol, 3.3 eq) in methanol (12 mL). The crude product was purified two times by flash column chromatography (10% methylene chloride in hexanes, 6% ethyl acetate in hexanes) to give terminal alkyne **119** as pale yellow solid (126 mg, 0.657 mmol, 55% over two steps).

R_f = 0.37 (10% ethyl acetate in hexanes).

Melting point = 140 °C.

^{1}H NMR (500 MHz, methylene chloride-d_2) δ (ppm) = 8.54 (s, 1H, NH), 8.16 – 8.06 (m, 2H, 4-H, 5-H), 7.57 (dd, *J* = 7.5, 1.1 Hz, 1H, 2-H), 7.53 (dt, *J* = 8.2, 0.9 Hz, 1H, 8-H), 7.47 (ddd, *J* = 8.1, 7.0, 1.2 Hz, 1H, 7-H), 7.28 (ddd, *J* = 7.9, 7.0, 1.1 Hz, 1H, 6-H), 7.21 (t, *J* = 7.6 Hz, 1H, 3-H), 3.55 (s, 1H, CCH).

^{13}C NMR (126 MHz, methylene chloride-d_2) δ (ppm) = 141.4 (C-9a), 139.7 (C-8a), 129.5 (C-2), 126.8 (C-7), 123.7 (C-4b), 123.4 (C-4a), 121.7 (C-4), 120.9 (C-5), 120.3 (C-6), 119.6 (C-3), 111.3 (C-8), 104.7 (C-1), 82.2 (C<u>C</u>H), 80.2 (<u>C</u>CH).

IR (ATR) $\tilde{\nu}$ (cm^{-1}) = 3401, 3276, 1595, 1494, 1453, 1422, 1317, 1238, 748, 682.

HRMS (EI) (*m/z*) = calculated for $C_{14}H_9N^{\cdot+}$ $[M]^{\cdot+}$ 191.0730, found 191.0730.

Purity (HPLC, method 2b) > 95% (λ = 210 nm), > 95% (λ = 254 nm).

5-(9*H*-Carbazol-1-yl)-3-phenylisoxazole (120)

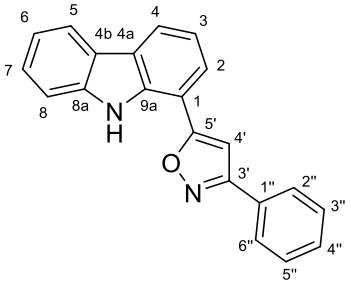

$C_{21}H_{14}N_2O$

M_r = 310.36 g/mol

Similar to **General Procedure IIIa**, alkyne **119** (95.6 mg, 0.500 mmol, 1.0 eq), (*E*)-benzaldehyde oxime (91 mg, 0.75 mmol, 1.5 eq) and [bis(trifluoroacetoxy)iodo]benzene (0.32 g, 0.75 mmol, 1.5 eq) were used in methanol/water (5.0 mL). In contrast to the general procedure, after stirring for 16 h, another amount of (*E*)-benzaldehyde oxime (91 mg, 0.75 mmol, 1.5 eq) and [bis(trifluoroacetoxy)iodo]benzene (0.32 g, 0.75 mmol, 1.5 eq) were added. After stirring for additional 20 h, the reaction was completed. The crude product was purified by flash column chromatography (7% ethyl acetate in hexanes) and subsequent recrystallization (from methylene chloride/hexanes) to give isoxazole **120** as pale yellow solid (31.8 mg, 0.102 mmol, 21%).

R_f = 0.17 (7% ethyl acetate in hexanes).

Melting point = 168 °C.

^{1}H NMR (400 MHz, methylene chloride-d_2) δ (ppm) = 9.55 (s, 1H, NH), 8.21 (dt, *J* = 7.7, 0.9 Hz, 1H, 4-H), 8.14 (dt, *J* = 7.8, 1.0 Hz, 1H, 5-H), 7.97 – 7.91 (m, 2H, 2‘‘-H, 6‘‘-H), 7.85 (dd, *J* = 7.6, 1.0 Hz, 1H, 2-H), 7.59 (dt, *J* = 8.2, 0.9 Hz, 1H, 8-H), 7.57 – 7.47 (m, 4H, 7-H, 3‘‘-H, 4‘‘-H, 5‘‘-H), 7.36 (t, *J* = 7.7 Hz, 1H, 3-H), 7.30 (ddd, *J* = 8.0, 7.1, 1.1 Hz, 1H, 6-H), 7.05 (s, 1H, 4‘-H).

^{13}C NMR (101 MHz, methylene chloride-d_2) δ (ppm) = 171.1 (C-5‘), 163.2 (C-3‘), 140.3 (C-8a), 136.4 (C-9a), 130.6 (C-4‘‘), 129.4 (C-3‘‘, C-5‘‘), 129.4 (C-1‘‘), 127.3 (C-2‘‘, C-6‘‘), 127.1 (C-7), 125.3 (C-4a), 124.1 (C-2), 123.0 (C-4b), 122.9 (C-4), 120.8 (C-5), 120.4 (C-6), 119.8 (C-3), 111.6 (C-8), 110.7 (C-1), 97.9 (C-4‘).

IR (ATR) $\tilde{\nu}$ (cm^{-1}) = 3435, 1611, 1597, 1564, 1442, 1427, 1397, 1322, 1270, 1231, 911, 757, 682.

HRMS (EI) (*m/z*) = calculated for $C_{21}H_{14}N_2O^{\cdot+}$ $[M]^{\cdot+}$ 310.1101, found 310.1110.

Purity (HPLC, method 2b) > 95% (λ = 210 nm), > 95% (λ = 254 nm).

7,8-Dichloro-1-ethynyl-9*H*-pyrido[3,4-*b*]indole (125)

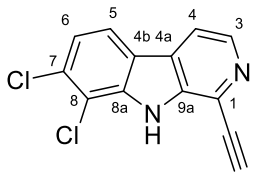

$C_{13}H_6Cl_2N_2$

M_r = 261.11 g/mol

1-Bromo-7,8-dichloro-9*H*-pyrido[3,4-*b*]indole (**124**) (63.2 mg, 0.200 mmol, 1.0 eq) was dissolved under N_2 atmosphere in anhydrous triethylamine (0.75 mL) and anhydrous DMF (0.55 mL) and the reaction mixture was stirred at room temperature. CuI (7.6 mg, 0.040 mmol, 0.2 eq) was added and the mixture was purged with N_2 for 5 min. Then, Pd(dppf)Cl_2 (7.3 mg, 0.010 mmol, 0.05 eq) was added and the mixture was purged again with N_2 for 5 min. A degassed solution of trimethylsilylacetylene (0.035 mL, 0.24 mmol, 1.2 eq, dissolved in 0.2 mL anhydrous DMF) was added dropwise and the reaction mixture stirred at room temperature for 4 h. Then, the mixture was partitioned between sat. aq. NaCl solution (25 mL) and ethyl acetate (25 mL). The aq. phase was further extracted with ethyl acetate (2 x 25 mL) and the combined organic layers were dried over Na_2SO_4, filtered and concentrated *in vacuo*. The crude TMS-protected intermediate (R_f = 0.72, 2% methanol in methylene chloride) was desilylated, following **General Procedure II**, with K_2CO_3 (109 mg, 0.660 mmol, 3.3 eq) in methanol (2.0 mL). The crude product was purified by flash column chromatography (35% ethyl acetate in hexanes) to give terminal alkyne **125** as light brown solid (27.1 mg, 0.104 mmol, 52% over two steps).

R_f = 0.30 (40% ethyl acetate in hexanes).

Melting point = 178 °C.

^{1}H NMR (500 MHz, chloroform-*d*) δ (ppm) = 8.62 (s, 1H), 8.50 (d, *J* = 5.2 Hz, 1H, 3-H), 7.91 (d, *J* = 8.4 Hz, 1H, 5-H), 7.88 (d, *J* = 5.2 Hz, 1H, 4-H), 7.38 (d, *J* = 8.4 Hz, 1H, 6-H), 3.61 (s, 1H, CCH).

^{13}C NMR (126 MHz, chloroform-*d*) δ (ppm) = 141.0 (C-3), 138.4 (C-8a), 137.8 (C-9a), 132.5 (C-7), 129.0 (C-4a), 126.5 (C-1), 122.8 (C-6), 121.5 (C-4b), 120.8 (C-5), 116.0 (C-8), 115.4 (C-4), 83.1 (C<u>C</u>H), 79.2 (<u>C</u>CH).

IR (ATR) $\tilde{\nu}$ (cm^{-1}) = 3265, 2107, 1620, 1568, 1461, 1420, 1305, 1261, 1231, 1158, 1071, 801, 773.

HRMS (EI) (*m/z*) = calculated for $C_{13}H_6{}^{35}Cl_2N_2{}^{\cdot+}$ $[M]^{\cdot+}$ 259.9908, found 259.9903.

Purity (HPLC, method 2c) > 95% (λ = 210 nm), > 95% (λ = 254 nm).

5-(7,8-Dichloro-9*H*-pyrido[3,4-*b*]indol-1-yl)-3-phenylisoxazole (126)

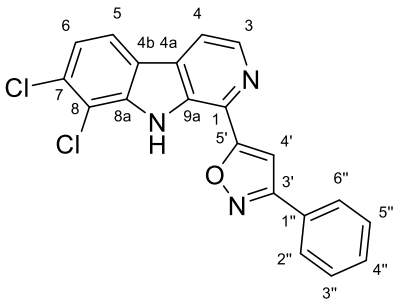

$C_{20}H_{11}Cl_2N_3O$

M_r = 380.23 g/mol

Following **General Procedure IIIa**, alkyne **125** (65.3 mg, 0.250 mmol, 1.0 eq), (*E*)-benzaldehyde oxime (45 mg, 0.38 mmol, 1.5 eq) and [bis(trifluoroacetoxy)iodo]benzene (161 mg, 0.375 mmol, 1.5 eq) were used in methanol/water (2.5 mL). After stirring for additional 16 h, the reaction was completed. The crude product was purified by flash column chromatography (20% → 25% ethyl acetate in hexanes) to give isoxazole **126** as white solid (83.4 mg, 0.219 mmol, 88%).

R_f = 0.43 (40% ethyl acetate in hexanes).

Melting point = 210 °C.

^{1}H NMR (400 MHz, methylene chloride-d_2) δ (ppm) = 9.50 (s, 1H, NH), 8.56 (d, *J* = 5.1 Hz, 1H, 3-H), 7.99 – 7.92 (m, 4H, 4-H, 5-H, 2''-H, 6''-H), 7.55 – 7.50 (m, 3H, 3''-H, 4''-H, 5''-H), 7.42 (s, 1H, 4'-H), 7.40 (d, *J* = 8.4 Hz, 1H, 6-H).

^{13}C NMR (101 MHz, methylene chloride-d_2) δ (ppm) = 170.8 (C-5'), 163.5 (C-3'), 140.9 (C-3), 139.4 (C-8a), 133.2 (C-7 or C-9a), 132.9 (C-7 or C-9a), 131.4 (C-1 or C-4a), 131.2 (C-1 or C-4a), 130.9 (C-4''), 129.6 (C-3'', C-5''), 129.2 (C-1''), 127.5 (C-2'', C-6''), 123.1 (C-6), 121.4 (C-4b), 121.2 (C-5), 116.7 (C-4), 116.4 (C-8), 101.0 (C-4').

IR (ATR) $\tilde{\nu}$ (cm^{-1}) = 3193, 1610, 1554, 1458, 1441, 1421, 1398, 1162, 919, 911, 796, 759.

HRMS (EI) (*m/z*) = calculated for $C_{20}H_{11}{}^{35}Cl_2N_3O^{\cdot+}$ $[M]^{\cdot+}$ 379.0274, found 379.0277.

Purity (HPLC, method 2a) > 95% (λ = 210 nm), > 95% (λ = 254 nm).

3-(2-(2-Methoxyphenyl)hydrazineylidene)piperidin-2-one (129)[227]

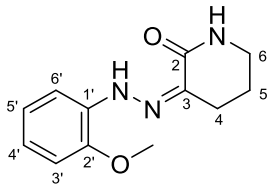

$C_{12}H_{15}N_3O_2$

M_r = 233.27 g/mol

Similar to literature[227], 3-ethoxycarbonyl-2-piperidone (4.32 g, 25.0 mmol, 1.0 eq) was dissolved in aq. KOH solution (0.5 M, 50 mL) and stirred at 35 °C for 16 h, then aq. HCl (6 M, 2.5 mL) was added dropwise at 0 °C. At the same time, 2-methoxyaniline (3.08 g, 25.0 mmol, 1.0 eq) was dissolved in aq. HCl (2.7 M, 48 mL) and at 0 °C a solution of $NaNO_2$ (1.76 g, 25.5 mmol, 1.02 eq) in water (12.4 mL) was added over 10 min and stirred for further 15 min. The piperidone solution was transferred dropwise to the diazotized aniline at 0 °C and sodium acetate (11.2 g, 137 mmol, 5.5 eq) was added to adjust pH 4 – 5. After stirring the suspension for 5 h at 0 °C, the precipitate was filtered, washed with water (100 mL) and dried to give pure hydrazone **129** as yellow solid. Additionally, the filtrate was extracted with ethyl acetate (3 x 100 mL). The combined organic layers were washed with sat. aq. $NaHCO_3$ solution and dried using a phase separation filter. The solvent was removed *in vacuo* and the crude product purified by flash column chromatography (40% ethyl acetate in hexanes) to give further hydrazone **129** as yellow solid (in total 3.98 g, 17.1 mmol, 68%).

R_f = 0.31 (65% ethyl acetate in hexanes).

Melting point = 163 °C (lit.[227] 162 – 164 °C).

^{1}H NMR (400 MHz, chloroform-*d*) δ (ppm) = 12.95 (s, 1H, NNH), 7.54 – 7.47 (m, 1H, 6'-H), 6.96 – 6.90 (m, 1H, 5'-H), 6.89 – 6.82 (m, 2H, 3'-H, 4'-H), 5.90 (s, 1H, CONH), 3.88 (s, 3H, OCH_3), 3.41 – 3.33 (m, 2H, 6-H), 2.76 – 2.69 (m, 2H, 4-H), 2.04 – 1.93 (m, 2H, 5-H).

^{13}C NMR (101 MHz, chloroform-*d*) δ (ppm) = 164.1 (C-1), 146.4 (C-2'), 133.7 (C-1'), 126.6 (C-3), 121.4 (C-5'), 120.7 (C-4'), 112.1 (C-6'), 110.5 (C-3'), 55.8 (OCH_3), 42.2 (C-6), 31.3 (C-4), 23.0 (C-5).

IR (ATR) $\tilde{\nu}$ (cm^{-1}) = 3208, 3150, 1644, 1595, 1540, 1506, 1399, 1336, 1228, 1150, 1100, 1029, 804, 741, 715.

HRMS (EI) (*m/z*) = calculated for $C_{12}H_{15}N_3O_2^{\cdot+}$ $[M]^{\cdot+}$ 233.1159, found 233.1156.

Purity (HPLC, method 2e) > 95% (λ = 210 nm), > 95% (λ = 254 nm).

8-Methoxy-2,3,4,9-tetrahydro-1*H*-pyrido[3,4-*b*]indol-1-one (130)[227]

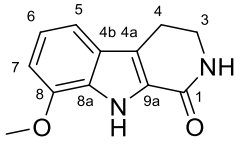

$C_{12}H_{12}N_2O_2$

M_r = 216.24 g/mol

Hydrazone **129** (3.97 g, 17.0 mmol) was dissolved in formic acid (17 mL) and stirred at 80 °C for 1 h. After cooling to room temperature, the solvent was cautiously removed *in vacuo* and the crude product purified by flash column chromatography (65% ethyl acetate in hexanes) to give tetrahydro-*β*-carboline **130** as light brown solid (1.94 g, 8.95 mmol, 53%).

R_f = 0.49 (100% ethyl acetate).

Melting point = 238 °C (lit.[227] 241 – 242 °C).

^{1}H NMR (400 MHz, chloroform-*d*) δ (ppm) = 9.24 (s, 1H, NH), 7.19 (dt, *J* = 8.2, 0.8 Hz, 1H, 5-H), 7.07 (t, *J* = 7.9 Hz, 1H, 6-H), 6.73 (dd, *J* = 7.7, 0.8 Hz, 1H, 7-H), 6.06 (s, 1H, CONH), 3.97 (s, 3H, OCH_3), 3.70 (td, *J* = 7.0, 2.6 Hz, 2H, 3-H), 3.05 (t, *J* = 7.0 Hz, 2H, 4-H).

^{13}C NMR (101 MHz, chloroform-*d*) δ (ppm) = 163.1 (C-1), 147.0 (C-8), 128.3 (C-8a), 126.7 (C-4b), 126.1 (C-9a), 121.0 (C-6), 120.2 (C-4a), 112.8 (C-5), 104.5 (C-7), 55.7 (OCH_3), 42.3 (C-3), 21.2 (C-4).

IR (ATR) $\tilde{\nu}$ (cm^{-1}) = 3206, 2922, 1650, 1576, 1501, 1389, 1329, 1254, 1099, 992, 785, 735.

HRMS (EI) (*m/z*) = calculated for $C_{12}H_{12}N_2O_2^{\cdot+}$ $[M]^{\cdot+}$ 216.0894, found 216.0889.

Purity (HPLC, method 2e) > 94% (λ = 210 nm), > 95% (λ = 254 nm).

8-Methoxy-2,9-dihydro-1*H*-pyrido[3,4-*b*]indol-1-one (131)

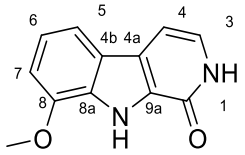

$C_{12}H_{10}N_2O_2$

M_r = 214.22 g/mol

Tetrahydro-*β*-carboline **130** (1.93 g, 8.90 mmol, 1.0 eq) and *p*-chloranil (3.28 g, 13.40 mmol, 1.5 eq) were suspended in toluene (90 mL). After the reaction mixture was stirred at 145 °C for 20 h, another portion of *p*-chloranil (1.09 g, 4.45 mmol, 0.5 eq) was added. The suspension was stirred at 145 °C for further 24 h and, after cooling to room temperature, the solvent was removed *in vacuo*. The crude product was purified by flash column chromatography (100% ethyl acetate → 5% methanol in ethyl acetate) to give *β*-carboline **131** as taupe solid (1.07 g, 4.98 mmol, 56%).

R_f = 0.31 (100% ethyl acetate).

Melting point = 155 °C.

^{1}H NMR (400 MHz, DMSO-d_6) δ (ppm) = 11.89 (s, 1H, NH), 11.33 (s, 1H, CONH), 7.57 (d, *J* = 8.0 Hz, 1H, 5-H), 7.10 (t, *J* = 7.9 Hz, 1H, 6-H), 7.06 (d, *J* = 6.7 Hz, 1H, 3-H), 6.98 – 6.89 (m, 2H, 4-H, 7-H), 3.93 (s, 3H, OCH_3).

^{13}C NMR (101 MHz, DMSO-d_6) δ (ppm) = 155.7 (C-1), 146.8 (C-8), 129.6 (C-8a), 127.9 (C-9a), 124.7 (C-4a), 124.6 (C-3), 123.4 (C-4b), 120.2 (C-6), 113.3 (C-5), 106.3 (C-7), 99.6 (C-4), 55.5 (OCH_3).

IR (ATR) $\tilde{\nu}$ (cm^{-1}) = 2957, 1644, 1606, 1435, 1419, 1259, 1246, 1076, 994, 771, 756.

HRMS (EI) (*m/z*) = calculated for $C_{12}H_{10}N_2O_2^{\cdot+}$ $[M]^{\cdot+}$ 214.0737, found 214.0732.

Purity (HPLC, method 2e) > 95% (λ = 210 nm), > 95% (λ = 254 nm).

8-Methoxy-9*H*-pyrido[3,4-*b*]indol-1-yl trifluoromethanesulfonate (132)

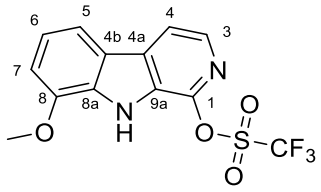

$C_{13}H_9F_3N_2O_4S$

M_r = 346.28 g/mol

β-Carbolinone **131** (107 mg, 0.500 mmol, 1.0 eq) was dissolved in anhydrous pyridine (5.0 mL) under N_2 atmosphere. The solution was cooled to 0 °C and purged with N_2 for 5 min. Trifluoromethanesulfonic anhydride (0.17 mL, 1.0 mmol, 2.0 eq) was added dropwise over 15 min. Then the reaction mixture was warmed up to room temperature and stirred for 1 h. The solution was partitioned between ethyl acetate (50 mL) and a mixture of water (100 mL) and aq. HCl (2 M, 10 mL). The aq. phase was further extracted with ethyl acetate (2 x 50 mL), the combined organic layers were washed with aq. HCl (2 M, 30 mL) and dried using a phase separation filter. The solvent was removed *in vacuo* and the crude product purified by flash column chromatography (15% ethyl acetate in hexanes) to give triflate **132** as white solid (162 mg, 0.467 mmol, 93%).

R_f = 0.60 (35% ethyl acetate in hexanes).

Melting point = 157 °C.

^{1}H NMR (500 MHz, chloroform-*d*) δ (ppm) = 8.60 (s, 1H, NH), 8.14 (d, J = 5.2 Hz, 1H, 3-H), 7.97 (dd, J = 5.3, 0.7 Hz, 1H, 4-H), 7.69 (dt, J = 8.1, 0.7 Hz, 1H, 5-H), 7.28 (t, J = 7.9 Hz, 1H, 6-H), 7.06 (dd, J = 7.9, 0.8 Hz, 1H, 7-H), 4.06 (s, 3H, OCH_3).

^{13}C NMR (126 MHz, chloroform-*d*) δ (ppm) = 146.6 (C-8), 141.3 (C-1), 136.4 (C-3), 134.9 (C-4a), 131.4 (C-8a), 125.2 (C-9a), 122.5 (C-4b), 122.0 (C-6), 118.9 (q, J_{CF} = 320.8 Hz, CF_3), 116.5 (C-4), 113.9 (C-5), 109.0 (C-7), 55.9 (OCH_3).

IR (ATR) $\tilde{\nu}$ (cm^{-1}) = 3420, 1583, 1474, 1406, 1395, 1263, 1202, 1126, 1051, 965, 838, 783.

HRMS (EI) (*m/z*) = calculated for $C_{13}H_9F_3N_2O_4S^{\cdot+}$ $[M]^{\cdot+}$ 346.0230, found 346.0225.

Purity (HPLC, method 2c) > 95% (λ = 210 nm), > 95% (λ = 254 nm).

1-Ethynyl-8-methoxy-9*H*-pyrido[3,4-*b*]indole (133)

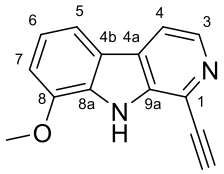

$C_{14}H_{10}N_2O$

M_r = 222.25 g/mol

Following **General Procedure Ib**, triflate **132** (104 mg, 0.300 mmol, 1.0 eq), LiCl (38 mg, 0.90 mmol, 3.0 eq), $Pd(PPh_3)_2Cl_2$ (17 mg, 0.024 mmol, 0.08 eq), CuI (6 mg, 0.03 mmol, 0.1 eq) and trimethylsilylacetylene (0.30 mL, 2.1 mmol, 7.0 eq) were used in anhydrous DMF/triethylamine (5.8 mL).

The crude TMS-protected intermediate (R_f = 0.66, 40% ethyl acetate in hexanes; HRMS (EI) (*m/z*) = calculated for $C_{17}H_{18}N_2OSi^{\cdot+}$ $[M]^{\cdot+}$ 294.1183, found 294.1183) was desilylated, following **General Procedure II**, with K_2CO_3 (0.16 g, 0.99 mmol, 3.3 eq) in methanol (1.0 mL). The crude product was purified by flash column chromatography (40% ethyl acetate in hexanes) to give terminal alkyne **133** as light brown solid (45.0 mg, 0.204 mmol, 68% over two steps).

R_f = 0.25 (40% ethyl acetate in hexanes).

Melting point = 159 °C.

^{1}H NMR (500 MHz, chloroform-*d*) δ (ppm) = 8.63 (s, 1H, NH), 8.45 (d, *J* = 5.2 Hz, 1H, 3-H), 7.92 (dd, *J* = 5.3, 0.8 Hz, 1H, 4-H), 7.70 (dd, *J* = 8.0, 0.8 Hz, 1H, 5-H), 7.23 (t, *J* = 7.9 Hz, 1H, 6-H), 7.03 (dd, *J* = 7.8, 0.8 Hz, 1H, 7-H), 4.05 (s, 3H, OCH_3), 3.57 (s, 1H, CCH).

^{13}C NMR (126 MHz, chloroform-*d*) δ (ppm) = 146.4 (C-8), 139.9 (C-3), 137.6 (C-9a), 130.9 (C-8a), 129.3 (C-4a), 126.1 (C-1), 122.8 (C-4b), 121.2 (C-6), 115.6 (C-4), 114.2 (C-5), 108.6 (C-7), 82.2 (C<u>C</u>H), 79.8 (<u>C</u>CH), 55.8 (OCH_3).

IR (ATR) $\tilde{\nu}$ (cm^{-1}) = 3393, 3274, 2106, 1574, 1461, 1424, 1323, 1265, 1224, 1051, 959, 839, 791, 769.

HRMS (EI) (*m/z*) = calculated for $C_{14}H_{10}N_2O^{\cdot+}$ $[M]^{\cdot+}$ 222.0788, found 222.0793.

Purity (HPLC, method 2e) > 95% (λ = 210 nm), > 95% (λ = 254 nm).

5-(8-Methoxy-9*H*-pyrido[3,4-*b*]indol-1-yl)-3-phenylisoxazole (128)

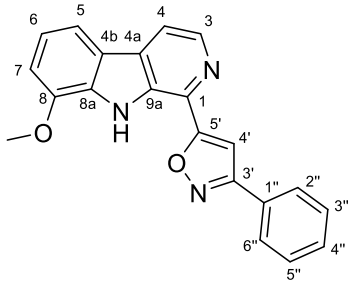

$C_{21}H_{15}N_3O_2$

M_r = 341.37 g/mol

Following **General Procedure IIIa**, alkyne **133** (267 mg, 1.20 mmol, 1.0 eq), (*E*)-benzaldehyde oxime (218 mg, 1.80 mmol, 1.5 eq) and [bis(trifluoroacetoxy)iodo]benzene (774 mg, 1.80 mmol, 1.5 eq) were used in methanol/water (12 mL). After stirring for additional 2 h, the reaction was completed. The crude product was purified by flash column chromatography (25% ethyl acetate in hexanes) to give isoxazole **128** as yellow solid (351 mg, 1.03 mmol, 86%).

R_f = 0.34 (25% ethyl acetate in hexanes).

Melting point = 174 °C.

^{1}H NMR (400 MHz, methylene chloride-d_2) δ (ppm) = 9.78 (s, 1H, NH), 8.64 (d, *J* = 5.5 Hz, 1H, 3-H), 8.17 (dd, *J* = 5.4, 0.7 Hz, 1H, 4-H), 7.97 – 7.92 (m, 2H, 2‘‘-H, 6‘‘-H), 7.80 – 7.75 (m, 2H, 5-H, 4‘-H), 7.57 – 7.51 (m, 3H, 3‘‘-H, 4‘‘-H, 5‘‘-H), 7.32 (t, *J* = 7.9 Hz, 1H, 6-H), 7.12 (dd, *J* = 7.8, 0.8 Hz, 1H, 7-H), 4.07 (s, 3H, OCH_3).

^{13}C NMR (101 MHz, methylene chloride-d_2) δ (ppm) = 167.7 (C-5‘), 163.7 (C-3‘), 146.9 (C-8), 136.7 (C-3), 133.6 (C-4a), 133.0 (C-8a), 132.4 (C-9a), 131.0 (C-4‘‘), 129.5 (C-3‘‘, C-5‘‘), 128.7 (C-1‘‘), 128.1 (C-1), 127.4 (C-2‘‘, C-6‘‘), 122.5 (C-6), 121.8 (C-4b), 117.2 (C-4), 114.3 (C-5), 110.2 (C-7), 102.6 (C-4‘), 56.2 (OCH_3).

IR (ATR) $\tilde{\nu}$ (cm^{-1}) = 3461, 2230, 1558, 1427, 1434, 1320, 1257, 1220, 1054, 1029, 9718, 762, 722.

HRMS (EI) (*m/z*) = calculated for $C_{21}H_{15}N_3O_2^{\cdot+}$ $[M]^{\cdot+}$ 341.1159, found 341.1152.

Purity (HPLC, method 2a) > 95% (λ = 210 nm), > 95% (λ = 254 nm).

1-(3-Phenylisoxazol-5-yl)-9*H*-pyrido[3,4-*b*]indol-8-ol (134)

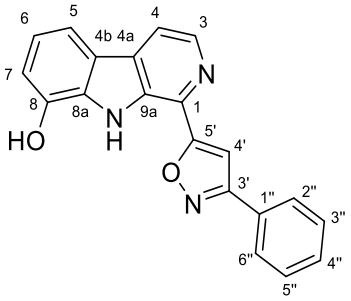

$C_{20}H_{13}N_3O_2$

M_r = 327.34 g/mol

Methyl ether **128** (307 mg, 0.900 mmol) was dissolved in glacial acetic acid (4.5 mL) and HBr (48% in water, 4.5 mL) was slowly added. The reaction mixture was stirred at 135 °C for 6 h and, after cooling to room temperature, diluted with water (35 mL) and cooled to 0 °C. The precipitate was filtered, washed with cold water (50 mL), resuspended in aq. NaOH solution (2 M, 200 mL) and extracted with ethyl acetate (4 x 100 mL). The combined organic layers were dried using a phase separation filter and the solvent was removed *in vacuo* to give sufficiently pure phenol **134** (186 mg, 0.569 mmol, 63%).

R_f = 0.23 (25% ethyl acetate in hexanes).

Melting point = 269 °C.

^{1}H NMR (500 MHz, DMSO-d_6) δ (ppm) = 11.27 (s, 1H, NH), 10.11 (s, 1H, OH), 8.53 (d, *J* = 5.0 Hz, 1H, 3-H), 8.28 (d, *J* = 5.0 Hz, 1H, 4-H), 8.11 – 8.06 (m, 2H, 2‘‘-H, 6‘‘-H), 7.86 (s, 1H, 4‘-H), 7.81 – 7.77 (m, 1H, 5-H), 7.62 – 7.55 (m, 3H, 3‘‘-H, 4‘‘-H, 5‘‘-H), 7.18 (t, *J* = 7.7 Hz, 1H, 6-H), 7.04 (dd, *J* = 7.6, 1.0 Hz, 1H, 7-H).

^{13}C NMR (126 MHz, DMSO-d_6) δ (ppm) = 169.6 (C-5‘), 162.5 (C-3‘), 143.6 (C-8), 138.6 (C-3), 132.0 (C-9a), 131.0 (C-1 or C-4a), 130.5 (C-8a, C-4‘‘), 129.6 (C-1 or C-4a), 129.2 (C-3‘‘, C-5‘‘), 128.4 (C-1‘‘), 126.9 (C-2‘‘, C-6‘‘), 122.4 (C-4b), 121.4 (C-6), 116.7 (C-4), 114.0 (C-7), 112.5 (C-5), 100.8 (C-4‘).

IR (ATR) $\tilde{\nu}$ (cm^{-1}) = 3324, 3063, 1560, 1463, 1436, 1399, 1374, 1288, 1265, 1240, 1226, 812, 763, 686.

HRMS (ESI) (*m/z*) = calculated for $C_{20}H_{14}N_3O_2^+$ $[M+H]^+$ 328.1081, found 328.1082.

Purity (HPLC, method 2c) > 95% (λ = 210 nm), > 95% (λ = 254 nm).

1-(3-Phenylisoxazol-5-yl)-9*H*-pyrido[3,4-*b*]indol-8-yl trifluoromethanesulfonate (127)

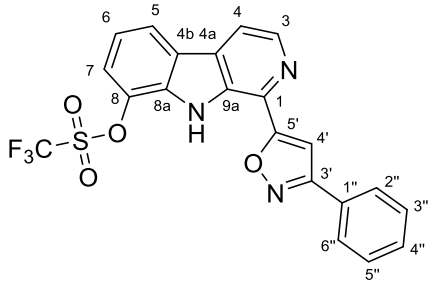

$C_{21}H_{12}F_3N_3O_4S$

M_r = 459.40 g/mol

Phenol **134** (131 mg, 0.400 mmol, 1.0 eq) was suspended in anhydrous methylene chloride/pyridine (2:1, 6.0 mL) under N_2 atmosphere. The suspension was cooled to 0 °C and purged with N_2 for 5 min. A solution of trifluoromethanesulfonic anhydride (0.080 mL, 0.48 mmol, 1.2 eq) in anhydrous methylene chloride (0.1 mL) was added dropwise over 10 min. The reaction mixture was stirred for 15 min at 0 °C, then warmed up to room temperature and stirred for further 1 h. The mixture was partitioned between methylene chloride (40 mL) and sat. aq. NaCl solution (40 mL). The aq. phase was further extracted with methylene chloride (2 x 40 mL), the combined organic layers were dried using a phase separation filter and the solvent removed *in vacuo*. The crude product was purified by flash column chromatography (30% → 40% methylene chloride in hexanes) to give triflate **127** as white solid (124 mg, 0.269 mmol, 67%).

R_f = 0.23 (50% methylene chloride in hexanes).

Melting point = 177 °C.

^{1}H NMR (400 MHz, methylene chloride-d_2) δ (ppm) = 9.70 (s, 1H, NH), 8.64 (d, J = 5.1 Hz, 1H, 3-H), 8.24 (dt, J = 7.9, 0.8 Hz, 1H, 5-H), 8.10 (dd, J = 5.1, 0.7 Hz, 1H, 4-H), 7.99 – 7.96 (m, 2H, 2‘‘-H, 6‘‘-H), 7.63 (dd, J = 8.1, 0.9 Hz, 1H, 7-H), 7.56 – 7.52 (m, 3H, 3‘‘-H, 4‘‘-H, 5‘‘-H), 7.48 (s, 1H, 4‘-H), 7.41 (t, J = 8.0 Hz, 1H, 6-H).

^{13}C NMR (101 MHz, methylene chloride-d_2) δ (ppm) = 170.7 (C-5‘), 163.5 (C-3‘), 140.9 (C-3), 135.2 (C-8), 133.3 (C-9a), 132.6 (C-8a), 131.4 (C-1 or C-4a), 130.9 (C-1 or C-4a), 130.8 (C-4‘‘), 129.5 (C-2‘‘, C-6‘‘), 129.0 (C-1‘‘), 127.4 (C-3‘‘, C-5‘‘), 125.5 (C-4b), 122.5 (C-5), 121.6 (C-6), 121.5 (C-7), 119.2 (q, J_{CF} = 320.8 Hz, CF_3), 116.7 (C-4), 100.9 (C-4‘).

IR (ATR) $\tilde{\nu}$ (cm^{-1}) = 3418, 1560, 1436, 1420, 1399, 1298, 1282, 1222, 1208, 1193, 1131, 1000, 934, 831, 800, 766.

HRMS (ESI) (*m/z*) = calculated for $C_{21}H_{13}F_3N_3O_4S^+$ $[M+H]^+$ 460.0573, found 460.0575.

Purity (HPLC, method 2a) > 95% (λ = 210 nm), > 95% (λ = 254 nm).

1-(3-Phenylisoxazol-5-yl)-9*H*-pyrido[3,4-*b*]indol-8-yl acetate (135)

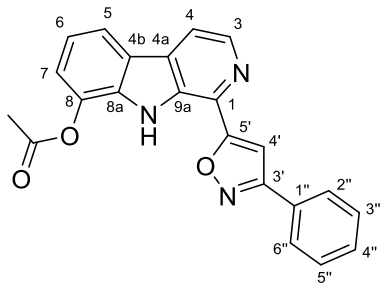

$C_{22}H_{15}N_3O_3$

M_r = 369.38 g/mol

In the synthesis of triflate **127**, flash column chromatography (40% methylene chloride in hexanes → 100% methylene chloride) gave also side product **135** as yellow solid (33.5 mg, 0.0907 mmol, 23%).

R_f = 0.10 (50% methylene chloride in hexanes).

Melting point = 249 °C.

^{1}H NMR (500 MHz, methylene chloride-d_2) δ (ppm) = 9.44 (s, 1H, NH), 8.57 (d, *J* = 5.0 Hz, 1H, 3-H), 8.08 – 8.05 (m, 2H, 4-H, 5-H), 7.97 – 7.94 (m, 2H, 2‘‘-H, 6‘‘-H), 7.56 – 7.51 (m, 3H, 3‘‘-H, 4‘‘-H, 5‘‘-H), 7.45 (s, 1H, 4‘-H), 7.44 (dd, *J* = 7.9, 1.0 Hz, 1H, 7-H), 7.33 (t, *J* = 7.8 Hz, 1H, 6-H), 2.53 (s, 3H, CH_3).

^{13}C NMR (126 MHz, methylene chloride-d_2) δ (ppm) = 171.3 (C-5‘), 169.6 (CO), 163.6 (C-3’), 140.4 (C-3), 137.1 (C-8), 133.5 (C-8a or C-9a), 133.3 (C-8a or C-9a), 131.6 (C-1 or C-4a), 130.9 (C-1 or C-4a), 130.9 (C-4’’), 129.6 (C-3’’, C-5’’), 129.3 (C-1’’), 127.5 (C-2’’, C-6’’), 124.3 (C-4b), 122.1 (C-7), 121.4 (C-6), 119.7 (C-5), 116.8 (C-4), 100.8 (C-4’), 21.8 (CH_3).

IR (ATR) $\tilde{\nu}$ (cm^{-1}) = 3383, 1746, 1556, 1442, 1424, 1399, 1278, 1200, 1164, 1013, 765, 690.

HRMS (ESI) (*m/z*) = calculated for $C_{22}H_{16}N_3O_3^+$ $[M+H]^+$ 370.1187, found 370.1190.

Purity (HPLC, method 2a) > 95% (λ = 210 nm), > 95% (λ = 254 nm).

3-Phenyl-1*H*-pyrazole (136)[302]

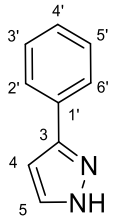

$C_9H_8N_2$

M_r = 144.18 g/mol

Following **General Procedure VIb**, phenyl triflate (45.2 mg, 0.200 mmol, 1.0 eq), 1*H*-pyrazol-3-ylboronic acid hydrate (31 mg, 0.24 mmol, 1.2 eq), Na_2CO_3 (64 mg, 0.60 mmol, 3.0 eq) and $Pd(PPh_3)_4$ (12 mg, 0.010 mmol, 0.05 eq) were used in degassed 1,4-dioxan/water (2.5 mL). The reaction was completed after 16 h and the extraction was performed with sat. aq. NaCl solution (15 mL) and ethyl acetate (3 x 15 mL). The crude product was purified by flash column chromatography (35% ethyl acetate in hexanes) to give biaryl **136** as colourless oil (20.1 mg, 0.139 mmol, 70%), which solidified in the cold (2 – 8°C).

R_f = 0.48 (50% ethyl acetate in hexanes).

Melting point = 60 °C (lit.[302] 60 – 62 °C).

^{1}H NMR (400 MHz, chloroform-*d*) δ (ppm) = 10.10 (s, 1H, NH), 7.71 – 7.65 (m, 2H, 2'-H, 6'-H), 7.52 (d, *J* = 2.3 Hz, 1H, 5-H), 7.35 – 7.29 (m, 2H, 3'-H, 5'-H), 7.28 – 7.22 (m, 1H, 4'-H), 6.53 (d, *J* = 2.2 Hz, 1H, 4-H).

^{13}C NMR (101 MHz, chloroform-*d*) δ (ppm) = 149.3 (C-3), 133.4 (C-5), 132.3 (C-1'), 128.9 (C-3', C-5'), 128.2 (C-4'), 126.0 (C-2', C-6'), 102.8 (C-4).

IR (ATR) $\tilde{\nu}$ (cm^{-1}) = 3159, 2921, 1456, 1441, 1353, 1072, 1048, 953, 918, 826, 749, 693.

HRMS (EI) (*m/z*) = calculated for $C_9H_8N_2^{\cdot+}$ $[M]^{\cdot+}$ 144.0682, found 144.0681.

Purity (HPLC, method 2e) > 95% (λ = 210 nm), > 95% (λ = 254 nm).

2-((Trimethylsilyl)ethynyl)-9*H*-carbazole (138)[223]

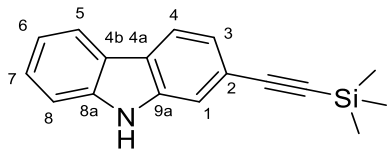

$C_{17}H_{17}NSi$

M_r = 263.42 g/mol

Following **General Procedure Ic**, 9*H*-carbazol-2-yl trifluoromethanesulfonate (**137**) (94.6 mg, 0.300 mmol, 1.0 eq), tetra-*n*-butylammonium iodide (0.33 g, 0.90 mmol, 3.0 eq), $Pd(PPh_3)_2Cl_2$ (21 mg, 0.030 mmol, 0.1 eq), CuI (17 mg, 0.090 mmol, 0.3 eq) and trimethylsilylacetylene (0.085 mL, 0.60 mmol, 2.0 eq) were used in anhydrous DMF/triethylamine (1.7 mL). The crude product was purified by flash column chromatography (5% ethyl acetate in hexanes) to give alkyne **138** as beige solid (78.5 mg, 0.298 mmol, 99%).

R_f = 0.58 (25% ethyl acetate in hexanes).

Melting point = 217 °C (lit.[223] 218 °C).

^{1}H NMR (400 MHz, DMSO-d_6) δ (ppm) = 11.36 (s, 1H, NH), 8.16 – 8.06 (m, 2H, 4-H, 5-H), 7.56 (dd, *J* = 1.5, 0.7 Hz, 1H, 1-H), 7.51 (dt, *J* = 8.2, 1.0 Hz, 1H, 8-H), 7.41 (ddd, *J* = 8.2, 7.0, 1.2 Hz, 1H, 7-H), 7.22 (dd, *J* = 8.0, 1.4 Hz, 1H, 3-H), 7.18 (ddd, *J* = 7.9, 7.1, 1.0 Hz, 1H, 6-H), 0.26 (s, 9H, $Si(CH_3)_3$).

^{13}C NMR (101 MHz, DMSO-d_6) δ (ppm) = 140.5 (C-8a), 139.1 (C-9a), 126.3 (C-7), 122.9 (C-4a), 122.1 (C-3), 121.9 (C-4b), 120.6 (C-4 or C-5), 120.4 (C-4 or C-5), 119.0 (C-6), 118.6 (C-2), 114.1 (C-1), 111.2 (C-8), 106.8 (SiC<u>C</u>), 93.0 (Si<u>C</u>C), 0.0 ($Si(CH_3)_3$).

IR (ATR) $\tilde{\nu}$ (cm^{-1}) = 3405, 2956, 2154, 1607, 1458, 1440, 1327, 1246, 836, 725.

HRMS (ESI) (*m/z*) = calculated for $C_{17}H_{17}NSi^{\cdot+}$ $[M]^{\cdot+}$ 263.1125, found 263.1125.

Purity (HPLC, method 2c) > 95% (λ = 210 nm), > 95% (λ = 254 nm).

tert-Butyl (3-(9*H*-carbazol-2-yl)prop-2-yn-1-yl)carbamate (140)

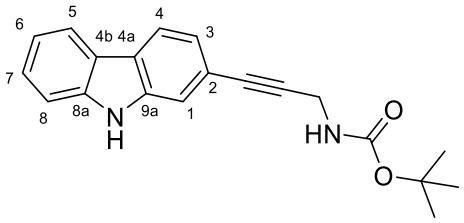

$C_{20}H_{20}N_2O_2$

M_r = 320.39 g/mol

Following **General Procedure Ic**, 9*H*-carbazol-2-yl trifluoromethanesulfonate (**137**) (94.6 mg, 0.300 mmol, 1.0 eq), tetra-*n*-butylammonium iodide (0.33 g, 0.90 mmol, 3.0 eq), $Pd(PPh_3)_2Cl_2$ (21 mg, 0.030 mmol, 0.1 eq), CuI (17 mg, 0.090 mmol, 0.3 eq) and *N*-Boc-propargylamine (93 mg, 0.60 mmol, 2.0 eq) were used in anhydrous DMF/triethylamine (1.7 mL). The crude product was purified two times by flash column chromatography (2% methanol in methylene chloride, 20% → 40% ethyl acetate in hexanes) to give alkyne **140** as beige solid (67.4 mg, 0.21 mmol, 70%).

R_f = 0.41 (25% ethyl acetate in hexanes).

Melting point = 161 °C.

^{1}H NMR (400 MHz, chloroform-*d*) δ (ppm) = 8.14 (s, 1H, 9-NH), 8.05 (d, *J* = 7.8 Hz, 1H, 5-H), 7.99 (d, *J* = 8.0 Hz, 1H, 4-H), 7.49 (d, *J* = 1.3 Hz, 1H, 1-H), 7.45 – 7.40 (m, 2H, 7-H, 8-H), 7.29 (dd, *J* = 8.0, 1.4 Hz, 1H, 3-H), 7.25 – 7.22 (m, 1H, 6-H, collapses with chloroform peak), 4.83 (s, 1H, CONH), 4.21 (d, *J* = 5.4 Hz, 2H, CH_2), 1.49 (s, 9H, $C(CH_3)_3$).

^{13}C NMR (101 MHz, chloroform-*d*) δ (ppm) = 155.5 (CONH), 140.2 (C-8a), 139.1 (C-9a), 126.5 (C-7), 123.6 (C-4a), 123.4 (C-3), 123.1 (C-4b), 120.7 (C-5), 120.3 (C-4), 119.9 (C-6), 119.7 (C-2), 114.1 (C-1), 110.9 (C-8), 84.9 ($CH_2\underline{C}C$), 84.3 ($CH_2C\underline{C}$), 80.2 ($\underline{C}(CH_3)_3$), 31.5 (CH_2), 28.6 ($C(\underline{C}H_3)_3$).

IR (ATR) $\tilde{\nu}$ (cm^{-1}) = 3398, 3361, 1690, 1514, 1459, 1440, 1368, 1327, 1283, 1246, 1160, 1139, 816, 750, 730.

HRMS (ESI) (*m/z*) = calculated for $C_{20}H_{20}N_2O_2^{\cdot+}$ $[M]^{\cdot+}$ 320.1520, found 320.1520.

Purity (HPLC, method 2c) > 95% (λ = 210 nm), > 95% (λ = 254 nm).

3-(9*H*-Carbazol-2-yl)prop-2-yn-1-ol (141)

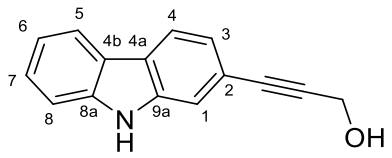

$C_{15}H_{11}NO$

M_r = 221.26 g/mol

Following **General Procedure Ic**, 9*H*-carbazol-2-yl trifluoromethanesulfonate (**137**) (94.6 mg, 0.300 mmol, 1.0 eq), tetra-*n*-butylammonium iodide (0.33 g, 0.90 mmol, 3.0 eq), $Pd(PPh_3)_2Cl_2$ (21 mg, 0.030 mmol, 0.1 eq), CuI (17 mg, 0.090 mmol, 0.3 eq) and propargyl alcohol (0.035 mL, 0.60 mmol, 2.0 eq) were used in anhydrous DMF/triethylamine (1.7 mL). The crude product was purified two times by flash column chromatography (2% methanol in methylene chloride, 20% → 40% ethyl acetate in hexanes) to give alkyne **141** as beige solid (55.5 mg, 0.251 mmol, 84%).

R_f = 0.33 (2% methanol in methylene chloride).

Melting point = 199 °C.

^{1}H NMR (500 MHz, DMSO-d_6) δ (ppm) = 11.35 (s, 1H, NH), 8.17 – 8.06 (m, 2H, 4-H, 5-H), 7.53 (d, *J* = 1.3 Hz, 1H, 1-H), 7.50 (d, *J* = 8.1 Hz, 1H, 8-H), 7.40 (ddd, *J* = 8.2, 7.0, 1.2 Hz, 1H, 7-H), 7.22 – 7.15 (m, 2H, 3-H, 6-H), 5.33 (t, *J* = 5.9 Hz, 1H, OH), 4.35 (d, *J* = 5.8 Hz, 2H, CH_2).

^{13}C NMR (126 MHz, DMSO-d_6) δ (ppm) = 140.3 (C-8a), 139.3 (C-9a), 126.1 (C-7), 122.5 (C-4a), 122.0 (C-4b), 121.8 (C-3), 120.5 (C-4 or C-5), 120.4 (C-4 or C-5), 119.0 (C-2), 118.9 (C-6), 113.8 (C-1), 111.1 (C-8), 89.0 ($CH_2\underline{C}C$), 84.9 ($CH_2C\underline{C}$), 49.6 (CH_2).

IR (ATR) $\tilde{\nu}$ (cm^{-1}) = 3396, 2922, 1606, 1458, 1438, 1325, 1231, 1022, 822, 746, 726.

HRMS (EI) (*m/z*) = calculated for $C_{15}H_{11}NO^{\cdot+}$ $[M]^{\cdot+}$ 221.0836, found 221.0830.

Purity (HPLC, method 2e) > 95% (λ = 210 nm), > 95% (λ = 254 nm).

3-(1-(3-Phenylisoxazol-5-yl)-9*H*-pyrido[3,4-*b*]indol-8-yl)prop-2-yn-1-ol (142)

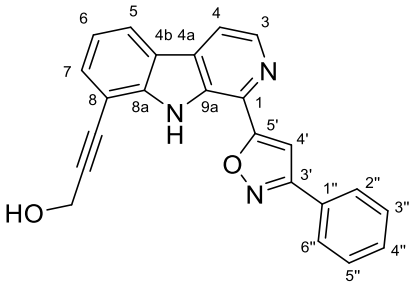

$C_{23}H_{15}N_3O_2$

M_r = 365.39 g/mol

Following **General Procedure Ic**, triflate **127** (50.1 mg, 0.109 mmol, 1.0 eq), tetra-*n*-butylammonium iodide (121 mg, 0.327 mmol, 3.0 eq), $Pd(PPh_3)_2Cl_2$ (8 mg, 0.01 mmol, 0.1 eq), CuI (6 mg, 0.03 mmol, 0.3 eq) and propargyl alcohol (0.013 mL, 0.22 mmol, 2.0 eq) were used in anhydrous DMF/triethylamine (1.2 mL). After the extraction, the combined organic layers were additionally washed with water (2 x 50 mL). The crude product was purified two times by flash column chromatography (25% ethyl acetate in hexanes → 100% ethyl acetate, 100% methylene chloride → 1.0% methanol in methylene chloride) to give alkyne **142** as off-white solid (34.4 mg, 0.0941 mmol, 86%).

R_f = 0.15 (25% ethyl acetate in hexanes).

Melting point = 236 °C.

^{1}H NMR (500 MHz, DMSO-d_6) δ (ppm) = 10.90 (s, 1H, NH), 8.61 (d, *J* = 5.0 Hz, 1H, 3-H), 8.41 – 8.36 (m, 2H, 4-H, 5-H), 8.10 – 8.06 (m, 2H, 2‘‘-H, 6‘‘-H), 7.84 (s, 1H, 4‘-H), 7.72 (dd, *J* = 7.4, 1.1 Hz, 1H, 7-H), 7.62 – 7.56 (m, 3H, 3‘‘-H, 4‘‘-H, 5‘‘-H), 7.36 (t, *J* = 7.6 Hz, 1H, 6-H), 5.50 (t, *J* = 5.9 Hz, 1H, OH), 4.51 (d, *J* = 5.8 Hz, 2H, CH_2).

^{13}C NMR (101 MHz, DMSO-d_6) δ (ppm) = 169.2 (C-5’), 162.4 (C-3’), 141.5 (C-8a), 139.5 (C-3), 132.7 (C-9a), 132.3 (C-7), 130.9 (C-4a), 130.5 (C-4’’), 130.3 (C-1), 129.3 (C-3’’, C-5’’), 128.4 (C-1’’), 126.8 (C-2’’, C-6’’), 122.6 (C-5), 121.1 (C-4b), 120.7 (C-6), 116.7 (C-4), 107.1 (C-8), 101.4 (C-4’), 95.1, ($CH_2\underline{C}C$), 79.6 ($CH_2C\underline{C}$), 50.0 (CH_2).

IR (ATR) $\tilde{\nu}$ (cm^{-1}) = 3464, 3253, 1608, 1559, 1441, 1430, 1398, 1305, 1294, 1283, 1168, 1031, 948, 765, 739, 691.

HRMS (ESI) (*m/z*) = calculated for $C_{23}H_{16}N_3O_2^+$ $[M+H]^+$ 366.1238, found 366.1235.

Purity (HPLC, method 2c) > 95% (λ = 210 nm), > 95% (λ = 254 nm).

5-(8-(1*H*-Pyrazol-3-yl)-9*H*-pyrido[3,4-*b*]indol-1-yl)-3-phenylisoxazole (143)

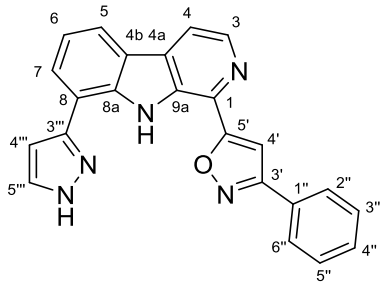

$C_{23}H_{15}N_5O$

M_r = 377.41 g/mol

Following **General Procedure VIb**, triflate **127** (59.7 mg, 0.130 mmol, 1.0 eq), 1*H*-pyrazol-3-ylboronic acid hydrate (34 mg, 0.26 mmol, 2.0 eq), Na_2CO_3 (64 mg, 0.60 mmol, 3.0 eq) and $Pd(PPh_3)_4$ (6 mg, 0.005 mmol, 0.04 eq) were used in degassed 1,4-dioxan/water (2.0 mL). The reaction was completed after 20 h and the extraction was performed with sat. aq. NaCl solution (100 mL) and ethyl acetate (4 x 50 mL). The crude product was purified two times by flash column chromatography (100% methylene chloride → 10% methanol in methylene chloride, 0.1% → 1.0% methanol in methylene chloride) to give pyrazole **143** as pale yellow solid (20.1 mg, 0.0533 mmol, 41%).

R_f = 0.38 (0.5% methanol in methylene chloride).

Melting point = 315 °C (decomposition).

^{1}H NMR (400 MHz, DMSO-d_6) δ (ppm) = 13.54 (s, 1H, 1'''-NH), 11.75 (s, 1H, 9-NH), 8.61 (d, *J* = 5.1 Hz, 1H, 3-H), 8.40 (d, *J* = 5.1 Hz, 1H, 4-H), 8.33 (d, *J* = 7.8 Hz, 1H, 5-H), 8.14 (dd, *J* = 7.5, 1.1 Hz, 1H, 7-H), 8.12 – 8.07 (m, 2H, 2''-H, 6''-H), 8.01 (dd, *J* = 2.5, 1.0 Hz, 1H, 5'''-H), 7.86 (s, 1H, 4'-H), 7.64 – 7.57 (m, 3H, 3''-H, 4''-H, 5''-H), 7.45 (t, *J* = 7.6 Hz, 1H, 6-H), 7.11 (t, *J* = 2.0 Hz, 1H, 4'''-H).

^{13}C NMR (101 MHz, DMSO-d_6) δ (ppm) = 170.4 (C-5'), 162.6 (C-3'), 149.5 (C-3'''), 139.2 (C-3), 137.3 (C-8a), 132.0 (C-9a), 130.6 (C-5'''), 130.4 (C-4a), 130.2 (C-4''), 129.4 (C-1), 129.3 (C-3'', C-5''), 128.3 (C-1''), 126.9 (C-2'', C-6''), 125.9 (C-7), 121.1 (C-5), 121.0 (C-4b), 120.7 (C-6), 117.3 (C-8), 116.9 (C-4), 102.2 (C-4'''), 100.6 (C-4').

IR (ATR) $\tilde{\nu}$ (cm^{-1}) = 3379, 3160, 2921, 1608, 1561, 1459, 1425, 1400, 1278, 1222, 1212, 1058, 951, 796, 750, 738.

HRMS (ESI) (*m/z*) = calculated for $C_{23}H_{16}N_5O^+$ $[M+H]^+$ 378.1350, found 378.1350.

Purity (HPLC, method 2a) > 95% (λ = 210 nm), > 95% (λ = 254 nm).

Ethyl 3-(3-nitropyridine-4-yl)-2-oxopropanoate /
ethyl 2-hydroxy-3-(3-nitropyridin-4-yl)acrylate (146[a])[303]

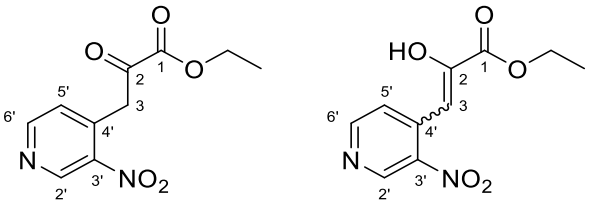

$C_{10}H_{10}N_2O_5$

M_r = 238.20 g/mol

Sodium (1.21 g, 52.5 mmol, 2.5 eq) was dissolved in absolute ethanol (38 mL) under N_2 atmosphere. Diethyl oxalate (5.7 mL, 42 mmol, 2.0 eq) was added and the reaction mixture stirred for 15 min at room temperature. Then a solution of 4-methyl-3-nitropyridine (2.36 mL, 21.0 mmol, 1.0 eq) in absolute ethanol (38 mL) was added dropwise and the reaction mixture stirred for further 17 h. Water (0.5 mL) was added and the solvent removed *in vacuo*. The residue was redissolved in water (150 mL) and the pH adjusted to 4 with acetic acid. The precipitate was filtered, washed with cold water (50 mL) and dried to give a mixture of keto-enol tautomers **146[a]** (ratio 1.0:0.35 determined *via* ^{1}H NMR spectrum) as red solid (3.52 g, 14.8 mmol, 70%).

R_f = 0.35 (50% ethyl acetate in hexanes).

Melting point = 133 °C (lit.[303] 132 – 133 °C).

^{1}H NMR (500 MHz, chloroform-*d*) δ (ppm) = 9.37 (s, 1H, 2'-H (keto)), 9.14 (s, 1H, 2'-H (enol)), 8.82 (d, *J* = 5.0 Hz, 1H, 6'-H (keto)), 8.77 (d, *J* = 5.3 Hz, 1H, 6'-H (enol)), 8.21 (d, *J* = 5.4 Hz, 1H, 5'-H (enol)), 7.31 (d, *J* = 5.1 Hz, 1H, 5'-H (keto)), 6.98 (s, 1H, 3-H (enol)), 4.60 (s, 2H, 3-H (keto)), 4.47 – 4.38 (m, 4H, OCH_2 (keto), OCH_2 (enol)), 1.42 (t, *J* = 7.2 Hz, 3H, CH_3 (enol)), 1.41 (t, *J* = 7.1 Hz, 3H, CH_3 (keto)). Signal for OH (enol) not observed.

^{13}C NMR (126 MHz, chloroform-*d*) δ (ppm) = 188.0 (C-2 (keto)), 165.0 (C-1 (enol)), 160.1 (C-1 (keto)), 154.2 (C-6' (keto)), 153.1 (C-6' (enol)), 146.8 (C-2' (keto)), 146.0 (C-2' (enol)), 145.0 (C-2 (enol)), 144.8 (C-3' (keto)), 144.0 (C-3' (enol)), 138.2 (C-4' (keto)), 136.3 (C-4' (enol)), 127.8 (C-5' (keto)), 124.7 (C-5' (enol)), 100.4 (C-3 (enol)), 64.0 (OCH_2 (enol)), 63.5 (OCH_2 (keto)), 43.9 (C-3 (keto)), 14.3 (CH_3 (enol)), 14.1 (CH_3 (keto)),

IR (ATR) $\tilde{\nu}$ (cm^{-1}) = 2981, 1709, 1654, 1591, 1519, 1493, 1465, 1424, 1324, 1276, 1214, 1140, 110, 1017, 832, 790.

HRMS (ESI) (*m/z*) = calculated for $C_{10}H_9N_2O_5^-$ $[M-H]^-$ 237.0517, found 237.0515.

Purity (HPLC, method 2g) > 93% (λ = 210 nm), > 95% (λ = 254 nm).

Ethyl 1*H*-pyrrolo[2,3-*c*]pyridine-2-carboxylate (147^{a})[304]

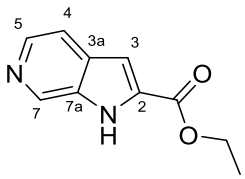

$C_{10}H_{10}N_2O_2$

M_r = 190.20 g/mol

Nitro compound **146^{a}** (1.55 g, 6.50 mmol, 1.0 eq) was dissolved in glacial acetic acid (35 mL) and iron powder (1.82 g, 32.50 mmol, 5.0 eq) was added. The reaction mixture was stirred at 60 °C for 4 h and, after cooling to room temperature, filtered through a pad of celite. The pad was washed with methanol (50 mL) and the solvent was removed *in vacuo*. The residue was resuspended in ethanol (50 mL) and solid $NaHCO_3$ (approx. 1.5 g) was cautiously added. The mixture was stirred for 15 min, then the solvent was again removed *in vacuo*. The crude product was purified by flash column chromatography (4% methanol in methylene chloride) to give 6-azaindole **147^{a}** as off-white solid (912 mg, 4.79 mmol, 74%).

R_f = 0.33 (35% ethyl acetate in hexanes).

Melting point = 211 °C (lit.[304] 212 – 214 °C).

^{1}H NMR (400 MHz, chloroform-*d*) δ (ppm) = 9.83 (s, 1H, NH), 8.97 (t, *J* = 1.1 Hz, 1H, 7-H), 8.34 (d, *J* = 5.6 Hz, 1H, 5-H), 7.61 (dd, *J* = 5.6, 1.2 Hz, 1H, 4-H), 7.21 (d, *J* = 0.9 Hz, 1H, 3-H), 4.46 (q, *J* = 7.1 Hz, 2H, CH_2), 1.43 (t, *J* = 7.1 Hz, 3H, CH_3).

^{13}C NMR (101 MHz, chloroform-*d*) δ (ppm) = 161.6 (COO), 139.5 (C-5), 136.0 (C-7), 133.6 (C-7a), 132.1 (C-3a), 131.0 (C-2), 116.6 (C-4), 107.3 (C-3), 61.8 (CH_2), 14.5 (CH_3).

IR (ATR) $\tilde{\nu}$ (cm^{-1}) = 3076, 2927, 2687, 1914, 1840, 1711, 1613, 1481, 1372, 1322, 1368, 1160, 1168, 1024, 972, 828, 789, 743.

HRMS (ESI) (*m/z*) = calculated for $C_{10}H_{11}N_2O_2^{+}$ $[M+H]^{+}$ 191.0815, found 191.0816.

Purity (HPLC, method 2e) > 95% (λ = 210 nm), > 95% (λ = 254 nm).

Ethyl 3-bromo-1*H*-pyrrolo[2,3-*c*]pyridine-2-carboxylate (148[a])[245]

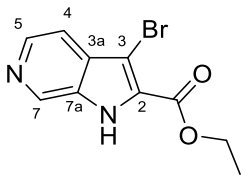

$C_{10}H_9BrN_2O_2$

M_r = 269.10 g/mol

6-Azaindole **147[a]** (1.43 g, 7.50 mmol, 1.0 eq) dissolved in anhydrous DMF (30 mL) under N_2 atmosphere and stirred at room temperature for 5 min, then *N*-bromosuccinimide (1.35 g, 7.50 mmol, 1.0 eq) was added in portions. After stirring for additional 3 h, the reaction mixture was cooled to 0 °C and diluted with ice water (100 mL). The precipitate was filtered, washed with cold water (100 mL) and dried to give bromide **148[a]** as pale yellow solid (1.87 g, 6.95 mmol, 93%).

R_f = 0.31 (50% ethyl acetate in hexanes).

Melting point = 260 °C.

^{1}H NMR (400 MHz, DMSO-d_6) δ (ppm) = 12.75 (s, 1H, NH), 8.88 (s, 1H, 7-H), 8.28 (d, *J* = 5.6 Hz, 1H, 5-H), 7.52 (dd, *J* = 5.6, 1.2 Hz, 1H, 4-H), 4.41 (q, *J* = 7.1 Hz, 2H, CH_2), 1.38 (t, *J* = 7.1 Hz, 3H, CH_3).

^{13}C NMR (101 MHz, DMSO-d_6) δ (ppm) = 159.8 (COO), 139.2 (C-5), 137.0 (C-7), 132.4 (C-7a), 131.0 (C-3a), 127.0 (C-2), 114.0 (C-4), 94.4 (C-3), 61.4 (CH_2), 14.1 (CH3).

IR (ATR) $\tilde{\nu}$ (cm^{-1}) = 3413, 3065, 2985, 2621, 1902, 1713, 1612, 1494, 1369, 1322, 1265, 1205, 1021, 928, 808, 744, 654.

HRMS (ESI) (*m/z*) = calculated for $C_{10}H_{10}{}^{79}BrN_2O_2$ $[M+H]^+$ 268.9921, found 268.9923.

Purity (HPLC, method 2e) > 95% (λ = 210 nm), > 95% (λ = 254 nm).

3-Bromo-1*H*-pyrrolo[2,3-*c*]pyridine-2-carboxylic acid (170[a])

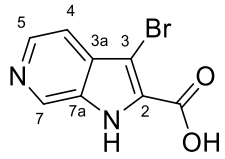

$C_8H_5BrN_2O_2$

M_r = 241.04 g/mol

Ester **148[a]** (404 mg, 1.50 mmol, 1.0 eq) was suspended in ethanol (20 mL) and aq. NaOH solution (2 M, 2.25 mL, 4.50 mmol, 3.0 eq) was added. The reaction mixture was stirred at 60 °C for 4.5 h and, after cooling to room temperature, the solvent was removed *in vacuo*. The residue was resuspended in water (15 mL) and the pH adjusted to 4 with acetic acid. The precipitate was filtered, washed with cold water (15 mL) and dried to give carboxylic acid **170[a]** as white solid (354 mg, 1.47 mmol, 98%).

R_f = 0.00 (3% methanol in ethyl acetate).

Melting point = 262 °C.

^{1}H NMR (400 MHz, DMSO-d_6) δ (ppm) = 12.64 (s, 1H, NH), 8.85 (s, 1H, 7-H), 8.26 (d, J = 5.7 Hz, 1H, 5-H), 7.53 (d, J = 5.6 Hz, 1H, 4-H). Signal for COOH not observed.

^{13}C NMR (101 MHz, DMSO-d_6) δ (ppm) = 161.3 (COOH), 138.8 (C-5), 136.6 (C-7), 132.2 (C-7a), 131.2 (C-3a), 128.6 (C-2), 114.0 (C-4), 93.7 (C-3).

IR (ATR) $\tilde{\nu}$ (cm^{-1}) = 3398, 3057, 3564, 2100, 1716, 1639, 1572, 1350, 1321, 1231, 1151, 915, 854, 804.

HRMS (ESI) (m/z) = calculated for $C_8H_6{}^{79}BrN_2O_2^+$ $[M+H]^+$ 240.9607, found 240.9606.

Purity (HPLC) n. d.

3-Bromo-1*H*-pyrrolo[2,3-*c*]pyridine-2-carboxamide (149[a])

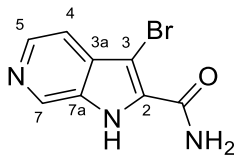

$C_8H_6BrN_3O$

M_r = 240.06 g/mol

Carboxylic acid **170[a]** (301 mg, 1.25 mmol, 1.0 eq) was suspended in anhydrous THF (50 mL) under N_2 atmosphere. *N*,*N*-Diisopropylethylamine (1.09 mL, 6.25 mL, 5.0 eq), 1-hydroxybenzotriazole (186 mg, 1.38 mmol, 1.1 eq), and 1-ethyl-3-(3-dimethylaminopropyl)carbodiimide hydrochloride (264 mg, 1.38 mmol, 1.1 eq) were added and the reaction mixture was stirred at room temperature for 15 min. Then, ammonium carbonate (961 mg, 10.0 mmol, 8.0 eq) was added and the suspension was stirred at room temperature for 22 h. The solvent was removed *in vacuo* and the residue partitioned between sat. aq. Na_2CO_3 solution (80 mL) and ethyl acetate (80 mL). The aqueous phase was further extracted with ethyl acetate (2 x 80 mL) and the combined organic layers were dried over Na_2SO_4, filtered and concentrated *in vacuo*. The crude product was purified by flash column chromatography (3% methanol in ethyl acetate) to give primary amide **149[a]** as off-white solid (183 mg, 0.762 mmol, 61%).

R_f = 0.17 (3% methanol in ethyl acetate).

Melting point = 264 °C.

^{1}H NMR (400 MHz, DMSO-d_6) δ (ppm) = 12.52 (s, 1H, NH), 8.82 (s, 1H, 7-H), 8.24 (d, *J* = 5.6 Hz, 1H, 5-H), 8.06 (s, 1H, $CONH_2$), 7.56 (s, 1H, $CONH_2$), 7.48 (d, *J* = 5.6 Hz, 1H, 4-H).

^{13}C NMR (101 MHz, DMSO-d_6) δ (ppm) = 161.2 ($CONH_2$), 138.8 (C-5), 136.2 (C-7), 131.9 (C-7a), 131.1 (C-3a), 129.4 (C-2), 113.6 (C-4), 89.2 (C-3).

IR (ATR) $\tilde{\nu}$ (cm^{-1}) = 3406, 3189, 2922, 2853, 1894, 1743, 1657, 1599, 1382, 1232, 1043, 919, 808, 765, 733, 696, 655.

HRMS (ESI) (*m/z*) = calculated for $C_8H_7{}^{79}BrN_3O^+$ $[M+H]^+$ 239.9767 found: 239.9767.

Purity (HPLC, method 2g) > 95% (λ = 210 nm), > 95% (λ = 254 nm).

Ethyl (*E*)-3-(2-ethoxyvinyl)-1*H*-pyrrolo[2,3-*c*]pyridine-2-carboxylate (152[a])

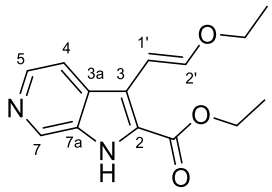

$C_{14}H_{16}N_2O_3$

M_r = 260.29 g/mol

Following **General Procedure VIc**, bromide **148[a]** (444 mg, 1.65 mmol, 1.0 eq), $Pd(PPh_3)_4$ (191 mg, 0.165 mmol, 0.1 eq), (*E*)-2-ethoxyvinylboronic acid pinacol ester (0.70 mL, 3.3 mmol, 2.0 eq) and Cs_2CO_3 (2.69 g, 8.25 mmol, 5.0 eq) were used in degassed 1,4-dioxane (10 mL) and water (3.3 mL). The reaction mixture was stirred at 95 °C for 18 h and the extraction was performed with sat. aq. NH_4Cl solution (100 mL) and ethyl acetate (3 x 100 mL). The crude product was purified by flash column chromatography (1% → 3% methanol in methylene chloride) to give enol ether **152[a]** as yellow solid (244 mg, 0.937 mmol, 57%).

R_f = 0.24 (3% methanol in methylene chloride).

Melting point = 204 °C.

^{1}H NMR (400 MHz, chloroform-*d*) δ (ppm) = 9.27 (s, 1H, NH), 8.88 (d, J = 1.1 Hz, 1H, 7-H), 8.32 (d, J = 5.7 Hz, 1H, 5-H), 7.70 (d, J = 5.6 Hz, 1H, 4-H), 7.32 (d, J = 13.4 Hz, 1H, 2'-H), 6.61 (d, J = 13.3 Hz, 1H, 1'-H), 4.46 (q, J = 7.1 Hz, 2H, $COOCH_2$), 4.01 (q, J = 7.0 Hz, 2H, OCH_2), 1.45 (t, J = 7.1 Hz, 3H, $COOCH_2\underline{CH_3}$), 1.40 (t, J = 7.0 Hz, 3H, $OCH_2\underline{CH_3}$).

^{13}C NMR (101 MHz, chloroform-*d*) δ (ppm) = 161.9 (COO), 150.4 (C-2'), 139.0 (C-5), 136.0 (C-7), 133.0 (C-7a), 129.9 (C-3a), 124.9 (C-2), 118.9 (C-3), 116.5 (C-4), 98.3 (C-1'), 65.4 (OCH_2), 61.6 ($COO\underline{CH_2}$), 14.9 ($OCH_2\underline{CH_3}$), 14.6 ($COOCH_2\underline{CH_3}$).

IR (ATR) $\tilde{\nu}$ (cm^{-1}) = 3081, 2976, 2846, 1713, 1641, 1613, 1455, 1330, 1268, 1172, 1028, 922, 796, 773, 663.

HRMS (ESI) (*m/z*) = calculated for $C_{14}H_{17}N_2O_3^+$ $[M+H]^+$ 261.1234, found 261.1235.

Purity (HPLC, method 2e) > 95% (λ = 210 nm), > 95% (λ = 254 nm).

2,9-Dihydro-1*H*-pyrrolo[2,3-*c*:5,4-*c'*]dipyridin-1-one (151[a2])

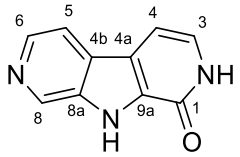

$C_{10}H_7N_3O$

M_r = 185.19 g/mol

Enol ether **152[a]** (234 mg, 0.900 mmol, 1.0 eq) was suspended in DMF (0.5 mL) in a pressure tube. Ammonium acetate (3.47 g, 45.0 mmol, 50 eq) was added and the mixture stirred for 72 h at 140 °C. Then it was transferred to a flask containing cold water (40 mL) and, after adjusting pH 8 with sat. aq. $NaHCO_3$ solution, the suspension was kept in the fridge for 48 h. The precipitate was collected by filtration, washed with water (20 mL) and ethyl acetate (10 mL) and dried to give pure pyridone **151[a]** as brown solid. Additionally, the filtrate was diluted with water (40 mL) and extracted with chloroform/isopropanol (3:1, 5 x 40 mL). The combined organic layers were dried using a phase separation filter and concentrated *in vacuo*. The crude product was purified by flash column chromatography (10% methanol in methylene chloride → 100% methanol) to give further pyridone **151[a]** as brown solid (in total 115 mg, 0.621 mmol, 69%).

R_f = 0.22 (10% methanol and 1% triethylamine in ethyl acetate).

Melting point = 250 °C (decomposition).

^{1}H NMR (400 MHz, DMSO-d_6) δ (ppm) = 12.38 (s, 1H, NH), 11.60 (s, 1H, CONH), 8.91 (s, 1H, 8-H), 8.31 (d, *J* = 5.4 Hz, 1H, 6-H), 8.03 (d, *J* = 5.3 Hz, 1H, 5-H), 7.14 (t, *J* = 6.2 Hz, 1H, 3-H), 7.04 (d, *J* = 6.8 Hz, 1H, 4-H).

^{13}C NMR (101 MHz, DMSO-d_6) δ (ppm) = 156.0 (C-1), 138.2 (C-6), 136.1 (C-8), 135.2 (C-8a), 130.0 (C-9a), 126.5 (C-4b), 125.2 (C-3), 122.8 (C-4a), 115.6 (C-5), 99.8 (C-4).

IR (ATR) $\tilde{\nu}$ (cm^{-1}) = 3061, 2981, 2842, 1645, 1442, 1354, 1275, 1202, 745, 660.

HRMS (EI) (*m/z*) = calculated for $C_{10}H_7N_3O^{\cdot+}$ $[M]^{\cdot+}$ 185.0584, found 185.0589.

Purity (HPLC, method 2i) > 95% (λ = 210 nm), > 95% (λ = 254 nm).

[2] Pyridone **151[a]** was first described within the master thesis of FRANCESCA DONÀ, but was not analytically pure.

1-Ethynyl-9*H*-pyrrolo[2,3-*c*:5,4-*c'*]dipyridine (157)

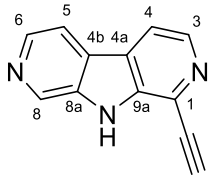

$C_{12}H_7N_3$

M_r = 193.21 g/mol

Pyridone **151[a]** (46.3 mg, 0.250 mmol, 1.0 eq) was dissolved in anhydrous pyridine (7.5 mL) under N_2 atmosphere. The solution was cooled to 0 °C and purged with N_2 for 5 min. Trifluoromethanesulfonic anhydride (0.042 mL, 0.25 mmol, 1.0 eq) was added dropwise over 15 min and the reaction mixture was warmed up to room temperature and stirred for 30 min. The mixture was again cooled to 0 °C and another amount of trifluoromethanesulfonic anhydride (0.021 mL, 0.13 mmol, 0.5 eq) was added dropwise. After stirring at room temperature for 30 min, another amount of trifluoromethanesulfonic anhydride (0.021 mL, 0.13 mmol, 0.5 eq) was added once more dropwise at 0 °C and the reaction mixture stirred at room temperature for further 1 h. The solution was partitioned between ethyl acetate (50 mL) and a mixture of water (100 mL) and aq. HCl (2 M, 10 mL). The aq. phase was further extracted with ethyl acetate (2 x 50 mL), the combined organic layers were washed with aq. HCl (2 M, 30 mL) and dried using a phase separation filter. The crude product was purified by flash column chromatography (50% ethyl acetate in hexanes) to give an inseparable mixture of mono- and ditriflated intermediates **155** (R_f = 0.50, 100% ethyl acetate; HRMS (EI) (*m/z*) = calculated for $C_{11}H_7F_3N_3O_3S^+$ $[M+H]^+$ 318.0155, found 318.0158) and **156** (R_f = 0.50, 100% ethyl acetate; HRMS (EI) (*m/z*) = calculated for $C_{12}H_6F_6N_3O_5S_2^+$ $[M+H]^+$ 449.9648, found 449.9649).

Following **General Procedure Ib**, the mixture of triflates **155** and **156**, LiCl (32 mg, 0.75 mmol, 3.0 eq), $Pd(PPh_3)_2Cl_2$ (14 mg, 0.020 mmol, 0.08 eq), CuI (4.8 mg, 0.025 mmol, 0.1 eq) and trimethylsilylacetylene (0.25 mL, 1.8 mmol, 7.0 eq) were used in anhydrous DMF/triethylamine (4.8 mL).

The crude TMS-protected intermediate (R_f = 0.30, 100% ethyl acetate; HRMS (EI) (*m/z*) = calculated for $C_{15}H_{15}N_3Si^{\cdot+}$ $[M]^{\cdot+}$ 265.1030, found 265.1032) was desilylated, following **General Procedure II**, with K_2CO_3 (0.14 g, 0.83 mmol, 3.3 eq) in methanol (1.0 mL). The crude product was purified by flash column chromatography (100% ethyl acetate → 2% methanol in ethyl acetate) to give terminal alkyne **157** as brown semi-solid (9.7 mg, 0.050 mmol, 20% over three steps).

R_f = 0.16 (100% ethyl acetate).

^{1}H NMR (400 MHz, methanol-d_4) δ (ppm) = 8.99 (d, J = 1.2 Hz, 1H, 8-H), 8.42 (d, J = 5.4 Hz, 1H, 6-H), 8.37 (d, J = 5.4 Hz, 1H, 3-H), 8.25 – 8.18 (m, 2H, 4-H, 5-H), 4.31 (s, 1H, CCH). Signal for NH not observed.

^{13}C NMR (101 MHz, methanol-d_4) δ (ppm) = 139.9 (C-9a), 139.9 (C-3), 139.7 (C-6), 138.5 (C-8a), 136.4 (C-8), 128.7 (C-1 or C-4a or C-4b), 128.6 (C-1 or C-4a or C-4b), 128.5 (C-1 or C-4a or C-4b), 118.0 (C-4), 117.7 (C-5), 85.6 (C<u>CH</u>), 79.6 (<u>C</u>CH).

IR (ATR) $\tilde{\nu}$ (cm^{-1}) = 3171, 2922, 2098, 1560, 1474, 1443, 1420, 1254, 1232, 1068, 1038, 818, 760.

HRMS (EI) (*m/z*) = calculated for $C_{12}H_7N_3^{\cdot+}$ $[M]^{\cdot+}$ 193.0635, found 193.0639.

Purity (HPLC, method 2e) > 82% (λ = 210 nm), > 95% (λ = 254 nm).

Ethyl 3-bromo-1-((2-(trimethylsilyl)ethoxy)methyl)-1*H*-pyrrolo[2,3-*c*]pyridine-2-carboxylate (171ª)

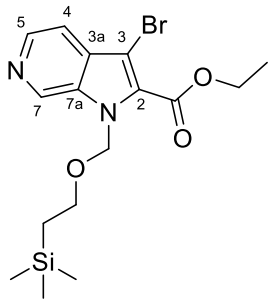

$C_{16}H_{23}BrN_2O_3Si$

M_r = 399.36 g/mol

Following **General Procedure VIIa**, 6-azaindole **148** (431 mg, 1.60 mmol, 1.0 eq), lithium bis(trimethylsilyl)amide (1 M in THF, 1.76 mL, 1.76 mmol, 1.1 eq) and SEM chloride (0.311 mL, 1.76 mmol, 1.1 eq) were used in anhydrous DMF (4.0 mL). The extraction was performed with sat. aq. NaCl solution (50 mL) and ethyl acetate (3 x 50 mL) and the crude product was purified by flash column chromatography (40% → 90% ethyl acetate in hexanes) to give *N*-SEM derivative **171ª** as yellow oil (464 mg, 1.16 mmol, 73%).

R_f = 0.16 (100% ethyl acetate).

^{1}H NMR (400 MHz, methylene chloride-d_2) δ (ppm) = 9.01 (d, J = 1.2 Hz, 1H, 7-H), 8.39 (d, J = 5.5 Hz, 1H, 5-H), 7.55 (dd, J = 5.5, 1.1 Hz, 1H, 4-H), 5.97 (s, 2H, NCH_2), 4.47 (q, J = 7.1 Hz, 2H, $O\underline{CH_2}CH_3$), 3.56 – 3.47 (m, 2H, $O\underline{CH_2}CH_2$), 1.46 (t, J = 7.1 Hz, 3H, $OCH_2\underline{CH_3}$), 0.89 – 0.84 (m, 2H, $SiCH_2$), -0.08 (s, 9H, $Si(CH_3)_3$).

^{13}C NMR (101 MHz, methylene chloride-d_2) δ (ppm) = 161.0 (COO), 140.9 (C-5), 135.9 (C-7), 134.8 (C-7a), 132.0 (C-3a), 128.8 (C-2), 115.0 (C-4), 98.9 (C-3), 74.6 (NCH_2), 66.8 ($O\underline{CH_2}CH_2$), 62.4 ($O\underline{CH_2}CH_3$), 18.1 ($SiCH_2$), 14.4 ($OCH_2\underline{CH_3}$), -1.5 ($Si(CH_3)_3$).

IR (ATR) $\tilde{\nu}$ (cm^{-1}) = 2953, 2896, 1713, 1451, 1324, 1243, 1218, 1097, 1077, 1028, 1016, 857, 833, 764.

HRMS (EI) (*m/z*) = calculated for $C_{16}H_{23}{}^{79}BrN_2O_3Si^{\cdot+}$ $[M]^{\cdot+}$ 398.0656, found 398.0656.

Purity (HPLC, method 2c) > 95% (λ = 210 nm), > 95% (λ = 254 nm).

Ethyl (*E*)-3-(2-ethoxyvinyl)-1-((2-(trimethylsilyl)ethoxy)methyl)-1*H*-pyrrolo[2,3-*c*]pyridine-2-carboxylate (158)

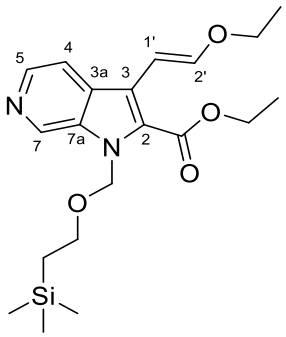

$C_{20}H_{30}N_2O_4Si$

M_r = 390.56 g/mol

Following **General Procedure VIc**, bromide **171[a]** (399 mg, 1.00 mmol, 1.0 eq), $Pd(PPh_3)_4$ (116 mg, 0.100 mmol, 0.1 eq), (*E*)-2-ethoxyvinylboronic acid pinacol ester (0.42 mL, 2.0 mmol, 2.0 eq) and Cs_2CO_3 (1.63 g, 5.00 mmol, 5.0 eq) were used in degassed 1,4-dioxane (6.0 mL) and water (2.0 mL). The reaction mixture was stirred at 95 °C for 18 h and the extraction was performed with sat. aq. NH_4Cl solution (30 mL) and ethyl acetate (3 x 20 mL). The crude product was purified by flash column chromatography (100% methylene chloride → 1% methanol in methylene chloride) to give enol ether **158** as yellow oil (296 mg, 0.757 mmol, 76%).

R_f = 0.19 (40% ethyl acetate in hexanes).

^{1}H NMR (400 MHz, methylene chloride-d_2) δ (ppm) = 8.97 (d, *J* = 1.1 Hz, 1H, 7-H), 8.31 (d, *J* = 5.6 Hz, 1H, 5-H), 7.69 (dd, *J* = 5.7, 1.2 Hz, 1H, 4-H), 7.19 (d, *J* = 13.3 Hz, 1H, 2'-H), 6.47 (d, *J* = 13.3 Hz, 1H, 1'-H), 5.94 (s, 2H, NCH_2), 4.43 (q, *J* = 7.1 Hz, 2H, $COO\underline{CH_2}CH_3$), 3.98 (q, *J* = 7.0 Hz, 2H, $O\underline{CH_2}CH_3$), 3.52 – 3.45 (m, 2H, $O\underline{CH_2}CH_2$), 1.44 (t, *J* = 7.1 Hz, 3H, $COOCH_2\underline{CH_3}$), 1.38 (t, *J* = 7.0 Hz, 3H, $OCH_2\underline{CH_3}$), 0.90 – 0.82 (m, 2H, $SiCH_2$), -0.08 (s, 9H, $Si(CH_3)_3$).

^{13}C NMR (101 MHz, methylene chloride-d_2) δ (ppm) = 162.5 (COO), 150.7 (C-2'), 140.3 (C-5), 136.0 (C-7a), 135.78 (C-7), 129.6 (C-3a), 126.4 (C-2), 120.4 (C-3), 116.2 (C-4), 98.8 (C-1'), 74.1 (NCH_2), 66.4 ($O\underline{CH_2}CH_2$), 65.8 ($O\underline{CH_2}CH_3$), 61.7 ($COO\underline{CH_2}CH_3$), 18.2 ($SiCH_2$), 15.0 ($OCH_2\underline{CH_3}$), 14.6 ($COOCH_2\underline{CH_3}$), -1.4 ($Si(CH_3)_3$).

IR (ATR) $\tilde{\nu}$ (cm^{-1}) = 2954, 2918, 1702, 1636, 1453, 1336, 1226, 1193, 1178, 1142, 1102, 1074, 1036, 932, 828.

HRMS (EI) (*m/z*) = calculated for $C_{20}H_{30}N_2O_4Si^{\cdot+}$ $[M]^{\cdot+}$ 390.1970, found 390.1964.

Purity (HPLC, method 2c) > 95% (λ = 210 nm), > 95% (λ = 254 nm).

((Trimethylsilyl)ethynyl)pyridin-3-amine (172^{b})[250]

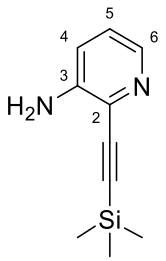

$C_{10}H_{14}N_2Si$

M_r = 190.32 g/mol

Similar to literature[250], $Pd(PPh_3)_4$ (1.2 g, 1.0 mmol, 0.10 eq), PPh_3 (0.26 g, 1.0 mmol, 0.11 eq) and CuI (0.19 g, 1.0 mmol, 0.10 eq) were dissolved in anhydrous triethylamine (50 mL) under N_2 atmosphere. Then 3-amino-2-bromopyridine (1.73 g, 10.0 mmol, 1.0 eq) and trimethylsilylacetylene (3.0 mL, 21 mmol, 2.1 eq) were added and the reaction mixture was stirred at 60 °C for 5 h. After cooling to room temperature, the mixture was filtered through a pad of celite. The pad was washed with ethyl acetate (400 mL) and the filtrate concentrated *in vacuo*. The crude product was purified by flash column chromatography (20% ethyl acetate in hexanes) to give TMS-protected alkyne **172^{b}** as dark brown solid (1.41 g, 7.40 mmol, 74%).

R_f = 0.63 (50% ethyl acetate in hexanes).

Melting point = 114 °C.

^{1}H NMR (400 MHz, chloroform-*d*) δ (ppm) = 7.98 (dd, *J* = 4.4, 1.6 Hz, 1H, 6-H), 7.03 (dd, *J* = 8.3, 4.4 Hz, 1H, 5-H), 6.99 (dd, *J* = 8.3, 1.6 Hz, 1H, 4-H), 4.22 (s, 2H, NH_2), 0.28 (s, 9H, $Si(CH_3)_3$).

^{13}C NMR (101 MHz, chloroform-*d*) δ (ppm) = 144.7 (C-3), 140.1 (C-6), 128.4 (C-2), 124.2 (C-5), 121.1 (C-4), 100.8 (C<u>C</u>Si), 100.6 (<u>C</u>CSi), 0.04 ($Si(CH_3)_3$).

IR (ATR) $\tilde{\nu}$ (cm^{-1}) = 3462, 3308, 3161, 2958, 2153, 1612, 1578, 1465, 1441, 1324, 1265, 1250, 1211, 1137, 1063, 887, 839, 800, 790, 758, 700.

HRMS (EI) (*m/z*) = calculated for $C_{10}H_{14}N_2Si^{\cdot+}$ $[M]^{\cdot+}$ 190.0921 found 190.0920.

Purity (HPLC) n.d.

2-Ethynylpyridin-3-amine (161^{b})[250]

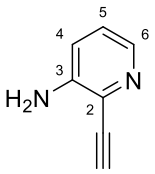

$C_7H_6N_2$

M_r = 118.14 g/mol

Similar to **General Procedure II**, TMS-protected alkyne **172^{b}** (1.41 g, 7.40 mmol, 1.0 eq) and K_2CO_3 (4.04 g, 24.4 mmol, 3.3 eq) were used in methanol (85 mL). In contrast to the general procedure, a modified work-up was performed. After stirring for 1 h, the solvent was removed *in vacuo*, the residue was resuspended in water (150 mL) and extracted with methylene chloride (3 x 150 mL). The combined organic layers were dried using a phase separation filter and concentrated *in vacuo* to give terminal alkyne **161^{b}** as light brown solid (872 mg, 7.38 mmol, 99%).

R_f = 0.35 (50% ethyl acetate in hexanes).

Melting point = 69 °C.

^{1}H NMR (400 MHz, chloroform-*d*) δ (ppm) = 7.99 (dd, *J* = 4.5, 1.5 Hz, 1H, 6-H), 7.07 (dd, *J* = 8.3, 4.5 Hz, 1H, 5-H), 7.00 (dd, *J* = 8.3, 1.5 Hz, 1H, 4-H), 4.25 (s, 2H, NH_2), 3.48 (s, 1H, CCH).

^{13}C NMR (101 MHz, chloroform-*d*) δ (ppm) = 145.1 (C-3), 140.2 (C-6), 127.4 (C-2), 124.5 (C-5), 121.3 (C-4), 82.8 (C<u>C</u>H), 79.9 (<u>C</u>CH).

IR (ATR) $\tilde{\nu}$ (cm^{-1}) = 3422, 3238, 3063, 2098, 1623, 1575, 1462, 1439, 1312, 1257, 1244, 1207, 1134, 1060, 963, 800, 792, 754, 695.

HRMS (EI) (*m/z*) = calculated for $C_7H_6N_2^{\cdot+}$ $[M]^{\cdot+}$ 118.0525, found 118.0526

Purity (HPLC, method 2i) > 95% (λ = 210 nm), > 95% (λ = 254 nm).

2-(3-Phenylisoxazol-5-yl)pyridin-3-amine (160^{b})

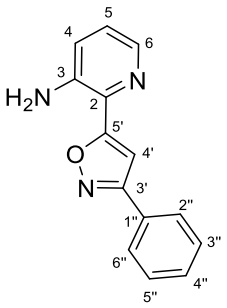

$C_{14}H_{11}N_3O$

M_r = 237.26 g/mol

Similar to **General Procedure IIIa**, alkyne **161^{b}** (59.1 mg, 0.500 mmol, 1.0 eq), (*E*)-benzaldehyde oxime (91 mg, 0.75 mmol, 1.5 eq) and [bis(trifluoroacetoxy)iodo]benzene (0.32 g, 0.75 mmol, 1.5 eq) were used in methanol/water (15 mL). In contrast to the general procedure, a modified work-up was performed. After stirring for additional 16 h, the solvent was removed in *vacuo*. Sat. aq. NaCl solution (20 mL) was added and the mixture extracted with ethyl acetate (3 x 20 mL). The combined organic layers were dried using a phase separation filter and concentrated *in vacuo*. The crude product was purified by flash column chromatography (25% ethyl acetate in hexanes) to give isoxazole **160^{b}** as pale yellow solid (78.5 mg, 0.331 mmol, 66%).

R_f = 0.45 (50% ethyl acetate in hexanes).

Melting point = 141 °C.

^{1}H NMR (400 MHz, chloroform-*d*) δ (ppm) = 8.11 (dd, *J* = 4.2, 1.6 Hz, 1H, 6-H), 7.96 – 7.82 (m, 2H, 2''-H, 6''-H), 7.56 – 7.41 (m, 3H, 3''-H, 4''-H, 5''-H), 7.22 (s, 1H, 4'-H), 7.15 (dd, *J* = 8.3, 4.2 Hz, 1H, 5-H), 7.10 (dd, *J* = 8.3, 1.5 Hz, 1H, 4-H), 4.96 (s, 2H, NH_2).

^{13}C NMR (101 MHz, chloroform-*d*) δ (ppm) = 172.0 (C-5'), 162.6 (C-3'), 141.4 (C-3), 139.7 (C-6), 130.3 (C-2), 130.3 (C-4''), 129.1 (C-3'', C-5''), 129.0 (C-1''), 127.1 (C-2'', C-6''), 125.5 (C-5), 124.7 (C-4), 100.5 (C-4').

IR (ATR) $\tilde{\nu}$ (cm^{-1}) = 3487, 3146, 1639, 1600, 1584, 1555, 1335, 1328, 1294, 1263, 1142, 1097, 1058, 960, 949, 924, 800, 771, 755, 689.

HRMS (ESI) (*m/z*) = calculated for $C_{14}H_{12}N_3O^+$ $[M+H]^+$ 238.0975 found 238.0976.

Purity (HPLC, method 2a) > 95% (λ = 210 nm), > 95% (λ = 254 nm).

N-Phenyl-2-(3-phenylisoxazol-5-yl)pyridin-3-amine (162^{b})

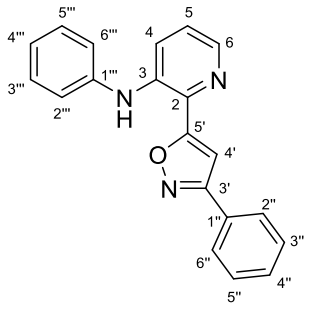

$C_{20}H_{15}N_3O$

M_r = 313.36 g/mol

Following **General Procedure XII**, aminopyridine **160^{b}** (50.2 mg, 0.210 mmol, 1.0 eq), $Pd(dba)_2$ (5 mg, 0.009 mmol, 0.04 eq), Xantphos (11 mg, 0.019 mmol, 0.09 eq), NaO*t*Bu (46 mg, 0.46 mmol, 2.2 eq) and iodobenzene (0.050 mL, 0.45 mmol, 2.1 eq) were used in anhydrous toluene (1.1 mL). The crude product was purified by flash column chromatography (25% ethyl acetate in hexanes) to give diarylamine **162^{b}** as yellow solid (56.6 mg, 0.181 mmol, 86%).

R_f = 0.81 (50% ethyl acetate in hexanes).

Melting point = 150 °C.

^{1}H NMR (400 MHz, chloroform-*d*) δ (ppm) = 8.19 (dd, *J* = 4.4, 1.4 Hz, 1H, 6-H), 7.95 – 7.86 (m, 2H, 2''-H, 6''-H), 7.65 (dd, *J* = 8.6, 1.4 Hz, 1H, 4-H), 7.63 (s, 1H, NH), 7.54 – 7.45 (m, 3H, 3''-H, 4''-H, 5''-H), 7.42 – 7.34 (m, 2H, 3'''-H, 5'''-H), 7.29 (s, 1H, 4'-H), 7.25 – 7.20 (m, 2H, 2'''-H, 6'''-H), 7.18 (ddd, *J* = 8.6, 4.3, 0.6 Hz, 1H, 5-H), 7.13 (tt, *J* = 7.1, 1.2 Hz, 1H, 4'''-H).

^{13}C NMR (101 MHz, chloroform-*d*) δ (ppm) = 171.8 (C-5'), 162.7 (C-3'), 140.7 (C-6), 140.5 (C-1'''), 139.7 (C-3), 132.5 (C-2), 130.4 (C-4''), 129.8 (C-3''', C-5'''), 129.2 (C-3'', C-5''), 128.9 (C-1''), 127.1 (C-2'', C-6''), 125.1 (C-5), 124.1 (C-4'''), 123.4 (C-4), 122.1 (C-2''', C-6'''), 101.4 (C-4').

IR (ATR) $\tilde{\nu}$ (cm^{-1}) = 3301, 3048, 1594, 1580, 1570, 1506, 1447, 1391, 1309, 1257, 1226, 1175, 1119, 948, 918, 807, 753, 694.

HRMS (ESI) (*m/z*) = calculated for $C_{20}H_{16}N_3O^+$ $[M+H]^+$ 314.1288, found 314.1289.

Purity (HPLC, method 2a) > 95% (λ = 210 nm), > 95% (λ = 254 nm).

2-(3-Phenylisoxazol-5-yl)-*N*-(pyridin-3-yl)pyridin-3-amine (163^{b})

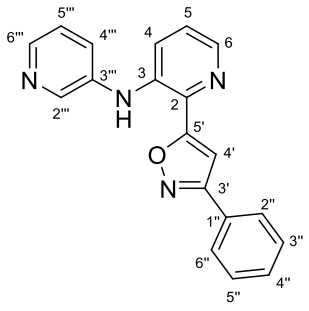

$C_{19}H_{14}N_4O$

M_r = 314.35 g/mol

Following **General Procedure XII**, aminopyridine **160^{b}** (50.9 mg, 0.215 mmol, 1.0 eq), $Pd(dba)_2$ (6 mg, 0.01 mmol, 0.05 eq), Xantphos (10 mg, 0.017 mmol, 0.08 eq), NaO*t*Bu (42 mg, 0.43 mmol, 2.0 eq) and 3-iodopyridine (53 mg, 0.26 mmol, 1.2 eq) were used in anhydrous toluene (1.1 mL). The crude product was purified by flash column chromatography (1% methanol in methylene chloride) to give diarylamine **163^{b}** as pale yellow solid (37.4 mg, 0.119 mmol, 57%).

R_f = 0.22 (50% ethyl acetate in hexanes).

Melting point = 187 °C.

^{1}H NMR (400 MHz, chloroform-*d*) δ (ppm) = 8.58 (d, *J* = 2.7 Hz, 1H, 2‘‘‘-H), 8.38 (dd, *J* = 4.7, 1.5 Hz, 1H, 6‘‘‘-H), 8.26 (dd, *J* = 4.4, 1.3 Hz, 1H, 6-H), 7.93 – 7.87 (m, 2H, 2‘‘-H, 6‘‘-H), 7.64 – 7.57 (m, 2H, 4-H, NH), 7.55 (ddd, *J* = 8.2, 2.7, 1.5 Hz, 1H, 4‘‘‘-H), 7.52 – 7.47 (m, 3H, 3‘‘-H, 4‘‘-H, 5‘‘-H), 7.33 – 7.28 (m, 2H, 4‘-H, 5‘‘‘-H), 7.22 (dd, *J* = 8.5, 4.4 Hz, 1H, 5-H).

^{13}C NMR (101 MHz, chloroform-*d*) δ (ppm) = 171.4 (C-5‘), 162.9 (C-3‘), 145.1 (C-6‘‘‘), 143.9 (C-2‘‘‘), 141.7 (C-6), 138.7 (C-3), 137.3 (C-3‘‘‘), 133.3 (C-2), 130.5 (C-4‘‘), 129.2 (C-3‘‘, C-5‘‘), 128.7 (C-1‘‘), 128.6 (C-4‘‘‘), 127.1 (C-2‘‘, C-6‘‘), 125.2 (C-5), 124.2 (C-5‘‘‘), 123.5 (C-4), 101.8 (C-4‘).

IR (ATR) $\tilde{\nu}$ (cm^{-1}) = 3241, 3155, 3025, 2978, 2912, 1572, 1456, 1429, 1393, 1319, 1313, 1266, 1181, 1120, 959, 951, 912, 799, 775, 765, 693.

HRMS (ESI) (*m/z*) = calculated for $C_{19}H_{15}N_4O^+$ $[M+H]^+$ 315.1240, found 315.1241.

Purity (HPLC, method 2a) > 95% (λ = 210 nm), > 95% (λ = 254 nm).

2-(3-Phenylisoxazol-5-yl)-*N*-(pyridin-4-yl)pyridin-3-amine (164[b])

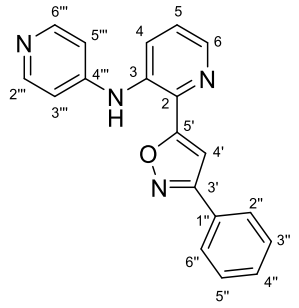

$C_{19}H_{14}N_4O$

M_r = 314.35 g/mol

The required 4-bromopyridine was prepared from its commercially available hydrochloride. Therefore, aq. NaOH solution (2 M, 20 mL) was added to 4-bromopyridine hydrochloride (300 mg, 1.54 mmol) and extracted with methylene chloride (3 x 10 mL). The combined organic phases were dried using a phase separation filter. The solvent was cautiously removed *in vacuo* (> 700 mbar) and further by applying a N_2 flow to receive the free base as yellow oil (100 mg, 0.633 mmol, 41%).

Following **General Procedure XII**, aminopyridine **160[b]** (50.6 mg, 0.213 mmol, 1.0 eq), $Pd(dba)_2$ (5 mg, 0.009 mmol, 0.04 eq), Xantphos (10 mg, 0.017 mmol, 0.08 eq), NaO*t*Bu (43 mg, 0.44 mmol, 2.1 eq) and 4-bromopyridine (100 mg, 0.63 mmol, 3.0 eq) were used in anhydrous toluene (1.1 mL). The crude product was purified by flash column chromatography (2% → 5% methanol in methylene chloride) to give diarylamine **164[b]** as pale yellow solid (46.8 mg, 0.149 mmol, 71%).

R_f = 0.20 (5% methanol in methylene chloride).

Melting point = 103 °C.

^{1}H NMR (400 MHz, chloroform-*d*) δ (ppm) = 8.44 – 8.40 (m, 3H, 6-H, 2‘‘‘-H, 6‘‘‘-H), 7.92 (dd, *J* = 8.4, 1.4 Hz, 1H, 4-H), 7.90 – 7.86 (m, 2H, 2‘‘-H, 6‘‘-H), 7.61 (s, 1H, NH), 7.50 (m, 3H, 3‘‘-H, 4‘‘-H, 5‘‘-H), 7.35 (dd, *J* = 8.4, 4.4 Hz, 1H, 5-H), 7.31 (s, 1H, 4‘-H), 7.02 – 6.96 (m, 2H, 3‘‘‘-H, 5‘‘‘-H).

^{13}C NMR (101 MHz, chloroform-*d*) δ (ppm) = 170.6 (C-5‘), 162.9 (C-3‘), 151.0 (C-2‘‘‘, C-6‘‘‘), 148.7 (C-4‘‘‘), 144.1 (C-6), 136.3 (C-2), 135.5 (C-3), 130.6 (C-4‘‘), 129.2 (C-3‘‘, C-5‘‘), 128.6 (C-1‘‘), 128.1 (C-4), 127.1 (C-2‘‘, C-6‘‘), 124.9 (C-5), 111.7 (C-3‘‘‘, C-5‘‘‘), 102.5 (C-4‘).

IR (ATR) $\tilde{\nu}$ (cm^{-1}) = 3241, 3051, 1594, 1578, 1569, 1453, 1441, 1392, 1330, 1307, 1212, 1123, 989, 947, 820, 808, 765, 695.

HRMS (ESI) (*m/z*) = calculated for $C_{19}H_{15}N_4O^+$ $[M+H]^+$ 315.1240, found 315.1241.

Purity (HPLC, method 2a) > 95% (λ = 210 nm), > 95% (λ = 254 nm).

N-(3-Methoxyphenyl)-2-(3-phenylisoxazol-5-yl)pyridin-3-amine (165^{b})

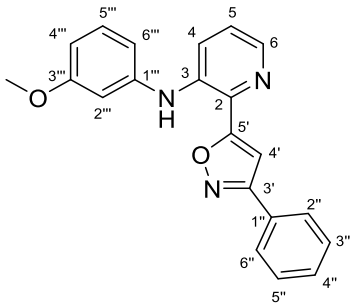

$C_{21}H_{17}N_3O_2$

M_r = 343.39 g/mol

Following **General Procedure XII**, aminopyridine **160^{b}** (49.9 mg, 0.210 mmol, 1.0 eq), $Pd(dba)_2$ (6 mg, 0.01 mmol, 0.05 eq), Xantphos (10 mg, 0.017 mmol, 0.08 eq), NaO*t*Bu (42 mg, 0.42 mmol, 2.0 eq) and 3-iodoanisole (0.050 mL, 0.42 mmol, 2.0 eq) were used in anhydrous toluene (1.1 mL). The crude product was purified by flash column chromatography (20% ethyl acetate in hexanes) to give diarylamine **165^{b}** as brown semi-solid (21.1 mg, 0.0614 mmol, 29%).

R_f = 0.32 (25% ethyl acetate in hexanes).

^{1}H NMR (400 MHz, chloroform-*d*) δ (ppm) = 8.20 (dd, *J* = 4.4, 1.4 Hz, 1H, 6-H), 7.92 – 7.88 (m, 2H, 2‘‘-H, 6‘‘-H), 7.71 (dd, *J* = 8.6, 1.4 Hz, 1H, 4-H), 7.60 (s, 1H, NH), 7.53 – 7.47 (m, 3H, 3‘‘-H, 4‘‘-H, 5‘‘-H), 7.29 – 7.26 (m, 2H, 4‘-H, 5‘‘‘-H), 7.19 (ddd, *J* = 8.6, 4.3, 0.6 Hz, 1H, 5-H), 6.82 (ddd, *J* = 8.0, 2.2, 0.9 Hz, 1H, 6‘‘‘-H), 6.76 (t, *J* = 2.3 Hz, 1H, 2‘‘‘-H), 6.67 (ddd, *J* = 8.3, 2.5, 0.9 Hz, 1H, 4‘‘‘-H), 3.82 (s, 3H, OCH_3).

^{13}C NMR (101 MHz, chloroform-*d*) δ (ppm) = 171.7 (C-5‘), 162.7 (C-3‘), 161.0 (C-3‘‘‘), 141.8 (C-1‘‘‘), 140.9 (C-6), 139.4 (C-3), 132.7 (C-2), 130.5 (C-5‘‘‘), 130.4 (C-4‘‘), 129.2 (C-3‘‘, C-5‘‘), 128.9 (C-1‘‘), 127.1 (C-2‘‘, C-6‘‘), 125.1 (C-5), 124.0 (C-4), 114.0 (C-6‘‘‘), 109.5 (C-4‘‘‘), 107.5 (C-2‘‘‘), 101.4 (C-4‘), 55.5 (OCH_3).

IR (ATR) $\tilde{\nu}$ (cm^{-1}) = 3426, 2934, 1594, 1577, 1489, 1456, 1441, 1399, 1317, 1281, 1247, 1214, 1155, 1119, 1039, 961, 949, 915, 843, 799, 765, 686.

HRMS (ESI) (*m/z*) = calculated for $C_{21}H_{18}N_3O_2^+$ $[M+H]^+$ 344.1394, found 344.1396.

Purity (HPLC, method 2a) > 95% (λ = 210 nm), > 95% (λ = 254 nm).

4-Chloro-*N*-(2-(3-phenylisoxazol-5-yl)pyridin-3-yl)pyridin-3-amine (166^{b})

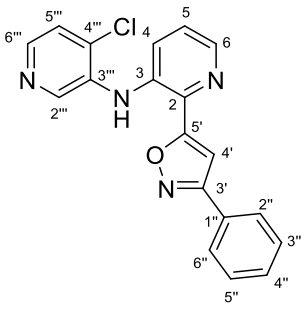

$C_{19}H_{13}ClN_4O$

M_r = 348.79 g/mol

Following **General Procedure XII**, aminopyridine **160^{b}** (142 mg, 0.600 mmol, 1.0 eq), $Pd(dba)_2$ (14 mg, 0.024 mmol, 0.04 eq), Xantphos (28 mg, 0.048 mmol, 0.08 eq), NaO*t*Bu (0.12 g, 1.2 mmol, 2.0 eq) and 4-chloro-3-iodo-pyridine (0.21 g, 0.90 mmol, 1.5 eq) were used in anhydrous toluene (3.0 mL). After filtration, the celite pad was additionally washed with methanol (50 mL). The crude product was purified by flash column chromatography (1% methanol in methylene chloride) to give diarylamine **166^{b}** as pale yellow solid (207 mg, 0.593 mmol, 99%).

R_f = 0.38 (50% ethyl acetate in hexanes).

Melting point = 144 °C.

^{1}H NMR (400 MHz, chloroform-*d*) δ (ppm) = 8.65 (s, 1H, 2‘‘‘-H), 8.34 (dd, *J* = 4.4, 1.4 Hz, 1H, 6-H), 8.24 (d, *J* = 5.2 Hz, 1H, 6‘‘‘-H), 7.95 – 7.86 (m, 2H, 2‘‘-H, 6‘‘-H), 7.71 (s, 1H, NH), 7.63 (dd, *J* = 8.5, 1.4 Hz, 1H, 4-H), 7.55 – 7.44 (m, 3H, 3‘‘-H, 4‘‘-H, 5‘‘-H), 7.42 (d, *J* = 5.2 Hz, 1H, 5‘‘‘-H), 7.33 (s, 1H, 4‘-H), 7.28 (m, 1H, 5-H, collapses with chloroform peak).

^{13}C NMR (101 MHz, chloroform-*d*) δ (ppm) = 171.0 (C-5‘), 162.9 (C-3‘), 144.6 (C-6‘‘‘), 142.8 (C-6), 142.2 (C-2‘‘‘), 137.2 (C-3), 135.3 (C-3‘‘‘), 135.3 (C-4‘‘‘), 134.5 (C-2), 130.5 (C-4‘‘), 129.2 (C-3‘‘, C-5‘‘), 128.7 (C-1‘‘), 127.1 (C-2‘‘, C-6‘‘), 125.1 (C-5), 125.1 (C-5‘‘‘), 124.9 (C-4), 102.1 (C-4‘).

IR (ATR) $\tilde{\nu}$ (cm^{-1}) = 3387, 2920, 2851, 1603, 1584, 1565, 1551, 1502, 1457, 1400, 960, 907, 792, 751, 698, 680, 675.

HRMS (ESI) (*m/z*) = calculated for $C_{19}H_{14}{}^{35}ClN_4O^+$ $[M+H]^+$ 349.0851, found 349.0852.

Purity (HPLC, method 2a) > 94% (λ = 210 nm), > 95% (λ = 254 nm).

4-Bromo-*N*-(2-(3-phenylisoxazol-5-yl)pyridin-3-yl)pyridin-3-amine (167)

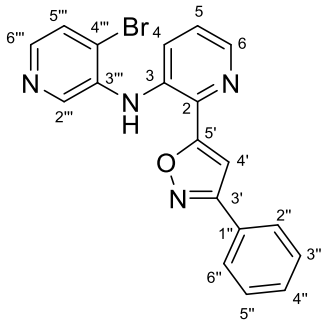

$C_{19}H_{13}BrN_4O$

M_r = 392.24 g/mol

Following **General Procedure XII**, aminopyridine **160[b]** (99.6 mg, 0.420 mmol, 1.0 eq), $Pd(dba)_2$ (10 mg, 0.017 mmol, 0.04 eq), Xantphos (19 mg, 0.034 mmol, 0.08 eq), NaO*t*Bu (83 mg, 0.84 mmol, 2.0 eq) and 4-bromo-3-iodo-pyridine (143 mg, 0.504 mmol, 1.2 eq) were used in anhydrous toluene (2.0 mL). After filtration, the celite pad was additionally washed with methanol (50 mL). The crude product was purified by flash column chromatography (1% methanol in methylene chloride) to give diarylamine **167** as pale beige solid (148 mg, 0.377 mmol, 90%).

R_f = 0.26 (2% methanol in methylene chloride).

Melting point = 158 °C.

^{1}H NMR (400 MHz, chloroform-*d*) δ (ppm) = 8.61 (s, 1H, 2'''-H), 8.34 (dd, *J* = 4.4, 1.4 Hz, 1H, 6-H), 8.13 (d, *J* = 5.2 Hz, 1H, 6'''-H), 7.93 – 7.88 (m, 2H, 2''-H, 6''-H), 7.72 (s, 1H, NH), 7.64 (dd, *J* = 8.5, 1.4 Hz, 1H, 4-H), 7.60 (d, *J* = 5.2 Hz, 1H, 5'''-H), 7.52 – 7.48 (m, 3H, 3''-H, 4''-H, 5''-H), 7.33 (s, 1H, 4'-H), 7.30 – 7.26 (m, 1H, 5-H, collapses with chloroform peak).

^{13}C NMR (101 MHz, chloroform-*d*) δ (ppm) = 171.0 (C-5'), 162.9 (C-3'), 144.6 (C-6'''), 142.8 (C-6), 142.0 (C-2'''), 137.2 (C-3), 136.7 (C-3'''), 134.5 (C-2), 130.5 (C-4''), 129.2 (C-3'', C-5''), 128.7 (C-1''), 128.4 (C-5'''), 127.1 (C-2'', C-6''), 126.2 (C-4'''), 125.2 (C-5), 124.9 (C-4), 102.1 (C-4').

IR (ATR) $\tilde{\nu}$ (cm^{-1}) = 3385, 1590, 1566, 1508, 1458, 1440, 1397, 1333, 1214, 1015, 922, 778, 765, 704.

HRMS (EI) (*m/z*) = calculated for $C_{19}H_{14}{}^{79}BrN_4O^+$ $[M+H]^+$ 393.0346, found 393.0352.

Purity (HPLC, method 2c) > 95% (λ = 210 nm), > 95% (λ = 254 nm).

3-Phenyl-5-(9*H*-pyrrolo[2,3-*c*:5,4-*c*']dipyridin-1-yl)isoxazole (144)

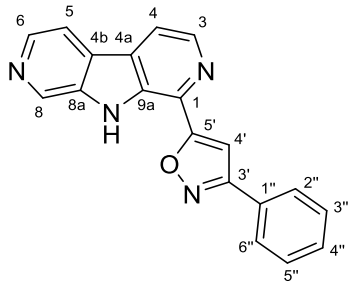

$C_{19}H_{12}N_4O$

M_r = 312.10 g/mol

Following **General Procedure XIII**, bromide **167** (138 mg, 0.350 mmol, 1.0 eq), $Pd(OAc)_2$ (16 mg, 0.070 mmol, 0.2 eq), CyJohnPhos (25 mg, 0.070 mmol, 0.2 eq) and DBU (0.1 mL, 0.7 mmol, 2.0 eq) were used in anhydrous DMA (0.7 mL). The crude product was purified two times by flash column chromatography (1% → 2% methanol in methylene chloride, 2% methanol in chloroform) to give 7-aza-*β*-carboline **144** as pale yellow solid (48.8 mg, 0.156 mmol, 45%).

R_f = 0.20 (3% methanol in methylene chloride).

Melting point = 270 °C (decomposition).

^{1}H NMR (500 MHz, DMSO-d_6) δ (ppm) = 12.21 (s, 1H, NH), 9.22 (d, *J* = 1.2 Hz, 1H, 8-H), 8.64 (d, *J* = 5.1 Hz, 1H, 3-H), 8.52 (d, *J* = 5.2 Hz, 1H, 6-H), 8.47 (d, *J* = 5.1 Hz, 1H, 4-H), 8.32 (d, *J* = 5.3 Hz, 1H, 5-H), 8.10 – 8.07 (m, 2H, 2''-H, 6''-H), 7.88 (s, 1H, 4'-H), 7.62 – 7.56 (m, 3H, 3''-H, 4''-H, 5''-H).

^{13}C NMR (126 MHz, DMSO-d_6) δ (ppm) = 169.2 (C-5‘), 162.5 (C-3‘), 139.3 (C-6), 138.9 (C-3), 137.3 (C-8a), 136.5 (C-8), 132.5 (C-9a), 130.9 (C-1), 130.6 (C-4‘‘), 129.3 (C-3‘‘, C-5‘‘), 128.8 (C-4a), 128.3 (C-1‘‘), 126.9 (C-2‘‘, C-6‘‘), 125.5 (C-4b), 118.0 (C-4), 115.9 (C-5), 101.1 (C-4‘).

IR (ATR) $\tilde{\nu}$ (cm^{-1}) = 3050, 1555, 1482, 1464, 1444, 1423, 1400, 1288, 1255, 1236, 1220, 978, 812, 758.

HRMS (ESI) (*m/z*) = calculated for $C_{19}H_{13}N_4O^+$ $[M+H]^+$ 313.1084, found 313.1085.

Purity (HPLC, method 2a) > 95% (λ = 210 nm), > 95% (λ = 254 nm).

3-Bromo-4-iodopyridine (168)[259]

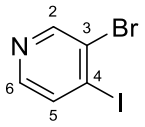

C_5H_3BrIN

M_r = 283.89 g/mol

LDA (2 M in THF, 1.5 mL, 3.0 mmol, 1.0 eq) was added to anhydrous THF (11 mL) under N_2 atmosphere and stirred at -78 °C for 30 min. Then, 3-bromopyridine (0.32 mL, 3.3 mmol, 1.1 eq) was added dropwise and stirred at -78 °C for 1 h. A solution of iodine (1.5 g, 6.0 mmol, 2.0 eq) in anhydrous THF (12.5 mL) was slowly added and the reaction mixture was stirred at -78 °C for 3 h, then slowly warmed up to room temperature and stirred for further 18 h. Subsequently, the reaction was quenched with sat. aq. $Na_2S_2O_3$ solution (75 mL) and extracted with ethyl acetate (2 x 75 mL). The combined organic layers were washed with sat. aq. $Na_2S_2O_3$ solution (50 mL), water (50 mL) and sat. aq. NaCl solution (50 mL) and dried using a phase separation filter. The solvent was removed *in vacuo* and the crude product was purified by flash column chromatography (50% → 66% methylene chloride in hexanes) to give iodide **168** as white solid (156 mg, 0.548 mmol, 18%).

R_f = 0.52 (100% methylene chloride).

Melting point = 112 °C (lit.[259] 112 – 113 °C).

^{1}H NMR (400 MHz, chloroform-*d*) δ (ppm) = 8.69 (s, 1H, 2-H), 8.12 (dd, *J* = 5.1, 0.5 Hz, 1H, 6-H), 7.81 (d, *J* = 5.2 Hz, 1H, 5-H).

^{13}C NMR (101 MHz, chloroform-*d*) δ (ppm) = 151.1 (C-2), 147.8 (C-6), 135.3 (C-5), 129.1 (C-3), 112.3 (C-4).

IR (ATR) $\tilde{\nu}$ (cm^{-1}) = 2922, 1553, 1541, 1447, 1388, 1265, 1113, 1056, 1008, 822, 707, 654.

HRMS (EI) (*m/z*) = calculated for $C_5H_3{}^{79}BrIN^{\cdot+}$ $[M]^{\cdot+}$ 282.8489, found 282.8489.

Purity (HPLC, method 2e) > 95% (λ = 210 nm), > 95% (λ = 254 nm).

_N_-(3-Bromopyridin-4-yl)-2-(3-phenylisoxazol-5-yl)pyridin-3-amine (169)

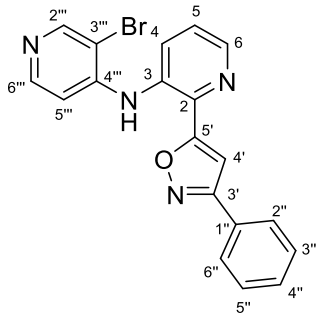

$C_{19}H_{13}BrN_4O$

M_r = 392.24 g/mol

Following **General Procedure XII**, aminopyridine **160[b]** (99.6 mg, 0.420 mmol, 1.0 eq), $Pd(dba)_2$ (10 mg, 0.017 mmol, 0.04 eq), Xantphos (19 mg, 0.034 mmol, 0.08 eq), NaO*t*Bu (83 mg, 0.84 mmol, 2.0 eq) and 3-bromo-4-iodo-pyridine (**168**) (0.14 g, 0.50 mmol, 1.2 eq) were used in anhydrous toluene (2.0 mL). After filtration, the celite pad was additionally washed with methanol (50 mL). The crude product was purified by flash column chromatography (1% methanol in methylene chloride) to give diarylamine **169** as pale yellow solid (129 mg, 0.329 mmol, 78%).

R_f = 0.38 (2% methanol in methylene chloride).

Melting point = 165 °C.

^{1}H NMR (400 MHz, chloroform-*d*) δ (ppm) = 8.62 (s, 1H, 2‘‘‘-H), 8.51 (dd, *J* = 4.5, 1.4 Hz, 1H, 6-H), 8.24 (d, *J* = 5.6 Hz, 1H, 6‘‘‘-H), 7.97 (s, 1H, NH), 7.91 (dd, *J* = 8.4, 1.4 Hz, 1H, 4-H), 7.90 – 7.87 (m, 2H, 2’’-H, 6’’-H), 7.51 – 7.46 (m, 3H, 3’’-H, 4’’-H, 5’’-H), 7.39 (dd, *J* = 8.4, 4.5 Hz, 1H, 5-H), 7.31 (s, 1H, 4’-H), 7.02 (d, *J* = 5.6 Hz, 1H, 5’’’-H).

^{13}C NMR (101 MHz, chloroform-*d*) δ (ppm) = 169.9 (C-5‘), 163.0 (C-3‘), 152.6 (C-2‘‘‘), 149.2 (C-6‘‘‘), 146.6 (C-4‘‘‘), 145.4 (C-6), 138.0 (C-2), 134.2 (C-3), 130.5 (C-4‘‘), 129.9 (C-4), 129.2 (C-3‘‘, C-5‘‘), 128.6 (C-1‘‘), 127.1 (C-2‘‘, C-6‘‘), 124.9 (C-5), 110.7 (C-3‘‘‘), 108.7 (C-5‘‘‘), 102.8 (C-4‘).

IR (ATR) $\tilde{\nu}$ (cm^{-1}) = 3385, 1574, 1566, 1508, 1458, 1440, 1397, 1333, 1214, 1015, 922, 778, 766, 704.

HRMS (ESI) (*m/z*) = calculated for $C_{19}H_{14}{}^{79}BrN_4O^+$ $[M+H]^+$ 393.0346, found 393.0345.

Purity (HPLC, method 2c) > 95% (λ = 210 nm), > 95% (λ = 254 nm).

3-Phenyl-5-(5*H*-pyrrolo[2,3-*c*:4,5-*c*']dipyridin-6-yl)isoxazole (145)

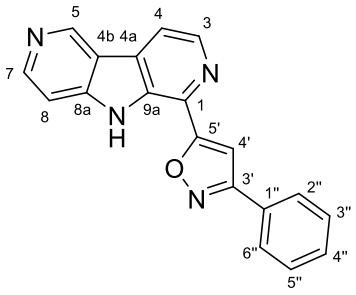

$C_{19}H_{12}N_4O$

M_r = 312.10 g/mol

Following **General Procedure XIII**, bromide **169** (98.3 mg, 0.250 mmol, 1.0 eq), $Pd(OAc)_2$ (11 mg, 0.050 mmol, 0.2 eq), CyJohnPhos (18 mg, 0.050 mmol, 0.2 eq) and DBU (0.075 mL, 0.50 mmol, 2.0 eq) were used in anhydrous DMA (0.5 mL). The crude product was purified two times by flash column chromatography (1% → 2.5% methanol in methylene chloride, 4% methanol in chloroform) to give 6-aza-*β*-carboline **145** as white solid (40.1 mg, 0.128 mmol, 51%).

R_f = 0.33 (5% methanol in methylene chloride).

Melting point = 304 °C (decomposition).

^{1}H NMR (500 MHz, DMSO-d_6) δ (ppm) = 12.25 (s, 1H, NH), 9.56 (d, *J* = 1.0 Hz, 1H, 5-H), 8.65 (d, *J* = 5.0 Hz, 1H, 3-H), 8.63 (d, *J* = 5.7 Hz, 1H, 7-H), 8.44 (d, *J* = 5.0 Hz, 1H, 4-H), 8.09 – 8.06 (m, 2H, 2''-H, 6''-H), 7.85 (s, 1H, 4'-H), 7.74 (dd, *J* = 5.7, 1.1 Hz, 1H, 8-H), 7.61 – 7.56 (m, 3H, 3''-H, 4''-H, 5''-H).

^{13}C NMR (126 MHz, DMSO-d_6) δ (ppm) = 169.3 (C-5'), 162.5 (C-3'), 147.3 (C-7), 145.5 (C-8a), 144.9 (C-5), 140.0 (C-3), 132.0 (C-9a), 130.5 (C-4''), 130.0 (C-1), 129.2 (C-3'', C-5''), 129.2 (C-4a), 128.3 (C-1''), 126.9 (C-2'', C-6''), 117.6 (C-4b), 116.9 (C-4), 108.0 (C-8), 101.1 (C-4').

IR (ATR) $\tilde{\nu}$ (cm^{-1}) = 3046, 1609, 1558, 1468, 1456, 1418, 1398, 1296, 1238, 1170, 1025, 899, 802, 759, 684.

HRMS (ESI) (*m/z*) = calculated for $C_{19}H_{13}N_4O^+$ $[M+H]^+$ 313.1084, found 313.1085.

Purity (HPLC, method 2a) > 95% (λ = 210 nm), > 95% (λ = 254 nm).

5.4 Procedures for biological testing

5.4.1 Thermal shift assay

The assay was performed as previously described[263, 305] employing SYPRO Orange as fluorescent dye. All potential inhibitors were tested at a concentration of 10 µM against a panel of the following 104 kinases (and bromodomains): AAK1, ABL1, AKT3, AURKB, BMP2K, BMPR2, BMX, BRAF, BRD4, BRPF1, CAMK1D, CAMK1G, CAMK2B, CAMK2D, CAMK4, CAMKK2, CASK, CDC42DPA, CDK2, CDKL1, CHEK2, CLK1, CLK3, CSNK1D, CSNK1E, CSNK2A1, CSNK2A2, DAPK1, DAPK3, DCAMKL1, DMPK1, DYRK1A, DYRK2, EPHA2, EPHA4, EPHA5, EPHA7, EPHB1, EPHB3, FESA, FGFR1, FGFR2, FGFR3, FLT1, GAK, GPRK5, GSG2, GSK3B, HIPK2, MAP2K1, MAP2K4, MAP2K6, MAP2K7, MAP3K5, MAPK10, MAPK13, MAPK14, MAPK15, MAPK1, MAPK8, MAPK9, MAPKAPK2, MARK3, MARK4, MELK, MERTK, MST3, MST4, NEK1, NEK2, NEK7, OSR1, PAK1, PAK4, PCTK1, PDK4, PHKG2, PIM1, PIM3, PKMYT1, PLK4, RIOK1, RPS6KA1, RPS6KA5, SLK, SPRK1, SRC, STK10, STK17A, STK17B, STK38L, STK39, STK3, STK4, STK6, TAF1, TIF1, TLK1, TOPK, TTK, ULK1, ULK3, VRK1, WNK1. All measurements were performed in the lab of PROF. DR. STEFAN KNAPP at the Goethe University Frankfurt (Germany).

5.4.2 Radiometric ^{33}PanQinase

All kinase assays (CLK1, CAMKK2, DYRK1A, DYRK2) were performed in 96-well plates from PerkinElmer in a 50 µL reaction volume. The reaction cocktail was pipetted in the following order: 25 µL of assay buffer (standard buffer/[γ-^{33}P]-ATP), 10 µL of ATP solution (in H_2O), 5 µL of test compound (in 10% DMSO) and 10 µL of enzyme/substrate mixture. The assay buffer for all protein kinases contained 70 mM, HEPES-NaOH pH 7.5, 3 mM $MgCl_2$, 3 mM $MnCl_2$, 3 µM Na-orthovanadate, 1.2 mM DTT, 50 µg/mL PEG20000, ATP (corresponding to the apparent ATP-K_m of the respective kinase) and [γ-^{33}P]-ATP (approx. 7 x 100^5 cpm per well). After an incubation time of 1 h at 30 °C, 50 µL of 2% H_3PO_4 was added, then the plates were aspirated and washed two times with 200 µL 0.9% NaCl. Incorporation of $^{33}P_i$ was determined with a microplate scintillation counter (Microbeta, Wallac). The residual activities for each concentration and the IC_{50} values were calculated using Quattro Workflow V3.1.1. All measurements were performed at Reaction Biology Europe GmbH (Freiburg, Germany).

5.4.3 MTT assay

HL-60 cells (DSM number: ACC 3) were purchased from the German Collection of Microorganisms and Cell Cultures GmbH (DSMZ, Braunschweig) and cultivated in RPMI 1640 medium supplemented with 10% fetal bovine serum (FBS).

For the MTT assay, cell density was adjusted to roughly 9 x 10^5 cells/mL. Cells were then seeded in 96-well plates by transferring 99 µL into each well and incubating for 24 h at 37 °C with 5% CO_2. The test compounds were used as 10 mM solutions in DMSO or, if IC_{50} values were determined, as a dilution series thereof (1:2, at least 5 dilution steps). 1.0 µL of test compound solution or Triton X-100 (0.1 mg/mL) as positive control or DMSO alone as negative control were transferred to each well and incubated for additional 24 h.

Then 10 µL MTT solution (5.0 mg/mL in PBS) were added to each well and incubated for 2 h. After this time, 190 µL DMSO was added and the plate was shaken for 1 h in the dark. The absorbance of each well was measured at 570 nm with a MRX Microplate Reader (Dynex Technologies). The software Prism 4 (GraphPad) was used to analyze all data and calculate IC_{50} values.

5.4.4 Agar diffusion assay

All tested germs were also purchased from the DSMZ and cultivated following their instructions in liquid culture.

The agar plates were filled with suitable culture media as follows. For *Escherichia coli* (DSM number: 426), *Pseudomonas marginalis* (DSM number: 7527) and *Yarrowia lipolytica* (DSM number: 1345) a mixture of 35.2 g all-culture agar (AC agar) and 20 g agar in 1.0 L water was used. For *Saccharomyces cerevisiae* (DSM number: 1333) 35.2 g AC agar in 1.0 L water was used. For *Straphylococcus equorum* (DSM number: 20675) and *Streptococcus entericus* (DSM number: 14446) a mixture of 10 g casein peptone, 5.0 g yeast extract, 5.0 g glucose, 5.0 g sodium chloride and 15 g agar in 1.0 L water was used. All agar media were autoclaved and filled in petri dished under aseptic conditions, while still hot and liquid. After cooling for at least 1 h at 8 °C, the agar plates were ready to use.

The test platelets (d = 6.0 mm, Macherey-Nagel) were impregnated with 3.0 µL of a 1% (m/V) solution of the respective compounds or the positive control tetracycline (as antibacterial) or clotrimazole (as antifungal agent) in DMSO. As negative control DMSO (3.0 µL) alone was used. All platelets were dried for 24 h at room temperature, then six were placed onto each agar plate, onto which germs were transferred before with cotton swabs: 4 test platelets impregnated with compounds, as well as 1 suitable positive and 1 negative control. The agar plates were sealed and incubated for 36 h at 32 °C (bacteria) or 28 °C (fungi). Then the antimicrobial effect was assessed by manually measuring the diameters of the zones of inhibition.

5.4.5 Y3H screening

The Y3H screening was performed as previously described[103, 287] and all measurements were performed in the lab of DR. SIMONE MOSER at the LMU Munich.

6 Appendices

6.1 Abbreviations

AAK1	adaptor-associated protein kinase 1
Ae.	*Aedes*
AKT1	RAC-alpha serine/threonine-protein kinase
APCI	atmospheric-pressure chemical ionization
approx.	approximately
aq.	aqueous
ASAP	atmospheric pressure solids analysis probe
ASN	asparagine
ASP	aspartic acid
ATP	adenosine triphosphate
ATR	attenuated total reflection
BCR-ABL	breakpoint cluster region Abelson
BMP2K	BMP-2-inducible protein kinase
Boc	*tert*-butyloxycarbonyl
BOP	benzotriazol-1-yloxytris(dimethylamino)phosphonium hexafluorophosphate
Bu	butyl
CAM	ceric ammonium molybdate
CAMK	Ca^{2+}/calmodulin-dependent protein kinase
CAMKK2	Ca^{2+}/calmodulin-dependent protein kinase kinase 2
CDI	1,1'-carbonyldiimidazole
CDK	cyclin-dependent kinase
cf.	*confer* (compare)
CHIKV	Chikungunya virus
CLK	Cdc2-like kinase, cell division cycle like kinase
CML	chronic myelogenous leukemia
COSY	correlation spectroscopy
COVID-19	coronavirus disease 2019
CSNK	casein kinase
d	doublet
DBU	1,8-diazabicyclo[5.4.0]undec-7-ene
DCC	*N*,*N*'-dicyclohexylcarbodiimide

DDQ	2,3-dichloro-5,6-dicyano-1,4-benzoquinone
DEPT	distortionless enhancement by polarization transfer
DIPEA	*N*,*N*-diisopropylethylamine
DMA	dimethylacetamide
DMAP	4-dimethylaminopyridine
DMF	dimethylformamide
DMSO	dimethyl sulfoxide
DNA	deoxyribonucleic acid
DNPH	2,4-dinitrophenylhydrazine
DPPA	diphenylphosphoryl azide
DSF	differential scanning fluorimetry
DYRK	dual specificity tyrosine-phosphorylation-regulated kinase
ECDC	European Centre for Disease Prevention and Control
EDC	1-ethyl-3-(3-dimethylaminopropyl)carbodiimide
e.g.	*exempli gratia* (for example)
EGF	epidermal growth factor
EI	electron ionisation
eq	equivalent
ESI	electrospray ionisation
Et	ethyl
et al.	*et alia* (and others)
EU/EEA	European Union/European Economic Area
FBS	fetal bovine serum
FDA	U.S. Food and Drug Administration
FMP	Leibniz-Forschungsinstitut für Molekulare Pharmakologie
GLU	glutamine
GLY	glycine
GSK	glycogen synthase kinases
GTP	guanosine triphosphate
HBTU	(2-(1*H*-benzotriazol-1-yl)-1,1,3,3-tetramethyluronium hexafluorophosphate
HEK	human embryonic kidney
HetAr	heteroarene
HMBC	heteronuclear multiple bond correlation
HMQC	heteronuclear multiple quantum coherence

HOBt	hydroxybenzotriazole
HPLC	high-performance liquid chromatography
HRMS	high-resolution mass spectroscopy
HSQC	heteronuclear single quantum correlation
IAV	influenza A virus
IC_{50}	half maximal inhibitory concentration
IR	infrared spectroscopy
IUPAC	International Union of Pure and Applied Chemistry
LDA	lithium diisopropylamide
LEU	leucine
LiHMDS	lithium bis(trimethylsilyl)amide
lit.	literature
LYS	lysine
m	multiplet
MAPK	mitogen-activated protein kinase
Me	methyl
MIDA	*N*-methyliminodiacetic acid
MPI	Max Planck Institute for Infection Biology
mRNA	messenger ribonucleic acid
MS	mass spectroscopy
mTOR	mammalian target of rapamycin
MTT	3-(4,5-dimethylthiazol-2-yl)-2,5-diphenyltetrazolium bromide
n	unbranched
NADH	nicotinamide adenine dinucleotide
NADPH	nicotinamide adenine dinucleotide phosphate
NBS	*N*-bromosuccinimide
NCS	*N*-chlorosuccinimide
n.d.	not determined
NMR	nuclear magnetic resonance
NOE	nuclear Overhauser effect
NQO2	quinone reductase 2
p	*para*
PDGF	platelet-derived growth factor
PG	protective group

Phe	phenylalanine
PIFA	[bis(trifluoracetoxy)iodo]benzene
PIM	proviral integration site for Moloney murine leukemia virus
pK_a	acid dissociation constant
PMB	*p*-methyoxybenzyl
PPA	polyphosphoric acid
q	quartet
quant.	quantitative
R_f	retardation factor
RNA	ribonucleic acid
rt	room temperature
s	singlet
SAR	structure-activity relationships
sat.	saturated
SEM	2-(trimethylsilyl)ethoxymethyl
siRNA	small interfering RNA
SRPK	SRSF protein kinase
SR protein	serine/arginine-rich protein
SRSF	serine/arginine-rich splicing factor
sta	staurosporine
STK	serine/threonine kinase
t	triplet
t	tertiary
TBAF	tetra-*n*-butylammonium fluoride
TBAI	tetra-*n*-butylammonium iodide
TBHP	*tert*-butyl hydroperoxide
temp.	temperature
TFA	trifluoroacetic acid
THF	tetrahydrofuran
TLC	thin-layer chromatography
TMS	trimethylsilyl
TRN-SR	transportin-3
UV	ultraviolet
Val	valine

VEGF	vascular endothelial growth factor
vol.	volume
vs.	versus
WNV	West Nile virus
Y3H	yeast three-hybrid

6.2 References

[1] P. Cohen, *Nat. Rev. Drug Discov.* **2002**, *1*, 309-315.

[2] T. Tamaoki, H. Nomoto, I. Takahashi, Y. Kato, M. Morimoto, F. Tomita, *Biochem. Biophys. Res. Com.* **1986**, *135*, 397-402.

[3] S. Omura, Y. Iwai, A. Hirano, A. Nakagawa, J. Awaya, H. Tsuchya, Y. Takahashi, R. Masuma, *J. Antibiot.* **1977**, *30*, 275-282.

[4] U.S. Food and Drug Administration, FDA approves new combination treatment for acute myeloid leukemia (https://www.fda.gov/news-events/press-announcements/fda-approves-new-combination-treatment-acute-myeloid-leukemia; accessed 22.04.2022).

[5] R. Capdeville, S. Silberman, S. Dimitrijevic, *Eur. J. Cancer* **2002**, *38*, 77-82.

[6] J. Heitman, N. R. Movva, M. N. Hall, *Science* **1991**, *253*, 905-909.

[7] P. Cohen, D. Cross, P. A. Janne, *Nat. Rev. Drug Discov.* **2021**, *20*, 551-569.

[8] C. C. Ayala-Aguilera, T. Valero, A. Lorente-Macias, D. J. Baillache, S. Croke, A. Unciti-Broceta, *J. Med. Chem.* **2022**, *65*, 1047-1131.

[9] Y. Pan, M. M. Mader, *J. Med. Chem.* **2022**, *65*, 5288-5299.

[10] G. Manning, D. B. Whyte, R. Martinez, T. Hunter, S. Sudarsanam, *Science* **2002**, *298*, 1912-1934.

[11] T. Winckler, I. Zündorf, T. Dingermann, *Pharm Unserer Zeit* **2008**, *37*, 370-380.

[12] J. Zhang, P. L. Yang, N. S. Gray, *Nat. Rev. Cancer* **2009**, *9*, 28-39.

[13] J. Yang, P. Cron, V. M. Good, V. Thompson, B. A. Hemmings, D. Barford, *Nat Struct Biol* **2002**, *9*, 940-944.

[14] L. A. Smyth, I. Collins, *J. Chem. Biol.* **2009**, *2*, 131-151.

[15] Y. Ben-David, K. Letwin, L. Tannock, A. Bernstein, T. Pawson, *EMBO J* **1991**, *10*, 317-325.

[16] B. W. Howell, D. E. Afar, J. Lew, E. M. Douville, P. L. Icely, D. A. Gray, J. C. Bell, *Mol. Cell. Biol.* **1991**, *11*, 568-572.

[17] O. Nayler, S. Stamm, A. Ullrich, *Biochem. J.* **1997**, *326*, 693-700.

[18] S. K. Hanks, T. Hunter, *FASEB J.* **1995**, *9*, 576-596.

[19] P. M. Moyano, V. Nemec, K. Paruch, *Int. J. Mol. Sci.* **2020**, *21*, 7549.

[20] UniProt Consortium, CLK1-4 (https://www.uniprot.org/; accessed 06.05.2022).

[21] P. I. Duncan, B. W. Howell, R. M. Marius, S. Drmanic, E. M. Douville, J. C. Bell, *J. Biol. Chem.* **1995**, *270*, 21524-21531.

[22] H. Menegay, F. Moeslein, G. Landreth, *Exp. Cell Res.* **1999**, *253*, 463-473.

[23] P. I. Duncan, D. F. Stojdl, R. M. Marius, J. C. Bell, *Mol. Cell. Biol.* **1997**, *17*, 5996-6001.

[24] W. Gilbert, *Nature* **1978**, *271*, 501.

[25] L. Frankiw, D. Baltimore, G. Li, *Nat. Rev. Immunol.* **2019**, *19*, 675-687.

[26] J. E. Mermoud, P. T. Cohen, A. I. Lamond, *EMBO J* **1994**, *13*, 5679-5688.

[27] A. George, B. E. Aubol, L. Fattet, J. A. Adams, *J. Biol. Chem.* **2019**, *294*, 9631-9641.

[28] K. Colwill, T. Pawson, B. Andrews, J. Prasad, J. L. Manley, J. C. Bell, P. I. Duncan, *EMBO J* **1996**, *15*, 265-275.

[29] B. E. Aubol, G. Wu, M. M. Keshwani, M. Movassat, L. Fattet, K. J. Hertel, X. D. Fu, J. A. Adams, *Mol. Cell* **2016**, *63*, 218-228.

[30] T. Haltenhof, A. Kotte, F. De Bortoli, S. Schiefer, S. Meinke, A. K. Emmerichs, K. K. Petermann, B. Timmermann, P. Imhof, A. Franz, B. Loll, M. C. Wahl, M. Preussner, F. Heyd, *Mol. Cell* **2020**, *78*, 57-69.

[31] S. Uzor, P. Zorzou, E. Bowler, S. Porazinski, I. Wilson, M. Ladomery, *Gene* **2018**, *670*, 46-54.

[32] Y. Zhang, J. Qian, C. Gu, Y. Yang, *Signal Transduct. Target. Ther.* **2021**, *6*, 78.

[33] B. K. Dredge, A. D. Polydorides, R. B. Darnell, *Nat. Rev. Neurosci.* **2001**, *2*, 43-50.

[34] I. Evsyukova, J. A. Somarelli, S. G. Gregory, M. A. Garcia-Blanco, *RNA Biol.* **2010**, *7*, 462-473.

[35] E. Hasimbegovic, V. Schweiger, N. Kastner, A. Spannbauer, D. Traxler, D. Lukovic, M. Gyongyosi, J. Mester-Tonczar, *Genes* **2021**, *12*, 1457.

[36] A. Mukha, E. Kalkhoven, S. W. C. van Mil, *Biochim. Biophys. Acta - Mol. Basis Dis.* **2021**, *1867*, 166183.

[37] S. Chen, C. Yang, Z. W. Wang, J. F. Hu, J. J. Pan, C. Y. Liao, J. Q. Zhang, J. Z. Chen, Y. Huang, L. Huang, Q. Zhan, Y. F. Tian, B. Y. Shen, Y. D. Wang, *J Hematol Oncol* **2021**, *14*, 60.

[38] M. Muraki, B. Ohkawara, T. Hosoya, H. Onogi, J. Koizumi, T. Koizumi, K. Sumi, J. Yomoda, M. V. Murray, H. Kimura, K. Furuichi, H. Shibuya, A. R. Krainer, M. Suzuki, M. Hagiwara, *J. Biol. Chem.* **2004**, *279*, 24246-24254.

[39] S. Uzor, S. R. Porazinski, L. Li, B. Clark, M. Ajiro, K. Iida, M. Hagiwara, A. A. Alqasem, C. M. Perks, I. D. Wilson, S. Oltean, M. R. Ladomery, *Sci. Rep.* **2021**, *11*, 7963.

[40] N. Babu, S. M. Pinto, M. Biswas, T. Subbannayya, M. Rajappa, S. V. Mohan, J. Advani, P. Rajagopalan, G. Sathe, N. Syed, V. D. Radhakrishna, O. Muthusamy, S. Navani, R. V. Kumar, G. Gopisetty, T. Rajkumar, P. Radhakrishnan, S. Thiyagarajan, A. Pandey, H. Gowda, P. Majumder, A. Chatterjee, *Gastric Cancer* **2020**, *23*, 796-810.

[41] D. Zhu, S. Xu, G. Deyanat-Yazdi, S. X. Peng, L. A. Barnes, R. K. Narla, T. Tran, D. Mikolon, Y. Ning, T. Shi, N. Jiang, H. K. Raymon, J. R. Riggs, J. F. Boylan, *Mol. Cancer Ther.* **2018**, *17*, 1727-1738.

[42] H. Li, X. Cui, Q. Hu, X. Chen, P. Zhou, *OncoTargets Ther.* **2019**, *12*, 9201-9213.

[43] U.S. National Library of Medicine, A Study Evaluating the Safety and Pharmacokinetics of Orally Administered SM08502 in Subjects With Advanced Solid Tumors (https://clinicaltrials.gov/ct2/show/study/NCT03355066?term=SM08502&draw=2&rank=2https://clinicaltrials.gov/ct2/show/study/NCT03355066?term=SM08502&draw=2&rank=2; accessed 28.04.2022).

[44] U.S. National Library of Medicine, A Study Evaluating the Safety, Pharmacokinetics, and Preliminary Efficacy of Orally Administered SM08502 Combined With Hormonal Therapy or Chemotherapy in Subjects With Advanced Solid Tumors (https://clinicaltrials.gov/ct2/show/study/NCT05084859?cond=CLK&draw=2&rank=1; accessed 28.04.2022).

[45] B. Y. Tam, K. Chiu, H. Chung, C. Bossard, J. D. Nguyen, E. Creger, B. W. Eastman, C. C. Mak, M. Ibanez, A. Ghias, J. Cahiwat, L. Do, S. Cho, J. Nguyen, V. Deshmukh, J. Stewart, C. W. Chen, C. Barroga, L. Dellamary, S. K. Kc, T. J. Phalen, J. Hood, S. Cha, Y. Yazici, *Cancer Lett.* **2020**, *473*, 186-197.

[46] K. Huber, doctoral thesis, Ludwig-Maximilians-Universität (München), **2007**.

[47] O. Fedorov, K. Huber, A. Eisenreich, P. Filippakopoulos, O. King, A. N. Bullock, D. Szklarczyk, L. J. Jensen, D. Fabbro, J. Trappe, U. Rauch, F. Bracher, S. Knapp, *Chem. Biol.* **2011**, *18*, 67-76.

[48] N. Hilz, doctoral thesis, Ludwig-Maximilians-Universität (München), **2011**.

[49] G. Simic, M. Babic Leko, S. Wray, C. Harrington, I. Delalle, N. Jovanov-Milosevic, D. Bazadona, L. Buee, R. de Silva, G. Di Giovanni, C. Wischik, P. R. Hof, *Biomolecules* **2016**, *6*, 6.

[50] F. Liu, C. X. Gong, *Mol. Neurodegener.* **2008**, *3*, 8.

[51] D. C. Glatz, D. Rujescu, Y. Tang, F. J. Berendt, A. M. Hartmann, F. Faltraco, C. Rosenberg, C. Hulette, K. Jellinger, H. Hampel, P. Riederer, H. J. Moller, A. Andreadis, K. Henkel, S. Stamm, *J. Neurochem.* **2006**, *96*, 635-644.

[52] P. Jain, C. Karthikeyan, N. S. Moorthy, D. K. Waiker, A. K. Jain, P. Trivedi, *Curr. Drug Targets* **2014**, *15*, 539-550.

[53] K.-Y. Lee, A. W. Clark, J. L. Rosales, K. Chapman, T. Fung, R. N. Johnston, *Neurosci. Res.* **1999**, *34*, 21-29.

[54] J. Wegiel, C. X. Gong, Y. W. Hwang, *FEBS J* **2011**, *278*, 236-245.

[55] T. E. Lin, M.-W. Chao, W.-C. HuangFu, H.-J. Tu, Z.-X. Peng, C.-J. Su, T.-Y. Sung, J.-H. Hsieh, C.-C. Lee, C.-R. Yang, S.-L. Pan, K.-C. Hsu, *Biomed. Pharmacother.* **2022**, *146*, 112580.

[56] S. H. E. Kaufmann, A. Dorhoi, R. S. Hotchkiss, R. Bartenschlager, *Nat. Rev. Drug Discov.* **2018**, *17*, 35-56.

[57] A. Karlas, N. Machuy, Y. Shin, K. P. Pleissner, A. Artarini, D. Heuer, D. Becker, H. Khalil, L. A. Ogilvie, S. Hess, A. P. Maurer, E. Muller, T. Wolff, T. Rudel, T. F. Meyer, *Nature* **2010**, *463*, 818-822.

[58] R. Konig, S. Stertz, Y. Zhou, A. Inoue, H. H. Hoffmann, S. Bhattacharyya, J. G. Alamares, D. M. Tscherne, M. B. Ortigoza, Y. Liang, Q. Gao, S. E. Andrews, S. Bandyopadhyay, P. De Jesus, B. P. Tu, L. Pache, C. Shih, A. Orth, G. Bonamy, L. Miraglia, T. Ideker, A. Garcia-Sastre, J. A. Young, P. Palese, M. L. Shaw, S. K. Chanda, *Nature* **2010**, *463*, 813-817.

[59] M. N. Krishnan, A. Ng, B. Sukumaran, F. D. Gilfoy, P. D. Uchil, H. Sultana, A. L. Brass, R. Adametz, M. Tsui, F. Qian, R. R. Montgomery, S. Lev, P. W. Mason, R. A. Koski, S. J. Elledge, R. J. Xavier, H. Agaisse, E. Fikrig, *Nature* **2008**, *455*, 242-245.

[60] A. Karlas, S. Berre, T. Couderc, M. Varjak, P. Braun, M. Meyer, N. Gangneux, L. Karo-Astover, F. Weege, M. Raftery, G. Schonrich, U. Klemm, A. Wurzlbauer, F. Bracher, A. Merits, T. F. Meyer, M. Lecuit, *Nat. Commun.* **2016**, *7*, 11320.

[61] R. A. Lamb, P. W. Choppin, *Virology* **1981**, *112*, 729-737.

[62] R. A. Lamb, C. J. Lai, P. W. Choppin, **1981**, *78*, 4170-4174.

[63] A. Artarini, M. Meyer, Y. J. Shin, K. Huber, N. Hilz, F. Bracher, D. Eros, L. Orfi, G. Keri, S. Goedert, M. Neuenschwander, J. von Kries, Y. Domovich-Eisenberg, N. Dekel, I. Szabadkai, M. Lebendiker, Z. Horvath, T. Danieli, O. Livnah, O. Moncorge, R. Frise, W. Barclay, T. F. Meyer, A. Karlas, *Antiviral Res* **2019**, *168*, 187-196.

[64] European Centre for Disease Prevention and Control, Chikungunya virus disease Annual Epidemiological Report for 2019 (https://www.ecdc.europa.eu/sites/default/files/documents/chikungunya-annual-epidemiological-report-2019.pdf; accessed 02.05.2022).

[65] European Centre for Disease Prevention and Control, Chikungunya virus disease Annual Epidemiological Report for 2020 (https://www.ecdc.europa.eu/sites/default/files/documents/CHIK_AER_2020_Report_final.pdf; accessed 02.05.2022).

[66] F. Riccardo, G. Venturi, M. Di Luca, M. Del Manso, F. Severini, X. Andrianou, C. Fortuna, M. E. Remoli, E. Benedetti, M. G. Caporali, F. Fratto, A. D. Mignuoli, L. Rizzo, G. De Vito, V. De Giorgio, L. Surace, F. Vairo, P. Angelini, M. C. Re, A. Amendola, C. Fiorentini, G. Marsili, L. Toma, D. Boccolini, R. Romi, P. Pezzotti, G. Rezza, C. Rizzo, *Emerg Infect Dis* **2019**, *25*, 2093-2095.

[67] C. Calba, M. Guerbois-Galla, F. Franke, C. Jeannin, M. Auzet-Caillaud, G. Grard, L. Pigaglio, A. Decoppet, J. Weicherding, M. C. Savaill, M. Munoz-Riviero, P. Chaud, B. Cadiou, L. Ramalli, P. Fournier, H. Noel, X. De Lamballerie, M. C. Paty, I. Leparc-Goffart, *Eurosurveillance* **2017**, *22*.

[68] M. U. G. Kraemer, R. C. Reiner, Jr., O. J. Brady, J. P. Messina, M. Gilbert, D. M. Pigott, D. Yi, K. Johnson, L. Earl, L. B. Marczak, S. Shirude, N. Davis Weaver, D. Bisanzio, T. A. Perkins, S. Lai, X. Lu, P. Jones, G. E. Coelho, R. G. Carvalho, W. Van Bortel, C. Marsboom, G. Hendrickx, F. Schaffner, C. G. Moore, H. H. Nax, L. Bengtsson, E. Wetter, A. J. Tatem, J. S. Brownstein, D. L. Smith, L. Lambrechts, S. Cauchemez, C. Linard, N. R. Faria, O. G. Pybus, T. W. Scott, Q. Liu, H. Yu, G. R. W. Wint, S. I. Hay, N. Golding, *Nat. Microbiol.* **2019**, *4*, 854-863.

[69] N. B. Tjaden, J. E. Suk, D. Fischer, S. M. Thomas, C. Beierkuhnlein, J. C. Semenza, *Sci. Rep.* **2017**, *7*, 3813.

[70] J. H. Strauss, E. G. Strauss, *Microbiol. Rev.* **1994**, *58*, 491-562.

[71] M. C. Robinson, *Trans. R. Soc. Trop. Med. Hyg.* **1955**, *49*, 28-32.

[72] World Health Organization, Fact sheet Chikungunya (https://www.who.int/news-room/factsheets/detail/chikungunya; accessed 06.05.2022).

[73] D. M. Vu, D. Jungkind, L. Angelle Desiree, *Clin. Lab. Med.* **2017**, *37*, 371-382.

[74] K. A. Tsetsarkin, D. L. Vanlandingham, C. E. McGee, S. Higgs, *PLOS Pathog.* **2007**, *3*, 1895-1906.

[75] European Centre for Disease Prevention and Control, Information for travellers to areas with chikungunya transmission (https://www.ecdc.europa.eu/en/chikungunya/threats-and-outbreaks/information-travellers; accessed 06.05.2022).

[76] O. Schwartz, M. L. Albert, *Nat. Rev. Microbiol.* **2010**, *8*, 491-500.

[77] Valneva SE, Valneva Successfully Completes Pivotal Phase 3 Trial of Single-Shot Chikungunya Vaccine Candidate (https://valneva.com/press-release/valneva-successfully-completes-pivotal-phase-3-trial-of-single-shot-chikungunya-vaccine-candidate/?lang=de; accessed 06.05.2022).

[78] B. Pohl, doctoral thesis, Ludwig-Maximilians-Universität (München), **2002**.

[79] B. Ströde, doctoral thesis, Ludwig-Maximilians-Universität (München), **2008**.

[80] O. Kast, doctoral thesis, Ludwig-Maximilians-Universität (München), **2003**.

[81] A. Ritter, doctoral thesis, Ludwig-Maximilians-Universität (München), **2006**.

[82] A. Wurzlbauer, doctoral thesis, Ludwig-Maximilians-Universität (München), **2013**.

[83] A. Gehring, doctoral thesis, Ludwig-Maximilians-Universität (München), **2013**.

[84] N. Dekel, Y. Eisenberg-Domovich, A. Karlas, T. F. Meyer, F. Bracher, M. Lebendiker, T. Danieli, O. Livnah, *Protein Expr. Purif.* **2020**, *176*, 105742.

[85] C. Aigner, doctoral thesis, Ludwig-Maximilians-Universität (München), **2017**.

[86] T. Tremmel, F. Bracher, *Tetrahedron* **2015**, *71*, 4640-4646.

[87] F. Bracher, D. Hildebrand, *Liebigs Ann.* **1992**, *1992*, 1315-1319.

[88] C. M. Roggero, J. M. Giulietti, S. P. Mulcahy, *Bioorg. Med. Chem. Lett.* **2014**, *24*, 3549-3551.

[89] G. La Regina, V. Famiglini, S. Passacantilli, S. Pelliccia, P. Punzi, R. Silvestri, *Synthesis* **2014**, *46*, 2093-2097.

[90] F. Bracher, D. Hildebrand, *Tetrahedron* **1994**, *50*, 12329-12336.

[91] T. Tremmel, doctoral thesis, Ludwig-Maximilians-Universität (München), **2016**.

[92] S. Crosignani, A. Pretre, C. Jorand-Lebrun, G. Fraboulet, J. Seenisamy, J. K. Augustine, M. Missotten, Y. Humbert, C. Cleva, N. Abla, H. Daff, O. Schott, M. Schneider, F. Burgat-Charvillon, D. Rivron, I. Hamernig, J. F. Arrighi, M. Gaudet, S. C. Zimmerli, P. Juillard, Z. Johnson, *J. Med. Chem.* **2011**, *54*, 7299-7317.

[93] S. Caddick, V. M. Delisser, V. E. Doyle, S. Khan, A. G. Avent, S. Vile, *Tetrahedron* **1999**, *55*, 2737-2754.

[94] F. Bracher, D. Hildebrand, L. Ernst, *Arch. Pharm.* **1994**, *327*, 121-122.

[95] D. Hildebrand, doctoral thesis, Philips-Universität Marburg (Marburg/Lahn), **1994**.

[96] W. J. Scott, J. K. Stille, *J. Am. Chem. Soc.* **1986**, *108*, 3033-3040.

[97] X. Zheng, M. A. Kerr, *Org. Lett.* **2006**, *8*, 3777-3779.

[98] R. Huisgen, *Angew. Chem.* **1963**, *75*, 604-637.

[99] R. Huisgen, *Angew. Chem.* **1963**, *75*, 742-754.

[100] S. B. Bharate, A. K. Padala, B. A. Dar, R. R. Yadav, B. Singh, R. A. Vishwakarma, *Tetrahedron Lett.* **2013**, *54*, 3558-3561.

[101] A. M. Jawalekar, E. Reubsaet, F. P. Rutjes, F. L. van Delft, *Chem. Commun.* **2011**, *47*, 3198-3200.

[102] E. Plesch, doctoral thesis, Ludwig-Maximilians-Universität (München), **2018**.

[103] P. Wang, T. Klassmüller, C. A. Karg, M. Kretschmer, S. Zahler, S. Braig, F. Bracher, A. M. Vollmar, S. Moser, *Biol. Chem.* **2022**, *403*, 421-431.

[104] B. Lohrer, F. Bracher, *Tetrahedron Lett.* **2019**, *60*, 151327.

[105] J. K. Howard, K. J. Rihak, A. C. Bissember, J. A. Smith, *Chem.: Asian J.* **2016**, *11*, 155-167.

[106] S. M. Bhosale, A. A. Momin, R. L. Gawade, V. G. Puranik, R. S. Kusurkar, *Tetrahedron Lett.* **2012**, *53*, 5327-5330.

[107] A. A. Akhrem, F. A. Lakhvich, V. A. Khripach, *Chem. Heterocycl. Compd.* **1981**, *17*, 853-868.

[108] K. C. Coffman, V. Duong, A. L. Bagdasarian, J. C. Fettinger, M. J. Haddadin, M. J. Kurth, *Eur. J. Org. Chem.* **2014**, *2014*, 7651-7657.

[109] E. Noelting, O. Michel, *Ber. Dtsch. Chem. Ges.* **1893**, *26*, 86-87.

[110] R. Lindsay, C. Allen, *Org. Synth.* **1942**, *22*, 96.

[111] C.-Z. Tao, X. Cui, J. Li, A.-X. Liu, L. Liu, Q.-X. Guo, *Tetrahedron Lett.* **2007**, *48*, 3525-3529.

[112] V. K. Aggarwal, J. de Vicente, R. V. Bonnert, *J. Org. Chem.* **2003**, *68*, 5381-5383.

[113] Y. Wang, X. Wen, X. Cui, L. Wojtas, X. P. Zhang, *J. Am. Chem. Soc.* **2017**, *139*, 1049-1052.

[114] W. R. Bamford, T. S. Stevens, *J. Chem. Soc.* **1952**, 4735-4740.

[115] A. Secrieru, P. M. O'Neill, M. L. S. Cristiano, *Molecules* **2020**, *25*, 42.

[116] E. Tyrrell, J. Allen, K. Jones, R. Beauchet, *Synthesis* **2005**, *2005*, 2393-2399.

[117] C. S. McKay, J. Moran, J. P. Pezacki, *Chem. Commun.* **2010**, *46*, 931-933.

[118] H. Seidl, R. Huisgen, R. Knorr, *Chem. Ber.* **1969**, *102*, 904-914.

[119] G. Wang, S. Sun, R. Chen, S. Zhao, L. Yang, Q. Li, Q. Chen, CN106986840 A, China, **2017**.

[120] T. Ohmoto, K. Koike, *Chem. Pharm. Bull.* **1984**, *32*, 3579-3583.

[121] V. Singh, S. Hutait, S. Batra, *Eur. J. Org. Chem.* **2009**, *2009*, 6211-6216.

[122] W. Chen, G. Zhang, L. Guo, W. Fan, Q. Ma, X. Zhang, R. Du, R. Cao, *Eur. J. Med. Chem.* **2016**, *124*, 249-261.

[123] T. R. Kelly, X. Wei, J. Sundaresan, *Tetrahedron Lett.* **1993**, *34*, 6173-6176.

[124] T. Veysoglu, L. A. Mitscher, J. K. Swayze, *Synthesis* **1980**, *1980*, 807-810.

[125] A. Puzik, doctoral thesis, Ludwig-Maximilians-Universität (München), **2003**.

[126] D. Singh, N. Devi, V. Kumar, C. C. Malakar, S. Mehra, R. K. Rawal, B. S. Kaith, V. Singh, *RSC Adv.* **2016**, *6*, 88066-88076.

[127] M. A. Ponce, O. I. Tarzi, R. Erra-Balsells, *J. Heterocycl. Chem.* **2003**, *40*, 419.

[128] A. Kamlah, doctoral thesis, Ludwig-Maximilians-Universität (München), **2018**.

[129] J. W. Scheeren, P. H. J. Ooms, R. J. F. Nivard, *Synthesis* **1973**, *1973*, 149-151.

[130] D. N. McGregor, U. Corbin, J. E. Swigor, L. C. Cheney, *Tetrahedron* **1969**, *25*, 389-395.

[131] F. J. McEvoy, G. R. Allen, *J. Org. Chem.* **1969**, *34*, 4199-4201.

[132] S. Samanta, R. R. Donthiri, M. Dinda, S. Adimurthy, *RSC Adv.* **2015**, *5*, 66718-66722.

[133] R. Robinson, *J. Chem. Soc., Trans.* **1909**, *95*, 2167-2174.

[134] S. Gabriel, *Ber. Dtsch. Chem. Ges.* **1910**, *43*, 1283-1287.

[135] G. Klimsha, B. Distanoc, N. Kudinova, SU973539 A1, Soviet Union, **1982**.

[136] G. S. Reddy, K. Rajasekhar, C. Praveen, K. Mukkanti, P. P. Reddy, *Synth. Commun.* **2008**, *38*, 3884-3893.

[137] P. G. M. Wuts, *Greene's protective groups in organic synthesis (5th ed.)*, John Wiley & Sons, Inc., Hoboken (New Jersey), **2014**.

[138] L.-H. Du, S.-J. Zhang, Y.-G. Wang, *Tetrahedron Lett.* **2005**, *46*, 3399-3402.

[139] R. Orth, S. A. Sieber, *J. Org. Chem.* **2009**, *74*, 8476-8479.

[140] W. Huang, J. Pei, B. Chen, W. Pei, X. Ye, *Tetrahedron* **1996**, *52*, 10131-10136.

[141] T. Sharonova, V. Pankrat'eva, P. Savko, S. Baykov, A. Shetnev, *Tetrahedron Lett.* **2018**, *59*, 2824-2827.

[142] W. Caneschi, K. B. Enes, C. Carvalho de Mendonca, F. de Souza Fernandes, F. B. Miguel, J. da Silva Martins, M. Le Hyaric, R. R. Pinho, L. M. Duarte, M. A. Leal de Oliveira, H. F. Dos Santos, M. T. Paz Lopes, D. Dittz, H. Silva, M. R. Costa Couri, *Eur. J. Med. Chem.* **2019**, *165*, 18-30.

[143] D. Singh, S. K. Tiwari, V. Singh, *New J. Chem.* **2019**, *43*, 93-102.

[144] T. D. Aicher, B. Balkan, P. A. Bell, L. J. Brand, S. H. Cheon, R. O. Deems, J. B. Fell, W. S. Fillers, J. D. Fraser, J. Gao, D. C. Knorr, G. G. Kahle, C. L. Leone, J. Nadelson, R. Simpson, H. C. Smith, *J. Med. Chem.* **1998**, *41*, 4556-4566.

[145] C. Du, L. Li, Y. Li, Z. Xie, *Angew. Chem.* **2009**, *121*, 7993-7996.
[146] S. W. Youn, *Org. Prep. Proced. Int.* **2006**, *38*, 505-591.
[147] N. Sudzukovic, J. Schinnerl, L. Brecker, *Bioorg. Med. Chem.* **2016**, *24*, 588-595.
[148] B. Zheng, T. H. Trieu, T.-Z. Meng, X. Lu, J. Dong, Q. Zhang, X.-X. Shi, *RSC Adv.* **2018**, *8*, 6834-6839.
[149] F. Hadjaz, S. Yous, N. Lebegue, P. Berthelot, P. Carato, *Tetrahedron* **2008**, *64*, 10004-10008.
[150] W. Jiang, Z. Sui, X. Chen, *Tetrahedron Lett.* **2002**, *43*, 8941-8945.
[151] M. Jawdosiuk, J. M. Cook, *J. Org. Chem.* **1983**, *49*, 2699-2701.
[152] T. Szabó, V. Hazai, B. Volk, G. Simig, M. Milen, *Tetrahedron Lett.* **2019**, *60*, 1471-1475.
[153] S. Rajkumar, S. Karthik, T. Gandhi, *J. Org. Chem.* **2015**, *80*, 5532-5545.
[154] Y. Zhang, Z. Zhang, B. Wang, L. Liu, Y. Che, *Bioorg. Med. Chem. Lett.* **2016**, *26*, 1885-1888.
[155] B. Radzisewski, *Ber. Dtsch. Chem. Ges.* **1882**, *15*, 2706-2708.
[156] M. Mao, S. Xiao, J. Li, Y. Zou, R. Zhang, J. Pan, F. Dan, K. Zou, T. Yi, *Tetrahedron* **2012**, *68*, 5037-5041.
[157] A. O. Eseola, M. Zhang, J.-F. Xiang, W. Zuo, Y. Li, J. A. O. Woods, W.-H. Sun, *Inorg. Chim. Acta* **2010**, *363*, 1970-1978.
[158] B. Khalili, T. Tondro, M. M. Hashemi, *Tetrahedron* **2009**, *65*, 6882-6887.
[159] A. Ritzén, J. Kehler, M. Langgård, J. Nielsen, J. P. Kilburn, M. M. Farah, WO2009/152825 A1, **2009**.
[160] L. He, S. Y. Liao, C. P. Tan, R. R. Ye, Y. W. Xu, M. Zhao, L. N. Ji, Z. W. Mao, *Chemistry* **2013**, *19*, 12152-12160.
[161] D. C. Baker, S. R. Putt, *ChemInform* **1978**, *9*, 478-479.
[162] V. Dal Piaz, S. Pinzauti, P. Lacrimini, *Synthesis* **1975**, *1975*, 664-665.
[163] H. Kawai, K. Tachi, E. Tokunaga, M. Shiro, N. Shibata, *Angew Chem Int Ed Engl* **2011**, *50*, 7803-7806.
[164] H. Zhao, G. Liu, Z. Xin, M. D. Serby, Z. Pei, B. G. Szczepankiewicz, P. J. Hajduk, C. Abad-Zapatero, C. W. Hutchins, T. H. Lubben, S. J. Ballaron, D. L. Haasch, W. Kaszubska, C. M. Rondinone, J. M. Trevillyan, M. R. Jirousek, *Bioorg. Med. Chem. Lett.* **2004**, *14*, 5543-5546.
[165] F. Bracher, D. Hildebrand, *Pharmazie* **1995**, *50*, 182-183.
[166] E. Winterfeldt, *Chem. Ber.* **1964**, *97*, 1952-1958.
[167] A. W. McCulloch, A. G. McInnes, *Can. J. Chem.* **1974**, *52*, 3569-3576.
[168] E. Rajanarendar, K. G. Reddy, S. R. Krishna, M. Srinivas, *J. Heterocycl. Chem.* **2015**, *52*, 660-668.
[169] C. L. Peck, J. A. Calderone, W. L. Santos, *Synthesis* **2015**, *47*, 2242-2248.
[170] M. Christl, R. Huisgen, R. Sustmann, *Chem. Ber.* **1973**, *106*, 3275-3290.
[171] J. M. Muchowski, D. R. Solas, *J. Org. Chem.* **1984**, *49*, 203-205.
[172] D. Heerdegen, doctoral thesis, Ludwig-Maximilians-Universität (München), **2020**.
[173] N. Papaioannou, S. J. Fink, T. A. Miller, G. W. Shipps Jr., J. M. Travins, D. E. Ehmann, A. Rae, J. M. Ellard, US2019/0284182 A1, United States, **2019**.
[174] T. Curtius, *J. prakt. Chem.* **1894**, *50*, 275-294.
[175] T. Curtius, *Ber. Dtsch. Chem. Ges.* **1890**, *23*, 3023-3033.
[176] T. Shioiri, K. Ninomiya, S. Yamada, *J. Am. Chem. Soc.* **1972**, *94*, 6203-6205.
[177] L. A. Reiter, *J. Org. Chem.* **1987**, *52*, 2714-2726.
[178] SciFinder (CAS), 3-Phenyl-5-(2-pyridinyl)-4-isoxazolamine (https://scifinder-n.cas.org/searchDetail/substance/6284e0f1e3120c1726f8f1ba/substanceDetails; accessed 18.05.2022).
[179] SciFinder (CAS), 4-isoxazolamine (https://scifinder-n.cas.org/searchDetail/substance/6284e1e6e3120c1726f8f3dc/substanceDetails; accessed 18.05.2022).
[180] C. A. Busacca, M. C. Eriksson, Y. Dong, A. S. Prokopowicz, A. M. Salvagno, M. A. Tschantz, *J. Org. Chem.* **1999**, *64*, 4564-4568.
[181] E. Sawatzky, A. Drakopoulos, M. Rolz, C. Sotriffer, B. Engels, M. Decker, *Beilstein J. Org. Chem.* **2016**, *12*, 2280-2292.

[182] A. Greenberg, N. Molinaro, M. Lang, *J. Org. Chem.* **2002**, *49*, 1127-1130.

[183] *Europäisches Arzneibuch (Ph. Eur., 10th ed.), Hydrochlorothiazid*, Deutscher Apotheker Verlag, Stuttgart, **2020**.

[184] Y. Yang, Y. Ling, Y. Guo, F. Liu, Y. Zhao, CN103145705 A, China, **2013**.

[185] S. G. Abdel-Moty, S. Sakai, N. Aimi, H. Takayama, M. Kitajima, A. El-Shorbagi, A. N. Ahmed, N. M. Omar, *Eur. J. Med. Chem.* **1998**, *32*, 1009-1017.

[186] P. O. Venkataramana Reddy, S. Mishra, M. P. Tantak, K. Nikhil, R. Sadana, K. Shah, D. Kumar, *Bioorg. Med. Chem. Lett.* **2017**, *27*, 1379-1384.

[187] Y. Murakami, T. Watanabe, A. Kobayashi, Y. Yokoyama, *Synthesis* **1984**, *1984*, 738-740.

[188] A. A. Haddach, A. Kelleman, M. V. Deaton-Rewolinski, *Tetrahedron Lett.* **2002**, *43*, 399-402.

[189] Y. Miki, H. Hachiken, Y. Kashima, W. Sugimura, N. Yanase, *Heterocycles* **1998**, *48*, 1-4.

[190] I. T. Forbes, C. N. Johnson, M. Thompson, *J. Chem. Soc., Perkin Trans. 1* **1992**, 275-281.

[191] C. Willemann, R. Grunert, P. J. Bednarski, R. Troschutz, *Bioorg. Med. Chem.* **2009**, *17*, 4406-4419.

[192] S. Mathieu, S. N. Gradl, L. Ren, Z. Wen, I. Aliagas, J. Gunzner-Toste, W. Lee, R. Pulk, G. Zhao, B. Alicke, J. W. Boggs, A. J. Buckmelter, E. F. Choo, V. Dinkel, S. L. Gloor, S. E. Gould, J. D. Hansen, G. Hastings, G. Hatzivassiliou, E. R. Laird, D. Moreno, Y. Ran, W. C. Voegtli, S. Wenglowsky, J. Grina, J. Rudolph, *J. Med. Chem.* **2012**, *55*, 2869-2881.

[193] M. Jumppanen, S. M. Kinnunen, M. J. Valimaki, V. Talman, S. Auno, T. Bruun, G. Boije Af Gennas, H. Xhaard, I. B. Aumuller, H. Ruskoaho, J. Yli-Kauhaluoma, *J. Med. Chem.* **2019**, *62*, 8284-8310.

[194] J. W. Lee, Y.-s. Son, J.-Y. Lee, M. H. Kim, S.-K. Woo, K. C. Lee, Y. J. Lee, G. T. Hwang, *Tetrahedron* **2016**, *72*, 5595-5601.

[195] S. B. King, B. Ganem, *J. Am. Chem. Soc.* **2002**, *116*, 562-570.

[196] M. Untergehrer, docotoral thesis, Ludwig-Maximilians-Universität (München), **2020**.

[197] K. Thees, doctoral thesis, Ludwig-Maximilians-Universität (München), **in preparation**.

[198] E. D. Cox, J. M. Cook, *Chem. Rev.* **2002**, *95*, 1797-1842.

[199] H. Liu, M. Qiao, H. Xu, Z. Dou, CN107973796 A, China, **2018**.

[200] Y. Zhao, F. Ye, J. Xu, Q. Liao, L. Chen, W. Zhang, H. Sun, W. Liu, F. Feng, W. Qu, *Bioorg. Med. Chem.* **2018**, *26*, 3812-3824.

[201] F. Donà, master thesis, Sapienza Università (Roma), **2020**.

[202] N. G. Gaylord, *J. Chem. Educ.* **1957**, *34*, 367-374.

[203] P. Ábrányi-Balogh, A. Dancsó, D. Frigyes, B. Volk, G. Keglevich, M. Milen, *Tetrahedron* **2014**, *70*, 5711-5719.

[204] A. Kim, M. Yu, J.-T. Sim, S.-G. Kim, *Bull. Korean Chem. Soc.* **2016**, *37*, 1529-1532.

[205] F. Bracher, *Mini-Rev. Org. Chem.* **2020**, *17*, 47-66.

[206] G. Bianchi, A. Cogoli, P. Grünanger, *J. Organomet. Chem.* **1966**, *6*, 598-602.

[207] M. W. Davies, R. A. J. Wybrow, J. P. A. Harrity, C. N. Johnson, *Chem. Commun.* **2001**, 1558-1559.

[208] J. E. Moore, M. W. Davies, K. M. Goodenough, R. A. J. Wybrow, M. York, C. N. Johnson, J. P. A. Harrity, *Tetrahedron* **2005**, *61*, 6707-6714.

[209] M. Ellermann, G. Valot, G. Y. Cancho, J. Hassfeld, T. Kinzel, J. Köbberling, K. Beyer, S. Röhrig, M. Sperzel, J. Stampfuss, I. Meyer, M. Köllnberger, N. Burkhardt, K. Schlemmer, C. Stegmann, J. Schuhmacher, M. Werner, J. Heiermann, W. J. Hengeveld, WO2016/071216 A1, **2016**.

[210] D. Gretzke, O. Ritzeler, U. Heinelt, V. Wehner, F. Schmidt, WO2018/083157 A1, **2018**.

[211] K. Mautner, doctoral thesis, Ludwig-Maximilians-Universität (München), **2016**.

[212] J. E. Grob, J. Nunez, M. A. Dechantsreiter, L. G. Hamann, *J. Org. Chem.* **2011**, *76*, 10241-10248.

[213] C. Bodea, M. Raileanu, *Liebigs Ann.* **1960**, *631*, 194-198.

[214] A. Hallberg, A. R. Martin, *Synth. Commun.* **1983**, *13*, 467-470.

[215] H. Gilman, D. A. Shirley, P. R. V. Ess, *J. Am. Chem. Soc.* **1944**, *66*, 625-627.

[216] G. Wittig, G. Harborth, *Ber. Dtsch. Chem. Ges.* **1944**, *77*, 306-314.

[217] Christa S. Krämer, Thomas J. J. Müller, *Eur. J. Org. Chem.* **2003**, *2003*, 3534-3548.

[218] X. Liu, X. Liu, M. Zhuang, M. Li, Y. He, H. Zheng, H. Sun, W. Liu, C. Li, K. Wei, CN111072702 A, China, **2020**.

[219] R. Barret, M. Daudon, *Monatsh. Chem.* **1991**, *122*, 323-325.

[220] E. Fischer, F. Jourdan, *Ber. Dtsch. Chem. Ges.* **1883**, *16*, 2241-2245.

[221] W. Borsche, *Liebigs Ann.* **1908**, *359*, 49-80.

[222] B. M. Barclay, N. Campbell, *J. Chem. Soc.* **1945**, 530-533.

[223] R. A. Al-Balushi, A. Haque, M. Jayapal, M. K. Al-Suti, J. Husband, M. S. Khan, O. F. Koentjoro, K. C. Molloy, J. M. Skelton, P. R. Raithby, *Inorg. Chem.* **2016**, *55*, 6465-6480.

[224] M. S. Bennington, H. L. Feltham, Z. J. Buxton, N. G. White, S. Brooker, *Dalton Trans.* **2017**, *46*, 4696-4710.

[225] F. R. Japp, F. Klingemann, *Ber. Dtsch. Chem. Ges.* **1887**, *20*, 2942-2944.

[226] F. R. Japp, F. Klingemann, *Ber. Dtsch. Chem. Ges.* **1887**, *20*, 3284-3286.

[227] F. Sóti, M. Incze, Z. Kardos-Balogh, M. Kajtár-Peredy, C. Szántay, *Synth. Commun.* **1993**, *23*, 1689-1698.

[228] J. F. W. McOmie, M. L. Watts, D. E. West, *Tetrahedron* **1968**, *24*, 2289-2292.

[229] R. Filler, B. T. Khan, C. W. McMullen, *J. Org. Chem.* **2002**, *27*, 4660-4662.

[230] R. L. Burwell, M. E. Fuller, *J. Am. Chem. Soc.* **1956**, *79*, 2332-2336.

[231] M. Maftouh, R. Besselievre, B. Monsarrat, P. Lesca, B. Meunier, H. P. Husson, C. Paoletti, *J. Med. Chem.* **1985**, *28*, 708-714.

[232] J. Reniers, S. Robert, R. Frederick, B. Masereel, S. Vincent, J. Wouters, *Bioorg. Med. Chem.* **2011**, *19*, 134-144.

[233] T. Choshi, T. Sada, H. Fujimoto, C. Nagayama, E. Sugino, S. Hibino, *J. Org. Chem.* **1997**, *62*, 2535-2543.

[234] T. R. Forbus, S. L. Taylor, J. C. Martin, *J. Org. Chem.* **1987**, *52*, 4156-4159.

[235] N. Bruno, Sigma-Aldrich, Cross-Coupling Reaction Manual: Desk Reference, **2017**.

[236] S. Yamamoto, T. Shibata, K. Abe, K. Oda, T. Aoki, Y. Kawakita, H. Kawamoto, *Chem. Pharm. Bull.* **2016**, *64*, 1321-1337.

[237] Z. Liu, J. J. Swidorski, B. Nowicka-Sans, B. Terry, T. Protack, Z. Lin, H. Samanta, S. Zhang, Z. Li, D. D. Parker, S. Rahematpura, S. Jenkins, B. R. Beno, M. Krystal, N. A. Meanwell, I. B. Dicker, A. Regueiro-Ren, *Bioorg. Med. Chem.* **2016**, *24*, 1757-1770.

[238] L. K. Crevatín, S. M. Bonesi, R. Erra-Balsells, *Helv. Chim. Acta* **2006**, *89*, 1147-1157.

[239] S. Rondeau-Gagné, C. Curutchet, F. Grenier, G. D. Scholes, J.-F. Morin, *Tetrahedron* **2010**, *66*, 4230-4242.

[240] N. A. Powell, S. D. Rychnovsky, *Tetrahedron Lett.* **1996**, *37*, 7901-7904.

[241] A. Kamlah, F. Lirk, F. Bracher, *Tetrahedron* **2016**, *72*, 837-845.

[242] A. Reissert, *Ber. Dtsch. Chem. Ges.* **2006**, *30*, 1030-1053.

[243] M. Tabart, E. Bacque, F. Halley, B. Ronan, P. Desmazeau, F. Viviani, C. Souaille, US2008/0139606 A1, United States, **2008**.

[244] A. Boruah, S. Chitty Venkata, S. Hosahalli, S. K. Panigrahi, WO2014/125408, **2014**.

[245] W. Stensen, F. Schevenels, Marko Istvan, S. John, WO2014/198848, **2014**.

[246] V. Spano, I. Frasson, D. Giallombardo, F. Doria, B. Parrino, A. Carbone, A. Montalbano, M. Nadai, P. Diana, G. Cirrincione, M. Freccero, S. N. Richter, P. Barraja, *Eur. J. Med. Chem.* **2016**, *123*, 447-461.

[247] R. Schütz, S. Schmidt, F. Bracher, *Tetrahedron* **2020**, *76*, 131150.

[248] F. Bracher, *Arch. Pharm.* **1989**, *322*, 293-294.

[249] L. Finger, bachelor thesis, Ludwig-Maximilians-Universität (München), **2021**.

[250] C. Gege, O. Kinzel, E. Hambruch, M. Birkel, C. Kremoser, U. Deuschle, WO2020/002611 A1, **2020**.

[251] K. Tanaka, S. Inoue, N. Murai, S. Shirotori, K. Nakamoto, S. Abe, T. Horii, M. Miyazaki, K. Hata, N. Watanabe, M. Asada, M. Matsukura, *Chem. Lett.* **2010**, *39*, 1033-1035.

[252] G. Abbiata, A. Arcadi, F. Marinelli, E. Rossi, *Eur. J. Org. Chem.* **2003**, 1423-1427.

[253] T. K. Mazu, J. R. Etukala, M. R. Jacob, S. I. Khan, L. A. Walker, S. Y. Ablordeppey, *Eur. J. Med. Chem.* **2011**, *46*, 2378-2385.

[254] S. I. Purificacao, M. J. D. Pires, R. Rippel, A. S. Santos, M. M. B. Marques, *Org. Lett.* **2017**, *19*, 5118-5121.

[255] O. A. Namjoshi, A. Gryboski, G. O. Fonseca, M. L. Van Linn, Z. J. Wang, J. R. Deschamps, J. M. Cook, *J. Org. Chem.* **2011**, *76*, 4721-4727.

[256] D. Ellies, S. Kimball, R. Young, US 2020/0055853 A1, United States, **2020**.

[257] M. Mizuno, H. Mizufune, M. Sera, M. Mineno, T. Ueda, US2009/0326229 A1, United States, **2009**.

[258] M. J. Kim, T. Y. Park, S. M. Cho, J. H. Lee, KR2017/113319 A, Korea, **2017**.

[259] P. N. Baxter, *Chemistry* **2003**, *9*, 2531-2541.

[260] Perkin Elmer, LabChip EZ Reader MS Aassays (https://www.perkinelmer.com/de/lab-products-and-services/application-support-knowledgebase/labchip/labchip-ezreader.html#LabChipEZReaderMS Aassays-Proteinandlipidkinaseassays; accessed 29.03.2022).

[261] A. Card, C. Caldwell, H. Min, B. Lokchander, X. Hualin, S. Sciabola, A. V. Kamath, S. L. Clugston, W. R. Tschantz, W. Leyu, D. J. Moshinsky, *J. Biomol. Screen.* **2009**, *14*, 31-42.

[262] D. Perrin, T. Martin, Y. Cambet, C. Fremaux, A. Scheer, *Assay Drug Dev. Technol.* **2006**, *4*, 185-196.

[263] O. Fedorov, F. H. Niesen, S. Knapp, *Methods Mol. Biol.* **2012**, *795*, 109-118.

[264] K. Gao, R. Oerlemans, M. R. Groves, *Biophys. Rev.* **2020**, *12*, 85-104.

[265] T. Anastassiadis, S. W. Deacon, K. Devarajan, H. Ma, J. R. Peterson, *Nat. Biotechnol.* **2011**, *29*, 1039-1045.

[266] A. F. Rudolf, T. Skovgaard, S. Knapp, L. J. Jensen, J. Berthelsen, *PLOS ONE* **2014**, *9*, e98800.

[267] Reaction Biology, Kinase Panel Screening and Profiling Service (https://www.reactionbiology.com/services/kinase-assays/kinase-panel-screening; accessed 09.05.2022).

[268] Reaction Biology, Kinase Profiling & Screening (https://www.reactionbiology.com/sites/default/files/Images/Content/Kinase/White_paper_Choosing_a_Kinase_Assay_Platform.pdf; accessed 09.05.2022).

[269] F. Giraud, G. Alves, E. Debiton, L. Nauton, V. Thery, E. Durieu, Y. Ferandin, O. Lozach, L. Meijer, F. Anizon, E. Pereira, P. Moreau, *J. Med. Chem.* **2011**, *54*, 4474-4489.

[270] A. F. Abdel-Magid, *ACS Med. Chem. Lett.* **2017**, *8*, 595-597.

[271] H. Zhou, M. Xu, Q. Huang, A. T. Gates, X. D. Zhang, J. C. Castle, E. Stec, M. Ferrer, B. Strulovici, D. J. Hazuda, A. S. Espeseth, *Cell Host Microbe* **2008**, *4*, 495-504.

[272] Y. Subbannayya, N. Syed, M. A. Barbhuiya, R. Raja, A. Marimuthu, N. Sahasrabuddhe, S. M. Pinto, S. S. Manda, S. Renuse, H. C. Manju, M. A. Zameer, J. Sharma, M. Brait, K. Srikumar, J. C. Roa, M. Vijaya Kumar, K. V. Kumar, T. S. Prasad, G. Ramaswamy, R. V. Kumar, A. Pandey, H. Gowda, A. Chatterjee, *Cancer Biol. Ther.* **2015**, *16*, 336-345.

[273] C. E. Massie, A. Lynch, A. Ramos-Montoya, J. Boren, R. Stark, L. Fazli, A. Warren, H. Scott, B. Madhu, N. Sharma, H. Bon, V. Zecchini, D. M. Smith, G. M. Denicola, N. Mathews, M. Osborne, J. Hadfield, S. Macarthur, B. Adryan, S. K. Lyons, K. M. Brindle, J. Griffiths, M. E. Gleave, P. S. Rennie, D. E. Neal, I. G. Mills, *EMBO J* **2011**, *30*, 2719-2733.

[274] C. Fromont, A. Atzori, D. Kaur, L. Hashmi, G. Greco, A. Cabanillas, H. V. Nguyen, D. H. Jones, M. Garzon, A. Varela, B. Stevenson, G. P. Iacobini, M. Lenoir, S. Rajesh, C. Box, J. Kumar, P. Grant, V. Novitskaya, J. Morgan, F. J. Sorrell, C. Redondo, A. Kramer, C. J. Harris, B. Leighton, S. P. Vickers, S. C. Cheetham,

C. Kenyon, A. M. Grabowska, M. Overduin, F. Berditchevski, C. J. Weston, S. Knapp, P. M. Fischer, S. Butterworth, *J. Med. Chem.* **2020**, *63*, 6784-6801.

[275] L. W. Loo, Y. Wang, E. M. Flynn, M. J. Lund, E. J. Bowles, D. S. Buist, J. M. Liff, E. W. Flagg, R. J. Coates, J. W. Eley, L. Hsu, P. L. Porter, *Breast Cancer Res. Treat.* **2011**, *127*, 297-308.

[276] M. Flajolet, G. He, M. Heiman, A. Lin, A. C. Nairn, P. Greengard, *Proc. Natl. Acad. Sci. U.S.A.* **2007**, *104*, 4159-4164.

[277] P. Janovska, E. Normant, H. Miskin, V. Bryja, *Int. J. Mol. Sci.* **2020**, *21*, 9026.

[278] D. W. Litchfield, *Biochem. J.* **2003**, *369*, 1-15.

[279] J. Boni, C. Rubio-Perez, N. Lopez-Bigas, C. Fillat, S. de la Luna, *Cancers* **2020**, *12*, 2106.

[280] A. Correa-Saez, R. Jimenez-Izquierdo, M. Garrido-Rodriguez, R. Morrugares, E. Munoz, M. A. Calzado, *Cell. Mol. Life Sci.* **2020**, *77*, 4747-4763.

[281] H. Arrouchi, W. Lakhlili, A. Ibrahimi, *Bioinformation* **2019**, *15*, 40-45.

[282] T. Mosmann, *J. Immunol. Methods* **1983**, *65*, 55-63.

[283] M. V. Berridge, A. S. Tan, *Arch. Biochem. Biophys.* **1993**, *303*, 474-482.

[284] S. Kumar, A. Singh, K. Kumar, V. Kumar, *Eur. J. Med. Chem.* **2017**, *142*, 48-73.

[285] R. Cao, W. Peng, H. Chen, X. Hou, H. Guan, Q. Chen, Y. Ma, A. Xu, *Eur. J. Med. Chem.* **2005**, *40*, 249-257.

[286] M. R. Panice, S. M. M. Lopes, M. C. Figueiredo, A. L. T. Goes Ruiz, M. A. Foglio, A. S. Nazari Formagio, M. H. Sarragiotto, E. M. T. Pinho, *Eur. J. Med. Chem.* **2019**, *179*, 123-132.

[287] S. Moser, K. Johnsson, *ChemBioChem* **2013**, *14*, 2239-2242.

[288] Y. Fu, L. Buryanovskyy, Z. Zhang, *J. Biol. Chem.* **2008**, *283*, 23829-23835.

[289] E. Janda, F. Nepveu, B. Calamini, G. Ferry, J. A. Boutin, *Mol. Pharmacol.* **2020**, *98*, 620-633.

[290] J. A. Winger, O. Hantschel, G. Superti-Furga, J. Kuriyan, *BMC Struct. Biol.* **2009**, *9*, 7.

[291] M. Chhour, P. Perio, R. Gayon, H. Ternet-Fontebasso, G. Ferry, F. Nepveu, J. A. Boutin, J. Sudor, K. Reybier, *Front. pharmacol.* **2021**, *12*, 660641.

[292] W. O. Kermack, W. H. Perkin, R. Robinson, *J. Chem. Soc., Trans.* **1922**, *121*, 1872-1896.

[293] E. Bamberger, E. Demuth, *Ber. Dtsch. Chem. Ges.* **1901**, *34*, 4015-4028.

[294] X. Jiang, X. Xu, Y. Lin, Y. Yan, P. Li, R. Bai, Y. Xie, *Tetrahedron* **2018**, *74*, 5879-5885.

[295] P. P. T. Sah, *J. Am. Chem. Soc.* **1942**, *64*, 1487-1488.

[296] S. Ginsburg, I. B. Wilson, *J. Am. Chem. Soc.* **1957**, *79*, 481-485.

[297] J.-I. Nakaya, K. Mori, H. Kinoshita, S.-I. Ono, *Nippon kagaku zassi* **1959**, *80*, 1212-1215.

[298] G. Goto, K. Kawakita, T. Okutani, T. Miki, *Chem. Pharm. Bull.* **1986**, *34*, 3202-3207.

[299] R. M. Silverstein, E. E. Ryskiewicz, S. W. Chaikin, *J. Am. Chem. Soc.* **2002**, *76*, 4485-4486.

[300] H. M. Viart, A. Bachmann, W. Kayitare, R. Sarpong, *J. Am. Chem. Soc.* **2017**, *139*, 1325-1329.

[301] T. Itahara, *J. Org. Chem.* **1985**, *50*, 5272-5275.

[302] C. J. Moody, C. W. Rees, R. G. Young, *J. Chem. Soc., Perkin Trans. 1* **1991**, 329-333.

[303] D. J. Sheffield, K. R. Wooldridge, *J. Chem. Soc., Perkin Trans. 1* **1972**, 2506-2509.

[304] M. H. Fisher, G. Schwartzkopf, Jr., D. R. Hoff, *J. Med. Chem.* **1972**, *15*, 1168-1171.

[305] A. Krämer, C. G. Kurz, B. T. Berger, I. E. Celik, A. Tjaden, F. A. Greco, S. Knapp, T. Hanke, *Eur. J. Med. Chem.* **2020**, *208*, 112770.

6.3 List of figures

6.4 List of schemes

6.5 List of tables